WOODHEAD PUBLISHING SERIES IN COMPOSITES SCIENCE AND ENGINEERING

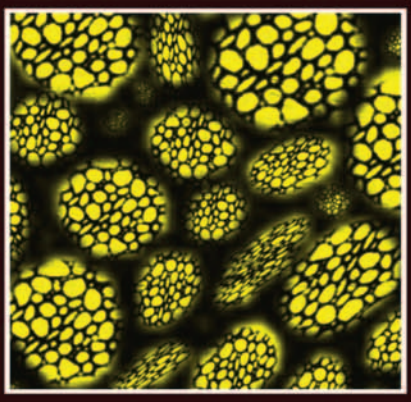

Biodegradable and Biocompatible Polymer Composites

Processing, Properties and Applications

Navinchandra Gopal Shimpi

WP
WOODHEAD PUBLISHING

Biodegradable and Biocompatible Polymer Composites

Related titles

Green Composites, 2e
(ISBN: 978-0-08-100783-9)

Advanced High Strength Natural Fibre Composites in Construction
(ISBN: 978-0-08-100411-1)

Natural Fibre-Reinforced Biodegradable and Bioresorbable Polymer Composites
(ISBN: 978-0-08-100656-6)

Woodhead Publishing Series in Composites Science and Engineering

Biodegradable and Biocompatible Polymer Composites

Processing, Properties and Applications

Edited by

Navinchandra Gopal Shimpi
Associate Professor
Department of Chemistry
University of Mumbai
Santa Cruz (E) India

WP
WOODHEAD
PUBLISHING
An imprint of Elsevier

Woodhead Publishing is an imprint of Elsevier
The Officers' Mess Business Centre, Royston Road, Duxford, CB22 4QH, United Kingdom
50 Hampshire Street, 5th Floor, Cambridge, MA 02139, United States
The Boulevard, Langford Lane, Kidlington, OX5 1GB, United Kingdom

Notices
Knowledge and best practice in this field are constantly changing. As new research and experience broaden our understanding, changes in research methods, professional practices, or medical treatment may become necessary.

Practitioners and researchers must always rely on their own experience and knowledge in evaluating and using any information, methods, compounds, or experiments described herein. In using such information or methods they should be mindful of their own safety and the safety of others, including parties for whom they have a professional responsibility.

To the fullest extent of the law, neither the Publisher nor the authors, contributors, or editors, assume any liability for any injury and/or damage to persons or property as a matter of products liability, negligence or otherwise, or from any use or operation of any methods, products, instructions, or ideas contained in the material herein.

Library of Congress Cataloging-in-Publication Data
A catalog record for this book is available from the Library of Congress

British Library Cataloguing-in-Publication Data
A catalogue record for this book is available from the British Library

ISBN: 978-0-08-100970-3 (print)
ISBN: 978-0-08-101058-7 (online)

Publisher: Matthew Deans
Acquisition Editor: Gwen Jones
Editorial Project Manager: Sabrina Webber
Production Project Manager: Surya Narayanan Jayachandran
Designer: Mark Rogers

Typeset by TNQ Books and Journals

Dedicated to my parents (Gopalrao and Bhanumati), wife (Harsha), kids (Shraddha & Omshree), elder brother (Sohan) and Sister's-Brother-in Law's with Nephew (Pratham). Finally to my GURU (S. Mishra).

This page intentionally left blank

Contents

List of contributors xiii
Biography xv
Preface xvii
Introduction xxi

Part One Characterization, synthesis and preparation of biodegradable composites 1

1 Natural and synthetic biocompatible and biodegradable polymers 3
Anand B. Balaji, Harshini Pakalapati, Mohammad Khalid, Rashmi Walvekar and Humaira Siddiqui
1.1 Introduction 3
1.2 Natural biopolymers 4
1.3 Synthetic biodegradable and biocompatible polymers 15
References 28

2 Surface modification techniques of biodegradable and biocompatible polymers 33
Feven M. Michael, Mohammad Khalid, Rashmi Walvekar, Humaira Siddiqui and Anand B. Balaji
2.1 Introduction 33
2.2 Physicochemical method 37
2.3 Mechanical method 48
2.4 Biological method 49
2.5 Summary 52
References 52

3 Characterization, testing, and reinforcing materials of biodegradable composites 55
Jignesh P. Patel and Parsotam H. Parsania
3.1 Introduction 55
3.2 Methods of fiber extraction and fiber cleaning 57
3.3 Fiber yielding plants and trees 58
3.4 Fiber modification 67
3.5 Chemical composition and physical properties of natural fibers 71

3.6 Characterization of natural fibers **74**
References **78**

Part Two Applications of biodegradable and biocompatible polymer composites 81

4 Medical applications 83
Ivan Djordjevic, Samira Hosseini and José I. Gómez Quiñones
4.1 Introduction **83**
4.2 Biodegradable composite biomaterials: implants and the concept of tissue engineering **86**
4.3 Release of filler components in physiological environment **100**
4.4 Composites as delivery mediators for bioactive components at the tissue interface **107**
4.5 Polymer/polymer composites and the concept of interpenetrated hydrogel networks **109**
4.6 Conclusion and future directions **111**
Acknowledgments **111**
References **112**

5 Surface modification of natural fibers 115
Anish M. Varghese and Vikas Mittal
5.1 Introduction **115**
5.2 Cotton fibers **118**
5.3 Flax fibers **122**
5.4 Hemp fibers **123**
5.5 Jute fibers **126**
5.6 Ramie fibers **128**
5.7 Kenaf fibers **129**
5.8 Bamboo fibers **130**
5.9 Coir fibers **131**
5.10 Oil palm fibers **133**
5.11 Sisal fibers **134**
5.12 Other lignocellulosic plant fibers **136**
5.13 Silk fibers **138**
5.14 Wool fibers **139**
5.15 Conclusions **141**
References **143**

6 Polymer composites with functionalized natural fibers 157
Anish M. Varghese and Vikas Mittal
6.1 Introduction **157**
6.2 Functionalized jute fiber–reinforced polymer composites **158**
6.3 Functionalized hemp fiber–reinforced polymer composites **161**
6.4 Functionalized kenaf fiber–reinforced polymer composites **163**

6.5 Functionalized flax fiber–reinforced polymer composites **165**
6.6 Functionalized ramie fiber–reinforced polymer composites **167**
6.7 Functionalized sisal fiber–reinforced polymer composites **168**
6.8 Functionalized bamboo fiber–reinforced polymer composites **170**
6.9 Functionalized coir fiber–reinforced polymer composites **172**
6.10 Functionalized oil palm fiber–reinforced polymer composites **174**
6.11 Polymer composites with other functionalized natural fibers **175**
6.12 Conclusions **177**
References **177**

7 Biocompatible and biodegradable Chitosan nanocomposites loaded with carbon nanotubes 187
Shadpour Mallakpour and Leila Khodadadzadeh
7.1 Introduction **187**
7.2 Synthesis and characterization of chit/carbon nanotube nanocomposites **189**
7.3 Applications of chit/carbon nanotube nanocomposites **201**
7.4 Conclusions **215**
Acknowledgments **216**
References **216**

8 Polycaprolactone/metal oxide nanocomposites: an overview of recent progress and applications 223
Shadpour Mallakpour and Nasrin Nouruzi
8.1 Introduction **223**
8.2 Polycaprolactone **224**
8.3 Metal oxides **226**
8.4 Polycaprolactone/metal oxide nanocomposites **228**
8.5 Conclusions **254**
Acknowledgments **255**
References **255**

9 Applications of biodegradable polymer/layered double hydroxide nanocomposites: current status and recent prospects 265
Shadpour Mallakpour and Elham Khadem
9.1 Introduction **265**
9.2 Polymer/layered double hydroxide nanocomposite **266**
9.3 Investigation biodegradability of polymer/layered double hydroxide nanocomposites **269**
9.4 Applications of biopolymer/layered double hydroxide nanocomposite **271**
9.5 Conclusions **289**
Acknowledgments **289**
References **289**

10 Poly(vinyl alcohol)/carbon nanotube nanocomposites: challenges and opportunities **297**
Shadpour Mallakpour and Shima Rashidimoghadam
10.1 Introduction **297**
10.2 Synthesis of poly(vinyl alcohol)/carbon nanotube nanocoposites **300**
10.3 Conclusions **311**
Acknowledgments **311**
References **312**

11 Bio-based aliphatic polyesters from dicarboxylic acids and related sugar and amino acid derivatives **317**
Jordi Puiggalí, Angélica Díaz and Ramaz Katsarava
11.1 Introduction **317**
11.2 Poly(alkylene dicarboxylate)s from renewable resources **318**
11.3 Poly(alkylene dicarboxylate)s and poly(ester amide)s from sugar-based monomers **320**
11.4 Biodegradable polymers composed of naturally occurring α-amino acids **323**
11.5 Nanocomposites from poly(alkylene dicarboxylate)s **331**
11.6 Nanocomposites from poly(ester amide)s **335**
11.7 Conclusions **341**
References **342**

12 Fundamentals of bionanocomposites **351**
Rajesh K. Saini, Anil K. Bajpai and Era Jain
12.1 Introduction **351**
12.2 Classification of composites **353**
12.3 Types of biopolymers used in bionanocomposites **355**
12.4 Preparation of nanocomposites **366**
12.5 Properties of bionanocomposites **369**
References **373**
Further reading **377**

13 Advances in bionanocomposites for biomedical applications **379**
Rajesh K. Saini, Anil K. Bajpai and Era Jain
13.1 Introduction **379**
13.2 Dental applications **379**
13.3 Orthopedic applications **381**
13.4 Tissue engineering **382**
13.5 Drug delivery **388**
13.6 Wound dressings **391**
13.7 Biosensors applications **395**
References **396**

14 Quality- and sustainability-related issues associated with biopolymers for food packaging applications: a comprehensive review **401**
Carlo Ingrao and Valentina Siracusa
14.1 Introduction **401**
14.2 Roles of food packaging **402**
14.3 Biodegradable polymers utilized in food packaging: a brief overview **403**
14.4 Packaging, sustainability, and the use of life cycle assessment **409**
14.5 Applications of life cycle assessment and related tools in the supply chains of packages made out of polylactic acid: a comprehensive review **413**
14.6 Conclusions **414**
References **415**

Index **419**

This page intentionally left blank

List of contributors

Anil K. Bajpai Government Model Science College, Jabalpur, India

Anand B. Balaji University of Nottingham Malaysia Campus, Semenyih, Malaysia

Angélica Díaz Escola d'Enginyeria de Barcelona Est-EEBE, Barcelona, Spain

Ivan Djordjevic Tecnologico de Monterrey, Monterrey, Mexico

José I. Gómez Quiñones Tecnologico de Monterrey, Monterrey, Mexico

Samira Hosseini Tecnologico de Monterrey, Monterrey, Mexico

Carlo Ingrao University of Catania, Catania, Italy

Era Jain Saint Louis University, Saint Louis, MO, United States

Ramaz Katsarava Agricultural University of Georgia, Tbilisi, Georgia

Elham Khadem Isfahan University of Technology, Isfahan, Islamic Republic of Iran

Mohammad Khalid Sunway University, Subang Jaya, Malaysia

Leila Khodadadzadeh Isfahan University of Technology, Isfahan, Islamic Republic of Iran

Shadpour Mallakpour Isfahan University of Technology, Isfahan, Islamic Republic of Iran

Feven M. Michael University of Nottingham Malaysia Campus, Semenyih, Malaysia

Vikas Mittal The Petroleum Institute, Abu Dhabi, United Arab Emirates

Nasrin Nouruzi Isfahan University of Technology, Isfahan, Islamic Republic of Iran

Harshini Pakalapati University of Nottingham Malaysia Campus, Semenyih, Malaysia

Parsotam H. Parsania Saurashtra University, Rajkot, India

Jignesh P. Patel Saurashtra University, Rajkot, India

Jordi Puiggalí Escola d'Enginyeria de Barcelona Est-EEBE, Barcelona, Spain

Shima Rashidimoghadam Isfahan University of Technology, Isfahan, Islamic Republic of Iran

Rajesh K. Saini Government Model Science College, Jabalpur, India

Humaira Siddiqui Taylor's University, Subang Jaya, Malaysia

Valentina Siracusa University of Catania, Catania, Italy

Anish M. Varghese The Petroleum Institute, Abu Dhabi, United Arab Emirates

Rashmi Walvekar Taylor's University, Subang Jaya, Malaysia

Biography

Dr. Navinchandra Gopal Shimpi has been working as an Associate Professor in the Department of Chemistry, University of Mumbai, Mumbai, since April 2014. Previously, he was associated with University Institute of Chemical Technology, Jalgaon. He has completed PhD from North Maharashtra University, Jalgaon, in 2006. He is the recipient of Young Scientist Award from Asian Polymer Association in 2014 and Dnyanjoti Puraskar in 2008 from Shirsathe Foundation, Jalgaon. So far, he has published more than 65 papers in international journals of good impact factor and delivered more than 40 lectures as an invited speaker. He has generated Rs 1.2 crores for outstanding research from various funding agencies. He is at present having one research project from UGC, New Delhi, and one consultancy project from Indofil Chemicals Ltd, Thane. So far, seven students have completed their PhD, two have submitted their thesis, and eight are doing their PhD under his guidance. He is having two granted patents and four are under examination. Moreover, he has guided 15 students for their MTech dissertation. Besides this, he has organized five national and international conferences with five staff development programs and four professional certificate courses. He is an associate editor of *International Journal of Chemical Studies* and worked as a lead guest editor for Advancement in Polymeric Nanomaterials and Nanocomposites, a special issue of *International Journal of Polymer Science*.

This page intentionally left blank

Preface

Biodegradable and Biocompatible Polymer Composites: Processing, Properties, and Applications deals with polymer composites of biodegradable and biocompatible polymers with their processing, properties, and applications. The book begins by discussing the state of the art, new challenges, and opportunities of various biodegradable and biocompatible polymer composite systems. Interfacial characterization of the composites is discussed in detail. The processing techniques for various systems and the influence of processing parameters on the properties of the composite are reviewed in detail. The characterizations of microstructure, elastic, viscoelastic, static and dynamic mechanical, thermal, rheological, optical, and electrical and barrier properties are highlighted, as well as their myriad applications. Biocomposites are often interpreted as either biomass-based or biomedical materials. The former have a wider meaning than the latter, because they are available for various industrial purposes. A biomass-based composite consists of biomass and/or biomass-derived substance. On the other hand, a biomedical composite is a specified material because it is limited merely to biomedical use. In this use, the constituents are not necessarily biomass based or biodegradable but should be biocompatible. In the present volume, as stated earlier, by biocomposites, we mean biomass-based composites. In this volume, the application of biocomposites is premised on structural use rather than functional one. From this point of view, we need to know exactly the mechanical properties, such as tensile strength and Young's modulus, of natural fibers and wood flours, similar to the case of artificial reinforcing materials such as carbon and glass fibers. Tensile properties of natural fibers such as cotton, flax, wool, and silk have been examined in detail in the field of textile engineering.

Intention behind editing this book is to introduce the readers with the recent outcomes and importance of biodegradable and biocompatible polymers and their composites, along with their processing, properties, and applications. This book will cover several aspects in terms of societal, academic, industrial, and research benefits.

This book is of great importance not only to the learners but also to the more experienced researchers, research scholars, and students of postgraduation and graduation. Based on particular theme of this book, this has been divided into two parts—*Part One: Characterization, Synthesis, and Preparation of Biodegradable composites*, which includes 3 chapters, and *Part Two: Applications of Biodegradable and Biocompatible Polymer Composites*, which includes 11 chapters.

Chapter 1 presents the introduction of natural and synthetic biopolymers, along with details of both types of polymers.

Chapter 2 presents surface modification techniques such as physicochemical and mechanical methods of biodegradable and biocompatible polymers, along with few of the biological methods of surface modifications.

Chapter 3 presents characterization, testing, and reinforcing materials of biodegradable composites and gives introduction and methods of fiber extraction and fiber cleaning. In addition this chapter gives idea about fiber yielding plants and trees with modification of fiber. Chemical composition and physical properties of natural fibers with characterization of natural fibers have also been given in detail.

Chapter 4 emphasizes on medical applications of biodegradable and biocompatible polymers. Initially, introduction about the chapter has been given. This chapter gives the idea about implants and the concept of tissue engineering in biodegradable composite biomaterials, along with release of filler components in physiological environment. This chapter also gives details of composites as delivery mediators for bioactive components at the tissue interface with polymer/polymer composites and the concept of interpenetrated hydrogel networks. Finally, the chapter has been concluded with future directions.

Chapter 5 covers surface modification of natural fibers such as cotton fibers, flax fibers, hemp fibers, jute fibers, ramie fibers, kenaf fibers, bamboo fibers, coir fibers, oil palm fibers, sisal fibers, other lignocellulosic plant fibers, silk fibers, and wool fibers. Finally, the chapter has been concluded by considering the above points.

Chapter 6 deals with polymer composites with functionalized natural fibers. In this chapter the detail explanation of functionalized jute fiber–reinforced polymer composites, hemp fiber–reinforced polymer composites, kenaf fiber–reinforced polymer composites, flax fiber–reinforced polymer composites, functionalized ramie fiber–reinforced polymer composites, sisal fiber–reinforced polymer composites, bamboo fiber–reinforced polymer composites, coir fiber–reinforced polymer composites, oil palm fiber–reinforced polymer composites, and polymer composites with other functionalized natural fibers have been discussed with effective concluding remarks.

Chapter 7 deals with biocompatible and biodegradable chitosan nanocomposites loaded with carbon nanotubes. In this chapter, synthesis and characterization of chit/carbon nanotubes nanocomposites with their applications of chit/carbon nanotubes nanocomposites has been discussed with concluding remarks.

Chapter 8 focuses on an overview of recent progress and applications of polycaprolactone/metal oxide nanocomposites, which mentions the metal oxides with their nanocomposites.

Chapter 9 deals with current status and recent prospects of applications of biodegradable polymer/layered double hydroxide nanocomposites. Moreover, investigation of biodegradability of polymer/layered double hydroxide nanocomposites with their applications of biopolymer/layered double hydroxide nanocomposites has been discussed.

Chapter 10 deals with challenges and opportunities of poly(vinyl alcohol)/carbon nanotubes nanocomposites. The synthesis of poly(vinyl alcohol)/carbon nanotubes nanocomposites has been discussed in detail with concluding remarks.

Chapter 11 deals with bio-based aliphatic polyesters from dicarboxylic acids and related sugar and amino acid derivatives, which includes poly(alkylene dicarboxylate)s from renewable resources, poly(alkylene dicarboxylate)s and poly(ester amide)s from sugar-based monomers, biodegradable polymers composed of naturally occurring α-amino acids, and nanocomposites from poly(alkylene dicarboxylate)s and poly(ester amide)s.

Chapter 12 summarizes fundamentals of bionanocomposites with classification of composites and types of biopolymers used in bionanocomposites with preparation of nanocomposites and properties of bionanocomposites.

Chapter 13 deals with advances in bionanocomposites for biomedical applications, which includes dental, orthopedic, tissue engineering, drug delivery, wound dressings, and biosensors applications.

Chapter 14 summarizes a comprehensive review of quality- and sustainability-related issues associated with biopolymers for food packaging applications.

Dr. Navinchandra Gopal Shimpi
Editor

This page intentionally left blank

Introduction

Navinchandra Gopal Shimpi
Department of Chemistry, University of Mumbai, Santa Cruz (E) India

1. Introduction to biodegradable polymers

We know that polymers are widely used in various industrial fields because of their merits, such as light weight, resistance to chemicals, resistance to the environment, and easy processing. It is difficult for polymers to be treated after use because of their resistance to the environment. When polymers are disposed of in a natural environment, they remain for a long time without degradation.

Biopolymers (bio-based and biodegradable) have become polymer matrices of interest in recent years. This may be because of the fear of depleting fossil resources, which are the largest sources of monomers from which the majority of synthetic polymers are generated till the date. Conventionally used common polymers such as polyethylene, polypropylene, polystyrene, and poly(methyl methacrylate) are nonbiodegradable, and recycling or reusing them is a very challenging task. This causes generation of huge amount of nonbiodegradable wastes all over the world. Composites generated from these polymers also become a part of this waste. Because most of the biodegradable polymers originated from other alternative renewable sources, their use in the polymer composites technology is fascinating; however, their substitution to commercial synthetic polymers has some serious challenges. Primarily, brittleness, low thermal stability, and poor barrier properties are some of them. Nowadays, biodegradable polymers are focused by many researchers because of their biodegradation ability that reduces synthetic waste [1]. After long time, these materials get decomposed into eco-friendly molecules [2–4]. The microorganisms present in the environment use the available carbon dioxide and water to biodegrade these polymers and are used for many applications [5–10].

Biodegradable polymers consist of ester, amide, or ether bonds. In general, biodegradable polymers can be grouped into two large groups based on their structure and synthesis (Fig. 1). One of these groups is agro-polymers, or those derived from biomass [11]. The other consists of biopolyesters, which are derived from microorganisms or synthetically made from either natural or synthetic monomers.

Agro-polymers include polysaccharides, such as starches found in potatoes or wood, and proteins, such as animal-based whey or plant-derived gluten. Polysaccharides consist of glycosidic bonds, which take a hemiacetal of a saccharide and bind it to an alcohol via loss of water. Proteins are made from amino acids, which contain various functional groups [12]. These amino acids come together again through condensation reactions to form peptide bonds, which consist of amide functional groups [12]. Examples of biopolyesters include polyhydroxybutyrate and polylactic acid.

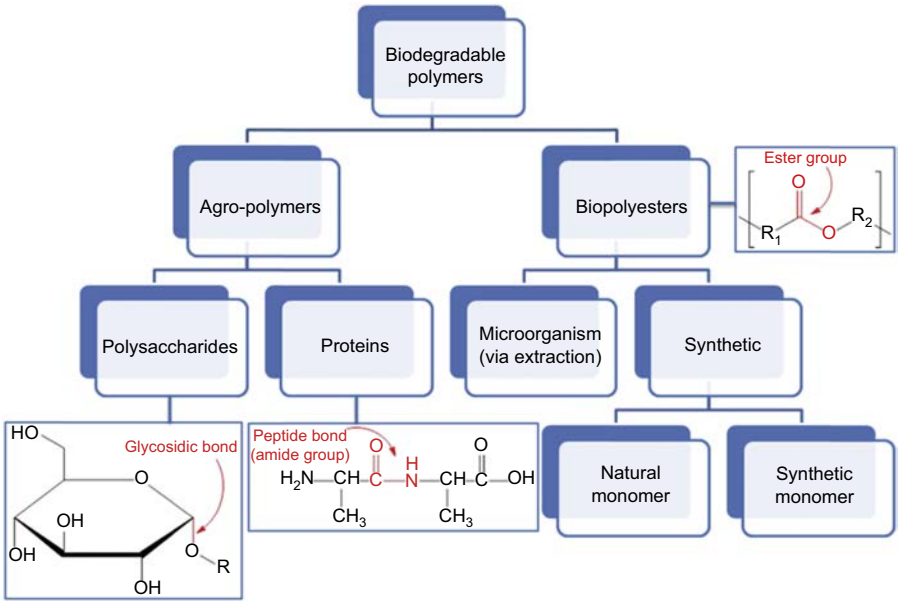

Figure 1 Organization of biodegradable polymers based on structure and occurrence [11].

2. Introduction to biocompatible polymers

Biocompatibility is one of the most important characteristics of a biomedical polymer material whose surface is required to interact with a biological system. Such interactions between polymer surfaces and organisms have been the focus of many studies.

A commonly used definition of biocompatibility is "the ability of a material to perform with an appropriate host response in a specific application". However, because the interaction between materials and biological systems occurs in a wide range of applications and molecular processes, there is no precise definition for a biocompatible material or accurate measurement of biocompatibility. Nevertheless, whether the materials will be accepted by a living body should be the criterion to evaluate the biocompatibility of materials. Biocompatible polymers have wide applications such as tissue culture, tissue scaffolds, implantable controlled drug delivery systems, catheters and dialysis tubing, artificial grafts, envelops for implantations of cardiac devices, wildlife vaccinations, and coatings on medical devices.

Considering the need and expectations of the readers in relevance with this field, this book has been divided into two parts having 14 chapters. Intention behind editing this book is to introduce the readers regarding recent outcomes and importance of biodegradable and biocompatible polymers and their composites along with their processing, properties, and applications. This book will cover several aspects in terms of societal, academic, industrial, and research benefits.

This book is of great importance not only to the learners but also to the more experienced researchers, research scholars, and students of postgraduation and graduation. Based on particular theme, this book has been divided into two parts: *Part One: Characterization, synthesis, and preparation of biodegradable composites*, which includes 3 chapters, and *Part Two: Applications of biodegradable and biocompatible polymer composites*, which includes 11 chapters. The details of each part along with the chapters included have been given in preface.

References

[1] T.T. Mohammad, A. Zahra, N. Zainab, Study of enzymatic degradation and water absorption of nanocomposites starch/polyvinyl alcohol and sodium montmorillonite clay, Journal of the Taiwan Institute of Chemical Engineers 43 (2012) 120–124.
[2] M.T. Taghizadeh, N. Nalbandi, A. Bahadori, Stabilizing effect of epoxidized sunflower oil as a secondary stabilizer for Ca/Hg stabilized PVC, Express Polymer Letters 2 (2008) 65–76.
[3] S. Mishra, N.R. Talele, Filler effect of potato starch and urea on degradation of linear low density polyethylene composites, Polymer-Plastics Technology and Engineering 41 (2002) 361–381.
[4] S.K. Rath, R.P. Singh, On the characterization of grafted and ungrafted starch, amylose, and amylopectin, Journal of Applied Polymer Science 70 (1998) 1795–1810.
[5] K. Fukushima, C. Abbate, D. Tabuani, M. Gennari, G. Camino, Biodegradation of poly(lactic acid) and its nanocomposites, Polymer Degradation and Stability 94 (2009) 1646–1655.
[6] N.G. Shimpi, M.D. Borane, S. Mishra, M. Kadam, Biodegradation of polystyrene (IPP)-poly(lactic acid) (PLA) nanocomposites using *Peudomonas aeruginosa*, Macromolecular Research 20 (2012) 181–187.
[7] N. Erika, L. Mazzucco, P. Gentile, T. Benko, V. Balbo, R. Mandrile, G. Ciardelli, Preparation and biodegradation of clay composites of PLA, Reactive and Functional Polymers 69 (2009) 371–379.
[8] R.B. Finkelman, Health benefits of geologic materials and geologic processes, International Journal of Environmental Research and Public Health 4 (2006) 338–342.
[9] M.A. Paul, C. Delcourt, M. Alexandre, P. Degee, F. Monteverde, P. Dubois, Polylactide/montmorillonite nanocomposites: study of the hydrolytic degradation, Polymer Degradation Stability 87 (2005) 535–542.
[10] C.P. Aguzzi, C. Viseras, C. Caramella, Use of clays as drug delivery systems: possibilities and limitations, Applied Clay Science 36 (2007) 22–36.
[11] L. Avérous, E. Pollet, Environmental silicate nano-biocomposites, Springer, London, 2012, ISBN: 978-1-4471-4108-2.
[12] M.L. Johnson, L. Brand (Eds.), Computer methods, first ed., Academic Press, San Diego, CA, 2011, ISBN: 9781118164792.

This page intentionally left blank

Part One

Characterization, synthesis, and preparation of biodegradable composites

This page intentionally left blank

Natural and synthetic biocompatible and biodegradable polymers

1

Anand B. Balaji[1], *Harshini Pakalapati*[1], *Mohammad Khalid*[2], *Rashmi Walvekar*[3], *Humaira Siddiqui*[3]
[1]University of Nottingham Malaysia Campus, Semenyih, Malaysia; [2]Sunway University, Subang Jaya, Malaysia; [3]Taylor's University, Subang Jaya, Malaysia

1.1 Introduction

Polymers whose basis of production is from natural resources including both animals and plants are termed as biopolymers. On the other hand, polymers that move with biological structures/system and assess, treat, supplement, or replace any unit of body are termed as biocompatible polymers. The polymers that break down into biologically acceptable molecules are classified as biodegradable polymers. In this chapter, the aforementioned polymer types are collectively termed as bio-based polymers. Typically, these polymers are classified into two types: natural and synthetic polymers. Natural biopolymers such as polysaccharides and proteins are from renewable or biological sources comprising of plant, animal, microbial, and marine sources, whereas synthetic polymers such as polyesters and aliphatic polymers are chemically synthesized. The commercial importance of these polymers are increasing due to their excellent biocompatibility and biodegradability. Biodegradation is usually catalyzed by enzymes and may involve both hydrolysis and oxidation. Biopolymers being used in tissue engineering, orthopedic replacements, and scaffold engineering have a demanding impact as they degrade into acids and other components that can either be digested or be eliminated by the animal body. However, the easy tailoring of mechanical, chemical, and thermal properties during their extraction, synthesis, or modification methods is an added advantage. Packaging industries, cosmetics, sutures, dental applications such as artificial tooth and filling pastes, photography, material manufacturing, food and beverage industries are some of the trades and commerce where bio-based polymers have established their roots of applications. As a result of the increased importance of biodegradable, biocompatible, and biopolymers in today's world, this chapter focuses on the source, structure, properties, biosynthetic or chemical synthesis pathways, extraction methods, and applications of few commercially important polymers.

Biodegradable and Biocompatible Polymer Composites. http://dx.doi.org/10.1016/B978-0-08-100970-3.00001-8

1.2 Natural biopolymers

Natural biopolymers are macromolecular compounds that occur naturally within various organisms. The biopolymers are synthesized by the living microorganisms consisting of repeating units connected by covalently bonded units. Natural polymers are found in microorganisms such as bacteria, fungi, and algae, whereas complex polymers such as proteins, nucleic acid, fats, and hydrocarbons are present in animals; cellulose, oils, starches, and even polyesters are found in plants and lower organisms. Although minute or large quantities, these polymers are finding their industrial importance due to their biodegradability, biocompatibility, and the ability to be synthetically modified. Several industrial extraction methods are being developed to make the natural polymers available for day-to-day consumption at affordable prices. The structure, biosynthesis, application, and extraction methods of few polymers are elaborated in subsequent sections.

1.2.1 Proteins

1.2.1.1 Collagen

Collagens are insoluble fibrous proteins, which are responsible for providing the structure for most of the animal bodies. Collagen has a triple helix structure, configured by the presence of three polypeptide alpha chains coiled around each other. Each alpha chain comprises more than 1000 amino acids featuring a sequence entailing glycine, proline, and hydroxyproline. Till date, more than 28 types of collagen have been identified and classified according to their assembly of polypeptide chains, various lengths and interruptions of helix structure, and differences in terminations of helix. However, 80%–90% of the collagen in animal body belongs to the classification of type 1–3. Collagens are found in ligaments, tissues, skin bones, cartilages, blood vessels, cornea, lungs, and muscle tissues.

Biosynthesis of collagens is a severe and complex system encompassing a number of intracellular and extracellular procedures (Fig. 1.1). Fibroblasts, chondrocytes, osteoblasts, ondoblasts, cementoblasts, epithelial cells are the few sites of biosynthesis of collagens. The transcription of RNA is the first step in the synthesis of the compounds. A 3D structure with the amino acids is assembled by posttranslational modifications to form procollagen. These steps include alteration of proline remains into hydroxyprolines, whereas the lysines are modified to hydroxylysines. Subsequently, they undergo N- and O-linked glycosylation and followed by trimerization. The disulfide bondings are formed ahead advocating for the strength of the procollagen. The compounds follow prolyl *cis–trans* isomerization to form helix structures, leading to the formation of procollagens. Furthermore, the procollagen passes to Golgi and unites with secretory vacuoles to move to the outside cell. Furthermore, the process follows the cleavage of C and N peptides by proteinase. The collagens then assemble themselves to form fibrils. These fibrils at this stage are weak and immature. As a final step, the covalent cross-links (including ester bonds, lysine bonds, hydroxylysine bonds, and other bonds with saccharides) are formed to stabilize the fibrils, thus forming collagens [1,2].

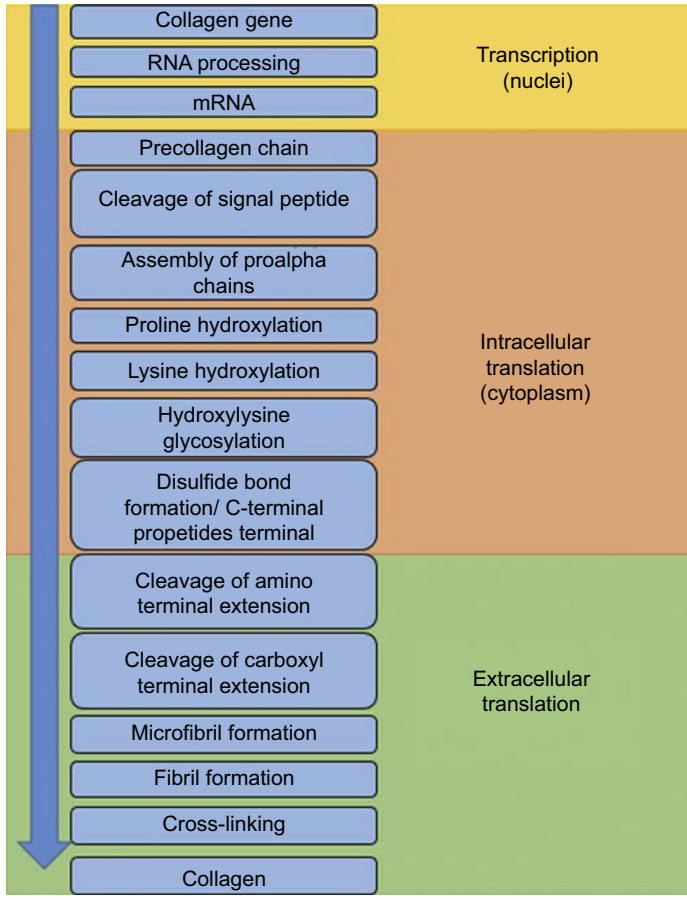

Figure 1.1 Biosynthetic pathway of collagen.

Collagens are mainly extracted by chemical hydrolysis or enzymatic hydrolysis. However, the raw material undergoes pretreatment process prior to hydrolysis. The pretreatment is necessary to remove the covalent cross-links formed during the biosynthesis [3]. Dilute acids such as acetic acid or bases such as sodium hydroxide are employed to the raw material to cleave the cross-links and for partial hydrolysis purposes. Furthermore, the hydrolysis of the collagen materials is performed using neutral saline solutions such as sodium chloride (NaCl), Tris-HCl (Tris(hydroxymethyl) aminomethanehydrochloride), phosphates, or citrates; organic acids such as acetic acid, citric acid, and lactic acid; inorganic acids such as hydrochloric acid [4–6]; and base solutions such as sodium hydroxide. Pepsin, Papain, pronase, alcalase, collagenases, bromelain, and trypsin are few enzymes used in enzymatic hydrolysis extraction of collagens [7,8].

Recently, collagens in short time are synthesized from gelatin by using protease enzymes for hydrolysis. Pancreatin, bromelain, papain, alcalase, propase E, Neutrase, Flavourzyme, and Protamex are some of the protease enzymes used in commercial

production of collagens from gelatin [9]. The extraction can also be enhanced using ultrasonication [10] and ultrafiltration systems [11], which are some advanced technologies used in enhanced extraction of collagens for commercial purposes. Collagens are used in cosmetics as antiaging creams, treatment of arthritis, dental composites as root canal filling, food and beverage industry to stabilize consistency and elasticity of food, photography, wound dressings, ophthalmic collagen shields, etc.

1.2.1.2 Gluten

Glutens are a viscoelastic prolamins extracted mainly from wheat flour, barley, triticale, rye, and oats. Based on the efficiency of extraction, gluten consists of 75%–85% protein and 5%–10% lipids and few amounts of starch. Gluten consists of hundreds of protein components either present as monomers or linked by interchain disulfide bonds. Gluten proteins have high molecular weight more than 30,000 Da and always found to be attached with starch in endosperm of the source. The wheat gluten proteins consist of two main fractions called gliadins and glutenins. Both the units comprise numerous proteins characterized by proline and glutamine. The gliadins are soluble in aqueous alcohols, whereas the glutenins are insoluble in aqueous alcohols. Cysteine and tyrosine cross-links; tyrosine–dehydroferulic acid, and arabinoxylans are few covalent bonds along with other noncovalent bonds found in the main structure of the gluten protein [12]. The biosynthesis of gluten is similar to other proteins with complex inter- and intracellular translations. The biosynthesis of gluten based on the postulates of Graham and Mortan is represented schematically in Fig. 1.2 [13]. The event of gluten proteins transcription coded by the genes takes place within the intercellular matter called endoplasmic reticulum. The N-terminal peptides are cleaved and transfer from the reticulum to the lumen. Furthermore, protein folds and undergoes disulfide bond formation. Enzymes such as protein disulfide isomerase and peptidyl–propyl cis–trans isomerase and molecular chaperons aid the

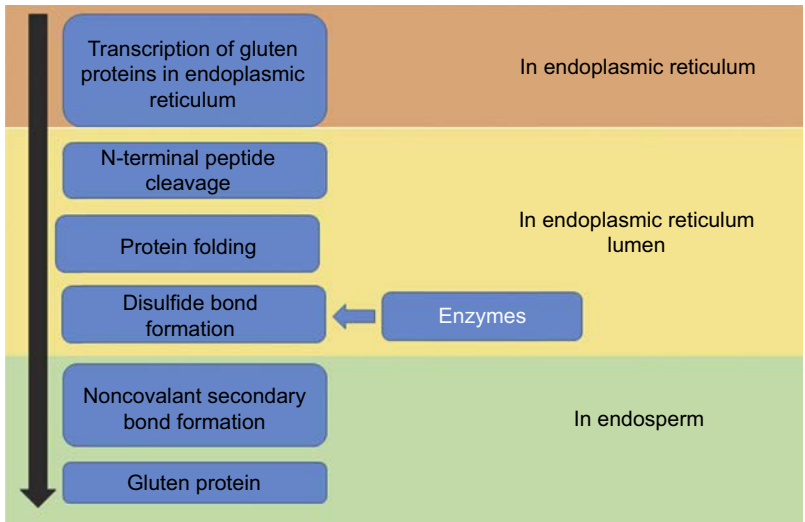

Figure 1.2 The synthesis of gluten in natural isolate.

disulfide formation in the biosynthesis of gluten proteins [14]. The nonsecondary advocates for the functionality of the gluten protein, which in turn is attached to the endoplasmic reticulum of the sources.

Commercially, the glutens are produced by Beccari process, Martin process, Batter process, and Laval Rasisio process [15]. However, the glutens are produced from these methods with the principle process of rinsing the starch from the kneaded dough (milled wheat flour with added water) and by hydrolysis. The glutens are mainly used in food industry in the manufacturing of breads and cookies. Furthermore, the modified glutens are also used as replacement of calf milk, as medical bandages and adhesive tapes, for binding heavy metals in industrial processes, for removing ink from waste paper; for solidifying waste oils, and in cosmetic industries [15].

1.2.1.3 Gelatin

Gelatin, a colorless, translucent, odorless, and rather tasteless substance, is entirely made up of amino acids linked by peptides. Gelatin contains 8%–13% moisture and has a relative density of 1.3–1.4. Gelatins are soluble in glycerol, propylene glycol, acetic acid, trifluoro ethanol, and formamide, whereas they are insoluble in less polar organic solvents such as benzene, acetone, primary alcohols, and dimethyl formamide. Gelatins are produced by partial hydrolysis and denaturation process of collagen, the most common protein in animal kingdom. Gelatins produced from collagens are extracted from cattle bones, hides, pig skins, mammals, and fish. The primary structure corresponding to the 18 groups of amino acids is the same for all gelatin types, with slight difference in their composition percentage due to the source of collagens (Fig. 1.3). The amino acid composition of gelatin from various sources is listed in Table 1.1. However, the secondary structure of

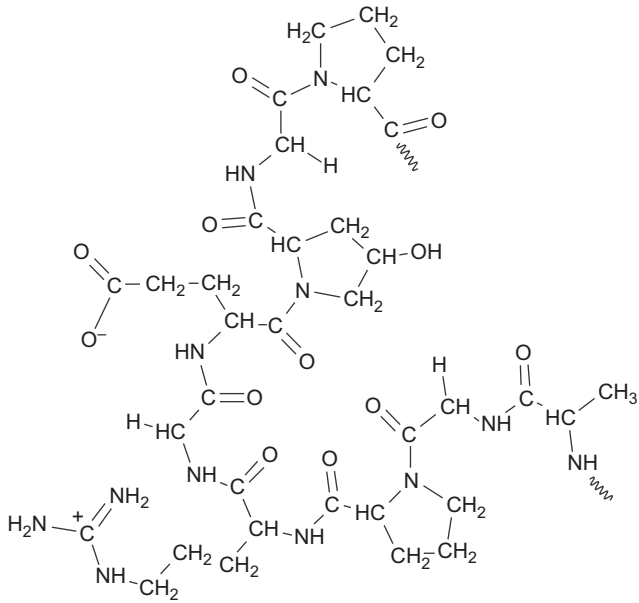

Figure 1.3 Gelatin structure.

Table 1.1 Amino acid compositions of various gelatin sources

Amino acid compositions (g/100 gm gelatin)	Pork skin	Calf skin	Bone	Sorghum bug	Melon bug	Red tilapia fish	Black tilapia fish
	Test [16]			Mariod and Adam [17]		Jamilah and Harvinder [18]	
Alanine	8.6	9.3	10.1	0.018	0.021	0.076	0.0903
Arginine	8.3	8.55	5.0	0.035	0.033	0.0295	0.0351
Aspartic acid	6.2	6.6	4.6	0.018	0.013	0.038	0.039
Cystine	0.1	Trace	Trace	Trace	Trace	0.0015	0.0029
Glutamic acid	11.3	11.1	11.6	0.043	0.027	0.071	0.0769
Glycine	26.3	26.9	28.8	0.048	0.051	0.38	0.30
Histidine	0.9	0.74	0.7	0.007	0.008	Not detected	
Hydroxylysine	1.0	0.91	0.9	Trace			
Hydroxyproline	13.5	14.0	13.4	Trace			
Isoleucine	1.4	1.7	1.5	0.009	0.010	0.0084	0.0094
Leucine	3.1	3.1	3.5	0.02	0.02	0.018	0.020
Lysine	4.1	4.5	4.4	0.021	0.018	0.0213	0.028
Methionine	0.8	0.8	0.6	0.0038	0.003	0.014	0.017
Phenylalanine	2.1	2.2	2.5	0.01	0.011	0.018	0.021
Proline	16.2	14.8	15.5	0.052	0.058	Not detected	0.0005
Serine	2.9	3.2	3.8	0.006	0.004	Not detected	
Threonine	2.2	2.2	2.4	0.0095	0.007	0.134	0.155
Tyrosine	0.4	0.2	0.2	0.0036	0.0032	0.005	0.0068
Valine	2.5	2.6	3.0	0.259	0.289	0.017	0.022

gelatins is made up of different polypeptide chains including α-chains, β chains (dimers of α-chain), and γ chains (trimers of α-chain), which attributes to the difference in molecular weight.

The collagens are subjected to thermal treatment at temperature of 40°C in presence of water where both hydrogen and electrostatic interactions (that stabilizes the collagen helix) are broken down. Subsequently, the process follows hydrolysis to break the intramolecular bonds between the three chains of the helix. The presence of any other additional retraining bonds between the chains can lead to formation of three different forms of gelatin during hydrolysis: (1) formation of three randomly coiled independent α-chains; (2) formation of a β-chain (two α-chains linked by one or more covalent bonds) and an independent α-chain; and (3) formation of a γ-chain (three chains linked by covalent bonds. The molecular weight for the α form varies from 80,000 to 125,000 and for the β form varies from 160,000 to 250,000. The molecular weight variation for the γ form is from 240,000 to 375,000 [17] (Fig. 1.4).

The manufacturing process of gelatin involves raw material preparation including degreasing and removing impurities that may have undesirable changes on physicochemical assets of the final gelatin product. The raw material is then subjected to acid or alkali treatment based on the source of raw collagen. The one extracted from an acid-treated is known as type A gelatin (typically used on pork), and resultant gelatin from an alkali-cured precursor is classified as type B (typically used on beef hides). The process is followed by multistage extraction to hydrolyze collagen into gelatin. Few decolorizing agents such as aluminum sulfate, aluminum hydroxide, monocalcium, sodium carbonate, hydrogen chloride, and disodium phosphate dodecahydrate are added in pretreatment process to prepare pigment-free gelatins and improve their transparency [19]. Finally, the refining and recovering treatments are carried out. Fig. 1.5 shows detailed production steps of gelatin. Gelatins are commonly used as emulsifiers, foaming agents, fining agents, and gelling agents in food, pharmaceuticals, photography, and cosmetic manufacturing.

1.2.2 Polysaccharides

1.2.2.1 Chitin and chitosan

Chitin is a rigid, simple polysaccharide, consisting of repeating units of *N*-acetyl glucosamine linked with β(1–4)glycosidic bonds. It is the second abundant natural biopolymer [20,21]. It is the essential constituent of cell walls of all fungi and also serves as the exoskeleton of crustaceans, arthropods, insects, and mollusks giving them a structure, strength, and maintaining the cell integrity. It is a white, inelastic, hard, nitrogenous hydrophobic polysaccharide. Commercially, chitin is obtained from crab and shrimp shells (Figs. 1.6 and 1.7).

Deacetylated form of chitin is chitosan. It has alternate D-glucosamine (deacetylated unit) and *N*-acetyl-D-glucosamine (acetylated unit) linked by β(1–4) linkage. It is colorless and has chelating ability for many transitional metal ions. It has reactive

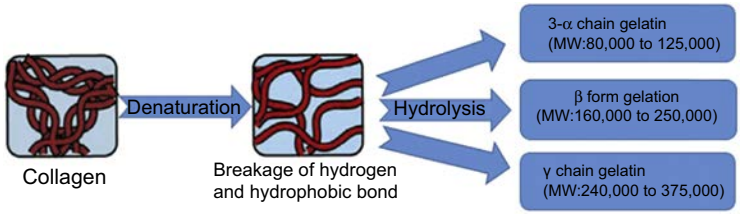

Figure 1.4 General schematic for extraction of gelatin from natural resources.

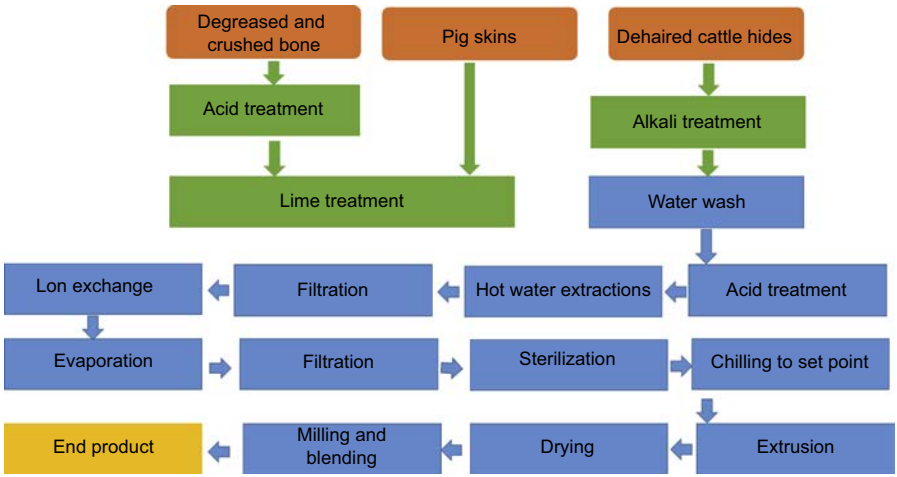

Figure 1.5 Steps involved in industrial extraction of gelatin.

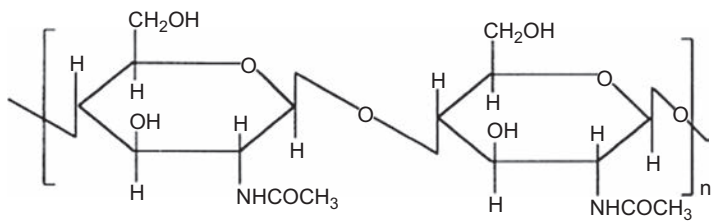

Figure 1.6 Schematics for chitin.

amine group making it possible to participate in chemical reactions (esterification and transesterification). The properties of chitosan vary with degree of deacetylation, acetyl groups, and also chain length.

Naturally occurring biopolymers are generally modified to make them more potential to become a part of industrial and medical applications. Chitin and chitosan are

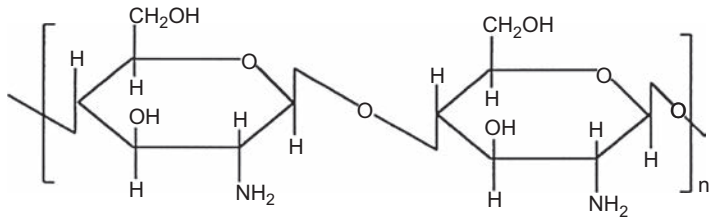

Figure 1.7 General structure of chitosan.

renewable biopolymers with biodegradable, biocompatible, and nontoxicity properties. Chitin is used in food processing industries as flavoring and coloring agent. In agriculture, chitin and chitosan are used for control release fertilizer and also reported to increase the crop yield. In medical field, chitin is used to prepare the suture threads due to its rigidity. Due to its biodegradable nontoxic properties, it is blended with many other polymers making its way into drug delivery and tissue engineering as well. Chitosan finds application as flocculants and antipollution agent due to its unique property (having pseudocationic nature) [21].

Chitin synthesis takes place in epidermis cells. The starting material for chitin synthesis is glycogen. First step is catalysis of glycogen phosphorylase enzyme, i.e., glycogen is converted to glucose-1-phosphate. Interconversion is next step catalyzed by phosphomutase forming glucose-6-P further converted to fructose-6-P by hexokinase. Further conversion from fructose-6-phosphate to *N*-acetyl glucosamine involves amination (glutamine to glutamic acid), acetylation (acetyl CoA to CoA), isomerization step (phosphate transfer to C6 to C1 catalyzed by a phospho-*N*-acetyl glucosamine mutase). Later, uridine diphosphate (UDP) *N*-acetyl glucosamine is formed by utilization of uridine triphosphate (UTP). Chitin synthase is an important enzyme finally forming chitin from UDP *N*-acetyl glucosamine (Fig. 1.8).

Commercially, chitin and chitosan are isolated by chemical process involving demineralization, deproteinization, and decolorization. Demineralization is achieved by removing the inorganic matter (calcium carbonate mainly) using HCl. Later the protein matter is extracted in alkaline medium, i.e., deproteinization, obtaining chitin. Temperature and alkali concentration are important for effective deproteinization. Further treatment using 50% NaOH results in deacetylation of chitin forming chitosan (Fig. 1.9).

1.2.2.2 Cellulose

Cellulose is the most abundant biopolymer available in nature. About 180 million tons of cellulose is produced in nature annually [22]. It is synthesized by a variety of living organisms, including plants, algae, bacteria, and animals. It is the main component of cell wall in plants and also in natural fibers such as cotton, wood (90% of wood consists of cellulose), flax, and jute. Of total plant tissues, cellulose occupies one-third part. It is synthesized in the form of microfibrils (in plants) and biofilms (in algae and bacteria).

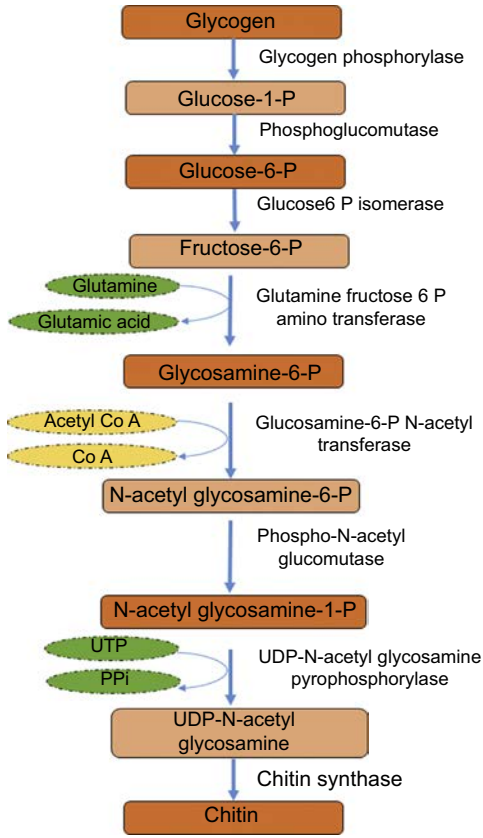

Figure 1.8 Natural synthesis pathway of chitin and chitosan. *UDP*, uridine diphosphate.

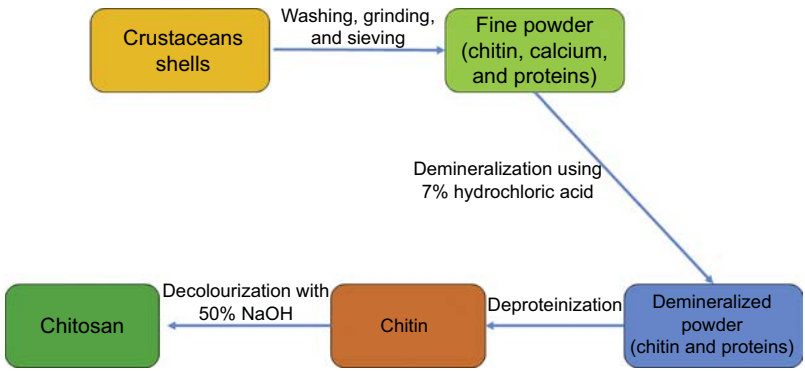

Figure 1.9 Extraction procedures for chitin and chitosan.

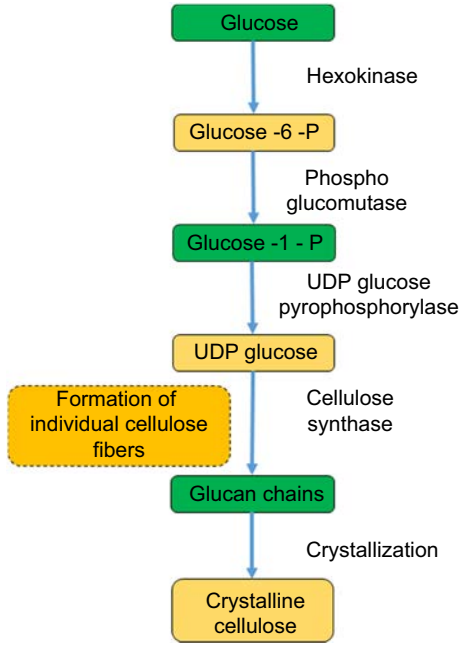

Figure 1.10 Biosynthetic pathways for cellulose synthesis. *UDP*, uridine diphosphate.

Cellulose is a crystalline polymer consisting of glucose units linked by β-1,4-glycosidic linkage organized in linear chains. It is colorless, odorless, hydrophilic, and insoluble in organic solvents. Its melting point is between 450 and 500°C [23]. It is mainly used to make paper and furniture.

Synthesis of cellulose occurs in plasma membrane in plants and Golgi apparatus in algae and obtained extracellularly in bacteria [24]. Formation of cellulose takes place in two stages: stage 1: polymerization, formation of glucan chains from UDP glucose residues catalyzed by cellulose synthase and stage 2: crystallization, where the individual glucan chains associate to form crystalline cellulose. The synthesis pathway of cellulose is depicted in Fig. 1.10.

Cellulose has huge potential applications in various industries such as pharmacy, biofuel production, and consumables. As a result, extracting cellulose from natural sources become significant. This process involves the treatment of natural fibers (with alkali/bisulfites and ionic solvents) and the separation of other components such as lignin. Extraction process can be done by different methods such as dissolution in ionic solvents (1-butyl-3-methylimidazolium chloride, 1-allyl-3-methylimidazolium chloride) [25], Jayme-wise method and digyme-HCl method [26], some classical methods modified using ultrasonication [27]. Each method has its advantages and disadvantages varying in amount and quality of cellulose. Cellulose should be modified to be processable. Cellulose acetate is an important derivative of cellulose with commercial importance. Tenite (United States), Bioceta (Italy), Fasal (Austria), and Natureflex (Germany) are trade names of cellulose-based polymers [28]. Ethers and some esters of cellulose derivatives also have commercial value.

1.2.2.3 Starch

Starch is a biodegradable, abundantly available, and one of the cheapest biopolymers. It is the major storage of carbohydrate in higher plants, readily available to generate energy when required (mainly during dormancy and growth). It is a common carbohydrate that serves as a major diet for human beings. Apart from nutrition, it also has various applications, used as adhesive in paper and textile industry, as starting material for ethanol production, for texturizing, and to provide specific functionalities in processed foods. It has branched structure with amylose (20%–30%) and amylopectin (70%–80%) arranged in layers linked by α(1–4) and (1–6) glycosidic linkages. It is white, odorless, and insoluble in cold water. Synthesis of starch takes place in leaves at daytime and mobilized at night. They are formed in meristems and root cap cells also. After the formation it is transported to organs such as tubers, seeds, and fruits, which perform the storage function.

Synthesis of starch takes place in cytosol and amyloplast of the cell. Repeating unit and starting material in starch is glucose. Series of reactions are depicted in Fig. 1.11. Glucose-6-P is transported from cytosol by glucose translocator. Source of glucose-6-P is from reductive pentose phosphate pathway (sucrose pathway). Phosphoglucomutase and ADP glucose pyrophosphorylase catalyze the formation of ADP glucose. Starch synthase enzyme catalyzes the next important step, formation of α(1–4) linkage between the preexisting glucan chains and the glucose moiety of ADP glucose, liberating ADP. Branching (formation of α(1–6) linkage is catalyzed by the branching enzyme. After the addition of minimum residues of glucose in the chains, branching occurs forming the α(1–6) linkage. Branching enzyme shows specificity for the length of the α(1–4) glucan chain that they will use as a substrate. Amylose and amylopectin are formed, finally resulting in the formation of starch [29].

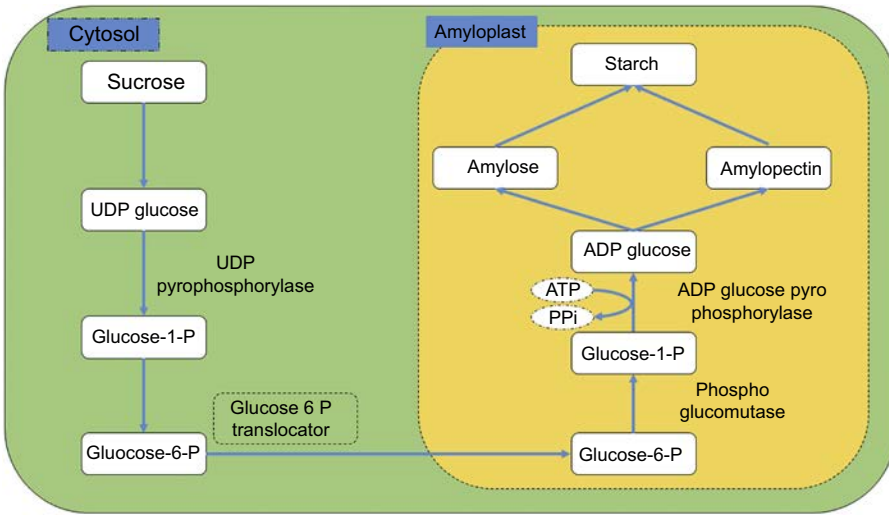

Figure 1.11 Starch synthesis in plant cells. *UDP*, uridine diphosphate.

Table 1.2 Different extraction methods for starch

Source	Method	Chemical used	References
Wheat	Pressing and decanting	NaCl	[30]
Pea	Pin milling and air classification	NaOH	[31]
Banana	Wet milling process	NaOH	[32]
Cassava		Ammonia	[33]
Potato	Washing with chemical followed by centrifugation and drying	Sodium thiosulfate and sodium chloride	[34]
Maize	Mixing and heating	Alcohols	[35]

Corn starch (maize, common corn), tuber starch (potato, cassava), and other cereals (rice, wheat, and barley) are the major source for industrial starch. Different methods and chemicals are implemented to extract the starch from different sources. Some references are mentioned in Table 1.2.

Poor mechanical properties, delicate nature, and sensibility are the disadvantages of starch-based products. Starch-based products suffer from water sensibility, brittleness, and poor mechanical properties. This problem is overcome by chemical modifications; usually the hydroxyl group is modified by acetylation. In another approach, starch is blended with synthetic biodegradable polymers.

1.3 Synthetic biodegradable and biocompatible polymers

Few polymers such as polylactic acid (PLA) are derived from renewable natural resources. Hence they can also be clarified under the category of biopolymers. Although they are derived from sources such as corn starch and cassava roots, they undergo chemical and enzymatic polymerization for large-scale production. However, a variety of biodegradable and biocompatible polymers are synthesized by chemical methods. Esters, anhydrides, diacids, and amides are few framework chemical compositions of these polymers. The weak hydrolyzable links forming the backbones of synthetic biopolymers are the prime source of biodegradability. They chemically or enzymatically break down into their monomer units, among which few are biologically acceptable by the human bodies, making their importance significant in various biomedical applications.

These polymers are generally synthesized by different polymerization techniques described in Fig. 1.12.

1.3.1 Polyglycolide

Polyglycolides (PGAs), the first synthetic biodegradable polymers, are prepared from polymerization of glycolic acids (Fig. 1.13). They are simple, linear, or aliphatic polyester chains with crystallinity of 45%–52%. PGAs were first synthesized to be used

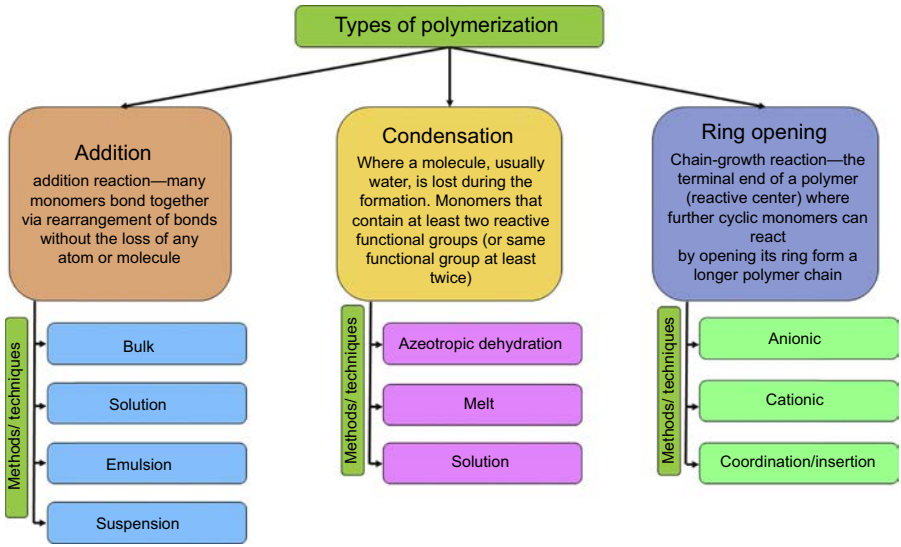

Figure 1.12 Types of polymerization.

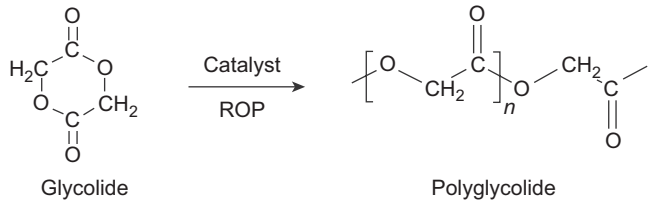

Figure 1.13 Ring-opening polymerization (ROP) of polyglycolide.

as sutures for medical applications. However, by various spinning techniques, PGAs are now used for numerous applications such as tissue engineering, scaffolds, drug delivery system, and textile technologies. These thermoplastic resins have high rate of degradation, where PGA is broken down by hydrolysis into its respective acids and alcohols. They tend to lose mechanical strength rapidly, over a period of 2–4 weeks after implantation.

PGAs are prepared by various methods based on the entrapment efficacy, rate of degradation, permanency of end product, and biocompatibility, required to engineer their application. PGAs are synthesized by simple polycondensation process of glycolic acid. Because of the thermal instability of the polymer formed and the equilibrium nature of the reaction as well as difficulties associated in removing water from the viscous polymer mass, only low-molecular-weight polymers are obtained. However, high-molecular-weight PGAs can be achieved by ring-opening polymerization (ROP), solution polymerization, and interfacial polymerization. The ROPs are

Table 1.3 Various methods for polyglycolide synthesis

Monomer	Method	Conditions	References
Sodium chloroacetate	Solid-state polycondensation	160–180°C	[37]
Glycolic acid	Melt polycondensation	220–230°C; catalyst: tin dichloride dehydrate	[38]
Glycolic acid	Melt–solid ring-opening polymerization	170°C; catalyst: $SnCl_2{\cdot}2H_2O$ and initiator: 1-dodecanol	[39]
Glycolic acid	Melt polycondensation	190°C ; catalyst: zinc acetate dehydrate,	[40]
Glycolide	Anionic ring-opening polymerization	17O°C for 2 h followed by 230°C for 0.5 h; catalyst: potassium hydroxide/potassium carbonate/pyridine	[41]
Glycolide	Ring-opening polymerization	l-Dodecanol as molecular weight regulator and tin (∏) 2-ethylhexanoate (Sn(Oct) 2)	[42]
Diglycolide	Ring-opening polymerization	130–150°C; catalyst: diphenyl bismuth bromide	[43]
Glycolide	Cationic ring-opening polymerization	100°C; catalyst: Montmorillonite clay	[44]

also facilitated by catalysts and initiators such as zinc chloride, ferric chloride, aluminum chloride, titanium tetrachloride, boron triflouride etherate, antimony triflouride, triphenyl phosphine, aluminum isopropoxide, calcium acetylacetonate, stannous octate, and several lanthanide alkoxides. PGAs can also be synthesized in one step by reacting triethylamine with bromoacetic acid in chloroform solution [36]. Recently, supercritical CO_2 has been used as a reaction medium to keep the PGAs soluble during polymerization, thus avoiding high reaction temperatures. Few PGAs with various polymerization techniques and monomers are listed in Table 1.3.

1.3.2 Poly(butylene succinate)

Poly(butylene succinates) (PBSs) are a class of aliphatic biodegradable polymers synthesized from succinic acid and butanediol. They have thermoplastic-like processing behaviour with a melting temperature of 90–120°C and a density of 125 g/cm^3. PBSs are mainly synthesized by transesterification process of dimethyl succinate with butanediol (in presence of a catalyst) followed by polycondensation or esterification process. The reaction mechanism is shown in Fig. 1.14.

PBS can also be synthesized by ROP, solution polymerization, and enzymatic polymerization. Titanium (IV) butoxide, titanium isopropoxide [45]; zirconium, tin, and germanium derivatives; p-toluenesulfonic acid; distannoxane; triflates of sodium, magnesium, bismuth, and aluminium [46]; tetrabutyl titanate [47]; and scandium(III) trifluoromethanesulfonate [48] are some of the catalysts used in producing PBS, whereas *Candida antarctica* (lipase B) is the most common enzyme used in the synthesis of PBS [49]. Moreover, as an additional step to polycondensation process, chain extenders having two functional groups can couple the PBS to increase their molecular weight. 2,2-(1,4-Phenylene)-bis(2-oxazoline) [50], adipoyl biscaprolactamate, hexamethylene diisocyanate [45], toluene-2,4-diisocyanate, benzoyl peroxide (BPO), BPO/ethylene glycol dimethacrylate (DF), and BPO/triallyl cyanurate (TF) [51] are few chain extenders used in production of extended PBS. PBSs are used in agriculture, packaging, drug delivery system, and construction engineering and textile sectors.

1.3.3 Poly(p-dioxanone)

Poly(p-dioxanone) (PDS) are biopolymer compounds with several ester–ether chains. They are crystalline and colorless materials used in the manufacturing of sutures for pediatric, ophthalmic, plastic, and gastrointestinal surgeries; drug delivery systems; and other orthopedic uses. They are of good interest in biomedical industries due to their biodegradability and extensive biocompatibility. PDS degrades into glycoxylate by hydrolysis. The degradation of PDS is slow to moderate, where it can retain its original strength up to 1–2 months [51a]. Although PDS hydrolyzes slower than the other synthetic absorbable sutures, external particle reactions with material are judged to be minimal (Fig. 1.15).

PDSs' are mainly polymerized by ROP of dioxane, synthesized by oxidative dehydrogenation of diethylene glycol. Similar to polymerization of other synthetic biopolymers (such as polycaprolactone (PCL) and PGA), metal derivative catalysts such as zinc diethyl, stannous octoate, triethylaluminum, and aluminum isopropoxide are few used in polymerization of PDS [51b].

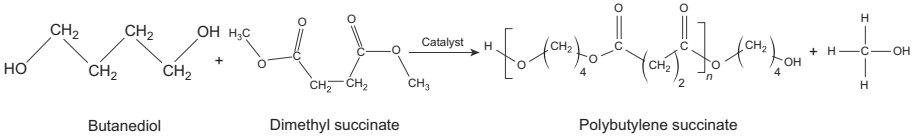

Figure 1.14 Poly(butylene succinate)synthesis.

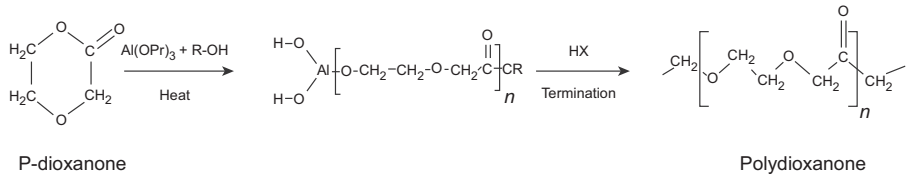

Figure 1.15 Ring-opening polymerization of polydioxanone.

1.3.4 Polyester amides

Polyester amides (PEAs) are synthetic biodegradable polymers with a combination of ester (–COO–) and amide groups (–NHCO–). The hydrolyzable ester groups advocate for the degradable character, whereas the amide linkages due to their strong intermolecular hydrogen bonding interactions provide the mechanical and thermal strength to the polymer. Various PEAs are developed from different monomers including α-amino acids, α-hydroxy acids, cyclic depsipeptides, fatty diacids, diols, α,ω-amino alcohols, diacyl chlorides, and carbohydrates. The PEAs are also produced from linseed oil, nahar seed oil, albizia benth oil, and pongamia glabra oil. A wide range of PEAs can be produced by varying the ester/amide ratio, aliphatic and aromatic ratio, hydrophilicity, stereochemistry, degree of functionalization, molecular architectures (e.g., linear or hyperbranched chains), and monomer distribution (e.g., ordered, blocky, or random) [52]. PEAs are modified with pendant carboxylic acid groups to produce polymers with high degradation rate. The carboxylic groups act as catalytic effect on hydrolytic scission of the ester bonds in the backbone of PEA.

PEAs have been synthesized by ROP and polycondensation methods. ROP has been mainly used in the synthesis from α-amino acids, α-hydroxy acids, and morpholine-2,5-diones. Production of PEAs by polycondensation has usually been performed by reacting diamide–diol, diester–diamine, ester–diamine, or diamide–diester monomers with dicarboxylic acid derivatives or diols. In addition, α,ω-amino alcohols can also be reacted with acid anhydrides or dicarboxylic acid derivatives to construct these polymers. Production of PEAs through thermal polycondensation of halogenoacetates is another route, where the by-product (metal salt) is removed at the end of the process. On the other hand, microwave radiations of sebacic acid and α,ω-amino alcohols (3-aminopropanol, 2-aminoethanol, and 6-aminohexanol) are applied to yield with higher-molecular-weight PGA. The microwave radiations provide volumetric heating as opposed to conventional heating methods.

1.3.5 Polyanhydride

Polyanhydrides are a group of biopolymers where the repeating units are connected by the anhydride bonds. They find increasing interest in biomedical applications due to their nature of degradation. Generally, the anhydride links undergo hydrolytic degradation to produce nontoxic diacidic units that either get metabolized or eliminated from the human body. Butcher and Slade [53] synthesized the first synthetic polyanhydride by treating acetic anhydride with isophthalic or terephthalic acid. Since then, hundreds of polyanhydrides are synthesized with various different building blocks, mostly being acidic groups. Based on the chemistry of the molecule between the anhydride bonds, they are classified into aliphatic, aromatic, unsaturated, and aliphatic–aromatic homopolyanhydrides. Aromatic polyanhydrides degrade slowly over a long period, whereas aliphatic polyanhydrides degrade in a few days. The monomer units with higher hydrophobicity degrade slower in comparison with building units with higher hydrophilicity.

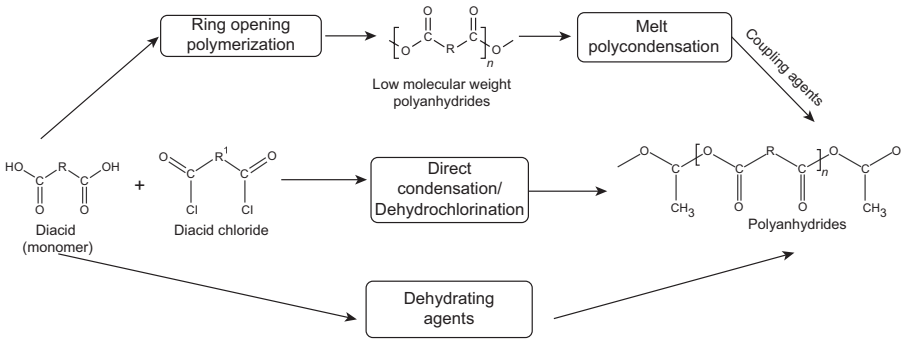

Figure 1.16 Synthetic pathways for the production of polyanhydrides.

Polyanhydrides are mainly synthesized by melt condensation, ROP, interfacial condensation, dehydrochlorination, and dehydrative coupling agents. Dichloromethane, chloroform dimethylformamide, benzene, and ethyl ether are few solvents used to produce polyanhydride by solution method. Dehydrochlorination (e.g., poly(terephthalic anhydride)) follows the Schotten–Baumann condensation, where the hydrochloric group is removed from the diacid chloride and a dicarboxylic acid in presence of a base to form polyanhydride [54]. However, the resultant polymers have less purity in comparison to the polyanhydrides synthesized from other methods. Although melt condensation results in high-purity polymers, it is not suitable to synthesize polyanhydrides from heat-sensitive acidic monomers. Furthermore, these biodegradable polymers with high molecular weights could also be produced by using coupling agents such as diacyl chloride, phosgene, and many other acid receptors including poly(4-vinylpyridine) (PVP) and potassium carbonate at ambient temperatures. Rapid synthesis of polyanhydrides is also facilitated by microwave and dielectric heating.

Polyanhydrides are modified accordingly to alter the degradation rate. For instance, fatty chain acids (such as stearic acid) are incorporated into polyanhydride to decrease the degradation rate. Amino acids (such as imide, glycine, β-alanine, γ-aminobutyric acid, L-leucine, L-tyrosine, 11-aminododecanoic acid, and 12-aminododecanoic acid)–based polymers are synthesized by melt condensation to be used as drug carriers. Similarly, photocross-linked polyanhydrides (e.g., dimethacrylated anhydride, 1,3-bis[p-carboxyphenoxypropane], and poly(dimer acid–sebacic acid)) are used for temporary medical implants and degradable orthopedic fixing devices (Fig. 1.16).

1.3.6 Poly(alkyl cyanoacrylate)

Poly(alkyl cyanoacrylates) are quick degrading polymers synthesized from alkyl cyanoacrylate monomers. Generally, polymers with high alkyl groups such as poly(octyl cyanoacrylate) or poly(hexyl cyanoacrylate) are used as biomaterial. The smaller alkyl group degrades in presence of aqueous ambience to produce toxic degradation products such as cyanoacetic acid and formaldehyde, which could lead to irritation [51a]. They are generally soft and flexible with very low tensile strengths. Anionic

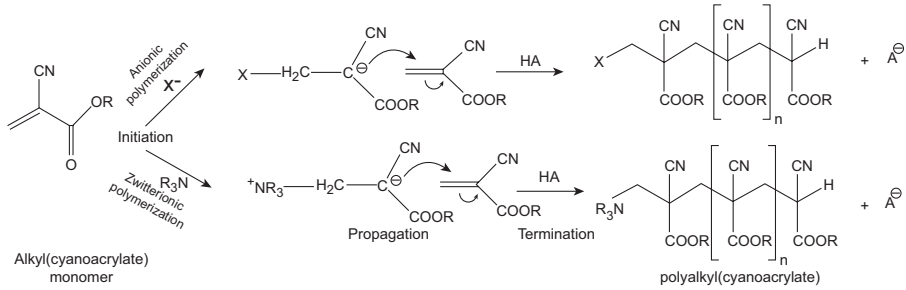

Figure 1.17 Anionic and cationic polymerization techniques of polyalkyl(cyanoacrylate).

and zwitterionic polymerization is the most preferred synthesis technique of these polymers due to their rapid chain growth and propagation. However, they can also be synthesized by free radical polymerization (very slow reaction) and bulk photoanionic polymerization. The reaction is initiated by the presence of initiators to form carbanions. The process propagates to react with another monomer to form polymer chains. The process is terminated by the formation of cation. The schematics of anionic and zwitterionic process are presented in Fig. 1.17. Phosphines and acyclic amines are most commonly used anionic initiators, whereas the others include Cl^-, $CH_3CO_2^-$, and OH^- species [54a]. Moreover, traces of moisture also act as initiator in anionic process. The free radical and zwitterionic polymerizations can be carried over by vinyl ethers, ethylene, furan, vinyl ketones, and so on [54b]. However, strong acids are required to inhibit the polymerization process. Without the presence of acids, no intrinsic termination reaction occurs.

These polymers are mainly used as skin and tissue adhesives in surgeries as a replacement of sutures due to their ability of quick polymerization in presence of moisture to form gluey nature. Recently, several copolymers and modified poly(alkyl cyanoacrylates) are finding their potential as nanoparticles in drug delivery systems for chemotherapy, as insulin administrator, and so on.

1.3.7 Polylactic acid

PLA is one of the highest consuming bioplastics in the world. It is an aliphatic polyester obtained from renewable sources such as corn sugar, starch, potato, and sugarcane. PLA has 37% crystallinity, elongation at break 30.7%, glass transition temperature of 53°C, and a melting temperature ranging between 170–180°C [28]. The polymers find their applications in fiber and textile industry, packaging, plasticulture, and most importantly in medical field and are used as a flavoring and preservative agent, bacterial inhibitor in many foods.

Basic building block of PLA is lactic acid, with asymmetric carbon atom existing in two optical active configurations (L & D). Lactic acid is derived from bacterial fermentation using *Lactobacillus* species, carbohydrates, proteins, and some nutrients such as vitamins.

Table 1.4 Catalyst and solvents used in polylactic acid synthesis

Catalyst	Solvents
Stannous octoate	Glycerol alcohols/carboxylic acids
Compounds of titanium and zirconium	Toluene
Aluminum isopropoxide	Tetrahydrofuran (THF)
Potassium naphthalenide	Toluene sulfonic acid
Tin chloride	Ethanol
Zn lactate	Ethers
Trifluoromethane sulfonate,	Methylene chloride
Mg, Al, Zn, titanium alkoxides	Isopropyl ether
Complexes of iron with acetic, butyric, isobutyric, and dichloroacetic acid	Toluene

Lactic acid having both carboxyl group and hydroxyl group easily forms polymer through polycondensation. The polycondensation of PLA can be achieved either by solution and melt polycondensation producing low-molecular-weight polymer. Various solvent systems (alcohols, organic solvents, ethers) and catalysts are used to synthesize the PLA, among which stannous octoate is mostly used [55]. Some of the solvents and catalysts used are mentioned in Table 1.4.

ROP is the most followed method to produce polymer with high molecular weight. Bulk or solution polymerization can be done; depending on the catalyst, the polymerization mechanism will occur (i.e., cationic, anionic, or coordination insertion). Higher-molecular-weight polymer is reported when the ROP is carried out (ranging from 2×10^4 to 6.8×10^5 MW) compared with polycondensation process (molecular weights lower than 1.6×10^4 MW) [55a]. Azeotropic dehydration is another method for PLA synthesis. High-molecular-weight PLA was reported using this method [56] at 138°C for 48–72 h using a drying agent and solvent xylene. Enzymatic polymerization, using enzyme as a catalyst, is considered to be environmental friendly, carried out in mild conditions, toxic free, and safer when used for medical purposes. The immobilized CALB (lipase from *C. antarctica*) gave a high-molecular-weight polymer when compared with lipase from PC and porcine pancreatic lipase [56a]. Synthesis methods of PLA are depicted in Fig 1.18.

1.3.8 Polycaprolactone

PCL is an aliphatic polyester with biodegradable and biocompatible properties. It is a semicrystalline polymer with repeating hexanoate units. Its glass transition temperature is −60°C, melting point ranges from 58 to 65°C, and degradation time is more than 24 months. Their property depends on its molecular weight and degree of crystallinity. PCL gained a lot of interest in recent decades with numerous diverse applications. It shows a rare property of being miscible and mechanically compatible with many other polymers such as PVC, PS, polybisphenol, polycarbonates, and natural rubber, which in turn improving their properties.

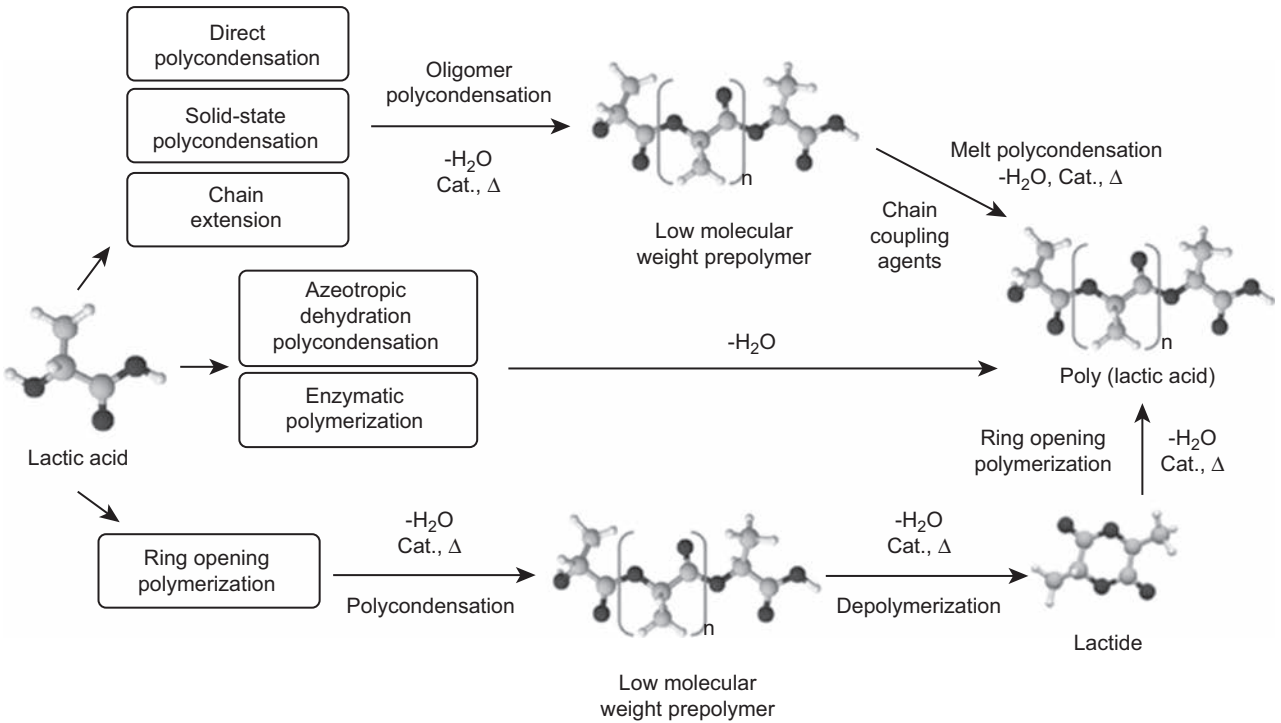

Figure 1.18 Synthesis methods of polylactic acid [57].

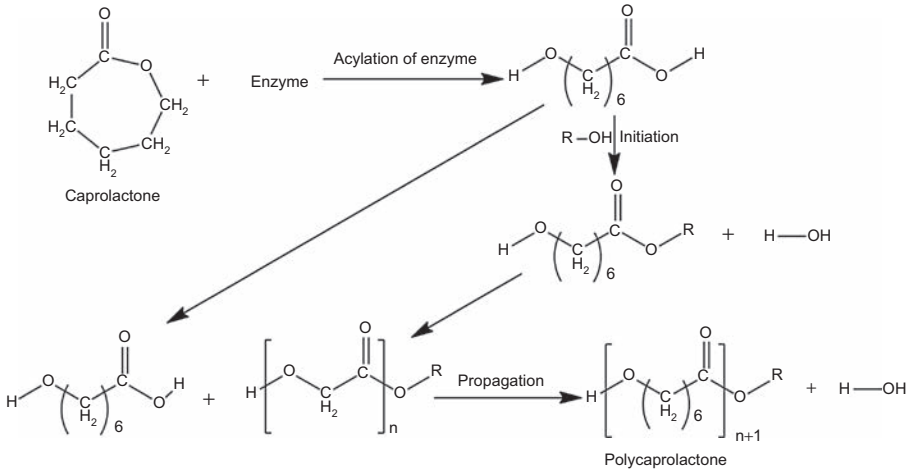

Figure 1.19 Synthesis of polycaprolactone.

Polycondensation and ROP are the two methods used to synthesize the PCL. In polycondensation method, the condensation of 6-hydroxyhexanoic acid is done under vacuum and water produced during the reaction is removed continuously. ROP is a preferred route for PCL synthesis. Conventionally the ROP of caprolactone is carried out by metal, and organometal catalysts (lithium, sodium, and potassium), rare earth metals, and transition metals have attracted considerable attention due to their high activity. Stannous octoate is the most used chemical catalyst for polymerization of caprolactone [58]. Due to the eco-friendly nature of enzymes, enzymatic polymerization came into existence being a good alternate and can also be carried out under mild conditions. There are many enzymes used to produce the PCL, maximum found to be lipases. Lipase from *Pseudomonas*, *Rhizopus*, *Yarrowia lipolytica*, and *Candida* species; cutinase from *Humicola insolens*; esterase from *Archaeoglobus fulgidus* are reported to synthesize the PCL. Of all *C. antarctica*, lipase B was reported to be a more effective catalyst than others [59] (Fig. 1.19).

PCL is synthesized conventionally by using magnetic stirrer. Recently, microwave irradiation, ultrasonication, and supercritical CO_2 technologies are used to synthesize the PCL. The advantages and disadvantages of these methods are mentioned in Table 1.5.

1.3.9 Polyurethanes

Polyurethanes are the most versatile and unique polymer material being a part of daily life. It is used in buildings, constructions, making furniture, transportation, packaging, appliances, textiles and apparels, electronics, footwear, and also medicine (implants to medical devices). Its physical and chemical properties are largely made suitable to meet the demands in modern technologies such as paintings, adhesives, fibers, and foams. Due to the fact that the composition and structure will be varied within wide

Table 1.5 Advantages and disadvantages of different methods used in polycaprolactone synthesis

Method	Advantages	Disadvantages	References
Conventional method (normal setup, magnetic stirrer for mixing)	Simple to set up	Temperature fluctuations	[60,61]
Microwave irradiation	Reaction rate enhancement Energy savings Direct heating High temperature homogeneity	Radiations may denature the enzymes	[62]
Ultrasonication	Diffusion rate is high	Chances affecting immobilization of enzymes	[63]
Superficial CO_2	Green method, no involvement of organic solvents	Low solubility of polymers	[64]

Table 1.6 Typical diisocyanates, polyols, and chain extenders used in polyurethane synthesis

Diisocyanates	Polyols	Chain extenders
Isophorone, diisocyanate	Polylactic acid	1,4-Butanediol
1,6-Diisocyanatohexane	Bis(hydroxymethyl) butyric acid	Hexane diol
1,4-Diisocyanatobutane	Polycaprolactones	Ethylene diol
Dicyclohexylmethane diisocyanate	Poly(ethylene oxide)	Diethylene diol
Lysine methyl ester diisocyanate	Poly(propylene oxide)	Ethylene diamine
4,4-Diphenylmethane diisocyanate	Poly(glycolide)	Propylene diamine
Toluene diisocyanate	Polytetramethylene oxide	
	Polyethylene adipate	

limits, there are no definite properties for polyurethanes. Polyurethanes are resistant to temperature extremes; any harsh condition will not cause its degradation easily. They exhibit good electrical insulating property.

Polyurethanes are prepared by condensation and addition reactions. Addition reaction of a diisocyanate with a diol is the commercially used method. A diisocyanate, a chain extender, and a polyol are the elements used to make polyurethane [65]. Some of these elements are given in Table 1.6.

Diisocyanates must be high purity to obtain high-molecular-weight polyurethanes. Polyesters, polyethers, hydrocarbon polymers, and polydimethylsiloxanes are

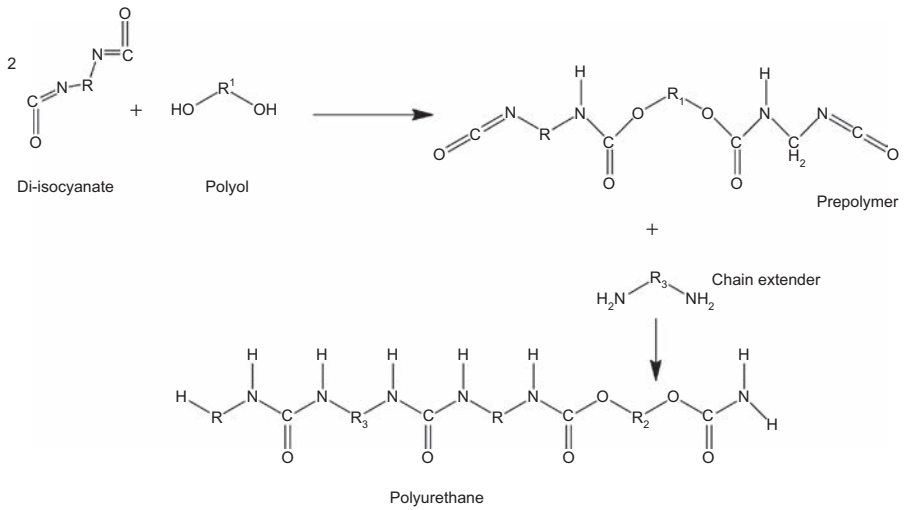

Figure 1.20 Synthetic pathways of polyurethane.

generally used as polyols. Diols and diamines (aliphatic and aromatic) and di- and polyfunctional active hydrogens are common chain extenders/cross-linkers used in polyurethane synthesis (Fig. 1.20).

Polyurethanes formed from these components (diisocyanates, polyols, and chain extenders) have hard and soft segments arranged in alternate manner. Hard constituent is usually contribution by diisocyanate, and chain extenders and polyols contribute soft segment of the polyurethane. Degradation of this polymer depends on ratio of hard and soft segments, which can be altered by selection of soft segment.

1.3.10 Polycarbonate

Polycarbonates are the aliphatic polyesters having carbonate groups in the structure with good biocompatibility and impact resistance. Traditionally they are combined with other polymers to enhance other properties such as thermal stability and biodegradation [66]. It is mainly used in electronic applications and construction industry, production of CD and DVD, automatic, aircraft industries, making common food and water containers. In medicine, few grades of polycarbonate are used but comparatively less application in medical field.

Its melting point is 100–110°C, glass transition temperature is nearly 150°C, the mechanical, thermal, and other processing parameters of polycarbonate will change with different molecular weight of the polymer.

Polycondensation, transesterification, and ROP are mechanisms used to synthesize the polycarbonate. Polycarbonate is synthesized mainly by interfacial polycondensation of bisphenol and phosgene [67]. Initially, bisphenol and phosgene are dissolved in aqueous and organic phase, and low pH values (9–11) are maintained to produce carbonate oligomers. Postformation of carbonate oligomers, catalysts (tertiary aliphatic amines)

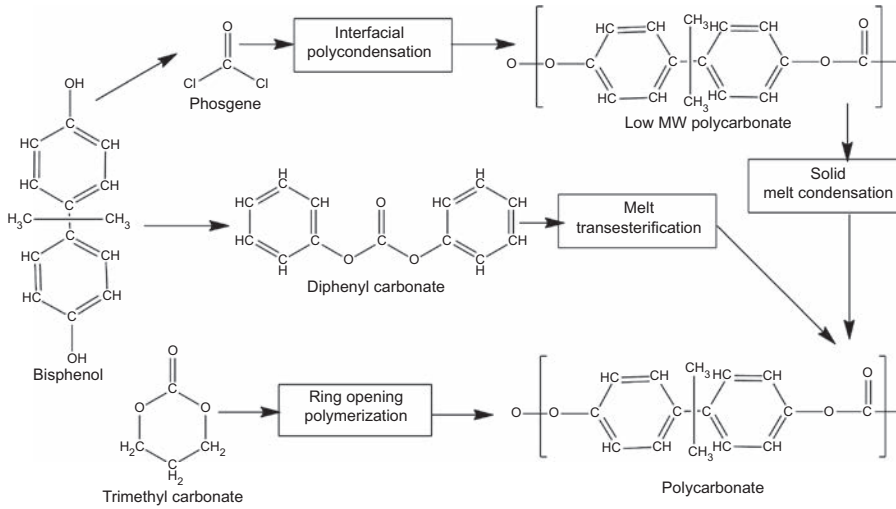

Figure 1.21 Various methods for production of polycarbonate.

are added, resulting in polymer. If the resultant polymer is low molecular weight, solid-state polymerization is carried out to obtain high-molecular-weight polymer.

Melt transesterification is also used to synthesize the polycarbonates. Polycarbonates are formed by transesterification reaction between diphenyl carbonate and bisphenol A. Usually catalyzed by alkali at low temperatures and reduced pressure initially, later the temperatures are kept increased.

ROP of cyclic oligomers at high temperatures is reported to produce polycarbonates. Trimethyl carbonate, 5-methyl-5benzyloxycarbonyl-1,3-dioxan-2-one are few monomers used for ROP using organometal catalyst. Enzymes are also used as catalyst to produce polycarbonate; lipase from *Pseudomonas fluorescents* was reported to give better monomers when compared with lipase from *C. antarctica*, *Candida rugose*, and *Mucor miehei* [68] (Fig. 1.21).

1.3.11 Polylactic glycolic acid

Polyester poly(lactic-co-glycolide) (PLGA) is a copolymer of PLA and polyglycolic acid (PGA). It gained interest due to its great potential application mainly in drug delivery. It is soluble in a wide range of common solvents including chlorinated solvents, tetrahydrofuran, acetone, or ethyl alcohol. Degree of crystallinity, melting point, and mechanical strength are determined on the molecular weight of the polymer. Besides, the properties can be easily adjusted to become better by altering the ratio (lactic acid/glycolic acid) and stereochemistry of the monomers, i.e., by modifying the composition and arrangement of chiral centers within the molecules of the polymers. The lactide content in the copolymer is inversely proportional to the degradation rate and also hydrophobicity of the polymer. PLGA degrades by hydrolysis of ester bonds.

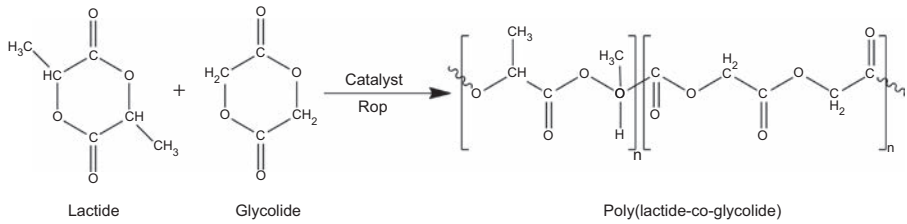

Figure 1.22 Copolymerization of poly(lactic-co-glycolide).

PLGA is synthesized by melt or solid polycondensation of PLA and PGA and the ROP of monomers such as lactide and glycolide. Stannous octoate and aluminum bromide are the most used catalysts used to synthesize the PLGA. Toluene, benzene, and chlorobenzene are some of the solvent systems used. High-molecular-weight polymers of 80,000 Da are reported [69] by polycondensation using methane sulfonic acid; solid polycondensate obtained is crushed into particles of various sizes and later subjected to solid postpolycondensation at 170°C for 10–20 h. Enzyme catalyst lipase from *Pseudomonas cepacia* is reported to catalyze the ROP of lactide and glycolide to form a cyclic polymer of PLGA [70] (Fig. 1.22).

References

[1] M.E. Grant, D.J. Prockop, The biosynthesis of collagen, New England Journal of Medicine 286 (1972) 291–300.
[2] D. Hulmes, Collagen diversity, synthesis and assembly, Collagen (2008) (Springer).
[3] E. Mocan, O. Tagadiuc, V. Nacu, Aspects of collagen isolation procedure, Clinical Research Studies 2 (2011) 3–5.
[4] M. Schmidt, R. Dornelles, R. Mello, E. Kubota, M. Mazutti, A. Kempka, I. Demiate, Collagen extraction process, International Food Research Journal 23 (2016).
[5] E. Skierka, M. Sadowska, The influence of different acids and pepsin on the extractability of collagen from the skin of Baltic cod (*Gadus morhua*), Food Chemistry 105 (2007) 1302–1306.
[6] L. Wang, B. Yang, X. Du, Y. Yang, J. Liu, Optimization of conditions for extraction of acid-soluble collagen from grass carp (*Ctenopharyngodon idella*) by response surface methodology, Innovative Food Science & Emerging Technologies 9 (2008) 604–607.
[7] M.I. Khan, M.S. Arshad, F.M. Anjum, A. Sameen, W.T. Gill, Meat as a functional food with special reference to probiotic sausages, Food Research International 44 (2011) 3125–3133.
[8] C. Wang, Y. Li, Z.-Y. Ma, W.-Q. Lan, Comparison study on extraction of collagen from porcine skin by different enzymes [J], Food Science 1 (2007) 046.
[9] A.W. Mohammad, N.M. Suhimi, A.G.K.A. Aziz, J.M. Jahim, Process for production of hydrolysed collagen from agriculture resources: potential for further development, Journal of Applied Sciences 14 (2014) 1319.
[10] H.K. Kim, Y.H. Kim, H.J. Park, N.H. Lee, Application of ultrasonic treatment to extraction of collagen from the skins of sea bass *Lateolabrax japonicus*, Fisheries Science 79 (2013) 849–856.

[11] M. Gómez-Guillén, B. Giménez, M.A. López-Caballero, M. Montero, Functional and bioactive properties of collagen and gelatin from alternative sources: a review, Food Hydrocolloids 25 (2011) 1813–1827.
[12] H. Wieser, Chemistry of gluten proteins, Food Microbiology 24 (2007) 115–119.
[13] T. Abonyi, I. Király, S. Tömösközi, O. Baticz, A. Guóth, S. Gergely, É. Scholz, D. Lásztity, R. Lásztity, Synthesis of gluten-forming polypeptides. 1. Biosynthesis of gliadins and glutenin subunits, Journal of Agricultural and Food Chemistry 55 (2007) 3655–3660.
[14] R. Lásztity, I. Király, O. Baticz, A. Guóth, T. Abonyi, S. Tömösközi, S. Gergely, Biosynthesis and in vivo and in vitro polymerization of glutenin subunits and its effect on quality of wheat, in: Proceedings of 3rd International Congress' Flour-Bread 05'and 5th Croatian Congress of Cereal Technologists, Opatija, 26–29 October 2005, Faculty of Food Technology, University of Josip Juraj Strossmayer, 2006, pp. 49–56.
[15] L. Day, M. Augustin, I. Batey, C. Wrigley, Wheat-gluten uses and industry needs, Trends in Food Science & Technology 17 (2006) 82–90.
[16] I. Test, Gelatin Manufacturers Institute of America, 2012 (New York).
[17] A.A. Mariod, H.F. Adam, Review: gelatin, source, extraction and industrial applications, Acta Scientiarum Polonorum Technologia Alimentaria 12 (2013) 135–147.
[18] B. Jamilah, K. Harvinder, Properties of gelatins from skins of fish—black tilapia (*Oreochromis mossambicus*) and red tilapia (*Oreochromis nilotica*), Food Chemistry 77 (2002) 81–84.
[19] K.B. Djagny, Z. Wang, S. Xu, Gelatin: a valuable protein for food and pharmaceutical industries: review, Critical Reviews in Food Science and Nutrition 41 (2001) 481–492.
[20] P.K. Dutta, J. Dutta, V. Tripathi, Chitin and chitosan: chemistry, properties and applications, Journal of Scientific and Industrial Research 63 (2004) 20–31.
[21] M. Rinaudo, Chitin and chitosan: properties and applications, Progress in Polymer Science 31 (2006) 603–632.
[22] M.B. Sticklen, Plant genetic engineering for biofuel production: towards affordable cellulosic ethanol, Nature Reviews Genetics 9 (2008) 433–443.
[23] C. Krumm, J. Pfaendtner, P.J. Dauenhauer, Millisecond pulsed films unify the mechanisms of cellulose fragmentation, Chemistry of Materials 28 (2016) 3108–3114.
[24] I.M. Saxena, R.M. Brown, Cellulose biosynthesis: current views and evolving concepts, Annals of Botany 96 (2005) 9–21.
[25] S. Zhu, Y. Wu, Q. Chen, Z. Yu, C. Wang, S. Jin, Y. Ding, G. Wu, Dissolution of cellulose with ionic liquids and its application: a mini-review, Green Chemistry 8 (2006) 325–327.
[26] L.E. Cullen, C. Macfarlane, Comparison of cellulose extraction methods for analysis of stable isotope ratios of carbon and oxygen in plant material, Tree Physiology 25 (2005) 563–569.
[27] C. Pappas, P. Tarantilis, I. Daliani, T. Mavromoustakos, M. Polissiou, Comparison of classical and ultrasound-assisted isolation procedures of cellulose from kenaf (*Hibiscus cannabinus* L.) and eucalyptus (*Eucalyptus rodustrus* Sm.), Ultrasonics Sonochemistry 9 (2002) 19–23.
[28] I. Vroman, L. Tighzert, Biodegradable polymers, Nature Materials 2 (2009) 307–344.
[29] A.M. Smith, The biosynthesis of starch granules, Biomacromolecules 2 (2001) 335–341.
[30] A. Mohammadkhani, F.L. Stoddard, D.R. Marshall, M.N. Uddin, X. Zhao, Starch extraction and amylose analysis from half seeds, Starch-Starke 51 (1999) 62–65.
[31] W.S. Ratnayake, R. Hoover, T. Warkentin, Pea starch: composition, structure and properties—a review, Starch-stärke 54 (2002) 217–234.

[32] P. Zhang, R.L. Whistler, J.N. Bemiller, B.R. Hamaker, Banana starch: production, physicochemical properties, and digestibility—a review, Carbohydrate Polymers 59 (2005b) 443–458.
[33] S.N. Moorthy, Physicochemical and functional properties of tropical tuber starches: a review, Starch-stärke 54 (2002) 559–592.
[34] M. Yusuph, R.F. Tester, R. Ansell, C.E. Snape, Composition and properties of starches extracted from tubers of different potato varieties grown under the same environmental conditions, Food Chemistry 82 (2003) 283–289.
[35] W. Morrison, A. Coventry, Extraction of lipids from cereal starches with hot aqueous alcohols, Starch-stärke 37 (1985) 83–87.
[36] A. Pinkus, R. Subramanyam, New high-yield, one-step synthesis of polyglycolide from haloacetic acids, Journal of Polymer Science: Polymer Chemistry Edition 22 (1984) 1131–1140.
[37] K. Schwarz, M. Epple, A detailed characterization of polyglycolide prepared by solid-state polycondensation reaction, Macromolecular Chemistry and Physics 200 (1999) 2221–2229.
[38] K. Shen, S.L. Yang, Preparation of high-molecular-weight poly (glycolic acid) by direct melt polycondensation from glycolic acid, Advanced Materials Research (2013) 1023–1026 Trans Tech Publ.
[39] H. Sato, F. Kobayashi, Y. Ichikawa, Y. Oishi, Synthesis and characterization of polyglycolic acid *via* sequential melt-solid ring-opening polymerization of glycolide, KOBUNSHI RONBUNSHU 69 (2012) 60–70.
[40] K. Takahashi, I. Taniguchi, M. Miyamoto, Y. Kimura, Melt/solid polycondensation of glycolic acid to obtain high-molecular-weight poly (glycolic acid), Polymer 41 (2000) 8725–8728.
[41] K. Chujo, H. Kobayashi, J. Suzuki, S. Tokuhara, M. Tanabe, Ring-opening polymerization of glycolide, Die Makromolekulare Chemie 100 (1967) 262–266.
[42] X.-L. Xia, W.-T. Liu, X.-Y. Tang, X.-Y. Shi, L.-N. Wang, S.-Q. He, C.-S. Zhu, Degradation behaviors, thermostability and mechanical properties of poly (ethylene terephthalate)/polylactic acid blends, Journal of Central South University 21 (2014) 1725–1732.
[43] Y. Lu, C. Schmidt, S. Beuermann, Fast synthesis of high-molecular-weight polyglycolide using diphenyl bismuth bromide as catalyst, Macromolecular Chemistry and Physics 216 (2015) 395–399.
[44] H. Amine, O. Karima, B.M. El Amine, M. Belbachir, R. Meghabar, Cationic ring opening polymerization of glycolide catalysed by a montmorillonite clay catalyst, Journal of Polymer Research 12 (2005) 361–365.
[45] V. Tserki, P. Matzinos, E. Pavlidou, C. Panayiotou, Biodegradable aliphatic polyesters. Part II. Synthesis and characterization of chain extended poly(butylene succinate-co-butylene adipate), Polymer Degradation and Stability 91 (2006) 377–384.
[46] P. Buzin, M. Lahcini, G. Schwarz, H.R. Kricheldorf, Aliphatic polyesters by bismuth triflate-catalyzed polycondensations of dicarboxylic acids and aliphatic diols, Macromolecules 41 (2008) 8491–8495.
[47] J. Du, Y. Zheng, J. Chang, L. Xu, Synthesis, characterization and properties of high molecular weight poly (butylenes succinate) reinforced by mesogenic units, European Polymer Journal 43 (2007) 1969–1977.
[48] A. Takasu, Y. Oishi, Y. Iio, Y. Inai, T. Hirabayashi, Synthesis of aliphatic polyesters by direct polyesterification of dicarboxylic acids with diols under mild conditions catalyzed by reusable rare-earth triflate, Macromolecules 36 (2003) 1772–1774.

[49] H. Azim, A. Dekhterman, Z. Jiang, R.A. Gross, Candida a ntarctica lipase B-catalyzed synthesis of poly (butylene succinate): shorter chain building blocks also work, Biomacromolecules 7 (2006) 3093–3097.
[50] C.Q. Huang, S.Y. Luo, S.Y. Xu, J.B. Zhao, S.L. Jiang, W.T. Yang, Catalyzed chain extension of poly (butylene adipate) and poly (butylene succinate) with 2, 2′-(1, 4-phenylene)-bis (2-oxazoline), Journal of Applied Polymer Science 115 (2010) 1555–1565.
[51] Y.-H. Zhang, X.-L. Wang, Y.-Z. Wang, K.-K. Yang, J. Li, A novel biodegradable polyester from chain-extension of poly(p-dioxanone) with poly(butylene succinate), Polymer Degradation and Stability 88 (2005a) 294–299.
[51a] L.S. Nair, C.T. Laurencin, Biodegradable polymers as biomaterials, Progress in Polymer Science 32 (2007) 762–798.
[51b] K.-K. Yang, X.-L. Wang, Y.-Z. Wang, Poly (p-dioxanone) and its copolymers, Journal of Macromolecular Science, Part C: Polymer Reviews 42 (2002) 373–398.
[52] R.A. Rodríguez Galán, M.L. Franco García, J. Puiggalí Bellalta, Biodegradable Poly (Ester Amide) S: Synthesis and Applications, 2011.
[53] J.E. Bucher, W.C. Slade, The anhydrides of isophthalic and terephthalic acids, Journal of the American Chemical Society 31 (1909) 1319–1321.
[54] K. Leong, V. Simonte, R. Langer, Synthesis of polyanhydrides: melt-polycondensation, dehydrochlorination, and dehydrative coupling, Macromolecules 20 (1987) 705–712.
[54a] B. Burns, Polycyanoacrylates, in: Encyclopedia of Polymer Science and Technology, 2016.
[54b] J. Woods, Polycyanoacrylates, in: Encyclopedia of Polymer Science and Technology, John Wiley & Sons, Inc, 2002.
[55] K.M. Nampoothiri, N.R. Nair, R.P. John, An overview of the recent developments in polylactide (PLA) research, Bioresource Technology 101 (2010) 8493–8501.
[55a] S.-H. Hyon, K. Jamshidi, Y. Ikada, Synthesis of polylactides with different molecular weights, Biomaterials 18 (1997) 1503–1508.
[56] A.J. Lasprilla, G.A. Martinez, B.H. Lunelli, A.L. Jardini, R. Maciel Filho, Poly-lactic acid synthesis for application in biomedical devices—a review, Biotechnology Advances 30 (2012) 321–328.
[56a] V. Lassalle, M.L. Ferreira, Lipase-catalyzed synthesis of polylactic acid: an overview of the experimental aspects, Journal of Chemical Technology and Biotechnology 83 (2008) 1493–1502.
[57] D. Garlotta, A literature review of poly (lactic acid), Journal of Polymers and the Environment 9 (2001) 63–84.
[58] A. Kowalski, A. Duda, S. Penczek, Kinetics and mechanism of cyclic esters polymerization initiated with tin (II) octoate, 1. Polymerization of ε-caprolactone, Macromolecular Rapid Communications 19 (1998) 567–572.
[59] M. Hunsen, A. Azim, H. Mang, S.R. Wallner, A. Ronkvist, W. Xie, R.A. Gross, A cutinase with polyester synthesis activity, Macromolecules 40 (2007) 148–150.
[60] M. Hunsen, A. Abul, W. Xie, R. Gross, Humicola insolens cutinase-catalyzed lactone ring-opening polymerizations: kinetic and mechanistic studies, Biomacromolecules 9 (2008) 518–522.
[61] J. Ma, Q. Li, B. Song, D. Liu, B. Zheng, Z. Zhang, Y. Feng, Ring-opening polymerization of ε-caprolactone catalyzed by a novel thermophilic esterase from the archaeon *Archaeoglobus fulgidus*, Journal of Molecular Catalysis B: Enzymatic 56 (2009) 151–157.
[62] P. Kerep, H. Ritter, Influence of microwave irradiation on the lipase-catalyzed ring-opening polymerization of ε-caprolactone, Macromolecular Rapid Communications 27 (2006) 707–710.

[63] A. Gumel, M. Annuar, Y. Chisti, T. Heidelberg, Ultrasound assisted lipase catalyzed synthesis of poly-6-hydroxyhexanoate, Ultrasonics Sonochemistry 19 (2012) 659–667.
[64] C. Jérôme, P. Lecomte, Recent advances in the synthesis of aliphatic polyesters by ring-opening polymerization, Advanced Drug Delivery Reviews 60 (2008) 1056–1076.
[65] S.A. Guelcher, Biodegradable polyurethanes: synthesis and applications in regenerative medicine, Tissue Engineering B: Reviews 14 (2008) 3–17.
[66] J. Tao, C. Song, M. Cao, D. Hu, L. Liu, N. Liu, S. Wang, Thermal properties and degradability of poly (propylene carbonate)/poly (β-hydroxybutyrate-co-β-hydroxyvalerate) (PPC/PHBV) blends, Polymer Degradation and Stability 94 (2009) 575–583.
[67] S.E. Morgan, J. Li, Polycarbonate (PC), World 10 (2006) 12.
[68] T.F. Al-Azemi, K.S. Bisht, Novel functional polycarbonate by lipase-catalyzed ring-opening polymerization of 5-methyl-5-benzyloxycarbonyl-1, 3-dioxan-2-one, Macromolecules 32 (1999) 6536–6540.
[69] S.I. Moon, K. Deguchi, M. Miyamoto, Y. Kimura, Synthesis of polyglactin by melt/solid polycondensation of glycolic/L-lactic acids, Polymer International 53 (2004) 254–258.
[70] S. Huijser, B.B. Staal, J. Huang, R. Duchateau, C.E. Koning, Topology characterization by MALDI-ToF-MS of enzymatically synthesized poly (lactide-co-glycolide), Biomacromolecules 7 (2006) 2465–2469.

Surface modification techniques of biodegradable and biocompatible polymers

2

Feven M. Michael[1], Mohammad Khalid[2], Rashmi Walvekar[3], Humaira Siddiqui[3], Anand B. Balaji[1]

[1]University of Nottingham Malaysia Campus, Semenyih, Malaysia; [2]Sunway University, Subang Jaya, Malaysia; [3]Taylor's University, Subang Jaya, Malaysia

2.1 Introduction

Polymers are the largest class of biomaterials, which are being extensively studied for different applications due to their unique properties such as viscosity, malleability, moldability, and their mechanical strength. These polymers are either natural or synthetic. Natural polymers (collagen and chitosan) are usually abundant and biodegradable and offer good biocompatibility. Synthetic polymers (biodegradable and nonbiodegradable) are human-made polymers. In this chapter, special focus is given to the biodegradable synthetic polymers; in particular polyesters such as polyglycolide acid (PGA), polylactic acid (PLA), and polylactic-co-glycolic acid (PLGA). Other aliphatic polyesters such as poly(3-hydroxybutyrate) (PHB), poly(ε-caprolactone) (PCL), and polybutylene succinate (PBS) are also among the biodegradable synthetic polymers. These biodegradable polymers are considered as environmentally friendly polymers because they convert into CO_2 and water when in contact with soil that contains microorganisms. In addition, the bulk properties of the biodegradable polymers such as mechanical, thermal, electrical as well as biocompatibility and biodegradability are greatly influenced by their surface properties. These surface properties include hydrophilicity/hydrophobicity, ionic charge or pH, adsorption of molecules, adhesion of microorganisms, permeation of molecules, chemical or biological reaction kinetics, roughness or friction, and their impurities. Thus, any alteration in the surface properties can ultimately impact the bulk properties of the polymer, widening the applications of polymers. However, the most crucial property in determining the application is the surface hydrophilicity/hydrophobicity also known as wettability, which is also related to the surface roughness, adhesion, adsorption, and chemical compositions of the polymer.

Polymer wettability is a fundamental surface property that plays important roles in different industries. Consequently, surface wettability of a polymer can be measured in terms of the polymer surface contact angle; a parameter that characterizes the drop shape on the solid (polymer) surface. The water contact angle varies from 0 to 150 degrees, in which below 90 degrees is an indication of hydrophilic nature,

Biodegradable and Biocompatible Polymer Composites. http://dx.doi.org/10.1016/B978-0-08-100970-3.00002-X

whereas above 90 degrees is hydrophobic, as shown in Fig. 2.1. In general, most of the polymers are hydrophobic in nature, i.e., they repel water. In other words, they are nonwetting, whereby water and aqueous fluids will not spread but form drops on the polymer surface. Some polymers are hydrophilic to some extent (wetting); allow water to spread on the surface; and absorb into the bulk.

Subsequent to surface wettability, another surface property that is important is adhesion: the ability of biodegradable polymers to attach with another material, for instance, any of the biodegradable polymers attaching to either metals, ceramics, or biomolecules. However, it is not easy to join these two different materials due to the fact that biodegradable polymers are mostly hydrophobic, whereas the other materials (metals, ceramics, and biomolecules) are hydrophilic. As a result, prior to mixing these two opposite materials, either one of the materials should be surface-modified to acquire similar hydrophilic or hydrophobic chains. This is where the surface ionic charge or pH, adsorption, permeation, chemical or biological reaction kinetics, and roughness of the biodegradable polymer play important roles. Altering these surface properties allows the hydrophobic biodegradable polymer to have hydrophilic chain that can easily attach with the hydrophilic material.

Mostly, biodegradable polymers are suitable for medical industries especially for medical implant devices. In here, the interaction of these polymers with the body (cells), that is biocompatibility, is a key importance for the successful long-term implantation of medical devices. Among the main parameters of the cell–polymer interaction are cell adhesion and spreading. The cell adhesion involves the cell growth, migration, and differentiation processes. Moreover, the cell–polymer interaction is significantly influenced by the surface roughness, wettability, and chemical compositions. In general, the rough surfaces enhance the cell adhesion, while slowing down the cell spreading. This indicates the cells are constrained when the high surface roughness enhances the level of adhesion as illustrated in Fig. 2.2.

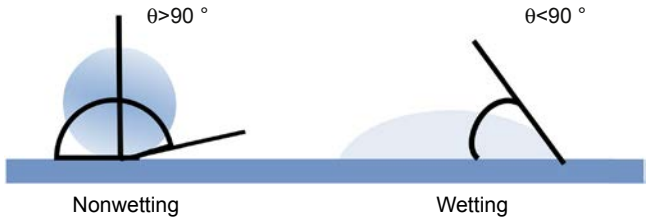

Figure 2.1 Water contact angle for hydrophobic (nonwetting) and hydrophilic (wetting) surfaces.

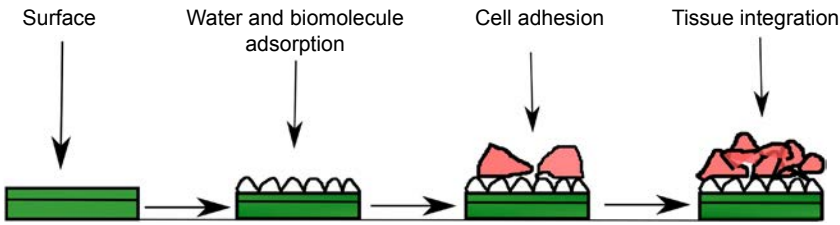

Figure 2.2 Schematic of cell adhesion and tissue integration on a polymer surface.

For instance, J.W. Lee et al. [1], reported on the surface modification of three different biodegradable polymers: PLGA, PLA, and PCL by roughening the surfaces. The measured water contact angle of the PLA, PLGA, and PCL was 79 ± 3, 74.4 ± 1.1, and 78 ± 2 degrees, respectively. This in turn indicated that the hydrophilic nature of these biodegradable polymers has improved after surface modification (attaining water contact angle below 90 degrees). In addition, J.W. Lee et al. [1] also observed the surface topography. Figs. 2.3 and 2.4 depict the surface morphology and roughness of surface-modified biodegradable polymers examined by field emission scanning electron and atomic force (AFM) micrographs, respectively. The average roughness measured by AFM was 3.6 Å (PLGA), 2.6 Å (PLA), and 198 Å (PCL). Among these three biodegradable polymers, PCL-coated surface showed higher roughness, whereas there was no significant difference between the PLGA and PLA. However, J.W. Lee et al. [1] also reported that both the surface roughness and wettability of the biodegradable polymers had no significant influence on the cell–polymer interaction due to the polymers lacking biological component (spacer), which can induce early cell–polymer interaction.

Considering the importance of surface modification, over the years, many polymer surface modification techniques have been adapted as illustrated in Fig. 2.5. These techniques can be categorized mainly into three groups: physicochemical, mechanical, and biological methods. Physicochemical technique mainly deals with the enhancement of surface hydrophilicity by attaching coupling agents with hydrophilic chains. Moreover, the impurities at the surface of the polymers are removed by desorption process, leaving more ions on the polymer surface to be attached with the coupling agents. This helps in improving the interaction between the hydrophobic polymers and hydrophilic fillers, resulting in the fabrication of homogenous composites. Meanwhile, the mechanical methods improve the surface roughness and friction by altering the surface topography using roughening techniques. This also improves the wettability and adhesion properties of the polymer. Biological method on the other hand enhances the interaction between biomolecules and the polymers by adding a compound that acts as spacer, linking the

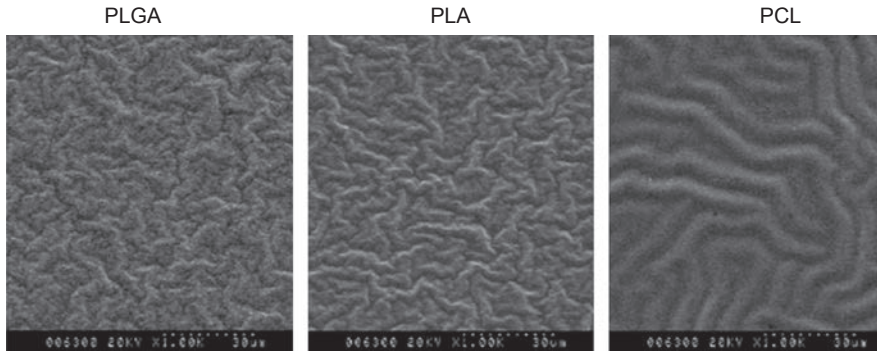

Figure 2.3 Surface topography images of the biodegradable polymers using field emission scanning electron microscopy [1]. *PCL*, poly(ε-caprolactone); *PLA*, polylactic acid; *PLGA*, polylactic-co-glycolic acid.

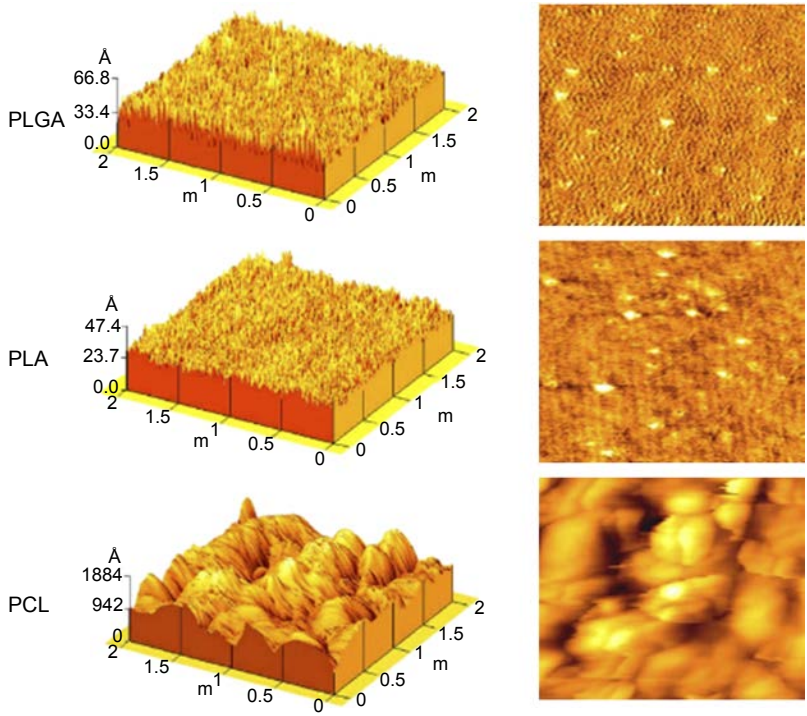

Figure 2.4 Atomic force microscopic image of the measured surface roughness of the biodegradable polymers [1]. *PCL*, poly(ε-caprolactone); *PLA*, polylactic acid; *PLGA*, polylactic-co-glycolic acid.

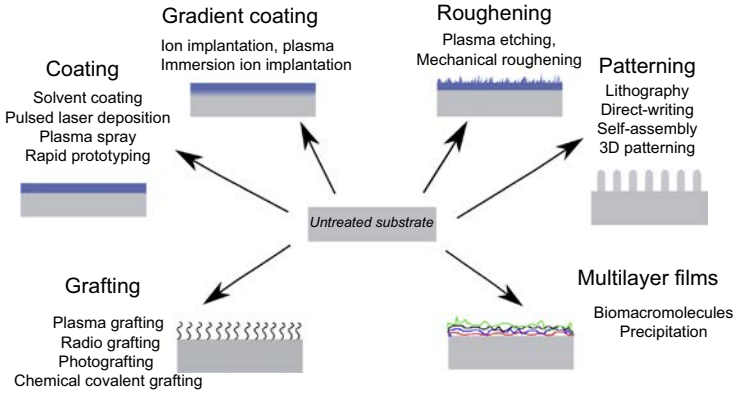

Figure 2.5 Schematic representation of the surface modification techniques [2].

polymer with the biomolecule or cells. In addition, biological surface treatment further allows the polymers to venture in medical-related applications by improving the biocompatibility and hemocompatibility and by promoting vascularization. Therefore, in this chapter, the three different surface modifying methods

(physicochemical, mechanical, and biological) are discussed. Special focus is given to the procedures and the schematic representation of the surface modification.

2.2 Physicochemical method

Surface modification of polymers through physicochemical method involves either surface coating, polishing, grit blasting, etching, vapor deposition, or self-assembly methods. As a result, the physicochemical methods can further be categories into (1) gas phase or radiation method, (2) liquid and bulk phase methods, and (3) combination of (1) and (2). In most of these methods, the polymer surface topography can be tailored by attaching new molecules/elements/ions via physical interactions such as van der Waals forces, hydrogen bonding, and/or hydrophobic interactions.

2.2.1 Gas phase or radiation

It includes the use of gases containing active species such as free radicals, electrons, ions, and molecules. Moreover, electromagnetic radiations such as visible light, UV, and gamma rays are used.

2.2.1.1 Chemical vapor deposition

Chemical vapor deposition (CVD) is the widely used surface modifying method. A thin polymer film is formed by evaporating the monomers under ultrahigh vacuum conditions and depositing the film on the surface of the polymer as shown in Fig. 2.6. The process involves passing a precursor gas or gases into a chamber containing one or more heated materials to be coated. Chemical reaction occurs on and near the hot surfaces, resulting in the deposition of thin film on the surface. This is accompanied by the production of chemical by-products that are exhausted out of the chamber along with unreacted precursor gases. CVD is done in hot wall reactors (200–300°C) and cold wall reactors (20–50°C), at sub-torr total pressures to above atmospheric pressures.

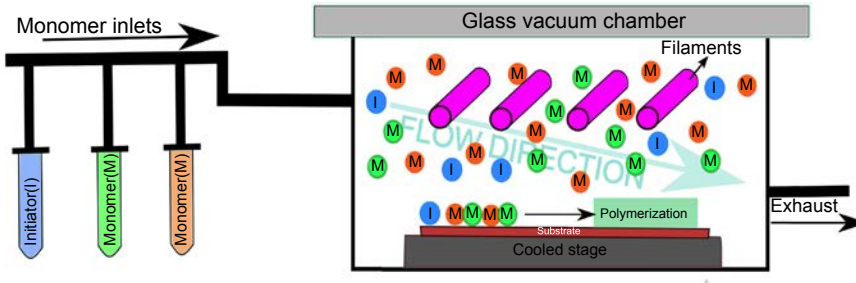

Figure 2.6 Surface modification of polymer by deposition of thin-film substrate on the surface of the polymer using chemical vapor deposition [3].

CVD method was first developed by Prof. Karen K. Gleason [3]. CVD occurs in three stages: initiation, propagation, and termination. These reactions take place on the surface of the cooled substrate and form a polymer film. The details of the reactions are presented in Eqs. (2.1)–(2.5), where I is initiator and M is monomer. Initiation arises when the initiator free radical attacks the vinyl bond of the monomer (Eq. 2.1). The resulting radical then adds to another vinyl monomer during the propagation stage (Eq. 2.2). Termination occurs when two of the propagating radicals react (Eq. 2.3) or through primary radical termination (Eq. 2.4) and primary radical recombination (Eq. 2.5).

Initiation: $I^{*}\,(ad) + M\,(ad) \rightarrow M_1{}^{*}\,(ad)$ (2.1)

Propagation: $M_n{}^{*}\,(ad) + M\,(ad) \rightarrow M_{n+1}{}^{*}\,(ad)$ (2.2)

Termination: $M_n{}^{*}\,(ad) + M_m{}^{*}\,(ad) \rightarrow M_{n+m}\,(ad)$ (2.3)

Primary Radical Termination: $M_n{}^{*}\,(ad) + I^{*}\,(ad) \rightarrow M_n\,(ad)$ (2.4)

Primary Radical Recombination: $I^{*}\,(ad) + I^{*}\,(ad) \rightarrow I_2\,(ad)$ (2.5)

CVD has a number of advantages, primarily being that the films are quite conformal. This means that films can be applied to elaborately shaped pieces, including the insides and undersides of features, and that high-aspect ratio holes and other features can be completely filled. CVD has good reproducibility. Moreover, CVD can be used to deposit various materials with high purity and deposition rate. CVD also has many disadvantages, especially with the properties of the precursors and film deposition temperature. Ideally, the precursors need to be volatile at room temperatures. CVD precursors can also be highly toxic, explosive, or corrosive. The by-products of the reactions can be also hazardous. CVD uses high temperature to deposit the films, hence restricting the kind of substrates to be coated. Last, CVD leads to stresses in films deposited on materials with different thermal expansion coefficients, which can cause mechanical instabilities in the deposited films.

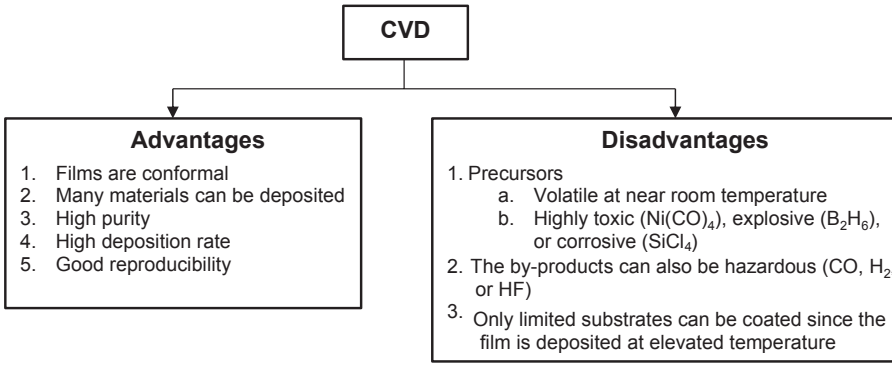

2.2.1.2 Plasma treatment

Plasma treatment shown in Fig. 2.7 is probably the most versatile method for the surface modification of polymers. It is relatively simple, easy to implement, and cost-effective. Apart from being a surface-sensitive modification method, plasma treatment does not have toxic waste as in the case of CVD. The plasma used to modify the surface of the polymers can be defined as a gas containing charged and neutral species, including electrons, positive and negative ions, radicals, atoms, metastables, and molecular fragments. In the plasma, the average electron temperature ranges between 1 and 10 eV, the electron density varies from 10^9 to 10^{12} cm^{-3}, and the degree of ionization can be as low as 10^{-6} or as high as 0.3. An AC frequency of 50–100 kHz and above can provide a continuous discharge.

Plasmas are capable of exerting four major effects through surface cleaning (removal of organic contamination from the surface), surface ablation or etching (removal of weak boundary layer and increase the surface area), surface cross-linking (strengthening the surface layer), and modification of the surface (chemical structure). The interaction of the polymer surface with plasma can cause hydrogen separation from polymeric chains and free radical creation. The reaction of the gas plasma with polymer surfaces can be classified into the following:

1. **Surface and interfacial reactions**: Reactions between the energetic species in the plasma and the substrate surface produce the surface functional groups, and reactions among the activated surface species can produce further changes such as cross-linking at the surface. These reactions involve treatments by argon, ammonia, carbon monoxide, carbon dioxide, fluorine, hydrogen, nitrogen, nitrogen dioxide, oxygen, and water plasmas.
2. **Dry etching**: Materials are removed from the polymer surface in the form volatiles by plasma-induced chemical reactions and physical etching at the surface. The etching process can also be used to remove organic contaminants from polymer surfaces. Oxygen plasma and

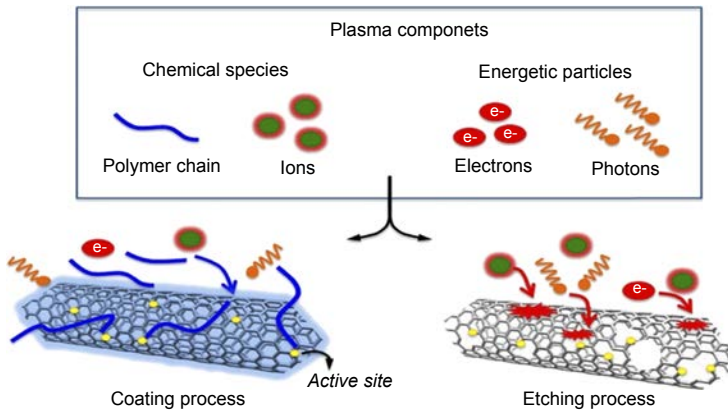

Figure 2.7 Surface modification of polymer using plasma treatment, etching, and coating process [4].

oxygen–fluorine-containing plasmas are frequently used for etching and cleaning of polymer surfaces.

3. **Plasma polymerization and deposition**: A thin film of polymer can be deposited on the surface of a polymer substrate via polymerization of organic monomers or molecules, derived from hydro- and fluorocarbons, in plasma.

2.2.1.3 Radiation

Radiation is a form of energy that comes from a source and travel through some medium or space. It is emitted from an atom when electrons drop from higher energy to lower energy. Hence, based on energy and ionizing power, radiation is categorized as ionizing and nonionizing radiation. Ionizing radiations (X-ray, gamma, alpha, beta, and neutron) are high-energy radiations, which are able to remove the electrons from an atom or a molecule to form an ion. In contrast to ionizing radiation, nonionizing radiations (UV, infrared, visible light, microwaves, radio waves, very low frequency, extremely low frequency, thermal radiation, and black body radiation) are electromagnetic radiations that do not have sufficient energy to remove electrons from an atom or molecule to form an ion during collision.

Among all the radiation methods, the most used ones are gamma, UV, and electron beam radiation. Gamma and electron beam radiations are mainly used for sterilization and cross-linking purpose. However, comparing the two, the electron beam is friendlier to polymers used for medical and packaging. This could be due to electron beam radiation consisting of corpuscular particles with limited penetrative depth. UV on the other hand is mainly used for its cross-linking as well as its photooxidization effects. Hence, as of now, many studies have reported the surface modification of polymers by exposing to radiation.

Generally, on radiation, the degradation rate of the polymers is seen to deteriorate, whereas other properties such as hydrophilicity, adhesion, roughness, and biocompatibility have shown to improve. For instance, gamma radiation has shown to enhance the heat stability, processability, and the biocompatibility of PCL because of improved cross-linking and sterilization [5,6]. In another study, electron beam radiation was used to alter the degradation rate of PLA and PLGA to meet the requirement of medical application [7]. Furthermore, with the help of UV (ozone) radiation, a hydrophobic PLA was modified to give hydrophilic and dyeable PLA [8]. This was due to breakage of the ester linkage in the PLA, resulting in reduction in the molecular weight and increasing the oxygen content on the PLA surface. As a result, the degradation rate increases while the water contact angle decreases, i.e., confirming the deterioration in the biodegradation rate and increase in hydrophilicity of PLA on UV radiation, respectively. In another study, Azevedo et al. [9] compared the effect of UV and gamma radiation on the surface properties of PU. They found hardness and elastic modulus of PU were significantly influenced by UV radiation due to both cross-linking and oxidation, while gamma radiation imparted marginal increase due to cross-linking.

2.2.2 Liquid and bulk phases

It is important to note that as fabricated polymers usually do not have the same composition as the bulk phase. This is due to adsorption of contaminates/impurities from the surrounding followed by desorption of these impurities and surface-active compounds from the bulk phase or oxidation or hydrolysis of surface groups. As a result, it is desirable to modify the surface of the polymer through sorption (adsorption) and desorption processes. Adsorption is the adhesion of atoms, molecules, or ions from the bulk phase to the surface. In contrast to adsorption, desorption is a phenomenon by which the atoms, molecules, or ions are released from or through the bulk to the surface of the polymer. Both these processes affect the surface tension of the polymer. Thus, given that this chapter focuses on the surface modification, we will discuss on the adsorption and desorption processes.

2.2.2.1 Solution adsorption of polymers

The purpose of polymer adsorption is to modify the interaction between the surfaces, which in turn improves the dispersion of particles, flocculation processes, and surface properties. It is most commonly measured through the concentration depletion of a solution after being in contact with the surface. Polymer adsorption takes place generally through three steps, which are (1) diffusion, (2) attachment, and (3) rearrangement. The first step, diffusion, involves polymer transport from the bulk to the surface. The second step, attachment, involves the attachment of the polymer to the surface (either by hydrophobic or electrostatic interaction). The final step is rearrangement or relaxation of polymer at the surface where optimization of polymer segments at the surface sites takes place. However, the adsorption process is dependent on the (1) solvent quality, (2) polymer molecular weight, (3) pH, (4) polymer density, (5) ionic strength, (6) surface-to-volume ratio, and (7) pressure and temperature. Generally, strong adsorption takes place when the interaction between the solvent and the polymer is weak. In addition, adsorption favors higher-molecular-weight polymers over low molecular weight, polymers with large surface-to-volume ratio and polymers with high density. Lastly, pressure and temperature also play vital role whereby higher pressure and lower temperature are preferred for maximum adsorption.

From literature, the solvents used to immerse the polymers are organic solvents such as acetonitrile, dimethylformamide (DMF), chloroform, or toluene [10,11]. Among these solvents, DMF will be used for illustration in this section. DMF is odorless and a polar (hydrophilic) compound that happens to be soluble in water. However, as mentioned earlier, the biodegradable polymers happen to be hydrophobic. Hence, the polymer is mixed in water in presencs of DMF to improve its hydrophilic nature. DMF contains one oxygen atom that can accept proton and make a hydrogen bond with polymer. The interaction between the polymer and DMF solvent is presented in Fig. 2.8. Alternatively, the C—H bonds in the DMF solvents can also interact with the C—H bond of the polymer matrix through hydrophobic interaction as depicted in Fig. 2.9. Hence, with the help of organic solvent (DMF) the surface properties of the polymer (PLA) is being modified.

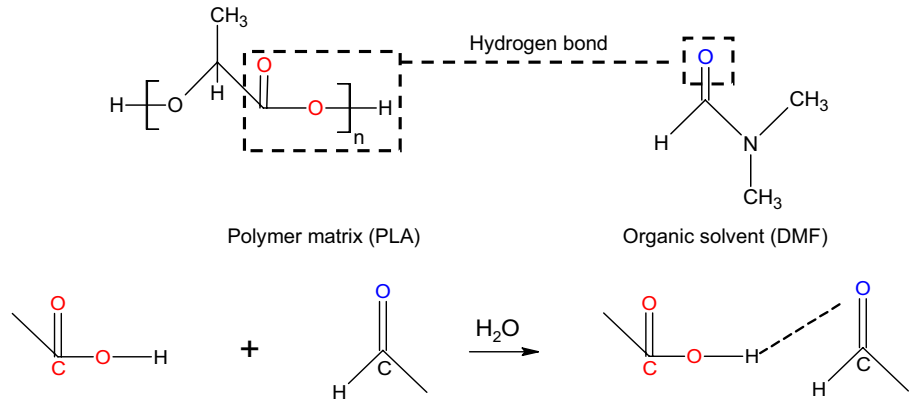

Figure 2.8 Schematic representation of the interaction between the carboxylate group of the polymer matrix (polylactic acid (PLA)) and the dimethylformamide (DMF) solution.

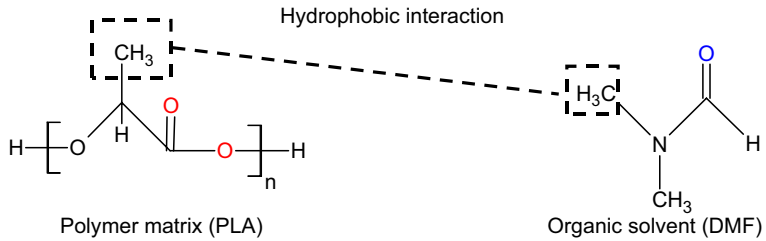

Figure 2.9 Schematic representation of the hydrophobic interaction between the polymer matrix (polylactic acid (PLA)) and the dimethylformamide (DMF) solution.

2.2.2.2 Desorption of surface active compounds from bulk to surface

Desorption is the opposite of adsorption process. Hence, polymers can be forced to desorb from a surface in three manners, including (1) adding second component with strong affinity for the surface and can displace the polymer from the surface, (2) reducing the driving force for adsorption, and (3) altering the solubility of the polymer. Thus, desorption process is conducted through addition of surface-active agents known as surfactant. Surfactants are substances used to reduce the surface tension or interfacial tension. Hence, on addition of surfactants the surface and interfacial tension between surface and the polymer is lowered. This further leads to the dissolution of polymer in the liquid phase followed by desorption and removal from the surface.

Moreover, surfactants can help in enhancing the wettability of the polymer because surfactants have a hydrophilic (an anionic, cationic, or polar group) and a hydrophobic part (long hydrocarbon chain). In which, the hydrophobic part of the surfactant can strongly bond to the hydrophobic part of the polymer through hydrophobic interaction as shown in Fig. 2.10(a). This polymer–surfactant interaction can contribute to a lower surface tension and interfacial tension of the polymer, which in turn enhances

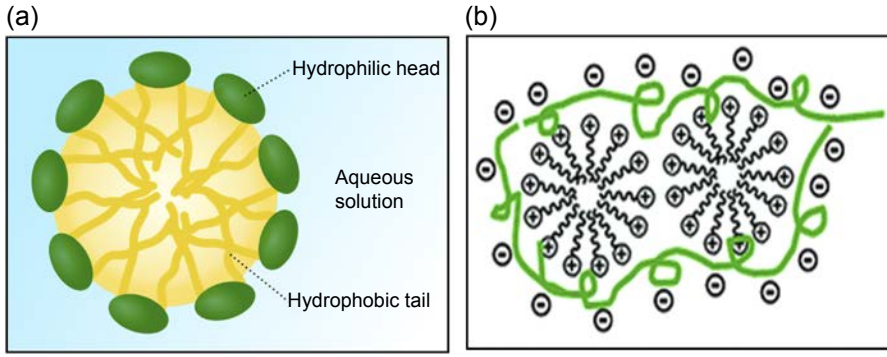

Figure 2.10 Interaction between the surfactant and polymer by (a) hydrophobic interaction and (b) electrostatic interaction.

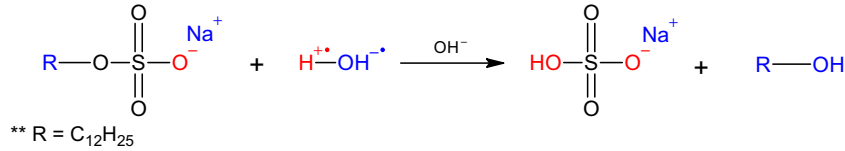

Figure 2.11 Schematic representation of the hydrolysis process of the surfactant (sodium dodecyl sulfate (SDS)).

the wettability of the polymer. In other words, due to the presence of the hydrophilic part in the surfactant, treated polymer can become partially or completely wetting biomaterial. Moreover, polymers can also bond with the oppositely charged surfactant using electrostatic interaction as shown in Fig. 2.10(b). Among the most used surfactants include sodium lauryl sulfate (SLS) or sodium dodecyl sulfate (SDS) [12,13], centrimonium bromide (CTAB) [14], and zwitterionic [15,16].

Among these surfactants, SDS is used to elaborate the surface modification mechanism of the polymer. SDS is an anionic surfactant that lowers the surface tension of the polymer. SDS consists of a sodium salt and a polar hydrocarbon tail, R ($C_{12}H_{25}$) attached to a sulfate group. When the SDS is added to water, it undergoes hydrolysis to yield sodium hydrogen sulfate and dodecanol as shown in Fig. 2.11. The by-products can then form bond with the polymer matrix using two different interaction mechanisms. The reactions involved are illustrated in Figs. 2.12 and 2.13, respectively. The carboxylate group of the polymer matrix has a weak bond (C—O) that can be easily broken and replaced by the anionic group of the sodium hydrogen sulfate using electrostatic interaction (Fig. 2.12). As a result, the polymer will end up with an ionic charged chain. The second by-product known as dodecanol has high surface activities and hence can bind with the polymer using hydrophobic bond (Fig. 2.13). This in turn increases the hydrophilic nature of the polymer, attaining more —OH group in the polymer matrix.

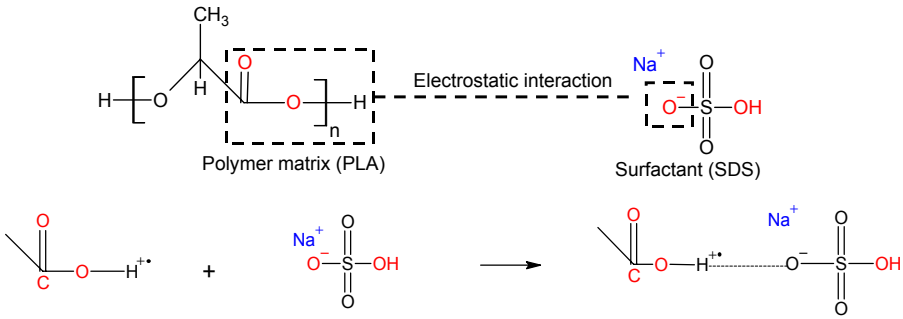

Figure 2.12 Schematic representation of the interaction between the carboxylate group of the polymer matrix (polylactic acid (PLA)) and the anionic group of the sodium dodecyl sulfate (SDS).

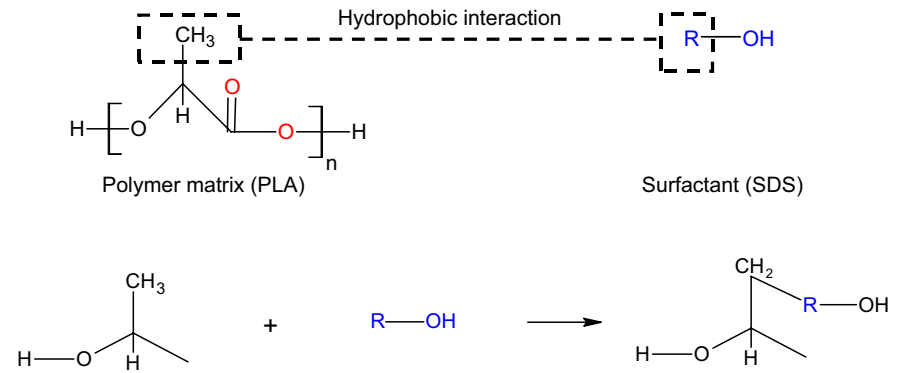

Figure 2.13 Schematic representation of the hydrophobic interaction between the polymer matrix (polylactic acid (PLA)) and the surfactant (sodium dodecyl sulfate (SDS)).

2.2.2.3 Chemical conjugation of molecules to surface groups

The most common way to improve the interfacial adhesion of polymers with other biomaterials is by using silane coupling agents. Silane coupling agents belong to a class of organosilane compounds having at least two reactive groups of different types bonded to the silicon atom in a molecule as shown in Fig. 2.14. The hydrophilic chain of the silane coupling agent is the hydrolyzable alkoxy group (methoxy and ethoxy), which reacts with water to form silanol groups. The other part of the silane coupling agent includes the hydrophobic organofunctional groups (vinyl-, amino-, epoxy-, mercapto-, glycidoxy-, methacryloxy-), which forms oligomers through self-condensation. All silane coupling agents with three X groups (X_3) on the Si should bond equally with any filler. However, matching the organofuctional group on the Si with the polymer matrix will dictate which silane coupling agent should be used for a particular application.

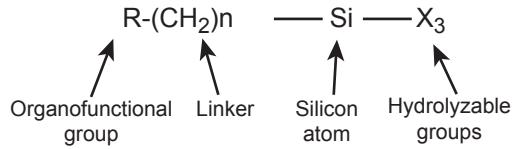

Figure 2.14 Silane coupling agent.

One of the advantages of silane coupling agents is the fact that they can bond with both hydrophobic polymer (through the organofunctional group) and hydrophilic filler (through the hydrolyzable groups). Moreover, treating the polymer or filler with silane coupling agents will lower viscosities during mixing of the polymer with the filler, produce smoother surfaces of the composites, as well as have less catalyst inhabitation on composites surface. As a result, several studies have reported on the use of silane coupling agents to improve the adhesion of the hydrophobic polymers with hydrophilic fillers. For example, the adhesion of PLA with fillers such as kenaf [17], hydroxyapatite [18], cellulose [19], clay [20], and so on was improved. Similarly, the adhesion of other polymers including PCL [21–23], PBS [24–26], PVA [27–29], polyamide [30], and PLGA [31–33] have improved with hydrophilic fillers. The improvement in adhesion further contributed in the enhancement of mechanical and thermal properties as well as the biocompatibilities of the composites. This in turn opened up avenue for these biocompatible and biodegradable polymers to be used in medical application mainly tissue engineering.

Among the silane coupling agents used, aminosilanes especially γ-aminopropyltriethoxysilane (APS) are most extensively reported in the literature [34–39]. Other silane coupling agents such as vinyl–saline and acryl–saline are also able to establish covalent bonds with polymers in presence of peroxide initiators [40]. APS is used as an example to illustrate the reaction schematic between the polymer matrix and the silane coupling agent. APS has two functional groups, represented by OR_1 (C_2H_5OH) and R_2 ($C_3H_7NH_2$). Generally, the reactive amine group, $R_{2,}$ is bonded to silicon atom via short aliphatic chain, whereas the OR_1 group is the hydrolyzing alcohol group. The reaction schematics to activate APS prior to adding to the polymer are shown in Fig. 2.15. Thus, when APS is mixed in water at a high temperature, 3-aminopropyl silanetriol is formed through hydrolysis process by liberating ethanol (Fig. 2.15(a)). Then the APS undergoes a self-condensation process, forming —Si—O—Si— and —Si—O—C— bonds (Fig. 2.15(b)). It is important to minimize the excess self-condensation process to leave the APS free for absorption with the polymer matrix.

On mixing the activated APS with the polymer, there are two possible interactions taking place. First interaction is between the carboxylate group of the polymer and the amine group of the APS as presented in Fig. 2.16. In this interaction, the carboxylic group of the polymer reacts with amine group of APS to form a stable covalent bond. The second interaction is between the hydrolyzed groups of

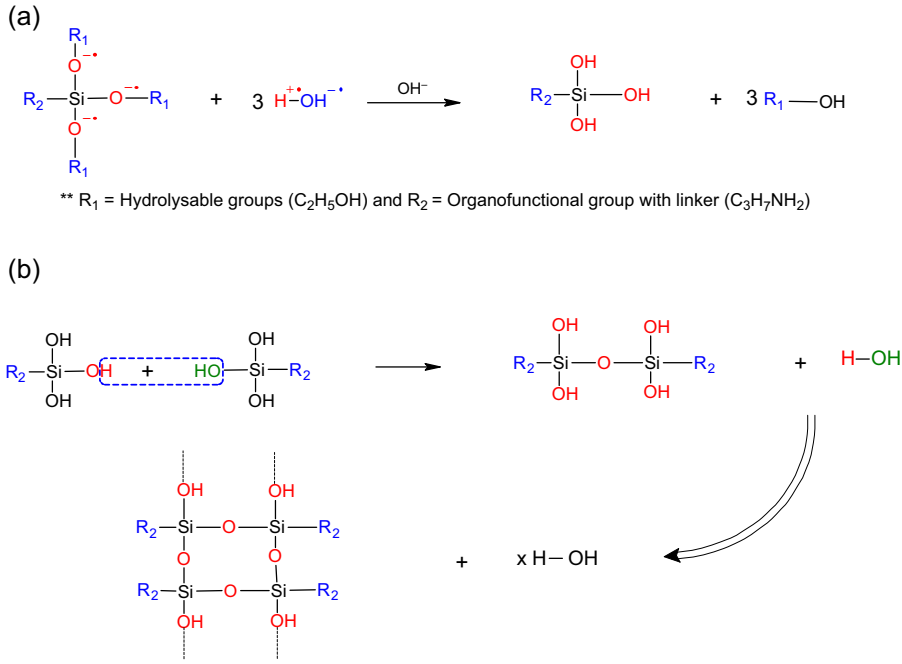

Figure 2.15 Schematic representation of the (a) hydrolysis and (b) self-condensation of silane coupling agent (aminopropyltriethoxysilane).

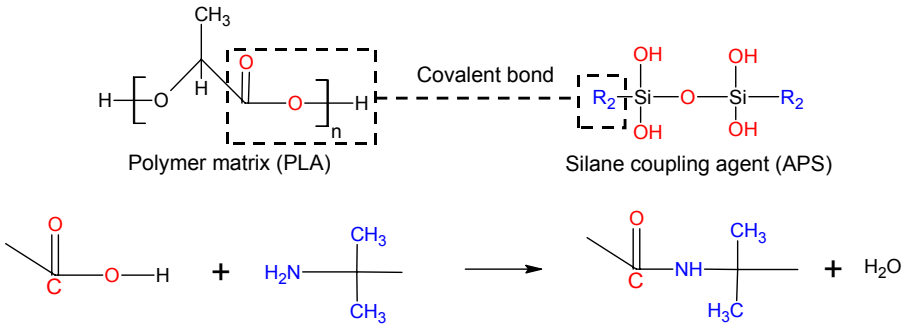

Figure 2.16 Schematic representation of the interaction between the carboxylate group of the polymer matrix (polylactic acid (PLA)) and the amine group of the saline coupling agent (aminopropyltriethoxysilane (APS)).

both the polymer and the APS as depicted in Fig. 2.17. Due to the high affinity of the APS, the —Si—O—Si— bonds of APS will link with the hydroxyl bond of the polymer through hydrogen bond. During heating, these hydrogen bonds are converted to covalent bonds, forming —R_2—Si—O— bonds by liberating water.

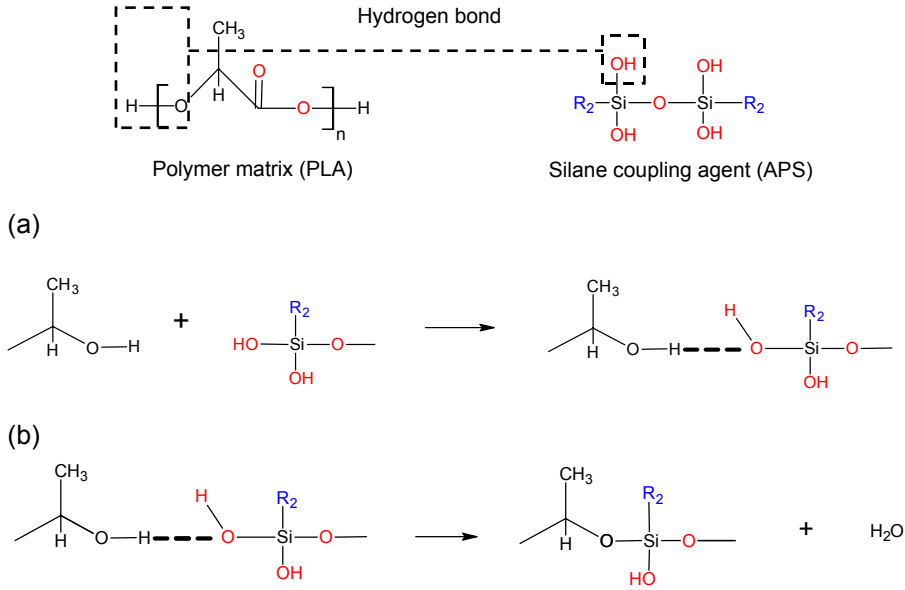

Figure 2.17 Schematic representation of the interaction between the hydroxyl groups of the polymer matrix (polylactic acid (PLA)) and the saline coupling agent (aminopropyltriethoxysilane (APS)): (a) absorption and (b) chemical grafting.

2.2.3 Combination

2.2.3.1 Grafting and polymerization

Grafting is a method used to link two monomers through covalent bonding, whereas polymerization is a process of reacting monomer molecules to form polymer chains. Thus, combination of both grafting and polymerization is an attractive method to impart various functional groups into the polymer, hence modifying the surface of the polymer as presented in Fig. 2.18. This process involves the application of ionizing radiation, UV, or ozone followed by polymerization.

2.2.3.2 Patterns

Patterns also known as microlithography are techniques used to deposit specific patterns onto the polymer surface, for instance, hydrophilic regions on a hydrophobic polymer. In addition, lithography is one of the well-known methods to develop 3D structure with patterns generated on the surface of the polymer. These patterns are created by two steps as illustrated in Fig. 2.19. First step includes the exposure of the polymer surface to UV irradiation. This allows the polymerization and/or cross-linking processes to take place. Followed by the second step, the unreacted surface (i.e., the surface of the polymer that was not UV irradiated) is removed by dissolving in a solvent, thus creating a 3D polymer surface with patterns. Consequently, the patterned 3D polymer surfaces have found many applications. For instance, due to their controlled geometrical patterns (lanes, squares,

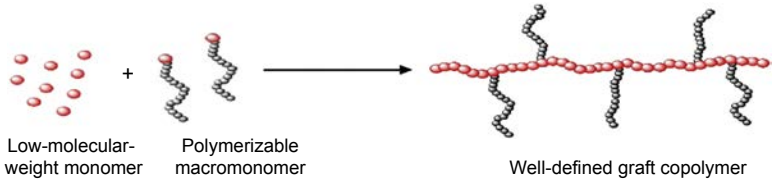

Figure 2.18 Surface modification of polymer by combination of grafting and polymerization method.

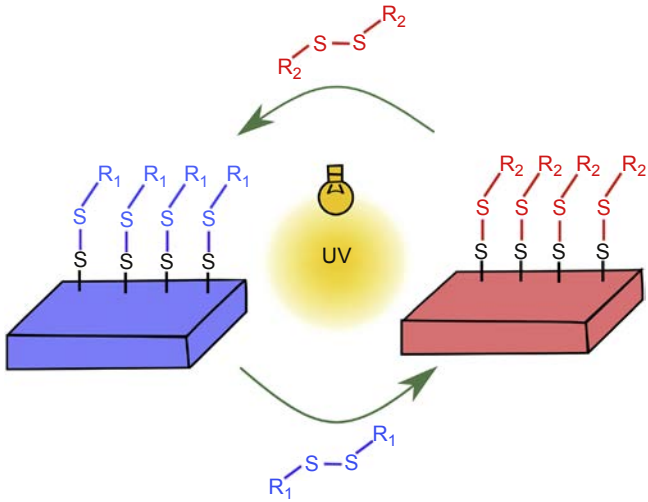

Figure 2.19 Surface modification of polymer using patterns.

triangles, or circles), the 3D polymers have the ability to manipulate the cellular behavior and interactions between the cells and the polymer matrix. Moreover, the lithographically treated polymer surface has also found application in semiconductor industries.

2.3 Mechanical method

The surface of the biodegradable polymers can also be modified using mechanical methods, namely, roughening and micromanipulation. In here, similar to the physicochemical methods, these mechanical methods also clean off the polymer surface and modify the surface chemistry through mechanical process and in the absence of chemicals.

2.3.1 Roughening

Modification of polymer surface through mechanical roughening technique implicates the change of the polymer surface topography from microrough to porous surface.

Unlike plasma treatment and chemical etching, this takes place only by altering the geometry of the surface through mechanical process.

2.3.2 Micromanipulation

Micromanipulation is a mechanical process that involves physical interaction with the polymer surface with the aid of microscope. In here, the polymer surface is carved at a microlevel or nanolevel with high precision for surface modification under scanning tunneling microscope or atomic force microscope, which are equipped with manipulator and tip of scanning probe. However, the feasibility of micromanipulation to modify the surface of biodegradable polymers is limited due to high cost and can only be used for polymers with high conductive surface.

2.4 Biological method

Polymer surfaces can also be modified biologically by immobilizing biomolecules and cells onto the polymer surface. Subsequently, a large and diverse family of polymer–biomolecule hybrid that can respond well to biological environment is developed. It is important to note the term "immobilization" refers to either to a temporary or to a long-term localization of the biomolecules on or within a polymer. Thus, biomolecules including enzyme, antibodies, affinity proteins, living cells, cell receptor ligands, and drugs have been immobilized through (1) physical adsorption, (2) physical entrapment, and (3) chemical or covalent attachment. These methods are illustrated in Fig. 2.20. However, just like the physicochemical and mechanical methods, biological method also has its pros and cons. Some of the advantages include enhanced stability, can modify the microenvironment of the biomaterials and can be reused again, lower cost and higher purity product, and most importantly no immunogenic responses. Therefore, it is very difficult to sterilize; there is resistance in mass transfer between the substrate and product as well as greater potential for products to inhibit. In addition, polymers modified through biological methods are used mainly in medical-related applications.

2.4.1 Physical adsorption and self-cross-linking of biomolecules

Physical adsorption is the simplest method to treat the surface of the polymer by incubating the polymer in solutions containing biomolecules. Here, the biomolecules attach to the polymer surface using van der Waal forces, electrostatic forces, hydrophobic interactions, and hydrogen bonds. The advantage of treating the surface of the polymer through physical adsorption is that no additional coupling reagents nor chemical modification of the biomolecules is needed. However, the interaction between the polymer and the biomolecules is weak, thus developing long-term unstable polymer–biomolecule material.

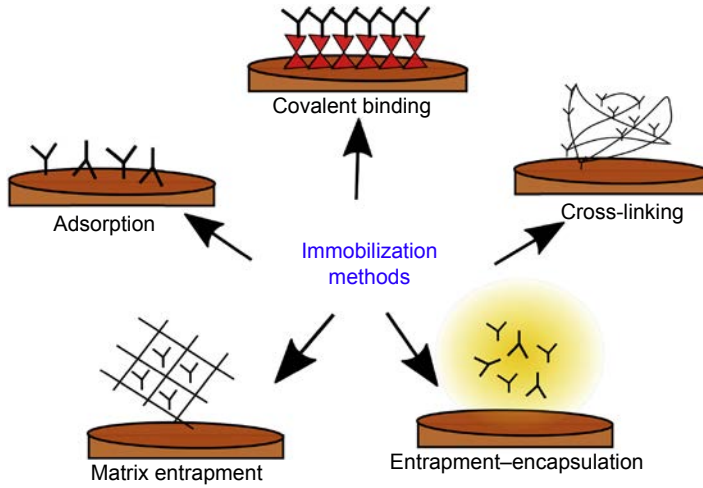

Figure 2.20 Illustration of different methods by which biomolecules can be immobilized on the surface [41].

2.4.2 Chemical conjugation of biomolecules to surface groups

As an alternative to physical adsorption, biomolecules can be attached to the surface of the polymer by covalent immobilization, developing a more stable polymer–biomolecule material. In here, a chemically immobilized biomolecule is attached to the polymer surface with the help of a spacer group. The spacer groups include common functional groups: amines, thiols, carboxylic acids, and alcohols. Such functional groups can bond to the polymer surface via electrostatic or hydrophobic interactions, which will then form a strong covalent bond between the polymer surface and the biomolecules. The immobilization of biomolecules on the polymer surface is illustrated briefly in Fig. 2.21. The selected spacer group possesses an amine functional group, whereas the selected polymer matrix is PLA. As described in Section 2.2.2.3, the polymer is bonded to the spacer using hydrogen bond that converted into covalent bond upon heating. Thus, the biomolecule (DNA strand) is then immobilized onto the polymer surface by linking with the amine group of the spacer as indicated in Fig. 2.21.

2.4.3 Cell seeding and growth to confluence

Generally, cells repel when seeded onto the biodegradable polymers because cells adhere well onto moderately hydrophilic surface. As a result, the surface of the biodegradable polymers is initially modified to acquire hydrophilic surfaces. Then, the cells are seeded onto the polymer surface once the cells reach confluency. It is important to note that the term "seeding" means to spread a defined amount (volume or cell number) of a cell suspension onto polymer surface and "confluency" is when cells are connected with each other through cell-to-cell adhesion when cultured in a controlled environment (Fig. 2.22).

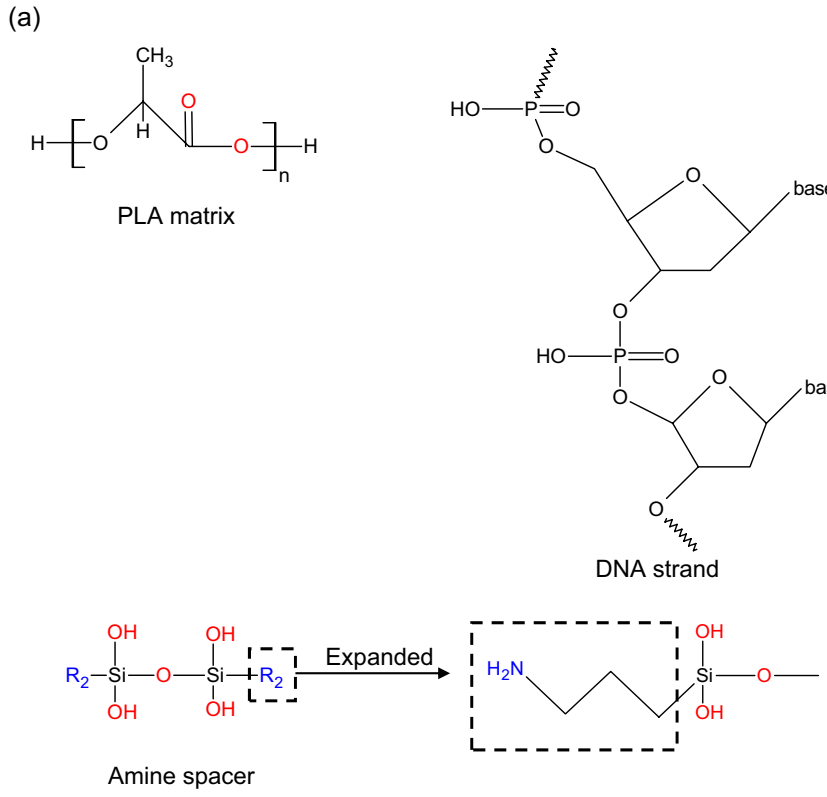

Figure 2.21 The interaction between polymer (polylactic acid (PLA)) and biomolecule (DNA) using covalent attachment in presence of a spacer (aminopropyltriethoxysilane (APS)). (a) Interaction between the hydroxyl group of the polymer (PLA) and the biomolecule (DNA) in presence of amine spacer (APS). (b) Immobilization of DNA onto the PLA surface.

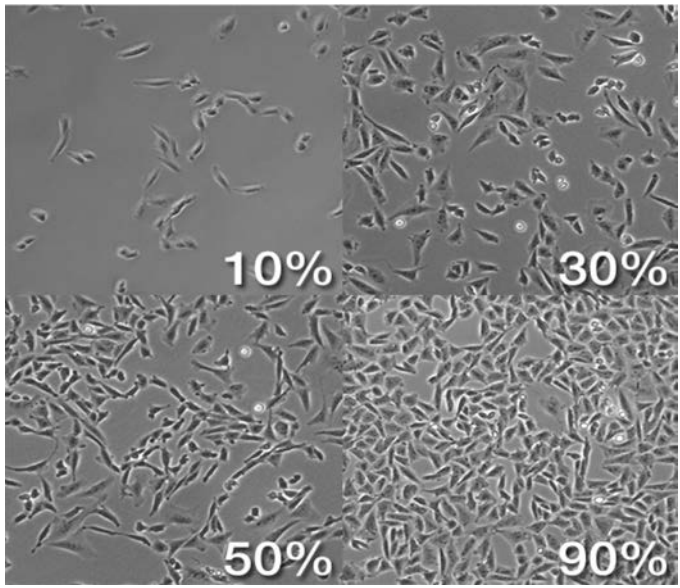

Figure 2.22 Different level of cell confluency.

2.5 Summary

Biodegradable and biocompatible polymers have proven to be useful in different applications, including medical industries (drug delivery, gene delivery, and regenerative medicine) and food industries. These polymers are human-made and require further surface modification to meet the specific bulk properties required for the proposed applications. The surface modifications involve alteration in the surface wettability, surface roughness, adhesion, and adsorption of biomolecules by the polymers. As a result, in this chapter, different surface modification techniques have been highlighted. Generally, these techniques aim to increase the surface roughness and surface wettability of the polymers to enhance the adhesion and adsorption of materials or biomolecules through physicochemical, mechanical, and biological methods.

References

[1] J.W. Lee, et al., Importance of integrin β1-mediated cell adhesion on biodegradable polymers under serum depletion in mesenchymal stem cells and chondrocytes, Biomaterials 25 (10) (2004) 1901–1909.

[2] Z.-Y. Qiu, et al., Advances in the surface modification techniques of bone-related implants for last 10 years, Regenerative Biomaterials 1 (1) (2014) 67–79.

[3] K.K. Gleason, CVD Polymers: Fabrication of Organic Surfaces and Devices, John Wiley & Sons, 2015.

[4] C.A. Ávila-Orta, et al., Toward Greener Chemistry Methods for Preparation of Hybrid Polymer Materials Based on Carbon Nanotubes. Syntheses and Applications of Carbon Nanotubes and Their Composites, InTech, Rijeka, 2013, p. 167.

[5] F. Yoshii, et al., Crosslinking of poly(ε-caprolactone) by radiation technique and its biodegradability, Radiation Physics and Chemistry 57 (3–6) (2000) 417–420.
[6] E. Cottam, et al., Effect of sterilisation by gamma irradiation on the ability of polycaprolactone (PCL) to act as a scaffold material, Medical Engineering & Physics 31 (2) (2009) 221–226.
[7] D.J. Leonard, et al., The modification of PLA and PLGA using electron-beam radiation, Journal of Biomedical Materials Research Part A 89A (3) (2009) 567–574.
[8] G.-H. Koo, J. Jang, Surface modification of poly (lactic acid) by UV/Ozone irradiation, Fibers and Polymers 9 (6) (2008) 674–678.
[9] E.C. Azevedo, et al., UV and gamma irradiation effects on surface properties of polyurethane derivate from castor oil, Polímeros 23 (2013) 305–311.
[10] T. Serizawa, et al., Layer-by-layer assembly of poly (vinyl alcohol) and hydrophobic polymers based on their physical adsorption on surfaces, Langmuir 18 (22) (2002) 8381–8385.
[11] W.Y. Ayen, K. Garkhal, N. Kumar, Doxorubicin-loaded (PEG)3-PLA nanopolymersomes: effect of solvents and process parameters on formulation development and in vitro study, Molecular Pharmaceutics 8 (2) (2011) 466–478.
[12] G. Nitya, et al., In vitro evaluation of electrospun PCL/nanoclay composite scaffold for bone tissue engineering, Journal of Materials Science: Materials in Medicine 23 (7) (2012) 1749–1761.
[13] W. Pon-On, S. Meejoo, I.M. Tang, Formation of hydroxyapatite crystallites using organic template of polyvinyl alcohol (PVA) and sodium dodecyl sulfate (SDS), Materials Chemistry and Physics 112 (2) (2008) 453–460.
[14] T.-M. Wu, C.-Y. Wu, Biodegradable poly(lactic acid)/chitosan-modified montmorillonite nanocomposites: preparation and characterization, Polymer Degradation and Stability 91 (9) (2006) 2198–2204.
[15] H. Jiang, et al., Improvement of hemocompatibility of polycaprolactone film surfaces with zwitterionic polymer brushes, Langmuir 27 (18) (2011) 11575–11581.
[16] Q. Li, et al., Functionalization of the surface of electrospun poly(epsilon-caprolactone) mats using zwitterionic poly(carboxybetaine methacrylate) and cell-specific peptide for endothelial progenitor cells capture, Materials Science and Engineering: C 33 (3) (2013) 1646–1653.
[17] M.S. Huda, et al., Effect of fiber surface-treatments on the properties of laminated biocomposites from poly (lactic acid)(PLA) and kenaf fibers, Composites Science and Technology 68 (2) (2008) 424–432.
[18] S. Rakmae, et al., Effect of silane coupling agent treated bovine bone based carbonated hydroxyapatite on in vitro degradation behavior and bioactivity of PLA composites, Materials Science and Engineering: C 32 (6) (2012) 1428–1436.
[19] A.N. Frone, et al., Morphology and thermal properties of PLA–cellulose nanofibers composites, Carbohydrate Polymers 91 (1) (2013) 377–384.
[20] M. Murariu, et al., Polylactide (PLA)—halloysite nanocomposites: production, morphology and key-properties, Journal of Polymers and the Environment 20 (4) (2012) 932–943.
[21] R.A. Khan, et al., Effectiveness of 3-aminopropyl-triethoxy-silane as a coupling agent for phosphate glass fiber-reinforced poly (caprolactone)-based composites for fracture fixation devices, Journal of Thermoplastic Composite Materials (2011)http://dx.doi.org/10.1177/0892705710391622.
[22] C. Deng, et al., Preparation and mechanical property of poly (ε-caprolactone)–matrix composites containing nano-apatite fillers modified by silane coupling agents, Journal of Materials Science: Materials in Medicine 21 (12) (2010) 3059–3064.
[23] H. Liu, et al., Isothermal crystallization kinetics of modified bamboo cellulose/PCL composites, Carbohydrate Polymers 79 (3) (2010) 513–519.

[24] B.P. Calabia, et al., Biodegradable poly (butylene succinate) composites reinforced by cotton fiber with silane coupling agent, Polymers 5 (1) (2013) 128–141.
[25] L. Liu, et al., Mechanical properties of poly (butylene succinate)(PBS) biocomposites reinforced with surface modified jute fibre, Composites Part A: Applied Science and Manufacturing 40 (5) (2009) 669–674.
[26] Y. Zhao, et al., The interfacial modification of rice straw fiber reinforced poly (butylene succinate) composites: effect of aminosilane with different alkoxy groups, Journal of Applied Polymer Science 125 (4) (2012) 3211–3220.
[27] B.S. Bae, et al., Inorganic-Organic Copolymer Using Polyvinylalcohol-silane Coupling Agent and Preparation Method Thereof, 2002 (Google Patents).
[28] S. Khoonsap, S. Amnuaypanich, Mixed matrix membranes prepared from poly (vinyl alcohol)(PVA) incorporated with zeolite 4A-graft-poly (2-hydroxyethyl methacrylate) (zeolite-g-PHEMA) for the pervaporation dehydration of water–acetone mixtures, Journal of Membrane Science 367 (1) (2011) 182–189.
[29] A. Sabetghadam, T. Mohammadi, Effect of annealing temperature and time on structure and performance of poly (vinyl) alcohol nanocomposite membranes, Polymer Engineering & Science 50 (12) (2010) 2392–2399.
[30] H. Wiebeck, et al., The effect of silane coupling agents on a composite polyamide-6/talc, Brazilian Journal of Chemical Engineering 15 (4) (1998) 406–409.
[31] A. Naik, S.M. Best, R.E. Cameron, The influence of silanisation on the mechanical and degradation behaviour of PLGA/HA composites, Materials Science and Engineering: C 48 (2015) 642–650.
[32] J. Liu, T. Xi, Enhanced anti-corrosion ability and biocompatibility of PLGA coatings on MgZnYNd alloy by BTSE-APTES pre-treatment for cardiovascular stent, Journal of Materials Science & Technology 32 (9) (2016) 845–857.
[33] F. Xin, et al., Effects of surface modification on the properties of poly (lactide-co-glycolide) composite materials, Polymer-Plastics Technology and Engineering 48 (6) (2009) 658–664.
[34] J. Kathi, K.-Y. Rhee, J.H. Lee, Effect of chemical functionalization of multi-walled carbon nanotubes with 3-aminopropyltriethoxysilane on mechanical and morphological properties of epoxy nanocomposites, Composites Part A: Applied Science and Manufacturing 40 (6) (2009) 800–809.
[35] C. Li, G.L. Wilkes, The mechanism for 3-aminopropyltriethoxysilane to strengthen the interface of polycarbonate substrates with hybrid organic–inorganic sol-gel coatings, Journal of Inorganic and Organometallic Polymers 7 (4) (1997) 203–216.
[36] H.J. Martin, et al., XPS study on the use of 3-aminopropyltriethoxysilane to bond chitosan to a titanium surface, Langmuir 23 (12) (2007) 6645–6651.
[37] T.P.T. Tran, J.-C. Bénézet, A. Bergeret, Rice and Einkorn wheat husks reinforced poly (lactic acid)(PLA) biocomposites: effects of alkaline and silane surface treatments of husks, Industrial Crops and Products 58 (2014) 111–124.
[38] P. Jandas, et al., Effect of surface treatments of banana fiber on mechanical, thermal, and biodegradability properties of PLA/banana fiber biocomposites, Polymer Composites 32 (11) (2011) 1689–1700.
[39] M. Hasan, et al., The influence of coupling agents on mechanical property retention and long-term cytocompatibility of phosphate glass fibre reinforced PLA composites, Journal of the Mechanical Behavior of Biomedical Materials 28 (2013) 1–14.
[40] Y. Xie, et al., Silane coupling agents used for natural fiber/polymer composites: a review, Composites Part A: Applied Science and Manufacturing 41 (7) (2010) 806–819.
[41] B.A. Rodriguez, et al., Nanomaterials for Advancing the Health Immunosensor, 2015.

Characterization, testing, and reinforcing materials of biodegradable composites

3

Jignesh P. Patel, Parsotam H. Parsania
Saurashtra University, Rajkot, India

3.1 Introduction

The biomass is used as a feedstock for the chemical industries, biomaterials, and bioenergy. Cash crops such as cocoa, cotton, rice, and oil palm generate large quantities of agricultural waste, which can be utilized as raw materials for bio-based industries. The burning of such waste causes air pollution. Judicious use of such material may be useful in making many valuable products in the chemical, energy, and biomaterial sectors.

The word "fiber" is derived from the Latin word *fibra*. Fiber is a natural or synthetic substance that is significantly longer than its width. Aspect ratio is defined as the ratio of fiber length to its diameter and it should be 100 times. Fibers are used in the manufacture of many engineering materials. Fibers are of two types: (1) short or discontinuous fibers with aspect ratio between 20 and 60 and (2) long or continuous fibers with aspect ratio between 200 and 500. Hairlike substances that can be derived from natural elements such as vegetable, animal, and mineral resources are known as natural fibers. Fibers can be converted into yarn after spinning and then into fabric. Natural fibers can be categorized into (1) cellulose/lignocellulose fibers/plant fibers, (2) animal fibers, and (3) mineral fibers.

3.1.1 Origin of natural fibers

Origins of natural fibers are based on plants and animals. Lignocellulosic fibers are also known as plant fibers, natural fibers, or vegetable fibers, which include bast (or stem or soft sclerenchyma) fibers, leaf or hard fibers, seed, fruit, wood, cereal straw, and other grass fibers. Plant-based natural fibers are derived from wood, pulp, cotton, bark, nut shells, bagasse, corn cobs, bamboo, cereal straw, and vegetable, e.g., flax, jute, hemp, sisal, ramie, okra, whereas wool and silk are animal-based natural fibers. Plant-based fibers are mainly composed of cellulose, hemicellulose, lignin, and pectin with a small quantity of extractives. The fiber constituents vary depending on their origin. Animal fibers are largely composed of proteins. Silk fibers are produced by a variety of insects such as silkworms and spiders. Silk and wool fibers are used

Biodegradable and Biocompatible Polymer Composites. http://dx.doi.org/10.1016/B978-0-08-100970-3.00003-1

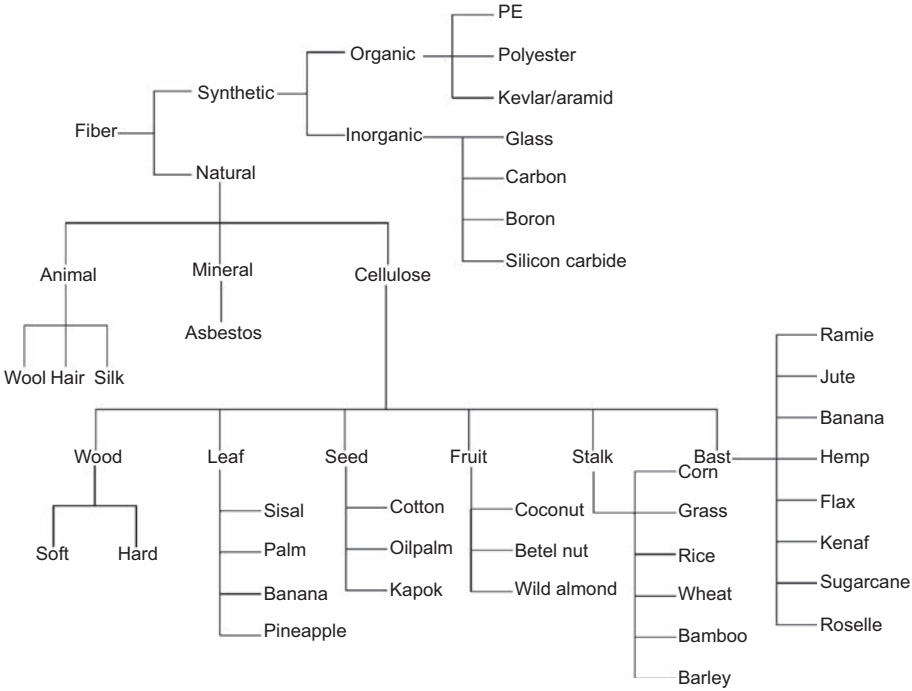

Figure 3.1 Classification of fibers.

in textiles. The energy consumption needed for the production of synthetic fibers is much more than that needed for a similar quantity of natural fibers. Unlike the synthetic fibers, natural fibers have a wide variation in diameter and length, which in turn affects the expected mechanical behavior of the composites. The variation in natural fiber dimensions is contributed to fiber type, fiber maturity, harvesting time, as well as processing methods adopted for the extraction of fibers, which all affect the diameter and stability of the fiber. Source, age, separating techniques, moisture content, and the history of fiber also play an important role in the filament and individual fiber properties. Fiber properties differ according to the source, location, and age of the plant and the extraction method used. The applications of natural fibers depend on their compositions and physical properties. The classification of the fibers is shown in Fig. 3.1.

3.1.2 Properties and advantages of natural fibers over conventional fibers

Natural fibers have low density, high specific strength, high stiffness, and high impact resistance, and relatively high tensile and flexural modulus, specific resistance, easily modified by a chemical agent, low wear resistance, minimal health hazards, and desirable fiber aspect ratio. Natural fibers have numerous advantages over conventional glass and carbon fibers. They are environmentally friendly/eco-friendly, abundance

availability, renewable, sustainable, economical, biodegradable, lightweight, nontoxic, neutral toward CO_2, and easily processible and require low energy inputs. However, most of the natural fibers are hydrophilic by nature and therefore show poor interfacial adhesion with hydrophobic matrices [1–22]. This bottleneck of the natural fibers can be overcome by fiber modification.

3.1.3 Composite

A composite is a material made from combination of two or more constituent materials with significantly different physical and chemical properties that produce a material with different characteristic properties from the individual components. The individual components remain separate and distinct within the finished structure. The new material may be stronger, lighter, or less expensive, when compared to traditional materials. Natural fibers such as jute, cotton, kenaf, bamboo, kapok, ramie, flax, hemp, sisal, coconut, banana, pineapple leaf, palmyra, rice straw, henequen, oil palm, and sugarcane fibers are potential candidates for replacing synthetic fibers in making advanced or medium-strength biodegradable composites also known as biocomposites. Recently, such materials are considered as new class of engineering materials having wide range of applications in transportation, construction, packaging, consumer products, automotive, and sporting industries.

3.2 Methods of fiber extraction and fiber cleaning

Fibers can be extracted by several retting processes such as mechanical retting (hammering), chemical retting (boiling with chemicals), steam/vapor/dew retting, and water/microbial retting. Water retting is the most popular process for the extraction of the fibers. Mechanical extraction is environmentally friendly, whereas other methods are not ecofriendly. In chemical retting, crop or deseeded straw is subjected to chemical or biological fermentation to make the fiber bundles more easily separable from the woody part of the stem. Decortication is the mechanical removal of nonfibrous material from retted stalks or from ribbons or strips of stem to extract the bast fibers. This is usually achieved by a manual operation, hammer mill, inclined plane/fluted rollers, or willower. Generally the natural fibers such as sisal, jute, and hemp are extracted by the decorticating process.

After extraction the natural fibers are washed thoroughly number of times by clean water and dried in the sunlight. Muddy particles can be removed by dipping dried fibers in dilute sodium hydroxide solution and washing thoroughly by clean water to get smooth fibers and then sun drying. Entangled fibers can be aligned by carding process. Entangled fibers are allowed to pass through between two loosely spaced and relatively moving surfaces clothed with pointed wire, pins, spikes, or saw teeth to get the product known as sliver. Gilling or pin drafting is combing of the sliver to decrease the mass per unit length. Spinning is the drafting and twisting of natural or human-made fibers to produce yarns also known as filaments, which can be spun into fabric or mat. The yarns can also be cut into different length manually.

3.3 Fiber yielding plants and trees

3.3.1 Jute

After cotton, jute is the second-most common natural fiber cultivated in the world. Jute is an annual plant and grows up to 2.5–4.5 m height (Fig. 3.2). Jute is primarily grown in Bangladesh, Brazil, China, India, and Indonesia (tropical regions). White jute (*Corchorus capsularis*) and brown jute (*Corchorus olitorius*) fibers are obtained from the bast layer of the plants. Jute fibers are used in thermoplastic matrix composites for automotive industry.

3.3.2 Kenaf

Kenaf (*Hibiscus cannabinus*) is an annual herbaceous fiber plant (Fig. 3.3) that grows in tropical regions (Africa and Asia). Kenaf plants grow up to 4–6 m height in about 4–5 months. Kenaf is known as mesta in India and Bangladesh, as stockroot in South Africa, as java jute in Indonesia, and as ambari in Taiwan.

3.3.3 Sisal

Sisal fibers (*Agave sisalana*) (Fig. 3.4) are extracted from sisal plant leaves by decortication. A rotating wheel having blunt knives is used to crush sisal leaves for the extraction of the fibers. Before sun drying, decorticated sisal fibers are washed thoroughly with water. Sisal fibers are most widely used in making various items such as mats, carpets, yarns, handcrafted articles, ropes, twines, cords, rugs, and mattresses. Sisal is used in cordage because of its strength, durability, ability to stretch, affinity for certain dyestuffs, and resistance to deterioration in saltwater. In paper industry, lower-grade sisal fibers are used due to their high cellulose and hemicellulose composition. In cordage industry, mainly medium-grade sisal fibers are used for the production of ropes, baler, binders twine, etc. Ropes and twines are mainly used for marine, agricultural, and general industrial uses. The higher-grade sisal fibers after treatment are used in carpet industry. Recently, sisal fiber–based many products such as furniture, wall tiles, car parts for cabin interiors, spa products, cat scratching posts, lumbar dartboards, buffing cloth, filters, geotextiles, mattresses, carpets, handicrafts, and wire rope cores are developed.

Figure 3.2 Jute plants and fibers.

Figure 3.3 Kenaf plants and fibers.

Figure 3.4 Sisal plants and fibers.

3.3.4 Roselle

The roselle (*Hibiscus sabdariffa*) is an herb or woody-based subshrub growing up to 2–2.5 m height (Fig. 3.5). Roselle leaves are deeply three to five lobed, 8–15 cm long, and arranged alternately on the stems. Roselle flowers are 8–10 cm in diameter and white to pale yellow in color with a dark red spot at the base of each petal, and have a stout fleshy calyx at the base, 1.5–2 cm wide, enlarging to 3–3.5 cm, fleshy, and bright red as the fruit matures.

Figure 3.5 Roselle plants and fibers.

Figure 3.6 Banana plants and fibers.

3.3.5 Banana

Banana plants (*Musa sapientum*) (Fig. 3.6) are normally tall and fairly sturdy. The leaves of banana plants are composed of a "stalk" (petiole) and a blade (lamina). The base of the petiole widens to form a sheath; the tightly packed sheaths make up the pseudostem, which is tall that supports the plant. Cultivated banana plants vary in height depending on the variety and growing conditions. Banana plants grow up to 3–7 m height. Leaves are spirally arranged and may grow up to 2.7 m long and 60 cm wide. Banana fibers are obtained from the pseudostem of banana plant. The "pseudostem" is a clustered, cylindrical aggregation of leaf stalk bases. Banana fiber at present is a waste product of banana cultivation. The banana plants are a source of fiber for high-quality textiles. Banana fibers are also used in the production of banana paper. The banana fibers are obtained from banana stem and leaves by retting process.

Figure 3.7 Hemp plants and fibers.

Figure 3.8 Flax plants and fibers.

3.3.6 Hemp

Hemp (*Cannabis sativa* L.) is an annual plant and grows in temperate regions (Fig. 3.7). Hemp grows up to 4 m height under suitable warm conditions. Hemp fibers are obtained from bast by retting process. True hemp fibers are fine, light colored, and lustrous. The color and cleanliness of hemp fibers vary in accordance to the method of preparation of the fibers. The lower-grade hemp fibers are dark cream and contain much nonfibrous matter. Hemp fibers range in length from 1.0 to 2.5 m and used in thermoplastic matrix composites for internal structures in automotive industry.

3.3.7 Flax

Flax grows up to 1 m in height in temperate regions (Fig. 3.8). In the UK, flax is normally sown in March–May. Flax fibers are obtained from bast by retting process. Flax

Figure 3.9 Okra plant and fibers.

can be stand-retted (before harvest), dew-retted (cut and left in the field), water-retted (immersed in tanks), or chemically retted (in process tanks). Enzymes (e.g., pectinase digests the pectin binder) may be used to assist the retting process. Termination of the retting process may be a problem, and failure to achieve this can result in reduced fiber properties. Preharvest stand retting of flax, when glyphosate is applied at the midpoint of flowering, depends on uniform desiccation of the entire stem and is difficult to achieve during a dry season. Both dew retting and stand retting of the desiccated flax in the field rely on invasion by natural microorganisms and are dependent on the weather conditions. Flax fibers are used in thermoplastic matrix composite panels for internal structures in the car industry including car door panels, car roof and boot linings, and parcel shelves.

3.3.8 Okra

Okra bamia (Lady's finger) plant (Fig. 3.9) is of the Malvaceae family. Okra fibers (*Abelmoschus esculentus*) are extracted from the barks of okra bamia plants. The color of okra fibers varies from whitish to yellowish depending on the action of the UV radiation. The stems are kept under water for 15–20 days for microbial degradation. The fibers are isolated from the degraded stems, washed well by clean water, tied with ropes, and dried in open air.

3.3.9 Betel nut

The betel nut fibers are extracted from the betel nut fruits (Fig. 3.10) after crushing and separating the seeds and then soaking in tap water for 48 h to ease the extraction of the fibers.

3.3.10 Oil palm

Oil palm (*Elaeis guineensis* Jacq.) (Fig. 3.11) is cultivated in many tropical countries, namely, Africa and Asia, and is the highest yielding edible oil crop

Figure 3.10 Betel nut tree and fibers.

Figure 3.11 Oil palm tree and fibers.

in the world. Empty fruit bunches, shell, and palm kernel are waste of oil palm cultivation and processing. Empty fruit bunches are usually burnt, disposed off in landfills, or composted to organic fertilizer. From oil palm tree, fibers are extracted from trunk, frond, fruit mesocarp, and empty fruit bunch. Empty fruit bunch is the fibrous mass left behind after separating the fruits. Oil palm fibers are extracted from empty fruit bunch by retting process and used in the production of composites, textiles, cellulose, and paper.

3.3.11 Wild almond

Wild almond (*Sterculia foetida*) tree (Fig. 3.12) is a soft-wooded tree that can grow up to 115 ft tall. The leaves and bark of the tree have some significant medicinal values. A gum that is obtained from the trunk and branches can be used for book binding and similar purposes. The seeds of the tree are also safe to eat. The oil of wild almond has

Figure 3.12 Wild almond tree.

been found to be comparable to sunflower, soybean, and rapeseed oils for the use of biofuels. Empty fruit bunch is the fibrous mass left behind after separating the fruits. Wild almond fibers are extracted from empty fruit bunch by retting process. Fruit bunch after crushing and separating the seeds is soaked in tap water for 15–20 days for microbial degradation. Extracted fibers are washed well by clean water and sun dried.

3.3.12 Coconut or coir

Coconut or coir fiber is extracted from the husk of coconut (Fig. 3.13). The individual fiber cells are narrow and hollow, with thick walls made of cellulose. They are pale when immature, but later become hardened and yellowed as a layer of lignin is deposited on their walls. Each cell is about 1 mm long and 10–20 μm in diameter. Fibers are typically 10–30 cm long. Coir is the fibrous material found between the hard, internal shell and the outer coat of a coconut. Brown coir, harvested from ripe coconuts, is used in upholstery padding, sacking and horticulture. White coir, harvested from unripe coconuts, is used for making finer brushes, strings, ropes, and fishing nets. Brown coir is thick and strong and has high abrasion resistance. Brown coir fibers contain more lignin and less cellulose. White coir fibers are smoother and finer, but they are weaker. They are spun to yarns for mats or ropes. The coir fibers are waterproof and resistant to damage by saltwater. Freshwater is used to process brown coir, whereas seawater and freshwater are both used in the production of white coir.

Brown fibrous layer of the fruit is separated manually from the hard shell by driving the fruit down onto a spike to split it (dehusking). The fibrous husks are soaked in pits or in nets in a slow-moving body of water to swell and soften the fibers. The long bristle fibers are separated from the shorter mattress fibers by wet-milling

Figure 3.13 Coconut tree and fibers.

process. The dirt and other rubbish are removed from the mattress fibers, dried in the sunlight, and packed into bales. Mattress fibers are allowed to retain more moisture to retain their elasticity for twisted fiber production. The longer bristle fibers are washed in clean water and dried before being tied into bundles or hanks. They may be cleaned and "hackled" by steel combs to straighten the fibers and remove any shorter fibers. Coir bristle fibers can be bleached and dyed to obtain hanks of different colors.

White coir is obtained by retting process. The immature husks are suspended in a river or water-filled pit for up to 10 months. During this time, microorganisms break down the plant tissues surrounding the fibers to loosen them. Segments of the husk are then beaten by hand to separate out the long fibers, which are subsequently dried and cleaned. The coir fibers can also be extracted from coconut husk by biological process without polluting the environment. This process involves enzymes to separate the fibers by converting and solubilizing plant compounds.

3.3.13 Sugarcane

Sugarcane (*Saccharum officinarum* L.) grows in all tropical and subtropical regions. Sugarcane (Fig. 3.14) is a renewable, natural agricultural resource because it provides sugar, besides biofuel, fiber, and fertilizer. Bagasse or sugarcane fiber is the fibrous material left after juice extraction. It is a dry pulpy residue left after the extraction of juice from sugarcane. Bagasse is utilized as a biofuel and in the manufacture of pulp and building materials. Bagasse is often used as a primary fuel source for sugar mills. Bagasse is commonly used as a substitute for wood for the production of pulp, paper, and board in many tropical and subtropical countries such as India, China, Colombia, Iran, Thailand, and Argentina.

3.3.14 Bamboo

Bamboo (Fig. 3.15) grows up to 5–30 m height and is used for building materials, as a food source and as a versatile raw product. Bamboo has a higher compressive strength

Figure 3.14 Sugarcane plants and fibers.

Figure 3.15 Bamboo plants and fibers.

than wood, brick, or concrete and tensile strength that competes steel. Bamboo can be cut and laminated into sheets and planks. Bamboo fibers are very short (less than 3 mm) and therefore they are not usually transformed into yarn by a natural process.

3.3.15 Ramie

Ramie (*Boehmeria nivea*) is commonly known as China grass. Ramie is the bast fiber crop that grows up to 1–2.5 m height (Fig. 3.16). The most suitable climate for ramie is warm and humid. China grass is also known as white ramie. The main producers of ramie are China, Brazil, Philippines, India, South Korea, and Thailand. Ramie fiber is durable and pure white in color and has a silky luster.

Resistant to bacteria, mildew, alkalis, rotting, light, insect attack, extremely absorbent, natural stain resisting ability, fairly good dyeability, and nonshrinkability are the advantages of the ramie fibers, whereas low elasticity, low abrasion resistance,

Figure 3.16 Ramie plants and fibers.

and easy wrinkle property are their disadvantages. Ramie fibers are stiff, brittle, and costly. Ramie fibers are well known as textile fibers and mainly used in apparel, home fashion, fire hoses, and filter cloth.

3.4 Fiber modification

Physical and chemical methods are available for the modification of natural fibers. Physical or chemical treatment to natural fibers improves the water resistance and the wettability by nonpolar polymers and hence promotes interfacial adhesion. Plasma discharge and corona discharge are physical treatments for natural fiber modification. Physical treatment may create hydrophilic or hydrophobic fiber surface that results in increase of the compatibility of the fiber with the polymer matrices. Physical surface treatment does not alter hydrophilic character of the fiber because it is very shallow surface of cell walls. Chemical treatment of natural fibers results into permanent change of the nature of fiber cell walls by grafting polymers onto the fibers, by cross-linking of the fiber cell walls, or by using coupling agents. The chemical modification of the fibers causes fiber cell walls to be more dimensionally stable, more water resistant, and increase resistance against fungal decay but may reduce impact strength due to embrittlement of the modified fibers. A coupling agent is a chemical that functions at the interface to create a chemical bridge between the reinforcement and matrix. It improves the interfacial adhesion. Extensively used coupling agents are copolymers containing maleic anhydrides, isocyanates, and silanes.

3.4.1 Mercerization (alkali treatment)

The alkali treatment promotes the removal of hemicellulose, lignin, waxes, and pectin and produces rough surface topography. In addition, alkali treatment leads to breakdown of the fiber bundles into smaller fibers, reduces fiber diameter, and increases

aspect ratio. This increases the effective surface available for wetting by the matrix material. Alkali-sensitive hydrogen bonds existing among the fibers break down, and new reactive hydrogen bonds form between the cellulose molecular chains. Due to this, hydrophilic hydroxyl groups are partially removed and moisture resistance property is improved.

Natural fibers are soaked in 5%–10% sodium hydroxide solution at room temperature or at 50–60°C in some cases for 6–8 h depending on required fiber strength. Then treated fibers are washed well with water to neutral pH and dried in an oven at 60°C for 3–4 h.

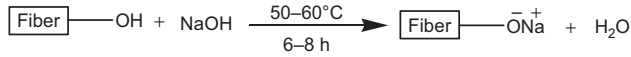

3.4.2 Acetylation

Acetylation of alkali-treated natural fibers is carried out using mixture of acetic acid and acetic anhydride at 50–60°C for 2–3 h. Acetylation of fibers causes reduction in hydrophilic nature of the fibers. This treatment provides rough surface topography and increases wetting by the resin.

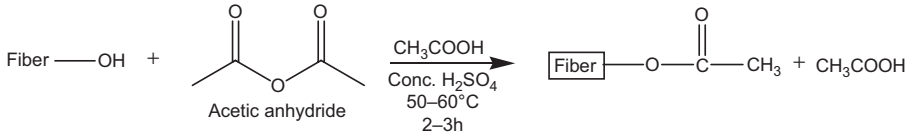

3.4.3 Benzoylation

Benzoylation of natural fibers involves benzoyl chloride to reduce the hydrophilicity of the fiber and improves fiber matrix adhesion, and as a consequence increases the mechanical strength of the composite. Benzoylation also increases thermal stability of the fiber. Before benzoylation, hydroxyl groups are activated by alkali pretreatment and then soaked in benzoyl chloride solution for 15–30 min. Unreacted benzoyl chloride can be removed by washing with ethanol followed by water and oven drying.

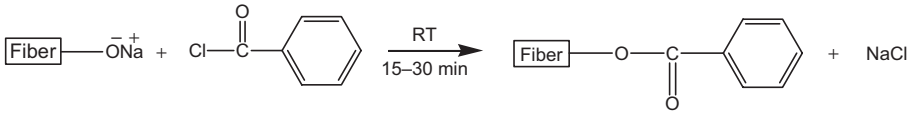

3.4.4 Malenization

Alkali-treated fibers are subjected to 5%–10% maleic anhydride in xylene and catalytic amount of concentrated sulfuric acid at reflux temperature for 4–6 h. Fibers are

washed well with methanol and dried in an oven at 80°C for 4–5 h. Possible reaction schemes are as follows:

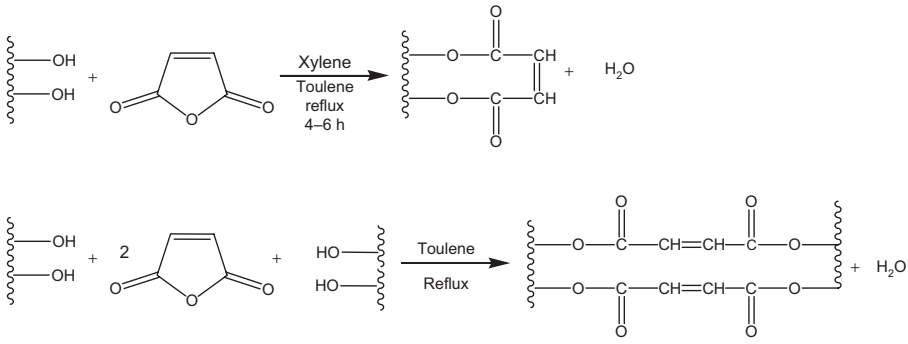

3.4.5 Silane treatment

Silane is used as a coupling agent for the modification of fiber surface. It undergoes hydrolysis, condensation, and bond formation during the treatment process. Silanols form in the presence of moisture and hydrolyzable alkoxy groups. It reacts with cellulose hydroxyl group of the fiber and improves fiber matrix adhesion to stabilize composite properties. The chemical composition of silane coupling agent (bifunctional siloxane molecules) allows forming a chemical link between the surface of the cellulose fiber and the resin through a siloxane bridge. This coreactivity provides molecular continuity across the interface region of the composite. It also provides the hydrocarbon chain that restrains fiber swelling into the matrix, natural fibers exhibit microspores on their surfaces, and silane coupling agent acts as a surface coating, which penetrates into the pores and develops mechanically interlocked coating on their surface. Silane-treated fiber-reinforced composite provides better tensile strength than the alkali-treated fiber composites.

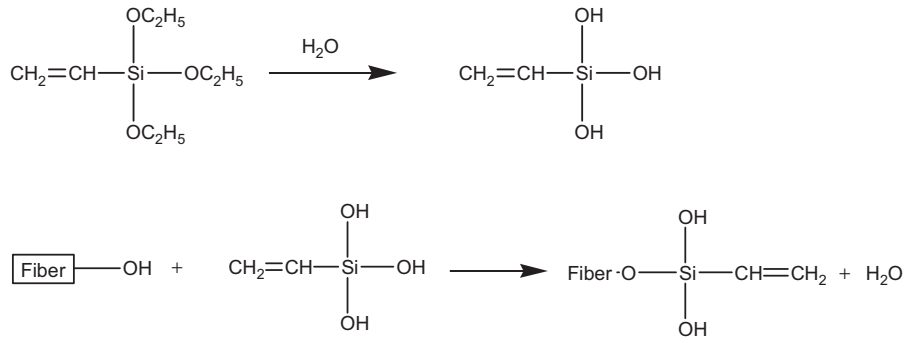

3.4.6 Benzylation

Benzylation is a Williamson nucleophilic substitution reaction of alkoxide or phenoxide ion and halide ion. Natural fibers are preswelled by concentrated sodium hydroxide (5–10 N) for 1 h and then reacted with benzyl chloride in presence of phase transfer catalyst at 120°C for different time interval (5–10 h) to get benzylated fibers after washing well with water and finally with ethanol. The treated fibers are dried under vacuum at 80°C.

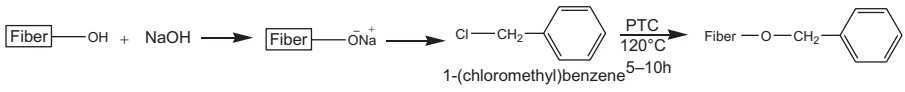

The side reactions

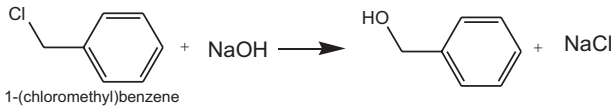

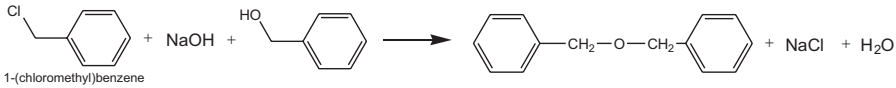

3.4.7 Scouring

Scouring is nothing but solvent treatment of textile materials in aqueous or other solvents to remove natural fats, waxes, proteins, dirt, oil, impurities, etc. This method is also known as solvent treatment of the fibers.

3.4.8 Bleaching

Any method other than scouring, for improving the whiteness of textile material by decolorizing it from the gray state, with or without the removal of natural coloring and/or extraneous substances, is known as bleaching. The removal of color from dyed or printed textiles is known as "stripping." Alkali-treated fibers are treated with NaOCl/H_2O (1:1) solution at 60°C for 4 h and then fibers are washed well with distilled water to eliminate remaining chemicals and dried in an oven at 60°C for 24 h. The active bleaching agent is the hypochlorite ion and the reactions are as follows:

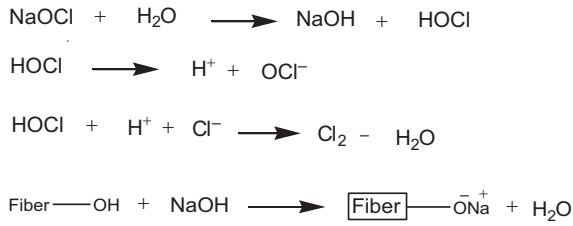

3.4.9 Treatment with compounds containing methylol group

This type of treatment is well known in textiles. Hydroxyl groups of cellulose form stable bonds with compounds containing methylol groups as shown below:

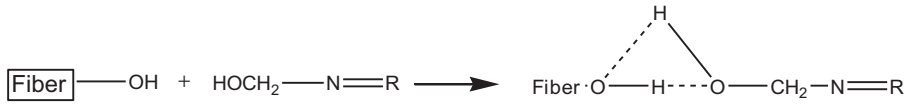

3.4.10 Toluene diisocyante treatment

Isocyanate groups are very susceptible to reaction with the hydroxyl groups of cellulose and lignin in the natural fibers.

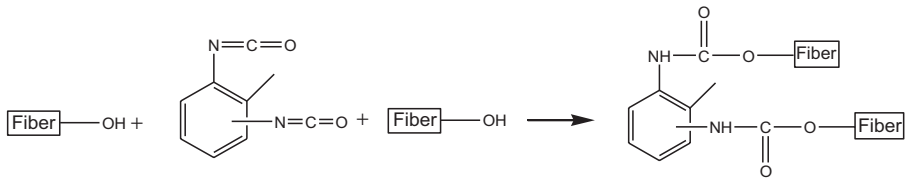

3.5 Chemical composition and physical properties of natural fibers

3.5.1 Chemical composition

Most plant fibers except cotton are composed of cellulose, hemicellulose, lignin, waxes, and some water-soluble compounds. Cellulose, hemicellulose, and lignin are the major constituents of the natural fibers. Chemical compositions of natural fibers are presented in Table 3.1.

3.5.1.1 Cellulose

Cellulose is the major component of the natural fiber, which gives the strength, stiffness, and structural stability. Cellulose has its own cell geometry, which is responsible for the high mechanical properties of plant fibers. Cellulose is a natural polymer consisting of D-anhydroglucose ($C_6H_{11}O_5$) repeating units joined by 1,4-D-glycosidic linkages at C1 and C4 positions. The degree of polymerization (DP) is ~10,000. Each repeating unit contains three hydroxyl groups. The hydroxyl groups form intra- and intermolecular hydrogen bonding as well as with moisture in the air. All natural fibers are hydrophilic in nature and absorb water ranging from 8% to 12.6%. The ability of hydrogen bond formation of the hydroxyl groups plays a major role in directing the crystalline packing and also governs the physical properties of cellulose. Cellulose structure is composed of crystalline and amorphous regions. Cellulose is also formed of slender rodlike

Table 3.1 Chemical composition of some natural fibers [1–22]

Fiber	Botanical name	Cellulose, %	Hemicellulose, %	Lignin, %	Pectin, %	Wax, %	Ash, %
Jute	*Corchorus olitoris*	61–71	12–20	12–13	04	0.5	2
Cotton		82.7	5.7	–	–	0.6	–
Kenaf	*Hibiscus cannabinus*	31–57	21.5	8–19	3.5	–	4.2
Bamboo	*Phyllostachys aurea*	26–43	15–26	21–31	–	–	–
Kapok	*Ceiba pentandra*	64	23	13	2.3	–	–
Ramie	*Boehmeria nivea*	68–76	13–17	0.6–0.7	1.9	0.3	–
Hemp	*Cannabis sativa*	70–74	17–22	3.7–5.7	0.9	0.8	2.5
Flax	*Linum usitatissimum* L.	64–72	17–21	2–2.2	1.8–2.3	1.7	3.8
Sisal	*Agave sisalana*	63–64	12	10–14	10	2	1
Coir	*Cocos nucifera*	32–43	0.1–0.2	40–45	–	–	0.8
Banana	*Musa acuminate*	65	19	5	–	–	–
Pineapple	*Pina*	81	–	12	–	–	–
Okra	*Abelmoschus esculentus*	60–70	15–20	5–10	3.7	3.9	–
Henequen	*Agave fourcroydes*	77.6	–	13.1	–	–	–
Sugarcane	*Blue agave*	32–55	20–25	18–24	10	<1	1–4
Rice husk	*Oryza sativa*	313	24.3	14.3	–	–	23.5
Groundnut	*Arachis hypogaea*	35.7	18.7	30.2	–	–	5.9
Betel nut	*Gossypium*	53.2	33	7.2	1.5	0.64	1.1
Mapple		45–50	22–30	22–30	–	–	–

crystalline microfibrils. The crystal nature (monoclinic sphenoid) of naturally occurring cellulose is known as cellulose I. Cellulose is resistant to strong alkali (17.5 wt%) but is easily hydrolyzed by acid to form water-soluble sugars. Cellulose is relatively resistant to oxidizing agents. Generally, tensile strength and Young's modulus of fibers increase with increasing cellulose content. The microfibrillar angle determines the stiffness of the fibers. Plant fibers are more ductile if the microfibrils have a spiral orientation to the fiber axis. If the microfibrils are oriented parallel to the fiber axis, the fibers will be rigid and inflexible and have high tensile strength.

3.5.1.2 Hemicellulose

The hemicellulose is responsible for considerable amount of moisture absorption, biodegradation, and thermal degradation of the fiber because of its least resistance. Hemicelluloses occur mainly in the primary cell walls and have branched and varied chemical structure. The branches are polymeric sugars. Hemicelluloses are comprised of a combination of 5- and 6-carbon ring sugars. Hemicellulose differs from cellulose in three aspects:

1. Hemicellulose molecule contains several different sugar units, whereas cellulose contains only 1,4–β-D-glucopyranose units.
2. Hemicellulose molecule contains a considerable degree of chain branching responsible for its noncrystalline nature, whereas cellulose is a linear polymer.
3. The degree of polymerization of native cellulose is 10–100 times higher than that of hemicellulose. The degree of polymerization of hemicellulose is ranging from 50 to 300.

Hemicelluloses are the supportive matrix for cellulose microfibrils. Hemicelluloses are highly hydrophilic, soluble in alkali, and easily hydrolyzed by acids. Mainly the acid groups of hemicelluloses make them highly hydrophilic and increase water uptake in the fibers and the risk of microbiological fiber degradation. Hemicelluloses are thermally degrading more at lower temperatures (150–180°C) than cellulose (200–230°C).

3.5.1.3 Lignin

Lignin is the cementing agent that binds individual fiber cells together. Lignin is thermally stable but prone to UV degradation. Lignin is a complex hydrocarbon polymer with both aliphatic and aromatic constituents, amorphous, and hydrophobic in nature. Lignin is totally insoluble in most solvents and cannot be broken down into monomeric units. The lignin content of the fibers affects its structure properties and morphology. It gives rigidity to the plants. Lignin contains five hydroxyl and five methoxyl groups per building unit. Lignin has a glass transition temperature of about 90°C and melting temperature of about 170°C. It is soluble in hot alkali, easily oxidizable, and condensable with phenol but does not hydrolyze by acids.

3.5.1.4 Pectin

The pectin is a heteropolysaccharide and its structure is complex. The side chains of pectin are often cross-linked with the calcium ions and arabinose sugars. The lignin, hemicelluloses, and pectin hold the cellulose framework structure of the fiber together. The pectin provides plant flexibility.

3.5.1.5 Extractive and ash

Natural fibers are also composed of a small amount of organic extractives and inorganic (ash) components. The color, odor, and decay resistance of the fibers are due to organic extractives. Inorganic matters enhance abrasive nature of the fiber.

3.5.1.6 Wax

Waxes are the last part of fibers and they consist of different types of alcohols, which are responsible for the wettability and adhesive characteristics of the fiber. The waxes can be extracted with organic solvents.

3.5.2 Physical properties

Physical properties of natural fibers are presented in Table 3.2.

3.6 Characterization of natural fibers

3.6.1 Fourier transform infrared spectroscopy

In infrared (IR) spectroscopy, IR radiations are allowed to interact with the substance and absorption or transmittance of the radiations is recoded. The vibrational frequencies

Table 3.2 Physical properties of natural fibers [1–22]

Fiber	Density, g/cm^3	Diameter, µm	Tensile strength, MPa	Tensile modulus, GPa	% Elongation	% Moisture absorption
Jute	1.39–1.52	25–200	307–1000	13–70	1.2–1.8	8.5–17
Cotton	1.51–1.55	–	287–840	9.4–22	3–10	7–25
Kenaf	1.193–1.4	18–22	240–1191	14–60	2.7	9.5–17
Bamboo	0.6–1.5	–	140–800	11–34	–	–
Kapok	–	15–35	93.3	4	1.2	–
Ramie	1.5	24	400–938	44–128	1.2–3.8	7.5–17
Roselle	0.75–0.8	–	170–350	10–17		
Hemp	1.48–1.52	28–38	550–920	30–70	1.6	6–12
Flax	1.4–1.53	20–25	345–1500	58–80	1.2–1.6	7–12
Mesta	1.47	200	157.38	12.62	–	–
Sisal	0.7–1.45	50–200	480–700	8–38	3–7	10–22
Palm	1.44	20–80	413–1627	34.5–82.5	1.6	–
Raphia	0.75	–	440–611	24–28	2.1–3.5	–
Coir	1.15–1.25	100–450	93–304	4–6	15–40	10–13
Banana	0.75–1.35	–	1.7–7.9	11–32	1.5–9	9–15
Pineapple	1.44	–	100–170	10–50	–	10–13
Oil palm	0.7–1.55	150–500	50–400	0.6–9	4–18	–
Sugarcane	0.5–1.2	300–400	170–290	15–19	3–7	–

and intensities are used to find the nature of the bond forces and molecular structure of the substance. Solid, liquid, gaseous samples or thin films can be used. Solids can be mixed with KBr powder and pelletized. Hydroxyl groups present in cellulose, hemicellulose, and lignin, which give strong and broad absorption peaks over the range from 3600 to 3000 cm^{-1}. C—H stretching peaks appear in the range 2900–2800 cm^{-1}. The important characteristic peaks for cellulose absorb in the range 1445–1414 cm^{-1} and for lignin absorption peaks observed in the range 1566–1250 cm^{-1}. Glycosidic C—O—C stretching appears at about 1022 cm^{-1}. Alkali-treated fibers show absence of peak at about 1700 and 1560 cm^{-1}, which confirms delignification and removal of hemicellulose. Partial treatment of natural fibers shows absorption peaks due to lignin and hemicellulose.

In the case of acetylated, benzoylated, and malenized natural fibers, new and strong absorption peak due to ester C═O stretching appears in the range 1700 cm^{-1}; isocyanate-treated fiber shows urethane stretching peaks due to NH, C═O and C—O groups; and benzylated fiber shows strong absorption peak due to C—O—C stretching, whereas peak due to OH stretching disappears practically.

3.6.2 Scanning electron microscopy

Scanning electron microscopy (SEM) is the most useful technique for the study of the surface morphology of the fiber by scanning it with a high energy beam of electrons. The electrons interact with the constituent atoms of the sample producing images of surface topography. SEM can produce very high-resolution images of a sample surface for understanding the surface structure of a sample. In this technique, special sample preparation is required. For SEM imaging the specimens must be electrically conductive at the surface. Before examining sample under electron microscope, sample is mounted on a double-sided carbon tape or an aluminum or copper stub. The sample is sputter coating with carbon vapor and finally with gold. The replica of the sample is taken on a copper grid and examined under electron microscope with suitable magnification. SEM micrographs reveal surface modification, fractured surfaces, cross-sectional area of the fibers, arrangement of the fibrils, adherence of minerals (silicon, potassium, calcium, magnesium, aluminum), porosity, fiber compactness, etc.

3.6.3 X-ray diffraction

X-ray diffraction is based on Bragg's law ($n\lambda = 2d\sin\theta$). A monochromatic beam of X-rays is allowed to incident on a sample, and reflected X-rays are detected by a detector. X-ray diffraction pattern is a characteristic of the substance under investigation. X-ray diffraction technique is useful in determining the percent crystallinity in the natural fibers before and after physical or chemical treatment. Generally, X-ray diffractogram of the sample is recorded on an X-ray diffractometer operating at known voltages and current using a Cu Kα X-rays ($\lambda = 0.15406$ nm) over the 2θ range from 10 to 100 degrees in the steps of 0.01 degree at room temperature in open quartz sample holders. Amorphous regions of the samples produce broad peak, whereas crystalline

regions produce sharp peaks. The degree of crystallinity (X_c) can be determined by determining the intensities of the crystalline (I_c) and amorphous (I_a) contents in the sample:

$$X_c = \frac{I_c}{I_a + I_c} \times 100$$

Alkali treatment reveals considerably broadening of the peak suggesting a higher level of transformation of the crystalline cellulose to amorphous cellulose.

3.6.4 Thermal analysis

Differential scanning calorimetry (DSC) and the combined thermogravimetric analysis (TGA) and differential thermal analysis (DTA) are very useful techniques for assessing crystallinity and thermal stability of the natural fibers. In DSC, sample and reference are placed on a separate identical sample and reference holders kept near to sensitive thermocouples and heated at a programmed heating rate under air or inert environment. When a transition occurs in the sample, thermal energy is added and is supplied to sample or reference to maintain same energy level. When sample absorbs energy, sample holder requires more power to maintain equal temperature to that of reference holder. Similarly if sample releases thermal energy, then less power is supplied to maintain same temperature as that of reference holder. Thus, DSC records the rate of energy change as a function of temperature. The area under the peak represents energy associated with the thermal transition. It is useful for the determination of glass transition, melting, crystallization transitions, etc. About 5–10 mg sample is required for the analysis. DTA records temperature difference between sample and reference as a function of temperature or time.

TGA records weight change of the sample as a function of time or temperature due to dehydration or decomposition reaction. A 3–5 mg of the sample is taken in a crucible, placed on an automatic high sensitivity balance, and heated continuously at a constant heating rate under air or inert environment. TGA thermogram is a characteristic curve for a given compound and therefore it is used for the identification of the polymers, fillers, etc. It is the most useful for polymer processing for end users.

The cellulose molecules are hydrophilic, and therefore the fiber properties are sensitive to the relative humidity of the environment in which they are processed and/or used. Around 100°C, DSC or DTA thermogram reveals endothermic transition due to moisture release and other endothermic transition at high temperature reveals cellulose degradation. Initial decomposition of cellulose fibers occurs primarily in the amorphous regions. For untreated jute fibers, decomposition temperature of α-cellulose is 362.2°C, whereas for mercerized fibers it is 348°C [22]. A small weight loss from room temperature to about 110–120°C reveals moisture release from the fibers. The thermal degradation of cellulose fibers occurs over the range from 200 to 310°C due to thermal

depolymerization of hemicellulose, pectin, and glycosidic linkages of cellulose. The degradation of α-cellulose occurs over the range 310–390°C. The structure of lignin is complex and composed of aromatic rings with various branches, and as a result degradation occurs slowly over the whole temperature range.

The natural fiber starts degrading at about 240°C. Structural constituents of the fiber (cellulose, hemicelluloses, lignin, etc.) are sensitive to the different range of temperatures. The lignin starts degrading at about 200°C. Hemicelluloses and celluloses degrade at higher temperatures. Thermal stability of the fiber can be enhanced by removing hemicelluloses and lignin by chemical treatment. The degradation of natural fiber is an important issue in the development of natural fiber composites in both composite manufacturing (curing, extrusion, or injection molding) and materials in service.

3.6.5 Mechanical properties

Tensile properties of the fibers are determined by tensile testing machine at a constant crosshead speed. Fiber is clamped between a stationary grip and a movable grip. Tensile strength and elongation at break can be determined according to following equations:

$$\text{Tensile strength, MPa} = \frac{\text{Maximum load}, N}{\text{Original cross sectional area}, \text{m}^2}$$

$$\text{Elongation at break}, \% = \frac{\text{Change in gauge length}}{\text{Original length}} \times 100$$

The modulus of elasticity (E) can be determined from the slope of initial linear portion of the stress–strain curve.

$$E = \frac{\text{Stress } (\sigma)}{\text{Strain } (\varepsilon)}$$

The structure, chemical composition, and microfibrillar angle are the most important variables that affect the overall properties of the fibers. A fiber is more ductile if the microfibrils have a spiral orientation to the fiber axis. If the microfibrils are oriented parallel to fiber axis, then the fibers are inflexible and rigid. The natural fibers exhibit considerable variation in diameter along with the length of individual filaments. The tensile strength of plant fiber is higher than other fibers. The natural fibers are used for durable yarns, fabrics, packaging, and paper.

3.6.6 Water absorption

Water absorption tendency of natural fibers increases biodegradation. Water absorption capability of untreated and chemically modified natural fibers can be determined

by a series of water absorption tests. Known weights of dried fibers with an approximate length of 45–50 mm are immersed in distilled water at constant temperature, say, 30°C. Weights of the moist fibers are determined at the interval of 24 h until equilibrium establishes. The percentage water absorption is expressed as

$$\% \text{ Water absorption} = \frac{(\text{Weight of moist sample} - \text{Weight of dry sample})}{\text{Weight of dry sample}} \times 100$$

References

[1] M.J. John, S. Thomas, Biofibers and biocomposite, Carbohydrate Polymers 71 (2008) 343–364.
[2] I.M. De Rosa, J.M. Kenny, D. Puglia, C. Santulli, F. Sarasini, Morphological, thermal and mechanical characterization of okra (*Abelmoschus esculentus*) fibres as potential reinforcement in polymer composites, Composites Science and Technology 70 (2010) 116–122.
[3] M.S. Alam, G.M. Arifuzzaman Khan, Chemical analysis of okra fiber (*Abelmoschus esculentus*) and its physico-chemical properties, Journal of Textile and Apparel, Technology and Management 5 (2007) 1–9.
[4] G.M. Arifuzzaman Khan, Md Shaheruzzaman, M.H. Rahman, S.M. Abdur Razzaque, Md Sakinul Islam, Md Shamsul Alam, Surface modification of okra fiber and its physico-chemical characteristics, Fibers and Polymers 10 (2009) 65–70.
[5] P.S. Mukherjee, K.G. Satyanarayana, Structure properties of some vegetable fibers, Part 1. Sisal fibre, Journal of Materials Science 19 (1984) 3925–3934.
[6] R. Murugan, S. Ramakrishna, Bioresorbable composite bone paste using polysaccharide based nano hydroxyapatite, Biomaterials 25 (2004) 3829–3835.
[7] S. Ramakrishna, J. Mayer, E. Winter Mantel, W. Leongk, Biomedical applications of polymer-composite materials: a review, Composites Science and Technology 61 (2001) 1189–1224.
[8] T. Sydenstricker, S. Mochnaz, S. Amico, Pull-out and other evaluations in sisal-reinforced polyester biocomposites, Polymer Testing 22 (2003) 375–380.
[9] N. Defoirdt, S. Biswas, L. De Vriese, Le.Q.N. Tran, J. Van Acker, Q. Ahsan, L. Gorbatikh, A. Van Vuure, I. Verpoest, Assessment of the tensile properties of coir, bamboo and jute fibre, Composites: Part A 41 (2010) 588–595.
[10] V.G. Geethamma, K.T. Mathew, R. Lakshminarayanan, S. Thomas, Composite of short coir fibres and natural rubber: effect of chemical modification, loading and orientation of fibre, Polymer 39 (1998) 1483–1491.
[11] P. Wambua, J. Ivens, I. Verpoest, Natural fibres: can they replace glass in fibre reinforced plastics, Composites Science and Technology 63 (2003) 1259–1264.
[12] J.E.G. Van Dam, M.J.A. van den Oever, E.R.P. Keijsers, J.C. van der Putten, C. Anayron, F. Josol, A. Peralta, Process for production of high density/high performance binder less boards from whole coconut husk. Part 2: coconut husk morphology, composition and properties, Industrial Crops and Products 24 (2006) 96–104.

[13] M.J. John, R.D. Anandjiwala, Recent developments in chemical modification and characterization of natural fiber-reinforced composites, Polymer Composites 29 (2008) 187–207.
[14] A.K. Bledzki, J. Gassan, Composites reinforced with cellulose based fibres, Progress in Polymer Science 24 (1999) 221–274.
[15] K.S. Ahmed, S. Vijayaraangan, A.C.B. Naidu, Elastic properties, notched strength and fracture criteria in untreated woven jute–glass fabric reinforced polyester hybrid composites, Material and Design 28 (2007) 2287–2294.
[16] F. Munder, H. Hempel, Mechanical and thermal properties of bast fibers compared with tropical fibers, Molecular Crystals and Liquid Crystals 448 (2006) 197–209.
[17] D.S. Varma, M. Varma, I.K. Varma, Coir fibres, part I: effect of physical and chemical treatments on properties, Textile Research Journal 54 (1984) 827–832.
[18] C. Baley, Analysis of the flax fibres tensile behaviour and analysis of the tensile stiffness increase, Composites Part A: Applied Science and Manufacturing 33 (2002) 939–948.
[19] E. Bodros, C. Baley, Study of the tensile properties of stinging nettle fibres (*Urtica dioica*), Materials Letters 62 (2008) 2143–2145.
[20] S. Shinoj, R. Visvanathan, S. Panigrahi, M. Kochubabu, Oil palm fiber (OPF) and its composites: a review, Industrial Crops and Products 33 (2011) 7–22.
[21] R. Malkapuram, V. Kumar, Y.S. Negi, Recent development in natural fiber reinforced polypropylene composites, Journal of Reinforced Plastics and Composites 28 (2009) 1169–1189.
[22] D. Ray, B.K. Sarkar, R.K. Basak, A.K. Rana, Study of the thermal behavior of alkali treated jute fibers, Journal of Applied Polymer Science 85 (2002) 2594–2599.

This page intentionally left blank

Part Two

Applications of biodegradable and biocompatible polymer composites

This page intentionally left blank

Medical applications

4

Ivan Djordjevic, Samira Hosseini, José I. Gómez Quiñones
Tecnologico de Monterrey, Monterrey, Mexico

4.1 Introduction

Standard definition of composite is a two-phase material consisting of polymer matrix and solid filler. Ever since the discovery of vulcanized rubber, fillers have evolved into advanced nanomaterials with specifically designed interfaces. In turn, advances in polymer science resulted in thousands of different polymers for various applications, ranging from space technology to sophisticated medical devices. Owing to their versatility and high level of control over material performance, composites have found their significant place as biomaterials [1–3].

A traditional definition of "biomaterial" accepted by experts in the field is *a biomaterial is nonviable material used in a medical device, intended to interact with biological systems (Williams, 1987)* [4]. By definition, biomaterial composite design requires particular choice of either polymer matrix or solid filler. Naturally, both components should possess minimal toxicity, and their fabrication should not include any toxic solvents.

Fig. 4.1 (left) shows schematic presentation of pure polymer matrix with indicated cross-linking points (red circles). Filler dispersion induces additional cross-linking within the matrix (dotted red circles in Fig. 4.1; right) causing changes in material properties. Heterogeneous interaction between polymers and solids is governed by the physicochemical properties at the interface between the matrix and the filler. The simplest route to produce the composite is to disperse filler material into prepolymer (or polymer solution) and to cure the mixture either by further polymerization of prepolymers (oligomers) or to evaporate the solvent from the casting mold. The result is the cross-linked composite with increased material strength due to the interfacial cross-links (Table 4.1).

Cross-links are either physical or chemical bonds (both intermolecular polymer bonds and interfacial bonds between the polymer and the filler), and their energies are presented in Table 4.1. There are various types of fillers produced in different sizes: rectangular or irregular shapes, spherical particles, nanoparticle (NP) aggregates, nanowires, etc. Nanomaterials generally have high specific surface area and therefore can achieve high level of contact with polymer matrices. This is possibly the most important feature of NP fillers making them materials of choice for future biomedical composite materials [5].

Composites have an advantage over pure polymers as they offer a high degree of control over material properties. There are several important factors that fundamentally define

Biodegradable and Biocompatible Polymer Composites. http://dx.doi.org/10.1016/B978-0-08-100970-3.00004-3

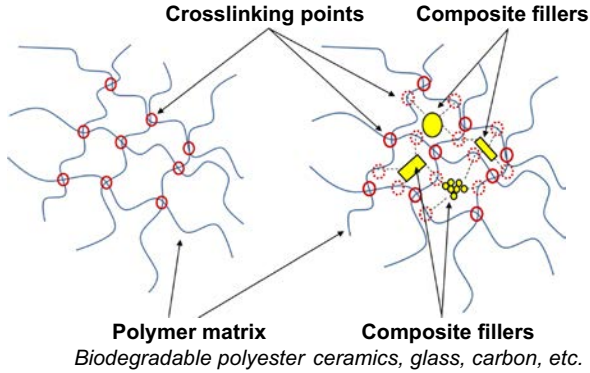

Figure 4.1 Schematic presentation of fundamental interactions in polymer composites. Left: pure polymer matrix with inherent intermolecular interaction (*full line circles*). Right: additional cross-linking points (*dotted red circles*) on mixture and interface with composite filler particles.

Table 4.1 The nature of intermolecular and matrix/filler forces in composite materials

Cross-linking bond	Dissociation energy (kJ/mol)
Covalent (single)	350
Ionic	100–1050
Hydrogen	8–42
Organometallic	150–400
Ion–dipole	20–200
Van der Waals	<50

composite biomaterials as a result of increased interfacial cross-linking. In turn, biomaterials' performance in medical devices is strongly dependent on the following factors:

- **Increased Young's modulus proportional to the filler concentration**: This particular feature is advantageous as the amount of filler can be carefully tuned to match the modulus of treated tissues. Mechanical match between implants and tissues is an important design parameter for all biomaterials [6].
- **Altered biodegradation rate**: Generally slower degradation kinetics is a result of increased cross-linking density in composites. Similar to the Young's modulus, biodegradation rate can be controlled by the physicochemical properties of individual components and matrix/filler concentrations [7].
- **Tissue exposure to filler on biodegradation**: As the polymer degrades the filler becomes more exposed to the medium. For that reason the filler should be carefully chosen to avoid an injury on the treated site and/or toxic effect on surrounding tissue [8].

Tissues such as bones, tendons, or blood vessels are hierarchically ordered composite materials. The most obvious one is bone that mainly consists of calcium

phosphate mineral dispersed into protein matrix. Mechanical behavior of tissues is anisotropic and possibly the most important advantage of composite materials is that they can be fabricated to mimic tissue response to mechanical stimulation [9]. Composites have been used for various biomaterial applications, such as tissue replacement (implants) or tissue engineering templates (scaffolds). However, possibly the most explored research area of composite biomaterials is for degradable bone fixation devices [1].

The application of degradable bone screws eliminates the necessity to perform second surgery for removal of metallic fixation devices. Another advantage is the choice of bioactive fillers that can be used to either prevent the bacterial infection around the implant or to induce tissue growth and subsequent bone regeneration through the biodegradation of the implants. Different types of polymers, fillers, and clinical strategies for bone implant and porous tissue engineering scaffolds are explained further in this chapter with examples from the latest published literature.

Degradation kinetics and the type of degradation products from polymer matrix are equally important parameters that would determine biological response. For instance, polylactic acid (PLA), polyglycolic acid (PGA), and their copolymers (PLGA) are produced from nontoxic lactic acid or glycolic acid monomer units bound with ester bonds. Those ester bonds are prone to hydrolytic and enzymatic degradation, which results in lactic acid release into the environment. The situation is not that simple as accumulation of acid around the implant might cause several detrimental consequences such as inflammation, interfacial bone cleavage, and implant migration [10]. Considering the fact that both polymer degradation products and filler release can have a strong effect on surrounding tissue, a careful choice of both components together with the production method are crucial for their performance.

This chapter explains fundamental interfacial properties of synthetic biodegradable polymer composites in regards to their performance as surgical implants, tissue engineering scaffolds, and protein delivery carriers. The chapter begins with the basic outlines of three important types of composite fillers and their properties, namely (1) ceramic and glass materials used as fillers in combination with biodegradable polymers; (2) composites with NPs as fillers; (3) ion release from the filler component and implications on physiological environment. Furthermore, some new aspects and strategies for biological activation of fillers by protein surface attachment are highlighted in separate section. At the end of the chapter, we introduce a new type of polymer composite hydrogels, called “double networks (DN)” or “interpenetrated networks” with their unique properties.

Outlined composite systems from the published literature are explained in detail through four major sections for their specific design of interfacial properties, biodegradation kinetics, influence of biodegradation on biological response, and controlled release of filler components. Selected examples are highlighted to present the major discoveries of polymer composites as multifunctional biomaterials to the readers. This chapter only deals with synthetic polymers that are specifically designed to interact with human body. Natural polymer systems such as polysaccharides (alginate, chitosan, etc.) are not covered in this chapter.

4.2 Biodegradable composite biomaterials: implants and the concept of tissue engineering

There is a tendency in implant medicine to replace prosthetic materials (metals and nondegradable plastics) with biodegradable ones. Current clinical bone surgery and tissue fixation procedure involves implant removal once the bone function is restored and ready to sustain biomechanical load without support from implanted screws. Those implants should support tissue growth and should be able to withstand substantial dynamical variation of biomechanical stresses. Regardless of the potential benefits, metallic implants are still predominant materials of bone fixation because of persistent clinical complications detected for biodegradable polymer implants. Put simply, *current polymers are still not a match for biomechanical robustness and biocompatibility of standardized metallic bone implants* [10].

Ever since the first reported tests on bioresorbable material made of PLA was reported in 1966 [11], there have been thousands of published studies proposing various engineering solutions from materials made of polylactide carbonate (PLC), PLA, PGA, or PLGA [12–14]. Physicochemical properties of those materials are well known, but the clinical applications of biodegradable polymers are still challenged by unpredictable immunological response to biomaterials. The situation with biodegradable composites is even more complex as individual properties of filler and matrix components influence implant response in close proximity to the biomaterial surface. Nevertheless, biodegradable implants are still subject of extensive research that so far established following strategies in tissue repair:

1. *Surgical implants* that are used to "bridge" or "fix" the affected tissue. Biodegradable materials serve as temporary prosthetics (mechanical support) while the naturally regenerated tissue slowly restores the biomechanical and physiological balance.
2. *Tissue engineering* concept requires a temporary matrix (scaffold) that mimics natural extracellular matrix (ECM) to mediate special tissue reconstruction. Scaffolds can be produced from biodegradable composites into various sizes and structures. Porous scaffolds allow three-dimensional (3D) cell migration, proliferation, and tissue regeneration supported by scaffold interface.

Both medical applications for biocompatible polymeric composites are discussed further in this section. For instruction purposes, here we present a basic laboratory experiment design to measure the rate of degradation in predetermined time intervals. The example is a composite scaffold, prepared with different percentages (w/w) of filler component. This method is universal and standard in published literature and is not limited to the shape, size, or type of the samples (i.e., composite films, coatings, scaffolds, ready-to-use machined implants, etc.).

4.2.1 Biodegradation kinetics of composite scaffolds: experimental protocol

Standard biodegradation experiment is a measurement of mass loss of the sample over the set period of time spent in either simulated physiological environment (in vitro)

or in living organism (in vivo). The "mass loss" or "degradation percentage" (%) is calculated from Eq. (4.1):

$$DEG.\ (\%) = \frac{M_0 - M_d}{M_0} \times 100 \tag{4.1}$$

where M_0 = mass of dry sample before degradation (g) and M_d = mass of dry sample after degradation (g).

In vitro degradation experiment is a setup of water thermostat (37°C) and centrifuge tubes filled with phosphate buffer saline (PBS) solution (10 mL). Prepared polymer composite scaffolds (Fig. 4.2(a) and (b)) are cut to approximate diameter = 6 mm and thickness = 3–5 mm [15]. Multiple samples are soaked in PBS (n = 5) and agitated

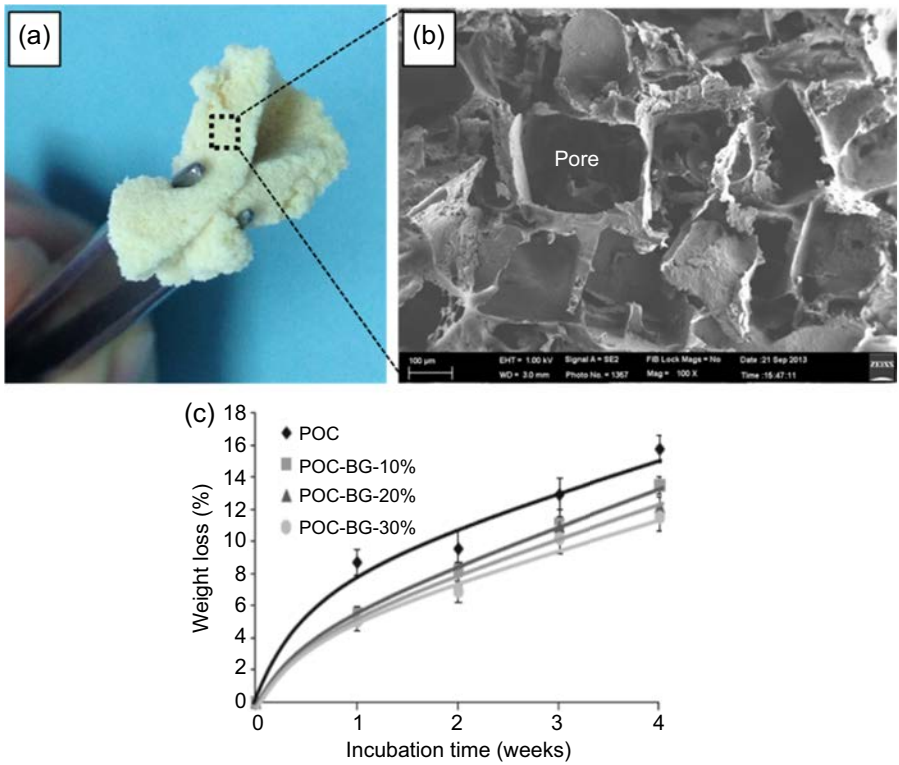

Figure 4.2 In vitro degradation experiment for composite scaffolds. (a and b) digital photography and SEM images of polyoctanediol citrate (POC)-bioglass (BG) scaffold sample; (c) in vitro biodegradation kinetics of composites with different percentages of filler (BG) in comparison to control POC scaffold (phosphate buffer saline; 37°C).
With permission from Springer, E. Zeimaran, S. Pourshahrestani, I. Djordjevic, B. Pingguan-Murphy, N.A. Kadri, A.W. Wren, M.R. Towler, Antibacterial properties of poly (octanediol citrate)/gallium-containing bioglass composite scaffolds, Journal of Materials Science. Materials in Medicine 27 (1) (2015) 1–11.

in shaker under physiological temperature of 37°C. Samples are removed from the centrifuge tubes and dried to measure the constant weight (M_d) at set periods of time (i.e., weekly). The experiment is usually set on duration of 28 days (Fig. 4.2(c)).

Note that the slower degradation rate of polyoctanediol citrate (POC)-bioglass (POC-BG) composite scaffolds (the chemical structure of POC is shown in Fig. 4.6) was recorded in comparison to pure POC scaffolds fabricated by the same method. Slower degradation of composites is a result of increased cross-linking density (Fig. 4.1) as the samples become less prone to hydrolytic attack.

In many cases the impact on biomechanical properties has to be recorded over time in physiological environment. Material cut in shapes required by international standards for mechanical tests (i.e., American Society for Testing and Materials; ASTM) can be soaked in PBS and measured on periods of incubation [16]. Another important information from this experiment is about chemical identification of organic polymer degradation products detected with chromatography techniques [17]. It is crucial to acknowledge the fact that in vivo responses are complex, and degradation products secreted from the implant surface will most certainly influence the surrounding cells on implantation (fundamental aspect of in vivo foreign body response is explained in Section 2.2.2).

4.2.2 Material interface with biological systems

The first biological entities that encounter the biomaterial on implantation are the cells. Cells attach to the materials' surface thus understanding their behavior is a crucial step in optimization of any biomaterial, including composites. The cell–material interface is influenced by material surface properties, such as surface chemistry, morphology, micromechanical characteristics, and leaching components (i.e., impurities, traces of solvent, biodegradation products). The two-component consistency of composite materials (Fig. 4.1) adds to the complexity of data interpretation as both polymer matrix and filler surfaces influences cell behavior at the intimate contact.

4.2.2.1 In vitro assessment of biomaterials

One of the standard biocompatibility assessments is the in vitro cell culture tests. Cell suspension in medium is normally pipetted on the biomaterial samples, and cell behavior is observed with different microscopy techniques [i.e., standard optical, confocal, scanning electron microscopy (SEM), etc.] and quantitative methods (i.e., cell culture assays: MTT, resazurin AlamarBlue colorimetric analysis, etc.). One of the most popular methods for cell assessment on material surface is the visual examination of cell morphology. Healthy cells (i.e., fibroblasts, osteoblasts), in most cases, assume spread-shape morphology on solid samples, and their proliferation pattern results in visually observed cell confluency within the period of days in cell culture [18]. In those measurements, the choice of experimental "controls" is crucial to make valid conclusions. In composite materials, pure polymer components (matrix and filler) are often used for data comparison to assess the influence of filler and possible improvement of pure polymeric biomaterial. The example of such experimental design is shown in Fig. 4.2.

As demonstrated in Fig. 4.1 the addition of filler increases the cross-linking density of the material by newly formed physicochemical bonds. Fig. 4.3(a) shows the elasticity of POC polymer with relatively low tensile modulus (E_t). This polymer was mixed with natural calcium phosphate ($Ca_3(PO_4)_2$)-type bone mineral (HA) to yield the composite material (POC-HA) suitable for fabrication of bone screws (example of bone screw is shown in Fig. 4.3(b) [19]). The addition of HA into the matrix resulted in 100 times increase of Young's modulus transforming the soft elastomer into a tough composite material that can be machined in sizes and shapes of choice (i.e., bone screws). The surface of bone implant was examined with SEM (Fig. 4.3(c)), and there was an obvious appearance of filler particles as a constituent part of material surface. Osteoblast cells were seeded on both POC-HA and pure POC (control) samples and their behavior was assessed after 3 days in culture. Few cells with healthy morphology appeared on POC surface while the situation with POC-HA was drastically different (Fig. 4.3(d) and (e)) [19].

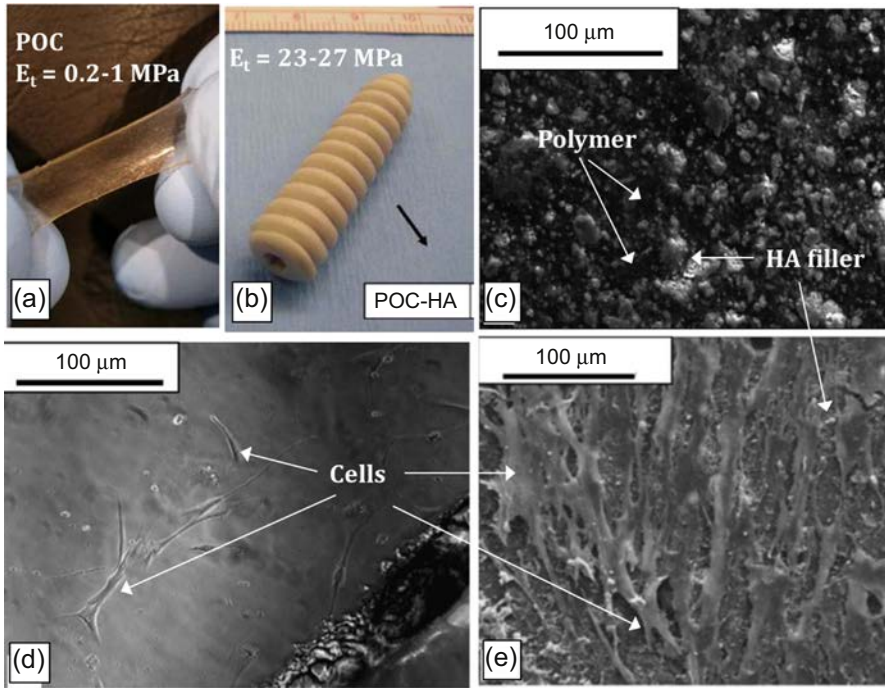

Figure 4.3 In vitro cell–material interface on biodegradable composite bone screws. (a) Pure polyoctanediol citrate (POC) elastomer and its value of tensile Young's modulus (E_t); (b) machined bone screw made of POC-HA composite. *SEM analysis of surface morphology and bone tissue cells (osteoblasts) on the substrate materials*: (c) as-prepared (no cells) POC-HA (40%); (d) cells on pure POC surface show a healthy spread morphology but with limited number of cells; (e) confluent multiple-cell layer on POC-HA (40%) composite surface. With permission from Elsevier, H. Qiu, J. Yang, P. Kodali, J. Koh, G.A. Ameer, A citric acid-based hydroxyapatite composite for orthopedic implants, Biomaterials 27 (34) (2006) 5845–5854.

Cells reached their confluency with the aid of HA showing a dual function in potential POC-HA implants: (1) HA served as effective composite filler that significantly reinforced the material and altered the micromechanical profile at the interface and (2) being a natural part of bone tissues, HA accelerated osteoblast proliferation and formation of cell layer that covered material surface.

In vitro cell culture tests are the first step in assessing newly developed biomaterials. Once the cell toxicity is eliminated and the material is optimized with cell cultures, it is important to investigate the material further with its in vivo reactions in living metabolisms. The situation in dynamic physiological environment is more complexed as the number of different interactions takes place within the window of natural immunological response.

4.2.2.2 *In vivo response to biomaterials*

The fundamental immunological or "foreign body" response that takes place over the period of time on surgical implantation is schematically illustrated in Fig. 4.4. *Note that the first event that takes place is the adsorption of sticky proteins from the blood to the implant surface.*

Monocytes detect accumulation of protein on the implant surface possibly through the formation of protein concentration gradient in the blood flow. Monocytes differentiate into macrophages that attack the implant as a result of natural tendency for phagocytosis: formation of giant cells that causes intercellular entrapment and digestion of foreign material. In case of a large implant dimensions (relative to cells), macrophages attach to the implant where the giant cells could only cover the surface without the possibility of intercellular entrapment. In turn, macrophages release the cytokine signal to fibroblasts, which produce the collagen protein, necessary for material encapsulation and separation of the intruder (implant) to protect the host tissue. From this step onward, collagen capsule either turns into vascularized scar tissues or results in severe inflammation (both chronical and acute) and possible implant rejection [12,20,21].

From Fig. 4.4, it is evident that material surface plays the crucial role in foreign body response. The situation explained in Fig. 4.4 could only be taken as a simplified model since the immunological response to implants involves many complex cell–cell or cell–material interactions that are not fully understood. For that reason one could not predict or construct the accurate model for immunological reaction to implants. Each newly developed material for clinical applications must be tested thoroughly with different animal models. In vivo results are then examined in comparison to appropriate controls or to already approved biomaterials for clinical use.

Similar to in vitro cellular interaction on composite materials, the in vivo data analysis should involve the influence of individual composite components: matrix and filler. As shown in micrographs in Fig. 4.3(c), both POC and HA surface components of the composite would be exposed to blood contact and therefore both would have an impact on surrounding tissue induced by the presence of biomaterial.

Regarding biodegradable materials, tissue interface could not be considered as static. The surface of material changes both chemically and physically in a dynamic

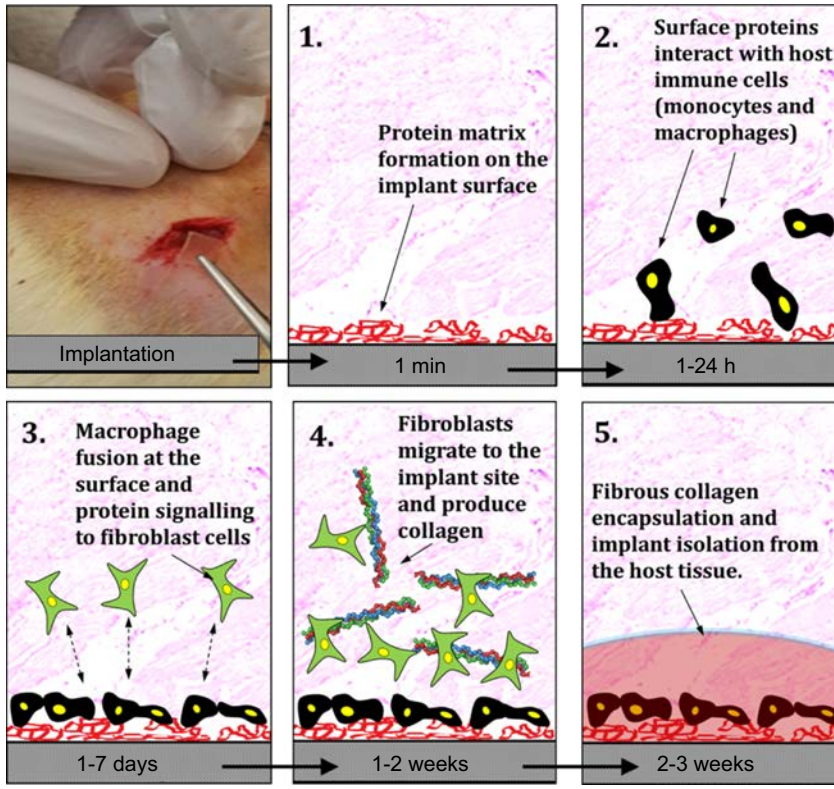

Figure 4.4 In vivo foreign body response initiated by surgical implantation of biomaterial. Schematic presentation of fundamental interaction between the blood flow and biomaterial implants: (1) Formation of fibrin predominant (provisional) protein film. (2) Macrophage interrogation of the implant and attachment on the protein surface film. (3) Formation of "giant cells" by fusion of macrophages and cytokine signal release that triggers the fibroblast migration to the implant site. (4) Fibroblasts gradually deposit the collagen layer that surrounds the implant. (5) Fibrous hydrogel-like matrix (collagen capsule/scar tissue) protects the host tissue from intrusion of the foreign body (biomaterial implant).

manner during the period of physiological degradation. This could cause positive and negative implications in patients. The general motivation for the research in this direction is the development of ideal implant that gradually degrades in controllable and monitored manner. Owing to enzymatic and hydrolytic cleavage of composite cross-links (i.e., biodegradation), a biomaterial loses the initial mechanical strength and causes the mismatch of biomechanical properties between the tissue and the implant. This mismatch could result in tissue fractures and loss of biomechanical support before the tissue is fully regenerated [8].

Degradation reaction of composite materials results in release of products from both polymers and fillers. Those products could be monomer (or oligomer) units from the polymer and filler fragments depending on the physicochemical composition of

either composite component. As a consequence, released chemicals affect the physiological environment. Standard quantification of that effect is performed in histological experiments with explanted biomaterials on animal sacrifice. Number/type of cells attached to the implant and the thickness of collagen capsule (Fig. 4.4, **Stage 5**) may be determined by histological staining as a measurement of the extent of foreign body response [22].

From the example of POC-HA in Fig. 4.3, the polymer phase (POC) was synthesized from octanediol (OD) and citric acid (CA) monomers. OD has minimal toxicity, and CA is part of metabolic cycle in humans. It was hypothesized that the potential release of either monomer (OD and CA) on biodegradation of POC ester bonds would cause minimal harm to the surrounding tissues and cells [23]. Although published results have shown promising performance of POC, both in vitro and in vivo, the exact chemical profile of POC biodegradation products has not yet been revealed. It is important to note that not only the monomers could be released from biodegradable polymer matrix. There is also a possibility of release of OD-CA oligomer units of which the exact molecular weight (i.e., chemical composition) and potential toxicity should be determined in future.

4.2.3 Tissue engineering strategy

Tissue engineering is *an interdisciplinary field that applies the principles of engineering and life sciences toward the development of biological substitutes that restore, maintain, or improve tissue function* [24]. The ultimate goal in tissue engineering is to discover and optimize processes, which produce completely functional substitutes that eventually would be used to replace damaged or diseased tissues in reconstructive surgery. One of the main strategies in tissue engineering today is to produce artificial matrices called scaffolds (Fig. 4.5(a) and (b)) that possess physical, chemical, and mechanical properties suitable for providing optimal conditions for tissue growth. Ideally, the scaffold material should be able to support the initial cell growth and further proliferation that is necessary for regeneration of the desired tissue (Fig. 4.5(c)).

Another important criterion for the synthesized biomimetic scaffolds is that the scaffolding material should biologically degrade over time, leaving a functional and regenerated tissue. In addition, the choice of scaffold material and its design are dictated by the target tissue. As a consequence, a close control over the mechanical and degradation properties is a highly desirable feature for the biomaterials to be used for tissue engineering applications [25–28].

Composite materials do not only offer a broad spectrum of performance including controlled mechanical properties and tunable surface of the material but also the available choice of different fillers allows us to introduce a “bioactive” filler component into the otherwise biologically inert polymer networks. For example, glass fillers are produced from metal oxides, and glasses from biodegradable composites always release metallic ions that have a substantial effect on biological environment [29] (discussed in Sections 2 and 3).

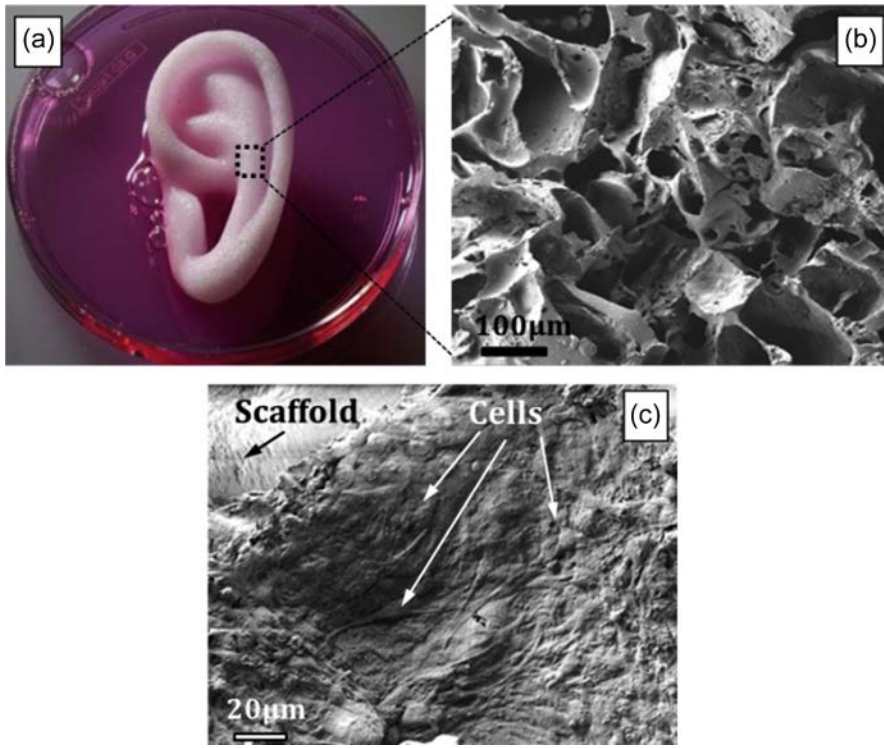

Figure 4.5 Scaffold-guided tissue engineering. (a) Example scaffold fabricated for human ear reconstruction; (b) SEM image of typical porous scaffold (>90% porosity) produced by solvent-casting/particulate leaching technique; (c) SEM image of confluent layer of tissue-specific cartilage cells (chondrocytes) covering the inner pore of the scaffold after 4–7 days in culture.

Bioactivity of fillers can be generally divided into two fundamental different categories that influence biological systems:

1. **Antibacterial effect**: Metallic ions released from glass filler particles (i.e., Zn^{2+}, Ag^{+}) cause bacterial depletion and offer a potential use in biomaterials as bacterial surface repellent on surgical intervention [29].
2. **Induced osteogenic effect**: Ionic dissolution products from inorganic fillers (i.e., Si^{4+}, Ca^{2+}) are reported to stimulate gene expression from osteoblast cells and to support angiogenesis, both in vitro and in vivo [29].
3. **Stimulation of cell proliferation by growth factor (GF) release**: In some cases, filler (or polymer) component can be loaded with GF molecules that are being released at biological interfaces thus stimulating surrounding cells or govern the stem cell differentiation [30].

Composites therefore present "smart materials" with wide spectrum of applications in tissue engineering. Multiple function scaffolds would not only facilitate new tissue formation but could also minimize the rate of implant rejection due to the local

infections caused by bacterial adsorption during and after the surgery. The influence of ion release and effect on bacterial life cycle in proximity of biomaterial surface is explained in more detail in Section 3.1.

4.2.4 Polymeric biomaterials and postsurgery implications of biodegradation

Chemical structures, nomenclature, and expected degradation times of the selected biodegradable polymers used for implants and tissue engineering devices are displayed in Fig. 4.6. Possibly the most prominent of those macromolecules are PLA, PGA, copolymer PLGA, and polycaprolactone (PCL) [12]. Extensive work with those materials has led to many approved medical devices, or devices that reached to the point of clinical trials [10,31]. There are possibly thousands of publications that involve those polymers and their applications as tissue reconnection (suturing) materials, medical implants, and tissue engineering scaffolds [12,31]. There are also a number of responsive polymers that have been used for controlled drug delivery [32].

Another two candidates for application as biomaterials are polyglycerol sebacate (PGS) and POC elastomers that are relatively new in comparison to standard biodegradable polymers presented in Fig. 4.6. These "biorubber" materials opened many possibilities for a fine-tuning of material properties and close mimicking of

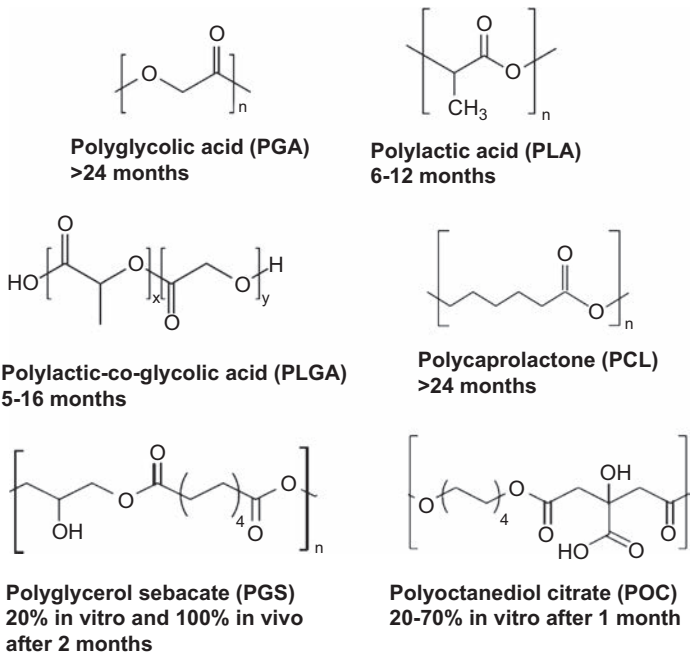

Figure 4.6 Biodegradable polymers. Chemical structures and estimated biodegradation times of the selected polymeric biomaterials used for production of biodegradable medical devices, composites, drug delivery vehicles, and tissue engineering scaffolds.

natural tissue mechanics in human body [33,34]. *Note that all of the compositions in* Fig 4.6 *contain ester bonds (—C—O—C═O) that are prone to hydrological/enzymatic attack and initiation of polymer scission (biodegradation).*

4.2.5 Clinical considerations

The strategical plan to replace orthopedic metal implants with biodegradable ones is still challenged by serious problems reported from clinical research. According to the clinical review, published in 2009 on knee reconstruction by biodegradable PLA/PGA fixation screws [10], there were persistent problems in the following symptoms and observations:

- **Prolonged degradation**: detectable implants in magnetic resonance imaging (MRI) longer than 3 years postoperatively.
- **Degradation products**: adverse effects presented either as acidic buildup (lactic and glycolic acids) or immunological response to broken implant down to particles.
- **Intra-articular migration of broken implant**: cases reported in the periods ranging from 3–4 months to 2 years postoperatively (arthroscopic implant removal is often required depending on the severity of symptoms).
- **Screw damage during the surgery (intraoperative)**: reported up to 9.6% cases where PLA screws broke during the surgical fixation procedure.
- **Prolonged effusion**: "water in knee" injury symptoms persisted up to 1 year postoperatively.
- **Inconsistent biodegradation rates in humans with results from animal trials**: a number of cases have been reported where the implant degradation rate in humans does not correspond to prior animal trails. Apart from differences in bone properties, metabolisms, and biomechanics between humans and animals, there is a significant age effect resulting in inconsistency of obtained results from patient's recovery. Unlike the wide range of ages in human trials, animal models are chosen in narrow age window.

The number of reported clinical results for biodegradable bone implants is limited in comparison to a number of studies performed with metallic implants. The data for biodegradable composites are even more limited. For instance, the clinical review from 2009 describes only two cases of surgical procedures with composite materials in comparison to more than 50 clinical trials performed on pure polymeric screws [10]. However, clinical data reported for biodegradable polymers are important for future directions in composite design. Put simply, the search goes on for perfect filler that would target clinical drawbacks of pure biodegradable polymers.

4.2.6 Composite ceramics and bioglass fillers

Bone is a composite material with major components of collagen-type polymer matrix and natural bone ceramic calcium phosphate (HA; see Section 2.1) with nominal composition of $Ca_{10}(PO_4)_6(OH)_2$ [8]. *As a constituent part of bone ECM, HA is often referred to as "bioactive ceramics" or "bioceramics" reflecting their ability to induce regeneration and new formation of interfacial bone tissue.* Bone tissue is a strong composite material with Young's modulus in the range of 5–27 GPa and hardness of ~0.7 GPa [35]. In respect to matching the anisotropic bone morphology and specific mechanical

profile, HA-based composites are considered to be as most prominent materials for bone implants and scaffold-guided tissue engineering. Flexibility of design by the choice of filler/polymer, with their particular physicochemical properties, and the predetermined composition offer high level of control over biomechanical performance.

Other types of fillers that are often used in orthopedic surgery are bioglass (BG) materials. These materials are multiple-component silicate or phosphate systems with unique osteoconductive properties that enable formation of HA mineral layer on exposure to biological fluid. Adsorbed HA layer enables BG substrates to form strong bonds with surrounding tissues and the release of ions from BG have shown dual effect: antibacterial and stimulation of tissue regeneration [1,29,36,37]. BG fillers are normally produced by traditional "melting/quenching" method where the raw components in the form of metal oxides are melted at 1000–1500°C and subsequently quenched in cold water. Solid glass is then grinded and sieved to obtain the BG particles in predetermined size. Thus prepared glass filler is mixed with polymer to obtain bone screws or scaffolds, similar to the case of POC-HA described in this chapter [7]. For thorough review on BG in medical applications, readers are referred to the cited references [2,3,29].

In this section we have shown the example of novel bone screw machined from POC-HA composite (Fig. 4.3(a) and (b)). The original elastomeric modulus of POC (0.2–1 MPa) [6] was drastically increased by addition of HA (40%; w/w) up to ~25 MPa [19]. The degradation rate of citrate elastomers (such as POC) can range within 20%–70% for a period of 4 weeks depending on their tunable molecular structure by the choice of diol as a monomer in polyesterification reaction with CA [38]. POC-HA composite (Fig. 4.3(b)) degrades at much slower rate (3%–6%; 4 weeks in vitro) due to the increased cross-linking density (Fig. 4.1) at POC/HA interface [19]. Ceramic fillers could also be used to produce composite tissue engineering scaffold by well-defined solvent-casting/particulate leaching technique with high scaffold porosity (>90%) as presented in Fig. 4.7(a) [39].

HA powder in fixed filler/polymer ratios is mixed with prepolymer solution prior to addition of salt particles used as water-soluble leachant [sodium chloride (NaCl) normally 90%, w/w = salt/composite mixture]. Salt particles are previously sieved (i.e., 200–300 μm) to produce a narrow window of pore size distribution. The mixture of polymer/HA/salt/solvent is casted into molds and left to cure at elevated temperature (80°C) for set period of time (5–7 days) [39]. Once the solvent has evaporated and polymer composite network is "wrapped" around salt particles, the casts are soaked in water for several days to dissolve NaCl particles with frequent replacement and constant stirring of water added in abundance (1 L of water is recommended for cylindrical scaffold cast: diameter = 5 cm; thickness = 1 cm). Once all the salt has been leached out, scaffolds are freeze-dried and used as prepared (Fig. 4.7(a) and (b)). *Note that the presence of filler in composite scaffold (POC-HA; Fig. 4.7(a)) could increase the compression modulus from 17 MPa for pure POC up to 33 MPa with addition of 30% (w/w) HA* [39].

In tissue engineering the primary target is formation of functional tissue within the scaffold porous network. Scaffold is not specifically designed for a bone biomechanical support such as the case with orthopedic implants (Fig. 4.3(b)). Cells are known to respond to surface micromechanics, and therefore "HA has a multiple function in

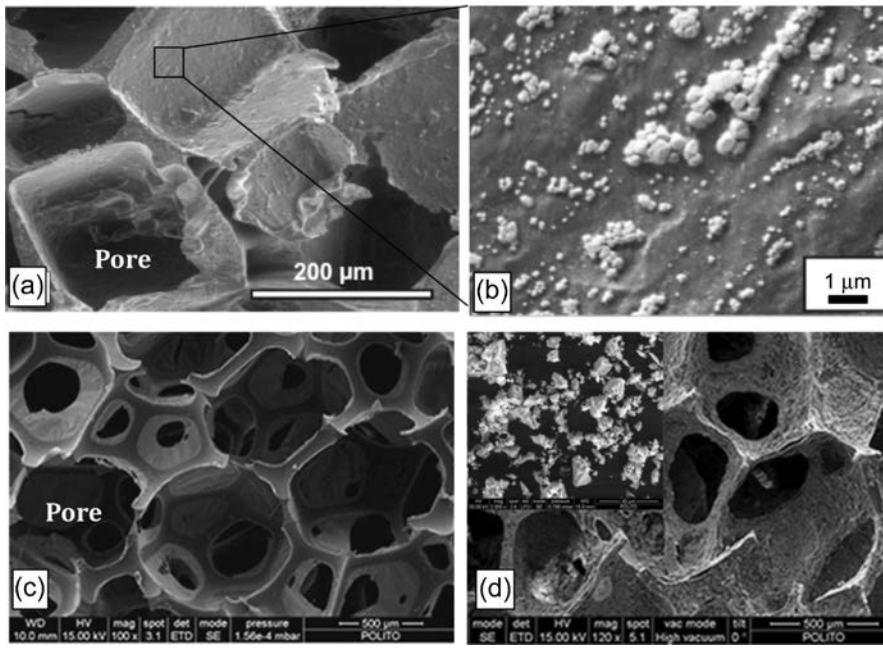

Figure 4.7 SEM analysis of ceramic and bioglass composite scaffolds. (a and b) polyoctanediol citrate (POC)-HA scaffold (20% HA, w/w) [39]; (c) commercial polyurethane (PU) sponge; (d) PU-silica bioglass (BG) composite scaffold produced by dip coating of PU sponge in glass-water slurry with the aid of polyvinyl alcohol hydrogel (inset showing pure BG: magnification bar = 40 µm; average particle size = 32 µm) [41].
With permission from Elsevier and Springer.

tissue engineering: (1) to adjust most suitable interfacial micromechanical properties; (2) to provide chemical cues from the surface to the cell that will eventually increase the cell proliferation rate; and (3) in some cases, HA-released ions serve the purpose to neutralize/modify acidic degradation products from polymer matrix" [2].

Apart from salt leaching method for composite fabrication [7,39,40] as-prepared polymer scaffolds can be enriched with BG filler by soaking the pure polymer into the glass/water slurry and subsequent drying (Fig. 4.7(c) and (d)). As a result of this method, the polymer-BG composite scaffold showed increased surface roughness due to the presence of BG particles (Fig. 4.7(d)) [41]. Interestingly, authors have used hydrogel polyvinyl alcohol (PVA) dispersed into the glass slurry for dip coating of polymer scaffold water to improve interfacial binding between BG and polymer (64% water; 30% BG; 6% PVA) [41]. PVA is a swollen gel network in water that attaches to the glass particle thus providing the surface hydroxyl (—OH) groups that most likely form hydrogen bonds with polyurethane used in experiments. This approach indicates the importance of appropriate binding and ordered dispersion of filler particles for better control over material properties. To obtain high degree of cross-linking in composite materials, scientists increasingly use NP fillers due to their high specific surface area. This strategy is presented in the following section.

4.2.7 Composite nanoparticle fillers

Owing to their unique properties such as high surface-to-volume ratio and increased contact with polymer matrices, NPs (or "nanofillers") in various shapes, sizes, and chemical structures have been utilized as composite fillers in biomedical research [29]. There is a tendency to replace conventional ceramic fillers with advanced nanomaterials that can be obtained with tailored multiple functions, including considerable reinforcement with minimal amount of NP filler. Some recent examples are shown in Fig. 4.8.

Carbon nanostructures are known for their high electron mobility, high strength-to-weight ratio, high conductivity, flexibility, and thermal stability. As a natural progression, such properties have placed carbon nanostructures in the hotspot of biomedical research science [42]. Ever since the first published reports on graphene-based materials in 1990s, carbon nanoparticle (CNP) structures became increasingly popular as composite fillers [5], particularly in development of multifunctional tissue engineering scaffolds and drug delivery devices. Apart from obvious benefits of using CNP materials as biocomposite fillers, there are some serious engineering obstacles that still remain a challenge. One of the general observations is the issue of limited dispersion and formation of NP aggregates in biodegradable polymer matrices. In terms of CNPs, surface functionalization with amine (—NH_2), carboxyl (—COOH), and —OH functional groups is always recommended to improve wettability and facilitate dispersion in polymer matrix [13]. Immobilization of organic compounds further extends the available strategies to produce highly dispersed CNP materials in biodegradable polymer composites [43]. Cited papers [35–37] provide detailed summary of all carbon functionalization techniques developed and reported up to date.

Fig. 4.7(a) and (b) shows the morphology of nanodiamond (ND) material used for production of fluorescent composite with prefunctionalized ND filler with hydrophobic octadecylamine (ODE) covalently attached to ND surface (ND-ODA) [35,44]. Thus functionalized nanofiller (Fig. 4.8(a)) can easily form stable colloidal solutions in chloroform (used to dissolve PLLA), and immobilized ODE provides optimal dispersion of ND in polymer matrix (Fig. 4.8(b)). The length of immobilized ODA on ND is approximately half of the ND diameter (2.5 nm) and therefore the single ND-ODA particle could be as large as 10 nm. From Fig. 4.8(b) the ND-ODA, dispersion in polymer matrix shows small ND-ODA agglomerates with ~10 nm in size that indicates optimal dispersion of carbon nanofiller. *Furthermore, the fluorescence signal originating from ND-ODA particles (Fig. 4.8(c)) opens new possibility for improvement of both clinical outcomes and fundamental understanding of composites through potential real-time monitoring of biodegradation process that occurs at the biological interfaces* [35]. Another type of NP filler made of zinc oxide (ZnO NP) is presented in Fig. 4.8(d)–(f). The main motivation to create such composite is a known biocompatibility of both polymer and filler pure components (Fig. 4.8(d) and (e)) [45].

Similar to other NP materials, ZnO also tends to form aggregates inside the polymer matrix (Fig. 4.8(f)). Degree of aggregation depends on the processing method used for composite fabrication. In most cases, simple mixing and dispersion of two components (filler and polymer) in solvent casting technique results in filler aggregation and precipitation.

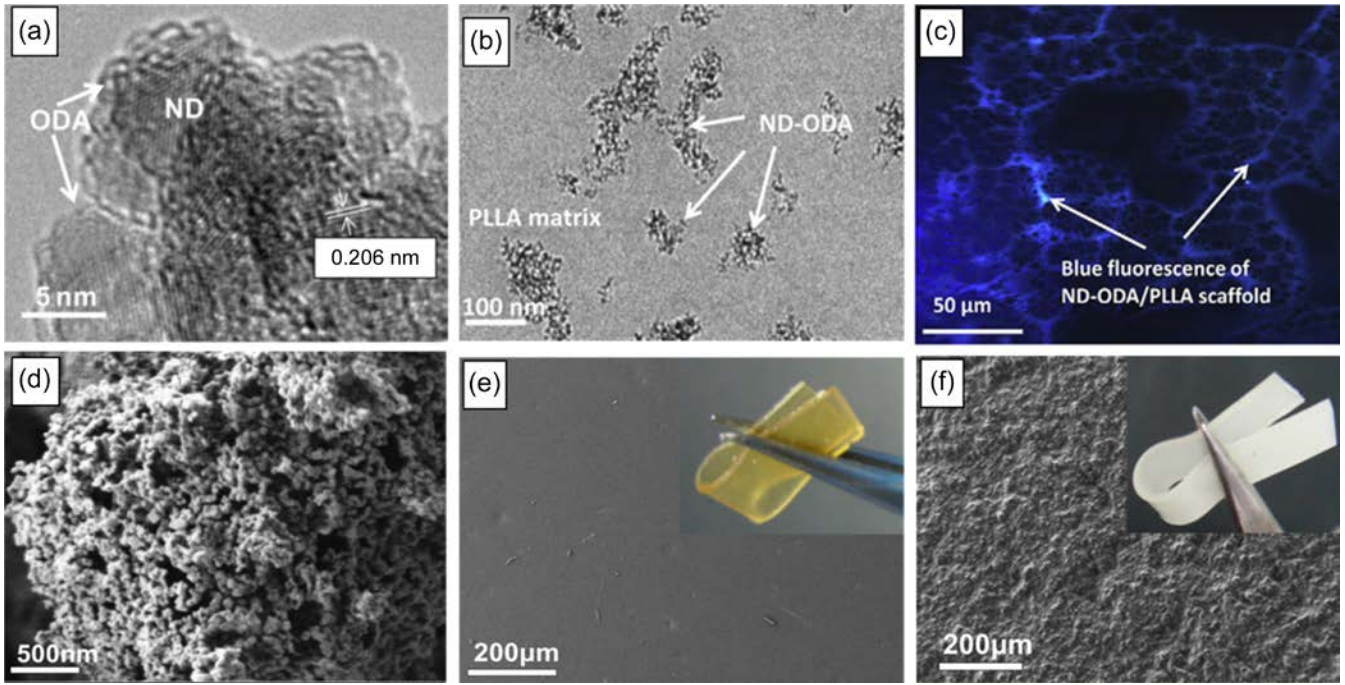

Figure 4.8 Filler nanostructures and dispersion into biodegradable polymer matrix. (a) TEM images of nanodiamond–octadecylamine (ND-ODA) filler and (b) dispersion of ND-ODA into PLLA matrix at 3% filler; (c) fluorescence imaging demonstrating possibility of composite real-time monitoring [35]. *SEM images of nanocomposite and the raw components*: (d) pristine ZnO nanoparticle (NP) aggregate; (e) pure polyoctanediol citrate (POC) film; (f) POC-ZnO NP composite film with 10% ZnO NP in POC matrix.
With permission from Elsevier, K. Kompany, E.H. Mirza, S. Hosseini, B. Pingguan-Murphy, I. Djordjevic, Polyoctanediol citrate–ZnO composite films: preparation, characterization and release kinetics of nanoparticles from polymer matrix, Materials Letters 126 (2014) 165–168.

Released Zn^{2+} from the composite (Fig. 4.8(f)) into physiological environment prevents bacterial adhesion on the implant and reduces the risks of infection [45]. Generally, inorganic filler particles release ions in proximity to the implant, and concentration of those ions has a strong influence on cell–material binding or exposure to blood. *Metal ions are beneficial as antibacterial agents; however, care must be taken in the choice of filler concentration, as the high concentration of ions tends to deplete healthy cells on transmembrane ion uptake.* The next section covers the fundamental aspect of such interactions and basic quantitative measurements of ion release from composite scaffolds.

4.3 Release of filler components in physiological environment

Ceramic and BG fillers release ions from swollen and degradable polymer matrix by ionic dissolution [29]. Quantitative information about released ions from biomaterial is crucial as those ions strongly influence the results from biocompatibility tests regardless of the type of experiment. Affected *biocompatibility tests* by released ions from composite biomaterials are summarized as follows:

- **In vitro interaction with cell cultures**: cell/material morphology and microscopical observation of cell attachment on material surface (Fig. 4.3); cell proliferation rate within the scaffold volume or on the surface of the implant; analysis of produced and extracted ECM molecules from the living cells on the surface of biomaterial (i.e., collagen).
- **In vivo implantation**: histological determination of cell type in close proximity to the material (i.e.,macrophages, giant cells, fibroblasts; see Fig. 4.4, **Stage 4**) and the thickness of fibrous capsule surrounding the material as a semiquantitative method to compare the degree of foreign body response to the selected controls (i.e., approved biomaterial in clinical practice; Fig. 4.4, **Stage 4**).

For instance, released ions such as gallium (Ga^{3+}) or zinc (Zn^{2+}) from polymer composite (Fig. 4.9(c) and (d)) can have a dual effect on biological systems. Ga^{3+} is a known chemotherapeutic ion, and its biological function has been approved by Food and Drug Administration (FDA) [7]. Ga-based BG materials can be used for bone cancer treatment as Ga^{3+} ions increase Ca^{2+} content of bone that prevents tissue resorption [7]. On the other hand, Zn^{2+} ions have a strong bactericidal effect and no significant harm to healthy tissue at the composite interface. ZnO is an inorganic compound, currently listed as a Generally Recognized as Safe (GRAS) material by FDA with established antimicrobial activity against different pathogens. This characteristic is of particular interest for in vivo tissue engineering and implant applications where the surgical procedure is always under attack from surrounding bacteria. Ion release from the implant could prevent initial bacterial attachment and significantly reduce the risk of infections during and after the surgery [45]. The fundamental aspect of bacterial attack and surface "biofilm" formation is discussed in the next section. In this section, we present the typical experimental setup for quantitative measurement of ion release from polymer-BG scaffolds.

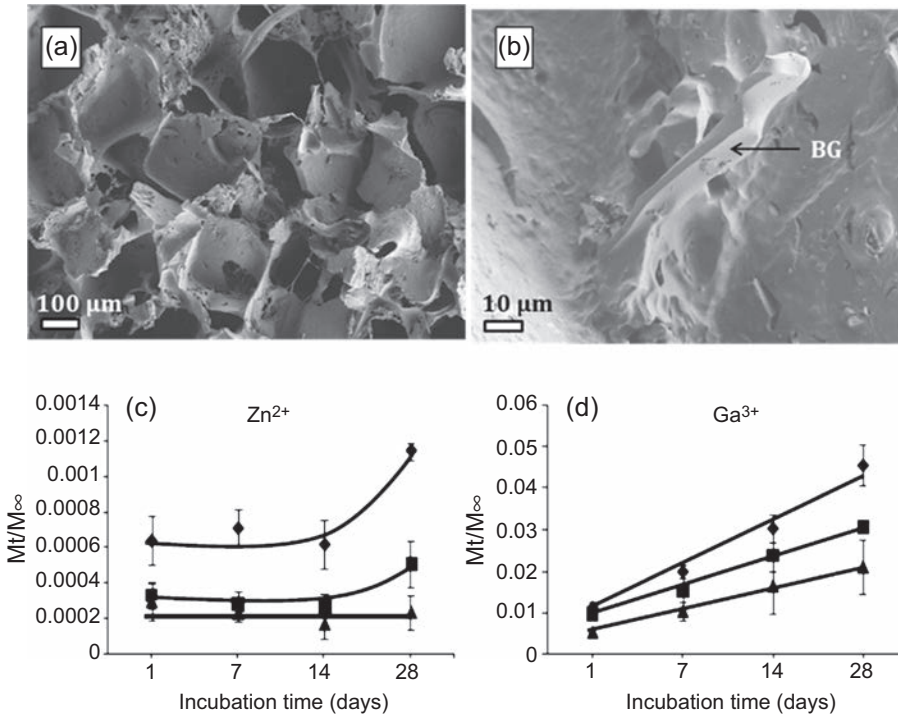

Figure 4.9 Ion release profile from composite polymer Ga–based BG scaffold. (a and b) SEM images of POC-BG scaffold indicating sharp features of grinded glass filler; (d and c) ion release profiles from POC-BG samples with different concentration of BG: (*diamond*) POC-BG 10%; (*square*) POC-BG 20%; and (*triangle*) POC-BG-30%, incubated in PBS at 37°C.

With permission from Springer, E. Zeimaran, S. Pourshahrestani, B. Pingguan-Murphy, N. Kadri, H. Rothan, R. Yusof, M. Towler, I. Djordjevic, Fabrication and characterization of poly(octanediol citrate)/gallium-containing bioglass microcomposite scaffolds, Journal of Materials Science 50 (5) (2015) 2189–2201.

4.3.1 Ion release kinetics from POC-BG composite scaffolds: experimental protocol

The experimental procedure for degradation experiment (Section 2; Fig. 4.2) is also used to monitor ion release from the POC-BG scaffold. Buffer medium is preserved after each degradation measurement and is analyzed for concentration of metallic ions released from soaked scaffolds by standard spectroscopy techniques. According to the standard methodology special care must be taken in the calibration range and selected medium for calibration standards. *In this example, the medium for standard solutions should always be PBS.*

In controlled release studies, concentrations are converted in absolute values of total ion mass released into the medium. If M_t is the mass of ion released at the

specified time intervals and M_∞ is the total mass of BG filler, the fractional ratio is calculated as:

$$\frac{M_t}{M_\infty} \tag{4.2}$$

where M_t = mass of ion released at the specified time intervals (g) and M_∞ = total mass of BG filler in prepared scaffold before degradation (g).

POC-BG scaffold porous morphology and release kinetics for Zn^{2+} and Ga^{3+} is presented in Fig. 4.9. Measured ion concentrations can be plotted directly against time to obtain semiquantitative or comparative results between composites prepared with different polymer/filler ratios [45]. For more accurate results, analyzed composites are compared to control samples, which are always pure composite components (polymer matrix and the filler). Controls should also be carefully prepared to extract the most accurate information from the experiment. For example, if the scaffold contains 40% (w/w) of filler and one sample weighs 15 mg, the average mass of dispersed filler in each sample is 6 mg. Therefore, measured ion concentrations released from pure filler (control) samples should be normalized to 6 mg.

In case of pure polymer control in described experiment, the samples must be fabricated with the same casting method as composites. Naturally, polymers are cut in the same dimensions (or mass, depending on the analyzed substrates) as composites and kept under the same conditions. Composite samples such as films, coatings, scaffolds, etc. can be tested with the method that we describe further; there are no limitations in terms of shapes and sizes.

Note that there is an overall decrease in released ions with increased concentration of BG filler (10%–30%). Similar to measured biodegradation rate for the same POC-BG scaffold samples presented in Fig. 4.2, the ion release is dependent on the cross-linking density [7]. High concentration of filler adds new cross-linking points from filler–matrix interface and therefore slows the degradation rate and subsequent ion release from the composite in simulated (in vitro) physiological environment [7]. *It is always recommended to obtain accurate data on ion release prior to biological tests to draw valid conclusions from either in vitro or in vivo results.*

4.3.2 Fillers as antibacterial agents and the battle against biofilm on the implant surface

Bacterial adhesion on implant during and after the surgery is the major cause of implant-associated infections. *When bacteria attach to the surface, they form protective biofilm layer that is extremely resistant to both the immune system and antibiotics* [46]. Chronological and metabolic stages of biofilm formation are schematically presented in Fig. 4.10.

From this picture, it is obvious that the prevention of initial bacterial adhesion (**Stage 1**; Fig. 4.10) is essential in combat against implant-associated infections [3].

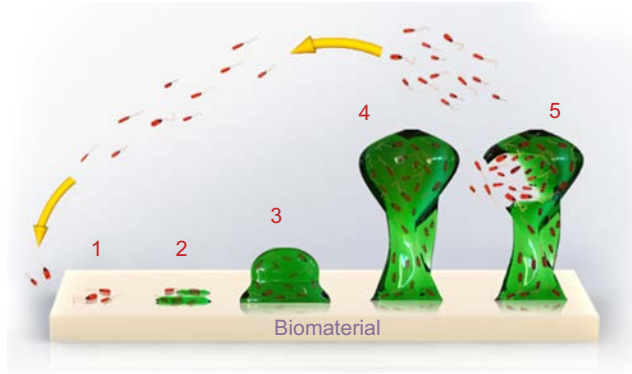

Figure 4.10 Biofilm life cycle on the biomaterial surface. (1) Bacteria adhere to the surface by protein attachment. (2) Proliferation of bacteria. (3) Formation of bacterial microcolonies. (4) Bacterial growth and encapsulation within hydrated protein/carbohydrate mixture. (5) Maturation/dispersal of bacterial cells and formation of "biofilm living cycle" on infected biomaterial surface.

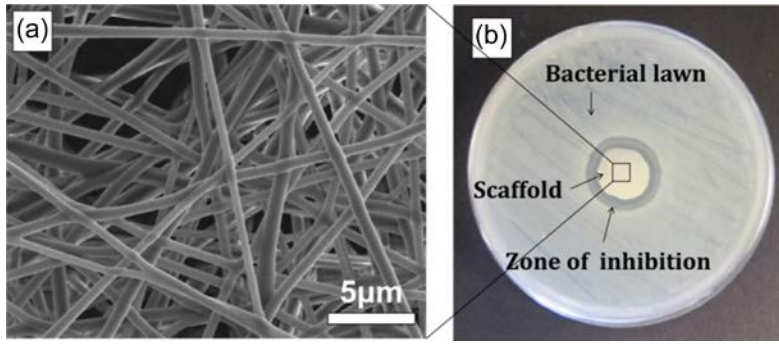

Figure 4.11 Antimicrobial properties of electrospun scaffold coated with Ag+ ions. (a) SEM image of fibrous polylactic acid scaffold treated by dip coating in $AgNO_3$ water/ethanol solution for 24 h; (b) scaffold in bacterial culture (silver-resistant *Escherichia coli*) and bacterial resistance closer to the surface.
With permission from Elsevier, M. Mohiti-Asli, B. Pourdeyhimi, E.G. Loboa, Novel, silver-ion-releasing nanofibrous scaffolds exhibit excellent antibacterial efficacy without the use of silver nanoparticles, Acta Biomaterialia 10 (5) (2014) 2096–2104.

Ions released from inorganic fillers [silver (Ag^+), Zn^{2+}, Ga^{3+} discussed in this chapter] in surrounding medium prevent bacterial adhesion. An example of the bacterial culture test performed on fibrous polymer scaffold that was previously treated in silver nitrate ($AgNO_3$) solution is shown in Fig. 4.11(a). Although this material could not exactly be defined as "composite" (more appropriate title would be "ion-doped polymer"), Fig. 4.11(b) shows typical test where the "zone of inhibition" is measured for polymer samples and reported as semiquantification of antibacterial effect [47].

POC-ZnO NP polymer samples (Fig. 4.8(d) and (e); Section 2.7) were prepared by simple solvent casting method where the polymer solution (50% w/v in dioxane) is mixed with precalculated percentage of ZnO NPs (by weight relative to the solvent-free polymer): POC-ZnO 2.5%; POC-ZnO 5%; and POC-ZnO 10%. The mixtures were casted and cured to yield films and their cross-sectional microprofiles are presented in Fig. 4.12(a) and (b). The ion release studies from the composite films revealed different kinetic profiles (Fig. 4.12(c)), and all the samples have shown excellent antibacterial properties in comparison to pure POC used as control (Fig. 4.12D(d)). *Note that the ZnO NPs precipitated significantly at 2.5% concentration. Particles simply sank at the bottom of the plate creating two distinctive layers observed in SEM analysis of material cross-sections* (Fig. 4.12(a)). Precipitation was not so obvious for higher concentration of ZnO NP (Fig. 4.12(b)). POC belongs

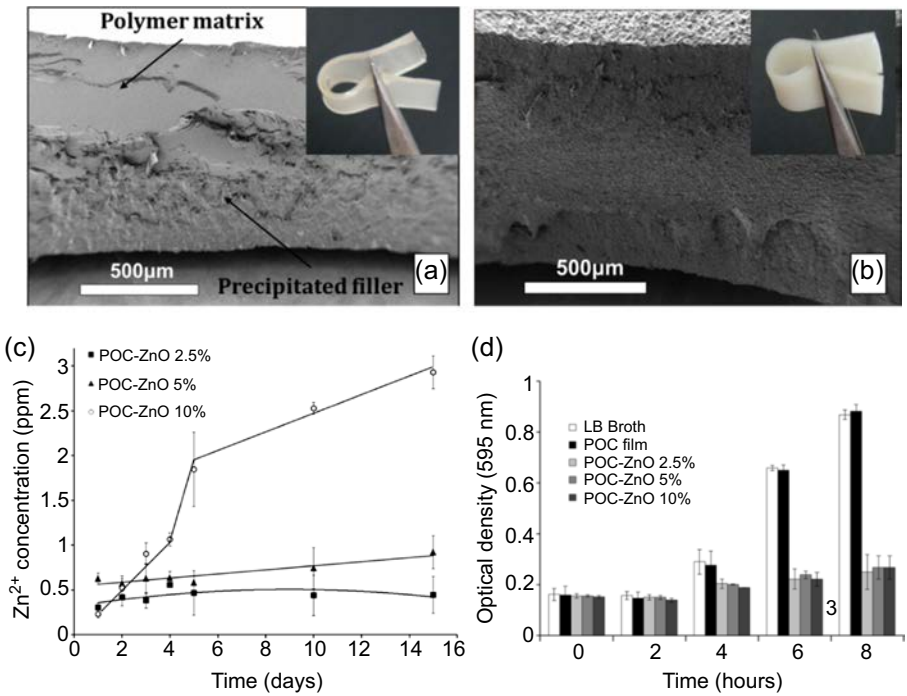

Figure 4.12 Phase separation at low filler concentration and antibacterial properties of POC-ZnO nanoparticle (NP) composite. SEM images of composite films: (a) NP concentration = 2.5%; (b) NP concentration = 10% (insets showing corresponding photographs of analyzed samples); (c) release kinetics of Zn^{2+} ions into buffer solution (phosphate buffer saline) at 37°C within 15 days; (d) antibacterial properties of POC-ZnO NP composite samples against *Escherichia coli*; the optical density at 595 nm corresponds to the bacterial growth. With permission from Elsevier, K. Kompany, E.H. Mirza, S. Hosseini, B. Pingguan-Murphy, I. Djordjevic, Polyoctanediol citrate–ZnO composite films: preparation, characterization and release kinetics of nanoparticles from polymer matrix, Materials Letters 126 (2014) 165–168.

to the group of "polycitrate" elastomers made of biocompatible and low-toxic monomers aimed mainly for soft tissue engineering (i.e., blood vessels, kidney, etc.) due to their elasticity comparable to natural collagen and other ECM components (Fig. 4.3(a)) [34]. Potential antibacterial composites made of POC matrix for soft tissue scaffolds should minimize the effect of increased Young's modulus with the presence of fillers (ZnO NP in this case).

Material should retain certain degree of elasticity (insets in Fig. 4.12(a) and (b)) and therefore the amount of filler should be brought to minimum. *Observing the precipitation of NPS from the example in Fig. 4.12(a), the optimization of composite material processing, where the elasticity is preserved and optimal NP dispersion maintained, seem like a task "easier said than done."* Future improvement of composite manufacturing relies both on processing method development and exploration of filler nanotechnology [1,29].

4.3.3 The impact of degradation on composite biomechanical properties

Properties of inorganic fillers influence both macroscopic (bulk) properties and the nanoscale interfacial phenomena. Those properties are both of chemical and physical in nature, influenced by chemical synthesis and material processing methods [1]. Commercially available HA ceramic products can be found in various conformations, from NPs to as-prepared ceramic formulations in standard laboratory setup. An example is given in Fig. 4.13 where two different HA morphologies were used to produce the composites with biodegradable polypropylene fumarate (PPF; Fig. 4.13(a) and (b)) [30]. As a result of surface morphology, HA formulations yielded composites with different cross-linking densities judging from the difference in Young's moduli presented in Fig. 4.13(a) and (b). The difference in modulus was more drastic for different HA morphologies after immediate hydrolytic attack in buffer solution (Fig. 4.13(c) and (d)).

Low biomechanical stability and loose packing of the filler could cause adverse effects in treated patients. Regarding the complexity of composite interfaces in physiological (or aqueous) environment, here we highlight some of the severe cases recorded in clinical trials with human subjects.

4.3.4 Clinical considerations

Similar to clinical cases selected for biodegradable polymer implants in Section 2.5, composite implants also resulted in prolonged degradation. The implants were still visible 2 years after implantation. Note that preclinical in vivo experiments on ovine model showed considerable success in terms of biodegradation in vivo and tissue integration.

Opposite to the promising results from the animal experiments performed on PLC (a mix of PLA and calcium carbonate, $CaCO_3$), investigated PLC composite knee

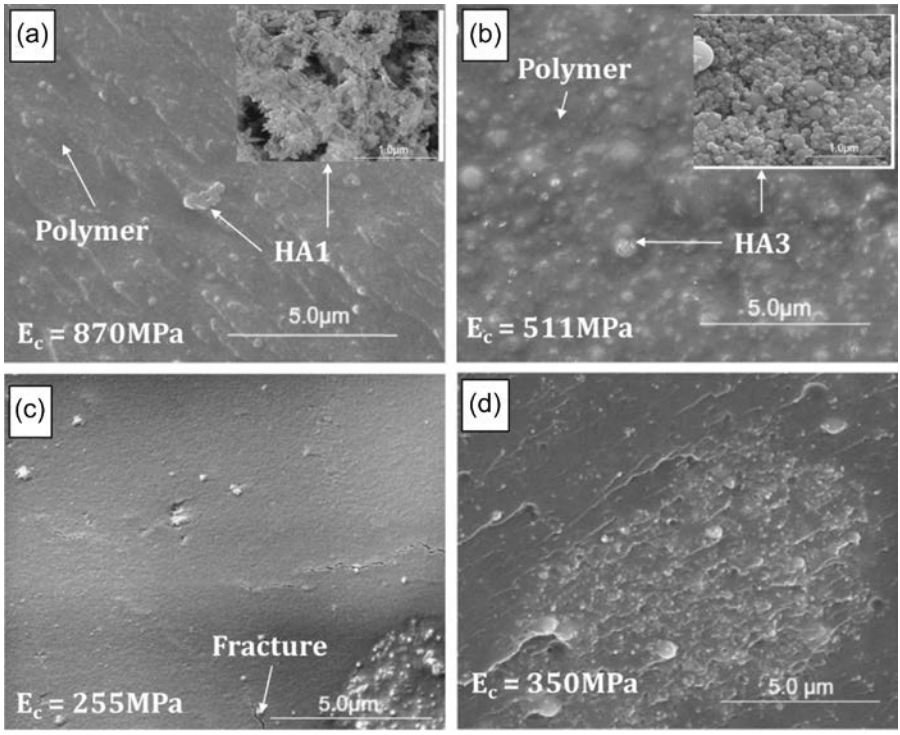

Figure 4.13 The impact of water on PPF-HA composite morphology (measured with SEM) and decrease in Young's moduli (Ec) determined by dynamic mechanical analysis (DMA). (a) As prepared PPF-HA1 and (b) PPF-HA3 (insets showing pure HA1 prepared by precipitation method and HA3 as a commercial product from Sigma, respectively); (c and d) PPF-HA1 and PPF-HA3 surface morphologies after immersion in PBS at 37°C and in situ DMA experiment (8 h), respectively.
With permission from Elsevier, M. Jayabalan, K.T. Shalumon, M.K. Mitha, K. Ganesan, M. Epple, Effect of hydroxyapatite on the biodegradation and biomechanical stability of polyester nanocomposites for orthopaedic applications, Acta Biomaterialia 6 (3) (2010) 763–775.

screws were withdrawn in 2007 due to the serious clinical implications summarized as follows [10]:

- **5% of patients were presented with tibial implant-side wound discharge**: in all affected patients the chalky white material was observed in tibial tunnel originating from implant degradation.
- **15% of patients showed swollen knee symptoms**: the swelling persisted for 6–8 weeks postoperatively.
- **6% of accumulation of filler substance at the wound site**: in 6% of patients the tibial tunnel (implant site) had to be curetted and the white debris washed out leaving an empty tunnel. The implant site had to be routinely filled with demineralized bone matrix (protein) and calcium phosphate.

Experimental mismatch between animals and humans is of serious concern as this type of error was also observed for knee implants produced from pure biodegradable polymers.

4.4 Composites as delivery mediators for bioactive components at the tissue interface

So far in this chapter we have covered fundamental concepts of composite biomaterials. Smart choice of both polymer matrix and the filler is always used to design material structures with high degree of control over bulk and interfacial properties. Nanotechnology research has resulted in various NP formulations used in biotechnology, from biosensor devices to smart drug delivery formulations. Classic definition of polymer composites (Fig. 4.1) is becoming more distorted with the development of new technologies. For instance, drug delivery polymer composites can be produced from standard biomaterial matrix (PLGA, PCL, etc. Fig. 4.6) and filler that is "bioactivated" by encapsulation of protein molecules within spherical PLGA particles (diameter ~ 2 μm) [48]. From physicochemical perspective, an introduction of protein practically transforms the composite from 2-phase to 3-phase systems. Preservation of protein activity plays a crucial role here. Hydrogels, in comparison to solid polymers, seem to be matrices of choice for protein-functionalized fillers as water-swollen gel networks would accommodate protein conformations and possibly preserve their activity for tissue interaction (see discussion in Section 5).

Prior to incorporation into composite systems, it is important to test neat NP fillers for the possibility of protein attachment and subsequent release in physiological environment. G. Xie et al. have investigated hydroxyapatite nanoparticles (HANPs) produced by precipitation method (Fig. 4.14(a)) for GF protein attachment. Bone morphogenic protein (BMP) GF (Fig. 4.14(b)) was loaded onto HANPs by simple dispersion in water solution of BMP (37°C; 30 min). Subsequent release in physiological environment was measured by monitoring the radioactive signal from labeled attached BMP protein (Fig. 4.14(c)) [30].

Authors have reported a thorough work in which the specific surface area of HANP [determined from Brunauer–Emmett–Teller (BET) method] and the total concentration of BMP loaded onto HANP surface were obtained. From this data set, one can calculate the average number of protein molecules attached to a single HANP [49]. Here in the following paragraph, we present a simplified model with the initial assumption of even distribution of the proteins over the total number of HANPs in measured system.

Average diameter (R_{avg}) of a single HANP was determined to be 10 nm from TEM analysis. One should bear in mind that specific surface area of particles in suspension accounts for the whole area exposed to the fluid. For example, HANP shapes in Fig. 4.14 are allowed to absorb proteins from both sides of the particle. HANP TEM image in Fig. 4.14(a) shows only the surface morphology of one side of the particle

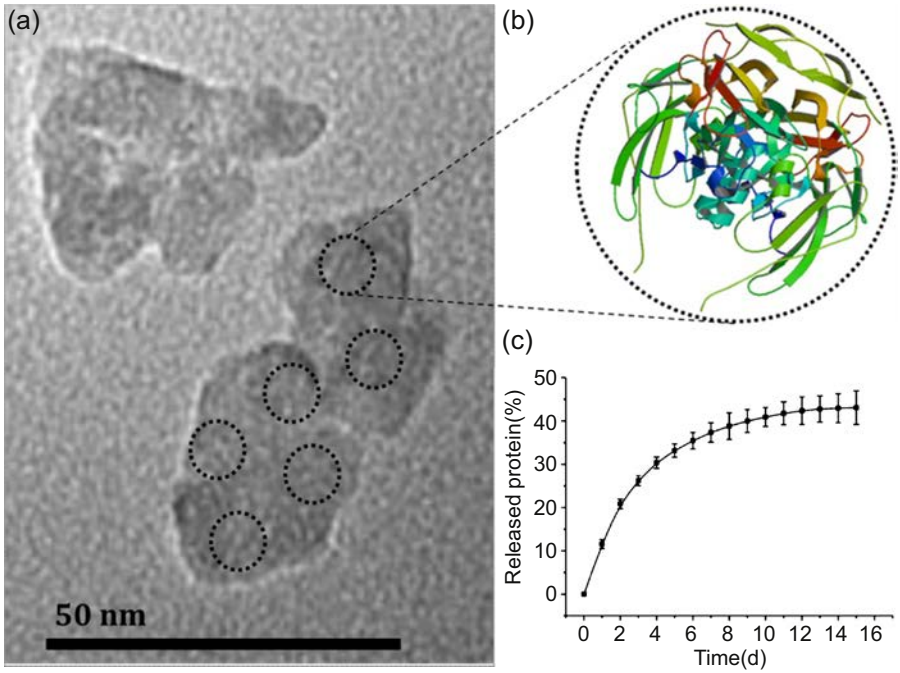

Figure 4.14 Hydroxyapatite nanoparticles (HANPs) as potential carriers for encapsulation/release of proteins that stimulate tissue regeneration (growth factors). (a) TEM image of HANP; (b) schematic presentation of bone morphogenic protein (BMP) growth factor protein structure and adsorption on HANP particle; (c) BMP release kinetics from protein-loaded HANPs incubated in buffer (phosphate buffer saline) at 37°C for 15 days.
With permission from Springer, M. Jayabalan, K.T. Shalumon, M.K. Mitha, K. Ganesan, M. Epple, Effect of hydroxyapatite on the biodegradation and biomechanical stability of polyester nanocomposites for orthopaedic applications, Acta Biomaterialia 6 (3) (2010) 763–775.

(or "flake"). One should bear in mind that reported case in Fig. 4.14 uses the experimental protocol in which the particles are dispersed into the protein solution in water, and therefore both sides of the HANP flake for all the treated particles are available for protein attachment.

Assuming the surface on the edges to be negligible, the approximated surface area of a single HANP with $R_{avg} = 10\,\text{nm}$ exposed to the protein is calculated as follows:

$$A_{avg} = 2 \times (R_{avg})^2 \ \pi = 628 \ \ nm^2 \tag{4.3}$$

The specific surface area (A_{sp}) is a collection of individual surface areas of all the particles contained in 1 g. Calculated A_{sp} from BET experiment was found to be 122.48 m^2/g. This result allows us to calculate the number of HANP particles (N_{HANP}) in 1 mg as follows:

$$N_{HANP}\left(mg^{-1}\right) = \frac{A_{sp}}{A_{avg}} = \frac{122.48 \times 10^{15}\left(nm^2/mg\right)}{628\ \left(nm^2\right)} = 2 \times 10^{14} \tag{4.4}$$

The maximum reported adsorption of BMP on HANP was 70 μg/mg. If the average M_w of BMP protein is taken to be 18 kDa, the number of BMP molecules in 70 μg is calculated by stoichiometric proportion:

$$N_{BMP}\left(mol^{-1}\right) = \frac{70\times10^{-6}\ (g)}{18000\ (g)}\times6.0233\times10^{23}\left(mol^{-1}\right) = 23.42\times10^{14} \tag{4.5}$$

Therefore, the average number of BMP molecules adsorbed on each NP can be calculated from the following ratio:

$$N_{ADS} = \frac{N_{BMP}}{N_{HANP}} = \frac{23.42\times10^{14}}{2\times10^{14}} = 12 \tag{4.6}$$

As presented in Fig. 4.14(a) there are six circles drawn on selected HANP that each circle corresponds to a single BMP molecule (6 molecules on each side of HANP gives a total number of 12 attached BMPs on a single particle). Knowing that the hydrodynamic radius (i.e., Stokes radius) of proteins is 5–10 nm, the diameter of dotted circles seems to provide realistic illustration of 2D space available for protein immobilization (see magnification bar on TEM image in Fig. 4.14).

Another possibility for tissue healing with composite systems is to incorporate protein-immobilized NPs into bioadhesive formulations used for tissue approximation in minimally invasive surgery procedures [50]. Incorporated NPs could deliver bioactive agents with multiple functions (i.e., antibacterial and regeneration-stimulated tissue reconstruction). From fundamental perspective, bioadhesives are the only materials that provide most intimate contact with tissue and therefore enable close monitoring of NP absorption from adhered polymer matrix. This feature of bioadhesives is of particular importance for fundamental understanding of NPs uptake from the living tissues [51]. However, synthetic bioadhesive systems are relatively new, and future clinical trials are yet to reveal their true benefits in this research direction.

4.5 Polymer/polymer composites and the concept of interpenetrated hydrogel networks

The DN hydrogels possess interpenetrating polymer network (IPN) structure where the properties of two individual networks are fundamentally different in chemical compositions, molecular weights, and cross-linking densities. IPN hydrogels are produced in the processes where either of the two polymer networks could be incorporated into a single composite polymer system by mixing and curing (less control over cross-linking) or by in situ polymerization of either network (more control over cross-linking). An example of IPN with individual polymer structures (PAMPS and PAAm) is presented in Fig. 4.15(a).

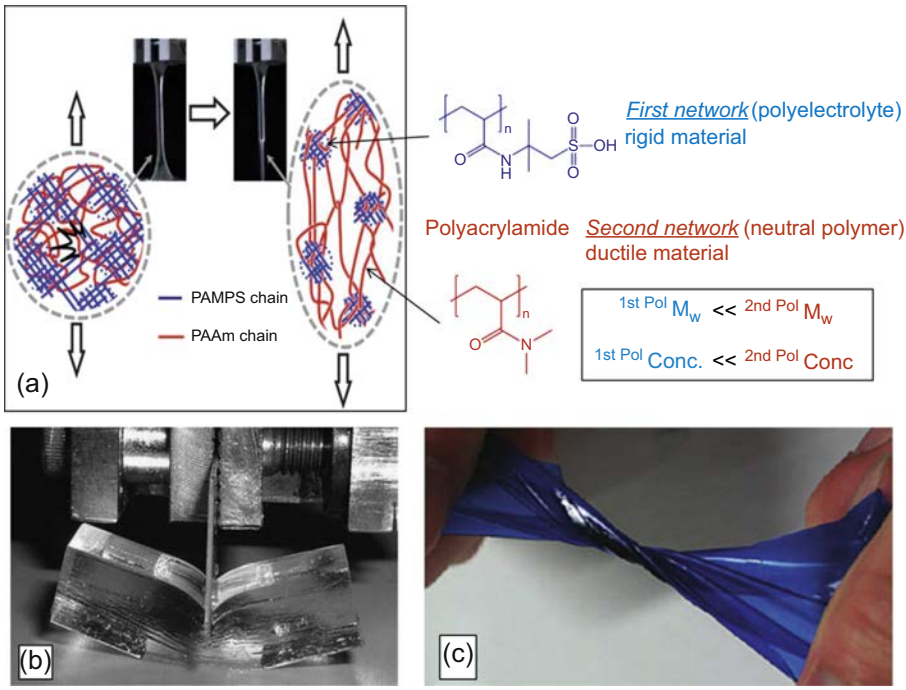

Figure 4.15 Polymer/polymer composites: interpenetrating polymer network (IPN). (a) Schematic picture of PAMPS/PAAm hydrogel morphology on tensile stress (left) and chemical structures of individual components (right); (b and c) toughness and elasticity demonstration of representative PAMPS/PAAm DN gels.
With permission from Royal Society of Chemistry, J.P. Gong, Why are double network hydrogels so tough?, Soft Matter 6 (12) (2010) 2583–2590; W. Dong, C. Huang, Y. Wang, Y. Sun, P. Ma, M. Chen, Superior mechanical properties of double-network hydrogels reinforced by carbon nanotubes without organic modification, International Journal of Molecular Sciences 14 (11) (2013) 22380–22394.

Reported literature generally defines individual polymers in IPNs as follows:

First Network: heterogeneous polyelectrolyte network.
Second Network: neutral polymer with high relative molecular weight.

The molar concentration of the *Second Network* is 20–30 times higher than the *First Network*. The cross-linking density of the *First Network* is higher than the *Second Network*. Because of that, the *Second Network* requires higher molecular weight in comparison to the *First Network*. So far, it is established that the IPN hydrogel mechanical strength increases with higher concentrations of the *Second Network* relative to the *First Network* [52].

Unlike pure hydrogel systems that are limited for drug delivery and soft tissue engineering due to their poor mechanical performance, IPN hydrogels in their swollen state (90% of water trapped inside cross-linked polymer network) can express mechanical moduli and hardness up to 1 MPa with the strength of 10 MPa, sustaining

high elongation of 1000%–2000% strain on applied mechanical stress. The superior mechanical strength of IPN materials could open new possibilities for tissue repair where load-bearing characteristics are crucial (i.e., tendons and ligaments) [53].

Generally, hydrogels have a high permeability and reversible volume due to the penetration of small molecules of water. Some hydrogels respond to changes in environment (pH, temperature, light, etc.) by absorption or release of water [26]. This particular feature has been explored for therapeutic delivery of water-soluble drugs and tissue engineering applications where the regenerative proteins can be loaded and subsequently released from hydrogel porous networks [26]. Knowing that the weak and brittle mechanical properties of conventional hydrogels could be surpassed by superior performance of IPN systems demonstrated in published literature, there are number of advantages of IPNs that are yet to be utilized in nanotechnology of advanced composite biomaterials.

4.6 Conclusion and future directions

Composites have a complex interaction with biological systems where the individual components (polymer matrices and fillers) equally contribute to the performance of the biomaterial. Biodegradability adds to the complexity of the process as the biodegradation products leach out from the material into the environment and influence sensitive biointerfaces. Owing to complexity and unpredictable behavior of composite biomaterials, there are a limited number of clinical results available in comparison to other biomaterial systems (i.e., pure polymers and metals). Biodegradable composites are almost exclusively made of established biocompatible polymer systems where either traditional hydroxyapatite ceramics or bioglass fillers are used to reinforce biodegradable polymers and to enhance the performance of surgical implants or tissue engineering devices. The progress in nanotechnology and development of novel, smart nanomaterials might change that picture in the future.

There are a number of studies that explore nanotechnology strategies for development of new biologically activated materials. Of particular interest is the possibility of surface functionalization of solid fillers (or polymer chains) that facilitate cell differentiation, modulate immunological response, and/or facilitate cell proliferation in immediate cell/material contact. The possibility of control over biological responses to composites used to fabricate tissue engineering scaffolds and surgical implants may open new strategical approaches for production of multifunctional biomaterials for successful clinical applications.

Acknowledgments

Authors would like to acknowledge Mr. Martin Francisco Jimenez Moreno for his generous help on artwork and Mr. Dan Morin for his intellectual feedback.

References

[1] A.R. Boccaccini, M. Erol, W.J. Stark, D. Mohn, Z. Hong, J.F. Mano, Polymer/bioactive glass nanocomposites for biomedical applications: a review, Composites Science and Technology 70 (13) (2010) 1764–1776.
[2] K. Rezwan, Q.Z. Chen, J.J. Blaker, A.R. Boccaccini, Biodegradable and bioactive porous polymer/inorganic composite scaffolds for bone tissue engineering, Biomaterials 27 (18) (2006) 3413–3431.
[3] A. Simchi, E. Tamjid, F. Pishbin, A.R. Boccaccini, Recent progress in inorganic and composite coatings with bactericidal capability for orthopaedic applications, nanomedicine: nanotechnology, Biology and Medicine 7 (1) (2011) 22–39.
[4] Front matter A2, in: B.D. Ratner, A.S. Hoffman, F.J. Schoen, J.E. Lemons (Eds.), Biomaterials Science, third ed., Academic Press, 2013, p. iii.
[5] Z. Spitalsky, D. Tasis, K. Papagelis, C. Galiotis, Carbon nanotube–polymer composites: chemistry, processing, mechanical and electrical properties, Progress in Polymer Science 35 (3) (2010) 357–401.
[6] I. Djordjevic, N.R. Choudhury, N.K. Dutta, S. Kumar, Synthesis and characterization of novel citric acid-based polyester elastomers, Polymer 50 (7) (2009) 1682–1691.
[7] E. Zeimaran, S. Pourshahrestani, B. Pingguan-Murphy, N. Kadri, H. Rothan, R. Yusof, M. Towler, I. Djordjevic, Fabrication and characterization of poly(octanediol citrate)/gallium-containing bioglass microcomposite scaffolds, Journal of Materials Science 50 (5) (2015) 2189–2201.
[8] C. Migliaresi, Composites A2, in: B.D. Ratner, A.S. Hoffman, F.J. Schoen, J.E. Lemons (Eds.), Biomaterials Science, third ed., Academic Press, 2013, pp. 223–241. Chapter I.2.9.
[9] L. Kupcsik, M.J. Stoddart, Z. Li, L.M. Benneker, M. Alini, Improving chondrogenesis: potential and limitations of SOX9 gene transfer and mechanical stimulation for cartilage tissue engineering, Tissue Engineering Part A 16 (6) (2010) 1845–1855.
[10] S. Konan, F.S. Haddad, A clinical review of bioabsorbable interference screws and their adverse effects in anterior cruciate ligament reconstruction surgery, The Knee 16 (1) (2009) 6–13.
[11] R.K. Kulkarni, K.C. Pani, C.C. Neuman, F.F. Leonard, Polylactic acid for surgical implants, Archives of Surgery 93 (5) (1966) 839–843.
[12] M.A. Woodruff, D.W. Hutmacher, The return of a forgotten polymer—polycaprolactone in the 21st century, Progress in Polymer Science 35 (10) (2010) 1217–1256.
[13] I. Manavitehrani, A. Fathi, H. Badr, S. Daly, A. Negahi Shirazi, F. Dehghani, Biomedical applications of biodegradable polyesters, Polymers 8 (1) (2016) 20.
[14] D.W. Hutmacher, Scaffolds in tissue engineering bone and cartilage, Biomaterials 21 (24) (2000) 2529–2543.
[15] E. Zeimaran, S. Pourshahrestani, I. Djordjevic, B. Pingguan-Murphy, N.A. Kadri, A.W. Wren, M.R. Towler, Antibacterial properties of poly (octanediol citrate)/gallium-containing bioglass composite scaffolds, Journal of Materials Science. Materials in Medicine 27 (1) (2015) 1–11.
[16] L. Tatai, T.G. Moore, R. Adhikari, F. Malherbe, R. Jayasekara, I. Griffiths, P.A. Gunatillake, Thermoplastic biodegradable polyurethanes: the effect of chain extender structure on properties and in-vitro degradation, Biomaterials 28 (36) (2007) 5407–5417.
[17] M.D. Timmer, H. Shin, R.A. Horch, C.G. Ambrose, A.G. Mikos, In vitro cytotoxicity of injectable and biodegradable poly(propylene fumarate)-based networks: unreacted macromers, cross-linked networks, and degradation products, Biomacromolecules 4 (4) (2003) 1026–1033.

[18] I. Djordjevic, E.J. Szili, N.R. Choudhury, N. Dutta, D.A. Steele, S. Kumar, Osteoblast biocompatibility on poly(octanediol citrate)/sebacate elastomers with controlled wettability, Journal of Biomaterials Science, Polymer Edition 21 (8–9) (2010) 1039–1050.
[19] H. Qiu, J. Yang, P. Kodali, J. Koh, G.A. Ameer, A citric acid-based hydroxyapatite composite for orthopedic implants, Biomaterials 27 (34) (2006) 5845–5854.
[20] Biological responses to materials, Annual Review of Materials Research 31 (1) (2001) 81–110.
[21] J.M. Anderson, A. Rodriguez, D.T. Chang, Foreign body reaction to biomaterials, Seminars in Immunology 20 (2) (2008) 86–100.
[22] C.J. Bettinger, J.P. Bruggeman, J.T. Borenstein, R.S. Langer, Amino alcohol-based degradable poly(ester amide) elastomers, Biomaterials 29 (15) (2008) 2315–2325.
[23] I. Djordjevic, N.R. Choudhury, N.K. Dutta, S. Kumar, Poly[octanediol-co-(citric acid)-co-(sebacic acid)] elastomers: novel bio-elastomers for tissue engineering, Polymer International 60 (3) (2011) 333–343.
[24] R. Langer, J. Vacanti, Tissue engineering, Science 260 (5110) (1993) 920–926.
[25] R. Langer, N.A. Peppas, Advances in biomaterials, drug delivery, and bionanotechnology, AIChE Journal 49 (12) (2003) 2990–3006.
[26] B.V. Slaughter, S.S. Khurshid, O.Z. Fisher, A. Khademhosseini, N.A. Peppas, Hydrogels in regenerative medicine, Advanced Materials 21 (32–33) (2009) 3307–3329.
[27] A.G. Mikos, G. Sarakinos, S.M. Leite, J.P. Vacant, R. Langer, Laminated three-dimensional biodegradable foams for use in tissue engineering, Biomaterials 14 (5) (1993) 323–330.
[28] M.S. Shoichet, Polymer scaffolds for biomaterials applications, Macromolecules 43 (2) (2010) 581–591.
[29] A. Hoppe, N.S. Güldal, A.R. Boccaccini, A review of the biological response to ionic dissolution products from bioactive glasses and glass-ceramics, Biomaterials 32 (11) (2011) 2757–2774.
[30] M. Jayabalan, K.T. Shalumon, M.K. Mitha, K. Ganesan, M. Epple, Effect of hydroxyapatite on the biodegradation and biomechanical stability of polyester nanocomposites for orthopaedic applications, Acta Biomaterialia 6 (3) (2010) 763–775.
[31] M. Martina, D.W. Hutmacher, Biodegradable polymers applied in tissue engineering research: a review, Polymer International 56 (2) (2007) 145–157.
[32] A.K. Bajpai, S.K. Shukla, S. Bhanu, S. Kankane, Responsive polymers in controlled drug delivery, Progress in Polymer Science 33 (11) (2008) 1088–1118.
[33] R. Rai, M. Tallawi, A. Grigore, A.R. Boccaccini, Synthesis, properties and biomedical applications of poly(glycerol sebacate) (PGS): a review, Progress in Polymer Science 37 (8) (2012) 1051–1078.
[34] R.T. Tran, J. Yang, G.A. Ameer, Citrate-based biomaterials and their applications in regenerative engineering, Annual Review of Materials Research 45 (1) (2015) 277–310.
[35] Q. Zhang, V.N. Mochalin, I. Neitzel, I.Y. Knoke, J. Han, C.A. Klug, J.G. Zhou, P.I. Lelkes, Y. Gogotsi, Fluorescent PLLA-nanodiamond composites for bone tissue engineering, Biomaterials 32 (1) (2011) 87–94.
[36] L.L. Hench, R.J. Splinter, W.C. Allen, T.K. Greenlee, Bonding mechanisms at the interface of ceramic prosthetic materials, Journal of Biomedical Materials Research 5 (6) (1971) 117–141.
[37] O. Bretcanu, A.R. Boccaccini, V. Salih, Poly-DL-lactic acid coated Bioglass® scaffolds: toughening effects and osteosarcoma cell proliferation, Journal of Material Science 47 (15) (2012) 5661–5672.
[38] J. Yang, A.R. Webb, S.J. Pickerill, G. Hageman, G.A. Ameer, Synthesis and evaluation of poly(diol citrate) biodegradable elastomers, Biomaterials 27 (9) (2006) 1889–1898.

[39] A. Moradi, A. Dalilottojari, B. Pingguan-Murphy, I. Djordjevic, Fabrication and characterization of elastomeric scaffolds comprised of a citric acid-based polyester/hydroxyapatite microcomposite, Materials & Design 50 (2013) 446–450.
[40] E.H. Mirza, C. Pan-Pan, W.M.A.B. Wan Ibrahim, I. Djordjevic, B. Pingguan-Murphy, Chondroprotective effect of zinc oxide nanoparticles in conjunction with hypoxia on bovine cartilage-matrix synthesis, Journal of Biomedical Materials Research Part A 103 (2015).
[41] F. Baino, E. Verné, C. Vitale-Brovarone, Feasibility, tailoring and properties of polyurethane/bioactive glass composite scaffolds for tissue engineering, Journal of Materials Science. Materials in Medicine 20 (11) (2009) 2189.
[42] V. Georgakilas, J.N. Tiwari, K.C. Kemp, J.A. Perman, A.B. Bourlinos, K.S. Kim, R. Zboril, Noncovalent functionalization of graphene and graphene oxide for energy materials, biosensing, catalytic, and biomedical applications, Chemical Reviews 116 (9) (2016) 5464–5519.
[43] S. Banerjee, T. Hemraj-Benny, S.S. Wong, Covalent surface chemistry of single-walled carbon nanotubes, Advanced Materials 17 (1) (2005) 17–29.
[44] V.N. Mochalin, Y. Gogotsi, Wet chemistry route to hydrophobic blue fluorescent nanodiamond, Journal of the American Chemical Society 131 (13) (2009) 4594–4595.
[45] K. Kompany, E.H. Mirza, S. Hosseini, B. Pingguan-Murphy, I. Djordjevic, Polyoctanediol citrate–ZnO composite films: preparation, characterization and release kinetics of nanoparticles from polymer matrix, Materials Letters 126 (2014) 165–168.
[46] J.W. Costerton, P.S. Stewart, E.P. Greenberg, Bacterial biofilms: a common cause of persistent infections, Science 284 (5418) (1999) 1318–1322.
[47] J.J. Elsner, I. Berdicevsky, M. Zilberman, In vitro microbial inhibition and cellular response to novel biodegradable composite wound dressings with controlled release of antibiotics, Acta Biomaterialia 7 (1) (2011) 325–336.
[48] B. Li, T. Yoshii, A.E. Hafeman, J.S. Nyman, J.C. Wenke, S.A. Guelcher, The effects of rhBMP-2 released from biodegradable polyurethane/microsphere composite scaffolds on new bone formation in rat femora, Biomaterials 30 (35) (2009) 6768–6779.
[49] G. Xie, J. Sun, G. Zhong, C. Liu, J. Wei, Hydroxyapatite nanoparticles as a controlled-release carrier of BMP-2: absorption and release kinetics in vitro, Journal of Materials Science. Materials in Medicine 21 (6) (2010) 1875–1880.
[50] P.J.M. Bouten, M. Zonjee, J. Bender, S.T.K. Yauw, H. van Goor, J.C.M. van Hest, R. Hoogenboom, The chemistry of tissue adhesive materials, Progress in Polymer Science 39 (7) (2014) 1375–1405.
[51] B.D. Ratner, Healing with medical implants: the body battles back, Science Translational Medicine 7 (272) (2015) 272fs4.
[52] J.P. Gong, Why are double network hydrogels so tough? Soft Matter 6 (12) (2010) 2583–2590.
[53] M.A. Haque, T. Kurokawa, J.P. Gong, Super tough double network hydrogels and their application as biomaterials, Polymer 53 (9) (2012) 1805–1822.
[54] M. Mohiti-Asli, B. Pourdeyhimi, E.G. Loboa, Novel, silver-ion-releasing nanofibrous scaffolds exhibit excellent antibacterial efficacy without the use of silver nanoparticles, Acta Biomaterialia 10 (5) (2014) 2096–2104.
[55] W. Dong, C. Huang, Y. Wang, Y. Sun, P. Ma, M. Chen, Superior mechanical properties of double-network hydrogels reinforced by carbon nanotubes without organic modification, International Journal of Molecular Sciences 14 (11) (2013) 22380–22394.

Surface modification of natural fibers

5

Anish M. Varghese, Vikas Mittal
The Petroleum Institute, Abu Dhabi, United Arab Emirates

5.1 Introduction

Natural fibers are growingly preferred in every sector of human activities in the last few decades as substitutes for conventional synthetic fibers. On account of higher environmental and ecological concerns, significant developments in natural fiber–based green materials in the discipline of polymer science and technology have been reported. In this respect, natural fiber–based biocomposites have gained considerable research attention due to their easy disposability after shelf life without any detrimental impacts on the environment [1,2]. Based on the renewable source, natural fibers are categorized into plant, animal, or mineral fibers (Fig. 5.1). Plant fibers are those fibers derived from any part of the plants, and this class mainly consists of bast fibers, leaf fibers, seed, fruit, wood, cereal straw, and other grass fibers. Their structure made up of cellulose, and they are considered as a composite structure of cellulose fibrils in lignin matrix. Chemical constituents of these fibers are cellulose, hemicellulose, lignin, pectin, and waxes, and their composition in particular fiber differs on account of their source, age, retting process used, and so on. These fibers also known as lignocellulosic fibers, and principal examples include flax, hemp, kenaf, sisal, henequen, banana, oil palm, jute, cotton, coir, etc. In the case of animal fibers, the major structural constituent is protein, and important members include hair, silk, and wool. Asbestos fiber is the one and only reported member of mineral fiber class [3–5].

Natural fibers are renewable materials that present combination of advantages such as biodegradability; exceptional precise properties such as strength, stiffness, impact resistance, and flexibility; free formability; low density; cheap, abundance and easily available; production needs only lower energy along with the absorption of CO_2 and the subsequent O_2 evolution; very low effusion of toxic products on heating and incineration; offer very low damage to processing machinery; notable corrosion as well as fatigue resistance; vibration damping; suitable fiber aspect ratio; minimal irritation to skin and respiratory system; provide safe and healthy environments; and so on [6–8]. Also, the ultimate properties of natural fibers can be tailored with respect to end use, and they greatly depend on fiber diameter, structure, type of constituents, extent of polymerization and crystallinity, crystal structure, void structure, and fiber origin [9]. These outstanding features along with good balance of environmental and economical aspects of natural fibers drive their applications in automotive, building, furniture, and

Biodegradable and Biocompatible Polymer Composites. http://dx.doi.org/10.1016/B978-0-08-100970-3.00005-5

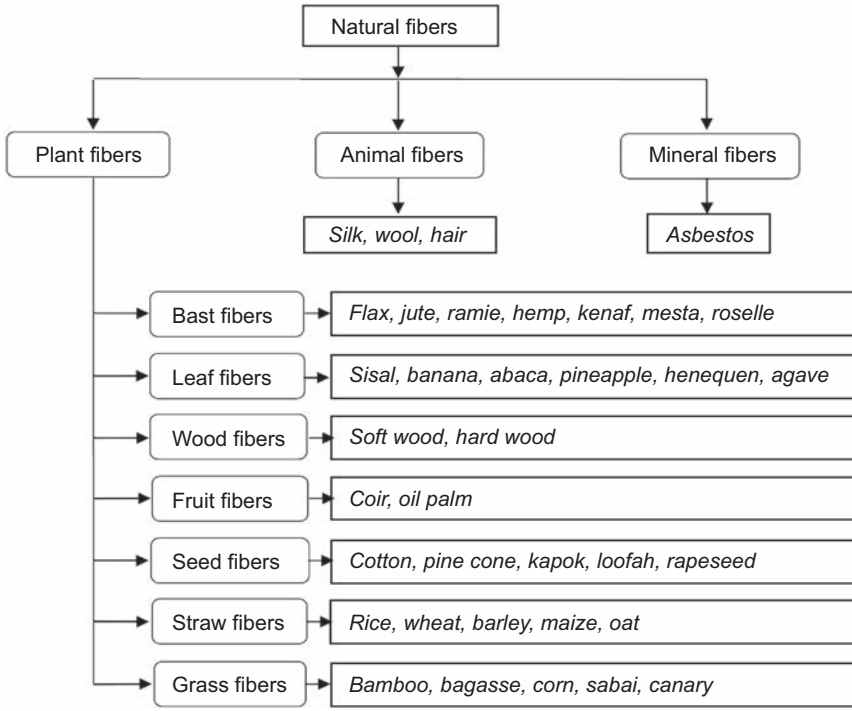

Figure 5.1 Categories of natural fibers.

packaging areas as polymer composites. Comparison between the mechanical properties of natural fibers and E-glass fiber is presented in Table 5.1 [5].

Notwithstanding this supremacy of natural fibers, these materials also show some disadvantages in mono or in composite form. The great rate of water/moisture intake and the corresponding swelling of natural fibers are due to their higher moisture affinity. This is related to the higher tendency of hydroxyl groups in the cellulose to form hydrogen bonding with the hydroxyl groups present in the air. Natural fibers prone to thermal degradation when undergoes polymer composite processing at a great temperature in extruder or compression molding machine, which is attributed to their high thermal sensitivity. In the biocomposites, the highly polar hydrophilic natural fibers present poor compatibility with the hydrophobic polymer matrices in account of their inadequate adhesion resulted from the poor wettability of natural fibers by nonpolar polymer matrices. This also creates uneven distribution of natural fibers in the polymer matrix and inferior stress transfer effectiveness from polymer matrix to natural fiber reinforcement in the biocomposites. The strong moisture sensitivity of natural fibers allows the growth of mold and decay fungi in the composites as well as the dimensional changes of the final biocomposite; these two effects finally cause to deteriorate the interfacial interactions of components in the biocomposite [10–15].

To overcome these drawbacks of natural fibers and thus to maintain enhanced physical and mechanical properties of resultant polymer biocomposites, innumerable

Table 5.1 Comparison of mechanical properties of natural fibers and glass fiber [5]

Fiber	Density (g/cm^3)	Length (mm)	Failure strain (%)	Tensile strength (MPa)	Young's modulus (GPa)	Specific tensile strength ($MPa/g/cm^3$)	Specific tensile strength ($GPa/g/cm^3$)
Ramie	1.5	900–1200	2.0–3.8	400–938	44–128	270–620	29–85
Flax	1.5	5–900	1.2–3.2	345–1830	27–80	230–1220	18–53
Hemp	1.5	5–55	1.6	550–1110	58–70	370–740	39–47
Jute	1.3–1.5	1.5–120	1.5–1.8	393–800	10–55	300–610	7.1–39
Harakeke	1.3	4–5	4.2–5.8	440–990	14–33	338–761	11–25
Sisal	1.3–1.5	900	2.0–2.5	507–855	9.4–28	362–610	6.7–20
Alfa	1.4	350	1.5–2.4	188–308	18–25	134–220	13–18
Cotton	1.5–1.6	10–60	3.0–10	287–800	5.5–13	190–530	3.7–8.4
Coir	1.2	20–150	15–30	131–220	4–6	110–180	3.3–5
Silk	1.3	Continuous	15–60	100–1500	5–25	100–1500	4–20
Feather	0.9	10–30	6.9	100–203	3–10	112–226	3.3–11
Wool	1.3	38–152	13.2–35	50–315	2.3–5	38–242	1.8–3.8
E-glass	2.5	Continuous	2.5	2000–3000	70	800–1400	29

studies relating surface modifications of natural fibers have been reported so far. These studies were aimed at reduction in moisture absorption, improvement in interaction with polymeric matrices, furtherance in wettability of natural fibers by nonpolar polymers, enhancement in antibacterial properties, etc. There are miscellaneous modification strategies that make redesigned natural fiber surfaces, and the available techniques are broadly classified into three basic methods, namely physical techniques, chemical techniques, and biological treatments. Physical techniques alter surface energies and structural features of natural fibers through the modification of shallow surfaces of cell wall without affecting their chemical composition. In this technique, the improved compatibility of natural fibers with polymer matrices can be achieved through stretching, calendaring, thermo-treatment, formation of hybrid yarns, electronic discharge from corona, and plasma treatments, and so on [16–20]. Chemical techniques improve the adhesion between natural fiber and hydrophobic polymeric surfaces by irreversibly changing the appearance of natural fiber cell walls through either altering their crystalline structure or eliminating weak components such as hemicellulose, lignin, etc. from the composition of natural fibers, cross-linking of fiber cell wall, grafting polymers, or functional groups and introducing coupling agents. These treatments also offer moisture resistance, dimensional stability, and fungal resistance to natural fibers. Silane treatment, alkaline treatment, acetylation, maleated coupling, enzyme treatment, etc. are the commonly used chemical techniques for natural fiber surface modifications [16,17,21–25]. Biological treatments results in the formation of enhanced interfacial interaction between natural fiber and polymer through the action of microorganisms especially bacteria [22,26]. The aim of this chapter is to overview the progresses in surface modification of natural fibers and also to investigate the impact of various techniques on the furtherance of their performances.

5.2 Cotton fibers

Cotton fiber is one of the highly acclaimed natural fibers under the genus of *Gossypium* made up of cellulose with 1,4-D-glucopyranose structural units. Many studies have been reported on surface modifications of cotton fibers to further enhance their performances, to introducing new features, and also to make compatibility with other surfaces. Among the various techniques, functionalizations through coating and grafting have received more interest. Generally, coatings can be applied over the surface of fibers with the help of various methods such as chemical vapor deposition, physical vapor deposition, electrochemical deposition, plasma polymerization, UV irradiation–induced polymerization, admicellar polymerization, etc. [27,28].

Gashti et al. [29] applied ozone gas treatment on the surface of cotton fibers to improve their contact with fluorocarbon monomer coating and thus their hydrophobicity. Combined effect of ozone gas treatment and fluorocarbon monomer on the surface of cotton fibers enhanced their contact angle to higher values on account of greater hydrophobic nature of fluorocarbon monomers. The effective grafting of fluorocarbon monomer on the surface of cotton fibers was further confirmed by weight changes observed. Fig. 5.2 presents scanning electron microscopical (SEM) images

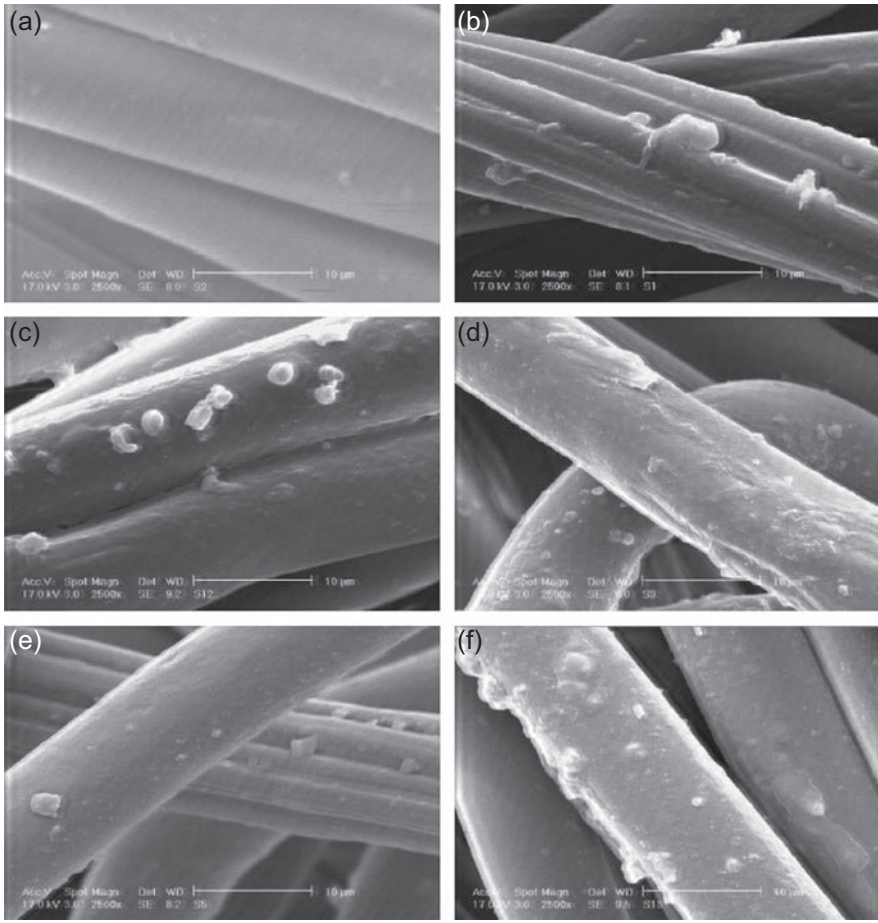

Figure 5.2 SEM images of cotton fibers: (a) untreated, (b) 90 min ozone treated, (c) 20 g/L fluoromonomer grafted, (d) 60 g/L fluoromonomer grafted, (e) 20 g/L fluoromonomer grafted on 90 min ozone treated and (f) 60 g/L fluoromonomer grafted on 90 min ozone treated [29].

of fluorocarbon monomer–grafted cotton fibers without any pretreatment and with ozone pretreatment. This kind of surface modifications does not need any kinds of solvents, so it can consider as an environmental friendly treatment [29]. In another study, Gashti et al. [30] developed silica–kaolinite-modified cotton fibers with the help of a cross-linking agent, succinic acid (SA), and a catalyst, sodium hypophosphite, using immersion of natural fibers in colloidal dispersion of additives and subsequent UV treatment. The improved interaction of inorganic particles with cellulose functional groups on the cotton fiber was confirmed using attenuated total reflectance-Fourier transform spectroscopical analysis. The impact of this modification on the contact angle of cotton fibers is presented in Fig. 5.3. Also, thermogravimetric analysis revealed the enhanced thermal stability of silica–kaolinite-modified cotton fibers on account of great heat resistance as well as mass transport barrier effect of silica–kaolinite [30].

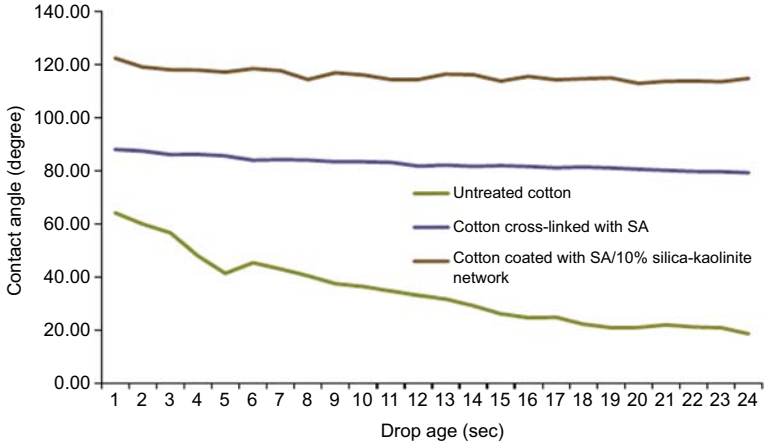

Figure 5.3 Variation in contact angles of untreated and modified cotton fibers [30].

Kang et al. [31] studied the effect of silver nanoparticles/3-mercaptopropyltrimethoxysilane (3-MPTMS) coating on the antibacterial activity of glycidyltrimethylammonium chloride (GTAC)–treated cotton fibers. In this process, cotton fibers were submerged into GTAC and then dry cured, followed by exertion of silver colloid/3-MPTMS solution on it at 43°C up to 90 min. An enhanced antibacterial properties against *Pseudomonas aeruginosa* on account of the combined effect of silver nanoparticles and GTAC were observed. Furthermore, SEM analysis revealed that the generation of rough surfaces after modifications is due to an improved surface attachment [31]. In another study, Varaprasad et al. [32] developed antibacterial cotton fibers by applying nano zinc oxide/sodium alginate coating over cotton fibers. The modified cotton fibers presented an excellent resistant against *Escherichia coli* and this recommends their use in biomedical applications [32].

Shafei et al. [33] observed higher antibacterial properties and UV resistance for cotton fibers modified with bionanocomposite coating composed of ZnO and carboxymethyl chitosan. Antibacterial properties were increased with increase in composite concentration while UV resistance improved with increase in curing temperature [33]. In another study, Selvam et al. [34] also attained improved antibacterial properties toward *Staphylococcus aureus* and *E. coli* bacterium as well as excellent reactive dyeability and color stability of cotton fibers by the application of poly-*N*-vinyl-2-pyrrolidone and ZnO nanoparticles [34]. The existence of greater dyeability for UV irradiated cotton fibers than mercerized one was reported by Bhatti et al. [35].

A study of Zakirov et al. [36] investigated the photoluminescence behavior of chemically surface modified and subsequent poly[2-methoxy-5-(2-ethylhexyloxy)-1,4-phenylenevinylene] (MEH-PPV)–coated cotton fibers. An enhanced photoluminescence for cotton fibers after chemical modification was observed and a blue photoluminescence when exposed to UV radiation was generated. The MEH-PPV coating on chemically modified cotton fibers caused to exhibit white-light emission, which was attributed to the generation of uniform as well as better adhesion of MEH-PPV coating on chemically modified cotton fibers through hydrogen bonding [36].

Ren et al. [37] fabricated 3-(4′-vinylbenzyl)-5,5-dimethylhydantoin (VBDMH) and applied over cotton fibers using admicellar polymerization in the presence of a cationic surfactant. Polymer-modified cotton generated a good stability toward *S. aureus* and *E. coli* after treatment with dilute sodium hypochlorite [37]. Tragoonwichian et al. [38] practiced admicellar polymerization of 2-hydroxy-4-acryloyloxybenzophenone (HAB) on the surface of cotton fibers using surfactant, sodium dodecylbenzene sulfonate with an aim to improve UV resistance. An enriched ultraviolet protection factor of 40 was observed for modified cotton fibers when compared to 4 of pure cotton fibers [38]. In another study, Tragoonwichian et al. [39] achieved combined UV and water resistance of cotton fibers by the use of double coating of HAB and methacryloxymethyltrimethylsilane through admicellar polymerization. Mao and coworkers [40] also developed UV-resistant cotton fibers by introducing ZnO nanoparticles on SiO_2-treated cotton fibers with the help of hydrothermal method.

A study of Pongprayoon et al. [41] reported an enhanced hydrophobicity for styrene-modified cotton fibers generated by admicellar polymerization. The resultant cotton fiber was stable against a droplet of water up to 30 min [41]. To boost the coverage of styrene film on the surface of cotton fiber, the authors used divinylbenzene (DVB) as a cross-linking agent, and a complete coating of cross-linked styrene on cotton fibers for 1 wt% of DVB [42] was found.

To improve flame retardancy of cotton fibers, Gashti et al. [43] applied multiwall carbon nanotubes (MWCNTs) on their surface with the help of vinylphosphonic acid monomer and benzophenone catalyst using UV irradiation. The occupancy of CNTs on the cotton fibers did result in the enhancement in thermal properties as well as flame retardancy on account of their high heat and mass transfer obstacle [43].

Jayasubramanyan et al. [44] fabricated superhydrophobic cotton fibers by applying a coating mixture consists of poly(vinyl chloride), copper stearate, and Fe_2O_3 or Cr_2O_3 nanoparticles. Polyvinyl chloride in the coating mixture acted as a binder and thus provided a strong adhesion of copper stearate and nanoparticles on cotton fibers. An enhanced water contact angle (WCA) of 147.5°C and 151.1°C for corresponding Fe_2O_3 and Cr_2O_3 nanoparticles–based coating was observed. This resulted in the generation of nonwettable surface roughened cotton fiber [44]. In another study, Yu et al. [45] utilized a combination of silica nanoparticles and perfluorooctylated quaternary ammonium silane coupling agent prepared by sol–gel process as a coating system to obtain superhydrophobic cotton fibers. As a result, the modified cotton fibers presented a WCA of 145°C and an oil contact angle of 131°C [45]. Bae and coworkers [46] also obtained superhydrophobicity of cotton fibers after treatment with a blend of silicon nanoparticles and commercial water repellant agent. A higher contact angle of more than 130 degrees for blend system with 0.1 wt% of water-repellant agent was obtained. Although, the individual effect of each component toward water resistance of cotton fiber was poor [46].

Andreozzi et al. [47] reported the grafting of methacrylates on the surface of cotton fibers through the radical sites generated after plasma treatment. In another study, Yeqiu et al. [48] successfully grafted blocked polyurethane on cotton fibers by simple immersion, which was ascribed to the reaction of hydroxyl group of cotton fibers with isocyanates formed from the blocked polyurethane. Janhom et al. [49] examined the

impact of poly(ethyleneimine) (PEI) and bovine serum albumin (BSA) on the surface of cotton fibers using zeta potential analysis. The presence of PEI on cotton fibers created more positive charges than that of BSA [49]. A study of Takacs et al. [50] compared the grafting yield of various monomers such as acrylamide (AAm), acrylic acid (Aac), 2-hydroxypropyl acrylate (HPA), 2-hydroxypropyl methacrylate (HPMA), and N,N′-methylene bisacrylamide (BAAm) on the preirradiated surface of cotton fibers. HPMA presented a greater grafting yield on the fiber surface [50].

Halim et al. [51] examined the effect of sodium chlorite/potassium permanganate ($KMnO_4$) redox bleaching system on the behavior of cotton fibers. The cotton fibers were first treated with $KMnO_4$ to create accumulation of Mn^{III} and then soaked in to a solution of sodium chlorite. The existence of adequate whiteness index as well as tensile strength of bleached cotton fibers was obtained for a bleaching system with a material to liquor ratio of 1:10 containing 0.01N $KMnO_4$ at 50°C and 5 g/L sodium chlorite solution [51]. In another study, Halim et al. [52] accomplished sufficient whiteness index and good tensile properties of cotton fibers through the treatment with thiourea-activated hydrogen peroxide.

5.3 Flax fibers

Flax fiber is a widely used natural fiber under the class of bast fibers with the scientific name *Linum usitatissimum*. The unique features such as low density and outstanding mechanical properties especially, moduli of flax fibers make them suitable for various applications as composite reinforcement as well as fiber. Functionalization of flax fibers needs to enrich their interactions with polymer matrices and hydrophobicity and thereby to broaden applications profile of renewable natural fibers [53,54].

Surface modification of flax fibers via grafting of glycidyl methacrylate (GMA) in an emulsion medium was reported by Moawia et al. [55] with the help of preirradiation treatment. FTIR and SEM analysis of modified fibers confirmed the successful grafting of GMA onto flax fibers. An optimal grafting degree of 148% was observed for 0.7% sodium chlorite solution–treated flax fibers compared with raw flax fibers. As a result of GMA grafting, modified flax fibers exhibited adequate hydrophobicity and mechanical strength [55]. In another study, Dorez et al. [56] used octadecylphosphonic acid (ODPA) to graft on the surface of flax fibers and the generation of about 5% ODPA grafting on the fibers was obtained after modification. This could be due to the strong reactions of ODPA with lignin and slightly reduced reaction with xylan (hemicellulose). There was no reaction of ODPA with cellulose in the flax fiber [56].

A study of Wang et al. [57] introduced nano-TiO_2 onto flax fiber surface through the grafting in a suspension consists of nano-TiO_2 and silane coupling agent by simple dipping. Functionalized flax fibers with about 2.34% of grafted nano-TiO_2 presented an increase of 23.1% in tensile strength (Fig. 5.4). Also, improvement in bonding as well as thermo-mechanical properties of nano-TiO_2 grafted flax fibers was noticed. This was attributed to the creation of Si—O—Ti and C—O—Si networks on the flax fiber surface on grafting [57]. Foruzanmehr et al. [58] grafted nano-TiO_2 onto flax fibers using sol–gel method and then investigated their influence on mechanical and physical properties. The existence of about 100-nm-thick TiO_2 coating over

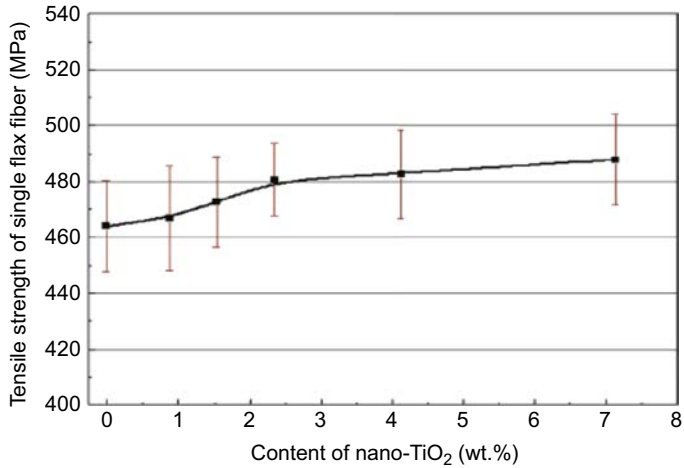

Figure 5.4 Modification in tensile strength of flax fibers with nano-TiO_2 content [57].

flax surface was detected. The appearance of nano-TiO_2 on flax fibers strengthened their mechanical properties and also caused to broaden wetting angles [58]. In another study, the authors introduced nano-TiO_2 coating over preoxidized flax fibers, which exhibited further enriched interactions and performances [59].

The surface behavior of scoured and bleached semiretted and retted flax fibers was evaluated by Halim et al. [60]. The effect of all these surface pretreatments resulted in the generation of negative zeta potential on the flax fiber surface. In contrast to semi-retted fibers, the existence of greater surface energies for retted fibers was observed. Also, the bleached fibers presented higher surface energies than that of the scoured one [60]. In another study, Martin et al. [61] investigated the role of retting degree on the properties of flax fibers. The increase in thermal stability, tensile strength, and Young's modulus as well as the decrease in water absorption of flax fibers with increase in degree of retting [61] was observed.

Pucci et al. [62] reported the chemical modifications of flax fiber surface through the use of thermal treatment at 80°C with an aim to improve their wettability. The dynamic apparent water wetting angle of modified flax fibers was lower than that of unmodified flax fibers, which created a much accelerated capillary ascension [62].

5.4 Hemp fibers

Hemp fibers are considered as one of the strong member of bast natural fibers family, which are derived from the hemp plant under the species of *Cannabis*. Nowadays, these fibers have received wide acceptance as reinforcements in composite materials on account of their biodegradability and low density compared with artificial fibers. Also these materials have inherent mechanical, thermal, and acoustic properties [63]. Surface functionalization of hemp fibers is of relevant importance to widen its applications.

A study of Troedec et al. [64] examined the compositional and structural impact of chemical treatments using NaOH, polyethyleneimine, ethylenediaminetetraacetic acid (EDTA), $Ca(OH)_2$, and $CaCl_2$ on hemp fibers. The treatments using 6% of NaOH contributed to increase the crystallinity of hemp fibers through the removal of amorphous aggregates. EDTA helped to dissociate fibers from the complex magnesium ion present in the pectin composition, whereas $Ca(OH)_2$ introduced calcium ions onto the fiber surface. The existence of in-between features was noticed for polyethyleneimine, but $CaCl_2$ had no significant effect [64]. In another study of Troidec et al. [65] investigated the influence of above-mentioned treatments on the adhesion properties of hemp fibers with a silica colloidal probe. The treatments using NaOH caused to create an optimal adhesion force of 174.2 nN on the surface of hemp fiber compared with 70.6 nN of unmodified hemp fiber, which was ascribed to the NaOH-induced hydrophilic nature of surface cellulose and the resultant higher capillary force and Van der Waal's forces [65].

Panaitescu et al. [12] observed the generation of hemp fiber bundle splitting as well as elementary fiber segregation after treatments with $KMnO_4$ and γ-methacryloxypropyltrimethoxysilane (MPS). MPS functionalization of hemp fiber enhanced their thermal stability, whereas $KMnO_4$ treatment decreased because of its mild oxidation tendency [12]. Beckermann et al. [66] reported the existence of enhanced tensile strength, Young's modulus, crystallinity index, and thermal stability as well as decreased lignin content for hemp fibers after alkali treatment using a system containing 5 wt% of NaOH and 2 wt% of Na_2SO_4 [66]. In another study, Pickering et al. [67] carried out alkali treatment of hemp fibers using 10 wt% of NaOH solution at a temperature of 160°C for 45 min. Hemp fibers with improved crystallinity index was obtained after NaOH treatment attributed to the ordered close packing of macromolecules of cellulose in the fibers caused by the elimination of amorphous compounds. This resulted in the further strengthening of hemp fibers along with separated structure having very low amount of lignin [67]. A study of Kostic et al. [68] reported an increase in flexibility and a decrease in water absorption for chemically modified hemp fibers using 5% NaOH solution [68].

Kabir et al. [69] practiced the impact of chemical treatments on the surface of hemp fibers using combination of chemicals such as alkali, acetyl, and silane. The action of highly concentrated solution of NaOH caused to remove most of the parts of hemicellulose and lignin in the hemp fibers, the remaining parts of these components were removed through subsequent acetylation using glacial acetic acid. Silane treatment by oligomeric siloxane solution in methyl alcohol had no role in the removal of hemicellulose and lignin from the hemp fiber surface, whereas it contributed to coupling reactions on the fiber surface [69]. It was observed that reduced tenacity for hemp fibers after NaOH treatment and some part of tenacity was retained after acetylation. Silane treatments created an increase in failure strain for hemp fibers [70].

Kostic et al. [71] reported the individual removal of hemicellulose and lignin constituents from the hemp fibers surface through the respective treatment with 17.5% NaOH and 0.7% $NaClO_2$. Enhanced absorption of moisture and iodine as well as electric resistance of hemp fibers was achieved through the removal of hemicellulose. But the removal of lignin decreased the absorption of moisture and iodine while electric

resistance presented a slight increase [71]. The removal of hemicellulose caused to increase the moisture absorption of hemp fibers, whereas lignin removal reduced the absorption of moisture [72].

A study of Li et al. [73] reported the use of chelator treatment and united chelator and enzyme treatments to the surface modification of hemp fibers. The effectiveness of all the treatments for the separation of fibers from the bundles and the removal of noncellulosic constituents was found. Modified hemp fibers exhibited improvement in crystallinity index and thermal degradation resistance. When comparing the modified properties of hemp fibers, treatment using chelator alone showed greater impact. The existence of more OH groups was observed on the fiber surface after treatments due to the removal of noncellulosic constituents [73]. In another study, George et al. [74] described the generation of further homogenized surface of hemp fibers via surface modifications with the help of enzymes such as hemicellulases, pectinases, and oxidoreductase. The enzymatically modified hemp fibers exhibited improvement in thermal stabilities on account of the effective removal of comparatively less stable pectic and hemicellulosic constituents [74].

Li et al. [75] examined the role of bag retting and white rot fungal treatments on to the surface modifications of hemp fibers. Both of these treatments generated highly ordered macromolecular arrangements of cellulose through the effective removal of noncellulosic components. Also, the modified hemp fibers presented more surface roughness along with increased number of active OH functional groups, which creates much better interactions on the fiber surface [75].

To enrich the flame retardancy of hemp fibers, Szlonoki et al. [76] introduced phosphorus comprising flame retardant on their surface by three various routes such as the dipping of pretreated fibers in a solution of phosphoric acid, fibers treated with the help of an aminosilane-type coupling agent, and the coating application onto fibers through the sol–gel method. Phosphorus modification of hemp fibers using all these routes exhibited enhanced LOI values and 25% decreased rate of heat release. The incorporation of amine-type phosphorus comprising curing agent onto treated hemp fibers displayed an enhanced flame retardancy rating of V0 on UL-94 test [76].

George et al. [77] grafted water-soluble sulfonic acid derivatives onto hemp fibers with an aim to make surface of hemp fibers for composite preparation. The existence of strong reaction between disubstituted benzene and amino groups during the treatment time was underlined by the results of FTIR analysis. X-ray photoelectron spectroscopical (XPS) analysis revealed the reduced O/C ratio and the increased C—C—O linkages on the surface of hemp fibers after grafting. The modified hemp fibers showed reduced surface polarity along with good improvement in thermal stability [77].

Dai et al. [78] developed nanocellulose from hemp fibers by oxidation hydrolysis under thorough sonication and then it was applied to functionalize the surface of dodecyltrimethylammonium bromide (DTAB) pretreated hemp fibers themselves. This created marked enhancement in mechanical properties such as 36.13% in modulus, 72.80% in tensile stress, and 67.89% in tensile strain on account of proper and efficient distribution of nanocellulose as well as interfibril bonding onto the fiber surface. Also, the crystallinity index and the resin adsorption of modified hemp fibers

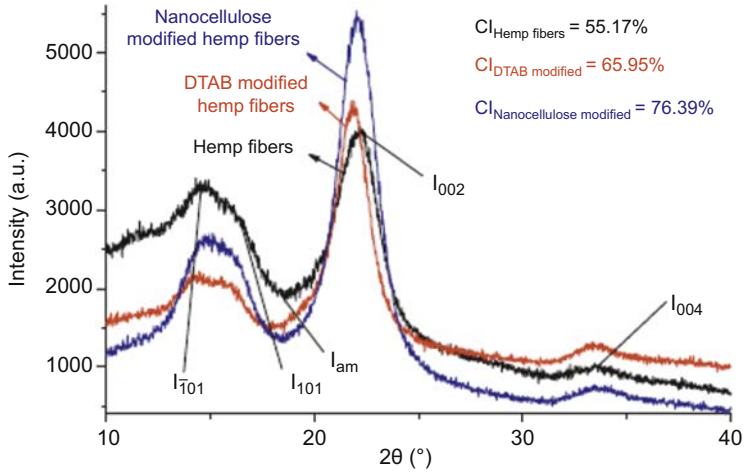

Figure 5.5 X-ray diffractogram of unmodified and modified hemp fibers [78]. *DTAB*, dodecyltrimethylammonium bromide.

increased by more than 20% and about 60%, respectively. The X-ray diffractogram presented in Fig. 5.5 shows developments in crystallinity index of hemp fibers after modifications [78].

Vukcevic et al. [79] fabricated carbonized hemp fibers using carbonization at 1000°C for 30 min under nitrogen atmosphere and subsequent stimulation using KOH at a temperature of 900°C for 30 min. Carbonization of hemp fibers exhibited an increase in specific surface area along with more surface oxygen groups, which correspondingly caused to enhance sorption properties [79].

5.5 Jute fibers

Jute fibers are lignocellulosic vegetable bast fibers obtained from the genus of *Corchorus.* These inexpensive natural fibers have gained more research concern to yield lightweight eco-friendly biocomposites [80]. Surface modification of jute fibers is important to overcome the limitations relating water absorption and mechanical performances. Gassen et al. [81] applied alkali treatments using different concentrations of NaOH onto the surface of jute fibers. The authors observed the strong influence of fiber shrinkage on the chemical treatments on the ultimate mechanical properties of jute fibers. The enhancements of 120% in tenacity and 150% in tensile modulus were obtained for treatment using 25% NaOH solution at a temperature of 20°C for 20 min [81].

Corrales et al. [82] used oleoyl chloride, a fatty acid derivate to chemically modify the surface of jute fibers with the help of solvents such as pyridine and dichloromethane. FTIR and elemental analysis revealed the generation of ester groups on the fiber surface through the reaction between oleoyl chloride and cellulosic OH group.

A greater functionalization degree was observed for oleoyl chloride in the pyridine swelling solvent than nonswelling solvent dichloromethane. The appearance of fatty acid derivate offered hydrophobicity to jute fibers along with good wettability [82].

Hossain et al. [83] investigated the impact of series of chemical treatments such as detergent washing, dewaxing, alkalization, and acetylation on the surface of jute fibers. These treatments caused to create an improved surface of jute fibers with enhanced adhesion tendency. Chemically modified fibers exhibited higher tensile properties than that of unmodified fibers [83]. In another study, Karaduman et al. [84] carried out the surface modification of jute fibers by treatment in 4 wt% NaOH solution at 30°C for 20 min with an objective to upgrade adhesion features [84].

Gao et al. [85] reported the modifications of jute fibers surface using pyromellitic dianhydride (PMDA) through the application of microwave treatments. The modified jute fibers presented an aniline adsorption capacity of 3 g/L at pH of 7. The adsorption capacity of modified fibers was further improved using desorption of aniline with the help of a solution containing 0.5 M HCl. These modified jute fibers are recommended for the aniline removal from the wastewater [85]. In another study, Hu et al. [86] obtained an aniline adsorption capacity of 96% for PMDA-modified jute fibers after three successive regeneration cycles. A study of Hassan et al. [87] fabricated acrylic acid–grafted jute fibers using gamma irradiation and then examined their feasibility to adsorb reactive dyes from the wastewater. The authors obtained an enhanced adsorption at comparatively low pH value of 3 (acidic medium) and its magnitude was increased with increase in time of contact [87].

Hong et al. [88] developed silane-modified surface of jute fibers through the treatment with a coupling agent, γ-glycidoxypropyl trimethoxy silane. The resultant fiber surface exhibited an enriched adhesion degree caused by the condensation reaction of hydroxyl silane with OH groups on the fiber surface [88]. A study of Acha et al. [89] described the chemical modification of jute fibers through esterification with the help of a commercial alkenyl succinic anhydride to impart the improved adhesion properties [89]. In another study, Gassen et al. [9] also modified jute fibers surface with an aim to enhance adhesion properties using maleic anhydride–grafted polypropylene in toluene [9]. The oxidation of jute fibers was carried out by Rahman et al. [90] with the help of 0.06 M sodium periodate solution. Goriparthi et al. [91] investigated the individual effect of alkali, permanganate, peroxide, and silane treatments onto the surface of jute fibers and an optimal modification for silane-treated jute fibers [91] was found.

Park et al. [92] reported the functionalization of jute fibers surface using NaOH and silane coupling agent. The reduced surface energy for silane-modified jute fibers was observed because of the obstruction of elevated energy domains. NaOH-modified jute fibers showed an enriched surface energy participated by the removal of weaker constituents. Tensile strength and modulus of jute fibers were observed to increase after both the treatments [92].

Tzounis et al. [93] prepared MWCNTs-coated jute fibers through the application of water-dispersed functionalized MWCNTs on to the alkali-treated water-dispersed jute fibers. Contact angle measurements exposed the enhanced hydrophobicity of MWCNTs-modified jute fibers. Also, adhesion properties were observed to increase after modification [93].

5.6 Ramie fibers

Ramie fibers are widely available powerful bast fibers under the family of Urticaceae with the genus of *Boehmeria*. These materials possess long durability and greater cellulose content. Compared to other members of bast fibers family, the chemical composition of ramie fibers needs further modifications to alleviate their limitations and thereby to widen applications range [94]. Zhou et al. [95] applied ethanol pretreatment and subsequent plasma treatment onto ramie fiber surface with an objective to enrich surface features and thus effective adhesion properties. Modification of ramie fibers was achieved through 10 min immersion in ethanol followed by helium plasma treatment. SEM analysis exposed the enhanced surface roughness of ramie fibers after plasma treatment. Enriched amount of carbon as well as hydrophobic C—C linkages on the surface of modified ramie fiber were observed using XPS analysis. Dynamic contact angle measurement revealed the enlarged WCA for plasma-treated ramie fibers. Furthermore, modified fibers presented an increase of 50% in shear strength to polypropylene due to the comprehensive impact of used treatments [95].

Liu et al. [96] grafted 2,2,2-trifluoroethyl methacrylate (TFEMA) onto ramie fiber surface through reversible addition–fragmentation chain transfer (RAFT) polymerization in supercritical carbon dioxide ($scCO_2$) with the help of a chain transfer agent 2-(ethoxycarbonyl)prop-2-yl dithiobenzoate (ECPDB). During the time of RAFT polymerization, surface OH groups of fibers were transformed into 2-dithiobenzoyl isobutyrate, this one also behaved as RAFT chain transfer agent. The modified ramie fiber exhibited an enhanced hydrophobicity along with an upgraded WCA of 149 degrees. The existence of controlled RAFT polymerization of TFEMA over ramie fibers surface was confirmed using the lower polydispersity (1.28) of grafted poly(TFEMA) [96].

To modify the surface properties, Li et al. [97] treated ramie fibers with epoxidized silicone oil at 160°C in the presence of argon gas. A reduced crystallinity for silicone-modified ramie fibers was observed on account of the creation of bond between some silicone chain and OH groups on the fiber surface. Also, modified fibers presented improved adhesion properties as well as thermal stability [97]. In another study, He et al. [98] observed change of surface behavior of ramie fibers from hydrophilic to hydrophobic after modifications by amino silicone oil (Fig. 5.6). The existence of strong intermolecular interactions between amino silicone oil and cellulose constituent of fibers was noted [98].

To obtain adhesion features of ramie fibers, Yu et al. [99] described the surface modification of ramie fibers with the help of NaOH and silane compounds such as 3-aminopropyltriethoxysilane and γ-glycidoxypropyltrimethoxysilane [99]. A study of Goda et al. [100] reported the impact of load introduction on the mercerization of ramie fibers on the tensile properties. The modification of fibers was carried out with the application of 0.049 N and 0.098 N loads in 15% NaOH solution for 2 h. An increase of 4%–18% in tensile strength was observed for modified ramie fibers while Young's modulus was decreased. Also, the fracture strains of ramie fibers were improved to 0.045–0.072 (about threefolds) after modification due to the removal of microcrystallines and other noncellulose materials on mercerization [100].

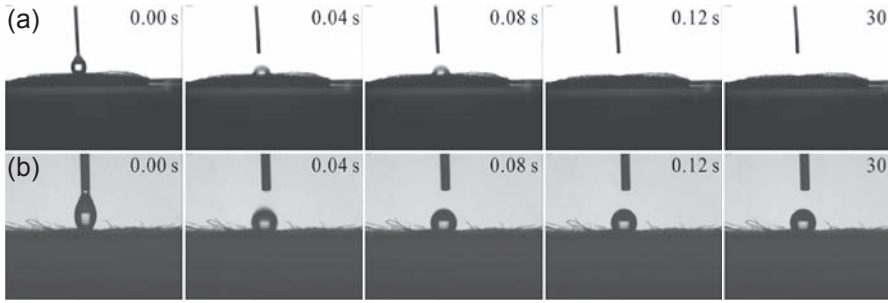

Figure 5.6 Behavior of water droplets on the surface of (a) unmodified ramie fiber and (b) amino silicone oil–modified ramie fiber [98].

Yuan et al. [101] modified ramie fibers by applying thermal treatments at 200°C in nitrogen and air atmosphere. Thermal treatments of ramie fibers under nitrogen atmosphere exhibited shrinkage, which was ascribed to the deterioration of thermally unstable constituents such as hemicellulose and pectin as well as the hydrophilic group reduction. This contributed to increase the adhesion properties of ramie fibers. Thermal treatments at air atmosphere caused to increase hydrogen bond intensities, lateral order indices, and IR crystallinity ratios of ramie fibers. However, crystallinity indices of hemp fibers decreased on account of the oxidation during the thermal treatment at air atmosphere. Also, ramie fibers presented shrinkage only up to 100°C and afterward expansion [101]. In another study, He et al. [102] used isocyanate group back titration (IBT) method to functionalize the surface of ramie fibers using toluene-2,4-diisocyanate (TDI) and hexadecanol. The effective grafting of TDI and hexadecanol onto fibers was confirmed by FTIR analysis. IBT-modified ramie fibers offered good hydrophobicity along with nice adhesion properties [102].

5.7 Kenaf fibers

Kenaf fibers are one of the widely accepted natural fibers from the plant family of Malvaceae. These fibers are obtained from the bast and core of plants with the genus *Hibiscus* and around 300 species. Kenaf fibers possess outstanding flexural strength and superior tensile strength along with usual natural fiber features such as lightweight, low cost, nonabrasiveness, combustibility, nontoxicity, and biodegradability, which offer their applications in wide areas [103]. Various surface treatments have been used to further upgrade the performances of kenaf fibers.

Edeerozey et al. [104] reported the chemical modification of kenaf fibers surface using various concentrations of NaOH. The marked enhancement in mechanical properties was achieved through NaOH treatment and the optimal concentration of NaOH was 6% [104]. In another study, Yousif et al. [105] reported the chemical modification of kenaf fibers using 6% NaOH to enrich the adhesion properties. A study of Mahjoub et al. [106] evaluated the role of various conditions of NaOH treatments on the modifications of kenaf fiber. It was observed that the treatments

using 5% NaOH was suitable for fiber modifications while higher concentration of NaOH spoiled the texture of fibers. Increase in both NaOH concentration and treatment duration caused to reduce the tensile strength of kenaf fibers [106]. In another study, Fiore et al. [107] investigated the effect of two different immersion periods (48 and 144 h) of 6% NaOH treatments onto kenaf fiber surface. NaOH treatment for 48 h was well to remove unwanted constituents on the fiber surface, whereas treatment for 144 h had some harmful effects on surface and mechanical features of fibers [107].

A study of Meon et al. [108] fabricated NaOH–modified kenaf fibers using various concentration of NaOH include 3%, 6% and 9%. Following this, NaOH-modified kenaf fibers were further modified with the help of maleated polyethylene (MPE) and maleated polypropylene (MPP). The tensile properties of kenaf fibers were considerably increased after NaOH treatments and it was optimal for 6% of NaOH. The presence of MPE and MPP on the surface of NaOH-modified and NaOH-unmodified kenaf fibers caused to enrich the tensile properties [108].

In another study, Asumani et al. [109] observed the greater impact of combined system of NaOH and 3-aminopropyltriethoxysilane for the furtherance in surface behavior and thus performances of kenaf fibers than their individual effect [109]. In another study, Asim et al. [110] examined the individual and combined impacts of 6% NaOH and 2% triethoxy(ethyl)silane on the surface kenaf fibers. SEM and FTIR analysis of modified fibers exposed the well feasibility of all treatments for the removal of unwanted constituents from the fiber surface and thereby the surface preparation. The existence of higher tensile strength and interfacial stress strength was observed in the case of modification using silane alone [110].

The role of citric acid for the surface modification of kenaf fibers was studied by Sajab et al. [111] through esterification. Citric acid (0.06 M)–modified kenaf fibers offered greater efficiency toward the adsorption of methylene blue and it was obtained an optimal adsorption of 131.6 mg/g at 60°C [111]. In another study, Mahmoud et al. [112] treated kenaf fibers with 3 M HCl to fabricate highly adsorbing surface. A study of Datta et al. [113] modified the surface of kenaf fibers with the help of acetylation and treatments based on blocked isocyanate, maleic anhydride, and permanganate [113]. Krishna et al. [114] demonstrated the individual impact of glutamic acid and lysine on kenaf fibers, and the modifications were carried out at ambient temperature for 24 h. Both modifications of kenaf fibers caused to reduce their thermal stability. For kenaf fibers, treatments using lysine generated much better results when compared to glutamic acid treatments [114].

5.8 Bamboo fibers

Bamboo fiber is derived from leaves, branches, and hard trunk of abundantly available everlasting bamboo plants (Bambusoideae) using steam explosion followed by mechanical treatment. These fibers have an ability to absorb UV light and also possess comparatively good properties as compared to other natural fibers [115]. Nowadays more research interests have been given to synthesis bamboo fiber–based

biocomposite materials and biopolymers. The surface modifications of bamboo fibers are necessary to enrich these applications through improved hydrophobicity, wettability, and adhesion.

Liu et al. [116] reported the grafting of a water-soluble monomer *N*-methylol acyrlamide onto four kinds of bamboo fibers such as bamboo particles (PF), mechanical pulp fibers (MP), chemical pulp fibers (CP), and original bamboo fibers (OF) with the help of a catalyst, sulfuric acid. Based on the divergent fiber morphology and chemical constitution of bamboo fibers, the degree of *N*-methyl acrylamide grafting was in the order of CP > MP > PF > OF. The grafting of *N*-methylol acrylamide onto bamboo fibers surface yielded an inflated N content and a decreased O/C ratio. Moreover, *N*-methylol acyrlamide–grafted bamboo fibers possessed good adhesion features [116].

Luna et al. [117] compared the individual impacts of NaOH treatment and plasma treatment on the surface modification of bamboo fibers. Both modification techniques offered improvement in surface features. Plasma treatment had no detrimental effect on the mechanical strength of bamboo fibers, whereas NaOH treatment caused to reduce [117]. Lu et al. [118] studied the individual impact of treatments using NaOH and silane coupling agent on the surface modification of bamboo fibers. The effectiveness of these two treatments for the modification of bamboo fibers was confirmed by FTIR analysis. The treatment using NaOH resulted in the splitting of fibers on account of the successive removal of lignin part and amorphous cellulose. Silane coupling agent caused to form Si—O—C and Si—O—Si network on fiber surface, which could increase mechanical as well as thermal performances of fibers [118].

Lu et al. [119] evaluated the individual influence of NaOH, silane coupling agent, and maleic anhydride for the furtherance of bamboo fibers surface. The impact of each treatment on the bamboo fiber surface was different. Treatment using NaOH contributed to enhance tensile strength and modulus, whereas silane coupling agent caused to increase toughness and elongation. Maleic anhydride grafting on bamboo fibers offered good comprehensive properties along with good balance of stiffness and toughness [119]. In another study, Manalo et al. [120] also tried NaOH treatments with varying concentrations (4–8 wt%) to modify the surface of bamboo fibers. The optimal enhancement in surface features for 6 wt% of NaOH treatment [120] was observed.

Yu et al. [121] applied mechanical treatments on bamboo fibers using a pilot machine to fabricate oriented bamboo fiber mat. A higher yield of 92.54% for modified bamboo fibers was observed. Mechanically modified fibers showed enhancement in performances along with nice adhesion properties [121].

5.9 Coir fibers

Coir fiber also known as coconut fiber is considered as a principal lignocellulosic natural fiber acquired from the husk of coconut (*Cocus nucifera*). These fibers attained much scientific as well as industrial research interest due to the excellent properties such as hard-wearing quality, durability, and other features of natural fibers along with their inexpensive in nature [122]. Adequate surface modifications of coir fibers are crucial to upgrade the limitations such as hydrophilicity, inferior wetting, and inadequate adhesion.

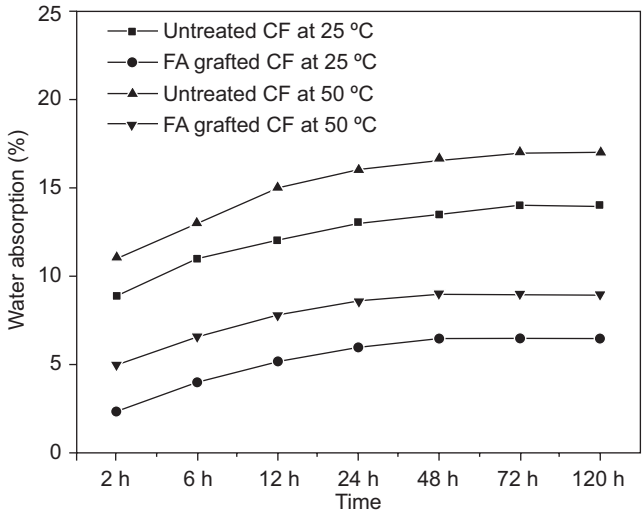

Figure 5.7 Water absorption behavior of untreated and furfuryl alcohol (FA)–grafted coir fibers (CF) as a function of time at two different temperatures [123].

Saw et al. [123] reported the surface modification of coir fibers through ClO_2 induced oxidation and subsequent grafting of furfuryl alcohol on ClO_2 pretreated surfaces of coir fibers. The formation of quinones on coir fibers was detected on ClO_2 treatment due to the oxidation of phenolic syringyl and guaiacyl units present in the lignin. Oxidized surfaces of coir fibers greatly supported the grafting of more furfuryl alcohol when compared to nonoxidized coir fibers. As a result, weight gain of 17.7% was noted in the case oxidized coir fibers, whereas it was only 2.2% in the case of nonoxidized coir fibers. Furfuryl alcohol grafting over coir fibers yielded more hydrophobicity as well as higher surface energy to coir fibers. Fig. 5.7 shows water absorption behavior of unmodified and furfuryl alcohol–grafted coir fibers at two different temperatures [123].

Praveen et al. [124] studied the impacts of weakly ionized oxygen plasma treatments on the surface modifications of coir fibers. An increase in water sorption from 39% to 100% of coir fibers was observed after plasma treatment. XPS analysis revealed about 14% increase in oxygen content on coir fibers surface after plasma treatment at 50 Pa. Plasma treatments on coir fibers caused to disengage the foremost layer, which was executed through atomic force microscopical analysis [124].

Gu et al. [125] modified the surface of coir fibers with NaOH and then investigated the impact of varying concentrations of NaOH (2–10) on their tensile properties. Tensile strength of NaOH–treated coir fibers decreased with increase in concentration of NaOH [125]. Nam et al. [126] attained an improvement of 55.6% in interfacial shear strength for coir fibers after chemical treatment in 5% NaOH at ambient temperature for 72 h. Route et al. [127] described the individual impact of NaOH treatment, bleaching, and acrylonitrile grafting on the surface modification of coir fibers. All treatments presented enriched surface performances and related properties.

Furthermore, these treatments also exhibited higher surface energy and thus good adhesion features [127]. Haque et al. [128] modified the coir fibers surface by chemical treatment with benzene diazonium salt to improve their adhesion features. A study of Islam et al. [129] reported improved performances of coir fibers through chemical treatment using *o*-hydroxybenzene diazonium salt. In another study, Rosa et al. [130] proposed the combination of water washing, alkali treatment, and bleaching to upgrade the surface features of coir fibers.

To modify the surface features of coir fibers, Rahman et al. [131] reported UV-induced grafting of ethylene dimethylacrylate (EMA) over pretreated coir fibers. Pretreatments of coir fibers were executed using respective NaOH and UV radiation and also the individual pretreatment impact on the grafting of EMA was evaluated. NaOH treatment at low temperature as well as treatment using 20% NaOH exhibited a greater shrinkage of coir fibers. Improved physicomechanical properties were observed for EMA-grafted coir fibers possessing greater shrinkage. Polymer grafts formation was observed to greater in NaOH pretreated coir fibers and it had about 56% higher polymer holding capability than pristine coir fibers, which caused to create about 27% higher tensile strength [131].

Thakur et al. [132] reported the surface functionalization of lignin-containing coir fibers via laccase-catalyzed biografting of ferulic acid with an aim to enhance moisture and microbial activity. The successful grafting of ferulic acid onto lignin in the coir fibers was observed with the help of FTIR, XRD, and SEM analysis. Also, the biografting caused to increase the thermal stability coir fibers [132]. In another study, Thakur et al. [133] utilized eugenol instead of ferulic acid in the abovementioned study to make biografting and thereby surface modifications of coir fibers.

5.10 Oil Palm fibers

Oil palm fiber is a foremost lignocellulosic fiber obtained from oil palm tree belongs to the family Arecaceae with the scientific name of *Elaeis guineensis*. Generally, fiber is derived from trunk, frond, fruit mesocarp, and empty fruit bunch of oil palm tree. Because of the many interesting advantages of natural fibers, oil palm fibers received growing acceptance as component of composite materials and other individual applications [134]. Surface modification of oil palm fibers aims to improve some common drawbacks of natural fibers and thus optimizing surface properties.

Sreekala et al. [135] modified the surface of oil palm fibers using miscellaneous techniques such as mercerization, latex coating, gamma irradiation, silane treatment, isocyanate treatment, acetylation, and peroxide treatment. The specific impact of each surface modifications technique on water absorption behavior of oil palm fibers was analyzed under various temperatures. An increased hydrophobicity of coir fibers for all techniques at all temperature ranges was observed, which indicated the decreased water absorption behavior after modifications. Also, the impact of water absorption on the mechanical performances of fibers was studied and found a decrease in mechanical performances with increase in water uptake and vice versa [135]. A study of Izani et al. [136] compared the effect of treatments using boiling water, 2% NaOH, and their fusion on the surface

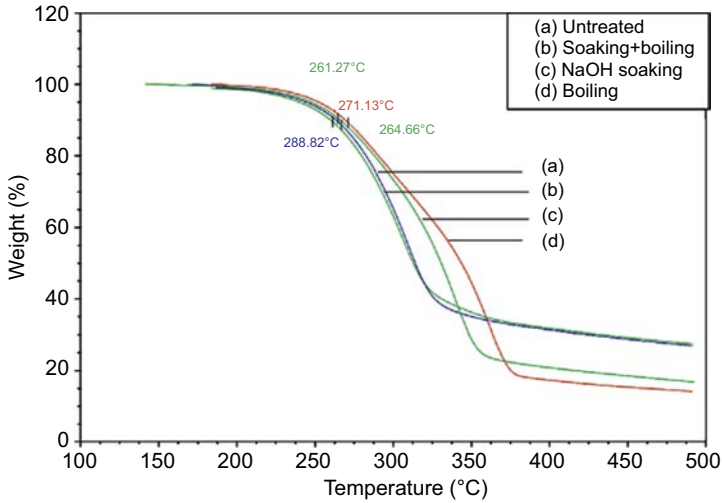

Figure 5.8 Thermogravimetric analysis thermograms of oil palm fibers (a) untreated, (b) combination of NaOH and boiling water treated, (c) NaOH treated, and (d) boiling water treated [136].

modification of oil palm fibers. NaOH treatment was found to efficient for surface modifications of oil palm fibers and caused to exhibit optimal tensile strength and Young's modulus. Application of both treatments increased thermal degradation resistance of oil palm fibers strongly (Fig. 5.8) [136]. To enrich polymer interaction of oil palm fibers, Essabir et al. [137] executed treatments in 1.6 mol/L NaOH solution.

To remove noncellulose constituents from the surface of oil palm fibers, Kim et al. [138] reported treatments using dilute sulfuric acid and followed by NaOH treatment. Acid treatment of oil palm fibers showed to remove 90% of hemicellulose and 32% of lignin content from the fiber surface. Alkali treatment was helpful to remove up to 70% of remaining lignin from the acid-treated oil palm fibers. As a result of acid/alkali treatment, the formation of more rough, porous, and irregularly ordered surface on oil palm fibers with high enzyme resistance was obtained [138]. In another study, Mamun et al. [139] used a blend of enzymes consisting of xylanase, laccase, and lipase to accomplish surface modification of oil palm fibers.

Sajab et al. [140] reported the modifications of oil palm fibers with the help of citric acid and PEI to enrich adsorption characteristics. Citric acid–modified oil palm fibers were effective to adsorb cationic methylene blue, whereas PEI-modified oil palm fibers exhibited great anionic phenol red adsorption. These two modified oil palm fibers possessed more than 70% adsorption capacity up to seven sequences [140].

5.11 Sisal fibers

Sisal fiber is a widely accepted biocellulose fiber extracted from the leaves of sisal plants with the scientific name *Agave sisalana* and these fibers comprised of around 65% cellulose, 12% hemicellulose, 10% lignin, 0.8% pectin, 0.3% wax, and some

other water-soluble constituents. Decortication is used to obtain fibers from leaves of sisal plants, and these fibers are quiet stiff in nature [141–143]. Many researchers have been practiced the surface modifications of sisal fibers in respect to overcome some common issues of natural fibers.

Kim et al. [144] reported mercerization of sisal fibers with an objective to enhance tensile properties and adhesion features. The application of tension on mercerization was found useful to reduce the shrinkage as well as microfibrillar angle of sisal fibers. Mercerization of sisal fibers increased their Young's modulus and fracture stress with the cost of toughness and fracture strain [144]. In another study, Mohan et al. [143] modified the surface of sisal fibers with the help of fused NaOH and clay treatments. The existence of about 20 wt% clays was observed on modified sisal fiber surfaces. A reduction of 2.6-folds in water absorption was obtained after NaOH-clay treatment. Moreover, the improvement in mechanical and thermal properties observed along with good adhesion properties [143]. Orue et al. [145] observed decrease in tensile strength for combined NaOH- and silane-modified sisal fibers.

Rong et al. [146] investigated the impact of various chemical treatments (alkalization, acetylation, cyanoethylation, and silane treatment) and one physical treatment (heating) on the surface modifications of sisal fibers. Chemical treatments were contributed to the removal of noncellulose constituents from the sisal fibers surface and thus created more flexibility. Also, chemical treatments generated higher surface energy on the fiber surface through the introduction of active groups on the fiber surface. Thermal treatment caused to increase the crystallinity of cellulose macromolecules in the sisal fibers, which increased their stiffness [146].

Zhou et al. [147] studied the effect of silane coupling agent (3-aminopropyltriethoxysilane (APS) and *N*-(2-aminoethyl)-3-aminopropyltrimethoxysilane (AAPTS)) on the modification of sisal fibers. On chemical treatment, silane adsorption on the fiber surface created a layer constitutes of siloxane and polysiloxane over it. Formation of strong chemical bonds between silane coupling agent and hydroxyl group on the fiber surface was confirmed using FTIR results, which correspondingly caused to increase the thermal stability of sisal fibers [147].

Fiore et al. [148] fabricated surface-modified sisal fibers using 10 wt% of sodium bicarbonate at ambient temperature with varying soaking period of 24, 120, and 240 h. Chemical treatment at a soaking time of 120 h presented maximum overall performances. The increase of about 198% and 115% in respective tensile strength and modulus for 120 h treatment was observed. This was attributed to the ejection of noncellulose attributes from the surface on chemical treatment [148]. A study of Wei et al. [149] obtained enhanced degradation stability of sisal fibers through treatments by Na_2CO_3 and thermal energy. In another study, Barra et al. [150] also attained degradation resistance of sisal fibers through methane cold plasma treatment.

Krishnaiah et al. [151] investigated the influence of combined NaOH and high-intensity ultrasound treatment on the surface modification of sisal fiber. Modification of sisal fibers led to removal of noncellulose constituents from the surface and was observed through FTIR and SEM analysis. Variations in FTIR spectra of unmodified and modified surfaces of sisal fibers are shown in Fig. 5.9. Crystallinity of fibers was improved with raise in amount of NaOH in the system. An increase of 38.5°C in thermal stability was reported for modified sisal fibers. Also, the existence of nice adhesion properties was noticed [151].

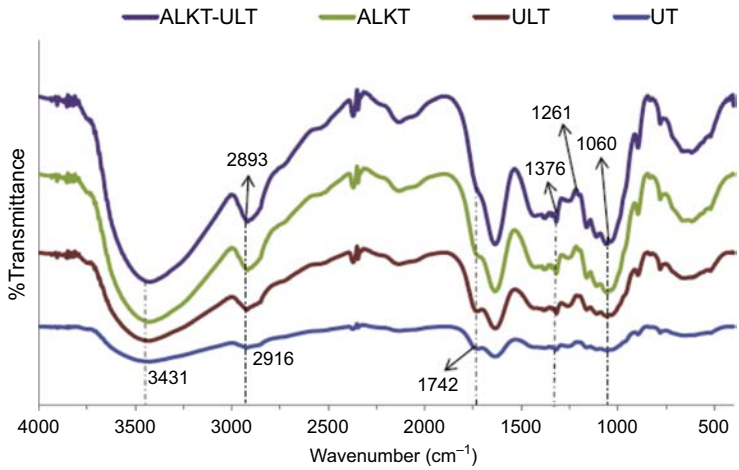

Figure 5.9 FTIR spectra of untreated (UT), ultrasound treated (ULT), alkali treated (ALKT), and the blend of alkali- and ultrasound-treated sisal fibers (ALKT-ULT) [151].

In another study, Pongprayoon et al. [152] applied poly(methyl methacrylate) (PMMA) coating over sisal fibers by admicellar polymerization to modify their surface properties. Formation of PMMA layer over sisal fiber was confirmed by FTIR and SEM analysis. PMMA-coated sisal fibers presented an enhanced hydrophobicity and this reflected in floating time, water absorption, and surface charge [152].

5.12 Other lignocellulosic plant fibers

This section covers the studies concerning the surface modifications of lignocellulosic fibers other than above discussed and includes abaca fibers, henequen fibers, pineapple leaf fibers, sugarcane fibers, pine corn fibers, date palm fibers, ijuk fibers, beech fibers, hyacinth fibers, *Xanthoceras sorbifolia* fibers, *Calotropis gigantea* fibers, *Luffa cylindrica* fibers, rice straw fibers, soybean straw fibers, and *Borassus* fruit fibers.

Cai et al. [153] described the surface modification of abaca fibers by 2 h alkali treatment in 5, 10, 15 wt% of NaOH solution with an objective to upgrade mechanical as well as adhesion features. Treatment in 5 wt% of solution caused to increase crystallinity, tensile strength, Young's modulus, and adhesion features of abaca fibers, whereas higher concentration of NaOH caused to deteriorate the fibers performances [153]. In another study, Cai et al. [154] examined the impact of 30 min NaOH treatment using various concentrations (5, 10, and 15 wt%) on the mechanical and the structural features of abaca fibers. An increase of 41% in Young's modulus was found for treatment in a solution comprising 5 wt% of NaOH, whereas further increase in NaOH concentration caused to deteriorate the mechanical performances. Also, the higher concentration of NaOH presented structural damages to abaca fibers [154]. In another study, Punyamurthy et al. [155] tried benzene diazonium chloride treatment on the abaca fibers surface with an objective to enrich interactions with polymers.

Gonzalez et al. [156] reported the surface modification of henequen fibers by alkali treatment and as a result, fine wetting of fibers was achieved. In another study, Gonzalez et al. [157] investigated the impact of silane coupling agent on the surface modification of henequen fibers. The results from XPS and FTIR analysis revealed the powerful interaction of silane coupling agents on fiber surface. Furthermore, this treatment was useful to partially detach the noncellulose constituents [157]. Threepopnatkul et al. [158] utilized NaOH pretreatment and successive treatment by silane coupling agents to modify surface features of pineapple leaf fibers. In another study, Panyasart et al. [159] examined the individual effect of NaOH and silane treatments on pineapple leaf fibers and the treatment using NaOH possessed more accessibility in terms of performances.

Liu et al. [160] reported the succinoylation of sugarcane bagasse fibers in an ionic solution containing 1-butyl-3-methylimidazolium chloride and dimethyl sulfoxide. In another study, Yue et al. [161] yielded sugarcane fibers with higher cellulose content through NaOH and subsequent $NaClO_2$ treatments. To detach the noncellulosic constituents from the surface of pine cone fibers and thus to enhance adhesion features, Arrakhiz et al. [162] practiced NaOH treatment. Luo et al. [163] carried out alkali and sizing treatments to improve the surface properties of corn fibers. A study of Taallah et al. [164] described the functionalization of date palm fibers with the help of NaOH treatment to enhance adhesion features. Zahari et al. [165] modified the surface of *ijuk* fibers (black sugar palm fibers) using vinyltrimethoxysilane with an aim to enhance mechanical performances and water resistance. Zierdt et al. [166] reported the chemical modification of beech fibers using treatment in NaOH solution and the modification caused to enhance the thermal stability of fibers [166].

Madrid et al. [167] reported the successful grafting of GMA on water hyacinth fibers surface using gamma irradiation and an optimal grafting yield of 58% was attained [167]. In another study, the authors replaced epoxy group of GMA-grafted hyacinth fibers with amine group using ethylenediamine solution to fabricate amine sort of adsorbent. The feasibility of this hyacinth-based amine sort of adsorbent toward the adsorption of Pb^{2+}, Cu^{2+}, and Cr^{3+} ions was evaluated and the strong influence of inceptive ion concentration and solution pH was inferred. The enhanced adsorption behavior of hyacinth fibers was resulted from the synergistic effect of gamma treatment and chemical amendment [168].

A study of Wang et al. [169] compared the effect of various surface treatments such as NaOH, silane coupling agent, their fusion and fusion of acetic acid, and hydrogen peroxide on husk fibers of *Xanthoceras sorbifolia*. The treatment using NaOH generated optimal cellulose content in fibers, whereas a system comprising of alkali and silane coupling agent created optimal thermal stability and tensile strength [169]. Zheng et al. [170] reported the existence of hydrophobic–oleophilic nature of *Calotropis gigantea* fibers after perfluorosilane treatment. The WCA of modified fiber was 130 degrees. Moreover, the increase of 112%, 52%, and 22% in absorbency of corresponding kerosene, soybean oil, and engine oil after modification [170] was obtained. Siqueira et al. [171] applied NaOH pretreatment and subsequent modification using 1,2,4,5-benzenetetracarboxylic dianhydride to enrich the surface behavior of *Luffa cylindrica* fibers. The existence of strong interaction between dianhydride and fibers surface was accomplished without any damage to fibers [171].

A study of Gong et al. [172] adapted the surface of rice straw fiber into high adsorbent of cationic dyes through the application of an esterifying agent, citric acid followed by treatment with sodium ions. In another study, Zhu et al. [173] yielded metal ion adsorbent surface on soybean straw fibers by acid/base wash followed by treatment with citric acid. The adsorption capacity of redesigned straw fiber surface toward Cu^{2+} was optimal at a solution pH of 6 [173].

Boopathi et al. [174] described the modification of Borassus fruit fibers by different concentrations of NaOH solutions such as 5%, 10%, and 15%. The removal of unwanted impurities from the fibers surface was executed through SEM analysis. The optimal advancement in tensile properties of fibers was accomplished in 5% NaOH solution [174]. In another study, Reddy et al. [175] also obtained the similar kind of results after 5% NaOH treatment on Borassus fruit fiber. The augmentation of 41% in tensile strength, 69% in tensile modulus, and 40% in elongation at break was achieved after 8 h of immersion in 5% NaOH solution [175].

5.13 Silk fibers

Silk is a naturally occurring protein containing high-molecular-weight fibrous polymer produced by arthropods, namely silkworms, spiders, scorpion, mites, fleas, and other insects. Among the diverse classes of silk fibers fraternity, mulberry silkworm silk fibers, *Bombyx mori* and wild nonmulberry silk fibers, *Antheraea pernyi* have received much scientific, industrial, and biomedical research attention. Silk is considered as a composite structure comprised of fibroin in sericin and also the fibroins are hold together by sericin in the silk structure. *Bombyx mori* silk is composed of about 70% fibroin and about 30% sericin. Silk fibers have some unique features such as superior tensile strength, good extensibility, nice hygroscopicity, competent appearance, and compatible to biological environments [176,177]. Studies concerning surface modifications of silk fibers have been reported to resolve some difficulties associated with them.

Lu et al. [178] applied nano-Ag on silk fibers surface using in situ method accommodated by UV light with an aim to improve bacterial resistance. An auspicious deposition of highly crystalline nano-Ag was attained on the surface of silk fibers. The modified silk fibers presented superior antibacterial properties along with improved thermal deterioration resistance on account of the high stability of nano-Ag on silk fibers resulted from the strong interaction between these two [178]. In another study, Lu et al. [179] reported the successful application of Ag nanoparticles over polydopamine-modified silk fibers via in situ synthesis. Polydopamine coating on silk fibers acted as reduction reagent and thus offered uniform dispersion of nano-Ag on it. Modified silk fibers offered outstanding resistance toward bacterial growth and it was assessed using bacterial growth rate and inhibition zone evaluation. The everlasting antibacterial effects of modified silk fibers were due to the elongated release of Ag^{+} ions [179]. A study of Meng et al. [180] also obtained a long-time Ag^{+} release of about 120 days for nano-Ag in situ functionalized double polymer layer of poly(acrylic acid) and poly(dimethyldiallylammonium chloride)-coated silk

fibers. This offered excellent antibacterial features [180]. To enrich antibacterial properties, a study of Xu et al. [181] applied hydroxyl functionalized nano-Ag over poly(amidoamine)-coated silk fibers using self-assembling route resulted from the strong intermolecular adhesion [181].

In another study, Xu et al. [182] fabricated hierarchical structured silk fibers by applying nanoparticles of Fe_3O_4 and Ag as dual coat with the help of a technology based on electrostatic self-assembly. The formation of regular and hierarchical coating over silk fibers was executed through XRD and SEM analysis. A higher magnetic behavior was reported for hierarchical structured silk fibers due to appearance of comparatively denser Fe_3O_4 [182].

Davarpanah et al. [183] evolved the effective grafting of chitosan, a polysaccharide on silk fibers with the help of anhydrides such as succinic anhydride and phthalic anhydride. The maximum grafting of chitosan on silk fiber was observed in the case of modifications at 50°C for 24 h using succinic acid along with dimethylformamide. FTIR results revealed the formation of amide functional groups during functionalization of silk fibers. The resultant functionalization of silk fibers created an outstanding dyeability, especially in the presence of acid dye [183].

Buga et al. [184] reported the treatment of 3-(trimethoxysilyl) propyl methacrylate (MPS) on silk fibers followed by grafting of methyl methacrylate (MMA) and tributylsilyl methacrylate (TBSiMA) through RAFT polymerization technique in the presence of a chain transfer agent, 2-cyanoprop-2-yl dithiobenzoate (CPDB) and an initiator, 2,2′-azobis(isobutyronitrile) (AIBN). The reaction was carried out at 70°C in toluene for 24 h. The nice grafting of both methacrylates onto silk fibers surfaces were confirmed using FTIR and SEM analysis, which created an excellent thermal stability [184].

Wei et al. [185] studied the effect of alcohol/water and inorganic salt treatments on the performances of silk fibers. The treatments using alcohol/water presented a great influence on the conversion of silk fibers conformation to β-sheet from random coil/α-helix when compared to treatment using inorganic salt. All treatments caused to improve the mechanical performances of silk fibers and a system containing 80 vol% of ethanol presented most favorable properties such as breaking stress of 199 MPa and elongation at break of 55% [185]. A study of Bai et al. [186] applied antimicrobial peptide (*Cecropin B*) onto silk fibers, which were pretreated in 60% ethanol solution. Peptide-modified silk fibers presented an enhanced surface roughness, antibacterial properties along with increased hydrophilicity due to the strong coupling of peptides with pretreated silk fiber surface [186].

5.14 Wool fibers

Wool fibers are strong member of protein fibers belongs to the group of α-keratin fibers. Their structure mimics as a composite material and it consists of keratin, cortical cells, cuticular cells, and cell membrane complex. These fibers are generally procured from sheep (*Ovis aries*), goats (*Capra aegagrus hircus*), muskoxen (*Ovibos moschatus*), rabbits (*Oryctolagus cuniculus*), and camelids (Camelidae). The existence of a monolayer

fatty acid over the outer cortical surface of wool fibers offers surface hydrophobicity to them [187,188]. There is an increasing demand to fabricate surface-modified wool fibers with much improved properties to tailor diverse applications.

To modify the surface features of wool fibers, Mohammadi et al. [189] introduced chitosan grafting on their surfaces with the help of anhydrides through acylation. The existence of proper grafting of chitosan onto the acylated wool surface was executed using FTIR, SEM, DSC, and weight gain test. The occupancy of chitosan on wool fibers caused to increase antibacterial as well as antifelting features of wool fibers [189]. In another study, Dev et al. [190] observed the strong influence of chitosan in the modified wool fibers to widen the antibacterial properties of dyes presented in the modified wool fibers. A study of Robert et al. [191] revealed the increase in antifelting characteristics of chitosan-modified wood fibers with increase in number of *N*-acyl groups in the chitosan [191].

Monier et al. [192] reported ethyl acrylate grafting on the wool fiber surface using redox initiator system of potassium persulfate and Mohr's salt followed by conversion of ester group presented in the ethyl acrylate grafts into hydrazide and then hydrazone using isatin to develop modified chelating wool fibers (Fig. 5.10). The authors examined the effectiveness of these chelating wool fibers toward the adsorption of Cu^{2+}, Hg^{2+}, and Ni^{2+} ions. A greater adsorption of Cu^{2+} was observed on chelating wool fibers compared to Hg^{2+} and Ni^{2+} and this recommends their applications in the area of water treatment [192].

Han et al. [193] studied the impact of curcumin (a natural colorant) on the antimicrobial properties of wool fibers. A greater improvements in bacterial resistance was obtained for home laundering when compared to light exposure conditions. The extent of improvement was about 45% toward *S. aureus* and 30% toward *E. coli*. However, the efficacy of curcumin was poor in light conditions [193]. In another study, Smith et al. [194] established considerable shrink resistance of wool fibers through the surface modifications using polypeptides extricated from wool protein by protease [194]. A study of Jus et al. [195] reported the use of PEG-modified proteases for the surface functionalization of wool fibers. This modification created much cleaner and smoother wool fibers surface with absence of any destruction [195].

A study of Gashti et al. [196] applied nano-ZrO_2 onto the wool fiber surface with the help of a cross-linking agent, citric acid, and a catalyst, sodium hypophosphite, by the application of UV irradiation. As a result, the powerful interactions of nano-ZrO_2 with the functional groups present on the surface of wool fibers were accomplished. The coating of nano-ZrO_2 over wool fibers caused to generate a higher thermal stability on account of their magnificent thermal resistance and mass barrier properties. Also, the feasibility of modified wool fibers to use as a photocatalyst [196] was found. In another study, the authors reported the enhanced flame retardancy and electromagnetic reflections for nano-ZrO_2 coated wool fibers [197].

Yu et al. [198] reported the generation of shrink-free wool fibers through the grafting of glycerol 1,3-diglycerolate diacrylate (GDA) onto prereduced wool fibers surface. The cross-links of GDA on the reduced wool fibers surface were formed by the thiol-ene click reaction between acrylate groups in the GDA and cysteine in reduced surface of wool. The GDA-grafted wool fibers exhibited higher shrink resistance as well as wet fracture strength. Also, increase in hydrophilicity of wool fibers was

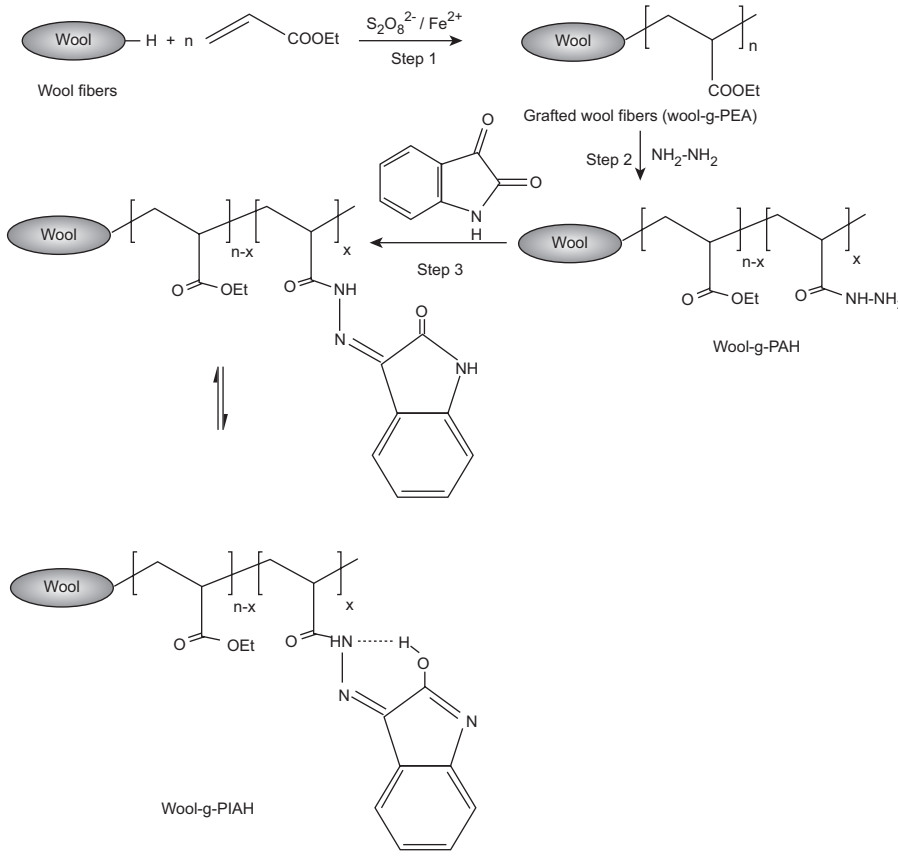

Figure 5.10 Schematic of the grafting mechanism for the preparation of wool-g-PIAH. Step 1: the reaction of wool with ethyl acrylate (EA) in the presence of potassium persulphate and Mohr's salt to form wool-g-PEA; Step 2: the addition of hydrazine hydrate into modified wool-g-PEA to form wool-g-poly(acrylic hydrazide) (wool-g-PAH); Step 3: the action of alcoholic isatin solution on wool-g-PAH to get wool-g-poly(isatin acrylic hydrazone) (wood-g-PIAH), a chelating fiber [192].

obtained [198]. In another study, Hu et al. [199] grafted thiol-acrylate quaternary ammonium salt with divinyl terminated onto prereduced wool fibers. This caused to generate excellent antibacterial and antistatic properties along with improved hydrophilicity [199]. Summary of some selected surface modification studies of natural fibers are presented in Table 5.2.

5.15 Conclusions

Nowadays, natural fibers have receiving considerable attention among academic and industrial researchers due to the growing environmental, ecological, and economical consciousness to succeed many nonbiodegradable, nonrenewable, synthetic, toxic

Table 5.2 Summary of some selected surface modification studies of natural fibers

Authors	Natural fiber	Surface modification	Achievements
Gashti et al. [29]	Cotton	Grafting fluorocarbon monomer	Improvement in hydrophobicity
Shafei et al. [33]	Cotton	Coating of ZnO and carboxymethyl chitosan	Higher antibacterial properties, UV resistance
Tragoonwichian et al. [39]	Cotton	Coating of 2-hydroxy-4-acryloyloxybenzophenone and methacryloxymethyltrimethylsilane	Water resistance, UV resistance
Gashti et al. [43]	Cotton	MWCNTs	Flame retardency
Moawia et al. [55]	Flax	Grafting of glycidyl methacrylate	Hydrophobicity, mechanical strength
Wang et al. [57]	Flax	Grafting of nano-TiO_2 in the presence of silane coupling agent	Thermomechanical properties.
Beckermann et al. [66]	Hemp	Alkali treatment using NaOH and Na_2SO_4	Tensile strength, Young's modulus, crystallinity index, thermal stability
Vukcevic et al. [79]	Hemp	Carbonization at 1000°C for 30 min using KOH	Increase in specific surface area, sorption characteristics
Gassen et al. [81]	Jute	NaOH treatment	Tensile strength, modulus
Gao et al. [85]	Jute	Pyromellitic dianhydride grafting	Adsorption capacity
Hong et al. [88]	Jute	Treatment with γ-glycidoxypropyl trimethoxy silane	Adhesion properties
He et al. [98]	Ramie	Amino silicone oil treatment	Hydrophobicity
Sajab et al. [111]	Kenaf	Esterification using citric acid	Greater absorption
Lu et al. [118]	Bamboo	Silane coupling agent	Improvement in mechanical and thermal properties
Rahman et al. [131]	Coir fiber	Grafting of ethylene dimethylacrylate	Improved physicomechanical properties
Sajab et al. [140]	Oil palm fibers	Treatment using citric acid and PEI (individual)	Increased adsorption capacity
Mohan et al. [143]	Sisal	Combined system of NaOH and clay	Mechanical, thermal and adhesion properties, water resistance
Fiore et al. [148]	Sisal	Treatment using sodium bicarbonate	Tensile strength and modulus
Lu et al. [179]	Silk	Grafting of nano-Ag	Antibacterial properties
Mohammadi et al. [189]	Wool	Grafting of chitosan	Antibacterial and antifelting characteristics
Gashti et al. [196]	Wool	Nano-ZrO_2 coating	Higher thermal stability

and costly materials with environment-friendly biodegradable, renewable, natural, nontoxic and low cost materials. The surface modifications of natural fibers are imperative to further enhancing the performance profile and also to make good compatibility with other materials. The present work discussed almost all reported studies concerning the surface modification of natural fibers using either physical or chemical techniques. In this respect, the current chapter overviewed the developments in surface modification of various natural fibers such as cotton fibers, flax fibers, hemp fibers, jute fibers, ramie fibers, kenaf fibers, bamboo fibers, coir fibers, oil palm fibers, other lignocellulosic plant fibers, silk fibers, and wool fibers. The surface modification of natural fibers was achieved through grafting of monomers/other materials, application of coating based on nano/micromaterials, incorporation of coupling agents, alkali treatments, acetylation, treatments using other chemicals, radiations/discharge from high energy sources such as UV, gamma, corona, plasma, etc., combination of either two or three abovementioned techniques, special treatments, and so on. The impact of each treatment on the surface modification of natural fibers is expressed in terms of any of the following parameters such as surface roughness, mechanical properties, water absorption, bacterial resistance, thermal stability, morphological characteristics, wetting features, adhesion properties, and so on. Also, the great influence of nature of material, technique, modifier, conditions, etc. on the extent of surface modification was observed. It could be seen that the surface modification of natural fibers was very effective to get high-performance material with nice adhesion properties.

References

[1] K.G. Satyanarayana, G.G. Arizaga, F. Wypych, Biodegradable composites based on lignocellulosic fibers—an overview, Progress in Polymer Science 34 (2009) 982–1021.
[2] F. La Mantia, M. Morreale, Green composites: a brief review, Composites Part A: Applied Science and Manufacturing 42 (2011) 579–588.
[3] M.J. John, S. Thomas, Biofibres and biocomposites, Carbohydrate Polymers 71 (2008) 343–364.
[4] T. Gurunathan, S. Mohanty, S.K. Nayak, A review of the recent developments in biocomposites based on natural fibres and their application perspectives, Composites Part A: Applied Science and Manufacturing 77 (2015) 1–25.
[5] V.K. Thakur, M.K. Thakur, Processing and characterization of natural cellulose fibers/thermoset polymer composites, Carbohydrate Polymers 109 (2014) 102–117.
[6] K.L. Pickering, M.A. Efendy, T.M. Le, A review of recent developments in natural fibre composites and their mechanical performance, Composites Part A: Applied Science and Manufacturing 83 (2016) 98–112.
[7] A. Rana, A. Mandal, S. Bandyopadhyay, Short jute fiber reinforced polypropylene composites: effect of compatibiliser, impact modifier and fiber loading, Composites Science and Technology 63 (2003) 801–806.
[8] N. Sgriccia, M. Hawley, M. Misra, Characterization of natural fiber surfaces and natural fiber composites, Composites Part A: Applied Science and Manufacturing 39 (2008) 1632–1637.

[9] J. Gassan, A.K. Bledzki, The influence of fiber-surface treatment on the mechanical properties of jute-polypropylene composites, Composites Part A: Applied Science and Manufacturing 28 (1997) 1001–1005.
[10] A. Mohanty, M. Misra, L. Drzal, Surface modifications of natural fibers and performance of the resulting biocomposites: an overview, Composite Interfaces 8 (2001) 313–343.
[11] A. Bledzki, S. Reihmane, J. Gassan, Properties and modification methods for vegetable fibers for natural fiber composites, Journal of Applied Polymer Science 59 (1996) 1329–1336.
[12] D.M. Panaitescu, C.A. Nicolae, Z. Vuluga, C. Vitelaru, C.G. Sanporean, C. Zaharia, D. Florea, G. Vasilievici, Influence of hemp fibers with modified surface on polypropylene composites, Journal of Industrial and Engineering Chemistry 37 (2016) 137–146.
[13] A. Rachini, G. Mougin, S. Delalande, J.-Y. Charmeau, C. Barrès, E. Fleury, Hemp fibers/polypropylene composites by reactive compounding: improvement of physical properties promoted by selective coupling chemistry, Polymer Degradation and Stability 97 (2012) 1988–1995.
[14] B. Singh, M. Gupta, A. Verma, Influence of fiber surface treatment on the properties of sisal-polyester composites, Polymer Composites 17 (1996) 910–918.
[15] M. Kazayawoko, J. Balatinecz, L. Matuana, Surface modification and adhesion mechanisms in woodfiber-polypropylene composites, Journal of Materials Science 34 (1999) 6189–6199.
[16] O. Faruk, A.K. Bledzki, H.-P. Fink, M. Sain, Biocomposites reinforced with natural fibers: 2000–2010, Progress in Polymer Science 37 (2012) 1552–1596.
[17] Y. Xie, C.A. Hill, Z. Xiao, H. Militz, C. Mai, Silane coupling agents used for natural fiber/polymer composites: a review, Composites Part A: Applied Science and Manufacturing 41 (2010) 806–819.
[18] E. Espino-Pérez, S. Domenek, N. Belgacem, C.C. Sillard, J. Bras, Green process for chemical functionalization of nanocellulose with carboxylic acids, Biomacromolecules 15 (2014) 4551–4560.
[19] D. Sun, G. Stylios, Investigating the plasma modification of natural fiber fabrics-the effect on fabric surface and mechanical properties, Textile Research Journal 75 (2005) 639–644.
[20] I. Sakata, M. Morita, N. Tsuruta, K. Morita, Activation of wood surface by corona treatment to improve adhesive bonding, Journal of Applied Polymer Science 49 (1993) 1251–1258.
[21] H.A. Khalil, Y. Davoudpour, M.N. Islam, A. Mustapha, K. Sudesh, R. Dungani, M. Jawaid, Production and modification of nanofibrillated cellulose using various mechanical processes: a review, Carbohydrate Polymers 99 (2014) 649–665.
[22] J. Cruz, R. Fangueiro, Surface modification of natural fibers: a review, Procedia Engineering 155 (2016) 285–288.
[23] X. Li, L.G. Tabil, S. Panigrahi, Chemical treatments of natural fiber for use in natural fiber-reinforced composites: a review, Journal of Polymers and the Environment 15 (2007) 25–33.
[24] M.K. Thakur, R.K. Gupta, V.K. Thakur, Surface modification of cellulose using silane coupling agent, Carbohydrate Polymers 111 (2014) 849–855.
[25] M.A. Sawpan, K.L. Pickering, A. Fernyhough, Effect of various chemical treatments on the fibre structure and tensile properties of industrial hemp fibres, Composites Part A: Applied Science and Manufacturing 42 (2011) 888–895.

[26] M. Pommet, J. Juntaro, J.Y. Heng, A. Mantalaris, A.F. Lee, K. Wilson, G. Kalinka, M.S. Shaffer, A. Bismarck, Surface modification of natural fibers using bacteria: depositing bacterial cellulose onto natural fibers to create hierarchical fiber reinforced nanocomposites, Biomacromolecules 9 (2008) 1643–1651.
[27] S. Gordon, Y.-L. Hsieh, Cotton: Science and Technology, Woodhead Publishing, 2006.
[28] K. Satyanarayana, J. Guimarães, F. Wypych, Studies on lignocellulosic fibers of Brazil. Part I: source, production, morphology, properties and applications, Composites Part A: Applied Science and Manufacturing 38 (2007) 1694–1709.
[29] M.P. Gashti, A. Pournaserani, H. Ehsani, M.P. Gashti, Surface oxidation of cellulose by ozone-gas in a vacuum cylinder to improve the functionality of fluoromonomer, Vacuum 91 (2013) 7–13.
[30] M.P. Gashti, A. Elahi, M.P. Gashti, UV radiation inducing succinic acid/silica–kaolinite network on cellulose fiber to improve the functionality, Composites Part B: Engineering 48 (2013) 158–166.
[31] C.K. Kang, S.S. Kim, S. Kim, J. Lee, J.-H. Lee, C. Roh, J. Lee, Antibacterial cotton fibers treated with silver nanoparticles and quaternary ammonium salts, Carbohydrate Polymers 151 (2016) 1012–1018.
[32] K. Varaprasad, G.M. Raghavendra, T. Jayaramudu, J. Seo, Nano zinc oxide–sodium alginate antibacterial cellulose fibres, Carbohydrate Polymers 135 (2016) 349–355.
[33] A.E. Shafei, A. Abou-Okeil, ZnO/carboxymethyl chitosan bionano-composite to impart antibacterial and UV protection for cotton fabric, Carbohydrate Polymers 83 (2011) 920–925.
[34] S. Selvam, M. Sundrarajan, Functionalization of cotton fabric with PVP/ZnO nanoparticles for improved reactive dyeability and antibacterial activity, Carbohydrate Polymers 87 (2012) 1419–1424.
[35] I.A. Bhatti, K.M. Zia, Z. Ali, M. Zuber, Modification of cellulosic fibers to enhance their dyeability using UV-irradiation, Carbohydrate Polymers 89 (2012) 783–787.
[36] A. Zakirov, S.U. Yuldashev, H. Wang, H. Cho, T. Kang, J. Khamdamov, A. Mamadalimov, Photoluminescence study of the surface modified and MEH-PPV coated cotton fibers, Journal of Luminescence 131 (2011) 301–305.
[37] X. Ren, L. Kou, H.B. Kocer, C. Zhu, S. Worley, R. Broughton, T. Huang, Antimicrobial coating of an N-halamine biocidal monomer on cotton fibers via admicellar polymerization, Colloids and Surfaces A: Physicochemical and Engineering Aspects 317 (2008) 711–716.
[38] S. Tragoonwichian, A. Edgar, N. Yanumet, Admicellar polymerization of 2-hydroxy-4-acryloyloxybenzophenone: the production of UV-protective cotton, Colloids and Surfaces A: Physicochemical and Engineering Aspects 329 (2008) 87–94.
[39] S. Tragoonwichian, A. Edgar, N. Yanumet, Double coating via repeat admicellar polymerization for preparation of bifunctional cotton fabric: ultraviolet protection and water repellence, Colloids and Surfaces A: Physicochemical and Engineering Aspects 349 (2009) 170–175.
[40] Z. Mao, Q. Shi, L. Zhang, H. Cao, The formation and UV-blocking property of needle-shaped ZnO nanorod on cotton fabric, Thin Solid Films 517 (2009) 2681–2686.
[41] T. Pongprayoon, N. Yanumet, A. Edgar, Admicellar polymerization of styrene on cotton, Journal of Colloid and Interface Science 249 (2002) 227–234.
[42] T. Pongprayoon, N. Yanumet, A. Edgar, W.E. Alvarez, D.E. Resasco, Surface characterization of cotton coated by a thin film of polystyrene with and without a cross-linking agent, Journal of Colloid and Interface Science 281 (2005) 307–315.

[43] M.P. Gashti, A. Almasian, UV radiation induced flame retardant cellulose fiber by using polyvinylphosphonic acid/carbon nanotube composite coating, Composites Part B: Engineering 45 (2013) 282–289.
[44] K. Jeyasubramanian, G. Hikku, A. Preethi, V. Benitha, N. Selvakumar, Fabrication of water repellent cotton fabric by coating nano particle impregnated hydrophobic additives and its characterization, Journal of Industrial and Engineering Chemistry 37 (2016) 180–189.
[45] M. Yu, G. Gu, W.-D. Meng, F.-L. Qing, Superhydrophobic cotton fabric coating based on a complex layer of silica nanoparticles and perfluorooctylated quaternary ammonium silane coupling agent, Applied Surface Science 253 (2007) 3669–3673.
[46] G.Y. Bae, B.G. Min, Y.G. Jeong, S.C. Lee, J.H. Jang, G.H. Koo, Superhydrophobicity of cotton fabrics treated with silica nanoparticles and water-repellent agent, Journal of Colloid and Interface Science 337 (2009) 170–175.
[47] L. Andreozzi, V. Castelvetro, G. Ciardelli, L. Corsi, M. Faetti, E. Fatarella, F. Zulli, Free radical generation upon plasma treatment of cotton fibers and their initiation efficiency in surface-graft polymerization, Journal of Colloid and Interface Science 289 (2005) 455–465.
[48] L. Yeqiu, H. Jinlian, Z. Yong, Y. Zhuohong, Surface modification of cotton fabric by grafting of polyurethane, Carbohydrate Polymers 61 (2005) 276–280.
[49] S. Janhom, R. Watanesk, S. Watanesk, P. Griffiths, O.-A. Arquero, W. Naksata, Comparative study of lac dye adsorption on cotton fibre surface modified by synthetic and natural polymers, Dyes and Pigments 71 (2006) 188–193.
[50] E. Takács, L. Wojnárovits, J. Borsa, J. Papp, P. Hargittai, L. Korecz, Modification of cotton-cellulose by preirradiation grafting, Nuclear Instruments and Methods in Physics Research Section B: Beam Interactions with Materials and Atoms 236 (2005) 259–265.
[51] E. Abdel-Halim, An effective redox system for bleaching cotton cellulose, Carbohydrate Polymers 90 (2012) 316–321.
[52] E. Abdel-Halim, S.S. Al-Deyab, One-step bleaching process for cotton fabrics using activated hydrogen peroxide, Carbohydrate Polymers 92 (2013) 1844–1849.
[53] M. Sumaila, A. Ibhadode, Technical properties of some plant fibres compared with glass fibre, International Journal of Engineering Research in Africa (2014) 11–26.
[54] B. Wang, S. Panigrahi, L. Tabil, W. Crerar, S. Sokansanj, L. Braun, Modification of flax fibers by chemical treatment, in: CSAE/SCGR, 2003, pp. 6–9.
[55] R.M. Moawia, M.M. Nasef, N.H. Mohamed, A. Ripin, Modification of flax fibres by radiation induced emulsion graft copolymerization of glycidyl methacrylate, Radiation Physics and Chemistry 122 (2016) 35–42.
[56] G. Dorez, B. Otazaghine, A. Taguet, L. Ferry, J. Lopez-Cuesta, Use of Py-GC/MS and PCFC to characterize the surface modification of flax fibres, Journal of Analytical and Applied Pyrolysis 105 (2014) 122–130.
[57] H. Wang, G. Xian, H. Li, Grafting of nano-TiO_2 onto flax fibers and the enhancement of the mechanical properties of the flax fiber and flax fiber/epoxy composite, Composites Part A: Applied Science and Manufacturing 76 (2015) 172–180.
[58] M. Foruzanmehr, P.Y. Vuillaume, M. Robert, S. Elkoun, The effect of grafting a nano-TiO_2 thin film on physical and mechanical properties of cellulosic natural fibers, Materials and Design 85 (2015) 671–678.
[59] M. Foruzanmehr, P.Y. Vuillaume, S. Elkoun, M. Robert, Physical and mechanical properties of PLA composites reinforced by TiO_2 grafted flax fibers, Materials and Design 106 (2016) 295–304.
[60] E. Abdel-Halim, Physiochemical properties of differently pretreated cellulosic fibers, Carbohydrate Polymers 88 (2012) 1201–1207.

[61] N. Martin, N. Mouret, P. Davies, C. Baley, Influence of the degree of retting of flax fibers on the tensile properties of single fibers and short fiber/polypropylene composites, Industrial Crops and Products 49 (2013) 755–767.
[62] M.F. Pucci, P.-J. Liotier, S. Drapier, Capillary effects on flax fibers–modification and characterization of the wetting dynamics, Composites Part A: Applied Science and Manufacturing 77 (2015) 257–265.
[63] Z. Li, X. Wang, L. Wang, Properties of hemp fibre reinforced concrete composites, Composites Part A: Applied Science and Manufacturing 37 (2006) 497–505.
[64] M. Le Troedec, D. Sedan, C. Peyratout, J.P. Bonnet, A. Smith, R. Guinebretiere, V. Gloaguen, P. Krausz, Influence of various chemical treatments on the composition and structure of hemp fibres, Composites Part A: Applied Science and Manufacturing 39 (2008) 514–522.
[65] M. Le Troëdec, A. Rachini, C. Peyratout, S. Rossignol, E. Max, O. Kaftan, A. Fery, A. Smith, Influence of chemical treatments on adhesion properties of hemp fibres, Journal of Colloid and Interface Science 356 (2011) 303–310.
[66] G. Beckermann, K.L. Pickering, Engineering and evaluation of hemp fibre reinforced polypropylene composites: fibre treatment and matrix modification, Composites Part A: Applied Science and Manufacturing 39 (2008) 979–988.
[67] K.L. Pickering, G. Beckermann, S. Alam, N.J. Foreman, Optimising industrial hemp fibre for composites, Composites Part A: Applied Science and Manufacturing 38 (2007) 461–468.
[68] M. Kostic, B. Pejic, P. Skundric, Quality of chemically modified hemp fibers, Bioresource Technology 99 (2008) 94–99.
[69] M. Kabir, H. Wang, K. Lau, F. Cardona, Effects of chemical treatments on hemp fibre structure, Applied Surface Science 276 (2013) 13–23.
[70] M. Kabir, H. Wang, K. Lau, F. Cardona, Tensile properties of chemically treated hemp fibres as reinforcement for composites, Composites Part B: Engineering 53 (2013) 362–368.
[71] M.M. Kostic, B.M. Pejic, K.A. Asanovic, V.M. Aleksic, P.D. Skundric, Effect of hemicelluloses and lignin on the sorption and electric properties of hemp fibers, Industrial Crops and Products 32 (2010) 169–174.
[72] B.M. Pejic, M.M. Kostic, P.D. Skundric, J.Z. Praskalo, The effects of hemicelluloses and lignin removal on water uptake behavior of hemp fibers, Bioresource Technology 99 (2008) 7152–7159.
[73] Y. Li, K.L. Pickering, Hemp fibre reinforced composites using chelator and enzyme treatments, Composites Science and Technology 68 (2008) 3293–3298.
[74] M. George, P.G. Mussone, D.C. Bressler, Surface and thermal characterization of natural fibres treated with enzymes, Industrial Crops and Products 53 (2014) 365–373.
[75] Y. Li, K. Pickering, R. Farrell, Analysis of green hemp fibre reinforced composites using bag retting and white rot fungal treatments, Industrial Crops and Products 29 (2009) 420–426.
[76] B. Szolnoki, K. Bocz, P.L. Sóti, B. Bodzay, E. Zimonyi, A. Toldy, B. Morlin, K. Bujnowicz, M. Wladyka-Przybylak, G. Marosi, Development of natural fibre reinforced flame retarded epoxy resin composites, Polymer Degradation and Stability 119 (2015) 68–76.
[77] M. George, P.G. Mussone, D.C. Bressler, Modification of the cellulosic component of hemp fibers using sulfonic acid derivatives: surface and thermal characterization, Carbohydrate Polymers 134 (2015) 230–239.

[78] D. Dai, M. Fan, P. Collins, Fabrication of nanocelluloses from hemp fibers and their application for the reinforcement of hemp fibers, Industrial Crops and Products 44 (2013) 192–199.
[79] M. Vukcevic, A. Kalijadis, M. Radisic, B. Pejic, M. Kostic, Z. Lausevic, M. Lausevic, Application of carbonized hemp fibers as a new solid-phase extraction sorbent for analysis of pesticides in water samples, Chemical Engineering Journal 211 (2012) 224–232.
[80] C. Stevens, J. Müssig, Industrial Applications of Natural Fibres: Structure, Properties and Technical Applications, vol. 10, John Wiley & Sons, 2010.
[81] J. Gassan, A.K. Bledzki, Possibilities for improving the mechanical properties of jute/epoxy composites by alkali treatment of fibres, Composites Science and Technology 59 (1999) 1303–1309.
[82] F. Corrales, F. Vilaseca, M. Llop, J. Girones, J. Mendez, P. Mutje, Chemical modification of jute fibers for the production of green-composites, Journal of Hazardous Materials 144 (2007) 730–735.
[83] M.K. Hossain, M.W. Dewan, M. Hosur, S. Jeelani, Mechanical performances of surface modified jute fiber reinforced biopol nanophased green composites, Composites Part B: Engineering 42 (2011) 1701–1707.
[84] Y. Karaduman, M. Sayeed, L. Onal, A. Rawal, Viscoelastic properties of surface modified jute fiber/polypropylene nonwoven composites, Composites Part B: Engineering 67 (2014) 111–118.
[85] D.-W. Gao, Q. Hu, H. Pan, J. Jiang, P. Wang, High-capacity adsorption of aniline using surface modification of lignocellulose-biomass jute fibers, Bioresource Technology 193 (2015) 507–512.
[86] Q. Hu, P. Wang, J. Jiang, H. Pan, D.-W. Gao, Column adsorption of aniline by a surface modified jute fiber and its regeneration property, Journal of Environmental Chemical Engineering 4 (2016) 2243–2249.
[87] M.S. Hassan, Removal of reactive dyes from textile wastewater by immobilized chitosan upon grafted jute fibers with acrylic acid by gamma irradiation, Radiation Physics and Chemistry 115 (2015) 55–61.
[88] C. Hong, I. Hwang, N. Kim, D. Park, B. Hwang, C. Nah, Mechanical properties of silanized jute–polypropylene composites, Journal of Industrial and Engineering Chemistry 14 (2008) 71–76.
[89] B.A. Acha, M.M. Reboredo, N.E. Marcovich, Creep and dynamic mechanical behavior of PP–jute composites: effect of the interfacial adhesion, Composites Part A: Applied Science and Manufacturing 38 (2007) 1507–1516.
[90] M.R. Rahman, M.M. Huque, M.N. Islam, M. Hasan, Improvement of physico-mechanical properties of jute fiber reinforced polypropylene composites by post-treatment, Composites Part A: Applied Science and Manufacturing 39 (2008) 1739–1747.
[91] B.K. Goriparthi, K. Suman, N.M. Rao, Effect of fiber surface treatments on mechanical and abrasive wear performance of polylactide/jute composites, Composites Part A: Applied Science and Manufacturing 43 (2012) 1800–1808.
[92] J.-M. Park, S.T. Quang, B.-S. Hwang, K.L. DeVries, Interfacial evaluation of modified Jute and Hemp fibers/polypropylene (PP)-maleic anhydride polypropylene copolymers (PP-MAPP) composites using micromechanical technique and nondestructive acoustic emission, Composites Science and Technology 66 (2006) 2686–2699.
[93] L. Tzounis, S. Debnath, S. Rooj, D. Fischer, E. Mäder, A. Das, M. Stamm, G. Heinrich, High performance natural rubber composites with a hierarchical reinforcement structure of carbon nanotube modified natural fibers, Materials and Design 58 (2014) 1–11.

[94] S. Nam, A.N. Netravali, Green composites. I. Physical properties of ramie fibers for environment-friendly green composites, Fibers and Polymers 7 (2006) 372–379.
[95] Z. Zhou, X. Liu, B. Hu, J. Wang, D. Xin, Z. Wang, Y. Qiu, Hydrophobic surface modification of ramie fibers with ethanol pretreatment and atmospheric pressure plasma treatment, Surface and Coatings Technology 205 (2011) 4205–4210.
[96] X. Liu, J. Chen, P. Sun, Z.-W. Liu, Z.-T. Liu, Grafting modification of ramie fibers with poly (2,2,2-trifluoroethyl methacrylate) via reversible addition–fragmentation chain transfer (RAFT) polymerization in supercritical carbon dioxide, Reactive and Functional Polymers 70 (2010) 972–979.
[97] X. Li, L. He, H. Zhou, W. Li, W. Zha, Influence of silicone oil modification on properties of ramie fiber reinforced polypropylene composites, Carbohydrate Polymers 87 (2012) 2000–2004.
[98] L. He, W. Li, D. Chen, D. Zhou, G. Lu, J. Yuan, Effects of amino silicone oil modification on properties of ramie fiber and ramie fiber/polypropylene composites, Materials and Design 77 (2015) 142–148.
[99] T. Yu, J. Ren, S. Li, H. Yuan, Y. Li, Effect of fiber surface-treatments on the properties of poly (lactic acid)/ramie composites, Composites Part A: Applied Science and Manufacturing 41 (2010) 499–505.
[100] K. Goda, M. Sreekala, A. Gomes, T. Kaji, J. Ohgi, Improvement of plant based natural fibers for toughening green composites—effect of load application during mercerization of ramie fibers, Composites Part A: Applied Science and Manufacturing 37 (2006) 2213–2220.
[101] J.-M. Yuan, Y.-R. Feng, L.-P. He, Effect of thermal treatment on properties of ramie fibers, Polymer Degradation and Stability 133 (2016) 303–311.
[102] L. He, X. Li, W. Li, J. Yuan, H. Zhou, A method for determining reactive hydroxyl groups in natural fibers: application to ramie fiber and its modification, Carbohydrate Research 348 (2012) 95–98.
[103] A.K. Mohanty, M. Misra, L.T. Drzal, Natural Fibers, Biopolymers, and Biocomposites, CRC Press, 2005.
[104] A.M. Edeerozey, H.M. Akil, A. Azhar, M.Z. Ariffin, Chemical modification of kenaf fibers, Materials Letters 61 (2007) 2023–2025.
[105] B. Yousif, A. Shalwan, C. Chin, K. Ming, Flexural properties of treated and untreated kenaf/epoxy composites, Materials and Design 40 (2012) 378–385.
[106] R. Mahjoub, J.M. Yatim, A.R.M. Sam, S.H. Hashemi, Tensile properties of kenaf fiber due to various conditions of chemical fiber surface modifications, Construction and Building Materials 55 (2014) 103–113.
[107] V. Fiore, G. Di Bella, A. Valenza, The effect of alkaline treatment on mechanical properties of kenaf fibers and their epoxy composites, Composites Part B: Engineering 68 (2015) 14–21.
[108] M.S. Meon, M.F. Othman, H. Husain, M.F. Remeli, M.S.M. Syawal, Improving tensile properties of kenaf fibers treated with sodium hydroxide, Procedia Engineering 41 (2012) 1587–1592.
[109] O. Asumani, R. Reid, R. Paskaramoorthy, The effects of alkali–silane treatment on the tensile and flexural properties of short fibre non-woven kenaf reinforced polypropylene composites, Composites Part A: Applied Science and Manufacturing 43 (2012) 1431–1440.
[110] M. Asim, M. Jawaid, K. Abdan, M.R. Ishak, Effect of alkali and silane treatments on mechanical and fibre-matrix bond strength of kenaf and pineapple leaf fibres, Journal of Bionic Engineering 13 (2016) 426–435.

[111] M.S. Sajab, C.H. Chia, S. Zakaria, S.M. Jani, M.K. Ayob, K.L. Chee, P.S. Khiew, W.S. Chiu, Citric acid modified kenaf core fibres for removal of methylene blue from aqueous solution, Bioresource Technology 102 (2011) 7237–7243.
[112] D.K. Mahmoud, M.A.M. Salleh, W.A.W.A. Karim, A. Idris, Z.Z. Abidin, Batch adsorption of basic dye using acid treated kenaf fibre char: equilibrium, kinetic and thermodynamic studies, Chemical Engineering Journal 181 (2012) 449–457.
[113] J. Datta, P. Kopczyńska, Effect of kenaf fibre modification on morphology and mechanical properties of thermoplastic polyurethane materials, Industrial Crops and Products 74 (2015) 566–576.
[114] K.V. Krishna, K. Kanny, The effect of treatment on kenaf fiber using green approach and their reinforced epoxy composites, Composites Part B: Engineering 104 (2016) 111–117.
[115] F.T. Wallenberger, N. Weston, Natural Fibers, Plastics and Composites, Springer Science & Business Media, 2003.
[116] W. Liu, T. Xie, R. Qiu, M. Fan, N-methylol acrylamide grafting bamboo fibers and their composites, Composites Science and Technology 117 (2015) 100–106.
[117] P. Luna, J. Lizarazo-Marriaga, A. Mariño, *Guadua angustifolia* bamboo fibers as reinforcement of polymeric matrices: an exploratory study, Construction and Building Materials 116 (2016) 93–97.
[118] T. Lu, M. Jiang, Z. Jiang, D. Hui, Z. Wang, Z. Zhou, Effect of surface modification of bamboo cellulose fibers on mechanical properties of cellulose/epoxy composites, Composites Part B: Engineering 51 (2013) 28–34.
[119] T. Lu, S. Liu, M. Jiang, X. Xu, Y. Wang, Z. Wang, J. Gou, D. Hui, Z. Zhou, Effects of modifications of bamboo cellulose fibers on the improved mechanical properties of cellulose reinforced poly (lactic acid) composites, Composites Part B: Engineering 62 (2014) 191–197.
[120] A.C. Manalo, E. Wani, N.A. Zukarnain, W. Karunasena, K.-T. Lau, Effects of alkali treatment and elevated temperature on the mechanical properties of bamboo fibre–polyester composites, Composites Part B: Engineering 80 (2015) 73–83.
[121] Y. Yu, X. Huang, W. Yu, A novel process to improve yield and mechanical performance of bamboo fiber reinforced composite via mechanical treatments, Composites Part B: Engineering 56 (2014) 48–53.
[122] A. Bismarck, A.K. Mohanty, I. Aranberri-Askargorta, S. Czapla, M. Misra, G. Hinrichsen, J. Springer, Surface characterization of natural fibers; surface properties and the water up-take behavior of modified sisal and coir fibers, Green Chemistry 3 (2001) 100–107.
[123] S.K. Saw, G. Sarkhel, A. Choudhury, Surface modification of coir fibre involving oxidation of lignins followed by reaction with furfuryl alcohol: characterization and stability, Applied Surface Science 257 (2011) 3763–3769.
[124] K. Praveen, S. Thomas, Y. Grohens, M. Mozetič, I. Junkar, G. Primc, M. Gorjanc, Investigations of plasma induced effects on the surface properties of lignocellulosic natural coir fibres, Applied Surface Science 368 (2016) 146–156.
[125] H. Gu, Tensile behaviours of the coir fibre and related composites after NaOH treatment, Materials and Design 30 (2009) 3931–3934.
[126] T.H. Nam, S. Ogihara, N.H. Tung, S. Kobayashi, Effect of alkali treatment on interfacial and mechanical properties of coir fiber reinforced poly (butylene succinate) biodegradable composites, Composites Part B: Engineering 42 (2011) 1648–1656.
[127] J. Rout, M. Misra, S. Tripathy, S. Nayak, A. Mohanty, The influence of fibre treatment on the performance of coir-polyester composites, Composites Science and Technology 61 (2001) 1303–1310.

[128] M.M. Haque, M. Hasan, M.S. Islam, M.E. Ali, Physico-mechanical properties of chemically treated palm and coir fiber reinforced polypropylene composites, Bioresource Technology 100 (2009) 4903–4906.
[129] M.N. Islam, M.R. Rahman, M.M. Haque, M.M. Huque, Physico-mechanical properties of chemically treated coir reinforced polypropylene composites, Composites Part A: Applied Science and Manufacturing 41 (2010) 192–198.
[130] M.F. Rosa, B.-S. Chiou, E.S. Medeiros, D.F. Wood, T.G. Williams, L.H. Mattoso, W.J. Orts, S.H. Imam, Effect of fiber treatments on tensile and thermal properties of starch/ethylene vinyl alcohol copolymers/coir biocomposites, Bioresource Technology 100 (2009) 5196–5202.
[131] M.M. Rahman, M.A. Khan, Surface treatment of coir (*Cocos nucifera*) fibers and its influence on the fibers' physico-mechanical properties, Composites Science and Technology 67 (2007) 2369–2376.
[132] K. Thakur, S. Kalia, D. Pathania, A. Kumar, N. Sharma, C.L. Schauer, Surface functionalization of lignin constituent of coconut fibers via laccase-catalyzed biografting for development of antibacterial and hydrophobic properties, Journal of Cleaner Production 113 (2016) 176–182.
[133] K. Thakur, S. Kalia, B. Kaith, D. Pathania, A. Kumar, P. Thakur, C.E. Knittel, C.L. Schauer, G. Totaro, The development of antibacterial and hydrophobic functionalities in natural fibers for fiber-reinforced composite materials, Journal of Environmental Chemical Engineering 4 (2016) 1743–1752.
[134] S. Shinoj, R. Visvanathan, S. Panigrahi, M. Kochubabu, Oil palm fiber (OPF) and its composites: a review, Industrial Crops and Products 33 (2011) 7–22.
[135] M. Sreekala, S. Thomas, Effect of fibre surface modification on water-sorption characteristics of oil palm fibres, Composites Science and Technology 63 (2003) 861–869.
[136] M.N. Izani, M. Paridah, U. Anwar, M.M. Nor, P.S. H'ng, Effects of fiber treatment on morphology, tensile and thermogravimetric analysis of oil palm empty fruit bunches fibers, Composites Part B: Engineering 45 (2013) 1251–1257.
[137] H. Essabir, R. Boujmal, M.O. Bensalah, D. Rodrigue, R. Bouhfid, A. el kacem Qaiss, Mechanical and thermal properties of hybrid composites: oil-palm fiber/clay reinforced high density polyethylene, Mechanics of Materials 98 (2016) 36–43.
[138] S. Kim, J.M. Park, J.-W. Seo, C.H. Kim, Sequential acid-/alkali-pretreatment of empty palm fruit bunch fiber, Bioresource Technology 109 (2012) 229–233.
[139] A.A. Mamun, H.-P. Heim, D.H. Beg, T.S. Kim, S.H. Ahmad, PLA and PP composites with enzyme modified oil palm fibre: a comparative study, Composites Part A: Applied Science and Manufacturing 53 (2013) 160–167.
[140] M.S. Sajab, C.H. Chia, S. Zakaria, P.S. Khiew, Cationic and anionic modifications of oil palm empty fruit bunch fibers for the removal of dyes from aqueous solutions, Bioresource Technology 128 (2013) 571–577.
[141] Y. Li, Y.-W. Mai, L. Ye, Sisal fibre and its composites: a review of recent developments, Composites Science and Technology 60 (2000) 2037–2055.
[142] S. Mishra, A.K. Mohanty, L.T. Drzal, M. Misra, G. Hinrichsen, A review on pineapple leaf fibers, sisal fibers and their biocomposites, Macromolecular Materials and Engineering 289 (2004) 955–974.
[143] T. Mohan, K. Kanny, Chemical treatment of sisal fiber using alkali and clay method, Composites Part A: Applied Science and Manufacturing 43 (2012) 1989–1998.
[144] J.T. Kim, A.N. Netravali, Mercerization of sisal fibers: effect of tension on mechanical properties of sisal fiber and fiber-reinforced composites, Composites Part A: Applied Science and Manufacturing 41 (2010) 1245–1252.

[145] A. Orue, A. Jauregi, U. Unsuain, J. Labidi, A. Eceiza, A. Arbelaiz, The effect of alkaline and silane treatments on mechanical properties and breakage of sisal fibers and poly (lactic acid)/sisal fiber composites, Composites Part A: Applied Science and Manufacturing 84 (2016) 186–195.
[146] M.Z. Rong, M.Q. Zhang, Y. Liu, G.C. Yang, H.M. Zeng, The effect of fiber treatment on the mechanical properties of unidirectional sisal-reinforced epoxy composites, Composites Science and Technology 61 (2001) 1437–1447.
[147] F. Zhou, G. Cheng, B. Jiang, Effect of silane treatment on microstructure of sisal fibers, Applied Surface Science 292 (2014) 806–812.
[148] V. Fiore, T. Scalici, F. Nicoletti, G. Vitale, M. Prestipino, A. Valenza, A new eco-friendly chemical treatment of natural fibres: effect of sodium bicarbonate on properties of sisal fibre and its epoxy composites, Composites Part B: Engineering 85 (2016) 150–160.
[149] J. Wei, C. Meyer, Improving degradation resistance of sisal fiber in concrete through fiber surface treatment, Applied Surface Science 289 (2014) 511–523.
[150] B. Barra, S. Santos, P. Bergo, C. Alves, K. Ghavami, H. Savastano, Residual sisal fibers treated by methane cold plasma discharge for potential application in cement based material, Industrial Crops and Products 77 (2015) 691–702.
[151] P. Krishnaiah, C.T. Ratnam, S. Manickam, Enhancements in crystallinity, thermal stability, tensile modulus and strength of sisal fibres and their PP composites induced by the synergistic effects of alkali and high intensity ultrasound (HIU) treatments, Ultrasonics Sonochemistry 34 (2017) 729–742.
[152] T. Pongprayoon, N. Yanumet, S. Sangthong, Surface behavior and film formation analysis of sisal fiber coated by poly (methyl methacrylate) ultrathin film, Colloids and Surfaces A: Physicochemical and Engineering Aspects 320 (2008) 130–137.
[153] M. Cai, H. Takagi, A.N. Nakagaito, Y. Li, G.I. Waterhouse, Effect of alkali treatment on interfacial bonding in abaca fiber-reinforced composites, Composites Part A: Applied Science and Manufacturing 90 (2016) 589–597.
[154] M. Cai, H. Takagi, A.N. Nakagaito, M. Katoh, T. Ueki, G.I. Waterhouse, Y. Li, Influence of alkali treatment on internal microstructure and tensile properties of abaca fibers, Industrial Crops and Products 65 (2015) 27–35.
[155] R. Punyamurthy, D. Sampathkumar, R.P.G. Ranganagowda, B. Bennehalli, C.V. Srinivasa, Mechanical properties of abaca fiber reinforced polypropylene composites: effect of chemical treatment by benzenediazonium chloride, Journal of King Saud University-Engineering Sciences 29 (2017) 289–294.
[156] A. Valadez-Gonzalez, J. Cervantes-Uc, R. Olayo, P. Herrera-Franco, Effect of fiber surface treatment on the fiber–matrix bond strength of natural fiber reinforced composites, Composites Part B: Engineering 30 (1999) 309–320.
[157] A. Valadez-Gonzalez, J. Cervantes-Uc, R. Olayo, P. Herrera-Franco, Chemical modification of henequen fibers with an organosilane coupling agent, Composites Part B: Engineering 30 (1999) 321–331.
[158] P. Threepopnatkul, N. Kaerkitcha, N. Athipongarporn, Effect of surface treatment on performance of pineapple leaf fiber–polycarbonate composites, Composites Part B: Engineering 40 (2009) 628–632.
[159] K. Panyasart, N. Chaiyut, T. Amornsakchai, O. Santawitee, Effect of surface treatment on the properties of pineapple leaf fibers reinforced polyamide 6 composites, Energy Procedia 56 (2014) 406–413.
[160] C. Liu, R. Sun, A. Zhang, J. Ren, Z. Geng, Structural and thermal characterization of sugarcane bagasse cellulose succinates prepared in ionic liquid, Polymer Degradation and Stability 91 (2006) 3040–3047.

[161] Y. Yue, J. Han, G. Han, G.M. Aita, Q. Wu, Cellulose fibers isolated from energycane bagasse using alkaline and sodium chlorite treatments: structural, chemical and thermal properties, Industrial Crops and Products 76 (2015) 355–363.
[162] F. Arrakhiz, M. El Achaby, K. Benmoussa, R. Bouhfid, E. Essassi, A. Qaiss, Evaluation of mechanical and thermal properties of pine cone fibers reinforced compatibilized polypropylene, Materials and Design 40 (2012) 528–535.
[163] H. Luo, G. Xiong, C. Ma, P. Chang, F. Yao, Y. Zhu, C. Zhang, Y. Wan, Mechanical and thermo-mechanical behaviors of sizing-treated corn fiber/polylactide composites, Polymer Testing 39 (2014) 45–52.
[164] B. Taallah, A. Guettala, The mechanical and physical properties of compressed earth block stabilized with lime and filled with untreated and alkali-treated date palm fibers, Construction and Building Materials 104 (2016) 52–62.
[165] W. Zahari, R. Badri, H. Ardyananta, D. Kurniawan, F. Nor, Mechanical properties and water absorption behavior of polypropylene/ijuk fiber composite by using silane treatment, Procedia Manufacturing 2 (2015) 573–578.
[166] P. Zierdt, T. Theumer, G. Kulkarni, V. Däumlich, J. Klehm, U. Hirsch, A. Weber, Sustainable wood-plastic composites from bio-based polyamide 11 and chemically modified beech fibers, Sustainable Materials and Technologies 6 (2015) 6–14.
[167] J.F. Madrid, G.M. Nuesca, L.V. Abad, Gamma radiation-induced grafting of glycidyl methacrylate (GMA) onto water hyacinth fibers, Radiation Physics and Chemistry 85 (2013) 182–188.
[168] J.F. Madrid, G.M. Nuesca, L.V. Abad, Amine functionalized radiation-induced grafted water hyacinth fibers for Pb^{2+}, Cu^{2+} and Cr^{3+} uptake, Radiation Physics and Chemistry 97 (2014) 246–252.
[169] H. Wang, X. Yao, G. Sui, L. Yin, L. Wang, Properties of *Xanthoceras sorbifolia* husk fibers with chemical treatment for applications in polymer composites, Journal of Materials Science and Technology 31 (2015) 164–170.
[170] Y. Zheng, E. Cao, Y. Zhu, A. Wang, H. Hu, Perfluorosilane treated *Calotropis gigantea* fiber: instant hydrophobic–oleophilic surface with efficient oil-absorbing performance, Chemical Engineering Journal 295 (2016) 477–483.
[171] É.J. Siqueira, V.R. Botaro, *Luffa cylindrica* fibres/vinylester matrix composites: effects of 1, 2, 4, 5-benzenetetracarboxylic dianhydride surface modification of the fibres and aluminum hydroxide addition on the properties of the composites, Composites Science and Technology 82 (2013) 76–83.
[172] R. Gong, Y. Jin, F. Chen, J. Chen, Z. Liu, Enhanced malachite green removal from aqueous solution by citric acid modified rice straw, Journal of Hazardous Materials 137 (2006) 865–870.
[173] B. Zhu, T. Fan, D. Zhang, Adsorption of copper ions from aqueous solution by citric acid modified soybean straw, Journal of Hazardous Materials 153 (2008) 300–308.
[174] L. Boopathi, P. Sampath, K. Mylsamy, Investigation of physical, chemical and mechanical properties of raw and alkali treated *Borassus* fruit fiber, Composites Part B: Engineering 43 (2012) 3044–3052.
[175] K.O. Reddy, C.U. Maheswari, M. Shukla, J. Song, A.V. Rajulu, Tensile and structural characterization of alkali treated *Borassus* fruit fine fibers, Composites Part B: Engineering 44 (2013) 433–438.
[176] O. Hakimi, D.P. Knight, F. Vollrath, P. Vadgama, Spider and mulberry silkworm silks as compatible biomaterials, Composites Part B: Engineering 38 (2007) 324–337.
[177] G. Li, H. Liu, T. Li, J. Wang, Surface modification and functionalization of silk fibroin fibers/fabric toward high performance applications, Materials Science and Engineering: C 32 (2012) 627–636.

[178] Z. Lu, M. Meng, Y. Jiang, J. Xie, UV-assisted in situ synthesis of silver nanoparticles on silk fibers for antibacterial applications, Colloids and Surfaces A: Physicochemical and Engineering Aspects 447 (2014) 1–7.
[179] Z. Lu, J. Xiao, Y. Wang, M. Meng, In situ synthesis of silver nanoparticles uniformly distributed on polydopamine-coated silk fibers for antibacterial application, Journal of Colloid and Interface Science 452 (2015) 8–14.
[180] M. Meng, H. He, J. Xiao, P. Zhao, J. Xie, Z. Lu, Controllable in situ synthesis of silver nanoparticles on multilayered film-coated silk fibers for antibacterial application, Journal of Colloid and Interface Science 461 (2016) 369–375.
[181] S. Xu, S. Chen, F. Zhang, C. Jiao, J. Song, Y. Chen, H. Lin, Y. Gotoh, H. Morikawa, Preparation and controlled coating of hydroxyl-modified silver nanoparticles on silk fibers through intermolecular interaction-induced self-assembly, Materials and Design 95 (2016) 107–118.
[182] S. Xu, J. Song, H. Morikawa, Y. Chen, H. Lin, Fabrication of hierarchical structured Fe_3O_4 and Ag nanoparticles dual-coated silk fibers through electrostatic self-assembly, Materials Letters 164 (2016) 274–277.
[183] S. Davarpanah, N.M. Mahmoodi, M. Arami, H. Bahrami, F. Mazaheri, Environmentally friendly surface modification of silk fiber: chitosan grafting and dyeing, Applied Surface Science 255 (2009) 4171–4176.
[184] M.-R. Buga, C. Zaharia, M. Bălan, C. Bressy, F. Ziarelli, A. Margaillan, Surface modification of silk fibroin fibers with poly (methyl methacrylate) and poly (tributylsilyl methacrylate) via RAFT polymerization for marine antifouling applications, Materials Science and Engineering: C 51 (2015) 233–241.
[185] W. Wei, Y. Zhang, Y. Zhao, H. Shao, X. Hu, Studies on the post-treatment of the dry-spun fibers from regenerated silk fibroin solution: post-treatment agent and method, Materials and Design 36 (2012) 816–822.
[186] L. Bai, L. Zhu, S. Min, L. Liu, Y. Cai, J. Yao, Surface modification and properties of *Bombyx mori* silk fibroin films by antimicrobial peptide, Applied Surface Science 254 (2008) 2988–2995.
[187] A.P. Negri, H. Cornell, D.E. Rivett, The modification of the surface diffusion barrier of wool, Journal of the Society of Dyers and Colourists 109 (1993) 296–301.
[188] S. Vilchez, A. Manich, P. Jovancic, P. Erra, Chitosan contribution on wool treatments with enzyme, Carbohydrate Polymers 71 (2008) 515–523.
[189] M. Ranjbar-Mohammadi, M. Arami, H. Bahrami, F. Mazaheri, N.M. Mahmoodi, Grafting of chitosan as a biopolymer onto wool fabric using anhydride bridge and its antibacterial property, Colloids and Surfaces B: Biointerfaces 76 (2010) 397–403.
[190] V.G. Dev, J. Venugopal, S. Sudha, G. Deepika, S. Ramakrishna, Dyeing and antimicrobial characteristics of chitosan treated wool fabrics with henna dye, Carbohydrate Polymers 75 (2009) 646–650.
[191] G.A. Roberts, F.A. Wood, A study of the influence of structure on the effectiveness of chitosan as an anti-felting treatment for wool, Journal of Biotechnology 89 (2001) 297–304.
[192] M. Monier, D. Ayad, A. Sarhan, Adsorption of Cu (II), Hg (II), and Ni (II) ions by modified natural wool chelating fibers, Journal of Hazardous Materials 176 (2010) 348–355.
[193] S. Han, Y. Yang, Antimicrobial activity of wool fabric treated with curcumin, Dyes and Pigments 64 (2005) 157–161.
[194] E. Smith, J. Shen, Surface modification of wool with protease extracted polypeptides, Journal of Biotechnology 156 (2011) 134–140.

[195] S. Jus, M. Schroeder, G.M. Guebitz, E. Heine, V. Kokol, The influence of enzymatic treatment on wool fibre properties using PEG-modified proteases, Enzyme and Microbial Technology 40 (2007) 1705–1711.
[196] M.P. Gashti, A. Almasian, Citric acid/ZrO_2 nanocomposite inducing thermal barrier and self-cleaning properties on protein fibers, Composites Part B: Engineering 52 (2013) 340–349.
[197] M.P. Gashti, A. Almasian, M.P. Gashti, Preparation of electromagnetic reflective wool using nano-ZrO_2/citric acid as inorganic/organic hybrid coating, Sensors and Actuators A: Physical 187 (2012) 1–9.
[198] D. Yu, J.Y. Cai, J.S. Church, L. Wang, Click chemistry modification of natural keratin fibers for sustained shrink-resist performance, International Journal of Biological Macromolecules 78 (2015) 32–38.
[199] Y. Hu, W. Wang, L. Xu, D. Yu, Surface modification of keratin fibers through step-growth dithiol-diacrylate thiol-ene click reactions, Materials Letters 178 (2016) 159–162.

This page intentionally left blank

Polymer composites with functionalized natural fibers

6

Anish M. Varghese, Vikas Mittal
The Petroleum Institute, Abu Dhabi, United Arab Emirates

6.1 Introduction

Natural fiber–reinforced polymer composites have been received considerable procurement in the research areas of polymer science and technology in the last few years due to the raising disquiet about the environmental, social, and economical issues of synthetic reinforcements such as glass fibers, carbon fibers, and aramid fibers. Natural fibers offer superior environmental performances along with good mechanical properties in cheap cost when compared to conventional synthetic fibers [1,2]. The unique features of natural fibers are biodegradable, combustible, nontoxic, precise mechanical properties such as strength, stiffness, toughness, and flexibility, free from corrosion as well as fatigue, nominal damage to processing machineries, lightweight, economical, easily accessible, acceptable fiber aspect ratio, fine surface finish, and so on [3–6].

Natural fibers are fibrous polymeric composite materials originated from the renewable sources such as plants and animals and thus they are considered as green fibers having thoroughly elucidated structure [7,8]. The main constituent of plant fibers is cellulose, whereas animal fibers are made up of proteins. Plant fibers also known as lignocellulosic fibers sourced from any part of plants such as bark, wood, leaf, seed, fruit, vegetable, straw, bagasse, root, and so on [9–11]. In addition to cellulose, other constituents of plant fibers are hemicellulose, lignin, pectin, and waxes. The composition of each component in the plant fibers varies depends on source, age, and preprocessing step [12,13]. So far, many plant fibers such as flax [14], jute [15,16], hemp [17], kenaf [18], ramie [19], banana [20], sisal [21,22], cotton [23], oil palm [24], and coir [25] have been reported as reinforcing agent for polymers. Another strong member of natural fibers fraternity is animal fiber and this class comprises silk [26], wool/hair [27,28], etc. Besides protein, silk contains sericin and wool contains keratin, and also some other constituents are present in small amount [29].

Even though the primacy of natural fibers is the polymer composite composition, the structural features of these biofibers also present some downside. Important among these include unsatisfactory adhesion with hydrophobic/polar polymer due to the pitiful wettability of biofibers; greater susceptibility to water/moisture resulted from the strong propensity of cellulose to form hydrogen bonding with hydroxyl in the open air; liable to thermal degradation when processed at the melting temperature polymers because of the superior heat susceptivity; possibility of shrinkage caused by the bacterial growth resulted from the greater water sensitivity [30–35].

Biodegradable and Biocompatible Polymer Composites. http://dx.doi.org/10.1016/B978-0-08-100970-3.00006-7

To achieve high performances of natural fiber–reinforced composites, numerous studies have been reported concerning the functionalization of natural fibers. Generally, the techniques used for the functionalization of natural fibers come under the categories of physical and chemical modifications. The ultimate goal of each functionalization technique belongs to any of the following aspects such as improvement in polymer interactions, wettability, moisture/water resistance, antibacterial properties, thermal stability, mechanical properties, and so on [30,36,37]. The treatments such as stretching, calendaring, thermotreatment, electronic discharge from corona and plasma sources, and formation of hybrid yarns are used to physically functionalize the surface and structural features of natural fibers without altering the chemical structure [9,33,38–41]. The functionalization using chemical techniques such as silylation, alkalization, acetylation, carboxymethylation, maleated coupling, grafting copolymerization, cross-linking, functional coatings, and enzyme treatment creates unchangeable appearance on the surface of fibers through either changing the crystalline structure or removing the noncellulosic constituents [37,42–46]. The goal of this study is to summarize the studies concerning the developments in functionalized natural fiber–based polymer composites and also to evaluate the influence of functionalization of natural fibers on the performances of resultant composites.

6.2 Functionalized jute fiber–reinforced polymer composites

Jute fibers are sourced from the genus of *Corchorus* and considered as one of the strongest lignocellulosic vegetable bast fibers. The usual advantages of natural fibers along with very inexpensiveness of these fibers drive their feasibility to generate lightweight eco-friendly biocomposites [35,47]. To conquer the difficulties relating the water absorption and the mechanical performances of jute fibers, functionalization acquired more interest. Polymer matrices such as epoxy resin, polypropylene (PP), poly(lactic acid) (PLA), natural rubber (NR), and biopol are reported to have reinforced with the help of functionalized jute fibers.

Gassan et al. [48] reported the preparation of epoxy composites with NaOH-functionalized jute fibers. The functionalization of jute fibers had no marked impact on the improvement in interfacial interactions with epoxy matrix. At the same time, improved mechanical features of jute fibers caused to enhance the strength and the stiffness of the resultant composite. About 20% higher Young's modulus was observed for epoxy composite based on NaOH-treated jute fibers when compared to composites based on untreated jute fibers. Unfortunately, the fatigue resistance of composites showed a slight reduction after NaOH treatment of jute fibers [48].

In another study, Gassan et al. [49] reported the modifications of jute fibers using maleic anhydride–grafted PP to strengthen the matrix of PP. An improved interfacial interactions of fibers and PP matrix after the functionalization of fibers were observed. This correspondingly caused to enhance flexural strength and dynamic strength of resultant composite [49]. Acha et al. [50] made use of alkenyl succinic anhydride–esterified

jute fibers to prepare composites with PP possessing higher interfacial bonding [50]. A study of Hong et al. [51] used silanized jute fibers to make composite with PP, and as a result, an improved interfacial bonding degree was observed. This subsequently increased the dynamic mechanical features and the tensile strength of PP/silanized jute fiber composite. Fig. 6.1 demonstrates schematic of reaction mechanism in a PP composite comprised of silane-treated jute fibers [51].

With an aim to enrich the bonding degree of jute fibers on PP matrix in the composite, Karaduman et al. [52] reported alkali treatment of jute fibers. Functionalization of jute fibers led to the generation of homogeneous composite structure. The resultant composite presented improved dynamic mechanical properties [52]. In another study, Sayeed et al. [53] observed enhancement in tensile and flexural moduli for PP/jute fiber composite made up of alkali-treated jute fibers [53]. Park et al. [54] compared the influence of alkaline- and silane-modified jute fibers on PP, and also the impact of a compatibilizer, maleated PP, was investigated. Both treatments were caused to increase the surface energy of PP, but it was strong in the case of composites containing alkaline-treated jute fibers due to the removal of noncellulosic constituents from fiber surface. The addition of small amount of maleated PP created further enhancement in surface energy [54].

Rahman et al. [55] functionalized the jute fibers surface through oxidation using sodium periodate solution and used to develop composite with PP, and also the influence of posttreatment by urotropine was evaluated. SEM images (Fig. 6.2) reveal the enhanced interactions of jute fibers on PP matrix after the functionalization of fibers. The enriched Young's modulus, flexural strength, flexural modulus, impact strength, and hardness for PP/oxidized jute fibers composite were observed but unfortunately, the tensile strength decreased. The peak properties

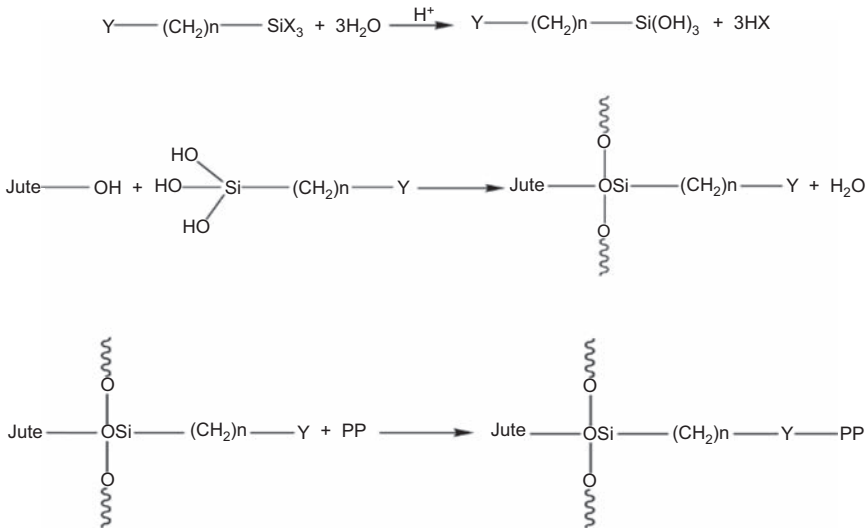

Figure 6.1 Schematic of reaction mechanism in a polypropylene composite comprised of silane-treated jute fibers [51].

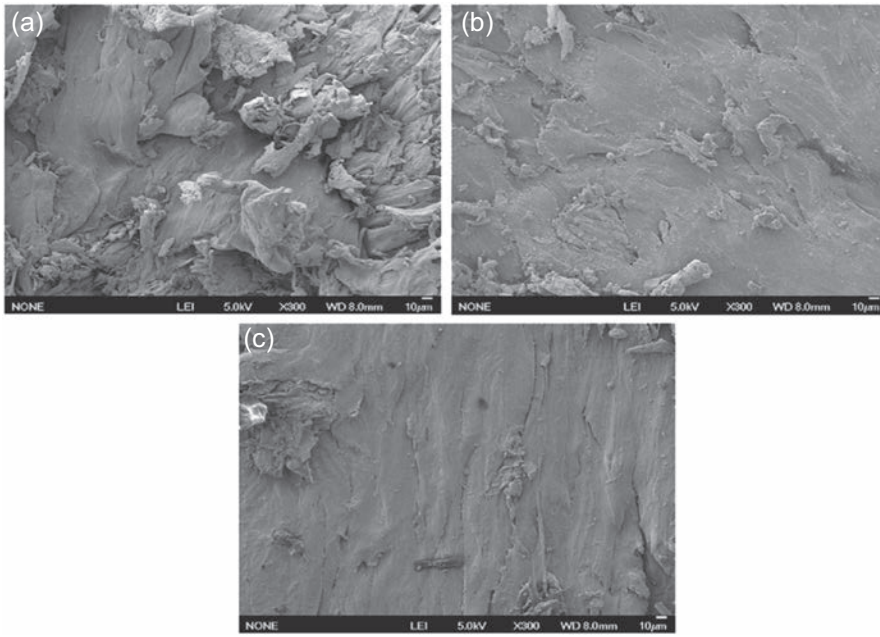

Figure 6.2 SEM images of polypropylene (PP) composites with 30 wt% of (a) untreated jute fibers and (b) 30 wt% oxidized jute fibers and (c) posttreated PP/30 wt% oxidized jute fiber composite [55].

were reported for composite comprised of 30 wt% oxidized fibers. The posttreatment of composite was useful to further enhance these properties and also to recuperate tensile strength [55].

Goriparthi and coworkers [56] studied the individual effect of alkali-, permanganate-, peroxide-, and silane-functionalized jute fibers on PLA. All treatments were effective to enrich the interface bonding of jute fibers on PLA matrix and consequently enhanced the tensile and the flexural properties of resultant composite. But unfortunately, the impact strength of composites presented a decreasing tendency after jute fiber modification. Moreover, PLA composites with silane-functionalized jute fiber exhibited an optimal resistance toward thermal degradation as well as abrasive wear [56].

Hossain et al. [57] reported a series of chemical treatments such as detergent washing, dewaxing, alkalization, and acetylation on jute fibers to functionalize their surface and thereby to improve the adhesion degree with biopol (poly(3-hydroxybutyrate-co-3-hydroxyvalerate)). The existence of strong bonding degree between biopol and jute fibers was obtained after series of chemical treatments, which was attributed to the creation of much rougher surface and the enlarged surface area of fibers. The composite consists of biopol and functionalized jute fibers exhibited higher modulus, flexural strength, and dynamic modulus than composites based on unmodified fibers. Also, the intensity of these properties was improved through the incorporation of nanoclay [57].

A study of Tzounis et al. [58] made functionalization of jute fibers through coating of multiwalled carbon nanotubes (MWCNTs) over the surface and then used to make composite with NR. The functionalization of jute fibers using MWCNTs created an excellent interfacial bonding with NR matrix through mechanical interlocking mechanism. This consequently improved tensile strength, tensile modulus, and thermal stability of composite [58].

6.3 Functionalized hemp fiber–reinforced polymer composites

Hemp fiber is one of the dominant classes of bast natural fibers, commonly procured from the hemp plant with the species of *Cannabis*. The common features of natural fibers along with inherent mechanical, thermal, and acoustic properties of hemp fibers make them beneficial for reinforcements in polymer composite materials [35,59,60]. Till now, matrices of PP and epoxy resin are reinforced using functionalized hemp fibers developed through chemical treatments, silanization, fungal treatment, chelator grafting, and so on.

Elkhaoulani et al. [61] made use of NaOH-treated hemp fibers to PP composite along with a compatibilizer, maleic anhydride–grafted styrene-ethylene-butene-styrene-block copolymer (SEBS-g-MA). The existence of strong interfacial adhesion of alkali-treated fibers on the PP matrix was observed even in the absence of compatibilizer and exhibited about 50% enhancement in Young's modulus. The addition of compatibilizer caused to further increase of 20% in Young's modulus of composite [61]. A study of Pickering et al. [62] obtained the enhanced tensile strength of 47.2 MPa and Young's modulus of 4.88 GPa for composites composed of PP, 3 wt% of maleated PP, and 40 wt% of 10% NaOH-treated hemp fibers [62]. Sgriccia et al. [34] reported greater water absorption for alkali-treated hemp fiber–based PP composite than that of silane-treated and untreated hemp fiber–based PP composites [34]. A study of Park et al. [54] observed greater surface energy for PP composite with alkaline-treated hemp fibers when compared to silane-treated one [54].

In another study, Beckermann et al. [63] reported the effects of chemical treatments using 10 wt% NaOH followed by combination of 5 wt% NaOH and 2 wt% Na_2SO_3 of hemp fibers on PP matrix. Also the effect of a compatibilizer, maleic anhydride–grafted PP, was studied. As expected, enhanced wetting of fibers on PP matrix was noted, which correspondingly caused to improve the interactions between hemp fiber and PP matrix. The maximum value of tensile strength and Young's modulus was reported for composite containing 40 wt% of modified fiber and 4 wt% of compatibilizer [63].

A study of Li et al. [64] fabricated composite containing PP matrix and chelator (ethylene diamine tetra methylene phosphonic acid pentasodium salt)-functionalized hemp fibers. The vigorous interactions of chelator-functionalized hemp fibers on the PP matrix were attained. An interesting thing is that the tensile strength of composites was increased with increase in chelator concentrations in the functionalized hemp fibers and an increase of up to 19% was observed [64].

To improve interfacial adhesion with PP, Li et al. [65] made functionalization of hemp fibers using white rot fungi *Schizophyllum commune*. Increased interfacial

adhesion between PP and functionalized hemp fibers created an improvement of 28% in tensile strength [65].

Panaitescu et al. [66] made a comparative study based on the effect of potassium permanganate (KP)- and γ-methacryloxypropyltrimethoxysilane (MPS)-functionalized hemp fibers on PP matrix. Both modifications of hemp fibers were effective to enhance the modulus of elasticity of resultant composites. About 69% and 67% increase in modulus of elasticity for PP composites based on respective KP- and MPS-functionalized hemp fibers were recorded [66].

Szolnoki et al. [67] developed a composite of epoxy resin with hemp fibers individually functionalized using phosphoric acid and aminosilane coupling agent with an objective to enrich flame retardancy. The great influence of phosphoric acid–modified hemp fibers to enhance the flame retardancy of epoxy was observed when compared with aminosilane-modified one [67]. Table 6.1 demonstrates the summary of some selected studies concerning the effect of functionalized hemp fibers on polymers.

Table 6.1 Summary of some selected studies concerning the effect of functionalized hemp fibers on polymers

Authors	Polymer matrix	Functionalization method	Major achievements
Elkhaoulani et al. [61]	Polypropylene (PP)	NaOH treatment	Strong interfacial adhesion degree and increase in Young's modulus
Pickering et al. [62]	PP	NaOH treatment	Increase in tensile strength and Young's modulus
Beckermann et al. [63]	PP	Combination of NaOH and Na_2SO_3 treatments	Improvement in interactions, tensile strength, and Young's modulus
Li et al. [64]	PP	Chelator functionalization	Increase in interactions and tensile strength
Li et al. [65]	PP	Fungal treatment	Increase in interfacial interactions and tensile strength
Panaitescu et al. [66]	PP	Individual treatment using potassium permanganate and silane compound	Enhancement in modulus of elasticity
Szolnoki et al. [67]	Epoxy resin	Individual treatment with phosphoric acid and aminosilane coupling agent	Increase in flame retardancy

6.4 Functionalized kenaf fiber–reinforced polymer composites

Kenaf fibers are derived from bast as well as core of plants with the genus *Hibiscus* and around 300 species. These fibers are also considered as vastly accepted natural fibers from the plant family of Malvaceae. Besides the usual natural fiber features such as lightweight, low cost, nonabrasiveness, combustibility, nontoxicity, and biodegradability, kenaf fiber exhibits excellent flexural strength and magnificent tensile strength [35,68,69]. To broaden the polymer composite reinforcing applications of these fibers, functionalization got keen interest. As per reported studies, functionalized kenaf fibers have made to reinforce polymer matrices of polyurethane (PU), PP, epoxy resin, and polyester.

Datta et al. [70] reported the functionalization of kenaf fibers through various chemical routes using acetic acid, blocked isocyanate, maleic anhydride, and KP and then used to fabricate composites with PU thermoplastic. SEM analysis revealed that the existence of much beneficial interaction of KP-modified kenaf fibers with PU matrix. The existence of great dynamic properties was noted for composites consist of acetic acid–modified and KP-modified kenaf fibers. Composites comprised of 10 wt% of functionalized fibers exhibited good comprehensive enhancement in characteristics such as tensile properties, resilience, hardness, and resistance to water. It was found that further increase in fiber content caused to strengthen hardness of composite, whereas tensile strength, resilience, and water resistance of composites weakened. The water uptake behavior of PU composites with untreated and treated kenaf fibers is shown in Fig. 6.3 [70].

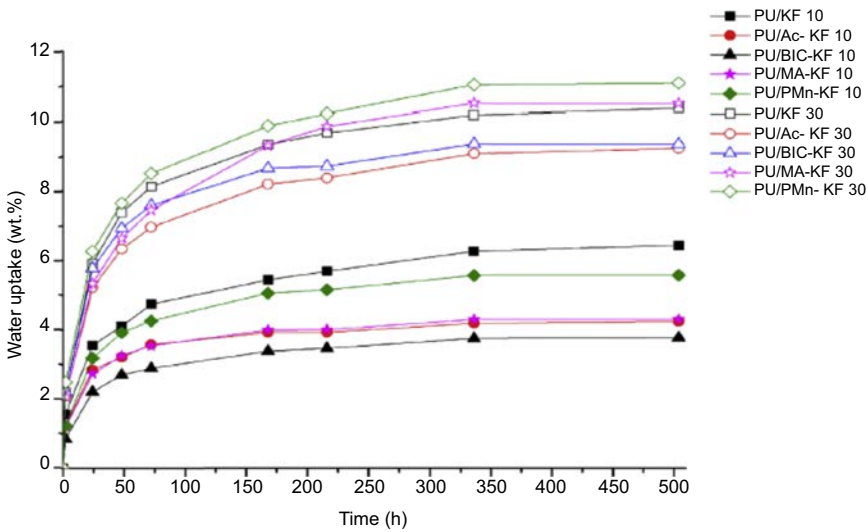

Figure 6.3 Water uptake behavior of polyurethane (PU) composites with 10 and 20 wt% of untreated (PU/KF 10 and PU/KF 30) and treated acetic acid (PU/Ac-KF 10 and PU/Ac-KF 30), blocked isocyanate (PU/BIC-KF 10 and PU/BIC-KF 30), maleic anhydride (PU/MA-KF 10 and PU/MA-KF 30), and potassium permanganate (PU/PMn-KF 10 and PU/PMn-KF 30) kenaf fibers [70].

A study of Xia et al. [71] made use of nano-magnesium carbonate (nano-$MgCO_3$)–infused kenaf fibers under high pressure to develop composite with polyester through vacuum-assisted resin transfer process. The increase in the yield of nano-$MgCO_3$ on kenaf fibers under higher pressure was observed. The occupancy of nano-$MgCO_3$-infused kenaf fibers on polyester matrix created the improvement of up to 277% in mechanical properties and a reduction of about 64% in water absorption [71].

Asumani et al. [72] prepared PP/functionalized kenaf fiber composites, and also the effect of functionalization of kenaf fibers by NaOH and combination of NaOH and 3-aminopropyltriethoxysilane on the mechanical properties of PP was established. It was observed that the existence of peak mechanical properties for composite composed of NaOH–silane modified kenaf fibers due to the strong adhesion of fibers on the matrix of PP. The composites of PP with 30 wt% of kenaf fibers exhibited almost similar mechanical features as that of PP composite composed of glass fiber (Fig. 6.4) [72]. A study of Meon et al. [73] applied NaOH-treated kenaf fibers on PP/3 wt% maleated PP and polyethylene (PE)/3 wt% maleated PE blend matrices to develop composites with upgraded interfacial bonding and tensile properties [73].

Fiore et al. [74] investigated the reinforcing effect of NaOH treatment of kenaf fibers on epoxy matrix. The generation improved compatibility between kenaf fiber and epoxy matrix, which caused to enrich the mechanical performances of composite. It was noticed that an improved modulus for composite consists of alkali-treated hemp fibers and its magnitude was more intensified in the case of composites with unidirectional layer of fibers. Moreover, the alkali treatment of kenaf fibers caused to reposition the tan δ peaks of composite to greater temperature along with lowering of magnitude [74]. In another study, Krishna et al. [75] utilized glutamic acid as well as lysine-modified kenaf fibers to reinforce epoxy resin. Both functionalized fibers presented increased adhesion degree on epoxy matrix and their intensities were

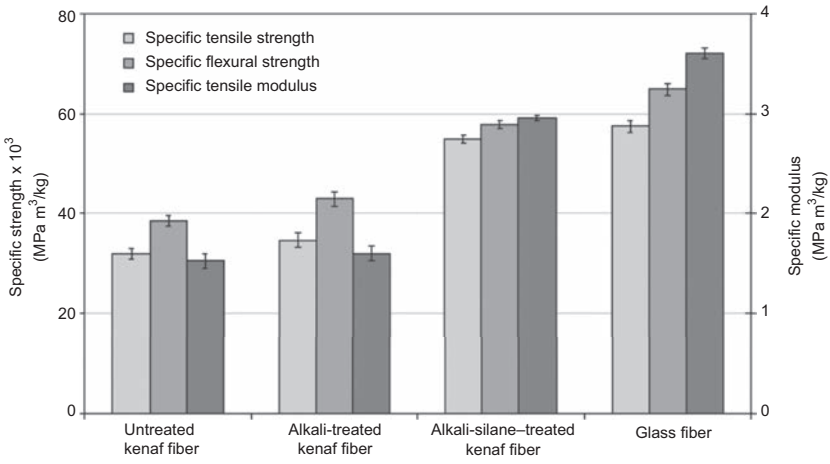

Figure 6.4 Comparison of specific mechanical properties of polypropylene (PP) composites comprised of untreated, alkali-treated and alkali–silane-treated kenaf fibers with PP/glass fiber composite [72].

quiet higher in the case of lysine-functionalized kenaf fibers. The enriched static and dynamic mechanical properties were observed for composites composed of glutamic acid as well as lysine-modified kenaf fibers [75]. Yousif et al. [76] reported the preparation of composite composed of epoxy resin and NaOH-functionalized kenaf fibers. Alkali treatment of fibers was beneficial to enhance the interfacial bonding with epoxy matrix and the porosity of resultant composite, which consequently caused to generate superlative properties. SEM images of cross-sectioned PP composites with untreated and alkalized kenaf fibers are demonstrated in Fig. 6.5, which underlined the existence of strong bonding between fibers and epoxy matrix after functionalization. The flexural strength of alkali-treated kenaf fiber–reinforced composite was 16% higher than one based on unmodified fiber [76]. Table 6.2 presents the summary of some selected studies concerning the effect of functionalized kenaf fibers on polymers.

6.5 Functionalized flax fiber–reinforced polymer composites

Flax fibers are much extensively used bast natural fibers with the binomial name *Linum usitatissimum*. These fibers are well suited for composite reinforcement as well as specific fiber applications due to the special features such as low density and outstanding mechanical properties, predominantly modulus [35,77–79]. Functionalization of flax fibers received keen research interest to intensify their interactions with polymer matrices and thereby related properties of resultant composite structure. So far, the functionalized flax fibers are mainly used to strengthen PLA and epoxy resin via graft polymerization or chemical treatment.

Foruzanmehr et al. [80] developed PLA composite using TiO_2-grafted flax fibers and obtained an enhanced interfacial adhesion between PLA and modified flax fibers. The oxidation of flax fibers before TiO_2 grafting was helpful to enhance the

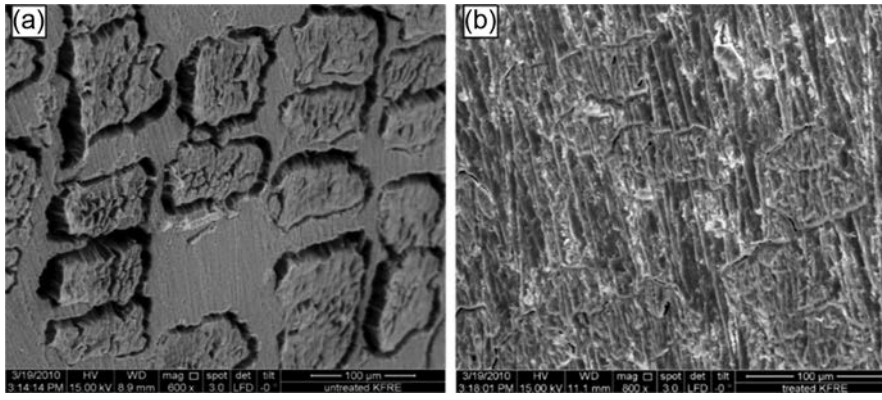

Figure 6.5 SEM images of cross-sectioned polypropylene (PP) composites with (a) untreated and (b) alkalized kenaf fibers [76].

Table 6.2 Summary of some selected studies concerning the effect of functionalized kenaf fibers on polymers

Authors	Polymer matrix	Functionalization method	Major achievements
Dutta et al. [70]	Polyurethane	Potassium permanganate treatment	Strong interfacial interactions and good dynamic properties
		Acetic acid treatment	Reduction in water absorption
Xia et al. [71]	Polyester resin	Infusion of nano-$MgCO_3$	Improvement in mechanical features and reduction in water uptake
Asumani et al. [72]	Polypropylene	NaOH–silane treatment	Good adhesion and increase in mechanical properties
Fiore et al. [74]	Epoxy resin	NaOH treatment	Increase in bonding and modulus
Krishna et al. [75]	Epoxy resin	Individual treatment using glutamic acid and lysine	Increase in adhesion degree and dynamic mechanical properties
Yousif et al. [76]	Epoxy resin	NaOH treatment	Improved adhesion degree and flexural strength

interactions with PLA matrix. Increased thermal stability and decreased water absorption for PLA composite based on TiO_2-grafted flax fibers were reported. An increase of about three times in impact strength was noted for modified flax fiber–based PLA composite. Also, the tensile strength of PLA/flax fiber composite was improved after modification of flax fibers [80].

In another study, Wang et al. [81] reported the impact of nano-TiO_2-grafted flax fibers on epoxy resin. The interactions between nano-TiO_2 and flax fibers were improved through the use of silane coupling agent. A marked improvement of 41% in interfacial shear strength on the matrix of epoxy was accomplished. It was believed that the presence of nano-TiO_2 and the existence of Ti—Si—O and C—O—Si linkages on the surface of flax fibers caused to improve the interaction degree and thereby performances. The tensile strength of resultant composite was improved by about 23% [81].

Yan et al. [82] functionalized the surface of flax fibers using 5 wt% of NaOH for 30 min with an aim to enrich the interfacial interactions with epoxy resin. The treatment of flax fibers caused to enhance the interfacial interactions with epoxy resin, which correspondingly increased the tensile strength to about 22% and the flexural strength to about 16% [82]. In another study, Triki et al. [83] also observed powerful adhesion of flax fibers on epoxy matrix after alkali treatment [83].

6.6 Functionalized ramie fiber–reinforced polymer composites

Ramie fibers are considered as one of the easily accessible strong bast fibers with the genus of *Boehmeria* under the family of Urticaceae. Compared to other natural fibers, these fibers have long durability and higher cellulose content [84]. To alleviate the difficulties of ramie fibers in the matrices of polymers such as PP and PLA, functionalization received great interest.

He et al. [85] made use of amino silicone oil–modified ramie fibers to generate composite with PP. Amino silicone–modified fibers exhibited good adhesion degree with PP, which correspondingly caused to exhibit greater mechanical properties. As a result, the optimal improvement of 16% in tensile strength, 7% in flexural strength, and 37% in impact strength was reported for resultant composite. Also, the modification of fibers created a reduction in water absorption degree [85]. In another study, Li et al. [86] investigated the role of epoxy silicone oil–modified ramie fibers on PP matrix. SEM analysis revealed the existence of beneficial interactions between PP matrix and functionalized ramie fibers. It was observed that the impact strength is increased by 17%, tensile strength by 27%, and elongation at break by 196% for modified ramie fiber–based PP composite. Further, PP composite with modified ramie fiber generated an improved thermal stability (Fig. 6.6) [86].

A study of Yu et al. [87] reported the functionalization of ramie fibers with the help of NaOH and two silane coupling agents such as 3-aminopropyltriethoxysilane and

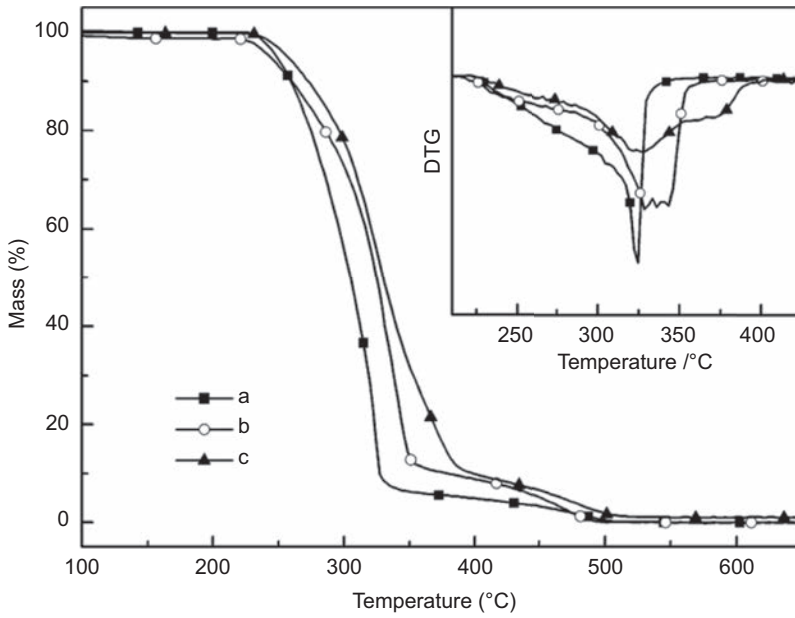

Figure 6.6 Thermogravimetric analysis thermograms of (a) polypropylene (PP) and PP composites with 30 wt% of (b) unmodified and (c) silicone oil modified ramie fibers [86].

γ-glycidoxypropyltrimethoxy silane and then the application of these functionalized fibers to generate composite with PLA. All functionalizations of ramie fibers resulted in powerful bonding of fibers on PLA matrix, which consequently increased tensile, impact, and flexural strength and dynamic mechanical properties. Moreover, the existence of enhanced thermal degradation resistance and Vicat softening temperature was reported for functionalized fiber-based PLA composite [87]. In another study, Yuan et al. [88] observed beneficial interfacial interaction of thermally treated ramie fibers at 200°C onto epoxy matrix [88].

6.7 Functionalized sisal fiber–reinforced polymer composites

Sisal fiber is a widely accepted biocellulose fiber comprised of about 65% cellulose, 12% hemicellulose, 10% lignin, 0.8% pectin, 0.3% wax, and some other water soluble constituents. These stiff fibers are sourced from the leaves of sisal plants with the scientific name *Agave sisalana* through decortication [35,89,90]. According to previous studies, functionalized sisal fibers are applied to polymer matrices of PP, PLA, polyester, epoxy resin, phenolic resin, and soy protein resin to enrich their performances.

To enhance the interfacial adhesion of sisal fibers on polyester matrix, Sreekumar et al. [91] investigated the role of various treatments such as mercerization, permanganate treatment, benzoylation, silanization, and thermal treatment at 100°C. All treatments of sisal fibers resulted in enhancement in interfacial bonding with polyester matrix, which consequently increased the tensile and the flexural performances. The enhancement of 36% in tensile strength and 53% in Young's modulus for composites composed of mercerized sisal fibers was observed. A rise of 25% in flexural strength was obtained for permanganate-treated fiber–based composite. As unexpected, all treatments of fibers caused to decrease the impact strength of composites. The water affinity of composites was reduced after fiber treatment using all abovementioned methods [91]. Sangthong et al. [92] reported the functionalization of sisal fiber surface by methyl methacrylate (MMA) coating via admicellar polymerization with an objective to upgrade the bonding degree on polyester resin and thereby mechanical performances. The presence of functionalized fibers in the polyester composite caused to exhibit intensified tensile and flexural performances, hardness, and impact strength, and these properties were optimal for composite containing 30 vol% of fibers. Fig. 6.7 presents variation in impact strength and hardness of polyester/sisal fiber composites with amount of MMA used to functionalize sisal fibers and amount of fiber [92].

Barreto et al. [93] made use of NaOH and subsequent sodium hypochlorite–treated sisal fibers to reinforce phenolic resin prepared using cashew nut shell liquid. As a result of fiber treatment, the composite presented an improvement in thermal stability and composite made of 10% NaOH-treated sisal fibers showed 15°C higher initial thermal degradation temperature than composite composed of untreated fibers [93].

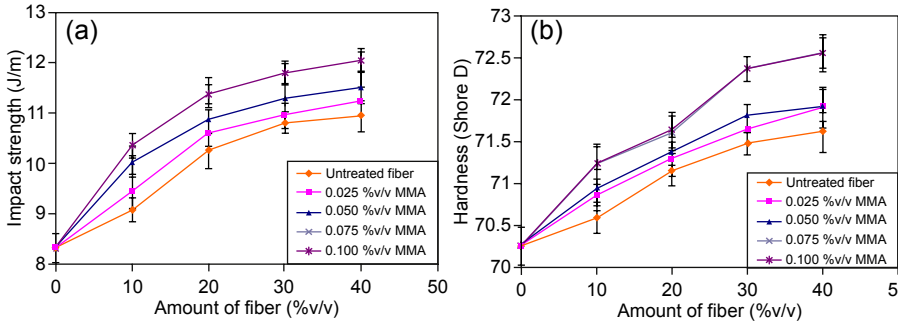

Figure 6.7 Variation in (a) impact strength and (b) hardness of polyester/sisal fiber composites with amount of methyl methacrylate (MMA) used to functionalize sisal fibers and amount of fibers [92].

A study of Orue et al. [94] modified the sisal fibers surface by various treatments such as alkali, silane, and fusion of these two with an objective to intensify their interfacial bonding with PLA. All treatments of fibers found to beneficial for enhancement of adhesion between fibers and PLA, which also resulted in increased interfacial shear strength in the composites, and minimal increment was 120%. Unfortunately, these treatments caused to reduce the tensile strength of resultant composites. Further, the enhanced hydrophobic nature of composites was executed through contact angle measurements [94]. In another study, the authors observed that the existence of higher tensile strength for composites comprised of alkali and combination of NaOH and silane-functionalized sisal fibers than one comprised of silane-modified fibers [95].

Composite containing epoxy matrix and sodium bicarbonate–functionalized sisal fiber reinforcement was developed by Fiore et al. [96], and also the effect of fiber treatment period on the characteristics of resultant composites was evaluated. The treatment for a period of 120 h generated the feasible adhesion of fibers with epoxy matrix and thereby created the existence of peak mechanical properties of composite [96]. Srisuwan et al. [97] evaluated the effect of alkali- and silane-treated sisal fibers on 1 wt% natural fiber–modified epoxy resin. Both fiber treatments increased the impact strength and the flexural modulus of composites. The maximum improvement in impact strength of 230% was observed for composite composed of 7 wt% of silanized sisal fibers. Regrettably, all treatments caused to reduce the flexural modulus of composites. Taking into considerations, silane-functionalized sisal fibers presented higher intensity of all properties [97]. In another study, Rong et al. [98] described the development of epoxy composites comprised of sisal fibers functionalized through various ways such as alkalization, acetylation, cyanoethylation, silanization, and thermal treatment at 150°C for 4 h [98].

Krishnaiah et al. [99] used sisal fibers functionalized using fusion of alkali and high-intensity ultrasound treatments to reinforce PP. Composite of PP with functionalized sisal fibers presented the improvement of 50% in tensile modulus and 10% in tensile strength due to the formation of good adhesion degree caused by the effect of combined treatment [99]. In another study, Mohan et al. [100] reinforced PP matrix by

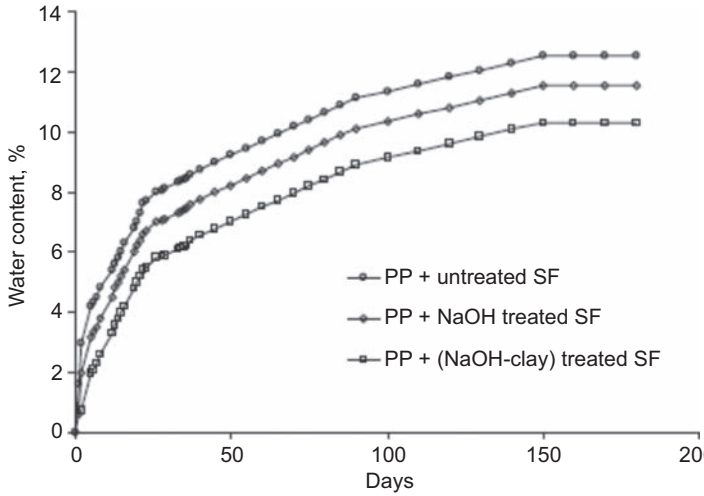

Figure 6.8 Impact of sisal fiber functionalization using NaOH alone and combination of NaOH and clay on water absorption behavior of polypropylene (PP)/sisal fiber (SF) composites [100].

sisal fiber functionalized through fusion of NaOH and clay treatments. The combined functionalization of sisal fibers caused to improve the interfacial bonding, tensile characteristics, and glass transition temperature of composite. Also, reduction in water absorption was achieved through the combined functionalization of NaOH and clay (Fig. 6.8) [100].

Kim et al. [101] reported the generation of green polymer composite consists of mercerized sisal fiber and biopolymer soy protein resin. It was executed that the powerful interaction of fibers on soy protein matrix, which consequently caused to exhibit the increase of 12% in fracture stress and 36% in stiffness [101].

6.8 Functionalized bamboo fiber–reinforced polymer composites

Bamboo fibers are abundantly available green fibers extracted from leaves, branches, and hard trunk of eternal bamboo plants (*Bambusoideae*) through steam explosion and subsequent mechanical treatment. Besides the usual natural fiber features, these fibers show UV light absorbency and much enhanced performances, which drive more interest as reinforcement material for polymer composites [102]. The application of functionalized bamboo fibers onto polymer matrices such as polyester resin, epoxy resin, phenolic resin, PLA, and PP is found to be beneficial to enhance composite performances.

Liu et al. [103] made use of *N*-methylol acrylamide (NMA)–grafted bamboo fiber to strengthen the matrix of polyester resin and also investigated the influence of four

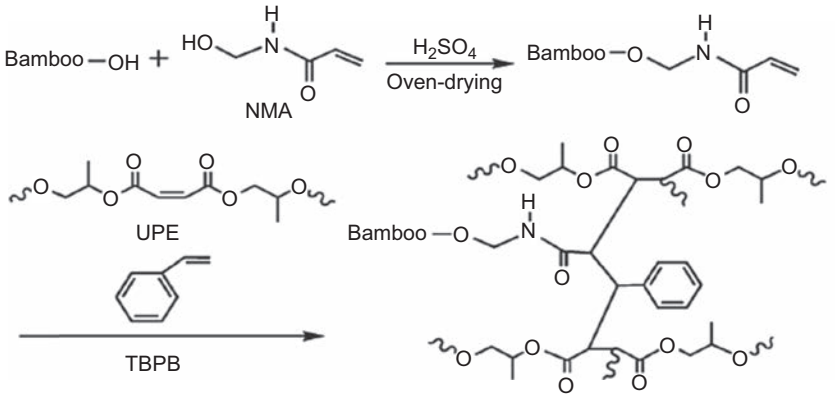

Figure 6.9 Schematic of reaction mechanism in a composite made up of unsaturated polyester resin and *N*-methylol acrylamide–functionalized bamboo fibers [103].

different kinds of bamboo fibers. Schematic of reaction mechanism in a composite made up of unsaturated polyester resin, and NMA-functionalized bamboo fibers is presented in Fig. 6.9. NMA-functionalized bamboo fiber containing composite exhibited beneficial compatibility of fibers with polyester resin by improving amount of N and reducing O/C ratio on the fiber surface. This correspondingly reflected in the betterment of mechanical properties. Also, an interesting thing inferred from this study was the great impact of fiber type used and grafting effectiveness on the furtherance of composite properties [103].

Lu et al. [104] reported the functionalization of bamboo fibers through alkalization and silanization to upgrade their interactions on epoxy matrix in the composite. Both treatments were effective to enrich the bonding as well as the mechanical characteristics of composites. Silanization of fibers improved the interaction with epoxy matrix through the formation of silicone linkages, while alkalization through the increased surface roughness of fibers. Composite based on silanized fibers exhibited slightly greater mechanical characteristics and it presented the enhancement of 71% in tensile strength and 53% in elongation at break while these were, respectively, about 34% and 31% in the case of alkalized bamboo fibers [104]. In another study, Manalo et al. [105] examined the impact of NaOH treatment of bamboo fibers on the mechanical properties of polyester/bamboo fiber composite. Alkaline solution with a concentration of 6% generated good mechanical properties for composite. Also, the mechanical characteristics of composite presented a decreasing tendency with increase in test temperature [105].

A study of Lu et al. [106] compared the effect of various functionalizations of bamboo fibers such as alkalization, silanization, and grafting of maleic anhydride on the matrix of PLA in the composite. The existence of optimal tensile strength and Young's modulus was reported for composite comprised of alkali-treated bamboo fibers. Impact strength and elongation of composites were maximal in the case of silane-treated fibers. Good balance of modulus and toughness along with nice comprehensive characteristics

for composite of maleic anhydride–grafted fibers was observed. These all resulted from the enhanced interfacial adhesion degree in the composites [106].

Yu et al. [107] reported the development of oriented bamboo fiber mat through functionalization using mechanical treatment in a pilot machine to reinforce phenol–formaldehyde (PF) resin. This mechanical treatment of bamboo fibers created considerable increase of all mechanical features of composite [107]. A study of Jayamani et al. [108] used NaOH-treated bamboo fibers along with jute fibers to strengthen the matrix of PP. The resultant composite generated lower dielectric constant and its intensity was increased by decreasing the amount of bamboo fiber in the hybrid system [108].

6.9 Functionalized coir fiber–reinforced polymer composites

Coir fiber or so-called coconut fiber is one of the major categories of lignocellulosic natural fiber, which is sourced from the husk of coconut (*Cocus nucifera*). The excellent properties such as hard-wearing quality, durability, and inexpensiveness along with usual natural fiber features of coir fibers make them suitable candidate for reinforcing polymers [109,110]. To upgrade the performances of coir fibers in the polymer matrices of PP, poly(butylene succinate) (PBS), polyester resin, and NR, functionalization of coir fibers was carried out.

Gu et al. [111] studied the impact of NaOH treatment of coir fibers on the tensile strength of PP/coir fiber composite. The alkali treatment of coir fibers created good adhesion on PP matrix, which correspondingly increased the tensile strength of composite. But higher concentration of NaOH (10%) caused a decrease in tensile strength due to the deterioration on the fiber surface [111]. A study of Haque et al. [112] yielded adequate mechanical properties for PP/coir fiber composite composed of benzene diazonium–functionalized coir fibers. The optimal properties were reported for composite containing 30 wt% of functionalized fiber [112]. In another study, Islam et al. [113] reported the use of *ortho*-hydroxybenzene diazonium to functionalize coir fibers in the PP/coir fiber composite. As a result, improved mechanical properties were observed for composite [113].

Nam et al. [114] utilized alkali-treated coir fibers to strengthen the matrix of PBS. The existence of enhanced interfacial shear strength and mechanical characteristics of composite through the usage of alkali-treated coir fibers was observed. Fig. 6.10 shows the impact of NaOH concentration and soaking time on the interfacial shear strength of composites. The enhancement of 55% in tensile strength, 142% in tensile modulus, 46% in flexural strength, and 97% in flexural modulus was reported for composite containing 25 wt% of alkalized coir fibers [114]. In another study, Thakur et al. [115] made use of eugenol-biografted coir fibers to strengthen the mechanical properties of PBS/coir fiber composite. As a result of biografting of coir fibers, composite exhibited considerable improvement in mechanical properties even at small amount of functionalized fibers. The variation in tensile stress–strain curve and tensile strength of composite after the functionalization of coir fibers is shown in Fig. 6.11 [115].

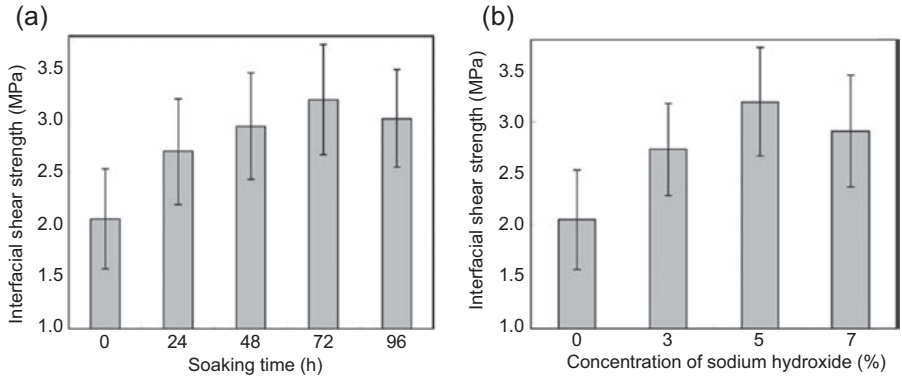

Figure 6.10 Impact of NaOH soaking time (a) and concentration (b) used to functionalize coir fibers on the interfacial shear strength of poly(butylene succinate)/coir fiber composites [114].

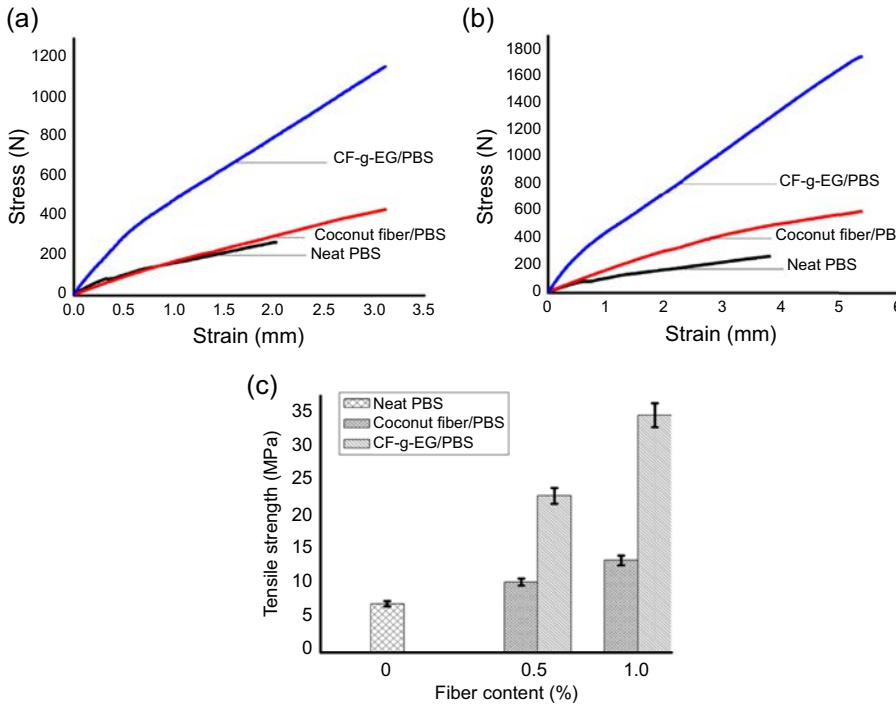

Figure 6.11 Variation in tensile stress–strain curve of neat poly(butylene succinate) (PBS) and PBS/coir fiber composites containing 0.5 wt% (a) and 1 wt% (b) of coir fibers before and after functionalization and tensile strength with the amount of functionalized coir fibers (c) [115].

A study of Rout et al. [116] investigated the impact of various treatments such as alkalization, bleaching, and vinyl grafting of coir fibers on the characteristics of polyester/coir fiber composites. All treatments created enriched interfacial interaction of fiber on polyester, and also the water affinity of resultant composite was

reduced. Composite with bleached coir fibers presented higher flexural strength, whereas one with alkalized coir fiber showed optimal tensile strength. Also, all these functionalized fibers were beneficial to enhance the flexural strength of glass fiber/polyester composites [116].

Mulinari et al. [117] made use of alkalized coir fibers as reinforcement for polyester resin. The fatigue life of resultant composite presented a decreasing tendency under tension, which was attributed to the poor interaction of alkali-treated coir fibers on polyester matrix [117]. In another study, Geethamma et al. [118] investigated the role of series of coir fiber chemical treatments such as alkalization, rubberization in NR, and depolymerized NR solution along with 1% of toluene diisocyanate on the mechanical characteristics of NR/coir fiber composite [118]. A study of Rosa et al. [119] achieved improvement in mechanical properties through the incorporation of mercerized coir fibers onto blend of starch and ethylene vinyl alcohol copolymer [119].

6.10 Functionalized oil palm fiber–reinforced polymer composites

Oil palm fiber (*Elaeis guineensis*) is a leading lignocellulosic fiber acquired from trunk, frond, fruit mesocarp, and empty fruit bunch of oil palm tree, which belongs to the family Arecaceae. These fibers have received growing acceptance as reinforcement for polymers on account of many interesting advantages of natural fibers [35,120]. Many researchers have tried functionalization of oil palm fibers to improve their performances on matrices of PP, PLA, PU, NR, high-density PE (HDPE), and phenolic resin.

Mamun et al. [121] reported the generation of composites of PP and PLA using enzyme (mixture of xylanase, laccase, and lipase)-modified oil palm fibers. The occupancy of enzyme-modified oil palm fibers in the composites of PP and PLA lowered the water absorption, and around 50% lightening was observed. In the case of PP composite, the enhancement of 18% in tensile strength, 27% in flexural strength, and 15% in heat deflection temperature were obtained through the functionalization of oil palm fibers. PLA composite also presented the improvement of 15% in tensile strength, 20% in flexural strength, and 7% in heat deflection temperature. The generation of all these improved properties was attributed to the increased adhesion of functionalized fibers onto the matrix of PP and PLA [121]. In another study, Rozman et al. [122] used maleic anhydride–functionalized oil palm fibers as reinforcement for PP. The enhanced flexural strength and toughness for composite comprised of functionalized fibers was observed [122].

Rozman et al. [123] investigated the effect of sequential toluene diisocyanate and hexamethylene diisocyanate functionalization of oil palm fibers on PU matrix in the composite. The enhancement in tensile and flexural strength and toughness was achieved through the functionalization of fibers, whereas tensile modulus of composite was decreased [123]. In another study, Essabir et al. [124] made use of alkali-functionalized oil palm fibers along with clay particles to reinforce the matrix of

HDPE. Alkalization of oil palm fibers was useful to enhance their interaction with HDPE. Hybrids containing equal amount of fiber and clay (12.5:12.5) possessed optimal mechanical properties [124].

A study of Jacob et al. [125] reported the strengthening of NR through the use of hybrid biofiber comprised of mercerized oil palm fibers and sisal fibers. Mercerization of fibers was beneficial to reduce the water uptake when compared to composite of unmodified fibers [125]. To enrich the adhesion of oil palm fibers with PF resin, Sreekala et al. [126] reported the functionalization of oil palm fibers through various methods such as mercerization, acetylation, acrylation, acrylonitrile grafting, latex coating, permanganate treatment, and peroxide treatment. These treatments of fibers were caused to enhance the mechanical performances of composites, especially impact strength [126]. A study of Eng et al. [127] used silanized oil palm fibers in combination with nanoclay to reinforce PLA/polycaprolactone (PCL) blend. The silanization of fiber caused to enhance the mechanical performances and the thermal stability of resultant composite [127].

6.11 Polymer composites with other functionalized natural fibers

This section summarizes the studies concerning the polymer composites developed using functionalized natural fibers other than the aforementioned and comprises of abaca fibers, pineapple leaf fibers, agave fibers, henequen fibers, corn fibers, pine cone fibers, date palm fibers, *Luffa cylindrica* fibers, ijuk fibers, beech fibers, betel nut fibers, and wool fibers.

Rahman et al. [128] prepared PP composite with benzenediazonium-functionalized abaca fibers. The generation of powerful interfacial adhesion degree of modified fibers on PP matrix was observed, which consequently improved the mechanical performances of composite [128]. A study of Punyamurthy et al. [129] also reported the improvement in mechanical properties of PP through the incorporation of benzenediazonium-functionalized abaca fibers. PP composite comprising 40 wt% of functionalized fiber exhibited peak mechanical properties [129]. Cai et al. [130] examined the impact of NaOH-functionalized abaca fibers on the eventual properties of abaca fiber–reinforced epoxy composite. The furtherance in crystallinity, tensile strength, Young's modulus, and interfacial shear strength was achieved through the use of 5% NaOH-functionalized abaca in the composite formulation. At the same time, fiber treatment using higher concentration of NaOH caused to deteriorate the improvement in composite features [130]. In another study, Liu et al. [131] made use of mercerized and silanized abaca fibers as reinforcement for epoxy resin. The resultant composite exhibited an improvement in transverse thermal conductivity due to the strengthening of infirm linkages as well as reduction of voids after treatment [131].

A study of Panyasart et al. [132] examined the effect of alkaline- and silane-functionalized pineapple leaf fibers on polyamide 6 matrix. Improved compatibility between fibers and polyamide 6 was achieved through both functionalizations

of fibers. Composites composed of both functionalized fibers generated higher thermal stability than one with unfunctionalized fibers. Also, functionalized composites had increased tensile strength and Young's modulus, but elongation showed a decreasing tendency [132]. In another study, Threepopnatkul et al. [133] fabricated polycarbonate/pineapple leaf fiber composite and investigated the effect of NaOH and silane functionalization. The functionalizations using NaOH and silane were effective to achieve the improved mechanical properties of the composites. The optimal tensile strength and impact strength were observed for polycarbonate composite of silanized fiber. Also, composite of NaOH-treated fibers presented peak Young's modulus. Unfortunately, the thermal stability of composites was decreased after modifications of fibers [133].

A study of Singha et al. [134] developed polystyrene composite that consists of MMA–grafted Agave (*Agave americana*) fibers. The composite with 20 wt% of functionalized fibers showed peak mechanical properties along with improved thermal stability [134]. Gonzalez et al. [135] tried various routes of henequen (*Agave fourcroydes*) fiber functionalizations to enrich its interfacial bonding with HDPE matrix. Alkaline treatment was helpful to enhance the interactions between fibers and HDPE matrix via improving the surface roughness as well as the surface cellulose content. Silane treatment also possessed some beneficial impact to improve the interfacial bonding between components in the composite system. Fiber preimpregnation in HDPE/xylene was very effective to get fine fiber wetting on HDPE matrix [135].

Luo et al. [136] reinforced PLA matrix using functionalized corn fibers developed through not only alkalization but also sizing. The degree of interfacial bonding was higher for composite containing sized corn fibers when compared to one based on alkalized corn fibers. Correspondingly, PLA composite with sized corn fibers presented greater mechanical and thermomechanical features [136]. Arrakhiz et al. [137] applied mercerized pine cone fibers along with clay onto the PP matrix and observed the contribution of fiber treatment to enrich the mechanical properties of hybrid composite [137]. In another study, the authors also reported the feasibility of alkali-treated pine cone fibers to improve the mechanical characteristics of compatibilized PP matrix [138]. A study of Alsaeed et al. [139] obtained optimal improvement in interfacial bonding and tensile strength for epoxy composite comprised of 6% NaOH-functionalized date palm fiber [139].

Siqueira et al. [140] carried out the functionalization of *L. cylindrica* fibers using 1,2,4,5-benzenetetracarboxylic dianhydride with an objective to enhance interfacial bonding with vinylester matrix. The resultant composite exhibited the improvement of 30% in tensile strength and 250% in impact strength [140]. A study of Zahari et al. [141] made use of silanized ijuk fibers to synthesize PP/ijuk fiber composite with enhanced interfacial adhesion. The occupancy of silanized ijuk fibers in the PP matrix increased the mechanical characteristics as well as decreased the water absorption degree [141]. Zierdt et al. [142] fabricated biocomposite composed of bio-based polyamide 11 and NaOH-functionalized beech fibers. The existence of enhanced tensile modulus, storage modulus, and thermal stability for functionalized fiber–based composite was reported. This was attributed to the multiplied hydrogen bonding of

functionalized fibers with matrix of biopolyamide 11 [142]. A study of Jayamani et al. [143] reported the development of polyester composite with NaOH-functionalized betel nut fibers. The resultant composite exhibited greater tensile strength and thermal stability when compared to one based on untreated fibers [143]. Conzatti et al. [144] made use of silanized as well as oxidized wool fibers to reinforce the matrix of PP. Both functionalizations of wool were advantageous to enhance the bonding with PP. Thermal stability of resultant composites was enhanced, and the intensity was higher for composite based on silanized wool fibers. The improvement in mechanical properties was underneath as anticipated [144].

6.12 Conclusions

Natural fiber–reinforced polymer composites have become growingly assertive in research areas of polymer science and technology because of the raising environmental, ecological, social, and economical concerns. The use of natural fibers offers some supremacy such as biodegradability, combustibility, nontoxicity, precise mechanical properties, absence of corrosion as well as fatigue, nominal damage to processing machineries, lightweight, economical, easily accessibility, nice surface finish, acceptable fiber aspect ratio, and so on. Functionalization of natural fibers is absolutely necessary to upgrade the interfacial bonding with polymers and thus to successfully obtain high-performance composite materials. The present work prosperously overviewed the available studies concerning the polymer composites fabricated from functionalized natural fibers such as jute fibers, hemp fibers, kenaf fibers, flax fibers, ramie fibers, sisal fibers, bamboo fibers, coir fibers, oil palm fibers, and other natural fibers. The effectiveness of natural fibers functionalization through either physical or chemical routes enriches the characteristics of resultant composites, namely, adhesion degree, interfacial shear strength, wetting, mechanical performances, thermal stability, dynamic mechanical features, thermomechanical properties, reduction in water absorption, antibacterial properties, and so on. This chapter contributes predominant guidance describing the polymer composites made up of functionalized natural fibers to upgrade their applications in future.

References

[1] A.N. Netravali, S. Chabba, Composites get greener, Materials Today 6 (2003) 22–29.
[2] A. May-Pat, A. Valadez-González, P.J. Herrera-Franco, Effect of fiber surface treatments on the essential work of fracture of HDPE-continuous henequen fiber-reinforced composites, Polymer Testing 32 (2013) 1114–1122.
[3] A. Shalwan, B. Yousif, In state of art: mechanical and tribological behaviour of polymeric composites based on natural fibres, Materials and Design 48 (2013) 14–24.
[4] A. Rana, A. Mandal, S. Bandyopadhyay, Short jute fiber reinforced polypropylene composites: effect of compatibiliser, impact modifier and fiber loading, Composites Science and Technology 63 (2003) 801–806.

[5] L. Mohammed, M.N. Ansari, G. Pua, M. Jawaid, M.S. Islam, A review on natural fiber reinforced polymer composite and its applications, International Journal of Polymer Science 2015 (2015).
[6] K.L. Pickering, M.A. Efendy, T.M. Le, A review of recent developments in natural fibre composites and their mechanical performance, Composites Part A: Applied Science and Manufacturing 83 (2016) 98–112.
[7] V.K. Thakur, Green Composites from Natural Resources, CRC Press, 2013.
[8] V.K. Thakur, M.K. Thakur, R.K. Gupta, Review: raw natural fiber–based polymer composites, International Journal of Polymer Analysis and Characterization 19 (2014) 256–271.
[9] O. Faruk, A.K. Bledzki, H.-P. Fink, M. Sain, Biocomposites reinforced with natural fibers: 2000–2010, Progress in Polymer Science 37 (2012) 1552–1596.
[10] Z. Xiao, L. Zhao, Y. Xie, Q. Wang, Review for development of wood plastic composites, Journal of Northeast Forestry University 31 (2002) 39–41.
[11] T. Gurunathan, S. Mohanty, S.K. Nayak, A review of the recent developments in biocomposites based on natural fibres and their application perspectives, Composites Part A: Applied Science and Manufacturing 77 (2015) 1–25.
[12] V.K. Thakur, M.K. Thakur, Processing and characterization of natural cellulose fibers/thermoset polymer composites, Carbohydrate Polymers 109 (2014) 102–117.
[13] M.J. John, S. Thomas, Biofibres and biocomposites, Carbohydrate Polymers 71 (2008) 343–364.
[14] Z. Liu, S.Z. Erhan, D.E. Akin, F.E. Barton, "Green" composites from renewable resources: preparation of epoxidized soybean oil and flax fiber composites, Journal of Agricultural and Food Chemistry 54 (2006) 2134–2137.
[15] C. Alves, A. Silva, L. Reis, M. Freitas, L. Rodrigues, D. Alves, Ecodesign of automotive components making use of natural jute fiber composites, Journal of Cleaner Production 18 (2010) 313–327.
[16] A. Rana, A. Mandal, B. Mitra, R. Jacobson, R. Rowell, A. Banerjee, Short jute fiber-reinforced polypropylene composites: effect of compatibilizer, Journal of Applied Polymer Science 69 (1998) 329–338.
[17] R. Hu, J.-K. Lim, Fabrication and mechanical properties of completely biodegradable hemp fiber reinforced polylactic acid composites, Journal of Composite Materials 41 (2007) 1655–1669.
[18] H. Akil, M. Omar, A. Mazuki, S. Safiee, Z.M. Ishak, A.A. Bakar, Kenaf fiber reinforced composites: a review, Materials and Design 32 (2011) 4107–4121.
[19] Y. Du, N. Yan, M. Kortschot, The use of ramie fibers as reinforcements in composites, in: Biofiber Reinforcements in Composite Materials, 2014, p. 104.
[20] M. Ramesh, T.S.A. Atreya, U. Aswin, H. Eashwar, C. Deepa, Processing and mechanical property evaluation of banana fiber reinforced polymer composites, Procedia Engineering 97 (2014) 563–572.
[21] Y. Li, H. Ma, Y. Shen, Q. Li, Z. Zheng, Effects of resin inside fiber lumen on the mechanical properties of sisal fiber reinforced composites, Composites Science and Technology 108 (2015) 32–40.
[22] K. Joseph, R.D. Tolêdo Filho, B. James, S. Thomas, L.H.D. Carvalho, A review on sisal fiber reinforced polymer composites, Revista Brasileira de Engenharia Agrícola e Ambiental 3 (1999) 367–379.
[23] X. Hou, F. Sun, D. Yan, H. Xu, Z. Dong, Q. Li, Y. Yang, Preparation of lightweight polypropylene composites reinforced by cotton stalk fibers from combined steam flash-explosion and alkaline treatment, Journal of Cleaner Production 83 (2014) 454–462.

[24] M. Abdullah, M. Nazir, M. Raza, B. Wahjoedi, A. Yussof, Autoclave and ultra-sonication treatments of oil palm empty fruit bunch fibers for cellulose extraction and its polypropylene composite properties, Journal of Cleaner Production 126 (2016) 686–697.
[25] D. Verma, B. Varanasi, P. Gope, The use of coir/coconut fibers as reinforcements in composites, in: Biofiber Reinforcements in Composite Materials, 2015, p. 285.
[26] K. Yang, R.O. Ritchie, Y. Gu, S.J. Wu, J. Guan, High volume-fraction silk fabric reinforcements can improve the key mechanical properties of epoxy resin composites, Materials and Design 108 (2016) 470–478.
[27] L. Conzatti, F. Giunco, P. Stagnaro, A. Patrucco, C. Marano, M. Rink, E. Marsano, Composites based on polypropylene and short wool fibres, Composites Part A: Applied Science and Manufacturing 47 (2013) 165–171.
[28] N. Kim, D. Bhattacharyya, Development of fire resistant wool polymer composites: mechanical performance and fire simulation with design perspectives, Materials and Design 106 (2016) 391–403.
[29] S. Vilchez, A. Manich, P. Jovancic, P. Erra, Chitosan contribution on wool treatments with enzyme, Carbohydrate Polymers 71 (2008) 515–523.
[30] A. Rachini, G. Mougin, S. Delalande, J.-Y. Charmeau, C. Barrès, E. Fleury, Hemp fibers/polypropylene composites by reactive compounding: improvement of physical properties promoted by selective coupling chemistry, Polymer Degradation and Stability 97 (2012) 1988–1995.
[31] A. Bledzki, S. Reihmane, J. Gassan, Properties and modification methods for vegetable fibers for natural fiber composites, Journal of Applied Polymer Science 59 (1996) 1329–1336.
[32] A. Mohanty, M. Misra, L. Drzal, Surface modifications of natural fibers and performance of the resulting biocomposites: an overview, Composite Interfaces 8 (2001) 313–343.
[33] M. Kazayawoko, J. Balatinecz, L. Matuana, Surface modification and adhesion mechanisms in woodfiber-polypropylene composites, Journal of Materials Science 34 (1999) 6189–6199.
[34] N. Sgriccia, M. Hawley, M. Misra, Characterization of natural fiber surfaces and natural fiber composites, Composites Part A: Applied Science and Manufacturing 39 (2008) 1632–1637.
[35] C. Nguong, S. Lee, D. Sujan, A review on natural fibre reinforced polymer composites, Proceedings of World Academy of Science, Engineering and Technology (2013) 1123.
[36] A.S. Singha, Surface Modification of Biopolymers, John Wiley & Sons, 2015.
[37] M.K. Thakur, R.K. Gupta, V.K. Thakur, Surface modification of cellulose using silane coupling agent, Carbohydrate Polymers 111 (2014) 849–855.
[38] Y. Xie, C.A. Hill, Z. Xiao, H. Militz, C. Mai, Silane coupling agents used for natural fiber/polymer composites: a review, Composites Part A: Applied Science and Manufacturing 41 (2010) 806–819.
[39] D. Sun, G. Stylios, Investigating the plasma modification of natural fiber fabrics-the effect on fabric surface and mechanical properties, Textile Research Journal 75 (2005) 639–644.
[40] D.M. Panaitescu, Z. Vuluga, M. Ghiurea, M. Iorga, C. Nicolae, R. Gabor, Influence of compatibilizing system on morphology, thermal and mechanical properties of high flow polypropylene reinforced with short hemp fibers, Composites Part B: Engineering 69 (2015) 286–295.
[41] I. Sakata, M. Morita, N. Tsuruta, K. Morita, Activation of wood surface by corona treatment to improve adhesive bonding, Journal of Applied Polymer Science 49 (1993) 1251–1258.

[42] J. Cruz, R. Fangueiro, Surface modification of natural fibers: a review, Procedia Engineering 155 (2016) 285–288.
[43] X. Li, L.G. Tabil, S. Panigrahi, Chemical treatments of natural fiber for use in natural fiber-reinforced composites: a review, Journal of Polymers and the Environment 15 (2007) 25–33.
[44] M.A. Sawpan, K.L. Pickering, A. Fernyhough, Effect of various chemical treatments on the fibre structure and tensile properties of industrial hemp fibres, Composites Part A: Applied Science and Manufacturing 42 (2011) 888–895.
[45] M.N. Belgacem, A. Gandini, The surface modification of cellulose fibres for use as reinforcing elements in composite materials, Composite Interfaces 12 (2005) 41–75.
[46] C. Hong, N. Kim, S. Kang, C. Nah, Y.-S. Lee, B.-H. Cho, J.-H. Ahn, Mechanical properties of maleic anhydride treated jute fibre/polypropylene composites, Plastics, Rubber and Composites 37 (2008) 325–330.
[47] C. Stevens, J. Müssig, Industrial Applications of Natural Fibres: Structure, Properties and Technical Applications, vol. 10, John Wiley & Sons, 2010.
[48] J. Gassan, A.K. Bledzki, Possibilities for improving the mechanical properties of jute/epoxy composites by alkali treatment of fibres, Composites Science and Technology 59 (1999) 1303–1309.
[49] J. Gassan, A.K. Bledzki, The influence of fiber-surface treatment on the mechanical properties of jute-polypropylene composites, Composites Part A: Applied Science and Manufacturing 28 (1997) 1001–1005.
[50] B.A. Acha, M.M. Reboredo, N.E. Marcovich, Creep and dynamic mechanical behavior of PP–jute composites: effect of the interfacial adhesion, Composites Part A: Applied Science and Manufacturing 38 (2007) 1507–1516.
[51] C. Hong, I. Hwang, N. Kim, D. Park, B. Hwang, C. Nah, Mechanical properties of silanized jute–polypropylene composites, Journal of Industrial and Engineering Chemistry 14 (2008) 71–76.
[52] Y. Karaduman, M. Sayeed, L. Onal, A. Rawal, Viscoelastic properties of surface modified jute fiber/polypropylene nonwoven composites, Composites Part B: Engineering 67 (2014) 111–118.
[53] M. Sayeed, A. Rawal, L. Onal, Y. Karaduman, Mechanical properties of surface modified jute fiber/polypropylene nonwoven composites, Polymer Composites 35 (2014) 1044–1050.
[54] J.-M. Park, S.T. Quang, B.-S. Hwang, K.L. DeVries, Interfacial evaluation of modified jute and hemp fibers/polypropylene (PP)-maleic anhydride polypropylene copolymers (PP-MAPP) composites using micromechanical technique and nondestructive acoustic emission, Composites Science and Technology 66 (2006) 2686–2699.
[55] M.R. Rahman, M.M. Huque, M.N. Islam, M. Hasan, Improvement of physico-mechanical properties of jute fiber reinforced polypropylene composites by post-treatment, Composites Part A: Applied Science and Manufacturing 39 (2008) 1739–1747.
[56] B.K. Goriparthi, K. Suman, N.M. Rao, Effect of fiber surface treatments on mechanical and abrasive wear performance of polylactide/jute composites, Composites Part A: Applied Science and Manufacturing 43 (2012) 1800–1808.
[57] M.K. Hossain, M.W. Dewan, M. Hosur, S. Jeelani, Mechanical performances of surface modified jute fiber reinforced biopol nanophased green composites, Composites Part B: Engineering 42 (2011) 1701–1707.
[58] L. Tzounis, S. Debnath, S. Rooj, D. Fischer, E. Mäder, A. Das, M. Stamm, G. Heinrich, High performance natural rubber composites with a hierarchical reinforcement structure of carbon nanotube modified natural fibers, Materials and Design 58 (2014) 1–11.

[59] Z. Li, X. Wang, L. Wang, Properties of hemp fibre reinforced concrete composites, Composites Part A: Applied Science and Manufacturing 37 (2006) 497–505.
[60] H. Dhakal, Z. Zhang, M. Richardson, Effect of water absorption on the mechanical properties of hemp fibre reinforced unsaturated polyester composites, Composites Science and Technology 67 (2007) 1674–1683.
[61] A. Elkhaoulani, F. Arrakhiz, K. Benmoussa, R. Bouhfid, A. Qaiss, Mechanical and thermal properties of polymer composite based on natural fibers: Moroccan hemp fibers/polypropylene, Materials and Design 49 (2013) 203–208.
[62] K.L. Pickering, G. Beckermann, S. Alam, N.J. Foreman, Optimising industrial hemp fibre for composites, Composites Part A: Applied Science and Manufacturing 38 (2007) 461–468.
[63] G. Beckermann, K.L. Pickering, Engineering and evaluation of hemp fibre reinforced polypropylene composites: fibre treatment and matrix modification, Composites Part A: Applied Science and Manufacturing 39 (2008) 979–988.
[64] Y. Li, K.L. Pickering, Hemp fibre reinforced composites using chelator and enzyme treatments, Composites Science and Technology 68 (2008) 3293–3298.
[65] Y. Li, K. Pickering, R. Farrell, Analysis of green hemp fibre reinforced composites using bag retting and white rot fungal treatments, Industrial Crops and Products 29 (2009) 420–426.
[66] D.M. Panaitescu, C.A. Nicolae, Z. Vuluga, C. Vitelaru, C.G. Sanporean, C. Zaharia, D. Florea, G. Vasilievici, Influence of hemp fibers with modified surface on polypropylene composites, Journal of Industrial and Engineering Chemistry 37 (2016) 137–146.
[67] B. Szolnoki, K. Bocz, P.L. Sóti, B. Bodzay, E. Zimonyi, A. Toldy, B. Morlin, K. Bujnowicz, M. Wladyka-Przybylak, G. Marosi, Development of natural fibre reinforced flame retarded epoxy resin composites, Polymer Degradation and Stability 119 (2015) 68–76.
[68] A. Bledzki, P. Franciszczak, Z. Osman, M. Elbadawi, Polypropylene biocomposites reinforced with softwood, abaca, jute, and kenaf fibers, Industrial Crops and Products 70 (2015) 91–99.
[69] A.K. Mohanty, M. Misra, L.T. Drzal, Natural Fibers, Biopolymers, and Biocomposites, CRC Press, 2005.
[70] J. Datta, P. Kopczyńska, Effect of kenaf fibre modification on morphology and mechanical properties of thermoplastic polyurethane materials, Industrial Crops and Products 74 (2015) 566–576.
[71] C. Xia, S.Q. Shi, Y. Wu, L. Cai, High pressure-assisted magnesium carbonate impregnated natural fiber-reinforced composites, Industrial Crops and Products 86 (2016) 16–22.
[72] O. Asumani, R. Reid, R. Paskaramoorthy, The effects of alkali–silane treatment on the tensile and flexural properties of short fibre non-woven kenaf reinforced polypropylene composites, Composites Part A: Applied Science and Manufacturing 43 (2012) 1431–1440.
[73] M.S. Meon, M.F. Othman, H. Husain, M.F. Remeli, M.S.M. Syawal, Improving tensile properties of kenaf fibers treated with sodium hydroxide, Procedia Engineering 41 (2012) 1587–1592.
[74] V. Fiore, G. Di Bella, A. Valenza, The effect of alkaline treatment on mechanical properties of kenaf fibers and their epoxy composites, Composites Part B: Engineering 68 (2015) 14–21.
[75] K.V. Krishna, K. Kanny, The effect of treatment on kenaf fiber using green approach and their reinforced epoxy composites, Composites Part B: Engineering 104 (2016) 111–117.

[76] B. Yousif, A. Shalwan, C. Chin, K. Ming, Flexural properties of treated and untreated kenaf/epoxy composites, Materials and Design 40 (2012) 378–385.
[77] B. Wang, S. Panigrahi, L. Tabil, W. Crerar, S. Sokansanj, L. Braun, Modification of flax fibers by chemical treatment, in: CSAE/SCGR, 2003, pp. 6–9.
[78] M. Sumaila, A. Ibhadode, Technical properties of some plant fibres compared with glass fibre, International Journal of Engineering Research in Africa (2014) 11–26.
[79] L. Yan, N. Chouw, K. Jayaraman, Flax fibre and its composites–a review, Composites Part B: Engineering 56 (2014) 296–317.
[80] M. Foruzanmehr, P.Y. Vuillaume, S. Elkoun, M. Robert, Physical and mechanical properties of PLA composites reinforced by TiO_2 grafted flax fibers, Materials and Design 106 (2016) 295–304.
[81] H. Wang, G. Xian, H. Li, Grafting of nano-TiO_2 onto flax fibers and the enhancement of the mechanical properties of the flax fiber and flax fiber/epoxy composite, Composites Part A: Applied Science and Manufacturing 76 (2015) 172–180.
[82] L. Yan, N. Chouw, X. Yuan, Improving the mechanical properties of natural fibre fabric reinforced epoxy composites by alkali treatment, Journal of Reinforced Plastics and Composites (2012)http://dx.doi.org/10.1177/0731684412439494.
[83] A. Triki, M. Karray, C. Poilâne, P. Picart, M. Gargouri, Dielectric analysis of the interfacial polarization of alkali treated woven flax fibers reinforced epoxy composites, Journal of Electrostatics 76 (2015) 67–72.
[84] S. Nam, A.N. Netravali, Green composites. I. Physical properties of ramie fibers for environment-friendly green composites, Fibers and Polymers 7 (2006) 372–379.
[85] L. He, W. Li, D. Chen, D. Zhou, G. Lu, J. Yuan, Effects of amino silicone oil modification on properties of ramie fiber and ramie fiber/polypropylene composites, Materials and Design 77 (2015) 142–148.
[86] X. Li, L. He, H. Zhou, W. Li, W. Zha, Influence of silicone oil modification on properties of ramie fiber reinforced polypropylene composites, Carbohydrate Polymers 87 (2012) 2000–2004.
[87] T. Yu, J. Ren, S. Li, H. Yuan, Y. Li, Effect of fiber surface-treatments on the properties of poly (lactic acid)/ramie composites, Composites Part A: Applied Science and Manufacturing 41 (2010) 499–505.
[88] J.-M. Yuan, Y.-R. Feng, L.-P. He, Effect of thermal treatment on properties of ramie fibers, Polymer Degradation and Stability 133 (2016) 303–311.
[89] Y. Li, Y.-W. Mai, L. Ye, Sisal fibre and its composites: a review of recent developments, Composites Science and Technology 60 (2000) 2037–2055.
[90] S. Mishra, A.K. Mohanty, L.T. Drzal, M. Misra, G. Hinrichsen, A review on pineapple leaf fibers, sisal fibers and their biocomposites, Macromolecular Materials and Engineering 289 (2004) 955–974.
[91] P. Sreekumar, S.P. Thomas, J. marc Saiter, K. Joseph, G. Unnikrishnan, S. Thomas, Effect of fiber surface modification on the mechanical and water absorption characteristics of sisal/polyester composites fabricated by resin transfer molding, Composites Part A: Applied Science and Manufacturing 40 (2009) 1777–1784.
[92] S. Sangthong, T. Pongprayoon, N. Yanumet, Mechanical property improvement of unsaturated polyester composite reinforced with admicellar-treated sisal fibers, Composites Part A: Applied Science and Manufacturing 40 (2009) 687–694.
[93] A. Barreto, D. Rosa, P. Fechine, S. Mazzetto, Properties of sisal fibers treated by alkali solution and their application into cardanol-based biocomposites, Composites Part A: Applied Science and Manufacturing 42 (2011) 492–500.

[94] A. Orue, A. Jauregi, C. Peña-Rodriguez, J. Labidi, A. Eceiza, A. Arbelaiz, The effect of surface modifications on sisal fiber properties and sisal/poly (lactic acid) interface adhesion, Composites Part B: Engineering 73 (2015) 132–138.
[95] A. Orue, A. Jauregi, U. Unsuain, J. Labidi, A. Eceiza, A. Arbelaiz, The effect of alkaline and silane treatments on mechanical properties and breakage of sisal fibers and poly (lactic acid)/sisal fiber composites, Composites Part A: Applied Science and Manufacturing 84 (2016) 186–195.
[96] V. Fiore, T. Scalici, F. Nicoletti, G. Vitale, M. Prestipino, A. Valenza, A new eco-friendly chemical treatment of natural fibres: effect of sodium bicarbonate on properties of sisal fibre and its epoxy composites, Composites Part B: Engineering 85 (2016) 150–160.
[97] S. Srisuwan, N. Prasoetsopha, N. Suppakarn, P. Chumsamrong, The effects of alkalized and silanized woven sisal fibers on mechanical properties of natural rubber modified epoxy resin, Energy Procedia 56 (2014) 19–25.
[98] M.Z. Rong, M.Q. Zhang, Y. Liu, G.C. Yang, H.M. Zeng, The effect of fiber treatment on the mechanical properties of unidirectional sisal-reinforced epoxy composites, Composites Science and Technology 61 (2001) 1437–1447.
[99] P. Krishnaiah, C.T. Ratnam, S. Manickam, Enhancements in crystallinity, thermal stability, tensile modulus and strength of sisal fibres and their PP composites induced by the synergistic effects of alkali and high intensity ultrasound (HIU) treatments, Ultrasonics Sonochemistry 34 (2017) 729–742.
[100] T. Mohan, K. Kanny, Chemical treatment of sisal fiber using alkali and clay method, Composites Part A: Applied Science and Manufacturing 43 (2012) 1989–1998.
[101] J.T. Kim, A.N. Netravali, Mercerization of sisal fibers: effect of tension on mechanical properties of sisal fiber and fiber-reinforced composites, Composites Part A: Applied Science and Manufacturing 41 (2010) 1245–1252.
[102] F.T. Wallenberger, N. Weston, Natural Fibers, Plastics and Composites, Springer Science & Business Media, 2003.
[103] W. Liu, T. Xie, R. Qiu, M. Fan, N-methylol acrylamide grafting bamboo fibers and their composites, Composites Science and Technology 117 (2015) 100–106.
[104] T. Lu, M. Jiang, Z. Jiang, D. Hui, Z. Wang, Z. Zhou, Effect of surface modification of bamboo cellulose fibers on mechanical properties of cellulose/epoxy composites, Composites Part B: Engineering 51 (2013) 28–34.
[105] A.C. Manalo, E. Wani, N.A. Zukarnain, W. Karunasena, K.-T. Lau, Effects of alkali treatment and elevated temperature on the mechanical properties of bamboo fibre–polyester composites, Composites Part B: Engineering 80 (2015) 73–83.
[106] T. Lu, S. Liu, M. Jiang, X. Xu, Y. Wang, Z. Wang, J. Gou, D. Hui, Z. Zhou, Effects of modifications of bamboo cellulose fibers on the improved mechanical properties of cellulose reinforced poly (lactic acid) composites, Composites Part B: Engineering 62 (2014) 191–197.
[107] Y. Yu, X. Huang, W. Yu, A novel process to improve yield and mechanical performance of bamboo fiber reinforced composite via mechanical treatments, Composites Part B: Engineering 56 (2014) 48–53.
[108] E. Jayamani, S. Hamdan, M.R. Rahman, M.K.B. Bakri, Comparative study of dielectric properties of hybrid natural fiber composites, Procedia Engineering 97 (2014) 536–544.
[109] A. Bismarck, A.K. Mohanty, I. Aranberri-Askargorta, S. Czapla, M. Misra, G. Hinrichsen, J. Springer, Surface characterization of natural fibers; surface properties and the water up-take behavior of modified sisal and coir fibers, Green Chemistry 3 (2001) 100–107.

[110] H.S.A. Khalil, M.S. Alwani, A.K.M. Omar, Chemical composition, anatomy, lignin distribution, and cell wall structure of Malaysian plant waste fibers, BioResources 1 (2007) 220–232.
[111] H. Gu, Tensile behaviours of the coir fibre and related composites after NaOH treatment, Materials and Design 30 (2009) 3931–3934.
[112] M.M. Haque, M. Hasan, M.S. Islam, M.E. Ali, Physico-mechanical properties of chemically treated palm and coir fiber reinforced polypropylene composites, Bioresource Technology 100 (2009) 4903–4906.
[113] M.N. Islam, M.R. Rahman, M.M. Haque, M.M. Huque, Physico-mechanical properties of chemically treated coir reinforced polypropylene composites, Composites Part A: Applied Science and Manufacturing 41 (2010) 192–198.
[114] T.H. Nam, S. Ogihara, N.H. Tung, S. Kobayashi, Effect of alkali treatment on interfacial and mechanical properties of coir fiber reinforced poly (butylene succinate) biodegradable composites, Composites Part B: Engineering 42 (2011) 1648–1656.
[115] K. Thakur, S. Kalia, B. Kaith, D. Pathania, A. Kumar, P. Thakur, C.E. Knittel, C.L. Schauer, G. Totaro, The development of antibacterial and hydrophobic functionalities in natural fibers for fiber-reinforced composite materials, Journal of Environmental Chemical Engineering 4 (2016) 1743–1752.
[116] J. Rout, M. Misra, S. Tripathy, S. Nayak, A. Mohanty, The influence of fibre treatment on the performance of coir-polyester composites, Composites Science and Technology 61 (2001) 1303–1310.
[117] D. Mulinari, C. Baptista, J.V.C.D. Souza, H. Voorwald, Mechanical properties of coconut fibers reinforced polyester composites, Procedia Engineering 10 (2011) 2074–2079.
[118] V. Geethamma, K.T. Mathew, R. Lakshminarayanan, S. Thomas, Composite of short coir fibres and natural rubber: effect of chemical modification, loading and orientation of fibre, Polymer 39 (1998) 1483–1491.
[119] M.F. Rosa, B.-S. Chiou, E.S. Medeiros, D.F. Wood, T.G. Williams, L.H. Mattoso, W.J. Orts, S.H. Imam, Effect of fiber treatments on tensile and thermal properties of starch/ethylene vinyl alcohol copolymers/coir biocomposites, Bioresource Technology 100 (2009) 5196–5202.
[120] S. Shinoj, R. Visvanathan, S. Panigrahi, M. Kochubabu, Oil palm fiber (OPF) and its composites: a review, Industrial Crops and Products 33 (2011) 7–22.
[121] A.A. Mamun, H.-P. Heim, D.H. Beg, T.S. Kim, S.H. Ahmad, PLA and PP composites with enzyme modified oil palm fibre: a comparative study, Composites Part A: Applied Science and Manufacturing 53 (2013) 160–167.
[122] H. Rozman, M. Saad, Z.M. Ishak, Flexural and impact properties of oil palm empty fruit bunch (EFB)–polypropylene composites—the effect of maleic anhydride chemical modification of EFB, Polymer Testing 22 (2003) 335–341.
[123] H. Rozman, K. Ahmad Hilme, A. Abubakar, Polyurethane composites based on oil palm empty fruit bunches: effect of isocyanate/hydroxyl ratio and chemical modification of empty fruit bunches with toluene diisocyanate and hexamethylene diisocyanate on mechanical properties, Journal of Applied Polymer Science 106 (2007) 2290–2297.
[124] H. Essabir, R. Boujmal, M.O. Bensalah, D. Rodrigue, R. Bouhfid, A. el kacem Qaiss, Mechanical and thermal properties of hybrid composites: oil-palm fiber/clay reinforced high density polyethylene, Mechanics of Materials 98 (2016) 36–43.
[125] M. Jacob, K. Varughese, S. Thomas, Water sorption studies of hybrid biofiber-reinforced natural rubber biocomposites, Biomacromolecules 6 (2005) 2969–2979.
[126] M. Sreekala, M. Kumaran, S. Joseph, M. Jacob, S. Thomas, Oil palm fibre reinforced phenol formaldehyde composites: influence of fibre surface modifications on the mechanical performance, Applied Composite Materials 7 (2000) 295–329.

[127] C.C. Eng, N.A. Ibrahim, N. Zainuddin, H. Ariffin, W.M.Z.W. Yunus, Impact strength and flexural properties enhancement of methacrylate silane treated oil palm mesocarp fiber reinforced biodegradable hybrid composites, The Scientific World Journal 2014 (2014).
[128] M.R. Rahman, M.M. Huque, M.N. Islam, M. Hasan, Mechanical properties of polypropylene composites reinforced with chemically treated abaca, Composites Part A: Applied Science and Manufacturing 40 (2009) 511–517.
[129] R. Punyamurthy, D. Sampathkumar, R.P.G. Ranganagowda, B. Bennehalli, C.V. Srinivasa, Mechanical properties of abaca fiber reinforced polypropylene composites: effect of chemical treatment by benzenediazonium chloride, Journal of King Saud University-Engineering Sciences 29 (2017) 289–294.
[130] M. Cai, H. Takagi, A.N. Nakagaito, Y. Li, G.I. Waterhouse, Effect of alkali treatment on interfacial bonding in abaca fiber-reinforced composites, Composites Part A: Applied Science and Manufacturing 90 (2016) 589–597.
[131] K. Liu, X. Zhang, H. Takagi, Z. Yang, D. Wang, Effect of chemical treatments on transverse thermal conductivity of unidirectional abaca fiber/epoxy composite, Composites Part A: Applied Science and Manufacturing 66 (2014) 227–236.
[132] K. Panyasart, N. Chaiyut, T. Amornsakchai, O. Santawitee, Effect of surface treatment on the properties of pineapple leaf fibers reinforced polyamide 6 composites, Energy Procedia 56 (2014) 406–413.
[133] P. Threepopnatkul, N. Kaerkitcha, N. Athipongarporn, Effect of surface treatment on performance of pineapple leaf fiber–polycarbonate composites, Composites Part B: Engineering 40 (2009) 628–632.
[134] A. Singha, R.K. Rana, Natural fiber reinforced polystyrene composites: effect of fiber loading, fiber dimensions and surface modification on mechanical properties, Materials and Design 41 (2012) 289–297.
[135] A. Valadez-Gonzalez, J. Cervantes-Uc, R. Olayo, P. Herrera-Franco, Effect of fiber surface treatment on the fiber–matrix bond strength of natural fiber reinforced composites, Composites Part B: Engineering 30 (1999) 309–320.
[136] H. Luo, G. Xiong, C. Ma, P. Chang, F. Yao, Y. Zhu, C. Zhang, Y. Wan, Mechanical and thermo-mechanical behaviors of sizing-treated corn fiber/polylactide composites, Polymer Testing 39 (2014) 45–52.
[137] F. Arrakhiz, K. Benmoussa, R. Bouhfid, A. Qaiss, Pine cone fiber/clay hybrid composite: mechanical and thermal properties, Materials and Design 50 (2013) 376–381.
[138] F. Arrakhiz, M. El Achaby, K. Benmoussa, R. Bouhfid, E. Essassi, A. Qaiss, Evaluation of mechanical and thermal properties of pine cone fibers reinforced compatibilized polypropylene, Materials and Design 40 (2012) 528–535.
[139] T. Alsaeed, B. Yousif, H. Ku, The potential of using date palm fibres as reinforcement for polymeric composites, Materials and Design 43 (2013) 177–184.
[140] É.J. Siqueira, V.R. Botaro, *Luffa cylindrica* fibres/vinylester matrix composites: effects of 1, 2, 4, 5-benzenetetracarboxylic dianhydride surface modification of the fibres and aluminum hydroxide addition on the properties of the composites, Composites Science and Technology 82 (2013) 76–83.
[141] W. Zahari, R. Badri, H. Ardyananta, D. Kurniawan, F. Nor, Mechanical properties and water absorption behavior of polypropylene/ijuk fiber composite by using silane treatment, Procedia Manufacturing 2 (2015) 573–578.
[142] P. Zierdt, T. Theumer, G. Kulkarni, V. Däumlich, J. Klehm, U. Hirsch, A. Weber, Sustainable wood-plastic composites from bio-based polyamide 11 and chemically modified beech fibers, Sustainable Materials and Technologies 6 (2015) 6–14.

[143] E. Jayamani, S. Hamdan, M.R. Rahman, M.K.B. Bakri, Investigation of fiber surface treatment on mechanical, acoustical and thermal properties of betelnut fiber polyester composites, Procedia Engineering 97 (2014) 545–554.
[144] L. Conzatti, F. Giunco, P. Stagnaro, A. Patrucco, C. Tonin, C. Marano, M. Rink, E. Marsano, Wool fibres functionalised with a silane-based coupling agent for reinforced polypropylene composites, Composites Part A: Applied Science and Manufacturing 61 (2014) 51–59.

Biocompatible and biodegradable Chitosan nanocomposites loaded with carbon nanotubes

7

Shadpour Mallakpour, Leila Khodadadzadeh
Isfahan University of Technology, Isfahan, Islamic Republic of Iran

7.1 Introduction

A biocompatible material is a synthetic or natural substance expected to interface with biological systems to assess, treat, enlarge, or substitute a special part of the body, and they can be viable or nonviable [1]. A biodegradable polymer is a synthetic or natural polymer, which can be easily degraded to smaller species and natural by-products under the action of microorganisms or enzymes [1,2]. Ester, amide, and ether are their main functional groups, which usually create via condensation reactions and ring-opening polymerization [1]. Biodegradable polymers can be classified into some categories depending on the synthesis and sources [3]. Although petroleum-based polymers have led to lots of satisfaction, their stability and resistance to degradation can cause accumulation of them in the environment at high rates. Biopolymers have been attracting special attention in the last decade to replace petroleum-based polymers. On the other hand, the mechanical and thermal properties and functionalities of biopolymers have to be improved to compete with the petroleum-based plastics. One of the most encouraging solutions to prevail over these disadvantages is the development of bionanocomposites (bio-NCs) [4]. NCs consist of two or more distinct components, including matrix and filler, and at least one phase is in nanosclae range (less than 100 nm) [5]. There are three types of NCs: metal NCs, ceramic NCs, and polymer NCs in which the matrix is metal, ceramic, and polymer, respectively. Compared with pure polymers, polymeric NCs have provided a wide range of promising applications because of their improved properties, such as mechanical [6] and thermal [7] behaviors, water permeability [8], and some useful applications such as removal of heavy metal ions and other pollutants from water [9], drug delivery [10], etc. These properties can be obtained by using only a very low amount of nanofiller compared to higher content in conventional composites [11].

Chit, poly-β(1,4)-2-amino-2-deoxy-D-glucose, is a nontoxic, semicrystalline, biodegradable, and biocompatible linear polysaccharide. It consists of irregularly dispersed glucosamine and N-acetyl glucosamine parts [12]. As shown in Fig. 7.1 the active functional groups of Chit are the free amine and hydroxyl groups. It's notable that Chit can solve in water media via protonation of $—NH_2$ group in acidic conditions, and under these conditions, Chit converts to a polycation. The charge density of Chit depends on the degree of amino group acetylation and pH [13].

Biodegradable and Biocompatible Polymer Composites. http://dx.doi.org/10.1016/B978-0-08-100970-3.00007-9

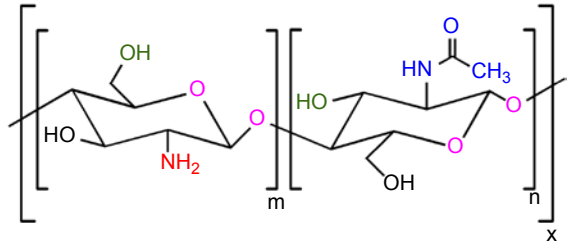

Figure 7.1 Chemical structure of Chit.
Adapted from R. Riva, et al., Chitosan and Chitosan Derivatives in Drug Delivery and Tissue Engineering, Chitosan for Biomaterials II, Springer, 2011, pp. 19–44, with kind permission of Springer.

Chit is the second most abundant polysaccharide, but it does not exist abroad in nature and cannot be directly extracted from natural resources. Typically, Chit is obtained by hydrolysis of amide parts of chitin under alkali conditions. This deacetylation process is seldom complete, and when the degree of acetylation reduces to 60 mol%, chitin converts to Chit. Unlike Chit, chitin is present in nature, especially in insects, crustaceans, and mushrooms, and a nonanimal origin is proved to be safer for biomedical applications [12]. Because of its biocompatibility, biodegradability, and containing several functional groups, Chit has been enticed notable interest in some important usages such as water treatment, separation membrane, food packaging, tissue engineering, and drug delivery [14]. Because of cationic structure, Chit chains can interact with negatively charged species via electrostatic interactions. Chit also can make nanoparticles (NPs) by ionic gelation with polyphosphates and nucleic acids [12]. However, low mechanical and thermal properties of Chit limit its usage for lots of industrial applications. Preparing Chit NCs containing nanofillers, such as carbon nanotube (CNT) [15,16], clay [17], hydroxyapatite [18], and metal oxides [19,20], has proved to be an important method to solve mentioned problems [14]. When the nanofillers are distributed uniformly in the Chit matrix, greatest mechanical improvements can be achieved.

Among nanofillers, CNTs have allured very great notice because of their extremely good physicochemical, mechanical, electrical, optical, and thermal properties [21,22]. CNTs can be creatively fabricated by rolling up a single layer of graphene sheet (to produce single-walled CNT (SWCNT)) or many layers (to produce multiwalled CNT (MWCNT)) to form concentric cylinders [23]. CNTs can be applied in many fields such as drug delivery [24], hydrogen storage [25], chemical sensor [23], and reinforcement applications in NCs [22,26,27]. Because of low density and extremely high aspect ratio, CNTs have outstanding outcome in improving the thermal, electrical, and mechanical properties of polymer NCs compared with pristine polymer [28–30]. There are various procedures for the preparation of CNTs such as arc discharge, laser ablation, carbon monoxide disproportionation, chemical vapor deposition (CVD), and hydrothermal method [31].

This chapter critically describes the latest (2014–16) methods used in the synthesis and characterization of biocompatible and biodegradable Chit/CNT NCs. Moreover, lately, the applications of Chit/CNTs are explained in detail.

7.2 Synthesis and characterization of chit/carbon nanotube nanocomposites

Generally, there are three procedures for the preparation of polymer NCs: solution mixing, melt mixing, and in situ polymerization in which solution mixing is the most common rout [32]. Low CNT value and large interface area are two important factors needed for the best performance of polymer/CNT NCs. On the other hand, CNTs are susceptible to aggregation due to inherent van der Waals attraction among tubes, high surface area, and high aspect ratio, so incorporation of individualized CNTs into the matrix is a main problem in terms of using CNT in NCs [33]. It has been indicated that only stirring in a solvent or even in a polymer melt is not enough to attain this goal. For this purpose, ultrasonication is a frequently applied method [34,35]. In addition, native CNTs have poor solubility and biocompatibility, whereas the properties of polymer/CNT NCs are highly dependent on the dispersion state of nanotubes and their interaction with the polymer matrix [36,37]. Surface modification of CNTs is a successful way to improve the solubility and compatibility of CNTs with polymer matrix [38]. Modification process introduces some kinds of polar groups, such as polar functional groups, small organic molecules, and macromolecules on the surface of CNTs, resulting in improvement in their hydrophilicity and decreasing agglomerations [39–42]. To further facilitate CNTs functionalization and their applications, some approaches, which are based on their high efficiency, energy-saving and environment-friendly chemical reaction such as green functionalization by using water [43,44] or ionic liquids [45,46] as solvents, nonsolvent reactions [47,48], sonication [34,35], and microwave-assisted functionalization [49–51], have been reported.

Structural and morphological properties of polymer NCs have been characterized to evaluate the dispersion state of fillers in polymer matrix. For characterization of NCs, various characterization methods can be used. Powder X-ray diffraction (XRD) is the usually applied method to probe the structure of NCs. Scanning electron microscopy (SEM) and transmission electron microscopy (TEM) are useful techniques for investigating the morphology and dispersion state of nanofillers. However, it is very difficult to estimate the real degree of distribution of nanofillers because the intrinsic resolution of most SEM tools is around 1 nm [13].

7.2.1 Chit/carbon nanotube nanocomposite films

1n 2014–15, Mallakpour and Madani synthesized different kinds of Chit/MWCNT NCs by using small organic molecules for further modification of MWCNT-COOH [15,16,52–54]. They enhanced the biocompatibility of MWCNTs with Chit by increasing their hydrophilicity. For this purpose, some biomolecules such as vitamins, amino acids, and carbohydrates were introduced to the surface of MWCNT-COOH. Using such biomolecules endows MWCNT the ability of using as biodegradable and biomedical materials. As an example, in 2015, they functionalized MWCNT-COOH with valine (Val) amino acid via creation of amide bond between carboxyl group of MWCNT and amino

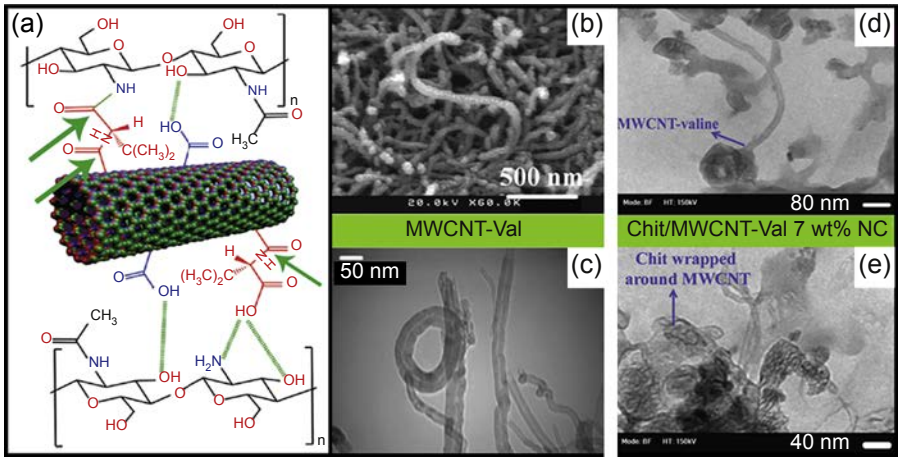

Figure 7.2 (a) Possible covalent and hydrogen bonding interactions between the Chit and MWCNT-Val, (amid bonds are shown by *green arrow*), (b) SEM image of MWCNT-Val, (c) TEM image of MWCNT-Val, and (d and e) Chit/MWCNT-Val 7 wt% NC with different magnifications.

group of Val [15]; (see Fig. 7.2(a)). The prepared Val-grafted MWCNTs were characterized using Fourier transform infrared (FT-IR) spectroscopy, XRD, field-emission SEM (FE-SEM), and TEM. Morphological characterizations revealed cylindrical shape and high surface roughness for modified nanotubes (see Fig. 7.2(b) and (c)). Homogenous Chit/MWCNT-Val acidic solutions with various percentages of MWCNT-Val (3, 5, and 7 wt% respect to polymer) were prepared with the aid of sonication and then the NC films were made by solution casting technique. As can be seen in Fig. 7.2(a), in addition to physical interactions (hydrogen bonding) between filler and matrix, the sonication process caused to covalently interact between them via formation of second amide bond between amino group of Chit and carboxyl group of Val on the surface of MWCNT. SEM, TEM, and XRD were used to characterize the obtained Chit/MWCNT-Val NCs. TEM images of 7 wt% NC (see Fig. 7.2(d) and (e)) showed wrapped Chit around nanotubes, which indicated that introduction of Val onto the surface of nanotubes caused relatively strong adhesion between MWCNT-Val and Chit, resulting in good compatibility and well distribution of MWCNT-Val in Chit matrix. It was observed that the thermal and mechanical properties of Chit/MWCNT-Val NCs were depended on MWCNT-Val value. The tensile strength and modulus of all Chit/MWCNT-Val NC films changed compared with pure Chit. Tensile strength was decreased for 3 wt% NC film, whereas it was improved in terms of 5 and 7 wt% NCs. The Young's modulus and strain (%) of 3 and 5 wt% NCs were higher and lower, respectively, compared with Chit, whereas they were vice versa for 7 wt% NC. It can be concluded that aggregation of nanotubes may be occurred in higher percentages of MWCNT-Val resulting in decrease of strength and modules of the NC films. On the other hand, results of thermogravimetric analysis (TGA) revealed that 3 wt% NC had the highest thermal stability and 5 wt% NC showed little increase, whereas for 7 wt% NC the thermal stability was lower than pure Chit, which is due to the aggregation of nanotubes in higher percentages.

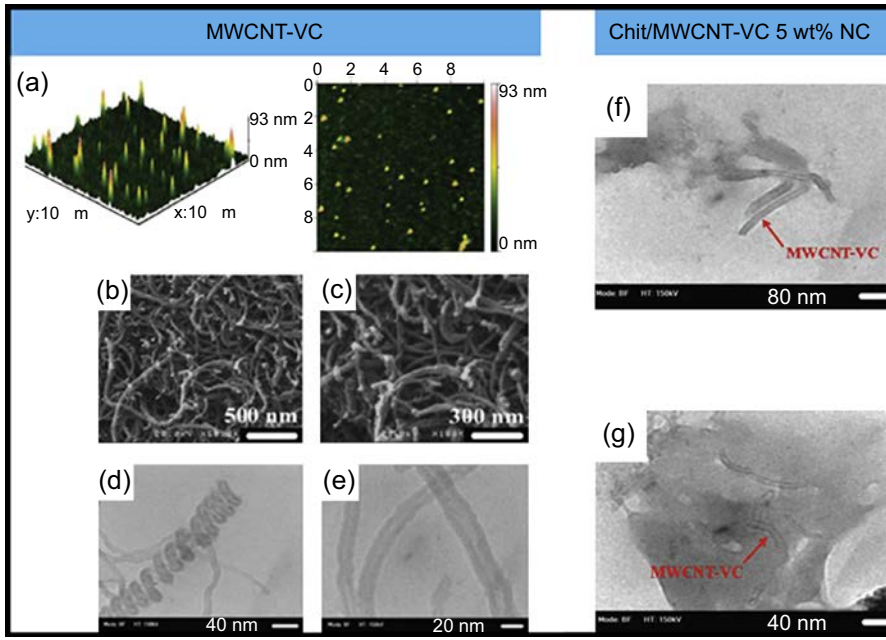

Figure 7.3 (a) AFM images of MWCNT-VC, (b and c) FESEM micrographs of MWCNT-VC with different magnification, and TEM micrographs of (d and e) MWCNT-VC and (f and g) Chit/MWCNT-VC NC 5 wt% with different magnification.

In another work, Mallakpour and Madani used vitamin C (VC) for surface modification of MWCNT-COOH [53]. In this process, an esteric bond was made via the reaction between the carboxyl group of MWCNT and hydroxyl group of VC. Then 3, 5, and 7 wt% of MWCNT-VC were added to the acidic solution of Chit, and after sonication, the NC films were obtained by casting these solutions. Morphological properties of MWCNT-VC and Chit/MWCNT-VC 5 wt% NC were investigated by atomic force microscopy (AFM), FE-SEM, and TEM (see Fig. 7.3). These characterizations revealed that MWCNT-VC has cylindrical (see Fig. 7.3(a)) and nontubular shape (see Fig. 7.3(d) and (e)) with rough surface (see Fig. 7.3(b) and (c)). Furthermore, TEM micrographs of Chit/MWCNT-VC NC with 5 wt% MWCNT-VC proved that nanotubes were well distributed in Chit as a result of hydrogen bonding between them (see Fig. 7.3(f) and (g)).

The effect of MWCNT-VC incorporated into the Chit was studied on the mechanical and thermal properties of NCs. TGA analysis showed that all Chit/MWCNT-VC NCs were less thermally stable compared with pure Chit. This observation is attributed to the semicrystalline structure of Chit. In fact, incorporation of MWCNT-VC into Chit causes to destroy the crystallinity of Chit via weakening the interchain interactions, consequently resulting to increase the mobility of chains and decrease thermal stability. In terms of mechanical properties, addition of MWCNT-VC increased the tensile strength of 5 and 7 wt% NCs whereas decreased it for 3 wt% NC, which may be due to the incomplete distribution of nanotubes.

This research work also used carbohydrates such as glucose (Gl) and fructose (Fr) for further modification of MWCNT-COOH [52,54]. They modified MWCNT-COOH with Gl in the presence of N,N'-carbonyldiimidazole (CDI) [52]. The CDI catalyzes an esterification reaction between the carboxylic acid group of MWCNT-COOH and hydroxyl group of Gl. Afterward, Chit/MWCNT-Gl NCs were prepared by solution casting technique and by the addition of 3, 5, and 7 wt% MWCNT-Gl in an acidic Chit solution followed by ultrasonication of mixture. Fig. 7.4 shows the AFM and TEM images of the pure Chit and Chit/MWCNT-Gl 7 wt% NC. As shown in Fig. 7.4(a), the existence of bulges proved that the Chit is crystalline, whereas, by the addition of MWCNT-Gl, the morphology of the surface was changed (see Fig. 7.4(b)). The TEM images of the Chit/MWCNT-Gl 7 wt% NC (see Fig. 7.4(c)) indicated that modified nanotubes were well distributed into the matrix. TGA analysis showed that NCs were less thermally stable than Chit due to semicrystalline structure of Chit as mentioned earlier. In terms of mechanical properties, the tensile strength increased with increasing MWCNT-Gl from 3 to 7 wt%. On the other hand, the tensile strength and Young's modulus of 3 and 5 wt% NCs were lower compared with pure Chit, whereas NCs they were higher in terms of 7 wt%. Actually, the Chit/MWCNT-Gl 7 wt% NC had best compatibility between filler and matrix and consequently had highest tensile strength.

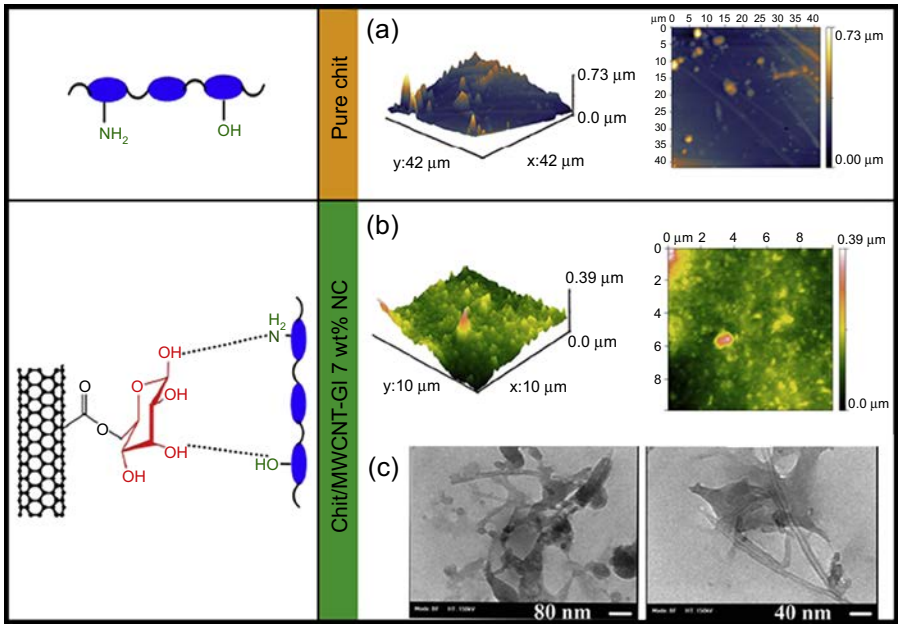

Figure 7.4 AFM images of (a) pure Chit and (b) Chit/MWCNT-Gl NC 7 wt%; (c) TEM images of Chit/MWCNT-Gl NC 7 wt% with different magnifications.
Adapted from S. Mallakpour, M. Madani, Effects of glucose-functionalized multiwalled carbon nanotubes on the structural, mechanical, and thermal properties of chitosan nanocomposite films, Journal of Applied Polymer Science 132 (23) (2015), with kind permission of John Wiley and Sons.

However, the elongation of all NCs increased than the pure Chit, which proved that the Chit/MWCNT-Gl NC films were more flexible compared with pure Chit.

Chit/MWCNT NCs were prepared by only carboxyl-modified MWCNT. Cheng et al. [55] prepared Chit/MWCNT-COOH NC films by adding 0.1, 0.3, 0.5, 0.7, and 0.9 wt% of MWCNT-COOH into the Chit matrix. Sonication and solution casting method were used to prepare NC films. Mechanical properties of pure Chit films and Chit/MWCNT-COOH NC films were compared. Tensile strength and Young's modulus were increased compared with Chit only in terms of Chit/MWCNT-COOH 0.1 wt% NC, whereas when the amount of MWCNT-COOH was increased rather than 1 wt%, they decreased, which may be attributed to the aggregation of nanotubes in higher values. The elongation at break of the NCs decreased when the amount of nanotubes increased. This observation can be a result of antiplasticizer effect of nanotubes, which can restrict the Chit elastic deformation behavior. Moreover, because of the hydrophobic characteristic of MWCNTs,NCs with higher percentages of nanotubes were more water resistant. This is despite the fact that water absorption of all NCs was considerable as a result of hydroxyl and free amino groups presented in the Chit. The biodegradation process of obtained NCs was studied in this work, and the effect of different factors such as buffer and enzyme concentration and MWCNT value was investigated. It was observed that the biodegradation rate of NCs was decreased when the amount of MWCNTs was increased. In addition, MWCNTs were recovered from degraded Chit/MWCNT NCs by physical base separation and new NCs were prepared using recovered MWCNTs. The recovery efficiency of MWCNTs was high. The derivative thermogravimetric (DTG) and SEM (see Fig. 7.5) results proved that structure and thermal properties of recovered MWCNTs were similar to initial MWCNTs.

It seems that in comparison between MWCNT-COOH and biomolecule (vitamin, carbohydrate, and amino acid)–modified MWCNT-COOH, the latter can cause improvements in the dispersion and hydrophilicity of CNTs and consequently further amounts of CNT can be incorporated into Chit matrix, so better mechanical and thermal properties can be achieved.

In 2015, Zaman et al. [56], studied the effect of gamma irradiation (γ-irradiation) on the properties of Chit/MWCNT NCs. Different kinds of Chit/MWCNT NC films using both pristine MWCNT (p-MWCNTs) and MWCNT-COOH were prepared via sonication and solution casting techniques. Then the prepared NCs were subjected to γ-irradiation and the properties of irradiated and nonirradiated NCs were compared. In terms of FT-IR analysis, it was observed that, for nonirradiated Chit/MWCNT-COOH NCs, the 1641 cm^{-1} band attributed to the carbonyl of ester was broadened and the Chit amino group band at 1562 cm^{-1} was weakened because of its reaction with carboxyl group of MWCNT-COOH. This is despite the fact that, in the irradiated NCs, the 1562 cm^{-1} band of amino group was broadened because of the deacetylation process. In TGA analysis, improved thermal stability was observed in terms of Chit/MWCNT-COOH NCs, which were supposed to irradiation due to cross-linking between Chit and MWCNT-COOH. The intensity of irradiation was affected on the mechanical properties of NCs. When the NCs were supposed to low-intensity irradiation, the tensile properties of the NCs were improved than the nonirradiated NCs as a result of cross-linking, but at further intensities, tensile properties were dropped off,

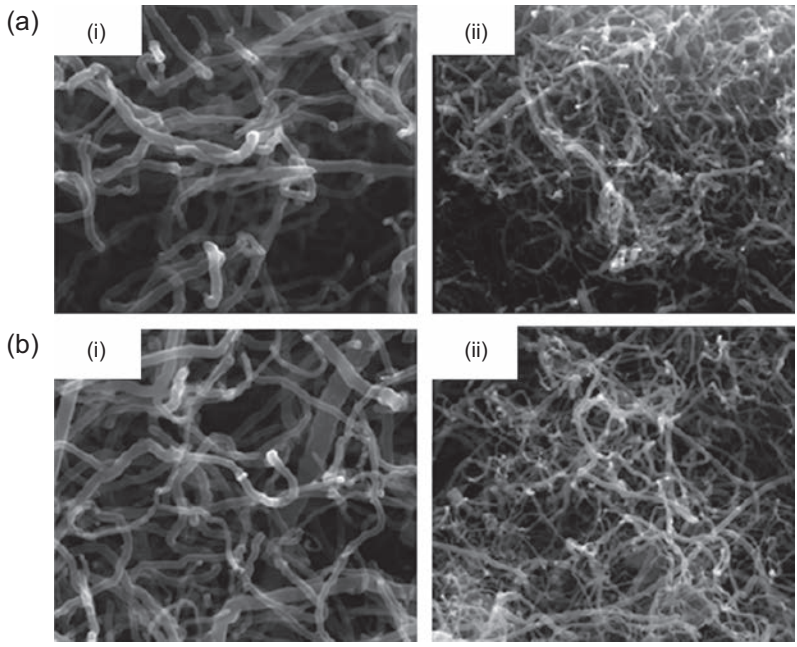

Figure 7.5 SEM with resolution (i) 100kX and (ii) 40kX: (a) oxidized MWCNTs and (b) recovered MWCNTs (second stage).
Adopted from Y.K. Cheng, et al., Study on the reusability of multiwalled carbon nanotubes in biodegradable chitosan nanocomposites, Polymer-Plastics Technology and Engineering 53 (12) (2014) 1236–1250, with kind permission of Taylor and Francis.

which is due to the chain scission of Chit. However, reverse results were found for the elongation at break. It was decreased at a lower intensity and increased at a higher intensity. It can be concluded that, cross-linking effects was a prevailing factor at lower intensities, whereas chain scission was predominant factor at higher intensities.

Using of Chit only for surface modification of MWCNT was done by Shariatzadeh and Moradi [50]. They prepared an organic/inorganic hydride material via the surface functionalization of MWCNT with two antimicrobial materials, Chit and magnesium oxide (MgO) NPs, by single-step microwave-assisted synthesis. FT-IR, SEM, TEM, X-ray probe microanalyzer, and TGA were used to identify the existence of MgO NPs and Chit on the surface of MWCNTs. The presence of MgO in NCs was proved by observing the band at 680 cm^{-1} in FT-IR spectrum, which is attributed to the heteropolar diatomic molecular vibrations. As can be seen in Fig. 7.6(a), electrostatic interactions and hydrogen bonding could conjugate the MgO NPs and Chit chains. Morphological characterizations (see Fig. 7.6(b) and (c)) of MWCNT–Chit, MgO NCs, showed a considerable increase in the diameter of MWCNTs, indicating that a large amount of Chit was grafted and covered the surface of nanotubes. The presence of MgO NPs connected to the surface of MWCNT–Chit was indicated by the TEM image. It can be expected that this NC with antibacterial properties can be useful in the pharmaceutical industry, such as drug delivery, dental, and orthopedic.

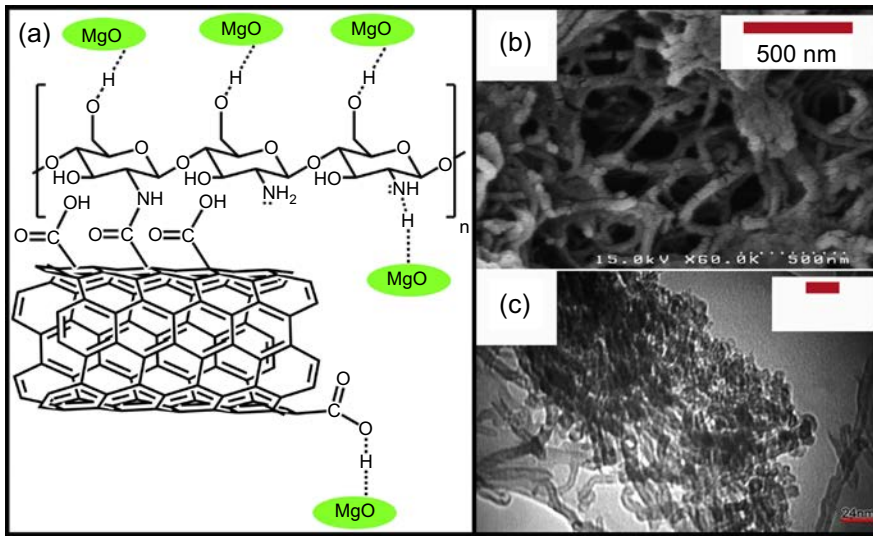

Figure 7.6 (a) Representation for MWCNT–Chit, MgO composite; (b) SEM image of MWCNT–Chit, MgO composite; and (c) TEM image of MWCNT–Chit, MgO composite. Adapted from B. Shariatzadeh, O. Moradi, Surface functionalization of multiwalled carbon nanotubes with chitosan and magnesium oxide nanoparticles by microwave-assisted synthesis, Polymer Composites 35 (10) (2014) 2050–2055, with kind permission of John Wiley and Sons.

7.2.2 Chit/carbon nanotube nanocomposite fiber

Fibers are useful in many applications such as textiles. Chit also can be shaped into fiber, but the mechanical properties of pure Chit fibers are not suitable for many industrial applications. Blending of Chit with other polymers or CNTs is an outstanding way to improve the properties of Chit fibers, although the mechanical strength and electrical conductivity of Chit/CNT NC fibers are relatively low ever. In 2016, Lee et al. [57] prepared biocompatible and macropore MWCNT/Chit-cross-linked polyurethane (PU) fiber with 4, 4′-methylenebis (phenylisocyanate) by the wet spinning method. At first, a solution of Chit/MWNT-COOH was made by formation of amide bond between Chit and MWCNT and then the cross-linking of PU into the macroscopic fibers was done via the wet spinning method. SEM images of obtained MWCNT/Chit-cross-linked PU fibers showed plentiful porous and rough grains on the inner and outer surfaces of fibers, which endow the flexible properties and large surface area of fibers (see Fig. 7.7(a) and (b)). Furthermore, Fig. 7.7(c) shows that MWCNTs were well distributed in the Chit matrix indicating good adhesion between them. The fabricated MWCNT/Chit-cross-linked PU had improved mechanical properties and electrical conductivity than the fibers without PU. The electrical conductivity of the fibers depended on the 4, 4′-methylenebis (phenylisocyanate) value for cross-linking. The tensile strength and electrical conductivity of the fibers improved when the amount of used 4, 4′-methylenebis (phenylisocyanate) was increased. Postspin twisting procedure was performed to increase the mechanical properties of the fibers (see Fig 7.7(d)). This technique can

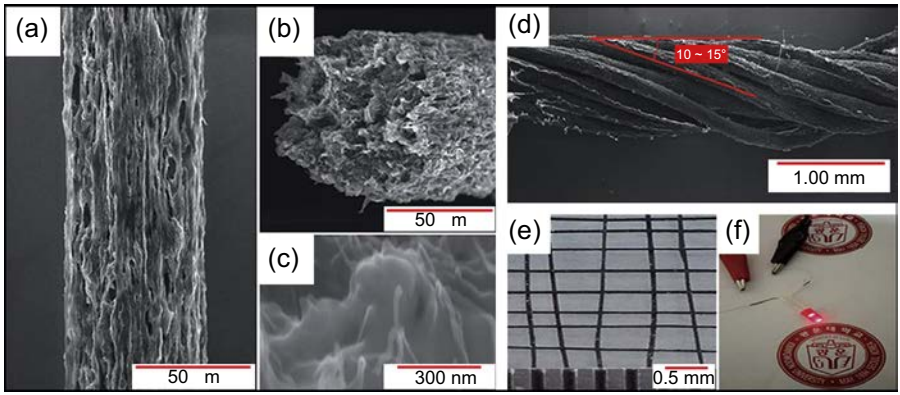

Figure 7.7 SEM images of (a) a fiber with the diameter of about 50 mm, (b) cross-sectional image, (c) fracture surface morphology of the Chit-based MWNT/PU composite fiber, (d) twisted fibers with yarn, (e) textile type, and (f) lighted LED lamp using CMPF composite fiber as the leads.
Adapted from H.U. Lee, et al., Highly conductive and flexible chitosan based multi-wall carbon nanotube/polyurethane composite fibers, RSC Advances 6 (3) (2016) 2149–2154, with kind permission of Royal Society of Chemistry.

cause stronger adhesion between nanotubes, resulting in higher van der Waals forces and friction, which can increase the load transfer between them. These MWCNT/Chit-cross-linked PU flexible fibers can be woven into different materials for many usages, such as sensors, energy harvesting, catalysts, and lead wires. As an example, the textile was woven by applying the MWCNT/Chit-cross-linked PU fibers for using as biosensor (see Fig. 7.7(e) and (f)).

CNT fibers have been attracting significant attentions because this kind of CNT can be handled more suitably compared with single nanotubes. These fibers have significant advantages than the other fibers such as modulus and strength, flexibility, and difficulty to break. CNT fibers can be made by various methods such as coagulation-based wet spinning, direct spinning from a CNT aerogel or from a preformed CNT film, and array spinning based on vertically aligned CNT arrays in which the latter is the most common method because the CNT fibers made by this method has outstanding properties such as high CNT alignment, low impurity, and low density. Liquid densification and polymer infiltration are important methods for the preparation of stronger CNT fibers. In terms of polymer infiltration, increasing the molecular weight of polymer terminates to stronger CNT fibers. However, penetration of such massive polymers into CNT gathering is very difficult. Ye et al. [58] reported a depolymerization process to penetrate Chit into CNT fiber. By depolymerization of Chit with H_2O_2 in an acidic medium (HCl), it changed to lower molecular weight polymer so that it could easily infiltrate into CNT fibers. The depolymerized Chit solution was added directly to the CNT fiber spinning and Chit-penetrated CNT fibers were obtained. Chit contains lots of —NH_2 and —OH groups, which can interact with nanotubes and consequently increase the strength the CNT fibers. Compared with polyvinyl alcohol (PVA) including only —OH groups, Chit could strengthen the

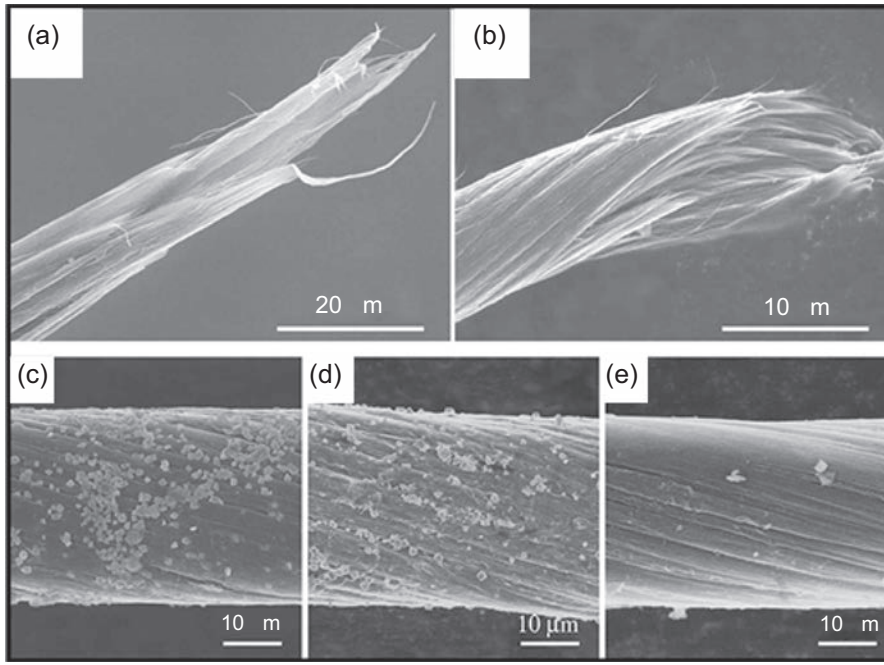

Figure 7.8 Fracture morphology of (a) CNT–PVA, (b) CNT–Chit composite fibers and SEM images of the surface morphology of (c and d). The two CdS-deposited Chit/CNT composite fibers; and (e) pure CNT fiber (unable to CdS deposition).
Adopted from Y. Ye, et al., Enhancing interfacial adhesion and functionality of carbon nanotube fibers with depolymerized chitosan, Journal of Materials Chemistry C 1 (10) (2013) 2009–2013, with kind permission of Royal Society of Chemistry.

CNT fibers significantly better, and it was confirmed by fracture mechanism as shown in Fig. 7.8(a) and (b). The depolymerization of Chit only causes shorter chains and does not influence the structure of Chit. Penetration of depolymerized Chit into CNT fibers enhanced the fiber strength double the strength of ethanol-densified fiber (liquid densification method). It was observed that depolymerization time affected the fiber strength and, by increasing this time, the strength was improved.

The effect of depolymerization process on polymer infiltration into the CNT fiber was proved by TGA analysis. It was observed that the amount of infiltrated Chit was significantly increased after shortening the chains under the depolymerization process; however, in the presence of CNTs, the decomposition temperature of Chit was dramatically decreased. Such a decrease can restrict the use of these fibers at high temperatures. Infiltration of Chit in CNT fibers also endow other abilities such as adsorption of heavy metal ions (functional groups of Chit can make complex with heavy metal ions) and photoluminescence of these fibers. As two sample tests, the adsorption of Cu(II) and the deposition of CdS NPs were performed by these fibers. The adsorption process also has effects on electrical properties of the Chit/CNT fibers. It was found that, after adsorption of Cu(II) and then drying the fibers, the conductivity of the CNT

fiber did not change while the conductivity of the Chit/CNT fibers was enhanced. The other effect of infiltrated Chit into the CNT fiber was observed during the deposition of CdS NPs, important optoelectronic, photosensitive, and photoluminescent materials, on the surface of pure CNT and Chit/CNT fibers. It was observed that CdS NPs were significantly deposited on the surface of fibers containing infiltrated Chit (see Fig. 7.8(c) and (d)), whereas there was no NPs on the surface of pure CNT fibers (see Fig. 7.8(e)), which indicates that Chit/CNT fibers can be photoluminescent.

7.2.3 Chit/carbon nanotube nanocomposite foam

Powders, films, and fibers are common forms of Chit although the porosity of these forms is not enough for some applications such as tissue engineering because it can cause fast tissue regeneration. Therefore, there is a certain need for the preparation of foams. Because the foams in tissue engineering suffer mechanical compression, thus, the desired foams must have recoverability against compressions while keeping enough porosity. Yan et al. [59] prepared pure Chit and Chit/CNT NC foams. These foams have ordered lamellar shape. Ice-templating procedure under various freezing rates (6 mm/min (low) and 10 cm/min (high)) was used for the preparation of foams and then the properties of Chit and Chit/CNT NC foams (Chit/CNT-L-x and Chit/CNT-H-x, where x is the fraction of CNTs and H and L are high and low freezing rates) were compared. As can be seen in Fig. 7.9(a), both two kinds of obtained foams were foamlike and self-standing.

SEM images of obtained foams in Fig. 7.9(b) and (c) show that foams were consisted of large amounts of lamellas or sheets that expanded at uniform direction. The interspace between these aligned parallel lamellas was at micron scale and their thickness was similar at submicron scale (see Fig. 7.9(d)). In terms of Chit/CNT NC foams, CNTs are well distributed in Chit in a separate Chit/CNT lamella (see Fig. 7.9(e)), whereas the surface of these lamellas is not smooth, and some antenna shapes is seen on their surfaces (see Fig. 7.9(e) and (g)). Creation of these antennas was stronger both in their density and length when the freezing rate was higher. Furthermore, the incorporation of CNTs into the Chit gave the elastic properties to the Chit/CNT NC foams, which was not observed when the CNT was absent (see Fig. 7.10). This outstanding elasticity can make this biocompatible Chit/CNT NC foam an excellent candidate for tissue engineering, orthopedics, and nanocarriers. On the other hand, the mechanical properties of these Chit/CNT foams were seriously influenced by freezing rate, density, and CNTs amount as follows. More elasticity was obtained at lower freezing rate and higher density. When the density of foams was constant, by increasing the CNT amount, an enhancement in elasticity was observed; however, by further addition of CNT, aggregation of nanotubes caused to decreasing the elasticity. The other benefit of CNT was improving in thermal stability of Chit/CNT foams.

In 2015, Oh et al. [60] prepared pure Chit and Chit/CNT NC foams by using sublimation-helped compression procedure at two different temperatures. To produce the foams, after casting the pure Chit and MWCNT/Chit (with different value of CNT) solutions, they were put into liquid nitrogen at −196 and −78°C and then the obtained solid mixtures were freeze-dried. In the second step, the prepared foams were pressed into multilayered films in vertical direction, which are shown in Fig. 7.11 as their SEM images.

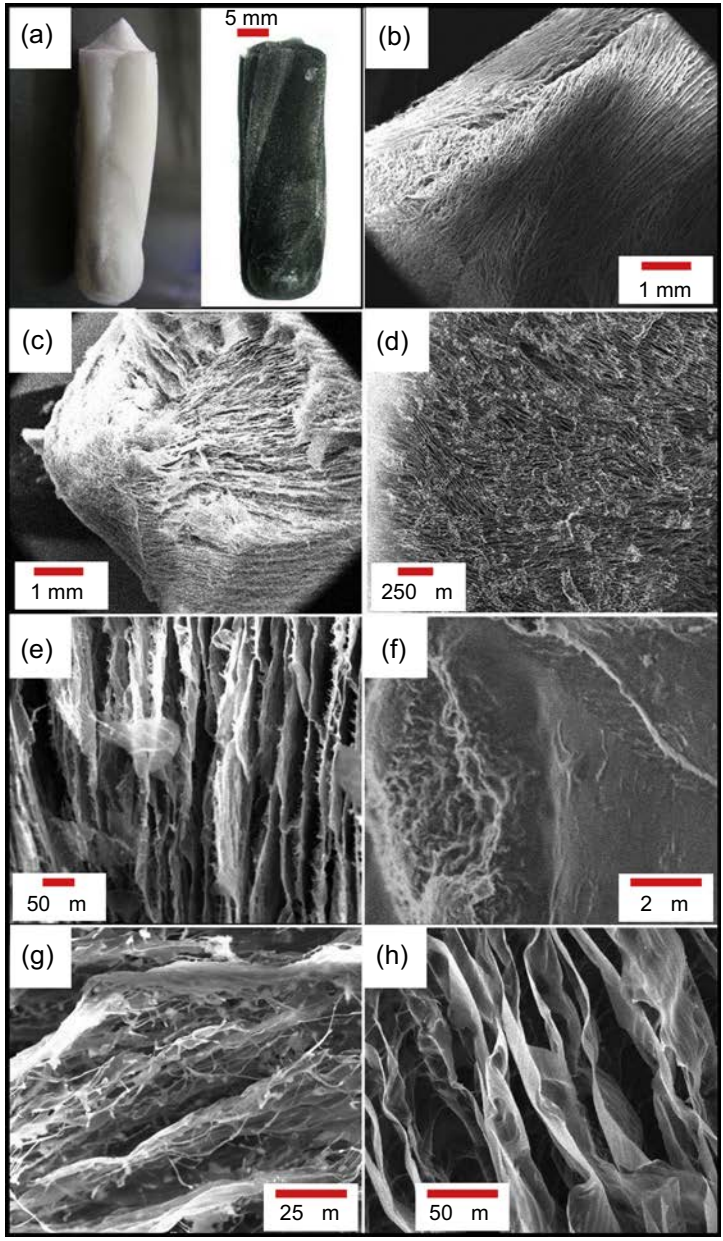

Figure 7.9 Digital photographs of the pure Chit foam (left in a) and CNTs/Chit composite foam (right in a), and SEM images of CNTs/Chit-L-0.5 (b–f), CNTs/Chit-H-0.5 (g) and the pure Chit foam prepared at low immersion rate (h). (b) Lateral surface of the sample block; (c–h) cross sections parallel (c and e–h) and perpendicular (d) to the direction of ice crystals growth (i.e., the direction of immersion into liquid nitrogen). The images in (e–h) were taken after cyclic compression tests.

Adapted from J. Yan, et al., Preparation and characterization of carbon nanotubes/chitosan composite foam with enhanced elastic property, Carbohydrate Polymers 136 (2016) 1288–1296, with kind permission of Elsevier.

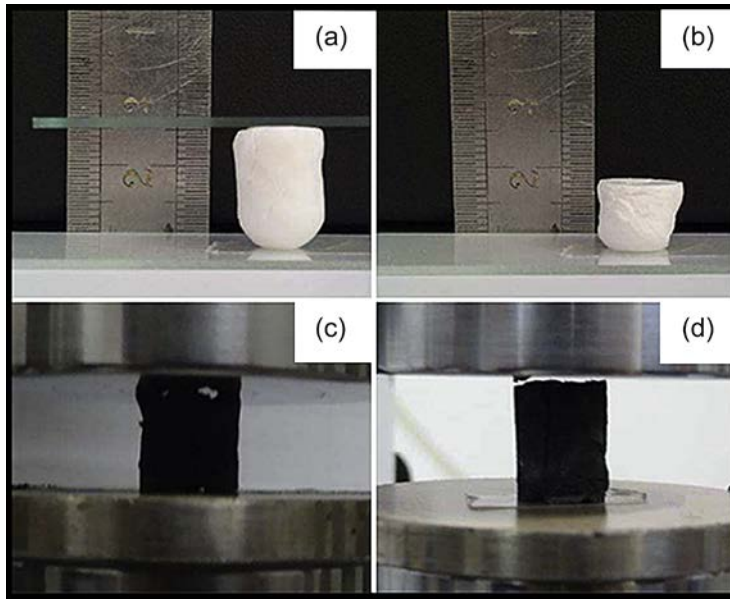

Figure 7.10 Digital photographs of pure Chit and Chit/CNT-L-0.5 composite foams (a and c) before and (b and d) after they were compressed to 50% of original length.
Adapted from J. Yan, et al., Preparation and characterization of carbon nanotubes/chitosan composite foam with enhanced elastic property, Carbohydrate Polymers 136 (2016) 1288–1296, with kind permission of Elsevier.

An individual layer of Chit/CNT multilayered film made at −196°C (see Fig. 7.11(f)) confirmed well dispersion of CNTs in Chit. On the other hand, pure Chit and Chit/CNT foams prepared at −196°C had more regularly aligned vertical direction than the foams prepared at −78°C. The vertically aligned direction in foams is ascribed to the heat flow direction during solidification. As can be seen in Fig. 7.11(d) and (e), the presence of CNTs can effect on the structure of porous Chit foams only when the foams were fabricated at higher temperatures, i.e., −78°C because at this temperature the structures of foams were more regular when CNTs were present compared with pure Chit. This is despite the fact that, at lower temperature (−196°C), such regular structures were formed when CNTs exist or not. It can be concluded that, at lower temperatures, polymer controls the microstructure of foam, notwithstanding of nanofiller. According to these results, in a sublimation-assisted compression method, higher changes in temperature can lead to highly directional heat flow and so preparation of more regular microstructures. It was also observed that high amount of CNTs prevented the formation of vertically aligned structure and therefore a serious decrease in elastic modulus and yield strength was occurred compared with pure Chit, whereas these properties improved when lower amount of CNTs were used. On the other hand, tensile and elongation were better in pure Chit foams compared with Chit/CNT because regular vertically aligned multilayered structure could act as a load-sustaining component.

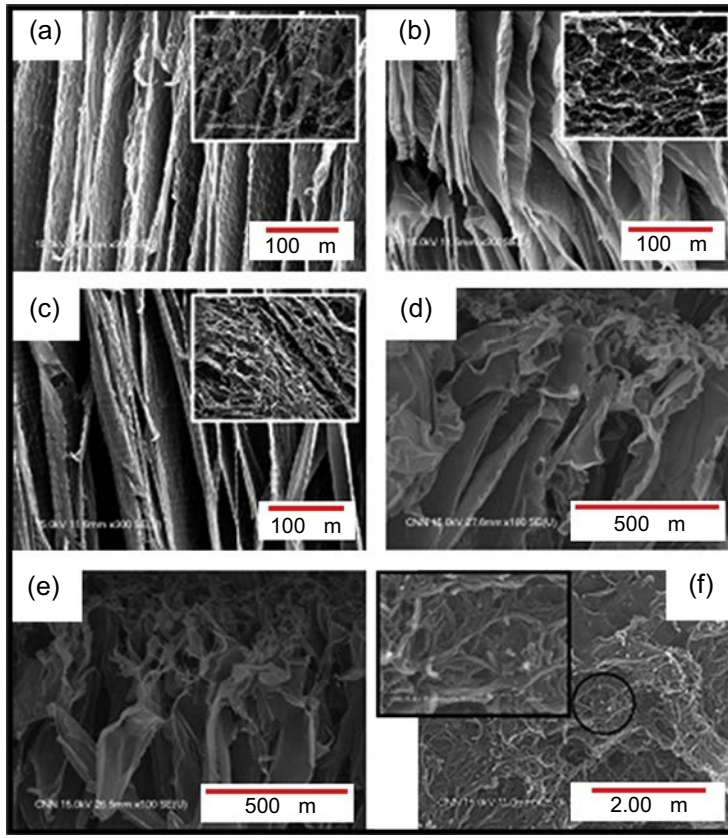

Figure 7.11 Cross-sectional and plane-view (insets) SEM images of (a) pure Chit specimens, (b and c) Chit/CNT (higher content of CNT in c) at −196°C, (d and e) pure Chit specimen and Chit/CNT NC, respectively, at −78°C, and (f) plane-view of Chit/CNT NCs fabricated in −196°C after removing a layer.
Adapted from M. Oh, et al., Vertically aligned multi-layered structures to enhance mechanical properties of chitosan–carbon nanotube films, Journal of Materials Science 50 (6) (2015) 2587–2593, with kind permission of Springer.

7.3 Applications of chit/carbon nanotube nanocomposites

7.3.1 Chit/carbon nanotube nanocomposites for adsorption and membrane

7.3.1.1 Using porous beads of chit/carbon nanotube nanocomposites

Porous NCs combine the advantages of a polymer matrix in forming a stable framework and the nanofillers that provide high surface area. Porous Chit beads are extensively applied as sorbent in many fields. Two main elements that impact the adsorption behavior

in Chit beads are microstructure and pore morphology. Moreover, Chit beads incorporated with NMs such as CNTs profit stronger porous structure and higher surface area, which can cause improved molecular adsorption. Currently reported works have applied procedures such as phase inversion, inverse phase suspension, and freeze casting procedures for preparation of Chit and Chit–CNT porous structures [61]. Ouyang and Liang [62] studied the adsorption of methyl orange (MO) and Au NPs by Chit beads. Dynamic adsorption (repeatedly compressing the Chit beads during the adsorption process) and bead surface modification with SWCNTs were two methods that are used in this study. For the preparation of Chit beads, a mixture of Chit solution and MWCNTs (for improving the porous structure) was freeze-casted by dropping in liquid nitrogen. The presence of many pores on the surface of prepared beads was confirmed by SEM images. These pores help diffusion and transportation of MO and Au NPs (see Fig. 7.12(a) and (b)). Furthermore, mechanical test showed that these porous Chit beads can retrieve to initial shape in both dry and wet conditions after compressing (see Fig. 7.12(c)). The elastic property of beads was improved in water media attributed to the adsorption of water during the unloading operation that allows the bead to enlarge and retrieve to initial shape. Adsorption properties of these porous Chit beads surveyed for an aqueous solution of MO under both dynamic and static (without compressing) conditions. Results showed better adsorption

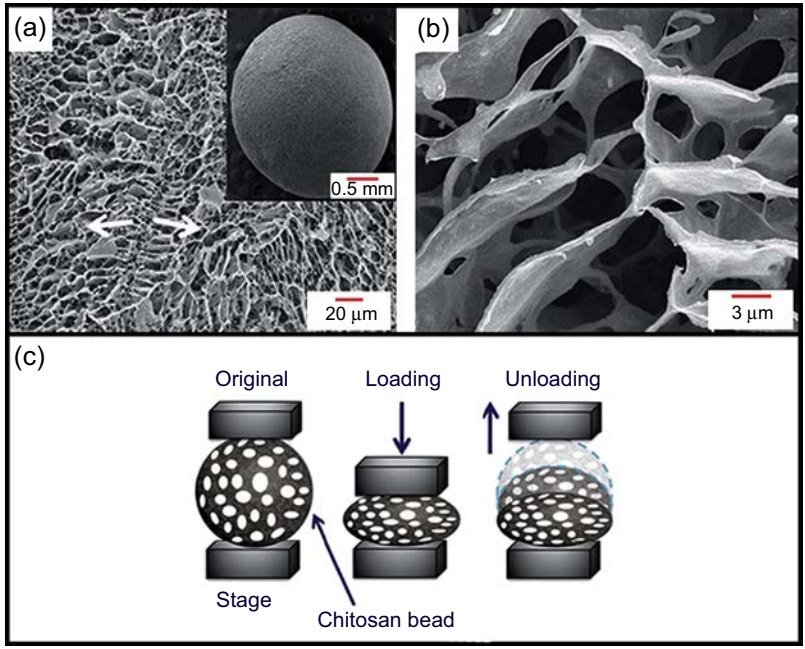

Figure 7.12 (a) SEM image of the Chit beads surface, in which the *arrows* show the direction of dendritic branches; inset, the entire bead; (b) detailed texture and pore structure on the bead surface; and (c) illustration of the dynamic process by compressing Chit beads cyclically. Adapted from A. Ouyang, J. Liang, Tailoring the adsorption rate of porous chitosan and chitosan–carbon nanotube core–shell beads, RSC Advances 4 (49) (2014) 25835–25842, with kind permission of American Chemical Society.

rate and capacity in dynamic conditions because compression of beads could ease the MO diffusion into inner pores via uptaking and extruding the solution again and again.

They also modified the surface of beads with SWCNT and this outside network can block or decrease the diffusion rate of larger size NPs without impacting the adsorption of small-sized molecules and NPs. For this purpose, an SWCNT film is cut into desired size to wrap separate Chit beads to make core–shell structures (see Fig. 7.13(a)). Spherical shape of Chit–SWCNT beads and attaching of SWCNT film to the surface of beads was confirmed by SEM images (see Fig. 7.13(b) and (c)). Its notably that these modified beads have different pore distribution at the surface (SWCNT) and core section (Chit) because the SWCNT shell has much smaller pores (tens to hundreds of nanometers) compared with the Chit pores (several millimeters).

A comparison between adsorption properties of MO and Au NPs (small (5 nm) or large (50 nm)) with Chit and Chit–SWCNT core–shell beads, was done. For MO and small Au NPs, both kinds of beads showed close adsorption rates, but for large Au NPs, a distinguishable difference was obtained and Chit beads had a higher adsorption rate. It is due to the presence of nanotube network shell, which could decrease the adsorption rate of large NPs into the Chit–SWCNT bead. This observation is attributed to the different roles of core and shell in adsorption. The adsorption process with Chit–SWCNT beads has two steps. The first step is diffusion by SWCNT shell and the second step is the adsorption of diffused species by the Chit bead core. Smaller species can simply enter to the SWNT shell and then enter to the Chit core. As a result,

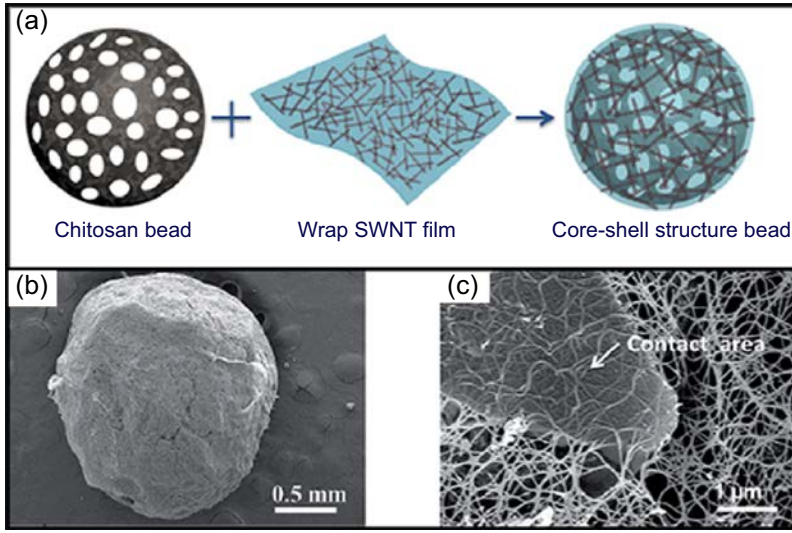

Figure 7.13 (a) Preparation of Chit–SWNT beads by wrapping an SWNT film onto a Chit bead; (b) SEM image of a Chit–SWNT bead; and (c) close view of the contact area showing well adhesion of SWNTs to the underlying bead.
Adapted from A. Ouyang, J. Liang, Tailoring the adsorption rate of porous chitosan and chitosan–carbon nanotube core–shell beads, RSC Advances 4 (49) (2014) 25835–25842, with kind permission of American Chemical Society.

for MO and small Au NPs, the adsorption by the Chit core bead is a main step so the adsorption capacity of Chit–SWCNT is close to beads without SWCNT shell for these two small species. By continuing the process, large Au NPs assembled onto the SWCNT shell so many of the pores blocked and caused to decrease the diffusion rate and adsorption capacity.

Another application of porous Chit/CNT beads for adsorption was reported by Ouyang et al. in 2015 [61]. They used various percentages of CNT-COOH (40, 80 wt%) for the preparation of spherical Chit/CNT beads. The performance of these Chit/CNT beads and Chit bead (without CNT) was compared for the adsorption of bilirubin (a metabolite of hemoglobin in blood). Freeze casting by dropping a mixed solution into liquid nitrogen was used and highly porous Chit/CNT beads including radially oriented channels were obtained. SEM results indicated that two definite morphologies related to the channel orientation and wall structure can be fabricated and the wall structure can be adapted by percentage of CNTs. Two kinds of walls (Chit controlling or CNT controlling) were fabricated at lower or higher CNT values. The Chit-controlling kind is promoted by isolated accumulations of CNT incorporated into the Chit, whereas the CNT-controlling kind includes continuously dispersed CNT stabilized by Chit as adhesives. Many micrometer-sized CNT aggregations were located randomly in Chit matrix when 40 wt% of CNT was used for the preparation of beads, while the wall thickness was below 1 mm. This morphology designates that even strong sonication of Chit/CNT could not reach to the well dispersion of CNT. On the other hand, these small CNT agglomerations located in the channel walls can act as outstanding sites for adsorption. By using 80 wt% of CNT, the radially aligned channels of Chit/CNT beads was remained while the channel walls were more curled compared with Chit beads or Chit/CNT beads with 40 wt% CNTs. This shape of walls caused to fragile beads due to decreasing of Chit as CNT adhesion agent and this role of Chit in stability of porous beads was confirmed by fabrication of very brittle Chit-free beads (CNT beads). Adsorption capacity of bilirubin for Chit/CNT was higher compared with the Chit beads because CNT-COOH could enhance the surface area, pore volume, and adsorption site (COOH group) of beads.

7.3.1.2 Using magnetically and other multifunctional chit/carbon nanotube nanocomposites

Magnetic separation is an outstanding method for the isolation of magnetic species. Separation of sorbents with magnetic properties after the adsorption process can be easily done by using only external magnetic field. Nonetheless, there are few works on the application of magnetic Chit/CNT adsorbents due to the deficiency of simple and dependable procedures for fabrication of magnetic Chit/CNT. However, there are some useful reports from 2014 on using magnetically Chit/CNT NCs for isolation of dyes and rare earth elements [63–65]. As an example, Wang et al. [65] prepared magnetically reusable Chit/CNT (mChit/CNT) by gathering Chit/CNT NC with magnetic NP for separation of acid red 18. As shown in Fig. 7.14 the Chit/CNT NC made via a

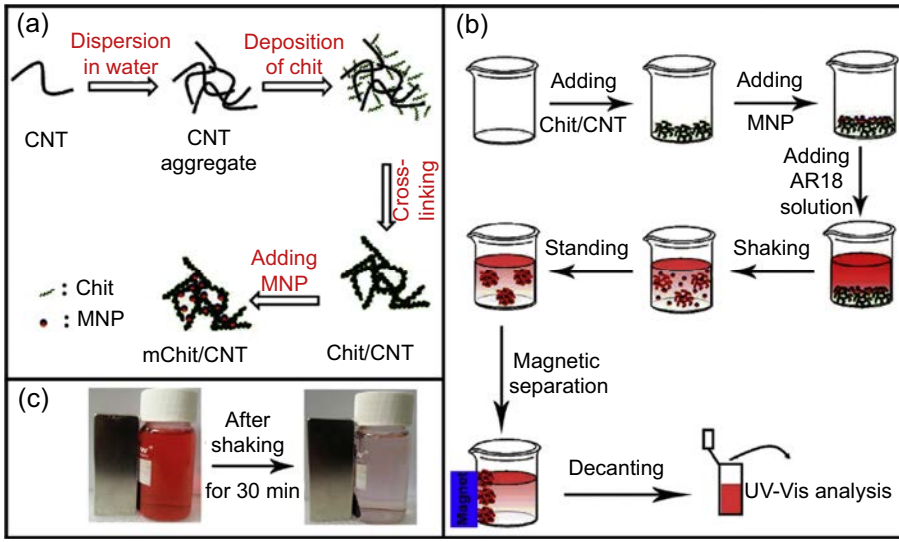

Figure 7.14 (a) Principle and process of mChit/CNT formation; (b) mChit/CNT directly formed in acid red 18 solution for acid red 18 removal; and (c) photographs of acid red 18 solution (120 mg/L) before (up) and after (down) adsorption by mChit/CNT.
Adapted from S. Wang, et al., Highly efficient removal of Acid Red 18 from aqueous solution by magnetically retrievable chitosan/carbon nanotube: batch study, isotherms, kinetics, and thermodynamics, Journal of Chemical & Engineering Data 59 (1) (2013) 39–51, with kind permission of American chemical society.

"surface deposition–cross-linking" rout and mChit/CNT was made in situ in acid red 18 solution (see Fig. 7.14), and after adsorption process, all of dye-adsorbed mChit/CNT was easily isolated by an external magnetic field.

The adsorption process was described using pseudo–second-order kinetics. Freundlich and Redlich–Peterson isotherm models fitted well the experimental data with $R^2 > 0.9137$. Thermodynamic constants such as $\Delta G°$ (−2.87 to −3.28 kJ/mol), $\Delta H°$ (3.39 kJ/mol), and $\Delta S°$ (20.61 J/K mol) indicated the spontaneous, endothermic, and entropy-driven nature of acid red 18 adsorption on mChit/CNT. Moreover, the reusability test showed that the adsorption of acid red 18 with mChit/CNT was kept relatively constant. The study indicated that the mChit/CNT is an encouraging adsorbent for the separation of anionic azo dyes.

Purification of rare earth elements has drawn significant attention due to their special properties, which are useful for some important technologies such as turbines, car engines, and petroleum. On the other hand, rare earth metals purification is difficult due to similar physical and chemical properties of these metals. Adsorption and especially adsorption by ion-imprinted polymers (IIPs), which has high selectivity for capturing a certain ion in terms of size, is an outstanding method for purification of rare earth metals. Generally, in imprinting method, a template-shaped cavity is made in polymer with the memory of the template. In 2015, Li et al. [63] fabricated a

magnetically retrievable IIP Chit/CNT NCs for selective separation of Gd^{3+} from an aqueous mixture of rare earth ions. For this purpose, a Gd^{3+}-imprinted Chit-coated CNT (IIP/CNT) NC was fabricated by surface deposition–cross-linking method (depositing the Gd^{3+}–Chit complex onto CNT surface and then cross-linking of Gd^{3+}–Chit) followed by magnetization by a simple blending method [simply adding Gd^{3+}-IIP-Chit/CNT and silica-coated magnetite NP (SiO_2—Fe_3O_4)] (see Fig. 7.15(a)). The SEM images of IIP-Chit/CNT and magnetically IIP-Chit/CNT (mIIP-Chit/CNT) are shown in Fig. 7.15(b) and (c).

Saturation adsorption capacity for Gd^{3+} by this mIIP-Chit/CNT and reusability of this adsorbent were notably bettered compared with other reported ion-imprinted adsorbents for Gd^{3+}; however, the selectivity relative to La^{3+} and Ce^{3+} were close to other reported IIP-Chit adsorbents.

As an another example of using magnetically Chit/CNT NCs, we can point to the magnetic CNT/C-Fe/Chit for the separation of organic pollutants, including dyes (methylene blue (MB) and MO), antibiotics (tetracycline (TC)), and organic arsenical compound (roxarsone (ROX)) [64]. This CNT/C-Fe/Chit had higher adsorption capacity for negatively charged pollutants. The equilibrium adsorption data were well matched with the Langmuir, Freundlich, and Temkin models. The kinetic study revealed that the adsorption process by this adsorbent was better matched with the pseudo–second-order kinetic model. Positive ΔH° proved the endothermic feature of adsorption. Negative ΔG° reflected that the adsorption process is feasible and spontaneous.

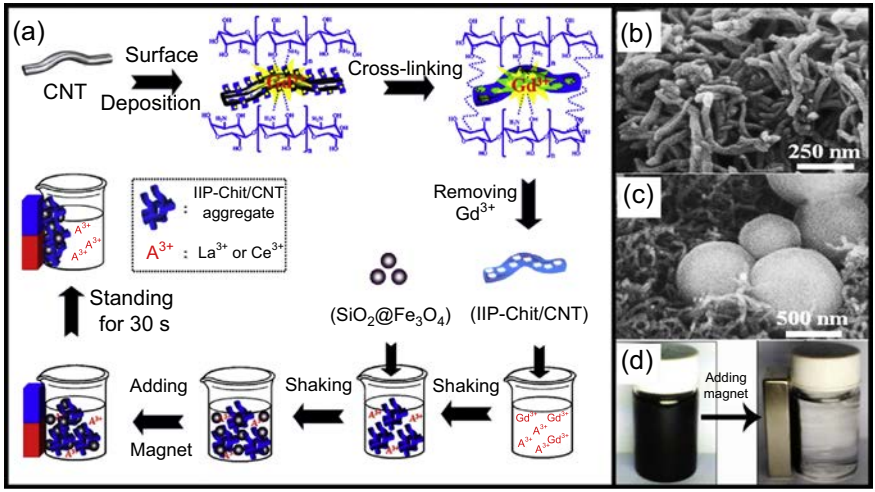

Figure 7.15 (a) Preparation of magnetically retrievable IIP-Chit/CNT and its application for selective adsorption of Gd^{3+}, SEM images of (b) IIP-Chit/CNT; (c) mIIP-Chit/CNT; and (d) photographs of mIIP-Chit/CNT solution before (left) and after (right) magnetic separation. Adopted from K. Li, et al., Selective adsorption of Gd^{3+} on a magnetically retrievable imprinted chitosan/carbon nanotube composite with high capacity, ACS Applied Materials & Interfaces 7 (38) (2015) 21047–21055, with kind permission of American Chemical society.

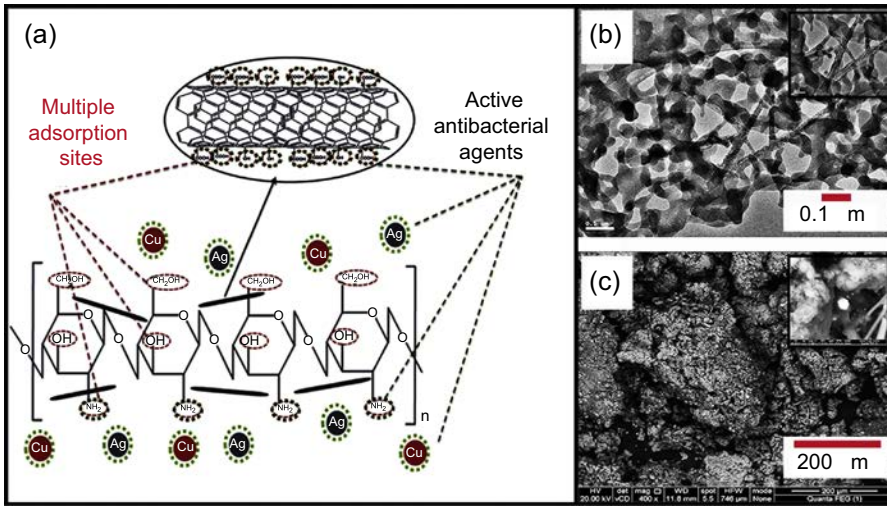

Figure 7.16 (a) Different active sites of the prepared multifunctional composite; (b) TEM image of the multifunctional composite; the insert shows higher magnification image; and (c) SEM image of the multifunctional composite; the insert shows a higher magnification image. Adapted from A.M. Alsabagh, et al., Preparation and characterization of chitosan/silver nanoparticle/copper nanoparticle/carbon nanotube multifunctional nano-composite for water treatment: heavy metals removal; kinetics, isotherms and competitive studies, RSC Advances 5 (69) (2015) 55774–55783, with kind permission of Royal Society of Chemistry.

Some other multifunctional Chit/CNT NCs for adsorption are reported in recent years. As an example, a multifunctional NC of Chit, Ag NPs, Cu NPs, and CNT was prepared by Alsabagh et al. in 2015 for the removal of heavy metals and microbes from water [66]. The structure of this Chit/Ag/Cu/CNT is shown in Fig. 7.16(a). Fig. 7.16(b) and (c) shows the SEM and TEM images of Chit/Ag/Cu/CNT and confirmed the adhesion of CNTs onto the Chit and the presence of spherical NPs.

The prepared Chit/Ag/Cu/CNT had a greater Cu^{2+}, Cd^{2+}, and Pb^{2+} adsorption efficiency than the pure Chit. Furthermore, results showed the reusability of this multifunctional composite in adsorption/desorption processes.

Chit cannot be used as a proton exchange membrane due to its low proton conductivity. Many modification methods including sulfonation, phosphorylation, chemical cross-linking, incorporation of inorganic particles, and blending with other polymers have been used to refine the proton conductivity of Chit; nonetheless, week mechanical and electrical properties of chemically modified Chit limit some of the applications. Incorporation of inorganic particles into the Chit is a promising solution for this problem. In 2015, Chit/silica-coated CNTs (Chit/SCNTs) membranes were fabricated by a solution blending followed by chemical cross-linking [67]. The presence of SCNTs prohibited the electron conduction through the Chit/SCNTs. The hydrophilic silica layer on the surface of CNT had two main roles: preventing the electronic short-circuiting and increasing the biocompatibility of CNT with Chit and consequently well distribution of CNT in Chit matrix. These Chit/SCNTs membranes had improved thermal and oxidative stability, mechanical properties, and proton conductivity compared with pure Chit membrane.

Lee et al. prepared surface wettability-controlled Chit/CNT membrane for selective separation of phenol from water [68]. For the preparation of Chit/CNT membranes, Chit as a hydrophilic shell was wrapped around CNT as a core followed by self-assembling of this core–shell structure. By modification of Chit shell using octanal (reaction between NH_2 group of Chit with COH group of octanal and creation of imine group), the octanal-modified Chit/CNT membrane (ocChit–CNT) was obtained, which has hydrophobic surface. Different CNT values (25, 50, and 75 wt%) were used to prepare both Chit–CNT and ocChit–CNT membranes. SEM and TEM images of both membranes showed lots of nanosized pores. All Chit–CNT membranes with various CNT values had very similar external appearance and the rough surfaces of membranes confirmed the adhesion of the Chit shell on CNT surfaces via hydrogen bonding. On the other hand, different Chit–CNT (Chit–CNT25, Chit–CNT50, Chit–CNT75) membranes showed different thicknesses of Chit shell. The thickness of Chit shell reduced when the value of Chit decreased. Nonetheless, Chit–CNT and ocChit–CNT did not show considerable difference about thicknesses and pore size. However, surface roughness of membranes was decreased after modification with octanal. Water contact angle of membranes showed different wettability before and after modification with octanal and presented in Fig. 7.17. This observation is attributed to the Chit shell nature in two kinds of membranes, which is hydrophilic in Chit/CNT due to the existence of free amine groups while it is hydrophobic in ocChit–CNT due to the presence of octyl chain and decreasing the free amine groups.

In addition, the effect of CNT value on wettability properties of membranes was studied. According to the results, the different Chit–CNT membranes showed a regular

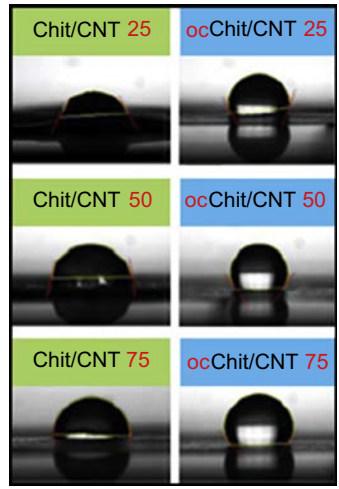

Figure 7.17 Water contact angles of Chit–CNT (Chit–CNT25, Chit–CNT50, Chit–CNT75) and ocChit–CNT (ocChit–CNT25, ocChit–CNT50, ocChit–CNT75) membranes.
Adapted from E.-J. Lee, et al., Wettability control on chitosan-wrapped carbon nanotube surface through simple octanal-treatment: selective removing phenol from water, Macromolecular Research 24 (5) (2016) 429–435, with kind permission of Springer.

enhance of water contact angle per 25 wt% of CNT percentage increase while irregular and weaker increases were observed for different ocChit–CNT membranes. It is noteworthy that ocChit–CNT membranes had better capacity and efficiency of phenol adsorption compared with Chit/CNT membranes. It is attributed to π–π stacking between CNT and phenol, van der Waals force between octyl chain and phenol, and the hydrogen bonding between Chit and phenol.

Shin and Kim also prepared a core–shell-structured Chit–CNT membrane that was used for drug delivery system and will be discussed in Section 7.3.3.

7.3.2 Chit/carbon nanotube nanocomposite for tissue engineering

Tissue engineering is an encouraging approach to regenerate the bone tissue. One of the most important approaches in tissue engineering is the fabrication of scaffolds. Preparation and application of scaffolds in many reported works is restricted by their low mechanical properties and biodegradation. Actually, fabrication of scaffolds with good mechanical and biodegradation properties at the same time is hard. According to excellent biocompatibility and biodegradability, biopolymers and specially Chit are encouraging candidates for the preparation of scaffolds. Unfortunately, mechanical strength and young's modulus of these biopolymers are not high enough for this purpose. Using ceramics together with biopolymer NCs is a good solution for this problem. Recently there are many reports for the application of Chit/CNT NCs for tissue engineering [69–72]. Shokri et al. [72] prepared NC scaffolds by using bioactive glass (a desired ceramic), CNT, and Chit. Cross-linking, pressing, and salt leaching are three steps for the fabrication of these NC scaffolds. Cross-linking of Chit was done with the aid of hexamethylene diisocyanate at high temperature and a urea group was created in Chit. The cross-linking procedure was pressurized so that the NC scaffolds could be more compressed and so the mechanical strength was enhanced. Mechanical properties of the scaffolds were improved by the addition of CNT-COOH to the Chit and bioactive glass matrix. All the NC scaffolds with different ratio of each component did not show toxicity in MTT assay. Existence of urea group in these NC scaffolds caused to slow degradation in biodegradability test.

Another example for using Chit/CNT NC for tissue engineering is fabrication of scaffold for the repair of heart defect [71]. This scaffold made to solve the main constraint of current myocardial patches that insulating polymeric scaffold walls delay the transfer of electrical signals between cardiomyocytes, causing arrhythmias. For the fabrication of this scaffold, small amount of SWCNTs (0–175 ppm; 00.0175% (w/v)) were incorporated into a gelatin–Chit hydrogel. Presence of SWCNT as electrical nanobridges between cardiomyocytes caused to enhance electrical coupling, synchronous beating, and cardiomyocyte function, while keeping biocompatibility. The value of SWCNT used in this work was appreciably lower compared with other works that used CNT as electrical conductor in hydrogels. Furthermore, as shown in Fig. 7.18(a), by incorporation of different amounts of SWCNT, the spongelike shape was maintained as well as hydrogel without SWCNT whereas in other reported works of using CNT in hydrogels,

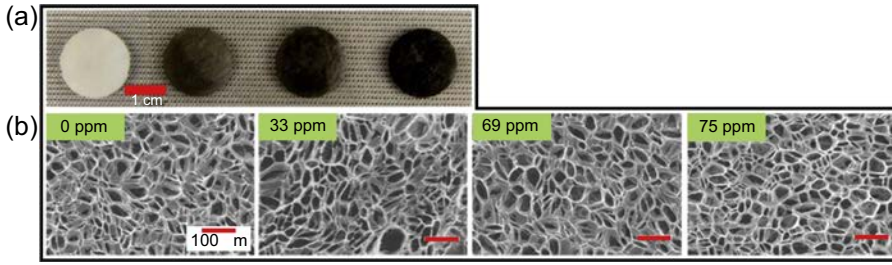

Figure 7.18 Macro- and microscopic structural properties of SWCNT-incorporated hydrogels: (a) macrograph and (b) SEM micrographs of SWCNT hydrogels with different concentrations of SWCNT.

the morphological properties of scaffold changed. Moreover, SEM analysis indicated desired properties for pores (see Fig. 7.18(b)) regardless of SWCNT amount.

On the other hand, mean pore diameter was not depended on SWCNT amount, but by increasing SWCNT, the distribution of pore size was more constant. In addition, there was a direct relationship between circularity of the pores and SWCNT amount.

7.3.3 Chit/carbon nanotube nanocomposite for drug delivery

Polymers are outstanding materials in drug delivery, which can restrict the release of pharmaceutical ingredients during the extended period and lead to reducing the side effects of them. Polymer NCs, nanocarriers, hydrogels, and micelles are most important polymeric drug delivery systems, which contain a polymer and a drug. Polymer in polymeric drug delivery system can be biodegradable or not, but biocompatible and biodegradable polymers are excellent candidates because they can remove after releasing the drug and have no toxicity. Natural polymers such as polysaccharides are mostly used for this purpose [12], and there are many reports for the application of Chit in drug delivery systems. It is very good for negatively charged drug according to its cationic feature [73]. On the other hand, there are many reports for the applications of CNTs in drug delivery. Hollow structure or inner cavities of CNT are very good places for various drugs. Small-sized drug molecules can form covalent bond with CNT and aromatic drugs can conjugate to CNT by noncovalent interactions (π–π stacking). The drug release from CNTs can be controlled by varying the pH value and temperature [31]. Surface modification of CNTs with polar molecules is a promising approach to overcome their hydrophobic nature and increasing their biocompatibility. There are many reports for the application of Chit/CNT NCs for drug delivery systems [74–78]. In 2016, Kim and Shin [74] prepared CNT buckypaper as a membrane, which has porous structure and positive surface and is capable for selective loading of negatively charged drug such as bovine serum albumin (BSA). This membrane was made by self-assembly of MWCNT fibers hybridized with Chit, and morphology images indicated the core–shell structure of Chit/CNT and the presence of Chit layer on the surface of

CNTs via strong hydrogen bonding. Among negatively charged BSA and positively charged cytochrome *c* (CC), Chit/CNT hybrid membrane was selective for loading BSA. The especially larger amount of loading capacities (LCs) for BSA is attributed to the positive surface of CNT fiber and pores of hybrid membrane.

Chit-modified CNT was used for the production of galactosylated Chit (LChit)–grafted oxidized MWCNT (O-CNT), as a nanocarrier for pH-dependent sustained release and targeted delivery of doxorubicin (DOX) [78]. Nanocarriers containing galactose residue are very useful for target drugs to hepatocytes via ligand–receptor interaction-mediated transmembrane transport due to successful identification of galactose. LChit, prepared from the reaction between the COOH of lactobionic acid and the NH_2 of Chit and its galactose residue, performed as a hepatic tumor–targeting agent. According to the high adsorption tendency of Chit on O-CNT, coating layers were created on the surface of O-CNT after modification of it with Chit. Actually with the presence of Chit containing polar functional groups (OH and NH_2) on the surface of O-CNT, the solubility and biocompatibility of the O-CNTs were increased. DOX was loaded successfully in O-CNTs-LChit via π–π stacking interaction between DOX and O-CNT, which determined the DOX LC. The presence of LChit in O-CNTs-LChit-DOX was confirmed by observation of a thicker coating layer on the surface of CNT in TEM images of O-CNTs-LChit-DOX. The presence of DOX in O-CNTs-LChit-DOX was confirmed by observing the absorption peak at 490 nm in UV–vis spectrum and emission band at 595 nm in fluorescence spectrum, which was not present in the spectrum of the O-CNTs-LChit. The zeta potential of O-CNT was negative because of the presence of COOH groups, but after modification with LChit, in addition to the increasing of the particle size, the zeta potential shifted to a positive value due to the presence of amino group of the Chit. The in vitro release of DOX was performed in different pH (5.5 (lysosomal pH), 6.5 (tumor pH), and 7.4 (physiological pH)). It was observed that release of DOX from O-CNTs-LChit-DOX was pH dependent and higher release percentage was obtained in relatively acidic pH (pH 6.5 and 5.5). The total amount of loaded DOX in O-CNTs-LChit-DOX was not released after 24 h, indicating that the strong adhesion between the O-CNTs and DOX is stable in the buffer solution. It can be concluded that the O-CNTs-LChit-DOX nanocarrier would be able to release higher amount of drug in acidic tumor compared with normal tissue. Estimating HepG2 cytotoxicity, vascular irritation and the maximum tolerated dose indicated biocompatibility and low toxicity of this nanocarrier. Moreover, these nanocarriers showed higher cellular uptake efficiency compared with free DOX. The estimation of cellular uptake of DOX and O-CNTs-LChit-DOX into HepG2 cells was done by the fluorescence method. As shown in Fig. 7.19(a), after incubating for 4 h, an enhancement in fluorescence intensity was observed for the cells treated with O-CNTs-LChit-DOX nanocarrier (DOX penetrated into the cancer cell nucleus and destroyed their DNA). Moreover, in vivo toxicity and anticancer therapeutic efficiency experiments were also performed on mice. As shown in Fig. 7.19(b) and (c), after intravenous administration in mice suffering H22 tumor, O-CNTs-LChit-DOX exhibited higher antitumor activity and higher fluorescent intensity in tumor tissue than the free DOX.

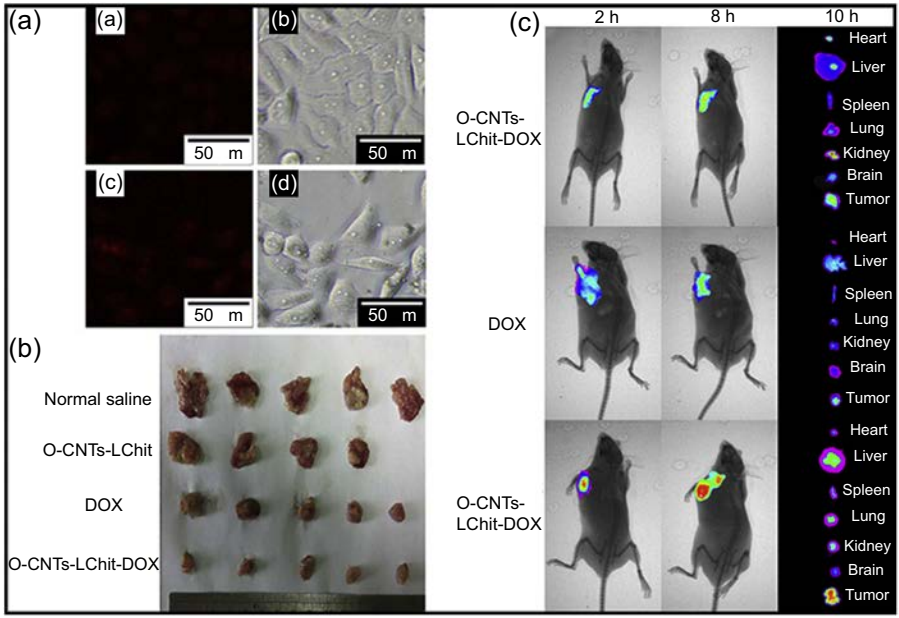

Figure 7.19 (a) Fluorescence microscopy images of HepG2 cells after incubation with DOX (a and b) and O-CNTs-LChit-DOX (c and d) for 4 h. (b) Images of tumors collected from each group after 12 days. (c) The in vivo imaging of H22 tumor-bearing mice after intravenous injection of DOX (control), O-CNTs-Chit-DOX, and O-CNTs-LChit-DOX. The images were taken at 2 and 8 h after administration. The tumor-bearing mice were sacrificed 10 h after in vivo injection and representative ex vivo fluorescence images of the major organs (heart, liver, spleen, lung, kidney, and brain) and tumor uptake of DOX (n = 5) are shown. Adopted from X. Qi, et al., Galactosylated chitosan-grafted multiwall carbon nanotubes for pH-dependent sustained release and hepatic tumor-targeted delivery of doxorubicin in vivo, Colloids and Surfaces B: Biointerfaces 133 (2015) 314–322, with kind permission of Elsevier.

7.3.4 Chit/carbon nanotube nanocomposites for electroanalytical sensors

Polymer NCs have used as transducer for electroanalytical sensors because of their special features such as morphology, variety, and facile preparation procedure. Their distinctive properties supply advantages containing inexpensive, better electronic features, a large edge/basal plane ratio, reversible doping/dedoping procedure, fast electrode kinetics, and biocompatibility [79]. According to excellent conductivity, large surface area, and catalytic activity, CNT is a magnificent applicant for sensors and modified electrodes and these modified sensors have improved properties collate to conventional carbon electrode such as better sensitivities, lower level of detection, and rapid electrode kinetics. Some polymer/CNT NCs such as Chit/CNT NCs can be used as a stable film on the surface of electrodes. There are many reports for the application of Chit/CNT NCs for sensors from 2014 [80–96] that we will point two important of them as follows.

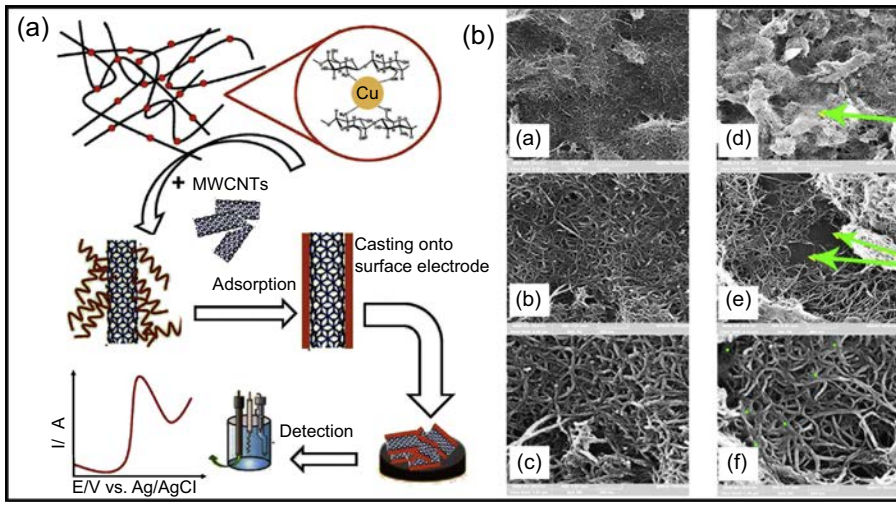

Figure 7.20 (a) The stepwise fabrication process of Cu-Chit/MWCNT/GC electrode and (b) SEM images of MWCNT/GCE (a–c) and Cu-Chit/MWCNT/GCE (d–f). The smooth surface of the Cu-Chit film is shown by *green arrows* and *dots*.
Adopted from M.B. Gholivand, et al., Application of a Cu–chitosan/multiwalled carbon nanotube film-modified electrode for the sensitive determination of rutin, Analytical Biochemistry 493 (2016) 35–43, with kind permission of Elsevier.

Using copper cross-linked Chit/MWCNT NC as a modifier for a glassy carbon electrode (Cu-Chit/MWCNT/GCE) is a prominent example of application of Chit/CNT NC film for sensor [84]. This electrode was applied for detection and determination of rutin in fruit samples. Rutin can be detected by electrochemical techniques because of its tendency to make complexes with transition metal ions and its electroactive feature. After dispersion of MWCNT in a solution of cross-linked Chit (Cu-Chit), appropriate amount of this Cu-Chit/MWCNT solution was dropped onto the surface of the GCE and allowed to drying (see Fig. 7.20). The SEM image of the MWCNT/GCE does not show any aggregation of nanotubes on the surface of electrode (see Fig. 7.20(a)–(c)). On the other hand, considerable changes were observed in the SEM image of Cu-Chit/MWCNT/GCE, which confirmed the modification of electrode with cross-linked Chit (see Fig. 7.20(d)–(f)).

Fig. 7.21(a) shows the electrochemical oxidation of rutin. The cyclic voltammograms (CVs) of rutin (see Fig. 7.21(b)) indicated, that when bare GCE was applied, slow electron transfer due to poor adsorption of rutin to the electrode caused ill-defined redox peaks and week response of rutin (curve a). By using Chit/GCE, two enhancements were observed: (1) increasing in anodic peak current (attributed to the adsorption of rutin to the surface of electrode) (curve b) and (2) increasing in peak-to-peak potential separation (caused by poor electron conductivity of Chit). The result being that the electron transfer procedure on the surface of electrode was restricted. On the other hand, MWCNT-modified GCE shows increase in the reversibility by reducing the peak potential separation (curve c)

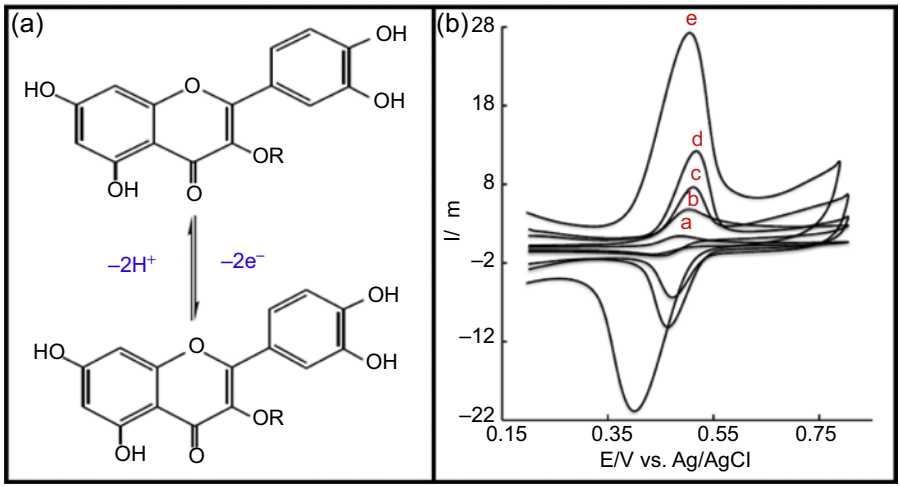

Figure 7.21 (a) The redox reaction mechanism of rutin; (b) the CVs of 0.04 M buffer solution (pH = 3) containing 10 μM rutin at bare GCE (A), Chit/GCE (B), MWCNT/GCE (C), Chit/MWCNT/GCE (D) and Cu-Chit/MWCNT/GCE (E), scan rates = 100 mV/s.
Adopted from M.B. Gholivand, et al., Application of a Cu–chitosan/multiwalled carbon nanotube film-modified electrode for the sensitive determination of rutin. Analytical Biochemistry 493 (2016) 35–43, with kind permission of Elsevier.

in addition to the increase in anodic and cathodic peak currents. This observation proved that MWCNT can considerably enhance electron transfer to the rutin on the surface of the electrode. By using both MWCNT and Chit as modifying agents, more increase in anodic and cathodic peak currents was occurred (curve d). Moreover by using Cu-Chit (curve e), a considerable enhancement in the redox peak current was observed compared with Chit (curve d). This enhancement is attributed to the Cu^{2+}, which can make the complex with rutin, causing an increase in the adsorption of it to the electrode. This tendency between rutin and Cu^{2+} could enhance the sensitivity of the electrode.

In 2016, Tabassum and Gupta [94] reported an approach to study the blood coagulation and anticoagulation. They fabricated cascaded channel multianalyte sensing probe for the concurrent evaluation of vitamin K_1 (VK_1) and heparin (Hep). For this purpose, two cascaded unclad regions on the fiber were fabricated. One of the unclad parts for the evaluation of VK_1 was coated with silver followed by an NC of MWCNT in Chit and the other unclad part for the evaluation of Hep was coated with copper followed by core shell nanostructure of polybrene (PB) and ZnO (see Fig. 7.22(a)). The surface morphology of the sensor was explored by TEM. As shown in Fig. 7.22(b), the large surface to volume ratio of MWCNT-Chit NC (special properties of nonomaterials) supplies more access to the analyte. The necessity for the presence of MWCNT-Chit hybrid in channel 1 and PB-ZnO composite in channel 2 was proved when experiments were done by probes, which were made with only one component of hybrid (Ag/MWCNT and Ag/Chit NPs in channel 1 and Cu/PB NPs and Cu/ZnO NPs in channel 2), because by the use of complete hybrids in each case (Ag/MWCNT-Chit

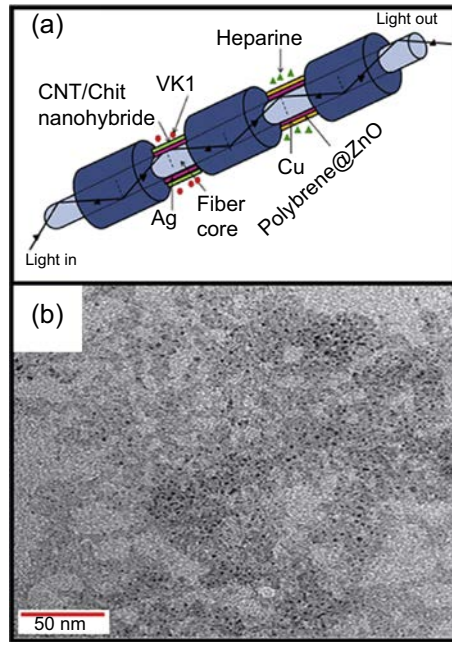

Figure 7.22 (a) Structure of fiber optic probe and (b) TEM image of CNT–Chit in channel 1. Adopted from R. Tabassum, B.D. Gupta, Simultaneous estimation of vitamin K1 and heparin with low limit of detection using cascaded channels fiber optic surface plasmon resonance, Biosensors and Bioelectronics 86 (2016), with kind permission of Elsevier.

for VK_1 and Cu/PB-ZnO for Hep), the maximum shift was attained. This observation is attributed to the special interaction/reaction of VK_1 and Hep with the sensing overlayer. Incorporated VK_1 into the MWCNT-Chit NC suffered oxidation and reduction, which enhanced its effective dielectric function, causing increase in shift. Moreover, reusability test indicated that the probe was reusable.

7.4 Conclusions

The present chapter has tried to highlight and describe some recent synthesis methods, characterization, properties, and applications of Chit NCs containing CNT as filler. Chit was chosen as valuable polymer because of eco-friendly, nontoxic, hydrophilic, degradable nature and the easiness of making films, fibers, and foams with CNTs. The –OH and $–NH_2$ groups in Chit can be a source of hydrogen bonding and therefore contribute to the formation of polymer composites. Recent applications of Chit/CNT NCs, which have been described in this chapter, are listed as follows:

- Sorbents and membranes
- Tissue engineering
- Drug delivery
- Electroanalytical sensors

According to the mentioned results, porous Chit/CNT beads, magnetically Chit/CNT NCs, and other multifunctional Chit/CNT NCs showed high efficiency in adsorption of dye molecules, NPs, heavy metal ions, and other organic pollutants such as antibiotics. IIP-Chit/CNT NCs are also used for the selective removal of rare earth metals. Chit/CNT NCs also showed significant applications in fabricating of scaffolds for the tissue engineering and the drug delivery. There are many literatures in using Chit/CNT NCs for analytical sensors and results showed high efficiency of these NCs for detection and determination of some important organics and biologic molecules such as vitamin K_1.

Acknowledgments

The authors acknowledge the Research Affairs Division of Isfahan University of Technology (IUT), Isfahan, Iran. We also appreciate the National Elite Foundation (NEF), Tehran, Iran, the Iran Nanotechnology Initiative Council (INIC), Tehran, Iran, and Center of Excellence in Sensors and Green Chemistry Research (IUT), Isfahan, Iran, for financial support.

References

[1] J.W. Gooch, Biocompatible Polymeric Materials and Tourniquets for Wounds, Springer Science & Business Media, 2010.
[2] S. Karlsson, A.C. Albertsson, Biodegradable polymers and environmental interaction, Polymer Engineering & Science 38 (8) (1998) 1251–1253.
[3] M.G.A. Vieira, et al., Natural-based plasticizers and biopolymer films: a review, European Polymer Journal 47 (3) (2011) 254–263.
[4] H.B. Yao, et al., Artificial nacre-like bionanocomposite films from the self-assembly of chitosan–montmorillonite hybrid building blocks, Angewandte Chemie International Edition 49 (52) (2010) 10127–10131.
[5] H. Ishida, et al., General approach to nanocomposite preparation, Chemistry of Materials 12 (5) (2000) 1260–1267.
[6] A. Hashemi, et al., Enhanced glassy state mechanical properties of polymer nanocomposites via supramolecular interactions, Nano Letters 15 (8) (2015) 5465–5471.
[7] B. Arash, et al., Mechanical properties of carbon nanotube/polymer composites, Scientific Reports 4 (2014).
[8] Z. Han, A. Fina, Thermal conductivity of carbon nanotubes and their polymer nanocomposites: a review, Progress in Polymer Science 36 (7) (2011) 914–944.
[9] L. Famá, et al., Biodegradable starch based nanocomposites with low water vapor permeability and high storage modulus, Carbohydrate Polymers 87 (3) (2012) 1989–1993.
[10] H.N.M.E. Mahmud, et al., The removal of heavy metal ions from wastewater/aqueous solution using polypyrrole-based adsorbents: a review, RSC Advances 6 (18) (2016) 14778–14791.
[11] A.A. Chavan, et al., Elastomeric nanocomposite foams for the removal of heavy metal ions from water, ACS Applied Materials & Interfaces 7 (27) (2015) 14778–14784.
[12] R. Riva, et al., Chitosan and Chitosan Derivatives in Drug Delivery and Tissue Engineering. Chitosan for Biomaterials II, Springer, 2011, pp. 19–44.

[13] V. Ojijo, S.S. Ray, Processing strategies in bionanocomposites, Progress in Polymer Science 38 (10) (2013) 1543–1589.
[14] X. Yang, et al., Well-dispersed chitosan/graphene oxide nanocomposites, ACS Applied Materials & Interfaces 2 (6) (2010) 1707–1713.
[15] S. Mallakpour, M. Madani, Valine amino acid-functionalized multiwalled carbon nanotube/chitosan green nanocomposite membranes synthesis and characterization, High Performance Polymers 27 (7) (2015) 793–801.
[16] S. Mallakpour, M. Madani, p-Amino phenol immobilized on multi-walled carbon nanotubes for the preparation of chitosan nanocomposites, Journal of Composite Materials 50 (3) (2016) 403–411.
[17] E.M. Azzam, et al., Preparation and characterization of chitosan-clay nanocomposites for the removal of Cu (II) from aqueous solution, International Journal of Biological Macromolecules 89 (2016) 507–517.
[18] L. Pighinelli, M. Kucharska, Chitosan–hydroxyapatite composites, Carbohydrate Polymers 93 (1) (2013) 256–262.
[19] S. Mallakpour, M. Madani, Effect of functionalized TiO_2 on mechanical, thermal and swelling properties of chitosan-based nanocomposite films, Polymer-Plastics Technology and Engineering 54 (10) (2015) 1035–1042.
[20] S. Mallakpour, M. Madani, Functionalized-MnO_2/chitosan nanocomposites: a promising adsorbent for the removal of lead ions, Carbohydrate Polymers 147 (2016) 53–59.
[21] D.F. Eckel, et al., Assessing organo-clay dispersion in polymer nanocomposites, Journal of Applied Polymer Science 93 (3) (2004) 1110–1117.
[22] S. Merino, et al., Nanocomposite hydrogels: 3D polymer–nanoparticle synergies for on-demand drug delivery, ACS Nano 9 (5) (2015) 4686–4697.
[23] A. Bianco, et al., Applications of carbon nanotubes in drug delivery, Current Opinion in Chemical Biology 9 (6) (2005) 674–679.
[24] C. Velasco-Santos, et al., Improvement of thermal and mechanical properties of carbon nanotube composites through chemical functionalization, Chemistry of Materials 15 (23) (2003) 4470–4475.
[25] D. Tasis, et al., Chemistry of carbon nanotubes, Chemical Reviews 106 (3) (2006) 1105–1136.
[26] A. Abdolmaleki, et al., Microwave-assisted treatment of MWCNTs with vitamin B 2: study on morphology, tensile and thermal behaviors of poly (vinyl alcohol) based nanocomposites, European Polymer Journal 87 (2017) 277–285.
[27] S. Mallakpour, A. Zadehnazari, Effect of amino acid-functionalized multi-walled carbon nanotubes on the properties of dopamine-based poly (amide-imide) composites: an experimental study, Bulletin of Materials Science 37 (5) (2014) 1065–1077.
[28] S.H. Aboutalebi, et al., Enhanced hydrogen storage in graphene oxide-MWCNTs composite at room temperature, Advanced Energy Materials 2 (12) (2012) 1439–1446.
[29] S. Mallakpour, V. Behranvand, Recycled PET/MWCNT-ZnO quantum dot nanocomposites: adsorption of Cd (II) ion, morphology, thermal and electrical conductivity properties, Chemical Engineering Journal 313 (2016).
[30] M.M. Rahman, et al., Chemical sensor development based on poly (o-anisidine) silverized–MWCNT nanocomposites deposited on glassy carbon electrodes for environmental remediation, RSC Advances 5 (87) (2015) 71370–71378.
[31] A. Kumari, et al., Nanoencapsulation for drug delivery, EXCLI Journal 13 (2014) 265.
[32] M. Moniruzzaman, K.I. Winey, Polymer nanocomposites containing carbon nanotubes, Macromolecules 39 (16) (2006) 5194–5205.

[33] S.H. Lee, et al., Rheological property and curing behavior of poly (amide-co-imide)/ multi-walled carbon nanotube composites, Korean Journal of Chemical Engineering 27 (2) (2010) 658–665.
[34] H. Bahrambeygi, et al., Nanofibers (PU and PAN) and nanoparticles (Nanoclay and MWNTs) simultaneous effects on polyurethane foam sound absorption, Journal of Polymer Research 20 (2) (2013) 1–10.
[35] P. Garg, et al., Effect of dispersion conditions on the mechanical properties of multi-walled carbon nanotubes based epoxy resin composites, Journal of Polymer Research 18 (6) (2011) 1397–1407.
[36] B. Koh, W. Cheng, Mechanisms of carbon nanotube aggregation and the reversion of carbon nanotube aggregates in aqueous medium, Langmuir 30 (36) (2014) 10899–10909.
[37] B. Rozenberg, R. Tenne, Polymer-assisted fabrication of nanoparticles and nanocomposites, Progress in Polymer Science 33 (1) (2008) 40–112.
[38] S. Mallakpour, S. Soltanian, Surface functionalization of carbon nanotubes: fabrication and applications, RSC Advances 6 (111) (2016) 109916–109935.
[39] S. Mallakpour, V. Behranvand, Improved solubilization of multiwalled carbon nanotubes (MWCNTs) in water by surface functionalization with d-glucose and d-fructose: properties comparison of functionalized MWCNTs/alanine-based poly (amide–imide) nanocomposites, High Performance Polymers 28 (8) (2016) 936–944.
[40] S. Mallakpour, S. Soltanian, Morphology and thermal properties of nanocomposites based on chiral poly (ester-imide) matrix reinforced by vitamin B1 functionalized multiwalled carbon nanotubes, Journal of Composite Materials (2016)http://dx.doi.org/10.1177/0021998316669856.
[41] S. Mallakpour, S. Soltanian, Vitamin C functionalized multi-walled carbon nanotubes and its reinforcement on poly (ester-imide) nanocomposites containing L-isoleucine amino acid moiety, Composite Interfaces 23 (3) (2016) 209–221.
[42] S. Mallakpour, A. Zadehnazari, Functionalized multi-walled carbon nanotubes with vitamin C structures: characterization and fabrication of thiazole containing poly (amide–imide)-based composites, Polymer-Plastics Technology and Engineering 54 (15) (2015) 1644–1652.
[43] C.A. Dyke, J.M. Tour, Unbundled and highly functionalized carbon nanotubes from aqueous reactions, Nano Letters 3 (9) (2003) 1215–1218.
[44] B.K. Price, J.M. Tour, Functionalization of single-walled carbon nanotubes on water, Journal of the American Chemical Society 128 (39) (2006) 12899–12904.
[45] B.K. Price, et al., Green chemical functionalization of single-walled carbon nanotubes in ionic liquids, Journal of the American Chemical Society 127 (42) (2005) 14867–14870.
[46] Y. Zhang, et al., Electrochemical functionalization of single-walled carbon nanotubes in large quantities at a room-temperature ionic liquid supported three-dimensional network electrode, Langmuir 21 (11) (2005) 4797–4800.
[47] R. Barthos, et al., Functionalization of single-walled carbon nanotubes by using alkyl-halides, Carbon 43 (2) (2005) 321–325.
[48] C.A. Dyke, J.M. Tour, Solvent-free functionalization of carbon nanotubes, Journal of the American Chemical Society 125 (5) (2003) 1156–1157.
[49] J. Liu, et al., Efficient microwave-assisted radical functionalization of single-wall carbon nanotubes, Carbon 45 (4) (2007) 885–891.
[50] B. Shariatzadeh, O. Moradi, Surface functionalization of multiwalled carbon nanotubes with chitosan and magnesium oxide nanoparticles by microwave-assisted synthesis, Polymer Composites 35 (10) (2014) 2050–2055.

[51] Y. Wang, et al., Microwave-induced rapid chemical functionalization of single-walled carbon nanotubes, Carbon 43 (5) (2005) 1015–1020.
[52] S. Mallakpour, M. Madani, Effects of glucose-functionalized multiwalled carbon nanotubes on the structural, mechanical, and thermal properties of chitosan nanocomposite films, Journal of Applied Polymer Science 132 (23) (2015).
[53] S. Mallakpour, M. Madani, Enhanced interfacial interaction for effective reinforcement of chitosan nanocomposites at different loading of modified multiwalled carbon nanotubes with vitamin C, Journal of Elastomers and Plastics (2015)http://dx.doi.org/10.1177/0095244315613618.
[54] S. Mallakpour, M. Madani, Synthesis, structural characterization, and tensile properties of fructose functionalized multi-walled carbon nanotubes/chitosan nanocomposite films, Journal of Plastic Film and Sheeting (2015)http://dx.doi.org/10.1177/8756087915578184.
[55] Y.K. Cheng, et al., Study on the reusability of multiwalled carbon nanotubes in biodegradable chitosan nanocomposites, Polymer-Plastics Technology and Engineering 53 (12) (2014) 1236–1250.
[56] A. Zaman, et al., Preparation and characterization of multiwall carbon nanotube (MWCNT) reinforced chitosan nanocomposites: effect of gamma radiation, BioNanoScience 5 (1) (2015) 31–38.
[57] H.U. Lee, et al., Highly conductive and flexible chitosan based multi-wall carbon nanotube/polyurethane composite fibers, RSC Advances 6 (3) (2016) 2149–2154.
[58] Y. Ye, et al., Enhancing interfacial adhesion and functionality of carbon nanotube fibers with depolymerized chitosan, Journal of Materials Chemistry C 1 (10) (2013) 2009–2013.
[59] J. Yan, et al., Preparation and characterization of carbon nanotubes/chitosan composite foam with enhanced elastic property, Carbohydrate Polymers 136 (2016) 1288–1296.
[60] M. Oh, et al., Vertically aligned multi-layered structures to enhance mechanical properties of chitosan–carbon nanotube films, Journal of Materials Science 50 (6) (2015) 2587–2593.
[61] A. Ouyang, et al., Carbon nanotube–chitosan composite beads with radially aligned channels and nanotube-exposed walls for bilirubin adsorption, Advanced Engineering Materials 17 (4) (2015) 460–466.
[62] A. Ouyang, J. Liang, Tailoring the adsorption rate of porous chitosan and chitosan–carbon nanotube core–shell beads, RSC Advances 4 (49) (2014) 25835–25842.
[63] K. Li, et al., Selective adsorption of Gd^{3+} on a magnetically retrievable imprinted chitosan/carbon nanotube composite with high capacity, ACS Applied Materials & Interfaces 7 (38) (2015) 21047–21055.
[64] J. Ma, et al., Equilibrium, kinetic and thermodynamic adsorption studies of organic pollutants from aqueous solution onto CNT/C@ Fe/chitosan composites, New Journal of Chemistry 39 (12) (2015) 9299–9305.
[65] S. Wang, et al., Highly efficient removal of Acid Red 18 from aqueous solution by magnetically retrievable chitosan/carbon nanotube: batch study, isotherms, kinetics, and thermodynamics, Journal of Chemical & Engineering Data 59 (1) (2013) 39–51.
[66] A.M. Alsabagh, et al., Preparation and characterization of chitosan/silver nanoparticle/copper nanoparticle/carbon nanotube multifunctional nano-composite for water treatment: heavy metals removal; kinetics, isotherms and competitive studies, RSC Advances 5 (69) (2015) 55774–55783.
[67] H. Liu, et al., Chitosan/silica coated carbon nanotubes composite proton exchange membranes for fuel cell applications, Carbohydrate Polymers 136 (2016) 1379–1385.
[68] E.-J. Lee, et al., Wettability control on chitosan-wrapped carbon nanotube surface through simple octanal-treatment: selective removing phenol from water, Macromolecular Research 24 (5) (2016) 429–435.

[69] E. Axpe, et al., Sub-nanoscale free volume and local elastic modulus of chitosan–carbon nanotube biomimetic nanocomposite scaffold-materials, Journal of Materials Chemistry B 3 (16) (2015) 3169–3176.
[70] K. Nawrotek, et al., Assessment of degradation and biocompatibility of electrodeposited chitosan and chitosan–carbon nanotube tubular implants, Journal of Biomedical Materials Research Part A 104 (11) (2016) 2701–2711.
[71] S. Pok, et al., Biocompatible carbon nanotube–chitosan scaffold matching the electrical conductivity of the heart, ACS Nano 8 (10) (2014) 9822–9832.
[72] S. Shokri, et al., A new approach to fabrication of Cs/BG/CNT nanocomposite scaffold towards bone tissue engineering and evaluation of its properties, Applied Surface Science 357 (2015) 1758–1764.
[73] A. Bernkop-Schnürch, S. Dünnhaupt, Chitosan-based drug delivery systems, European Journal of Pharmaceutics and Biopharmaceutics 81 (3) (2012) 463–469.
[74] H.S. Kim, U.S. Shin, Core–shell structured chitosan–carbon nanotube membrane as a positively charged drug delivery system: selective loading and releasing profiles for bovine serum albumin, Bulletin of the Korean Chemical Society 37 (4) (2016) 500–505.
[75] H. Moradian, et al., Poly (ethyleneimine) functionalized carbon nanotubes as efficient nano-vector for transfecting mesenchymal stem cells, Colloids and Surfaces B: Biointerfaces 122 (2014) 115–125.
[76] E. Nivethaa, et al., Fabrication of chitosan/MWCNT nanocomposite as a carrier for 5-fluorouracil and a study of the cytotoxicity of 5-fluorouracil encapsulated nanocomposite towards MCF-7, Polymer Bulletin 73(11) (2016) 3221–3236.
[77] K.D. Patel, et al., Nanostructured biointerfacing of metals with carbon nanotube/chitosan hybrids by electrodeposition for cell stimulation and therapeutics delivery, ACS Applied Materials & Interfaces 6 (22) (2014) 20214–20224.
[78] X. Qi, et al., Galactosylated chitosan-grafted multiwall carbon nanotubes for pH-dependent sustained release and hepatic tumor-targeted delivery of doxorubicin in vivo, Colloids and Surfaces B: Biointerfaces 133 (2015) 314–322.
[79] S. Shrivastava, et al., Next-generation polymer nanocomposite-based electrochemical sensors and biosensors: a review, TrAC Trends in Analytical Chemistry 82 (2016) 55–67.
[80] S. Afreen, et al., Functionalized fullerene (C 60) as a potential nanomediator in the fabrication of highly sensitive biosensors, Biosensors and Bioelectronics 63 (2015) 354–364.
[81] M.A. Ali, et al., Chitosan-modified carbon nanotubes-based platform for low-density lipoprotein detection, Applied Biochemistry and Biotechnology 174 (3) (2014) 926–935.
[82] S. Beiranvand, et al., A simple and label-free aptasensor based on amino group-functionalized gold nanocomposites-Prussian blue/carbon nanotubes as labels for signal amplification, Journal of Electroanalytical Chemistry 776 (2016) 170–179.
[83] S. El Ichi, et al., Chitosan improves stability of carbon nanotube biocathodes for glucose biofuel cells, Chemical Communications 50 (93) (2014) 14535–14538.
[84] M.B. Gholivand, et al., Application of a Cu–chitosan/multiwalled carbon nanotube film-modified electrode for the sensitive determination of rutin, Analytical Biochemistry 493 (2016) 35–43.
[85] N. Karadas-Bakirhan, et al., Determination of the anticancer drug sorafenib in serum by adsorptive stripping differential pulse voltammetry using a chitosan/multiwall carbon nanotube modified glassy carbon electrode, Electroanalysis 28 (2) (2016) 358–365.
[86] Y. Li, et al., Flexible chitosan/carbon nanotubes aerogel, a robust matrix for in-situ growth and non-enzymatic biosensing applications, Sensors and Actuators B: Chemical 232 (2016) 750–757.

[87] X. Meng, et al., A molecularly imprinted electrochemical sensor based on gold nanoparticles and multiwalled carbon nanotube–chitosan for the detection of tryptamine, RSC Advances 4 (73) (2014) 38649–38654.
[88] A. Numnuam, et al., An amperometric uric acid biosensor based on chitosan-carbon nanotubes electrospun nanofiber on silver nanoparticles, Analytical and Bioanalytical Chemistry 406 (15) (2014) 3763–3772.
[89] A. Pavinatto, et al., Layer-by-Layer assembled films of chitosan and multi-walled carbon nanotubes for the electrochemical detection of 17α-ethinylestradiol, Journal of Electroanalytical Chemistry 755 (2015) 215–220.
[90] A. Salimi, et al., Manganese oxide nanoflakes/multi-walled carbon nanotubes/chitosan nanocomposite modified glassy carbon electrode as a novel electrochemical sensor for chromium (III) detection, Electrochimica Acta 156 (2015) 207–215.
[91] C. Sengiz, et al., Multiwalled carbon nanotubes-chitosan modified single-use biosensors for electrochemical monitoring of drug-DNA interactions, Electroanalysis 27 (8) (2015) 1855–1863.
[92] F. Shahdost-fard, et al., Highly selective and sensitive adenosine aptasensor based on platinum nanoparticles as catalytical label for amplified detection of biorecognition events through H_2O_2 reduction, Biosensors and Bioelectronics 53 (2014) 355–362.
[93] Y.-T. Shieh, H.-F. Jiang, Graphene oxide-assisted dispersion of carbon nanotubes in sulfonated chitosan-modified electrode for selective detections of dopamine, uric acid, and ascorbic acid, Journal of Electroanalytical Chemistry 736 (2015) 132–138.
[94] R. Tabassum, B.D. Gupta, Simultaneous estimation of vitamin K 1 and heparin with low limit of detection using cascaded channels fiber optic surface plasmon resonance, Biosensors and Bioelectronics 86 (2016).
[95] B. Wu, et al., High aqueous solubility of carboxylated-carbon nanotubes as support for PtRu nanoparticles: enhanced dispersion and electrocatalytic performance, International Journal of Hydrogen Energy 39 (14) (2014) 7318–7325.
[96] L.-Y. Yu, et al., Chiral electrochemical recognition of tryptophan enantiomers at a multiwalled carbon nanotube–chitosan composite modified glassy carbon electrode, RSC Advances 5 (119) (2015) 98020–98025.

This page intentionally left blank

Polycaprolactone/metal oxide nanocomposites: an overview of recent progress and applications

8

Shadpour Mallakpour, Nasrin Nouruzi
Isfahan University of Technology, Isfahan, Islamic Republic of Iran

8.1 Introduction

Recently, there was an increasing interest in the progress of biodegradable macromolecules and biocomposites to diminish the need on fossil fuels and to change to the sustainable materials. This interest is also justified by the potential technological uses of these materials and by the environmental awareness and demand for green technology. Biopolymers possess several profits compared with other polymers, including mechanical properties, simplicity of shaping and manufacture, which enable appropriate pore sizes leading to tissue ingrowth, and controlled release of drugs that confined into the polymer [1–3]. Bionanocomposites are a family of materials formed by combination of biopolymer matrix and nanofillers (fiber, platelet, or particle) having one dimension on the nanometer scale [2,4].

As a result of the excellent physicochemical properties, metal oxide nanoparticles (MO NPs) have generated numerous scientific activities. By combining simultaneously mechanical, electrical, thermal, or even electrochemical performances, these NPs are generally considered as favorable candidates for wide series of applications. They are largely used as additive fillers in various nanocomposites (NCs), especially in polymer NCs. Besides the excellent physiochemical properties, they show a low density and a great aspect ratio useful to considerable strengthening of the matrices. Moreover, they can be dispersed in water and other organic solvents via different functionalization routes [5].

Polycaprolactone (PCL) is a semicrystalline polymer, which is already extensively used for numerous applications. Compared with other polymers, it is biodegradable, biocompatible, and easy to process from aqueous solutions. Therefore, it can be used in biopackaging and medical devices [6].

It was quite natural for researchers to try to mix nanofillers and polymer to improve the properties of the neat polymer. In this chapter, we will first examine the different methods that have been used to process PCL/MO NCs. Then we will consider the composite-enhanced properties and their applications in different fields, which have been extensively investigated in the literatures.

Biodegradable and Biocompatible Polymer Composites. http://dx.doi.org/10.1016/B978-0-08-100970-3.00008-0

8.2 Polycaprolactone

PCL, composed of hexanoate repeat units [7], is one of the first macromolecules prepared by the Carothers group in 1930 [3]. It is one of the most commonly studied biodegradable, hydrophobic, and nontoxic [8] macromolecule belonging to the linear aliphatic polyesters, with a melting point of 60°C and a high degradation temperature of 350°C [9]. It is a semicrystalline macromolecule with a grade of crystallinity up to 70% [10], that its crystallinity tends to decrease with increasing molecular weight (Mw) typically ranging from 3000 to 800,000 g/mol [3,11]. The crystal structure of PCL is described by an orthorhombic unit cell with parameters of $a = 7.47$ Å, $b = 4.98$ Å, $c = 17.05$ Å [12]. PCL is also a thermoplastic macromolecule with several appropriate characteristics, including high strength under ambient environments and ease of processability (thermal and solution). It has previously been permitted for usage in little products [13,14] and various devices for biomedical applications by the U.S. Food and Drug Administration (FDA) [1]. Its different properties rely on the Mw and crystallinity grade. Table 8.1 presents the reported property values [7]. These unique thermoplastic properties enable it to be processed into three-dimensional (3D) spongy scaffolds, with a completely unified pore system, using fused deposition modeling [15,16]. However, its large engineering applications and its commercialization have been limited because of its relative high cost [1], along with some intrinsic inferior properties [17] such as low thermal stability, inadequate mechanical strength, and barrier properties to gases [8]. Efforts on PCL mixed with other low-cost and biodegradable materials have been done to overcome the mentioned shortcomings and broaden PCL applications [18]. Three routes available were reported on this purpose including copolymerization, mixing with the nanofillers, and blending with many other macromolecules such as polylactide (PLA) to obtain new biocompatible materials with high performance [19]. The most effective way is the reinforcing of soft matrix with hard NPs.

Table 8.1 Polycaprolactone properties

Properties	Range
Number average molecular weight (M_n, g/mol)	530–630,000
Density (ϱ, g/mol)	1.071–1.200
Glass transition temperature (T_g, °C)	(−65)–(−60)
Melting temperature (T_m, °C)	56–65
Decomposition temperature (°C)	350
Inherent viscosity (η_{inh}, cm^3/g)	100–130
Intrinsic viscosity (η, cm^3/g)	0.9
Tensile Strength (σ, MPa)	4–785
Young modulus (E, GPa)	0.21–0.44
Elongation at break (ε, %)	20–1,000

Adapted from M. Labet, W. Thielemans, Synthesis of polycaprolactone: a review, Chemical Society Reviews 38 (12) (2009) 3484–3504. With kind permission of Royal Society of Chemistry.

The rigid nanofillers, such as single or multiwalled carbon nanotubes [20], clay [21], graphene [22], cellulose nanofiber or nanowhisker gels [23], and MO NPs [24], have been utilized to fabricate NCs, which show remarkable properties including electric conduction, high mechanical strengths, thermal stability, and gas-barrier characteristics [23]. Among the many possible types of nanofiller, metal oxide reinforcements have been revealed to effectively strengthen polymers. The most usual metal oxide NPs, used for the preparation of polymer NCs, are ZnO [25,26], TiO_2 [27], SiO_2 [28], ZrO_2 [29], and Al_2O_3 [30,31].

8.2.1 Polycaprolactone synthesis

PCL can be synthesized through two methods: step-growth polymerization including straight condensation of hydroxycaproic acid and chain-growth polymerization such as ring-opening polymerization (ROP). Condensation involves the consecutive addition of monomers to prepare the polymer [32], and the consequence of this route is that polymers with Mw up to 10,000 g/mol can be obtained at high conversion, by enzymes or by strongly forcing remotion of condensation of ancillary products to drive the equilibrium [11]. Some hydrolytic enzymes are unchanging in organic solvents and can be used to catalyze the condensation reactions, which are difficult to obtain in aqueous solution by other methods [33].

PCL is generally synthesized by the ROP of cyclic monomer, ε-caprolactone (ε-CL), in front of a catalyst and by using an alcohol (R–OH) as an initiator [34,35]. Advantages of the ROP over the polycondensation are the ability to achieve greater Mw, lower polydispersities, and higher monomer conversions [36]. For the ROP of ε-caprolactone, various cationic or anionic initiators have been used; therefore the ROP involves the polymerization through either an ionic or coordination insertion mechanism [35].

A wide number of catalyst including metal compounds, organic and enzymatic systems, and even some inorganic acids can promote the ROP of ε-caprolactone. So far, metal-based catalysts (Al, Sn, and earth-based metals) have been considered the most, but the removing of metal residues that appear as impurities and hinder the utilization of the materials in biomedicals and microelectronics is very hard. In this regards, enzyme-catalyzed ROP is a promising tool, which avoids the use of metal catalysts and brings green-chemistry appeal with it [37]. However, the availability of enzymes is even bounded, the polymerization is slow and the last macromolecule architecture is not well controlled. Thus, it is of great interest to develop new synthetic routes based on metal-free catalysts [38].

In addition to alcohols and the OH on the NP surfaces, metal alkoxides have also been shown to be efficient initiators for the ROP of various cyclic esters. The polymerization reaction generally proceeds through a "coordination–insertion" mechanism, in which ε-CL is entered into the M—O bond via the selective cleavage of the acyl-oxygen bond of the lactone chain (Fig. 8.1) [39,40]. The dead end of the growing chain is constituted by the alkoxide group. Because the other end is still active and the macromolecules do not lose their capability to grow, the polymerization of cyclic esters

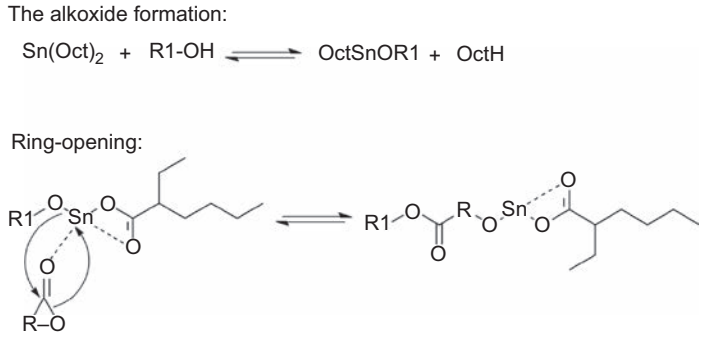

Figure 8.1 $Sn(Oct)_2$/alcohol coinitiated polymerization of lactones.
Adapted from A.C. Albertsson, I.K. Varma, Recent developments in ring opening polymerization of lactones for biomedical applications, Biomacromolecules 4 (6) (2003) 1466–1486. With kind permission of American Chemical Society.

with metal alkoxides is referred to "a living polymerization" [41]. As propagation is faster than initiation step and such initiators cause transesterification reactions, fine Mw distributions are not yielded [40].

8.3 Metal oxides

MOs have drawn heightening technological and industrial interest because of their different features, for instance, magnetic, optical, electrical combined with thermal stableness and chemical resistance. These NPs also attracted attention because of the properties linked to their nanometer size. Some extraordinary electrical and optical properties are due to a phenomenon that known as quantum confinement [42–44]. The mentioned properties, combined with large aspect ratios of MOs, make them a promising candidate for gas sensing, electroceramics, catalysis, or energy conversion and storage [42]. However, many of their properties depended on the synthetic methods. The properties of surface and interface also influence the overall properties. Therefore, the physicochemical properties of surfaces and interfaces should be analyzed carefully to control the reactivity [45].

The surface of many metal oxides is regarded as a condensed part of the crystal comprising coordinately unsaturated sites, anions and cations. Therefore, they incline to saturate by reacting with gas molecules when exposed to the atmosphere. One major process occurs is hydroxylation, a result of organic reactions among surface M—O bonds and H_2O molecules, and the ensuing hydroxyl group amounts relies powerfully on the MO nature. Another process that can take place simultaneously with hydroxylation is carbonation [45,46].

High surface energy, little particle size, and strong particle–particle interactions can induce a strong aggregation of surface metal oxide species, which results in decreased interfacial area and poor mechanical properties [47,48]. Preventing the presence of aggregation effects is not a trivial issue, especially when dispersing the hydrophilic NPs in hydrophobic matrices. This is principally because of the poor

hydrophilic NPs compatibility with the hydrophobic matrix [2]. Therefore, surface modification of the filler or the polymer matrix with surface-active molecules is required to improve the dispersion and the compatibility between the NPs and polymer matrices [49–53].

8.3.1 Metal oxide synthesis methods

The conventional and also traditional synthesis of MO NPs was the direct reactions of a mixture of powders. However, these solid-state reactions required harsh conditions such as high temperature and small particle sizes to impede subtle control of the reactions and prevent the organization of thermally labile and metastable solids [54]. For NP synthesis, the control over size and shape is a crucial factor in determining the properties, so other preparation methods have to be developed, in which proper control of the molecular precursor and the final product, high purity and homogeneity, and low processing temperatures can be obtained [55]. The next route for the NP preparation is chemical strategy involving the process of precipitation of a solid phase from a solution. This preparation method includes the nucleation and growth of particles in the solution, in which the NPs nucleation and growth must be controlled [56]. The chemical synthetic route can be separated into thermally decomposition of organometallic compounds and metal complexes, solvothermal and hydrothermal routes, micelle and sol–gel routes, and chemical precipitation [5].

The thermal decomposition route relies on the reactions between the precursor species and the solvent and is accomplished at moderate temperatures below 350°C [5]. This route is first introduced in the early 1990s and has been a common way to obtain monodisperse quantum dots [57].

Solvothermal method requires the use of a solvent under mild to harsh pressure and temperature that facilitates the contact of reactants throughout the synthesis. If H_2O is exploited as the solvent, the method is called hydrothermal synthesis [58]. This is a green process because of the closed system conditions and it has been extensively used for growing single crystals [59]. It also allows for the accurate control over the size, shape, distribution, and crystallinity of the metal NPs. These characteristics can be altered by changing experimental factors, for example, temperature, reaction time, solvent, surfactant, and precursor [60].

Reverse micelle or microemulsion is some other procedure for the synthesis of MO NPs. The reverse micelle is defined as a tiny drop of polar liquid restricted with the surfactant molecules, which act as a nanoreactor, distributed in an organic phase. The microemulsion can be elucidated as a thermodynamically steady organization of water, oil, and amphiphiles, which is the center of the reverse micelle and acts as a template for the growing nuclei into the uniform NPs [61].

Sol–gel route typically involves aqueous precipitation of the metal ion with base, washing, solvent exchange of the products, and the subsequent atmospheric or supercritical drying. This method comes about in room conditions with general laboratory equipment, making the process convenient and inexpensive [62].

Precipitation is the pathway in which the oxides themselves or their precursors are generated and it is really practicable for catalytic materials in the form of bulk oxides [63].

During the process, nucleation is the basic stage, and many small particles are generated. Afterward, another processes such as Ostwald ripening and aggregation dramatically influence the size of the NPs. Because of the simultaneous happening of nucleation, growth, coarsening, and agglomeration, a careful check of the process conditions is necessary for the synthesis of uniform NPs [56].

8.4 Polycaprolactone/metal oxide nanocomposites

8.4.1 Preparation of polycaprolactone/metal oxide nanocomposites and their properties

Polymer NCs are generally described as multiphase materials, in which one component must have nanometer length scale (<100 nm) [48]. Two essential characteristics of NCs can be responsible for their successful development, high specific interfacial area, and stress transfer across the interface. The large surface area of the NPs provides a greater surface/volume ratio, leading to wide bounding between the matrix and the NPs. Strong interfacial bonding is then required to transfer the excellent NP properties into the NCs [47]. This characteristic powerfully relies on the bonding energy at the interface that can be improved by hydrogen binding, covalent linkage, electrostatic interactions, and van der Waals interactions [64]. Most often the inorganic components act as filler for the macromolecule matrices. The reinforcing agent/filler can be of any dimension including zero dimensional such as metal oxides; one dimensional such as nanofibers; two dimensional such as layered materials and 3D framework systems (such as zeolites) [65]. PCL-based NCs as biomaterials for application in drug release and tissue engineering have been in the focus of attention, owing to the cytotoxicity or biocompatibility with tuned mechanical strength and biodegradation. Many kinds of PCL NCs and its copolymers have been reported [66]. Three different methods for the preparation of PCL/metal oxide NCs are presented: solution casting method, melt extrusion technique, and in situ polymerization [67].

8.4.1.1 Solution casting method

The solution casting or solvent evaporation technique is developed at the end of the 1970s [68]. Afterward, numerous studies on microencapsulation have been accounted on the basis of this technique. This method is based on the evaporation of the solvent from an emulsion by stirring. Initially, the polymeric material as the matrix phase should be dissolved in a volatile organic phase. The nanofillers to be encapsulated are distributed in the matrix solution, or they can be distributed in the organic solution to form a suspension, and subsequently the prepared suspension is poured into the polymer solution. The NPs can nicely be distributed in the polymer matrix after removing the solvent by fast evaporation [67,69–71].

Recently, Mallakpour et al. [72] have prepared PCL/ZnO NCs by solution casting technique. Firstly, they modified the ZnO NPs with poly(vinyl alcohol) under ultrasound irradiation. Then, the organically modified ZnO NPs was sonicated in dichloromethane (DCM) to achieve a good dispersion. In a separate pot, the PCL

was dissolved in DCM and was poured into the ZnO suspension. Finally, the mixture transferred onto a Petri dish and the PCL NC films were prepared through evaporation of the solvent. Field emission scanning electron microscopy (FE-SEM) images of the NCs (Fig. 8.2(a)–(c)) showed that the surface of neat PCL and NC by low content of modifier was tabulate, but increasing the NP percentages resulted in the rougher surfaces may be on account of ZnO NPs agglomerations. The NPs also influenced Elastic modulus (E-modulus) and yield tensile stress of the NCs (Fig. 8.2(e)). Low NP contents (2 wt%) resulted in a strong reinforcing effect and improved tensile modulus, but more filler percentages caused lower mechanical properties. This arises from the great surface energy of the NPs that led to their aggregation, as observed by FE-SEM images. Increasing the nanofiller content also led to a drop in thermal resistance of the NCs (Fig. 8.2(d)), because the interaction at the interface of the matrix and the nanofiller weakened the interactive force of PCL interchains and accelerated thermal decomposition of PCL in NCs. Moreover, ZnO NPs can accelerate the oxidative decomposition of surrounding carbon. In another similar work [73], the ZnO NPs were modified with optically active amino acid (*N*-trimellitylimido-L-alanine). The obtained NPs were used for reinforcing the PCL matrix that, for these NCs, the mechanical strength was also increased.

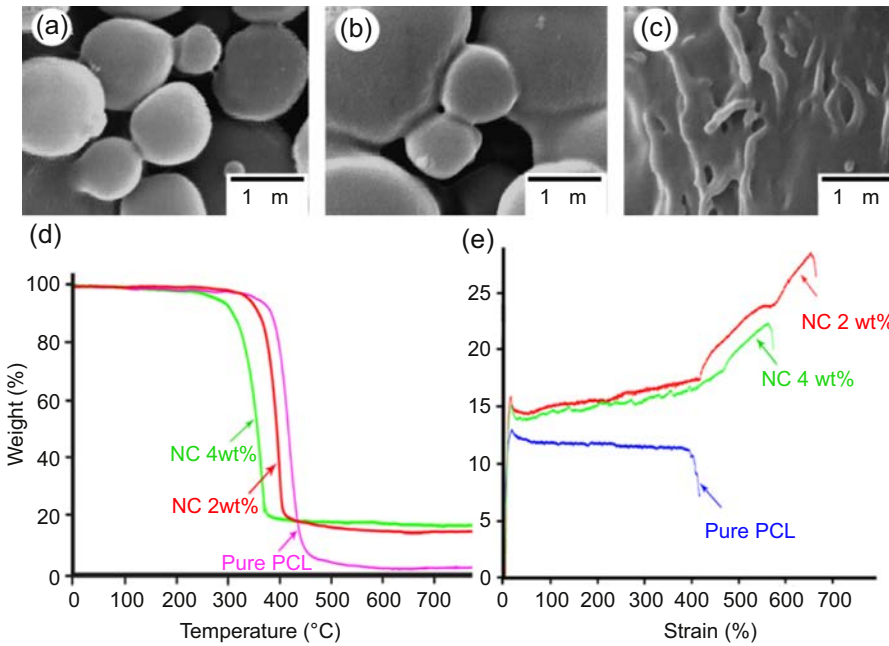

Figure 8.2 (a–c) FE-SEM images of Pure PCL, PCL/ZnO-PVA 2 wt%, 4 wt%, respectively; (d) TGA thermograms of PCL/ZnO-PVA NCs; and (e) stress–strain diagram of the PCL/ZnO-PVA NCs.
Adapted from S. Mallakpour, N. Nouruzi, Effect of modified ZnO nanoparticles with biosafe molecule on the morphology and physiochemical properties of novel polycaprolactone nanocomposites, Polymer 89 (2016) 94–101. With kind permission of Elsevier.

Shin et al. [74] have prepared porous PCL/silica hybrid NCs with patterned surface pores by casting a mixture of PCL solution and sol–gel derived silica sol. For this purpose, a desired amount of PCL was dissolved in a mixture of dichloroethane and *N*,*N*-dimethylformamide. In a separate preparation, the silica sol was synthesized using a sol–gel route at room conditions. Then, the prepared silica was added to the prepared solution and then it was stirred. The mixture was poured into Petri dishes and the solvent was evaporated. The porous structure of the hybrid membranes prepared with various initial tetraethyl orthosilicate ($Si(OC_2H_5)_4$;TEOS) contents in relation to the PCL content in the mixture that this ratio will impress the poriferous construction of hybrid membranes. The pure PCL membrane without a TEOS showed a rather dense structure and small pores that could be attributed to the slow evaporation of the nonsolvent on the surfaces. While, extremely poriferous construction with regular pores is formed by increasing the amount of TEOS content, in which the walls of the pores went denser. The size of the surface pores increased from 43 to 67 μm with raising original TEOS volume from 20 to 40 vol% (Fig. 8.3), whereas keeping the high mechanical strength and E-moduli.

8.4.1.2 *Melt extrusion*

Melt extrusion is the route of applying temperature and pressure to melt a polymer and force it through an orifice in a continuous process. In this technique, the NPs are mixed with the matrix in the molten state in a single/twin screw extruder. Polymer and NPs are mixed in a high speed mixer to formulate the premixture prior to extrusion [66].

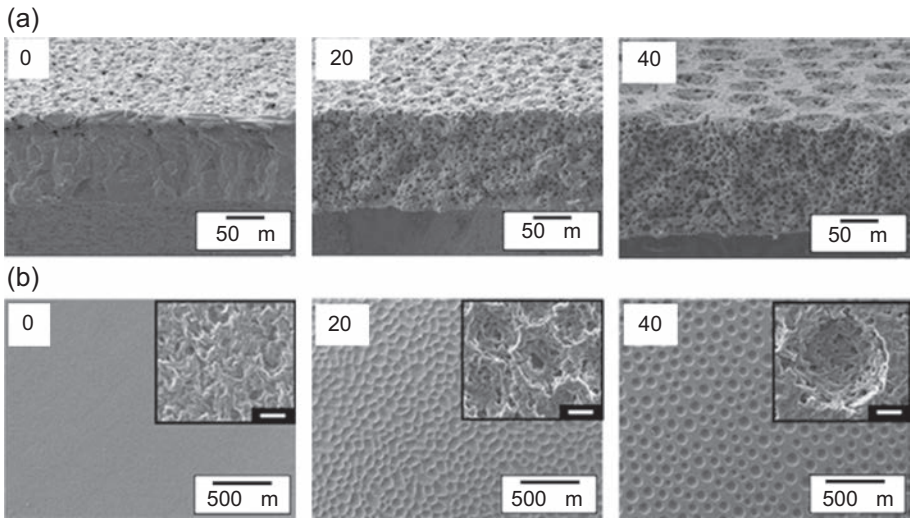

Figure 8.3 SEM micrographs of (a) cross sections and (b) top surfaces of the PCL/silica hybrid membranes with various TEOS contents in relation to the PCL (0, 20, and 40 vol%). Adapted from K.H. Shin, Y.H. Koh, W.Y. Choi, H.E. Kim, Production of porous poly (ε-caprolactone)/silica hybrid membranes with patterned surface pores, Materials Letters 65 (12) (2011) 1903–1906. With kind permission of Elsevier.

The most important advantage of melt extrusion is the possibility of working without solvents, thus debarring the necessity for subsequent drying steps [75]. Furthermore, it is relatively low cost allowing simple fabrication with low ecological footprint, improved product physical stability, and the capability to run continuously. Because PCL is thermoplastic in nature, it is possible to melt under reasonable conditions [76].

Mofokeng et al. [77] employed melt mixing technique for the preparation of PLA/PCL blend NCs (with different ratios) with TiO_2 as the filler. For preparation of the NCs, the mixtures were mixed at 170°C at a speediness of 50 rpm. The prepared samples were compression molded into 2-mm-thick sheets at the same temperature using a hydraulic press. From TEM images of PLA/PCL/TiO_2 NCs (Fig. 8.4), it was clear that the NPs were frequently dispersed in the PLA phase, with some small and large aggregates. In these figures, PCL was darker, and TiO_2 is clearly visible from the polymer. As shown in the figures, no substantial concentration of the NPs was existing on the interfaces between PLA and PCL. This was ascribed to the larger affinity between PLA and TiO_2, as they are similar in the term of polarity. TGA results showed that neat PLA had a lower thermal stability, but greater activation energy of erosion, owing to the more complex degradation mechanism(s). Blending the polymers reduced the thermal resistance of each polymer, but the existence of TiO_2 NPs increased the thermal stabilities of both polymers in the blends and affected the volatilization of the degradation products that can be ascribed to the combination of the catalytic influence of the NPs and their possible interaction with the volatile decomposition yields.

In a comprehensive study [78], poly(ε-caprolactone-co-D,L-lactide) copolymer (P[CL-co-LA]) was prepared through ROP of ε-caprolactone and D,L-lactide, catalyzed by *n*-heptanol and tin(II) octoate ($Sn(Oct)_2$) with a primary molar [alcohol]/$Sn(Oct)_2$

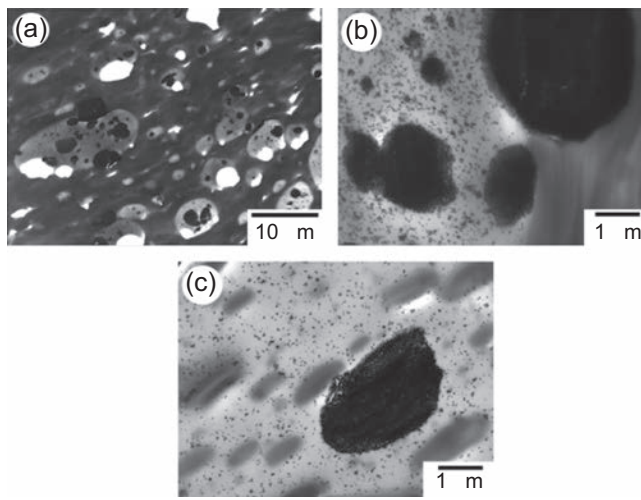

Figure 8.4 (a and b) TEM pictures of 30/70/5 w/w PLA/PCL/TiO_2, and (c) 70/30/5 w/w PLA/PCL/TiO_2.
Adopted from J. Mofokeng, A. Luyt, Morphology and thermal degradation studies of melt-mixed poly (lactic acid)(PLA)/poly (ε-caprolactone)(PCL) biodegradable polymer blend nanocompositeswith TiO_2 as filler, Polymer Testing 45 (2015) 93–100. With kind permission of Elsevier.

proportion of 100 (Fig. 8.5). The number-average Mw of the prepared copolyester was 35,400 g/mol with a dispersity index of 2.0. PLA-silica NPs as masterbatches were prepared through solvent casting using chloroform. The resulting masterbatches were melt-blended with poly(ε-caprolactone-co-D,L-lactide) copolyester using a twin-screw microcompounder. TEM analyses of the PLA-based substance with 10 wt% of the copolymer (Fig. 8.6(a)) revealed the presence of roundlike nodules frequently dispersed within the PLA matrix, and TEM images of the silica-containing materials (Fig. 8.6(b) and (c)) showed that the NPs are more likely located at the PLA/P[CL-co-LA] interface, exhibiting the affinity of NPs to be localized at the interface of the blend components. The two-step NC preparation route resulted in improved material toughness as attested by a 15-fold increase recorded in impact strength, while maintaining high level of transparency. Unfilled PLA behaved as stiff and glassy materials with high Young's

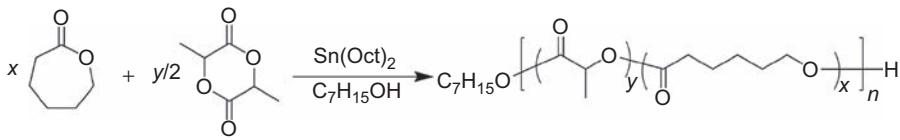

Figure 8.5 Ring-opening polymerization of ε-CL and D,L-lactide promoted by *n*-heptanol and $Sn(Oct)_2$.
Adapted from J. Odent, Y. Habibi, J.M. Raquez, P. Dubois, Ultra-tough polylactide-based materials synergistically designed in the presence of rubbery ε-caprolactone-based copolyester and silica nanoparticles, Composites Science and Technology 84 (2013) 86–91. With kind permission of Elsevier.

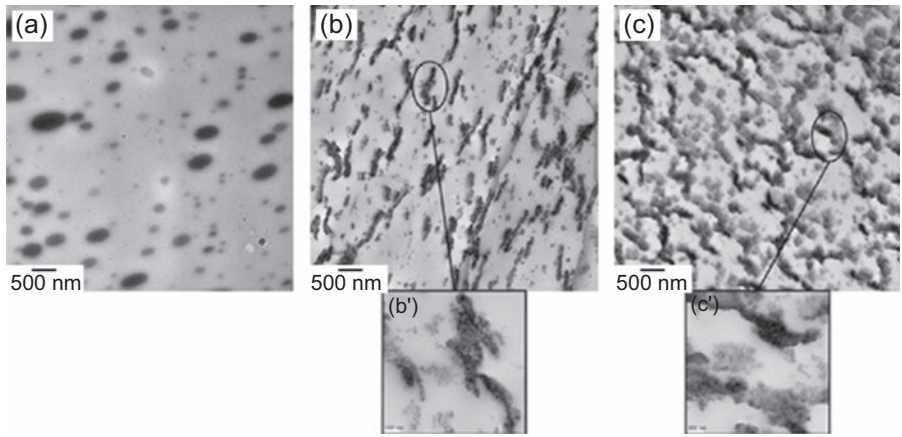

Figure 8.6 TEM images of room-temperature notched surfaces of PLA-based materials containing 10 wt% of poly(ε-caprolactone-co-D,L-lactide) copolyester (a) without silica NPs, (b) with 5 wt% (c) and 10 wt% of silica NPs.
Adapted from J. Odent, Y. Habibi, J.M. Raquez, P. Dubois, Ultra-tough polylactide-based materials synergistically designed in the presence of rubbery ε-caprolactone-based copolyester and silica nanoparticles, Composites Science and Technology 84 (2013) 86–91. With kind permission of Elsevier.

moduli and tensile strength and low elongation at failure. When loaded the PLA at the copolyester as impact modifier, a brittle–ductile performance was detected for the resultant blend that is distinctive of semicrystalline macromolecules toughened by rubbery materials. When silica NPs were loaded at the copolyester, the tensile properties of the NCs are not altered noticeably, but the impact strength increase, up to 10-fold.

8.4.1.3 *In situ polymerization*

In this technique, appropriate inorganic nanofiller contents were admixed with the monomers and they were polymerized using simple bulk or solution method in front of a low quantity of catalyst. Final dispersion of NPs in resulted NCs was better in this process because NPs can be homogeneously distributed in low viscous monomer [79]. This route is considered as a preferred method for polymer NCs containing different nanofillers, which simplifies the NPs dispersion and maximizes interfacial interaction of nanofillers in the matrix [40,79,80]. There are various examples of this category for PCL-based NCs. Wang et al. [82] have prepared PCL/Fe_3O_4 NCs via in situ polymerization method. The polymerization of ε-caprolactone was carried out through ROP with the OH groups on the surface of Fe_3O_4 NPs as initiators and $Sn(Oct)_2$ as the catalyst (Fig. 8.7). The certain amount of Fe_3O_4 NPs was suspended in a ε-caprolactone by means of ultrasound irradiation, then the suspension containing the NPs, $Sn(Oct)_2$, and ε-CL was added to a flask and it was refluxed. Although crystallization structure of PCL does not be altered by incorporation of Fe_3O_4 NPs, thermal stability of PCL is reduced by increasing the NPs content. Thus, Fe_3O_4 NPs caused the random pyrolysis of the PCL chains and accelerated thermal decomposition of the macromolecule.

In a different study [81], Fe_3O_4@graphene oxide NPs were produced through an inverse coprecipitation method, so that the GO nanosheets were decorated with Fe_3O_4 NPs. In the second step, superparamagnetic PCL/Fe_3O_4@GO NCs were prepared via in situ ROP of ε-CL in the presence of the Fe_3O_4 NPs immobilized on the GO surfaces. The

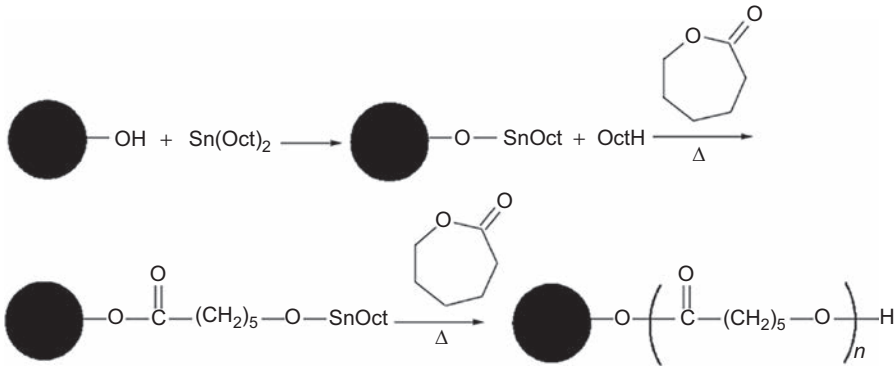

Figure 8.7 Schematic representation of fabrication process of PCL/Fe_3O_4 NCs.
Adapted from G.S. Wang, L. Wang, L. Sang, X.F. Dong, G.Y. Chen, Y. Chang, W.X. Zhang, Synthesis and characterization of poly (ε-caprolactone)/Fe_3O_4 nanocomposites by in situ polymerization, Chinese Journal of Polymer Science 31 (7) (2013) 1011–1021. With kind permission of Springer.

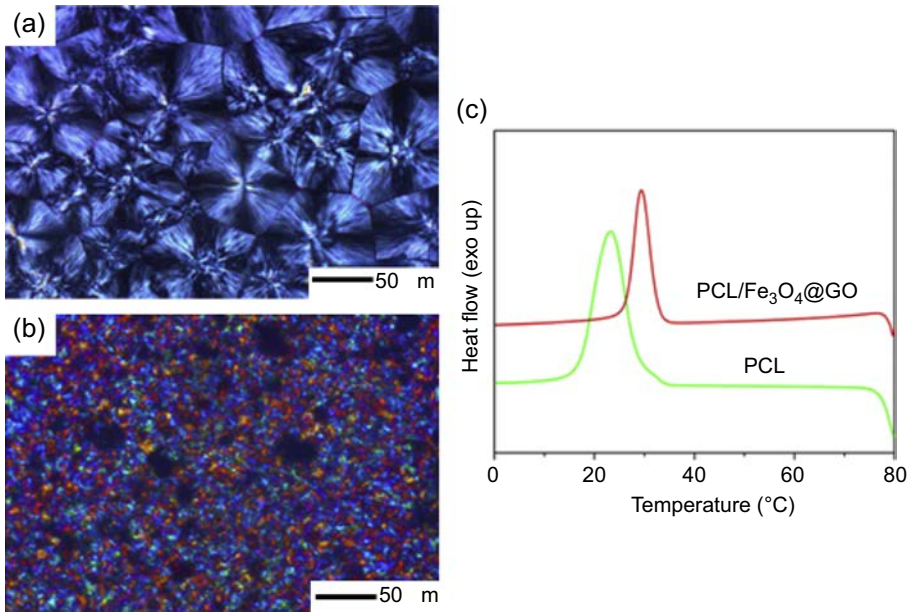

Figure 8.8 POM images of (a) PCL and (b) PCL/Fe_3O_4@GO NC, and (c) DSC traces of PCL and PCL/Fe_3O_4@GO NC.
Adapted from G. Wang, S. Yang, Z. Wei, X. Dong, H. Wang, M. Qi, Facile preparation of poly (ε-caprolactone)/Fe_3O_4@ graphene oxide superparamagnetic nanocomposites, Polymer Bulletin 70 (8) (2013) 2359–2371. With kind permission of Springer.

OH groups on the surface of Fe_3O_4@GO NPs and $Sn(Oct)_2$ were used as the ROP initiators and promoter, respectively. Fe_3O_4 NPs on the GO also acted as nanoscale spacers to prevent the aggregation of the nanosheets, avoiding/weakening the loss of their high active surface area. Differential scanning calorimeter (DSC) and polar optical microscopy (POM) showed that the crystallization temperature (T_c) increased from 23.1 to 29.4°C, and the spherulites size decreased (Fig. 8.8), when Fe_3O_4@GO NPs were embedded into the matrix, which indicates strong heterogeneous nucleating effect of NPs.

Wang et al. [83] modified the surface of TiO_2 NPs with aminopropyl trimethoxy silane to obtain grafted TiO_2 NPs (g-TiO_2) to improve the NPs dispersion. Subsequently, they introduced the NPs into the PCL matrix to prepare PCL/TiO_2 NCs via the in situ polymerization. It was obvious from the TEM images (Fig. 8.9) that the g-TiO_2 NPs showed finer dispersion and distribution. Incorporating the surface-treated NPs resulted in developed mechanical strength and Young's modulus and lower ductility with regard to the pure PCL, because of their well dispersion and strong interfacial interaction with PCL matrix.

Apart from the mentioned techniques to prepare PCL-based NC powders or films, the NCs can also be in the form of fibers. Extrusion of the PCL into monofilament and multifilament can be obtained through melt spinning, solution spinning, and electrospinning, each having its own advantages and drawbacks [85]. Among them, electrospinning process has been applied frequently and has received much interest for

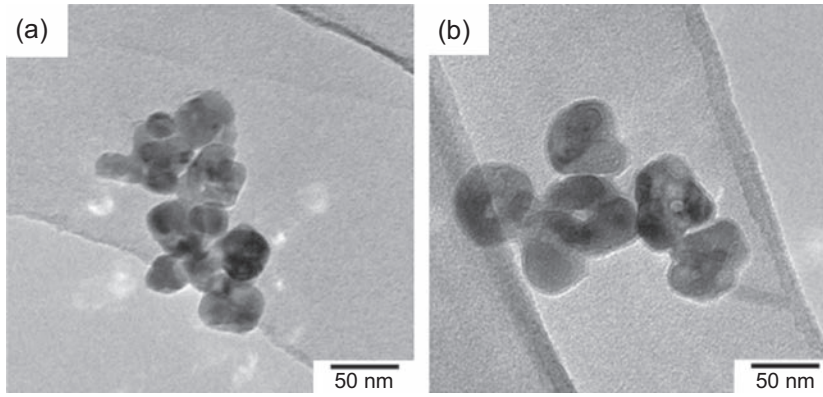

Figure 8.9 TEM micrographs of b-TiO_2 NPs (a) and g-TiO_2 NPs (b).
Adapted from G. Wang, G. Chen, Z. Wei, T. Yu, L. Liu, P. Wang, M. Qi, A comparative study of TiO_2 and surface-treated TiO_2 nanoparticles on thermal and mechanical properties of poly (ε-caprolactone) nanocomposites, Journal of Applied Polymer Science 125 (5) (2012) 3871–3879. With kind permission of John Wiley and Sons.

preparing PCL fibers. Electrospinning as a unique technique uses electrostatic interactions to yield good fibers; therefore, the produced fibers have a small diameter and a larger surface area with regard to those gained from other established spinning routes. In this process, a polymer solution or melt is exposed to robust electric fields; afterward the liquid phase macromolecule is cast out from a nozzle. Before arriving the collecting screen, its solvent vaporizes or it turns to a solid and is collected as a consistent network of little fibers. Thus, the fibers' diameter is reduced as they move in the direction of the collector. Fig. 8.10 shows an electrospinning scheme [86,87]. By changing electrospinning process, parameters including solvent, polymer concentration, and flow rate; nanofibers with various diameters can be achieved [88,89]. The biological properties of electrospun nanofibrous scaffolds such as hydrophilicity, mechanical property, and bioactivity are largely contingent on the composition of the polymers used [89].

There are an extensive variety of polymers that are used in electrospinning and are able to form fine nanofibers with the micron size and were exploited for diverse applications. Electrospun nanofibers are originated from different synthetic macromolecules, natural polymers, and a combination of both, involving proteins, nucleic acids [86,90], and even polysaccharides [91]. Electrospun membranes of PCL and its NCs are studied by many researchers for various tissue engineering applications [92]. A type of PCL-based scaffolds without the nanofiller was fabricated using the electrospinning technique by Gupta et al. [93]. For the preparation, PCL was dissolved in a mixture of chloroform and methanol at room temperature and was stirred for 1 h and sonicated. Then, TiO_2 was added in the solution and stirred. PCL/TiO_2 and the control PCL solution was taken in a syringe equipped with flat tip metal needle to produce the fibrous PCL. In 2010, Shin et al. [94] prepared silica sols using a sol–gel route at room condition via mixing TEOS, H_2O, and C_2H_5OH with the assistance of HCl as the catalyst. The prepared sols were heated to raise the viscosity via solvent evaporation, followed

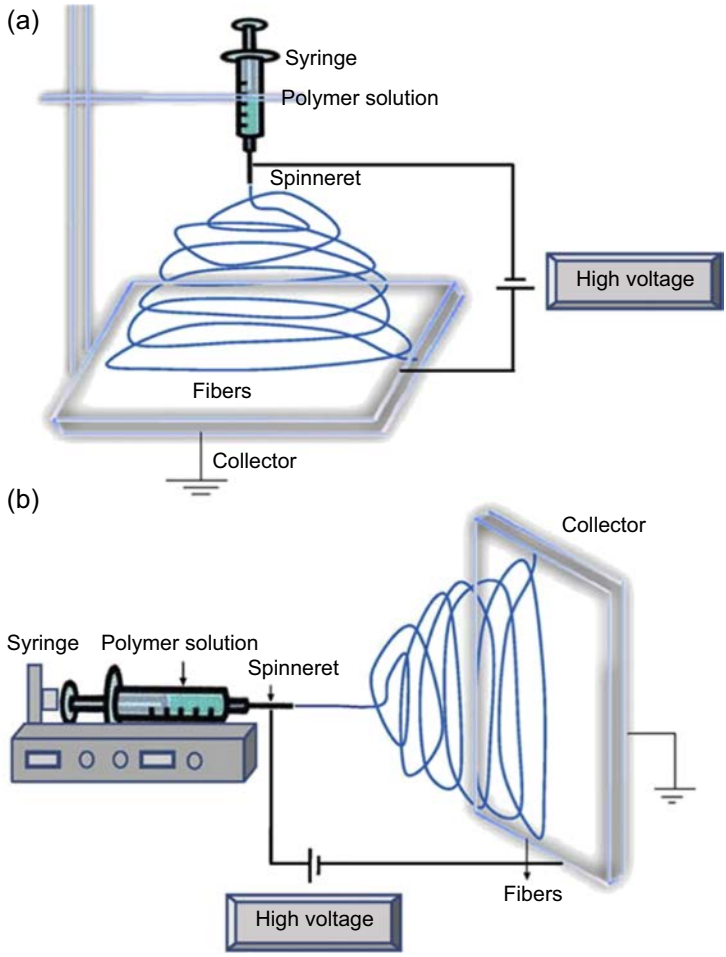

Figure 8.10 Schematic diagram of set up of electrospinning apparatus (a) typical vertical set up and (b) horizontal set up of electrospinning apparatus.
Adapted from N. Bhardwaj, S.C. Kundu, Electrospinning: a fascinating fiber fabrication technique, Biotechnology Advances 28 (3) (2010) 325–347. With kind permission of Elsevier.

by cooling to stop further reactions. A PCL solution was similarly ready through dissolving PCL into a mixture of dichloroethane and N,N-dimethylformamide as solvent and nonsolvent, respectively. Both solutions were individually poured into syringes and coelectrospinning was performed. Fig. 8.11(a) and (b) represents the SEM micrographs of the PCL nanofibers prepared using silica sols heated at 60°C for various times (0 and 3 h). After removing the PCL by thermal decomposition at 500°C, the sample showed partially collapsed silica nanofibers (Fig. 8.11(c)), exhibiting the lacking of silica coating layer. However, the scaffold was produced by a silica heated for 3 h showed some hollow beads with a trace of nanofibers (Fig. 8.11(d)), suggesting that the silica sol is conglomerated on the PCL nanofibers through the coelectrospinning process. TEM micrograph of the

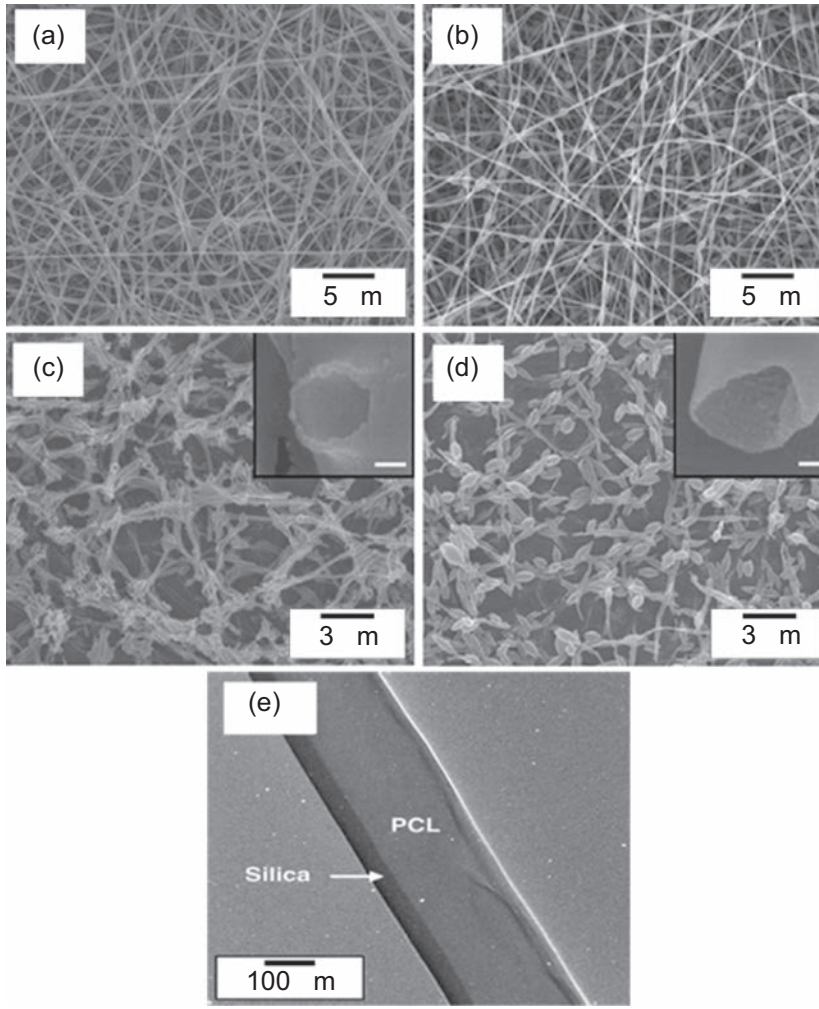

Figure 8.11 SEM micrographs of the PCL nanofibrous scaffolds prepared using various silica sols heat-treated at 60°C for (a) 0 h, (b) 3 h, and the samples after removing the PCL via thermal decomposition at 500°C for 1 h, produced using various silica sols heat-treated at 60°C for (c) 0 h, (d) 3 h, (e) typical TEM image of the PCL nanofiber with the silica coating layer. Adapted from K.H. Shin, J.H. Sung, Y.H. Koh, J.H. Lee, W.Y. Choi, H.E. Kim, Direct coating of bioactive sol–gel derived silica on poly (ε-caprolactone) nanofibrous scaffold using co-electrospinning, Materials Letters 64 (13) (2010) 1539–1542. With kind permission of Elsevier.

NCs (Fig. 8.11(e)) showed that a fine layer of ~26 nm in thickness was formed on the surface of the PCL nanofiber.

Many other valuable PCL-based nanofibers have also been reported, in which various NPs are used, such as TiO_2 nanopowder [95], ZnO NPs [96], and bioactive glass NPs [89,97].

8.4.2 Polycaprolactone/metal oxide nanocomposites degradation

Polymer degradation describes as a mixture of chemical processes and physical changes, occurring through the processing and storage resulting in the cleavage of main chain bonds. Therefore, shorter oligomers, monomers, and other decomposition productions with low Mw can be created [9]. The degradation can principally proceed via three pathways: degradation by biological agents, chemical routes, and physical means. As degradation would cause the creation of low Mw by-products, "erosion" would describe the passage of these low Mw produces. As postulated by Gopferich in 1996, erosion is defined as the loss of material owing to monomers and oligomers leaving the macromolecule [98].

One of the most important reasons of interest in PCL is that PCL materials are completely biodegradable [11]. The existence of five nonpolar methylene linkages in the repeat unity gives its unique properties; however the hydrolytically labile aliphatic-ester connection induces the PCL to be degradable. PCL can be hydrolytically degraded through bulk or surface erosion that 5-hydroxyhexanoic acid is the degradation produce. PCL degradation occurs more slowly than PLA and typically has a degradation period of 2 years that attributed to its hydrophobic nature [99]. PCL materials may be entirely degraded by microorganisms (including some phytopathogens), bacterial and fungal enzymes such as esterases, and lipase [100]. PCL is degraded in two stages. The first stage is a nonenzymatic hydrolytic ester cleavage, autocatalyzed by carbon end groups of the chains. As the Mw is declined to 5000, the next stage occurs with reducing the rate of chain scission and the beginning of weight loss, caused by the diffusion of oligomer sorts from the bulk. The macromolecule chains become ready to fragmentation, and either enzymatic surface erosion or phagocytosis contributes to the absorption process [101].

PCL degradation within the body is also feasible because the ester bonds are chemically labile and they tend toward hydrolysis, but ester hydrolysis under physiological conditions slows down with raising the carbon atoms numbers. This is a promising factor in employing the PCL for long-term biomaterial applications, but it is difficult to measure the long-time toxicities from its degradation. PCL has a low glass transition temperature and down melting temperatures of around 60°C and shows elastic behavior at room condition that make it easy to fabricate or process into highly structured forms [102]. The high solubility of PCL in a range of nonpolar solvents and its composition has also given it the exceptional features of being compatible with various polymers for effective blending. For instance, to synthesis of materials with specifically tailored properties (in terms of surface properties, degradation amount, mechanical properties, and biodegradation), PCL has been broadly explored by scholars as a copolymer or as a constituent in a macromolecule blends that are miscible with lots of other macromolecules such as poly(vinyl chloride), chlorinated polyethylene, and polycarbonate [11].

In 2016, Augustine et al. [103] have fabricated PCL/ZnO membranes by electrospinning of PCL NCs containing various concentrations of ZnO NPs (0.5–6 wt% of ZnO content). For investigation of the ZnO NPs influence on the degradation rate, the

in vitro test in simulated body fluid (SBF), at pH of 7.3 and temperature of 37°C, was performed. They put the samples in test tubes and then exposed them to degradation for 30 days in SBF and then freeze-dried. The percentages of weight loss have been considered as a measure of NC biodegradation. The NCs with higher percentages of the NPs showed higher weight losses.

8.4.3 Potential application of polycaprolactone/metal oxide nanocomposites

8.4.3.1 Polycaprolactone/metal oxide nanocomposites applied in tissue engineering

Within the broad discipline of biomaterials science, the area of tissue generation has one of the enormous economic impacts [104]. Tissue engineering is described as an interdisciplinary area, which uses the principles of engineering and sciences to realization of organization function relations in pathological mammalian tissue and the development of biological substitutes that restore, maintain, or improve tissue function or a whole organ [105]. Tissue engineering presents strategies to revolutionize therapies for the regeneration of various tissues, such as shell, bone, tendon, cardiac, and arteries, and to considerably enhancing the quality of patient's life [6]. Since the emerging of these fields, many researches have been distributed worldwide to the scientific community with the aim of generating an organ or part of it in vitro, or of inducing in vivo regeneration [106]. The tissue construct is categorized into two types, open systems and closed systems. The scaffold with attached cells implanted into the body is described as open system, whereas the implant that is employed as external organ support is specified as the closed system [105].

For regeneration of osseous tissue, the candidates should have several characteristics such as (1) bioresorbability and biocompatibility with manageable degradation degree to adjustment of cell/tissue growing in vitro/in vivo. It needs to be mentioned that one concern arises from using polymeric scaffold materials is that, after the breaking down the scaffold, the resulted byproducts and residues should be safely removed from the body by a biological system that this description for polymers is defined as a bioabsorbable polymer [9,85,105]; (2) osteoconductivity: the porous interconnected structure allows novel cellule to stick and transfer over the configuration, as well as permits the interchange of nutrient-waste and new blood vessel penetration; (3) osteoinductivity: the quality for possessing the essential proteins and growth factors to induce the progression of mesenchymal stem cells; (4) osteogenecity: the osteoblasts at the site of the generated bone that can produce minerals to harden the matrix to form the substrate for new bone; and (5) mechanical features of tissues to adjust in the site of implantation [105,107]. In general, for regeneration of organs, a polymeric scaffold is preferred. Both natural and synthetic macromolecules have been commonly applied as polymeric biomaterials. Although natural polymers have many advantages, including biodegradability and cytocompatibility [6], the physical traits of synthetic macromolecules, for instance mechanical features and degradation speed, can be changed consistent with the desires with fewer batch-to-batch variations than

usual with natural materials. Among the various synthetic biodegradable polymers, PCL and fibrous PCL are expansively examined for scaffold fabrication. PCL is a bioresorbable polymer and possess greater rheological properties; therefore it can be utilized by most of the macromolecule treating technology to prepare an enormous group of scaffolds [85]. Fibrous PCL has been prepared in various forms, as single, dual, hollow, and porous types. However, the important limitations in applying PCL fibers to bone regeneration are their low stiffness, hydrophobic nature, and relatively low bioactivity. To overcome these shortcomings, hybridization of PCL with inorganic substances have been devised by many researchers [108], which improves cell affinity while offering ideal mechanical properties for tissue engineering usages [109,110].

ZnO-containing films for directed tissue/bone revival were developed by Bottino group [111]. PCL and PCL/gelatin blend were filled by ZnO with diverse contents: 5, 15, and 30 wt%. The fibers were obtained through electrospinning by applying improved parameters and were analyzed with different techniques to understand whether the membranes were suitable for tissue engineering. TEM image of the fibers (Fig. 8.12) confirmed the existence of ZnO surrounded inside the matrix. Contact angle of the blend membrane showed hydrophilic surfaces that the incorporation of ZnO NPs resulted in the further improved hydrophilicity, compared with the aquaphobic membranes. The membranes also showed antibacterial activity against the bacteria tested (*Porphyromonas gingivalis* and *Fusobacterium nucleatum*) and satisfactory cytocompatibility, which was more pronounced with increased ZnO content; nonetheless, incorporation of 30 wt% of ZnO NPs resulted in a slight toxicant influence on the cells. The PCL/gelatin-based membrane produced the highest cytotoxic potential.

Bioactive glasses (BGs) are a group of surface reactive glass–ceramic materials that composed of SiO_2, CaO, Na_2O, and P_2O_5 with different percentages. BGs are

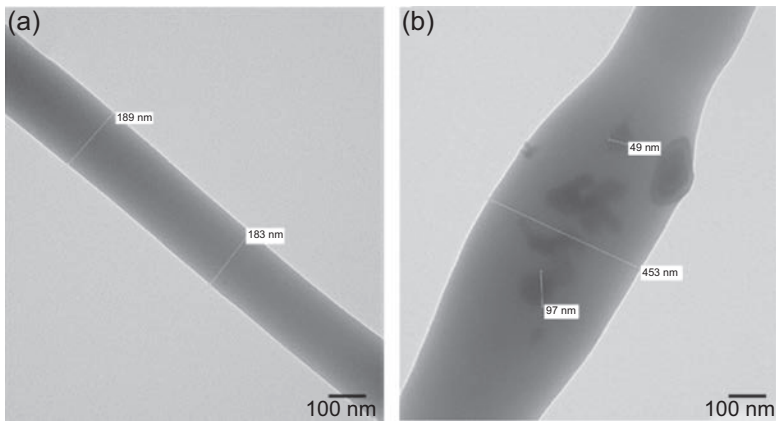

Figure 8.12 TEM images of (a) the neat PCL fibers and (b) ZnO-incorporated fibers. Adapted from E.A. Münchow, M.T.P. Albuquerque, B. Zero, K. Kamocki, E. Piva, R.L. Gregory, M.C. Bottino, Development and characterization of novel ZnO-loaded electrospun membranes for periodontal regeneration, Dental Materials 31 (9) (2015) 1038–1051. With kind permission of Elsevier.

excellent nanofillers due to their great bioactivity, which led to forming a hydroxyapatite on the NC surfaces, thus allowing direct attachment with natural bone tissue [89,110]. In a recent study by Gönen et al. [109], incorporation of BG into the gelatin/PCL mat was developed through the electrospinning technique. They showed that the prepared NC fibrous mat could be used as a scaffold for tissue engineering uses. They used surface methodology by using a three-level, four-variable Box–Behnken strategy to obtain the desired diameter. In best settings, the resultant fiber diameter was calculated 584 ± 337 nm. Surface morphology of the optimized NC mat revealed that it was involving randomly oriented, uniform, and bead free nanofibers. It was noticed that thermal degradation of NC mat was single-stage between 200 and 550°C, but for gelatin/PCL it was two-stage degradation in which the first stage at 240–364°C was accompanied by breaking the peptide bonds and the second between 364 and 560°C was attributed to the PCL decomposition. The change from two-stage degradation to single-stage degradation with the addition of BG could be caused by the presence of molecular interactions and the composite fabrication.

In an interesting study by Zhang et al. [112], 3D magnetic Fe_3O_4 NPs containing (2, 10 and 15 wt%) mesoporous BG/PCL (Fe_3O_4/MBG/PCL) composite scaffolds have been fabricated. The prepared scaffolds had uniform macropores, high porosity, and high compressive strength. The incorporation of Fe_3O_4 NPs into the MBG/PCL scaffolds did not affect their apatite precipitation ability in SBF, but induced high magnetic heating ability. The proliferation of human bone marrow mesenchymal stem cells (h-BMSCs) cultured on the scaffolds showed that all the scaffolds accelerated h-BMSCs proliferation, and no difference was noticed between the four scaffolds on the first and third days. However, the proliferation rates on the scaffold with high amount of Fe_3O_4 were higher than that on MBG/PCL scaffolds on day 7. In the gene expression investigation, significantly enhanced osteogenic separation of h-BMSCs was observed by incorporation of Fe_3O_4 NPs. There were no major variances in stimulated proliferation and alkaline phosphatase (ALP) activity of the h-BMSCs among all the scaffolds on day 7, but the Fe_3O_4 containing scaffolds improved the osteoblast phenotype expression of h-BMSCs at day 14 compared with the MBG/PCL scaffolds and also exhibited a positive correlation between ALP activity and Fe_3O_4 value of the scaffolds.

ALP is assayed by determining the released p-nitrophenol from p-nitrophenyl phosphate (p-NPP). The scaffolds cultured with mouse preosteoblast cells were rinsed gently with phosphate-buffered saline (PBS) and incubated in a buffer. Lysate was poured into a tissue culture plate comprising p-NPP solution. In the presence of ALP, p-NPP is transformed to p-nitrophenol and inorganic phosphate [113].

To investigate the effect of Si and Fe content on the solubility of phosphate-based glasses (PGs) containing calcium in the system ($50P_2O_5$-40CaO-10$x$$SiO_2$-$x$$Fe_2O_3$), SiO_2 was replaced with Fe_2O_3 that an improvement in the density and glass transition temperature of the PG was observed [114]. The resulted PG formulations, $50P_2O_5$-40CaO-10Fe_2O_3 (Fe10) and $50P_2O_5$-40CaO-5Fe_2O_3-5SiO_2 (Fe5Si5), were melt drawn into fibers and introduced into PCL. In deionized water, PCL-Fe5Si5 showed a greater ion delivery and weight loss, compared with PCL-Fe10. In addition, the

initial values of the mechanical strength and modulus of the composites were in the range of trabecular bone and they were remained within this region for the composites immersed in PBS during 7 and 28 days. At longer-term aging, the decrement of mechanical properties and storage modulus for PCL-Fe5Si5 was more than that of the PCL-Fe10. Therefore, the PCL-Fe10 was suitable for possible utilization as bone repairing devices.

Incorporation of BG-ceramic (BGC) along with bisphosphonate drug into a poly(lactide-co-caprolactone) was led to the formation of porous microspheric scaffolds, which were noncytotoxic and applied for the osteoporosis therapy such as bone defects [115]. Osteoconductivity of the scaffolds in SBF detected a hydroxycarbonate apatite layer on the surface that disclosed the bone bonding and bone revival capability of the scaffold. It was suggested that this approach can be a better approach to prevent osteoclast-mediated bone resorption phenomenon with the aid of bisphosphonate drug and to increase bone density by the incorporated BGC. Incorporation of BGC also promoted the cell adhesion of the composite microspheres toward the metabolically active cellules, whereas no cell adhesion was detected on the surfaces of the neat microspheres developed from the copolymer alone.

Dziadek et al. [116] have considered the influence of BG content and its chemical composition on physicochemical properties of the PCL-based composite films. The introduction of BG particles into the matrix increased the surface hydrophilicity that has been subjected to a glass substrate during casting. Therefore, by using different contents of BG particles, crystalline features of the matrix were modulated. The fillers also influenced the cellular response and degradation percentage of the composites. In the presence of BG particles in PCL matrix, the composites showed excellent in vitro biocompatibility, improved osteoblast-like cellules reproduction, and adjustable cell response.

In a fascinating study, in addition to investigating the physical and mechanical properties of the PCL/BG sheets, their ability to support nerve growth and survival were thoroughly studied [117]. For this reason, three different PCL composite sheets containing 50 wt% borate glass particles (B3), 50 wt% silicate glass particles (45S5), and a blend of B3 and 45S5 were composed. The NC with B3 had an advanced degradation rate with regard to the NC with 45S5, and the peak stress of the composites was lower than that of the neat polymer. Nonetheless, the neat polymer presented higher stiffness for long-run prereacting in cell media. To inquire whether the composites would preserve neuronal growth, dorsal root ganglia of embryonic chicks were isolated and cultured on the sheets and neurite outgrowth was measured. The incorporated BG particles in the composites showed no negative effects on neurite extension, and neurite extension enhanced on PCL:45S5 PCL:13–93 B3 when prereacted in media. Therefore, the composite sheets of PCL and BG particles offered a flexible biomaterial for neural tissue engineering.

Molecular level scale BG-PCL (MBG-PCL) hybrid monoliths with porous surface structure were successfully fabricated by Chen et al. [118], through a polydimethylsiloxane modified sol–gel technique. The hybrid monolith was porous with a crack-free morphology. The MBG-PCL hybrid structure exhibited high apatite-forming ability in SBF. The composition, holey arrangements, and excellent bioactivity of the monoliths

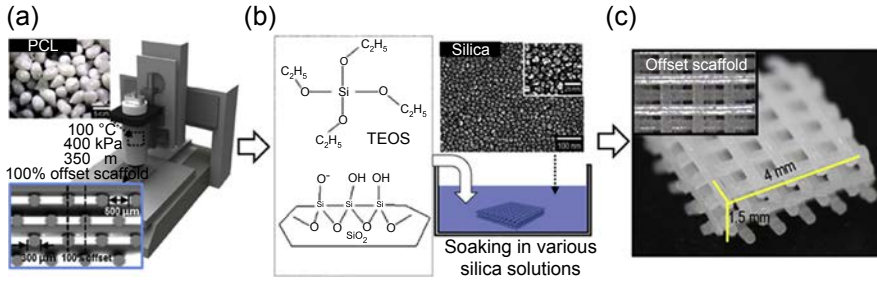

Figure 8.13 Schematic of the fabrication process of composite scaffolds. (a) Fabrication of multilayered PCL scaffolds having 100% offset structure to the thickness direction, (b) the process of coating with various silica solutions, and (c) an optical image of the fabricated pore structure of the composite scaffolds.
Adapted from H. Lee, H. Hwang, Y. Kim, H. Jeon, G. Kim, Physical and bioactive properties of multi-layered PCL/silica composite scaffolds for bone tissue regeneration, Chemical Engineering Journal 250 (2014) 399–408. With kind permission of Elsevier.

resulted in their application in bone tissue engineering as a bioactive implant. The soaking of the composites in SBF for 3 and 7 days induced the sedimentation of Ca-poor apatite layer. Similarly, Lei et al. [119] applied the PCL/BG scaffold in bone tissue renewal. During the composite synthesis, they added polyethylene glycol (PEG) as a template, which could be homogeneously dispersed in the PCL matrix, while generated pores in the PCL/NBG NCs.

The characteristic properties of nano-SiO_2, including high biocompatibility and hydrophilicity, have made it a potential component of materials for tissue engineering, whereas its low processability and low mechanical properties have been limited their extensive use as a tissue regenerative material [120]. For this purpose, composite scaffolds based on PCL and silica was fabricated by a melt-plotting/coating process [113]. By using the coating process with SiO_2 (Fig. 8.13), composite scaffolds with homogeneous surface roughness and improved wetting/water absorption with no mechanical loss were obtained. Biological activities of the composite scaffolds were significantly improved that the increase was depended on the weight percentages of silica. For instance, cell-seeding efficiency (~1.8-fold), cell viability (~5-fold) and ALP activity (~1.7-fold) demonstrated that even a low proportion of coating agent (i.e., silica) can noticeably increase in vitro cellular activities.

Lee et al. [108] have developed a fibrous membrane by electrospinning a uniform PCL–SiO_2 hybrid sol guided bone regeneration. The resulted membrane was reported to have nanosized uniform patterns, unique tensile strengths, and elastic modulus, and it was highly hydrophilic. However, the PCL–SiO_2 hybrid coatings on the surface of titanium plates were reported by Teng group via a sol–gel spin-coating technique [121]. SiO_2 content had influenced various features of the coatings, such as phase composition, surface morphology, wettability, and in vitro bioactivity that the last two properties were significantly improved. After incubation of the composites in SBF

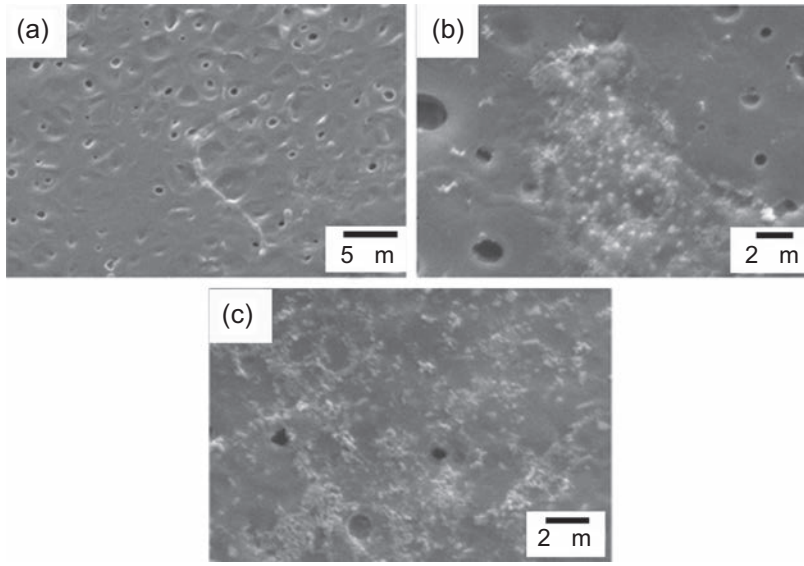

Figure 8.14 SEM images of (a) PCL, (b) PCL-10% SiO_2, and (c) PCL-30% SiO_2 after incubation in SBF solution for 3 days.
Adapted from S.H. Teng, P. Wang, J.Q. Dong, Bioactive hybrid coatings of poly (ε-caprolactone)–silica xerogel on titanium for biomedical applications, Materials Letters 129 (2014) 209–212. With kind permission of Elsevier.

solution for 3 days, vigorous sedimentation of the apatite crystals occurred on the NCs, especially on the NC with the high nanofiller content, whereas no mineral phase was formed on the pure PCL as seen in Fig. 8.14.

Besides all these experiments in the field of bone regeneration, the formation of an active blood vessel network through an implanted scaffold is one of the most important challenges [122]. The formation of an active blood vessel system is crucial for the accretion of the scaffold with existing host tissue that can occur mainly by angiogenesis. Angiogenesis is the development of new blood capillaries from current blood vessels for providing nutrients to cells that are away from the current blood vessels. Angiogenesis is described as a crucial reaction in growth, wound healing, and fabrication of granulation tissue, and it is mediated by the endothelial cellules that line blood vessels. It is a controlled process comprising a number of stimulators, for example fibroblast growth factor (FGF), vascular endothelial growth factor (VEGF), angiopoietins, activators of integrins, and inhibitors [123,124]. Thus, the usage of a material to accelerate of the cells growth can conquer the challenges. Reactive oxygen species (ROS) such as hydrogen peroxide can contribute in the cell multiplication and wound healing via the activation of growth factors [125] that play a significant role in angiogenesis by stimulation of the basic steps of cell proliferation, transfer, and tube constitution. Improvement of angiogenic property of electrospun PCL in tissue engineering scaffolds was studied by Augustine group [123]. They incorporated ZnO NPs in the polymer matrix that were able to generate H_2O_2 as the ROS, which induced

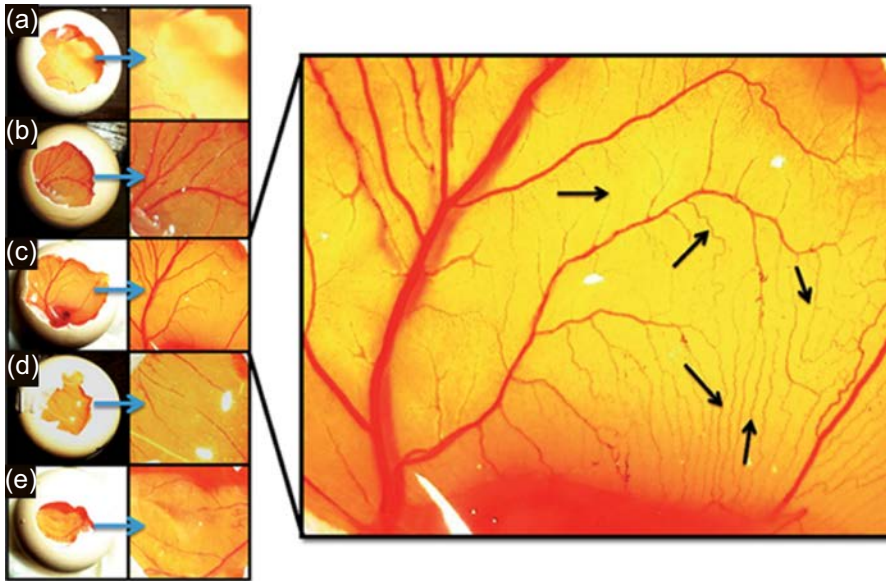

Figure 8.15 Illustrative images of CAM after placement of the scaffolds. Neat PCL membrane (a), PCL membrane with 0.5 wt% (b), 1 wt% (c), 2 wt% (d), and 4 wt% (e) ZnO NPs. Adapted from R. Augustine, E.A. Dominic, I. Reju, B. Kaimal, N. Kalarikkal, S. Thomas, Investigation of angiogenesis and its mechanism using zinc oxide nanoparticle-loaded electrospun tissue engineering scaffolds, RSC Advances 4 (93) (2014) 51528–51536. With kind permission of Royal Society of Chemistry.

angiogenesis through a growth factor–mediated mechanism. They used chicken chorioallantoic membrane (CAM) assay to study the ability of incorporated ZnO NPs to angiogenesis (Fig. 8.15). PCL membranes with 1 wt% of ZnO NPs exhibited the maximum matured blood vessels with highly branched capillary network, but higher concentration of the nanofiller did not remarkably improve the angiogenesis. In vivo implantation study disclosed that the fibrous PCL scaffolds were proangiogenic and also the enhanced angiogenic property of the scaffolds was due to the upregulation of key angiogenic factors, FGF and VEGF. As stated above, ROS can better wound healing by improving cell adhesion and cell migration through growth factor–mediated pathways. Therefore, the same group in another work [96] applied the prepared electrospun fibrous PCL/ZnO for wound healing without scar formation. Thus, the neat PCL membranes and that containing 1 wt% of the nanofiller were sutured in the full thickness wound in guinea pigs. On the first days, the wound was coated with the membranes. In between 15th and 20th days of implantation, outer regions of both neat membranes and NP incorporated membranes rejected from the healing wound accompanied by the debris. Afterward, the wound was clearly observable and there was a substantial change in healing between neat and NP containing PCL (Fig. 8.16(d) and (i)). On the 30th day, the wounds with PCL/ZnO membrane were entirely healed without any scar formation, but for neat membrane implanted wounds, hair formation

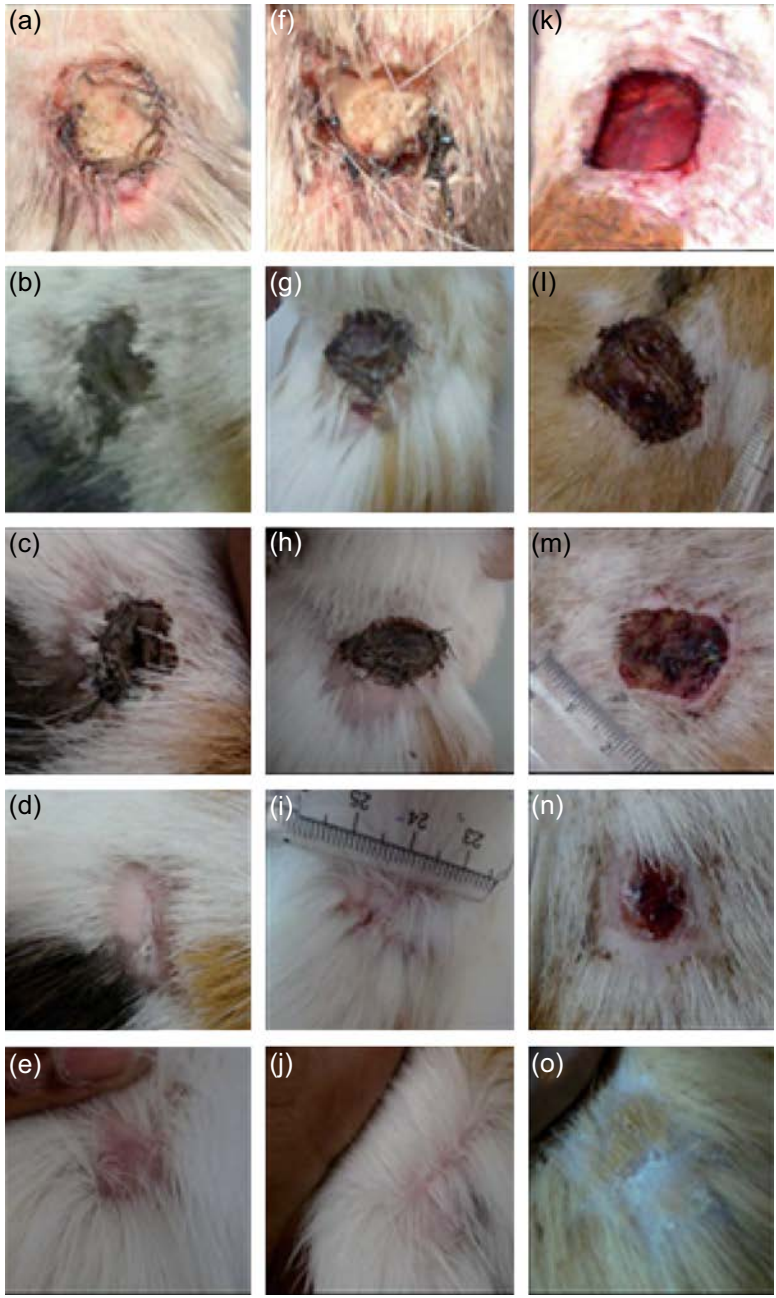

Figure 8.16 Wound healing activity of the membrane on the first day (a, f, and k), on 5th day (b, g, l, and q), on 10th day (c, h, and m), on 20th day (d, i, and n), and on 30th day (e, j, and o) of implantation. The first column (a–e) indicates neat PCL membranes, the second column (f–j) shows PCL membrane incorporated with 1 wt% ZnO NPs, and the third column (k–o) indicates povidone–iodine-treated wounds.
Adapted from R. Augustine, E.A. Dominic, I. Reju, B. Kaimal, N. Kalarikkal, S. Thomas, Electrospun polycaprolactone membranes incorporated with ZnO nanoparticles as skin substitutes with enhanced fibroblast proliferation and wound healing, RSC Advances 4 (47) (2014) 24777–24785. With kind permission of Royal Society of Chemistry.

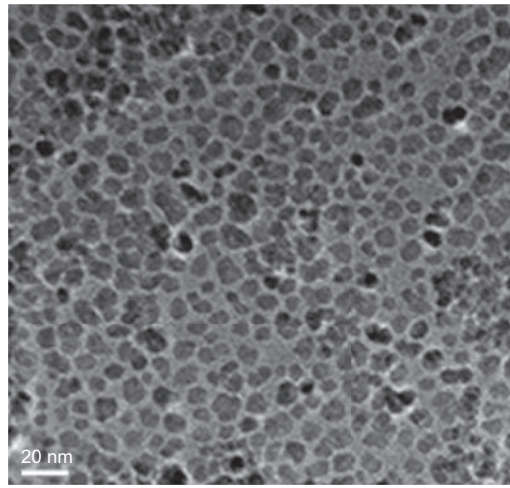

Figure 8.17 TEM image of the modified Fe_3O_4 NPs.
Adapted from J.J. Kim, R.K. Singh, S-J. Seo, T.H. Kim, J.H. Kim, E.J. Lee, H-W. Kim, Magnetic scaffolds of polycaprolactone with functionalized magnetite nanoparticles: physicochemical, mechanical, and biological properties effective for bone regeneration, RSC Advances 4 (33) (2014) 17325–17336. With kind permission of Royal Society of Chemistry.

on the healed area was lower compared with the other regions. For povidone-iodine treated wounds, thick scar formation was noticed. Negative controls did not heal the wound even after 30 days.

There are also other reports on the application of metal oxide NPs-filled PCL-based scaffolds for tissue engineering. Various NPs such as TiO_2 [108] and magnetic Fe_3O_4 [126] were encapsulated within the scaffolds to improve in vitro cellular responses in terms of reproduction and bone renewal ability. For further biocompatibility of the Fe_3O_4 NPs with the PCL as the matrix, the NP surfaces were modified with surfactants such as alcohols, oleic acids, and oleylamine that Fig. 8.17 shows the TEM image of the modified NPs.

8.4.3.2 Polycaprolctone/metal oxide nanocomposites applied in drug delivery

Current development in drug delivery caused the discovery and production of various therapeutic molecules with the ability to target and treats many diseases. Their use is relatively restricted by the limitations of the human body. Body is involving a complex network of compartments that the desired sites of action lie. To reach these targets, the drug molecules have to pass a series of boundaries, typically in the form of epithelial and mucosal barriers and face exposure to a strict media of degrading enzymes and varying pH levels [127]. However, hydrodynamic radius, charge, permeability, and hydrophilicity can occasionally influence movement [128]. Generally, the ability of the drug molecule to reach the target area is limited by obstacles such as drug solubility, drug stability, and physical barriers to absorption. Therefore, development of systems for improving drug delivery that lack stability and solubility is imperative

[129]. Drug carriers used in drug and gene release should have two preferences to avoid nonspecific capture at nontumor sites. First, they must be smaller than 200 nm to hinder uptake by the reticuloendothelial system, and the Mw should be more than approximately 40,000 Da to evade renal filtration. Second, they should not have strong interact or being taken up by means of organs, specially the reticuloendothelial system. Thus, hydrophobic or cationic carrier surfaces must be evaded, whereas hydrophilic carrier with neutral or weak negative surfaces will reduce random uptake [109,110].

Recently, significant advances in biomedical engineering has deduced in frequent commercially available macromolecular drugs. Biodegradable macromolecules have been widely used in biomedical utilization in the form of sutures, wound covering materials, and artificial skin [130]. Polymeric drug delivery systems are less complicated and they are small, because the drug can be loaded as powders within the polymer. It was reported that polymeric carriers are suitable for high Mw drugs and the drugs, which should be delivered in small quantities with zero-order kinetics [131]. Controlled drug release systems based on polymers, respond to variations in environmental conditions, such as temperature, pH, light, electric field, and certain chemicals, are being extensively explored. Such systems formulations have been applied in different forms relying on the end use specification that their major forms were NPs, microparticles, and hydrogels, respectively [132]. Various approaches for improved drug delivery relying on the polymer-based compounds are (1) implantable networks for controlled release; (2) NPs, liposomes, and micelles as the carrier systems for therapeutic encapsulation; and (3) macromolecule–drug conjugates [129]. PCL as a nontoxic and FDA-approved polyester has been used as a matrix for controlled delivery devices in a range of geometries. It is degraded slower than polyhydroxy acids and therefore is preferred for controlled delivery systems with a longer lifetime [133].

Zou et al. [134] have prepared magnetic complex micelles with temperature and redox responses based on amphiphilic PCL-SS-PDMAEMA copolymer, which was fabricated through a combination of atom transfer radical polymerization and ROP using the PCL and disulfide functionalized OH-SS-iBuBr. The prepared copolymer incorporated oleic acid–modified Fe_3O_4 NPs with good biocompatibility. Because water is a poor solvent for the NPs and the PCL block and a good solvent for the PDMAEMA block, the mixture of the PCL-SS-PDMAEMA copolymer and Fe_3O_4 NPs could self-assemble to micelles, with Fe_3O_4 and PCL block core and PDMAEMA block shell (Fig. 8.18(a)). The temperature response of the PDMAEMA block and the redox response of the disulfide bond allowed the magnetic micelles show dual responses. The magnetic micelles was used as a doxorubicin (DOX) carrier for controlled drug release that the release rate was controlled through the addition of an external alternating magnetic field and altering the DL-dithiothreitol (DTT) concentration. With the addition of DTT, the distributions of hydrodynamic radius (Rh) broadened with the appearance of aggregates. Fig. 8.18(b) shows the cumulative DOX release versus time under different conditions. The magnetic micellar capsules showed a rather low release level without an external magnetic field (EMF).

A redox response magnetic micelle with magnetic-guided and active-targeted functions was formed by self-assembly of four-arm PEG-PCL copolymers with disulfide bonds as intermediate linkers [135]. DOX and Fe_3O_4 NPs are simultaneously

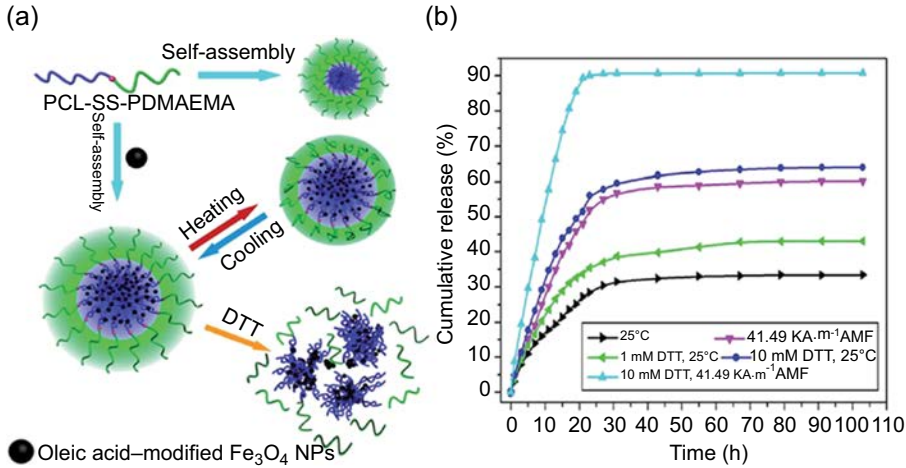

Figure 8.18 (a) Self-assembly of the PCL-SS-PDMAEMA copolymer, the preparation and dual responsive behaviors of the magnetic PCL-SS-PDMAEMA/Fe_3O_4 complex micelles. (b) Controlled release of DOX from the micelles under different conditions.
Adapted from H. Zou, W. Yuan, Temperature-and redox-responsive magnetic complex micelles for controlled drug release, Journal of Materials Chemistry B 3 (2) (2015) 260–269. With kind permission of Royal Society of Chemistry.

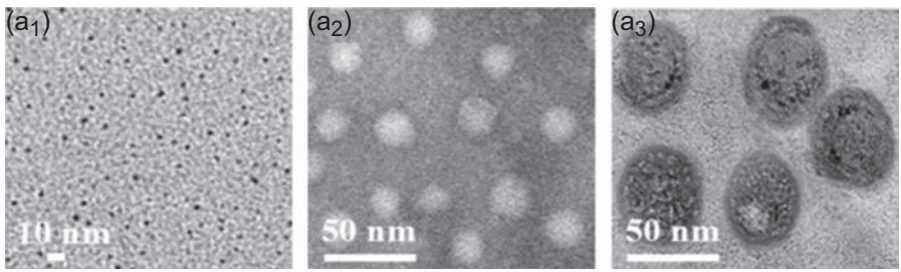

Figure 8.19 TEM images of (A_1) the modified Fe_3O_4 NPs, (A_2) the nonmagnetic micelles, and (A_3) the magnetic micelles.
Adapted from Z. Tang, L. Zhang, Y. Wang, D. Li, Z. Zhong, S. Zhou, Redox-responsive star-shaped magnetic micelles with active-targeted and magnetic-guided functions for cancer therapy, Acta Biomaterialia 42 (2016) 232–246. With kind permission of Elsevier.

incorporated into the hydrophobic cores. Phenylboronic acid (PBA) ligands are conjugated to the hydrophilic ends (PEG) segments, inducing the active targeting of nanocarriers. From the TEM images shown in Fig. 8.19, both the nonmagnetic and magnetic micelles had spherical shapes and small particle sizes, and the magnetic Fe_3O_4 NPs were well distributed in the micelles. Analyses of the intracellular uptake with salic acid (SA)–positive tumor cells and the negative cells in the presence of a magnetic field showed that PBA-targeted micelles can be accumulated round the

tumor cellules by magnetic guiding aim the SA-positive tumor cellules and facilitate the drug release within the cytoplasm. However, the absence of PBA-aiming ligands (in the single-aiming magnetic micelles) can weaken the binding ability compared with the PBA-aimed magnetic micelles. However, its accumulation was still better than free DOX and the nonaimed magnetic micelles. The in vivo outcomes were also in compromise with those of in vitro. Another example of self-assembled magnetic micelles for dual aiming of cancer cellules was reported by Yang et al. [136] that used diblock copolymers of PEG and PCL, bearing a tumor targeting ligand, folate. The DOX-containing micelles showed superparamagnetic behavior at room conditions; however, they were changed to ferromagnetic at 10K, in accordance with magnetic properties of primary used superparamagnetic NPs. Folate attachment caused the diagnosis of the micelles by tumor cells. Transport efficiency of the micelles within the tumor cellules can be also improved by using an EMF to the cellules.

Wang et al. [137] reported the preparation of hollow magnetic fibers for release of antifungal active "ketoconazole" (KCZ) that were fabricated by coaxial electrospinning. Fe_3O_4 NPs and the drug were encapsulated in the core–shell PCL matrix, during the electrospinning. Dimethyl silicone oil was used as the inner core, which consequently perfused out of the two-phase electrospun microstructures to form hollow fibers. An increase in hydrophilicity of membranes was occurred with increasing KCZ concentration. Advanced drug delivery through a low-sustained phase was achieved by applying an EMF. KCZ concentration in the electrospinning solutions affected drug loading and delivery efficiency of the resultant fibers. The lowest KCZ loaded fibers demonstrated the greater cumulative drug release among all three fiber types (0.5, 3, and 9 wt%). Another controlled drug-release system consisting PCL with a hollow interior was prepared in three steps [138]: (1) preparation of a mixture solution (polymer and Fe_3O_4 NPs); (2) mechanical agitating to acquire an aqueous emulsion; and (3) vaporization of the solvent by freeze-drying in vacuum (Fig. 8.20(a)). The surface hole of one particle resulted in the facile loading of the DOX molecules within the holes before thermal annealing of the particles. By exploiting an EMF, the volume of the hollow interior was decreased because of the heat generation of Fe_3O_4 NPs in response to the EMF that pump out the uptaken water, as well as the loaded DOX molecules. The percentage of the released drug at each pumping was controlled via the power of exploited field.

Two major difficulties for magnesium alloy implant are their high degradation rate and easy infection. For this purpose, Dong et al. [139] developed a surface drug delivery system (Mg/Epoxy resin-ZnO/PCL-Ibuprofen), which was capable of bidirectional controlled release of ibuprofen and Mg^{2+}. The system was prepared via a dip coating route followed by spraying. The in vitro study demonstrated that the ibuprofen release has constant release profiles in 22 days, which can efficiently solve the local cellular rejection and inflammation in early stage of the implantation. Moreover, the drug carrier exhibited better corrosion resistance against the high combining strength between epoxy resin–ZnO coating and magnesium alloy; hence Mg^{2+} can be released slowly at early stage and then speeded up.

Matos et al. [140] fabricated the PCL/SNP composites from PCL and mesoporous SNPs (MCM-41/SBA-15) by means of a supercritical CO_2 ($scCO_2$)–assisted foaming/

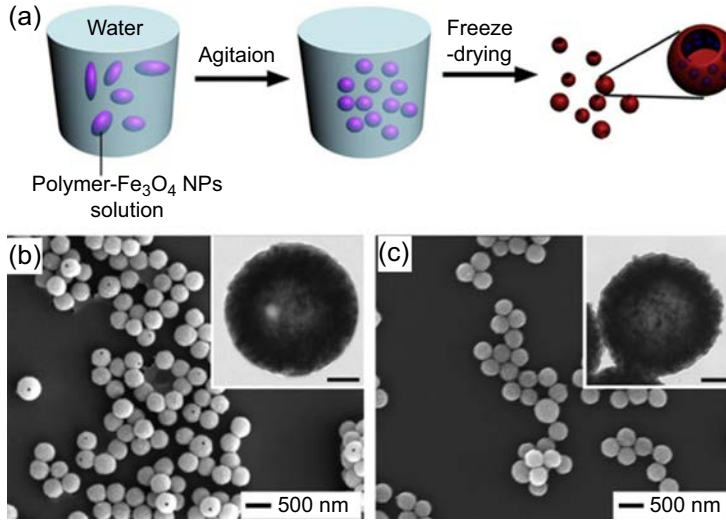

Figure 8.20 (a) The method for the synthesis of Fe_3O_4 containing PCL particles. (b) SEM image of the Fe_3O_4 containing PCL particles with holes created during freeze drying. (c) SEM image of the Fe_3O_4 NPs containing PCL particles that the holes were closed via thermal annealing at 50°C. The scale bars of the insets are 100 nm.
Adapted from D.C. Hyun, Magnetically-controlled, pulsatile drug release from poly (ε-caprolactone) (PCL) particles with hollow interiors, Polymer 74 (2015) 159–165. With kind permission of Elsevier.

mixing method (SFM) and then loaded DXMT into the SNPs by means of a $scCO_2$ solvent impregnation/deposition method and into the PCL/SNP NCs by SFM method. SBA-15 released greater quantities of DXMT compared with the MCM-41, related to the larger pore diameters of SBA-15, which led to the water diffusion within the pores and also allow the rapider DXMT desorption and delivery. In addition, PCL released lower DXMT values compared with PCL/SNPs, both operated at the same pressure. The processing at higher pressure led to higher released amounts for both of them. PCL/SBA-15 70:30 wt% composites released more DXMT than the 90:10 wt% composites, whereas the compositional effect was not obvious for PCL/MCM-41 samples. Another drug delivery system based on PCL and silica NPs was reported by Gao et al. [141] that applied cryomilling method (solvent free, low temperature processing) to generate a bio-NC film based on PCL and Dox containing silica NPs (Si-Dox). The variance between the pure PCL and the NCs was that the NC films contained many micron-sized pores and their Young's modulus was slightly superior to the PCL film due to the silica NPs ingredient (Fig. 8.21). They also showed a sustained release for Dox over 50 days.

Cationic PCL modified hollow porous silica was obtained via a postgrafting procedure by covalent bonding among the silanols on the silica surface and the trimethoxysilane groups of the poly(γ-(carbamic acid benzyl ester)-PCL) that the prepared cationic surface showed efficient drug delivery for ammonium glycyrrhizinate [142].

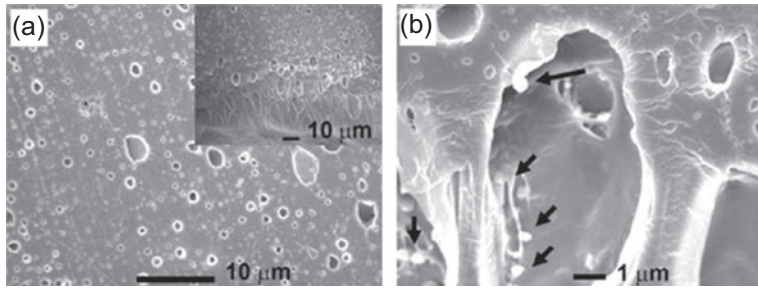

Figure 8.21 Characterization of the PCL/Si-Dox film: (a) representative SEM image of the surface and cross-section (insert) of the PCL/Si-Dox film; (b) representative SEM image of the microsized pore on the PCL/Si-Dox film. *Black arrows* point Si-Dox NPs.
Adapted from Y. Gao, J. Lim, Y. Han, L. Wang, M.S.K. Chong, S.H. Teoh, C. Xu, Cryomilling for the fabrication of doxorubicin-containing silica-nanoparticle/polycaprolactone nanocomposite films, Nanoscale 8 (5) (2016) 2568–2574. With kind permission of Royal Society of Chemistry.

8.4.3.3 *Polycaprolactone/metal oxide nanocomposites applied in water treatment*

With the rapid development of industrialization, noticeable attention has been focused on the removal of endocrine disrupting chemicals (EDCs) from water due to their various influence on mankind and animals through interacting with the normal functions of hormonal systems [143]. EDCs-contained compounds made naturally and man-made chemic materials in the environment. Between them, bisphenol A (BPA) is a toxic chemical that has estrogenic action. Yuan et al. [144] have prepared an amphiphilic star-shaped hybrid copolymer polyhedral oligomeric silsesquioxane-PCL-β-cyclodextrin (POSS-PCL-β-CD) by ROP and click chemistry. The amphiphilic copolymer self-assembled into the micelles with POSS-PCL encapsulating Fe_3O_4 NPs as the core and β-CD as the shell. TEM images of the NPs and POSS-PCL-β-CD/Fe_3O_4 micelles are shown in Fig. 8.22. In Fig. 8.22(d), the Fe_3O_4 NP is detected in the polymeric micelle. Because of the host–guest interaction of β-CD with BPA, the micelles could show high adsorption capacity for BPA elimination from aqueous solution.

Arsenic is another toxic chemical, existing mostly in the inorganic form, As(III) and As(V) in groundwater. All arsenic removal methods could be divided into four ways: ion exchange, chemical precipitation, membrane process, and adsorption. Various metal oxide NPs such as TiO_2, Fe_3O_4, CeO_2, and ZrO_2 have been exploited for arsenic removal, and showed great efficiency of extraction because of their larger surface area, as well as enhanced surface charges. In water treatment, spherical microcapsules showed a few superiority such as excellent surface area, high velocity in a moving fluid, the potential to be packed efficiently in a column, and simple removal through filtration [84,145,146]. Combining CeO_2 and Fe_3O_4 in a capsule leads to extract As(III) and As(V) within a wide range of pH. Setyono et al. [147] employed PCL and the polyvinylpyrrolidone to prepare microcapsules with big surface area and high

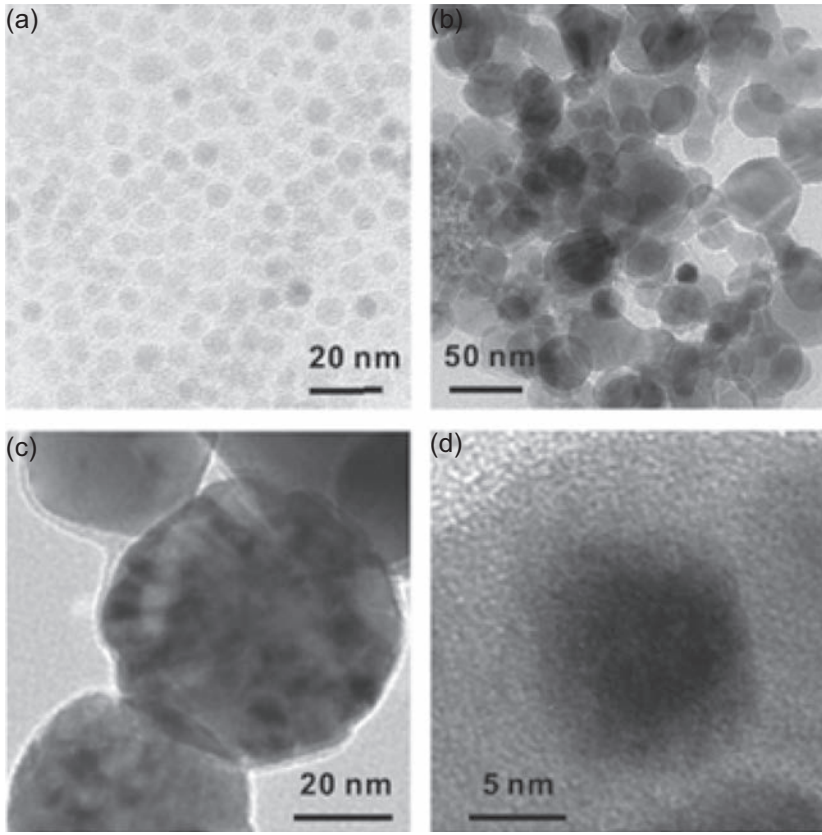

Figure 8.22 TEM images of (a) Fe_3O_4 NPs, (b) POSS-PCL-β-CD/Fe_3O_4 hybrid micelles, (c) enlarged POSS-PCL-β-CD/Fe_3O_4 hybrid micelles, and (d) Fe_3O_4 NP encapsulated into the POSS-PCL-β-CD micelle.
Adapted from W. Yuan, J. Shen, L. Li, X. Liu, H. Zou, Preparation of POSS-poly (ε-caprolactone)-β-cyclodextrin/Fe3O4 hybrid magnetic micelles for removal of bisphenol A from water, Carbohydrate Polymers 113 (2014) 353–361. With kind permission of Elsevier.

surface roughness. Modification of the microcapsule surfaces with metal oxide NPs (Ce and Fe oxides) increased the extraction efficiencies for As(III) and As(V) from water. The capsules were extracted and reused three cycles without losing extraction capacity. The prepared microcapsules displayed a maximum Langmuir adsorption of 32 and 28 mg/g for As(III) and As(V), respectively.

Sökmen et al. [148] developed the direct immobilization of anatase TiO_2 NPs into the PCL matrix, through solvent casting processes. The self-cleaning of the fabricated materials was studied by photocatalytic elimination of methylene blue (MB), and the antimicrobial activities were tested using *Candida albicans* as a microorganism. The TiO_2-immobilized polymer considerably removed dye from its aqueous solution without additional pH adjustment. Almost 83.2% of MB was removed and decomposed by a low content of TiO_2 immobilized into PCL, and even the removal percentage

reached to 94.2% with 5 wt% of TiO_2 fixed onto the PCL in a short exposure period. However, the removal percentage declined with enhancing ionic strength and using a visible light source.

8.4.3.4 Other applications of polycaprolactone/metal oxide nanocomposites

Elen et al. [149] have prepared biodegradable PCL containing ZnO NPs through varied morphologies of the NPs: disks, spheres, and rods. They realized that the dual action of the ZnO NPs suppressed the gas permeability of the NCs via two mechanisms: first by the creation of a tortuous path and second by gas adsorption. Enhances in barrier properties of all the NCs even with a small contents of ZnO NPs were observed. However, the variant morphologies of the NPs had an obvious result on the gas permeability. NC with ZnO nanorods indicated the higher gas barrier (the oxygen permeability reduced by 65%), but the permeability of the NCs containing spherical ZnO was very high, because the lower aspect ratio of the ZnO NPs induced a shorter diffusion pathway for the gas molecules. The permeability of the NC with disk-shaped ZnO NPs is also higher compared with the nanorods. Oxygen permeability of the NCs was depending on the particles morphology, and they can be reduced by more than 60%. In the case of tensile tests, the Young's moduli and tensile strength of the NCs with ZnO nanorods were the highest. Therefore, PCL NCs containing ZnO nanorods were considered high-performance biopackaging materials.

A composite film containing ZnO NPs, multiwalled carbon nanotube (MWNT), and PCL on glassy carbon electrode (ZnO–MWNT–PCL–GCE) was developed by Chekin et al. [150]. They used the prepared porous ZnO–MWNT–PCL film as a supporting matrix to entrap Co(II) ions. Immobilized cobalt ions as a biosensor showed high electrocatalytic properties in glucose oxidation, good recyclability, and long-time stability. They also applied the fabricated electrode for detection of glucose in human blood serum and analytical resumption of glucose.

8.5 Conclusions

This chapter is an overview of the synthesis, characterization, properties, processing, and biomedical uses of the PCL and its nanohybrids with MO NPs. Various films and fibers have been provided from metal oxides and PCL dispersions. Compared with other polymers, PCL exhibits particularly strong biodegradability and biocompatibility that are not observed in other metal oxide polymer NCs. Metal oxide can promote PCL biodegradability, cell adhesion, mechanical properties, and other physicochemical properties. These effects can be enhanced by the surface functionalization of metal oxides, in particular with hydroxyl or carboxyl groups, which display hydrogen bonds with PCL. A clear rising trend in PCL application in research during the recent decades indicates the recognition of this versatile resorbable polymer, especially in the fields of drug release, biomaterials and tissue engineering.

Based on the resulted given in this chapter, it can be deduced that PCL and its copolymers collectively provides a promising polymer platform for the production of longer term degradable implants with tunable mechanical, thermal, morphological, and biodegradation behavior.

Acknowledgments

The authors wish to acknowledge financial support for this research from Research Affairs Division, Isfahan University of Technology (IUT), Isfahan, Iran. They also thank the Iran Nanotechnology Initiative Council (INIC), Tehran, Iran, National Elite Foundation (NEF), Tehran, Iran, and Center of Excellence in Sensors and Green Chemistry (IUT), Isfahan, Iran for their support.

References

[1] A.V. García, M.R. Santonja, A.B. Sanahuja, M.D.C.G. Selva, Characterization and degradation characteristics of poly (ε-caprolactone)-based composites reinforced with almond skin residues, Polymer Degradation and Stability 108 (2014) 269–279.
[2] Y. Habibi, A.L. Goffin, N. Schiltz, E. Duquesne, P. Dubois, A. Dufresne, Bionanocomposites based on poly (ε-caprolactone)-grafted cellulose nanocrystals by ring-opening polymerization, Journal of Materials Chemistry 18 (41) (2008) 5002–5010.
[3] M.A. Woodruff, D.W. Hutmacher, The return of a forgotten polymer-polycaprolactone in the 21st century, Progress in Polymer Science 35 (10) (2010) 1217–1256.
[4] J.K. Pandey, A.P. Kumar, M. Misra, A.K. Mohanty, L.T. Drzal, R. Palsingh, Recent advances in biodegradable nanocomposites, Journal of Nanoscience and Nanotechnology 5 (4) (2005) 497–526.
[5] M. Niederberger, G. Garnweitner, Organic reaction pathways in the nonaqueous synthesis of metal oxide nanoparticles, Chemistry–A European Journal 12 (28) (2006) 7282–7302.
[6] D. Mondal, M. Griffith, S.S. Venkatraman, Polycaprolactone-based biomaterials for tissue engineering and drug delivery: current scenario and challenges, International Journal of Polymeric Materials and Polymeric Biomaterials 65 (5) (2016) 255–265.
[7] M. Labet, W. Thielemans, Synthesis of polycaprolactone: a review, Chemical Society Reviews 38 (12) (2009) 3484–3504.
[8] L. Hua, W.H. Kai, Y. Inoue, Crystallization behavior of poly (ε-caprolactone)/graphite oxide composites, Journal of Applied Polymer Science 106 (6) (2007) 4225–4232.
[9] C.X. Lam, S.H. Teoh, D.W. Hutmacher, Comparison of the degradation of polycaprolactone and polycaprolactone–(β-tricalcium phosphate) scaffolds in alkaline medium, Polymer International 56 (6) (2007) 718–728.
[10] M. Jenkins, K. Harrison, The effect of molecular weight on the crystallization kinetics of polycaprolactone, Polymers for Advanced Technologies 17 (6) (2006) 474–478.
[11] A.L. Sisson, D. Ekinci, A. Lendlein, The contemporary role of ε-caprolactone chemistry to create advanced polymer architectures, Polymer 54 (17) (2013) 4333–4350.
[12] L. Li, S. Zheng, Poly (ε-caprolactone)-grafted Fe_3O_4 nanoparticles: preparation and superparamagnetic nanocomposites with epoxy thermosets, Industrial & Engineering Chemistry Research 54 (1) (2014) 171–180.

[13] G. Ciapetti, L. Ambrosio, L. Savarino, D. Granchi, E. Cenni, N. Baldini, S. Pagani, S. Guizzardi, F. Causa, A. Giunti, Osteoblast growth and function in porous poly ε-caprolactone matrices for bone repair: a preliminary study, Biomaterials 24 (21) (2003) 3815–3824.
[14] H.L. Khor, K.W. Ng, J.T. Schantz, T.-T. Phan, T.C. Lim, S.H. Teoh, D. Hutmacher, Poly (ε-caprolactone) films as a potential substrate for tissue engineering an epidermal equivalent, Materials Science and Engineering: C 20 (1) (2002) 71–75.
[15] D.W. Hutmacher, T. Schantz, I. Zein, K.W. Ng, S.H. Teoh, K.C. Tan, Mechanical properties and cell cultural response of polycaprolactone scaffolds designed and fabricated via fused deposition modeling, Journal of Biomedical Materials Research 55 (2) (2001) 203–216.
[16] I. Zein, D.W. Hutmacher, K.C. Tan, S.H. Teoh, Fused deposition modeling of novel scaffold architectures for tissue engineering applications, Biomaterials 23 (4) (2002) 1169–1185.
[17] Q. Zhao, J. Tao, R.C. Yam, A.C. Mok, R.K. Li, C. Song, Biodegradation behavior of polycaprolactone/rice husk ecocomposites in simulated soil medium, Polymer Degradation and Stability 93 (8) (2008) 1571–1576.
[18] J. Cai, Z. Xiong, M. Zhou, J. Tan, F. Zeng, S. Lin, H. Xiong, Thermal properties and crystallization behavior of thermoplastic starch/poly (ε-caprolactone) composites, Carbohydrate Polymers 102 (2014) 746–754.
[19] D. Wu, Y. Zhang, M. Zhang, W. Yu, Selective localization of multiwalled carbon nanotubes in poly (ε-caprolactone)/polylactide blend, Biomacromolecules 10 (2) (2009) 417–424.
[20] L. Ci, J. Suhr, V. Pushparaj, X. Zhang, P. Ajayan, Continuous carbon nanotube reinforced composites, Nano Letters 8 (9) (2008) 2762–2766.
[21] A.L. Goffin, E. Duquesne, J.M. Raquez, H.E. Miltner, X. Ke, M. Alexandre, et al., From polyester grafting onto POSS nanocage by ring-opening polymerization to high performance polyester/POSS nanocomposites, Journal of Materials Chemistry 20 (42) (2010) 9415–9422.
[22] A.B. Kaiser, V. Skákalová, Electronic conduction in polymers, carbon nanotubes and graphene, Chemical Society Reviews 40 (7) (2011) 3786–3801.
[23] K. Li, J. Song, M. Xu, S. Kuga, L. Zhang, J. Cai, Extraordinary reinforcement effect of three-dimensionally nanoporous cellulose gels in poly (ε-caprolactone) bionanocomposites, ACS Applied Materials & Interfaces 6 (10) (2014) 7204–7213.
[24] A. Muñoz-Bonilla, M.L. Cerrada, M. Fernández-García, A. Kubacka, M. Ferrer, M. Fernández-García, Biodegradable polycaprolactone-titania nanocomposites: preparation, characterization and antimicrobial properties, International Journal of Molecular Sciences 14 (5) (2013) 9249–9266.
[25] S. Mallakpour, A. Abdolmaleki, M. Rostami, Morphological and thermal properties of poly(amide-imide)/ZnO nanocomposites derived from 4,4′-methylenebis(3-chloro-2,6-diethyl trimellitimidobenzene) and 3,5-diamino-N-(4-hydroxyphenyl) benzamide, Polymer-Plastics Technology and Engineering 53 (2014) 1615–1624.
[26] S. Mallakpour, M. Javadpour, The potential use of recycled PET bottle in nanocomposites manufacturing with modified ZnO nanoparticles capped with citric acid: preparation, thermal, and morphological characterization, RSC Advances 6 (2016) 15039–15047.
[27] S. Mallakpour, N. Jarang, Exploration of the role of modified titania nanoparticles with citric acid and vitamin C in improvement of thermal stability, optical property, and mechanical behavior of novel poly(vinyl chloride) nanocomposite films, Journal of Vinyl and Additive Technology (2015)http://dx.doi.org/10.1002/vnl.21526.

[28] S. Mallakpour, Z. Khani, Use of vitamin B_1 for the surface treatment of silica (SiO_2) and synthesis of poly(vinyl chloride)/SiO_2 nanocomposites with advanced properties, Polymer Bulletin (2017)http://dx.doi.org/10.1007/s00289-017-1911-8.
[29] S. Mallakpour, A. Nezamzadeh, Polymer nanocomposites based on modified ZrO_2 NPs and poly(vinyl alcohol)/poly(vinyl pyrrolidone) blend: optical, morphological and thermal properties, Polymer-Plastics Technology and Engineering (2016)http://dx.doi.org/10.1080/03602559.2016.1253741.
[30] C. Ashok, V. Rao, C. Shilpa Chakra, CuO/TiO_2 metal oxide nanocomposite synthesis via room temperature ionic liquid, Journal of Nanomaterials & Molecular Nanotechnology 5 (2016) 1 4, 12–15.
[31] S. Mallakpour, M. Dinari, Enhancement in thermal properties of poly(vinyl alcohol) nanocomposites reinforced with Al_2O_3 nanoparticles, Journal of Reinforced Plastics and Composites 32 (2013) 217–224.
[32] J.R. Fried, Polymer Science and Technology, Pearson Education, 2014, pp. 25–100.
[33] M.L. Foresti, M.L. Ferreira, Synthesis of polycaprolactone using free/supported enzymatic and non-enzymatic catalysts, Macromolecular Rapid Communications 25 (24) (2004) 2025–2028.
[34] S. Kobayashi, L.J. Hobson, J. Sakamoto, S. Kimura, J. Sugiyama, T. Imai, T. Itoh, Formation and structure of artificial cellulose spherulites via enzymatic polymerization, Biomacromolecules 1 (2) (2000) 168–173.
[35] V. Křen, J. Thiem, Glycosylation employing bio-systems: from enzymes to whole cells, Chemical Society Reviews 26 (6) (1997) 463–473.
[36] M. Heiny, J. Wurth, V. Shastri, Progress in functionalized biodegradable polyesters, in: Natural and Synthetic Biomedical Polymers, Elsevier Science, 2014, pp. 167–180.
[37] A.C. Albertsson, R.K. Srivastava, Recent developments in enzyme-catalyzed ring-opening polymerization, Advanced Drug Delivery Reviews 60 (9) (2008) 1077–1093.
[38] J. Xu, J. Song, S. Pispas, G. Zhang, Metal-free controlled ring-opening polymerization of ε-caprolactone in bulk using tris (pentafluorophenyl) borane as a catalyst, Polymer Chemistry 5 (16) (2014) 4726–4733.
[39] A.C. Albertsson, I.K. Varma, Recent developments in ring opening polymerization of lactones for biomedical applications, Biomacromolecules 4 (6) (2003) 1466–1486.
[40] A.A. Vassiliou, G.Z. Papageorgiou, D.S. Achilias, D.N. Bikiaris, Non-isothermal crystallisation kinetics of in situ prepared poly (ε-caprolactone)/surface-treated SiO_2 nanocomposites, Macromolecular Chemistry and Physics 208 (4) (2007) 364–376.
[41] A. Duda, S. Penczek, A. Kowalski, J. Libiszowski, Polymerizations of ε-caprolactone and L, L-dilactide initiated with stannous octoate and stannous butoxide-a comparison, Macromolecular Symposia 153 (2000) 41–53.
[42] M. Fernández-García, J.A. Rodriguez, Metal Oxide Nanoparticles, John Wiley & Sons, 2011.
[43] S. Mallakpour, E. Khadem, Carbon nanotube–metal oxide nanocomposites: fabrication, properties and applications, Chemical Engineering Journal 302 (2016) 344–367.
[44] S. Mallakpour, M. Madani, A review of current coupling agents for modification of metal oxide nanoparticles, Progress in Organic Coatings 86 (2015) 194–207.
[45] J.L.G. Fierro, Metal Oxides: Chemistry and Applications, CRC Press, 2005, pp. 111–128.
[46] T. Shirai, H. Watanabe, M. Fuji, M. Takahashi, Structural properties and surface characteristics on aluminum oxide powders, Annual Report of Ceramic Engineering Research Laboratory, Nagoya Institute of Technology 9 (2009) 23–31.
[47] K. Hu, D.D. Kulkarni, I. Choi, V.V. Tsukruk, Graphene-polymer nanocomposites for structural and functional applications, Progress in Polymer Science 39 (11) (2014) 1934–1972.

[48] T. Kuilla, S. Bhadra, D. Yao, N.H. Kim, S. Bose, J.H. Lee, Recent advances in graphene based polymer composites, Progress in Polymer Science 35 (11) (2010) 1350–1375.
[49] S. Mallakpour, A. Jarahiyan, An eco-friendly approach for the synthesis of biocompatible poly(vinyl alcohol) nanocomposite with aid of modified CuO nanoparticles with citric acid and vitamin C: mechanical, thermal and optical properties, Journal of the Iranian Chemical Society 13 (2015) 209–518.
[50] S. Mallakpour, E. Shafiee, The synthesis of poly(vinyl chloride) nanocomposite films containing ZrO_2 nanoparticles modified with vitamin B_1 with the aim of improving the mechanical, thermal and optical properties, Designed Monomers and Polymers 20 (1) (2017) 378–388.
[51] A. Nicolay, A. Lanzutti, M. Poelman, B. Ruelle, L. Fedrizzi, P. Dubois, M.-G. Olivier, Elaboration and characterization of a multifunctional silane/ZnO hybrid nanocomposite coating, Applied Surface Science 327 (2015) 379–388.
[52] J.-M. Raquez, Y. Habibi, M. Murariu, P. Dubois, Polylactide (PLA)-based nanocomposites, Progress in Polymer Science 38 (10) (2013) 1504–1542.
[53] S.S. Ray, M. Okamoto, Polymer/layered silicate nanocomposites: a review from preparation to processing, Progress in Polymer Science 28 (11) (2003) 1539–1641.
[54] M. Jansen, A concept for synthesis planning in solid-state chemistry, Angewandte Chemie International Edition 41 (20) (2002) 3746–3766.
[55] J. Livage, M. Henry, C. Sanchez, Sol-gel chemistry of transition metal oxides, Progress in Solid State Chemistry 18 (4) (1988) 259–341.
[56] H. Cui, Y. Feng, W. Ren, T. Zeng, H. Lv, Y. Pan, Strategies of large scale synthesis of monodisperse nanoparticles, Recent Patents on Nanotechnology 3 (1) (2009) 32–41.
[57] C. Murray, D.J. Norris, M.G. Bawendi, Synthesis and characterization of nearly monodisperse CdE (E=sulfur, selenium, tellurium) semiconductor nanocrystallites, Journal of the American Chemical Society 115 (19) (1993) 8706–8715.
[58] M. Rajamathi, R. Seshadri, Oxide and chalcogenide nanoparticles from hydrothermal/solvothermal reactions, Current Opinion in Solid State and Materials Science 6 (4) (2002) 337–345.
[59] S. Komarneni, Y.D. Noh, J.Y. Kim, S.H. Kim, H. Katsuki, Solvothermal/hydrothermal synthesis of metal oxides and metal powders with and without microwaves, Zeitschrift für Naturforschung B 65 (8) (2010) 1033–1037.
[60] R.C. Xie, J.K. Shang, Morphological control in solvothermal synthesis of titanium oxide, Journal of Materials Science 42 (16) (2007) 6583–6589.
[61] T. Ahmad, A.K. Ganguli, A. Ganguly, J. Ahmed, I.A. Wani, S. Khatoon, Chemistry of reverse micelles: a versatile route to the synthesis of nanorods and nanoparticles, Materials Research Society 1142 (2009) JJ05–59.
[62] A.E. Gash, T.M. Tillotson, J.H. Satcher Jr., L.W. Hrubesh, R.L. Simpson, New sol–gel synthetic route to transition and main-group metal oxide aerogels using inorganic salt precursors, Journal of Non-Crystalline Solids 285 (1) (2001) 22–28.
[63] J.L.G. Fierro, Metal Oxides: Chemistry and Applications, CRC Press, 2005, pp. 31–49.
[64] H. Fischer, Polymer nanocomposites: from fundamental research to specific applications, Materials Science and Engineering: C 23 (6) (2003) 763–772.
[65] A. Tiwari, M. Ramalingam, H. Kobayashi, A.P. Turner, Biomedical Materials and Diagnostic Devices, John Wiley & Sons, 2012, pp. 115–155.
[66] N.K. Singh, P. Maiti, Polycaprolactone based nanobiomaterials, John Wiley & Sons, Inc., 2012.
[67] D. Moura, J.F. Mano, M.C. Paiva, N.M. Alves, Chitosan nanocomposites based on distinct inorganic fillers for biomedical applications, Science and Technology of Advanced Materials 17 (1) (2016) 626–643.

[68] D.S. Jones, K.J. Pearce, An investigation of the effects of some process variables on the microencapsulation of propranolol hydrochloride by the solvent evaporation method, International Journal of Pharmaceutics 118 (2) (1995) 199–205.
[69] S. Mallakpour, M. Dinari, M. Hatami, Novel nanocomposites of poly(vinyl alcohol) and Mg–Al layered double hydroxide intercalated with diacid N-tetrabromophthaloyl-aspartic, Journal of Thermal Analysis and Calorimetry 120 (2015) 1293–1302.
[70] S. Mallakpour, M. Hatami, Production and evaluation of the surface properties of chiral poly(amide-imide)/TiO_2 nanocomposites containing *L*-phenylalanine units, Progress in Organic Coatings 74 (3) (2012) 564–571.
[71] S.J. Park, Y.J. Yang, H.B. Lee, Effect of acid–base interaction between silica and fragrant oil in the PCL/PEG microcapsules, Colloids and Surfaces B: Biointerfaces 38 (1) (2004) 35–40.
[72] S. Mallakpour, N. Nouruzi, Effect of modified ZnO nanoparticles with biosafe molecule on the morphology and physiochemical properties of novel polycaprolactone nanocomposites, Polymer 89 (2016) 94–101.
[73] S. Mallakpour, N. Nouruzi, Modification of morphological, mechanical, optical and thermal properties in polycaprolactone-based nanocomposites by the incorporation of diacid-modified ZnO nanoparticles, Journal of Materials Science 51 (13) (2016) 6400–6410.
[74] K.H. Shin, Y.H. Koh, W.Y. Choi, H.E. Kim, Production of porous poly (ε-caprolactone)/silica hybrid membranes with patterned surface pores, Materials Letters 65 (12) (2011) 1903–1906.
[75] L.D. Bruce, N.H. Shah, A.W. Malick, M.H. Infeld, J.W. McGinity, Properties of hot-melt extruded tablet formulations for the colonic delivery of 5-aminosalicylic acid, European Journal of Pharmaceutics and Biopharmaceutics 59 (1) (2005) 85–97.
[76] J. Thiry, P. Lebrun, C. Vinassa, M. Adam, L. Netchacovitch, E. Ziemons, et al., Continuous production of itraconazole-based solid dispersions by hot melt extrusion: preformulation, optimization and design space determination, International Journal of Pharmaceutics 515 (1) (2016) 114–124.
[77] J. Mofokeng, A. Luyt, Morphology and thermal degradation studies of melt-mixed poly (lactic acid)(PLA)/poly (ε-caprolactone)(PCL) biodegradable polymer blend nanocomposites with TiO_2 as filler, Polymer Testing 45 (2015) 93–100.
[78] J. Odent, Y. Habibi, J.M. Raquez, P. Dubois, Ultra-tough polylactide-based materials synergistically designed in the presence of rubbery ε-caprolactone-based copolyester and silica nanoparticles, Composites Science and Technology 84 (2013) 86–91.
[79] K. Chrissafis, G. Antoniadis, K. Paraskevopoulos, A. Vassiliou, D. Bikiaris, Comparative study of the effect of different nanoparticles on the mechanical properties and thermal degradation mechanism of in situ prepared poly (ε-caprolactone) nanocomposites, Composites Science and Technology 67 (10) (2007) 2165–2174.
[80] D. Chen, H. Zhu, T. Liu, In situ thermal preparation of polyimide nanocomposite films containing functionalized graphene sheets, ACS Applied Materials & Interfaces 2 (12) (2010) 3702–3708.
[81] G. Wang, S. Yang, Z. Wei, X. Dong, H. Wang, M. Qi, Facile preparation of poly (ε-caprolactone)/Fe_3O_4@ graphene oxide superparamagnetic nanocomposites, Polymer Bulletin 70 (8) (2013) 2359–2371.
[82] G.S. Wang, L. Wang, L. Sang, X.F. Dong, G.Y. Chen, Y. Chang, W.X. Zhang, Synthesis and characterization of poly (ε-caprolactone)/Fe_3O_4 nanocomposites by in situ polymerization, Chinese Journal of Polymer Science 31 (7) (2013) 1011–1021.
[83] G. Wang, G. Chen, Z. Wei, T. Yu, L. Liu, P. Wang, M. Qi, A comparative study of TiO_2 and surface-treated TiO_2 nanoparticles on thermal and mechanical properties of poly (ε-caprolactone) nanocomposites, Journal of Applied Polymer Science 125 (5) (2012) 3871–3879.

[84] L. Wang, J. Li, Q. Jiang, L. Zhao, Water-soluble Fe_3O_4 nanoparticles with high solubility for removal of heavy-metal ions from waste water, Dalton Transactions 41 (15) (2012) 4544–4551.
[85] B. Azimi, P. Nourpanah, M. Rabiee, S. Arbab, Poly (ε-caprolactone) fiber: an overview, Journal of Engineered Fabrics & Fibers (JEFF) 9 (3) (2014) 74–90.
[86] N. Bhardwaj, S.C. Kundu, Electrospinning: a fascinating fiber fabrication technique, Biotechnology Advances 28 (3) (2010) 325–347.
[87] Z.M. Huang, Y.Z. Zhang, M. Kotaki, S. Ramakrishna, A review on polymer nanofibers by electrospinning and their applications in nanocomposites, Composites Science and Technology 63 (15) (2003) 2223–2253.
[88] A. Abdal-hay, L.D. Tijing, J.K. Lim, Characterization of the surface biocompatibility of an electrospun nylon 6/CaP nanofiber scaffold using osteoblasts, Chemical Engineering Journal 215 (2013) 57–64.
[89] M. Kouhi, M. Morshed, J. Varshosaz, M.H. Fathi, Poly (ε-caprolactone) incorporated bioactive glass nanoparticles and simvastatin nanocomposite nanofibers: preparation, characterization and in vitro drug release for bone regeneration applications, Chemical Engineering Journal 228 (2013) 1057–1065.
[90] D.H. Reneker, I. Chun, Nanometre diameter fibres of polymer, produced by electrospinning, Nanotechnology 7 (3) (1996) 216.
[91] W.K. Son, J.H. Youk, W.H. Park, Preparation of ultrafine oxidized cellulose mats via electrospinning, Biomacromolecules 5 (1) (2004) 197–201.
[92] W. Zhao, Y.M. Ju, G. Christ, A. Atala, J.J. Yoo, S.J. Lee, Diaphragmatic muscle reconstruction with an aligned electrospun poly (ε-caprolactone)/collagen hybrid scaffold, Biomaterials 34 (33) (2013) 8235–8240.
[93] K.K. Gupta, A. Kundan, P.K. Mishra, P. Srivastava, S. Mohanty, N.K. Singh, et al., Polycaprolactone composites with TiO_2 for potential nanobiomaterials: tunable properties using different phases, Physical Chemistry Chemical Physics 14 (37) (2012) 12844–12853.
[94] K.H. Shin, J.H. Sung, Y.H. Koh, J.H. Lee, W.Y. Choi, H.E. Kim, Direct coating of bioactive sol–gel derived silica on poly (ε-caprolactone) nanofibrous scaffold using co-electrospinning, Materials Letters 64 (13) (2010) 1539–1542.
[95] S. Park, H. Lee, K. Ahn, J. Kim, J. Jin, J. Lee, et al., Enhanced photocatalytic activity of TiO_2-incorporated nanofiber membrane by oxygen plasma treatment, Thin Solid Films 519 (20) (2011) 6899–6902.
[96] R. Augustine, E.A. Dominic, I. Reju, B. Kaimal, N. Kalarikkal, S. Thomas, Electrospun polycaprolactone membranes incorporated with ZnO nanoparticles as skin substitutes with enhanced fibroblast proliferation and wound healing, RSC Advances 4 (47) (2014) 24777–24785.
[97] M. Otadi, D. Mohebbi-Kalhori, Evaluate of different bioactive glass on mechanical properties of nanocomposites prepared using electrospinning method, Procedia Materials Science 11 (2015) 196–201.
[98] A. Göpferich, Mechanisms of polymer degradation and erosion, Biomaterials 17 (2) (1996) 103–114.
[99] K. Ang, K. Leong, C. Chua, M. Chandrasekaran, Compressive properties and degradability of poly (ε-caprolatone)/hydroxyapatite composites under accelerated hydrolytic degradation, Journal of Biomedical Materials Research Part A 80 (3) (2007) 655–660.
[100] A. Kulkarni, J. Reiche, K. Kratz, H. Kamusewitz, I. Sokolov, A. Lendlein, Enzymatic chain scission kinetics of poly (ε-caprolactone) monolayers, Langmuir 23 (24) (2007) 12202–12207.

[101] K. Leja, G. Lewandowicz, Polymer biodegradation and biodegradable polymers—a review, Polish Journal of Environmental Studies 19 (2) (2010) 255–266.
[102] M. Karimi, M. Heuchel, T. Weigel, M. Schossig, D. Hofmann, A. Lendlein, Formation and size distribution of pores in poly (ε-caprolactone) foams prepared by pressure quenching using supercritical CO_2, The Journal of Supercritical Fluids 61 (2012) 175–190.
[103] R. Augustine, N. Kalarikkal, S. Thomas, Effect of zinc oxide nanoparticles on the in vitro degradation of electrospun polycaprolactone membranes in simulated body fluid, International Journal of Polymeric Materials and Polymeric Biomaterials 65 (1) (2016) 28–37.
[104] M.S. Shoichet, J.A. Hubbell, Polymers for Tissue Engineering, 1998, pp. 19–52. Utrecht, The Netherlands.
[105] N. Sultana, Biodegradable Polymer-Based Scaffolds for Bone Tissue Engineering, Springer Science & Business Media, 2012, pp. 1–17.
[106] C. Gualandi, Porous Polymeric Bioresorbable Scaffolds for Tissue Engineering, Springer Science & Business Media, 2011, pp. 1–30.
[107] D.W. Hutmacher, Scaffolds in tissue engineering bone and cartilage, Biomaterials 21 (24) (2000) 2529–2543.
[108] E.J. Lee, S.H. Teng, T.S. Jang, P. Wang, S.W. Yook, H.E. Kim, Y.H. Koh, Nanostructured poly (ε-caprolactone)–silica xerogel fibrous membrane for guided bone regeneration, Acta Biomaterialia 6 (9) (2010) 3557–3565.
[109] S.Ö. Gönen, M.E. Taygun, A. Aktürk, S. Küçükbayrak, Fabrication of nanocomposite mat through incorporating bioactive glass particles into gelatin/poly (ε-caprolactone) nanofibers by using Box–Behnken design, Materials Science and Engineering: C 67 (2016) 684–693.
[110] S.Ö. Gönen, M.E. Taygun, S. Küçükbayrak, Fabrication of bioactive glass containing nanocomposite fiber mats for bone tissue engineering applications, Composite Structures 138 (2016) 96–106.
[111] E.A. Münchow, M.T.P. Albuquerque, B. Zero, K. Kamocki, E. Piva, R.L. Gregory, M.C. Bottino, Development and characterization of novel ZnO-loaded electrospun membranes for periodontal regeneration, Dental Materials 31 (9) (2015) 1038–1051.
[112] J. Zhang, S. Zhao, M. Zhu, Y. Zhu, Y. Zhang, Z. Liu, C. Zhang, 3D-printed magnetic Fe_3O_4/MBG/PCL composite scaffolds with multifunctionality of bone regeneration, local anticancer drug delivery and hyperthermia, Journal of Materials Chemistry B 2 (43) (2014) 7583–7595.
[113] H. Lee, H. Hwang, Y. Kim, H. Jeon, G. Kim, Physical and bioactive properties of multi-layered PCL/silica composite scaffolds for bone tissue regeneration, Chemical Engineering Journal 250 (2014) 399–408.
[114] M.S. Mohammadi, I. Ahmed, N. Muja, S. Almeida, C. Rudd, M. Bureau, S. Nazhat, Effect of Si and Fe doping on calcium phosphate glass fibre reinforced polycaprolactone bone analogous composites, Acta Biomaterialia 8 (4) (2012) 1616–1626.
[115] T. Mondal, M. Sunny, D. Khastgir, H. Varma, P. Ramesh, Poly (L-lactide-co-Є caprolactone) microspheres laden with bioactive glass-ceramic and alendronate sodium as bone regenerative scaffolds, Materials Science and Engineering: C 32 (4) (2012) 697–706.
[116] M. Dziadek, E. Menaszek, B. Zagrajczuk, J. Pawlik, K. Cholewa-Kowalska, New generation poly (ε-caprolactone)/gel-derived bioactive glass composites for bone tissue engineering: Part I. Material properties, Materials Science and Engineering: C 56 (2015) 9–21.
[117] A. Mohammadkhah, L.M. Marquardt, S.E. Sakiyama-Elbert, D.E. Day, A.B. Harkins, Fabrication and characterization of poly-(ε)-caprolactone and bioactive glass composites for tissue engineering applications, Materials Science and Engineering: C 49 (2015) 632–639.

[118] J. Chen, W. Que, Y. Xing, B. Lei, Molecular level-based bioactive glass-poly (caprolactone) hybrids monoliths with porous structure for bone tissue repair, Ceramics International 41 (2) (2015) 3330–3334.
[119] B. Lei, K.H. Shin, D.Y. Noh, I.H. Jo, Y.H. Koh, H.E. Kim, S.E. Kim, Sol–gel derived nanoscale bioactive glass (NBG) particles reinforced poly (ε-caprolactone) composites for bone tissue engineering, Materials Science and Engineering: C 33 (3) (2013) 1102–1108.
[120] D. Arcos, M. Vallet-Regí, Sol–gel silica-based biomaterials and bone tissue regeneration, Acta Biomaterialia 6 (8) (2010) 2874–2888.
[121] S.H. Teng, P. Wang, J.Q. Dong, Bioactive hybrid coatings of poly (ε-caprolactone)–silica xerogel on titanium for biomedical applications, Materials Letters 129 (2014) 209–212.
[122] A.B. Ennett, D.J. Mooney, Tissue engineering strategies for in vivo neovascularisation, Expert Opinion on Biological Therapy 2 (8) (2002) 805–818.
[123] R. Augustine, E.A. Dominic, I. Reju, B. Kaimal, N. Kalarikkal, S. Thomas, Investigation of angiogenesis and its mechanism using zinc oxide nanoparticle-loaded electrospun tissue engineering scaffolds, RSC Advances 4 (93) (2014) 51528–51536.
[124] T.O. Daniel, D. Abrahamson, Endothelial signal integration in vascular assembly, Annual Review of Physiology 62 (1) (2000) 649–671.
[125] C.K. Sen, S. Khanna, B.M. Babior, T.K. Hunt, E.C. Ellison, S. Roy, Oxidant-induced vascular endothelial growth factor expression in human keratinocytes and cutaneous wound healing, Journal of Biological Chemistry 277 (36) (2002) 33284–33290.
[126] J.J. Kim, R.K. Singh, S.-J. Seo, T.H. Kim, J.H. Kim, E.J. Lee, H.-W. Kim, Magnetic scaffolds of polycaprolactone with functionalized magnetite nanoparticles: physicochemical, mechanical, and biological properties effective for bone regeneration, RSC Advances 4 (33) (2014) 17325–17336.
[127] J. Zuwała-Jagiełło, Endocytosis mediated by receptors–function and participation in oral drug delivery, Postepy Higieny i Medycyny Doswiadczalnej 57 (3) (2002) 275–291.
[128] V.V. Ranade, Drug delivery systems 5A. Oral drug delivery, The Journal of Clinical Pharmacology 31 (1) (1991) 2–16.
[129] R.A. Bader, D.A. Putnam, Engineering Polymer Systems for Improved Drug Delivery, John Wiley & Sons, 2014.
[130] A. Domb, A. Bentolila, D. Teomin, Biopolymers as drug carriers and bioactive macromolecules, Acta Polymerica 49 (10–11) (1998) 526–533.
[131] D.S. Hsieh, W.D. Rhine, R. Langer, Zero-order controlled-release polymer matrices for micro-and macromolecules, Journal of Pharmaceutical Sciences 72 (1) (1983) 17–22.
[132] M.N.R. Kumar, N. Kumar, A. Domb, M. Arora, Pharmaceutical polymeric controlled drug delivery systems, in: Filled Elastomers Drug Delivery Systems, Springer, 2002, pp. 45–117.
[133] D. Jones, Pharmaceutical Applications of Polymers for Drug Delivery, iSmithers Rapra Publishing, 2004, pp. 3–46.
[134] H. Zou, W. Yuan, Temperature-and redox-responsive magnetic complex micelles for controlled drug release, Journal of Materials Chemistry B 3 (2) (2015) 260–269.
[135] Z. Tang, L. Zhang, Y. Wang, D. Li, Z. Zhong, S. Zhou, Redox-responsive star-shaped magnetic micelles with active-targeted and magnetic-guided functions for cancer therapy, Acta Biomaterialia 42 (2016) 232–246.
[136] X. Yang, Y. Chen, R. Yuan, G. Chen, E. Blanco, J. Gao, X. Shuai, Folate-encoded and Fe_3O_4-loaded polymeric micelles for dual targeting of cancer cells, Polymer 49 (16) (2008) 3477–3485.

[137] B. Wang, H. Zheng, M.-W. Chang, Z. Ahmad, J.-S. Li, Hollow polycaprolactone composite fibers for controlled magnetic responsive antifungal drug release, Colloids and Surfaces B: Biointerfaces 145 (2016) 757–767.
[138] D.C. Hyun, Magnetically-controlled, pulsatile drug release from poly (ε-caprolactone) (PCL) particles with hollow interiors, Polymer 74 (2015) 159–165.
[139] H. Dong, Q. Li, C. Tan, N. Bai, P. Cai, Bi-directional controlled release of ibuprofen and Mg^{2+} from magnesium alloys coated by multifunctional composite, Materials Science and Engineering: C 68 (2016) 512–518.
[140] M. De Matos, A. Piedade, C. Alvarez-Lorenzo, A. Concheiro, M. Braga, H. De Sousa, Dexamethasone-loaded poly (ε-caprolactone)/silica nanoparticles composites prepared by supercritical CO_2 foaming/mixing and deposition, International Journal of Pharmaceutics 456 (2) (2013) 269–281.
[141] Y. Gao, J. Lim, Y. Han, L. Wang, M.S.K. Chong, S.H. Teoh, C. Xu, Cryomilling for the fabrication of doxorubicin-containing silica-nanoparticle/polycaprolactone nanocomposite films, Nanoscale 8 (5) (2016) 2568–2574.
[142] Y. Zhang, Z. Wang, W. Zhou, G. Min, M. Lang, Cationic poly (ε-caprolactone) surface functionalized mesoporous silica nanoparticles and their application in drug delivery, Applied Surface Science 276 (2013) 769–775.
[143] T. Basile, A. Petrella, M. Petrella, G. Boghetich, V. Petruzzelli, S. Colasuonno, D. Petruzzelli, Review of endocrine-disrupting-compound removal technologies in water and wastewater treatment plants: an EU perspective, Industrial & Engineering Chemistry Research 50 (14) (2011) 8389–8401.
[144] W. Yuan, J. Shen, L. Li, X. Liu, H. Zou, Preparation of POSS-poly (ε-caprolactone)-β-cyclodextrin/Fe_3O_4 hybrid magnetic micelles for removal of bisphenol A from water, Carbohydrate Polymers 113 (2014) 353–361.
[145] K. Hristovski, A. Baumgardner, P. Westerhoff, Selecting metal oxide nanomaterials for arsenic removal in fixed bed columns: from nanopowders to aggregated nanoparticle media, Journal of Hazardous Materials 147 (1) (2007) 265–274.
[146] R. Li, Q. Li, S. Gao, J.K. Shang, Exceptional arsenic adsorption performance of hydrous cerium oxide nanoparticles: Part A. Adsorption capacity and mechanism, Chemical Engineering Journal 185 (2012) 127–135.
[147] D. Setyono, S. Valiyaveettil, Multi-metal oxide incorporated microcapsules for efficient As (III) and As (V) removal from water, RSC Advances 4 (95) (2014) 53365–53373.
[148] M. Sökmen, İ. Tatlıdil, C. Breen, F. Clegg, C.K. Buruk, T. Sivlim, Ş. Akkan, A new nano-TiO_2 immobilized biodegradable polymer with self-cleaning properties, Journal of Hazardous Materials 187 (1) (2011) 199–205.
[149] K. Elen, M. Murariu, R. Peeters, P. Dubois, J. Mullens, A. Hardy, M. Van Bael, Towards high-performance biopackaging: barrier and mechanical properties of dual-action polycaprolactone/zinc oxide nanocomposites, Polymers for Advanced Technologies 23 (10) (2012) 1422–1428.
[150] F. Chekin, S. Bagheri, S.A. Hamid, Electrochemistry and electrocatalysis of cobalt (II) immobilized onto gel-assisted synthesized zinc oxide nanoparticle–multi wall carbon nanotube–polycaprolactone composite film: application to determination of glucose, Analytical Methods 4 (8) (2012) 2423–2428.

This page intentionally left blank

9 Applications of biodegradable polymer/layered double hydroxide nanocomposites: current status and recent prospects

Shadpour Mallakpour, Elham Khadem
Isfahan University of Technology, Isfahan, Islamic Republic of Iran

9.1 Introduction

The ever-growing environmental concern framed into an ever-stronger regulation is currently motivating intense research and attention throughout the world to replace petroleum-based plastic. Plastic products, due to their convenience and safety, low price, and good aesthetic qualities, usually have single-use applications, especially in food packaging and medical materials [1]. Nevertheless, polyplastics are not nature-friendly and they are persistent and accumulate in the ecosystem, creating a global environmental issues. Many remedies such as (1) the storage of wastes at landfill sites, (2) incineration, and (3) recycling were proposed for keeping the ecosystem free from these plastic wastes. But because of limited landfill sites, producing a large number of carbon dioxide and creating global warming, as well as requiring to considerable expenditure of labor and energy, these approaches are not very suitable [2]. Consequently, increasing attention has been turned to the development of green polymeric materials that would not comprise the use of toxic or noxious component in their manufacture and could be destroyed in the environment after being casted off [3,4]. Production of biodegradable blends or conventional composites using environmentally friendly filler is more and more considered as the "next generation" for improving some of the properties and performance of polymers. Various nanofillers are currently being developed, but the use of layered double hydroxide (LDH) mineral as the reinforcing phase is beneficial due to its easy availability, inexpensive, more eco-friendly, and also its versatility in chemical composition and tunable charge density, which permits interaction with the polymer [5]. Previously, some works have been published in the field of LDH, modified LDH, and their nanocomposites (NCs) [6–9], which reviewed this type of materials and biomaterials from various outlook, and most of them mainly focused on the introduction of the preparation methods, characterization, and application. In this chapter, after concise introduction of LDHs and biopolymers, we express the efficient synthetic pathways and some other synthetic approaches that have been applied in the biopolymer/LDH NCs over the last several years.

Biodegradable and Biocompatible Polymer Composites. http://dx.doi.org/10.1016/B978-0-08-100970-3.00009-2

Followed by, the important usages of the biopolymer/LDH NCs in biofields such as packaging, medical and drug deliver, biosensors, and removal of pollution from wastewater have been highlighted and discussed.

9.2 Polymer/layered double hydroxide nanocomposite

LDHs are attractive nanofillers for the reinforcement of biodegradable polymers obtained from renewable resources and other conventional polymers due to their high aspect ratio and specific surface area, which may be promising for the enhancement of certain properties. Usually, incorporation of LDH minerals in a polymer matrix can give rise to the formation of three morphologies of composite, namely, phase-separated, intercalated, and exfoliated composites (uniformly dispersed in an aqueous medium), which the last morphology is especially desirable for improving composite properties [10,11]. Synthesis of polymer/LDH NCs is the first step to explore its interesting properties and extensive applications. To date, different principle synthesis approaches have been described in the preparation of polymer/LDH NCs: (1) template synthesis (sol–gel technology), (2) hydrothermal [1,12], (3) in situ intercalative polymerization [13,14], (4) Melt intercalation [15–17], (5) intercalation of polymer or prepolymer from solution [18–20], (6) high-energy ball milling [21]. Complete explanations on these can be found in other works and will not be considered in the following discussion [9,11,21–23]. The delamination of LDHs and the intercalation of large anionic species by entrapping–restacking process is usually an interesting route for preexpanding the basal spacing of LDH and making new NCs based on LDH [20,24]. But LDHs compared to cationic clays are more difficult to be delamination into single sheets and it is not feasible in many cases. In LDH, the layered structure is stabilized not only by the high anion content and the strong interlayer electrostatic interactions between the host layers and intercalated anions but also by hydrogen bonding among hydroxide layers, intercalated anions, and interlayer moisture [9,25,26]. Consequently, virgin LDH is not appropriate for the penetration of giant polymer chains or chain segments into their gallery space. Therefore, to successfully delaminate and intercalate anions into LDH sheets, new approaches have been developed, including direct ion exchange, coprecipitation, reconstruction of calcined LDH, electrochemical reduction, ultrasound treatment, and delamination technology [8,27,28]. For instance, research group of Mallakpour synthesized chiral LDHs by the coprecipitation reaction of the $Al(NO_3)_3{\cdot}9H_2O$, $Mg(NO_3)_2{\cdot}6H_2O$, and various bioactive dicarboxylic acids based on L-amino acid (L-isoleucine, S-valine, L-leucine, and L-phenylalanine) in aqueous state [29,30]. The X-ray diffraction (XRD) results showed that the position of the peak of the modified LDHs shifted to a higher d value, which confirmed the intercalation of diacids between the LDH layered. There are other analytical methods such as in situ XRD, FT-IR, SEM-EDX, transmission electron microscopy (TEM), and thermogravimetry analysis (TGA) for characterization of prepared sample, and some review articles are devoted to this field [31–34].

9.2.1 Layered double hydroxide

LDHs as anionic clay are a class of host–guest lamellar compounds made up of structural similarity with $Mg(OH)_2$, where divalent magnesium ions occupy octahedral positions surrounded by six OH groups in a complex layered structure to form an infinite two-dimensional layer [19,28]. Replacement of some divalent ions with trivalent ions leads to the formation of a stacking of positive charged brucitelike layers balanced by interlayer counteranions and water molecules as stabilizer [35,36]. The general chemical formula of LDH materials is written as $(M^{2+}_{1-x}M^{3+}_{x}(OH)_2)^{x+}(A^{n-})_{x/n}\cdot mH_2O$, where M^{2+} as divalent cations may be common; Mg^{2+}, Zn^{2+}, or Ni^{2+} and M^{3+} as trivalent cations may be common; Al^{3+}, Ga^{3+}, Fe^{3+}, or Mn^{3+}, which may be partially or completely replaced by monovalent or tetravalent cations [121(3)] [37]. A^{n-} is an exchangeable anion with negative charge n, e.g., $CO_3{}^{2-}$, Cl^-, $SO_4{}^{2-}$, RCO^{2-}, and x is equal to the ratio $M^{3+}/(M^{2+}+M^{3+})$, generally ranging as $0.2<x<0.33$ [9,33,38].

LDHs have been known for more than 150 years by Hochstetter (in 1842) and synthesized 100 years later by Feitknecht. Since discovery of LDH up to now, comprehensive scientific report has been published to controlling synthesis and applications of LDH in various fields. Research-based LDHs can be produced from natural sources (such as dolomite as a magnesium source) or synthesized by various methods; the most common of them include coprecipitation, homogeneous precipitation, structure reconstruction, sol–gel, hydrothermal, and the anion exchange method [39–41]. The brucitelike sheets can be stacked either with a rhombohedral symmetry (two layers per unit cell) or a hexagonal symmetry (three layers per unit cell) or in less symmetrical arrangements [8,40]. The nature of the anions and their orientation into the hydroxide sheets are two main factors for adjusting the basal spacing of the LDH [42]. The layer thickness and lateral dimensions of LDHs vary widely depending on the concurrent presence of anions and water molecules and the synthesis method and conditions, respectively [3]. Therefore, the basal spacing of compounds can be increased from 0.48 nm in brucite to about 0.77 nm in Mg–Al LDH [43], and their lateral dimensions can be varied from 0.06 to 20 μm [39,44]. LDHs, due to their unique properties such as low cost, two-dimensional structure, high surface area, positive charge on the surface, high anion-exchange capacities, tunable interior architecture, and resistant to changes on heating, have hold a great promise for use in catalysis, flame retardants [44,45], adsorption, drug delivery, supercapacitors, water treatment agents, fuel cells, electrochemical sensors, and biosensors, and many other fields, which will be studied in following discussions [28,32,41,46].

9.2.2 Biodegradable polymers

Increasing concern of preservation of ecological system has resulted in a new generation of biopolymer materials, which has been expanded with the rapid growth of chemistry and biology, so that the first synthetic biopolymers were used in the 1960s [46a]. The term biodegradable was used for polymers, which are biologically degraded to by-products (including carbon dioxide, methane, water, inorganic compounds, and

biomass) [47,48] by enzyme generated in vitro or in living cell. Biocompatibility was known as a prerequisite for using biomaterials in the body tissues; however, the chemical, physical, and biological properties (shape and size of the material) should be studied before utilizing in the body [48a].

Biodegradable polymers can be categorized as (1) natural polymers including polymers made from biosources such as corn, wood cellulose, proteins (collagen, silk), which were first known by Anselm Payen in 1838 [48b], and polysaccharides (starch, alginate, chitosan); (2) synthetic polymers such as polymers synthesized by bacteria from small molecules such as butyric acid or valeric acid that give polyhydroxybutyrate (PHB) and polyhydroxyvalerate (PHV) and biodegradable polymers that are derived from the petroleum sources or that may be obtained from mixed sources of biomass and petroleum such as poly(3-caprolactone) (PCL), poly(lactic acid) (PLA), poly(glycolic acid) (PGA), and poly(vinyl alcohol) (PVA) [47–49] (Fig. 9.1). PGA was the first biodegradable synthetic polymer, which was produced in the 1950s. These two classes of biopolymers show different physicochemical properties.

Synthetic polymers have favorable mechanical strength and their shape (configuration, molecular weight, crystallinity, morphology, etc.) and degradation rate can be controlled, but they show hydrophobic surface and lack of cell recognition signals, whereas natural polymers have relatively poor mechanical performances, but they show capability to biological diagnosis, which completely protect cell adhesion and function [49,50].

The one of the main characterizations of biodegradation of polymers is the presence of labile linkages along the polymer backbone such as ester, orthoester, anhydride, carbonate, amide, urea, or urethane [50a]. Unlike most of the biodegradable polymers, PVA has only carbon in the backbone and can undergo both microbial and enzymatic oxidations.

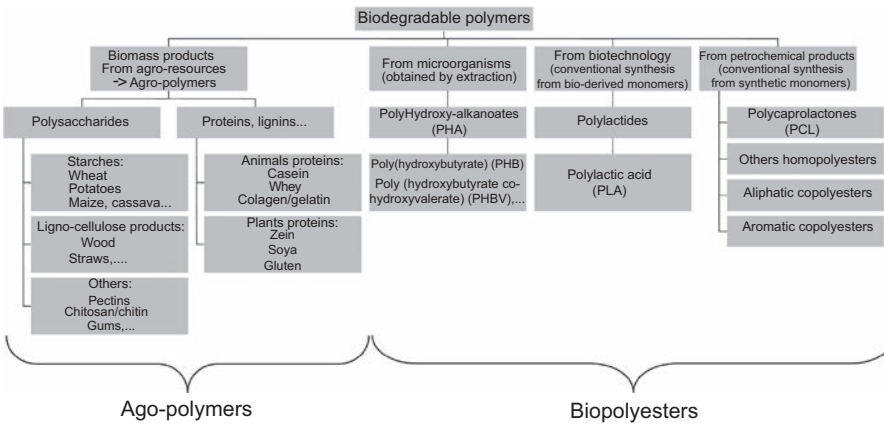

Figure 9.1 Classification of the main biodegradable polymers.
Adapted from L. Averous, E. Pollet, Biodegradable polymers, in: Environmental Silicate Nano-Biocomposites, Springer, 2012, pp. 13–39. With kind permission of Springer.

However, the preference for employing biodegradable materials is mainly to take excellence of their biodegradability and good biocompatibility, but the physical properties of the biopolymer will show an important influence in manufacturing and mechanical performance of the products developed [46a]. Blending and copolymerization of biodegradable polymers is one of the suitable approaches to improve the performance and particular properties, balance the high price of polymers, and expand their range of applications [51].

9.3 Investigation biodegradability of polymer/layered double hydroxide nanocomposites

Degradation is a process of polymer chain cleavage in which macromolecules loss the molecular weight during subsequent erosion of the biomaterial. Generally, the polymer erosion accomplishes enzymatically and hydrolytically sensitive bonds in the structure of natural polymers and synthetic polymers, respectively [50]. Two diverse erosion mechanisms, including homogeneous or bulk erosion and heterogeneous or surface erosion, have been introduced for biodegradable polymers. In bulk eroding polymers, the penetration of water into the polymer bulk is quicker than degradation of polymer; consequently, degradation occurs all over their cross section, whereas surface eroding polymers degrade principally from their surface, because of the phenomenon that degradation accomplishes faster than the penetration of water into the bulk [52]. Biodegradability of a biopolymer affects by the chemical composition, steric conformation, tacticity, melting point, and inherent degree of crystallinity of the materials [53]. C.-Y. Ciou et al. [53] studied the role of the m-LDH addition on the biodegradability of poly(3-hydroxybutyrate) (PHB) and poly (3-hydroxybutyrate-co-3-hydroxyvalerate) (PHBV5 and PHBV12 with PHV content of 5 and 12 wt%)-based film by using *Caldimonas manganoxidans* as a microbial catalyst. The result showed that PHBV5 and PHBV12 with different chemical composition compared with PHB indicated higher degradation rates that attributed to the reduced degree of crystallinity in PHBV. The field emission scanning electron microscopy (FESEM) images of microbial degraded PHB-based films indicated that the surface condition of samples is damaged by increasing time (Fig. 9.2). In these pictures, trace of the bacterial colonization is observed similar to hemirod shape on the surface of degraded films, where the footprint sizes are about several microns.

In other work, N. Gerds et al. [54] investigated the role of the catalytic depolymerization of laurate-modified magnesium aluminum LDH (Mg-Al-LDH-C_{12}) on the PLA/Mg-Al-LDH-C_{12} coprecipitation NCs prepared by melt compounding using bench-scale extrusion equipment. They outlined that the degree of dispersion, exfoliation, miscibility of the LDH, and also the accessibility of the hydroxide layer surfaces and Mg atomic sites (such as edges, step edges, corners, and step corners) are causative factors for Mg-catalyzed PLA degradation during melt processing. PLA mixed with Al^{3+} indicated far less reduction in molecular weight than the presence of Mg

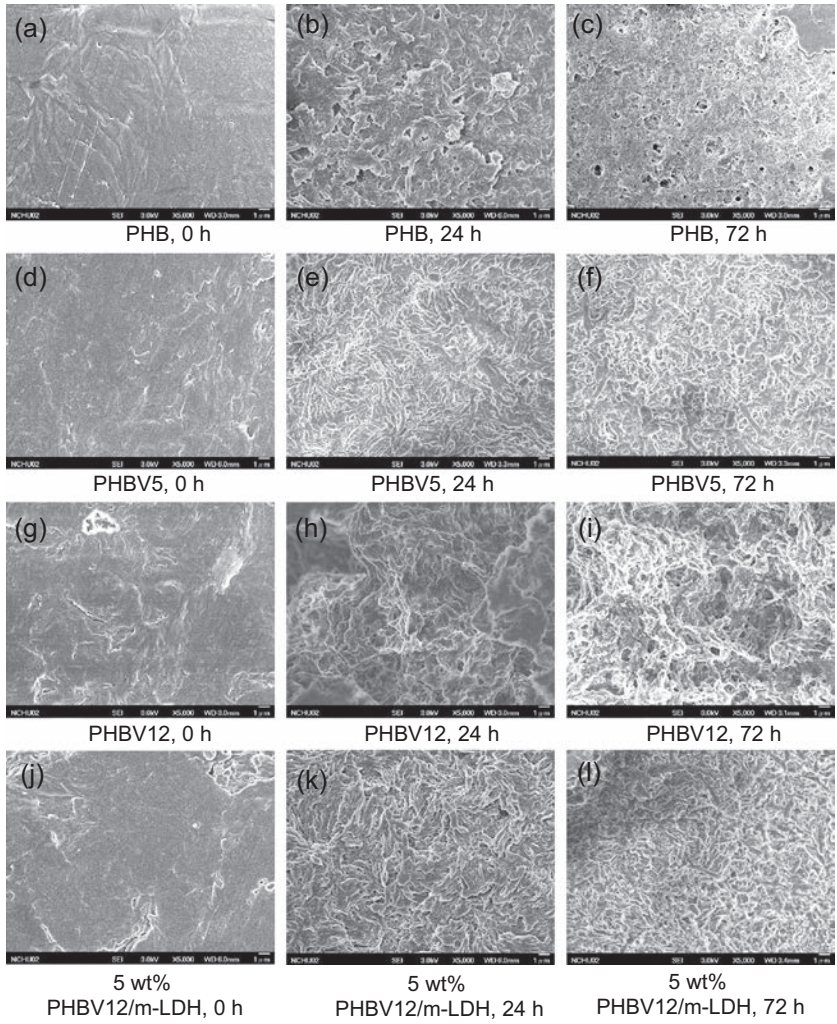

Figure 9.2 FESEM images of microbial degraded PHB-based films. (a–c) PHB; (d–f) PHBV5; (g–i) PHBV12; and (j–l) 5 wt% PHBV12/m-LDH.
Adapted from C.-Y. Ciou, S.-Y. Li, T.-M. Wu, Morphology and degradation behavior of poly (3-hydroxybutyrate-*co*-3-hydroxyvalerate)/layered double hydroxides composites, European Polymer Journal 59 (2014) 136–143. With kind permission of Elsevier.

compounds. Besides, S.S. Shafiei et al. [55] observed that the intercalation of LDH into PCL scaffold enhanced in vitro degradation rate and increased bulk degradation of the scaffolds, whereas in the neat PCL scaffold, the degradation was suffered by surface degradation mechanism. It may be due to decreased hydrophobicity of PCL-LDHs and penetration of more water into PCL chains during incubation. As showed in Fig. 9.3, scaffold with 10% LDH does not have any thinner fibers and only breakage of thicker fibers observed after 48 h.

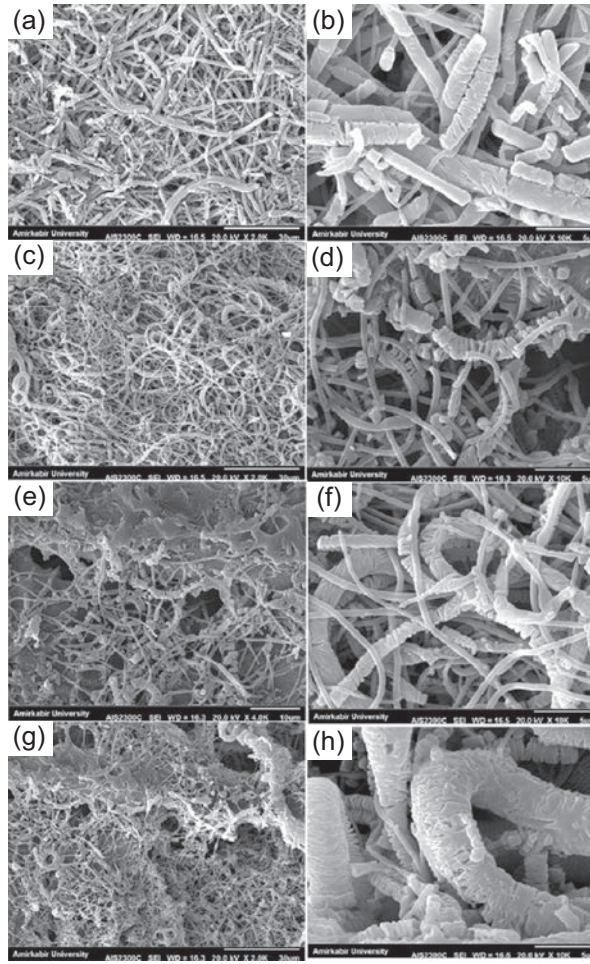

Figure 9.3 SEM micrographs of electrospun scaffolds immersed in accelerated degradation medium for 48 h. (a, b) PCL, (c, d) PCL + 0.1% LDH, (e, f) PCL + 1% LDH, and (g, h) PCL + 10% LDH.
Adapted from S.S. Shafiei, M. Shavandi, G. Ahangari, F. Shokrolahi, Electrospun layered double hydroxide/poly (ε-caprolactone) nanocomposite scaffolds for adipogenic differentiation of adipose-derived mesenchymal stem cells, Applied Clay Science 127 (2016) 52–63. With kind permission of Elsevier.

9.4 Applications of biopolymer/layered double hydroxide nanocomposite

9.4.1 Flame retardant

LDHs, due to their high smoke suppression, nontoxicity, or low toxicity, are used as second-generation additives in flame retardant with enhanced properties by either modification of the layers or intercalation of different anions [56].

The flame-retardant properties of polymer–LDH composites are mainly attributed to the physical barrier formed by the layered structure, the thermal degradation of LDHs, and the formation of a ceramic-like material, which slows down the release of flammable gases, thus inhibiting the polymer matrix from burning. Meanwhile, the characteristics and stoichiometry of the metal cations, the interlayer anions, the LDH particle size, and the dispersion of LDHs in the polymer matrix can have important role in appearance of these properties [37,57]. Compared with radical trapping and a barrier mechanism accepted for NCs containing of silicate clay, no mechanism has been proposed for the flame-retardant mechanism of LDH NCs. During burning process, LDHs can absorb the heat and produce H_2O and CO_2, which lowers the temperature of substrate and enhances foam char structure. Besides, the porous structure of the thermally decomposed products of LDHs with large specific surface area gives smoke suppression effects by absorbing the smoke and gases produced in the thermal decomposition. Therefore, the effects for these processes will decrease fuel accessible for combustion and increase the formation of an expanded carbonaceous coating or char, which protects the bulk polymer from exposure to air [58]. Based on literatures, different standards and indices such as microscale combustion calorimeter (MCC), limiting oxygen index (LOI), cone calorimeter (CONE), and UL-94 are used for considering the flame retardancy of a polymer [59,60]. Zhang et al. [17] investigated the thermal stability, thermal combustion, and thermomechanical properties for bio-NCs based on poly(3-hydroxybutyrate-co-4-hydroxybutyrate) (P(3,4)HB) and cobalt–aluminum LDH, which were prepared via melt intercalation. The result of thermogravimetric analysis showed that the thermal stability of the bio-NCs decreases with the addition of LDH amount, whereas thermal combustion properties indicated that the flame retardancy of P(3,4)HB/SS-LDH is improved with increasing loading of LDH. It is possibly attributed to the barrier effect of the nanosheets of dispersed LDH that can reduce the mass loss rate of polymer matrix and combustible gases. However, it is found that the peak heat release rate (PHRR), heat release capacity, and total heat release values are remarkably reduced from 761.9 to 435.7 W/g, from 743 to 451 J/g K, and from 13.6 to 11.8 kJ/g, respectively for P(3,4)HB/5 wt% SS-LDH compared to neat P(3,4)HB. The results of MCC and cone calorimetry test of biodegradable PLA revealed that loading of FR and ZnAl-LDH was very efficient in developing the flame retardancy of PLA composite. As shown in Fig. 9.4, pure PLA illustrates only Al foil and there is no residual of polymer after burning, whereas the PLA-FR and PLA-FR-ZnAl-LDH NC indicate intumescence. Examination of residues showed 2% LDH formed a consolidated and thick barrier from char layer, which significantly reduces heat transfer and air incursion, thus improving the flame-retardant performance of PLA-FR-ZnAl-LDH NC [61].

Li et al. [62] studied effect of LDH on flexible polyurethane foam and compared its results with montmorillonite clay (MMT) in similar work. Investigations suggested that LDH was the better option and produced a more effective fire-resistant coating than MMT. LDHs, because of producing additional pathways, not available by MMT, and diluting the fuel by releasing water in the gas phase, formed a protective residue layer between the polymer sample and the flame. LDH also provoked an endothermic dissociation reaction of the metal hydroxide layers and by adsorbing heat in the

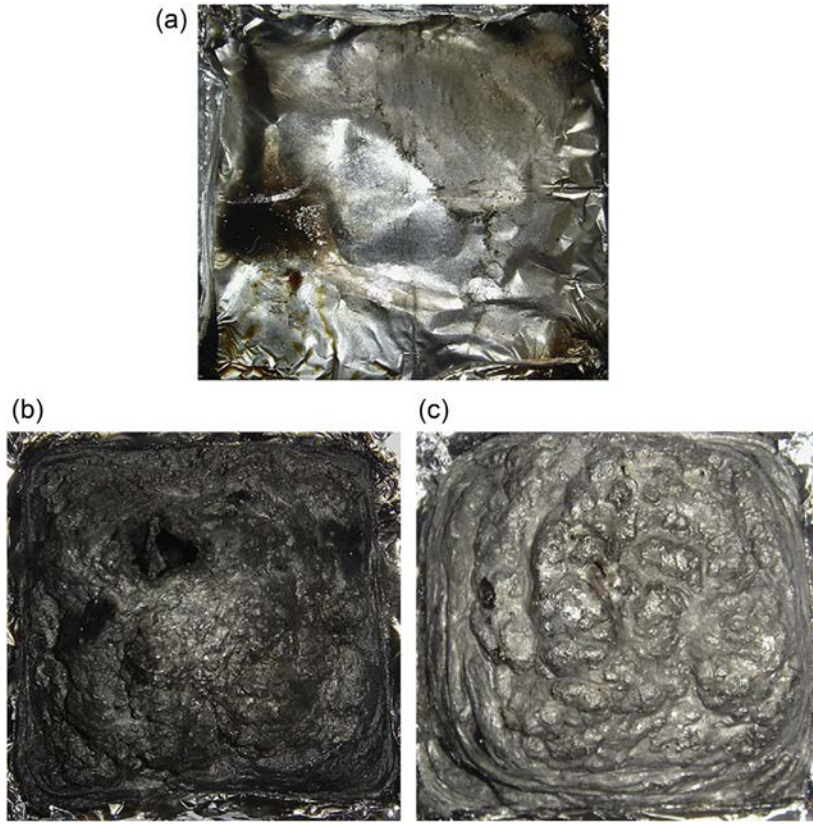

Figure 9.4 Photos of studied samples after cone calorimetry test: (a) neat PLA; (b) PLA-FR; and (c) PLA-FR-ZnAl-LDH.
Adapted from D.-Y. Wang, A. Leuteritz, Y.-Z. Wang, U. Wagenknecht, G. Heinrich, Preparation and burning behaviors of flame retarding biodegradable poly (lactic acid) nanocomposite based on zinc aluminum layered double hydroxide, Polymer Degradation and Stability 95 (2010) 2474–2480. With kind permission of Elsevier.

polymer decreases the temperature and slows down pyrolysis. For instance, LDH-based coating showed a 40% PHRR diminution that was at least 60% lighter and 50% faster to produce than the best MMT coating. Elbasuney [44] prepared $[Mg_6 AL_2 (OH)_{16}]CO_3{\cdot}4H_2O$ LDH with consistent product quality and then used poly (ethylene-co-acrylic acid) and dodecanedioic acid (DDA) as a polymeric surfactant and an organic ligand, respectively. They investigated the phase transition of LDH to corresponding oxides (MgO and AL_2O_3) during its endothermic decomposition using XRD. The XRD results confirmed that LDH began to go through phase transition to corresponding oxides over the temperature range 400–500°C. On the endothermic phase transition the obtained oxide layer migrates to the polymer surface during combustion and forms a protective oxide layer, which prevents further degradation. The formed oxide layer also absorbs soot leading to low smoke levels.

The presence of organic flame retardant with good char-forming ability can have vital role in the improvement of quality of char residue and the poor wetting of LDH. In other words, the relatively better dispersion state of functionalized LDH could increase the formation of intumescent and compact char residue and therefore facilitate the migration of LDH (or magnesium and aluminum) oxide (LDO) on the surface of condensed phase. During the process of combustion, LDO by forming a thermal insulating layer on the surface of condensed phase and adsorbing carbon small pieces in the gaseous phase plays a vital role in the improvement of flame retardancy efficiency [63]. Cai et al. [63] have considered the effect of functionalized LDH materials based on organic phosphorus flame retardant on the fire-retarding properties of unsaturated polyester (UP). Fig. 9.5 distinctly indicates the images of char residues and FESEM of LDH/UP composites after cone calorimetry testing. In comparison with UP NC containing 10 wt% of NO_3-LDH, the UP NC with 10 wt% of spirocyclic pentaerythritol bisphosphorate (SPDP)-LDH showed

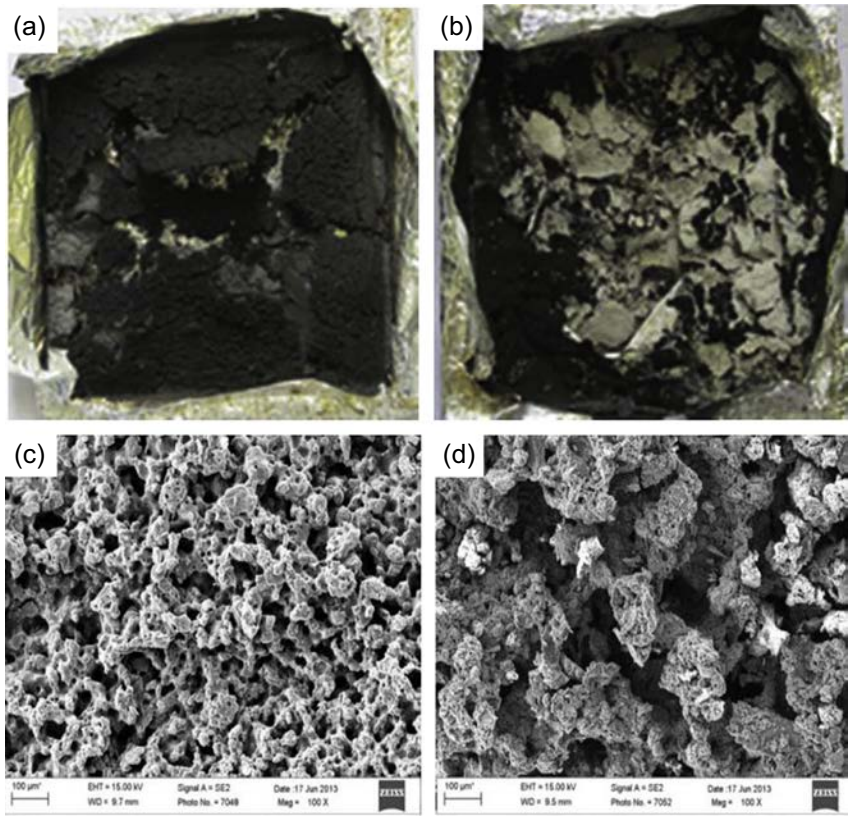

Figure 9.5 Photographs of the char residue after cone calorimetry testing: (a) 10%NO_3-LDH/UP; (b) 10%SPDP-LDH/UP and SEM images of the char residue after cone calorimetry testing: (c) 10%NO3-LDH/UP; (d) 10%SPDP-LDH/UP.
Adapted from J. Cai, H.-M. Heng, X.-P. Hu, Q.-K. Xu, F. Miao, A facile method for the preparation of novel fire-retardant layered double hydroxide and its application as nanofiller in UP, Polymer Degradation and Stability 126 (2016) 47–57. With kind permission of Elsevier.

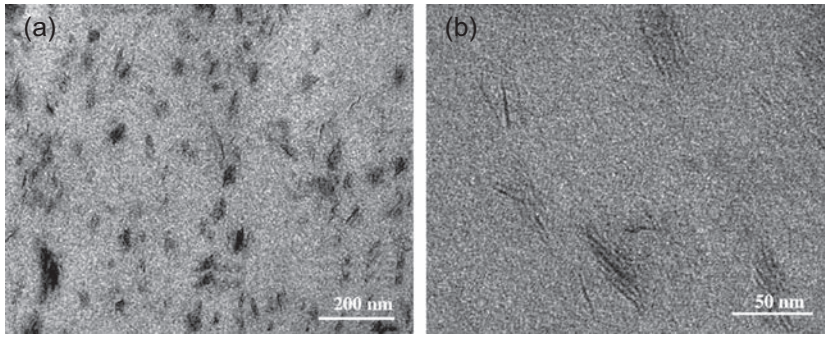

Figure 9.6 TEM micrographs of PPDO/LDH–DDS at low (a) and high (b) magnification. Adapted from M. Zubitur, A. Mugica, J. Areizaga, M. Cortázar, Morphology and thermal properties relationship in poly (p-dioxanone)/layered double hydroxides nanocomposites, Colloid and Polymer Science 288 (2010) 809–818. With kind permission of Elsevier.

an intact and fleecier char layer, so that a huge white scale like char was observed on the outer surface of char residue. Also, FESEM morphology of 10%SPDP-LDH/UP shows a swelling and dense network with least holes, which decreases the movement of heat and oxygen. Finally, it proposes that the existence of LDHs can improve the thermal degradation of UP, and SPDP-LDH is certainly superior to NO_3-LDH.

The same result was obtained in poly(p-dioxanone) (PPDO) NCs reinforced with sodium dodecyl sulfate (DDS)-LDH than the unmodified LDH, which attributed to the dispersion and high level of exfoliation of layers, which was confirmed by TEM images (Fig. 9.6) [64].

PVA is a flammable polymer with high PHRR. By increasing loading of the LDH/MoS_2 hybrids into PVA matrix, the PHRR of all the PVA composites is decreased gradually than the pure PVA. For example, the PHRR value is decreased from 288 W/g for neat PVA to 151 W/g for composite with 3 wt% LDH/MoS_2 hybrid, indicating the fire probability of the PVA reduced in the presence of the LDH/MoS_2 [65]. Zhao and coworkers [66] studied the impact of using ammonium polyphosphate (APP) and LDH on the flammability of PVA and reported an LOI value of up to 33 and UL-94 V-0 rating for most composites containing APP-based LDH. It has been related to the formation of a compact and intumescent charred layer on the surface of composite, which would act as an efficient shield and insulation that can prevent the underlying material contacting with heat, oxygen, and fire directly.

9.4.2 Catalyst and electrocatalyst

For the first time in 1973, LDHs composed from different metal ions were prepared for protecting of Ziegler catalysts for olefin polymerization. Calcined LDHs such as LDOs, because of having Brønsted-type base sites, are a suitable alternative to homogeneous base catalysts as environmentally friendly and recyclable catalysts for various organic reactions. The catalytic activity of LDHs is affected by factors such as kind of cations and their combination, selected anions, and uniform distribution of cations in the brucitelike layers and anions in the interlayer spacing [67,68]. Mahdi and coworkers [69]

studied the catalytic activity, the recyclability, and the storage of the beads composites prepared by using a hierarchical assembly of a recombinant fructose-6 phosphate aldolase (FSA_{wt}), LDH nanoplatelets, and polysaccharide beads. They observed that the presence of enzyme in the LDH supplies surface and anion exchange properties very appropriate to the efficient immobilization, thus increasing the loading and the activity of the catalyst. In addition, the use of the polysaccharide matrix (carrageenan) simplifies the separation of the catalyst and partially retains the structure and biological behaviors of the enzyme compared to FSAwt@Mg_2Al-LDH biohybrid. The recyclability result of beads displays a slight decrease in activity after four cycles (Fig. 9.7, left). Also, the activity of beads was measured for 12 days and shown a decrease of 60% and 28% for FSAwt@Mg_2AlLDH/ι-carr with or without KCl, respectively. This confirmed that KCl avoids the degeneration of the beads.

Kong et al. [70] showed that biprotein/LDH ultrathin film prepared by alternate assembly of hemoglobin (Hb) and horseradish peroxidase (HRP) molecules with LDH nanosheets can be used as an electrocatalyst for oxidation of catechol. Based on the synergistic effect of the two proteins, the modified electrode exhibits a favorable electrocatalytic activity with wide linear response range (6–170 μM, $r = 0.999$), low detection limit (5 μM), high sensitivity, and good reproducibility. Zhan et al. [71] used the Zn_2Al-LDH modified with hydroxyl-functionalized ionic liquid (HFIL) for immobilizing Hb. The result obtained from two methods of coprecipitation and adsorption showed that the Hb loading through coprecipitation was far higher than that the other method. Introduction of HFIL into LDH could particularly promote the electroactivity of HFIL–LDH–Hb_{cop} due to more adsorption sites and better conductivity and more favorable interface endowed by HFIL. Consequently, HFIL–LDH–Hb_{cop}/GCE exhibited the best electrocatalytic activity for H_2O_2 determination with a larger electroactive Hb percentage (6.76%), higher sensitivity (40.63 A/M cm^2), and lower detection limit (0.0054 μmol/L) and was suitable for fabrication of electrochemical biosensors. The photos of SEM and TEM of LDH–Hb_{cop} (thinner and irregular flaky particles with

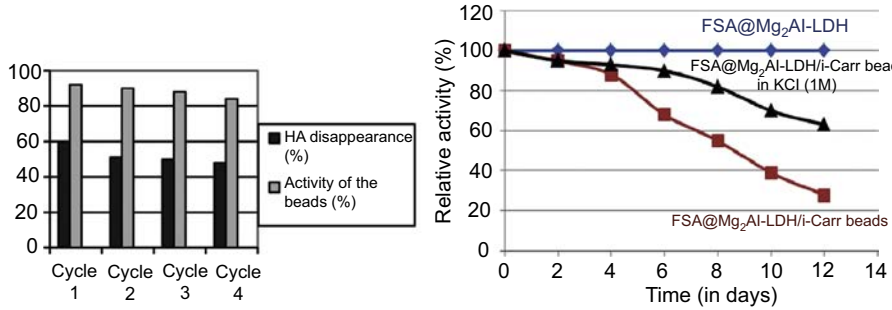

Figure 9.7 Left: Recyclability of the FSAwt@Mg2Al-LDH/ι-carr beads, 410 mg of beads (0.4 U) were used to perform aldolization between hydroxyacetone (0.12 mmol) and formaldehyde (0.2 mmol) in KCl (1 M), pH 8. Each run lasted 90 min. Right: Stability of the FSAwt@LDH/ι-carr beads with or without KCl compared with the FSAwt@Mg_2Al-LDH on storage. Adapted from R. Mahdi, C. Guérard-Hélaine, C. Laroche, P. Michaud, V. Prévot, C. Forano, M. Lemaire, Polysaccharide-layered double hydroxide–aldolase biohybrid beads for biocatalysed CC bond formation, Journal of Molecular Catalysis B: Enzymatic 122 (2015) 204–211. With kind permission of Elsevier.

stacked sheets) and HFIL–LDH–Hb_{cop} (thicker lamellar particles with dispersed colloidal flakelets) are shown in Fig. 9.8.

In a research work, poly(oligoethylene glycol methacrylate) (POEGMA)-grafted LDH was synthesized as a highly active and eco-friendly heterogeneous catalyst by a reversible addition–fragmentation chain transfer (RAFT) polymerization. Synthesized green catalyst, due to its significant properties such as cheapness, easiness, nonvolatile, reusability, high thermal stability, and good structural stability, is a good candidate for the synthesis of chromene-incorporated dihydroquinoline derivatives under solvent-free and mild reaction conditions (Fig. 9.9) [72].

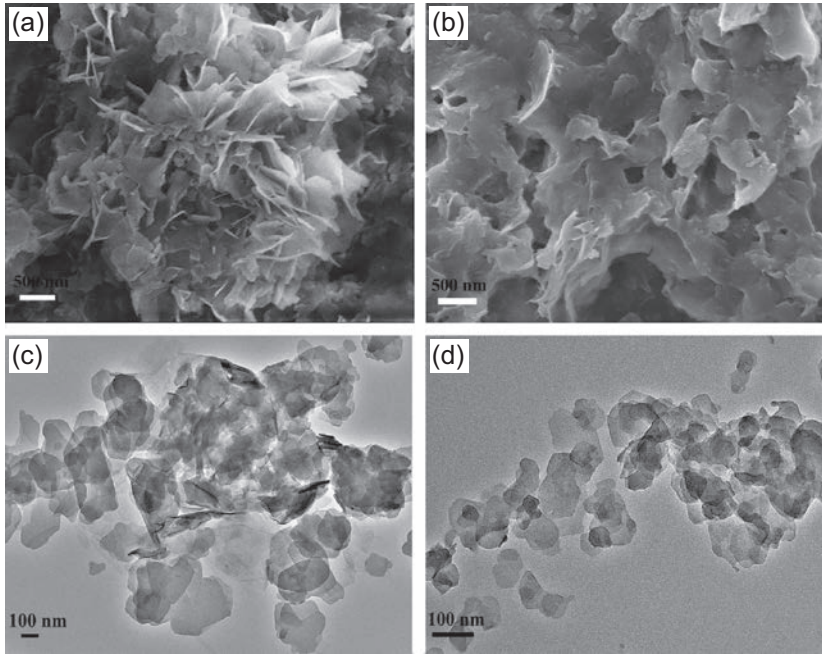

Figure 9.8 SEM (a and b) and TEM (c and d) images of LDH–Hbcop and HFIL–LDH–Hbcop. Adapted from T. Zhan, Q. Yang, Y. Zhang, X. Wang, J. Xu, W. Hou, Structural characterization andelectrocatalytic application of hemoglobin immobilized in layered double hydroxidesmodified with hydroxyl functionalized ionic liquid, Journal of Colloid and InterfaceScience 433 (2014) 49–57. With kind permission of Elsevier.

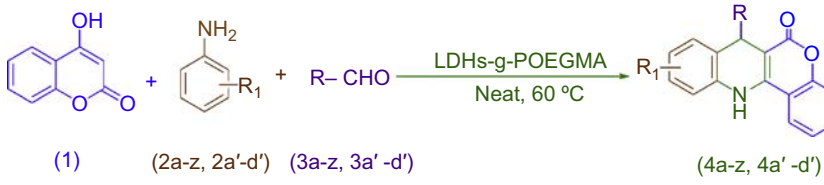

Figure 9.9 Synthesis of chromene-incorporated dihydroquinoline derivatives.
Adapted from M.V. Reddy, N.T.K. Lien, G.C.S. Reddy, K.T. Lim, Y.T. Jeong, Polymer grafted layered double hydroxides (LDHs-g-POEGMA): a highly efficient reusable solid catalyst for the synthesis of chromene incorporated dihydroquinoline derivatives under solvent-free conditions, Green Chemistry (2016). With kind permission of Royal Society of Chemistry.

9.4.3 Packaging

The environmental concern and landfill waste have been threatened to overwhelm landfills and created disposal problems. In this regard, worldwide effort has motivated to incorporate biodegradable and compostable biopolymers into common use, especially in the packaging industry [73]. Biopolymers such as PVA, PLA, and PCL have shown promising potential application in packaging industrials. Du et al. [74] fabricated PVA/LDH NCs with high mechanical performance, high transparency, and water resistance by directly dispersing PVA particles into LDH aqueous suspension. They observed that by loading 1.0 wt% LDH into the PVA matrix, tensile strength and Young's modulus of the NC films were enhanced by 93% and 144%, respectively, as compared to the neat PVA film. These composite films can potentially be used in the packaging industry. Higher water vapor permeability (WVP) and gas permeability are the main disadvantages that inhibit the use of polymers as packaging materials. It has been demonstrated that the introduction of nanofillers such as nanoplates in polymer matrix can reduce permeability. The relative permeability of NC is dependent on the volume fraction and dispersion nature of LDH layers, which might create a tortuous path, thereby extending the path length for the incoming water molecules through the polymer matrix surrounding the organomodified layered double hydroxide (OLDH) nanofillers [75,76]. Moreover, the appropriate dispersity of nanoplates provides hurdles to the entrance of gases, whereas virgin polymer may have voids for gas permeation. Chiang and Wu [75] fabricated PLLA composites, consisting of a fraction of unmodified LDH–NO_3 and γ-polyglutamate-modified LDH (γ-LDH), using the melt blending process. They found that the presence of either LDH–NO_3 or γ-LDH platelets within the PLLA results in a reduction in WVP and the higher barrier property was observed for the matrix reinforced with 5 wt% γ-LDH (54%) compared to that of the PLLA-LDH-NO_3 composites. This is mainly related to the dispersion of impermeable LDH sheets with less aggregate in the PLLA matrix. TEM images confirmed the intercalated structure of PLLA-γ-L NCs (Fig. 9.10).

The same result was observed by Xie et al. [77]. They prepared bio-NC films based on OLDH and poly(butylene adipateco-terephthalate) (PBAT) through the solvent casting method. The result showed that the low content addition of OLDH (1%) within the PBAT matrix with well delamination, uniform dispersion, and strong interaction can induce higher tensile and tear properties, higher optical and hydrophilic performances, and lower water vapor transmission rate than the pristine PBAT film. These observations are useful to develop eco-friendly packaging films. The presence of dispersed LDH in biodegradable polymers such as starch [1] and glycerol-plasticized starch [78] was effective in improving mechanical properties and decreasing water vapor permeability of polymers and can be used in packaging films. In a different method, Dou et al. [79] synthesized a self-healing film with excellent oxygen barrier performances and enhanced durability simultaneously, via layer-by-layer assembly of poly(sodium styrene-4-sulfonate) (PSS) and highly oriented LDH nanoplatelets followed by PVA coating. Most importantly, the obtained film due to hydrogen bonding interaction is capable of self-healing crack area and excellent gas barrier properties. For example, the oxygen transmission rate (OTR) value of the pristine polyester (PET) film decreases

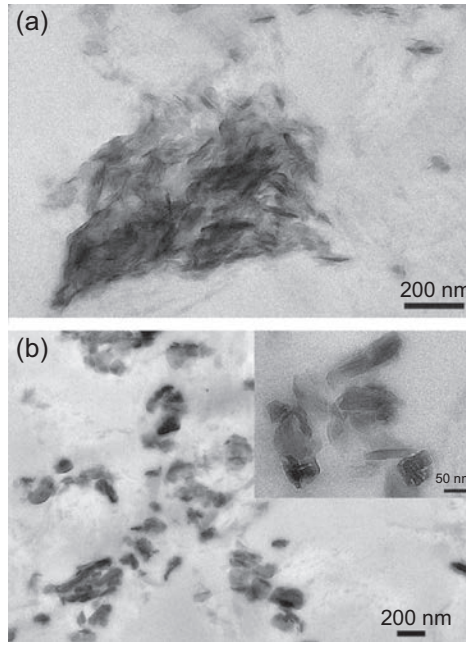

Figure 9.10 Bright-field TEM micrographs of (a) 5 wt% PLLA-L and (b) 5 wt% PLLA-γL. The inset in (b) is the high-magnification TEM images of 5 wt% PLLA-γL.
Adapted from M.-F. Chiang, T.-M. Wu, Preparation and characterization of melt processed poly (L-lactide)/layered double hydroxide nonocomposites, Composites Part B: Engineering 43 (2012) 2789–2794. With kind permission of Elsevier.

from 50.28 to 8.71 cm^3/m^2 day atm for $(LDH–PSS)_{20}$–PET film and almost 0.72 cm^3/m^2 day atm after incorporation of PVA. This occurrence can be attributed to the more condensed film and tortuous diffusion path and strong diffusion resistance, which proposed for application in the flexible display, druggery, and food packaging field. Pan et al. [80] prepared the superior gas barrier film via spin coating of hierarchical layered double hydroxide/chitosan (H-LDH/CTS) onto a precleaned poly(ethylene terephthalate) (PET) substrate (Fig. 9.11). In contrast to the pristine PET with OTR of ~8.431 cm^3/m^2 day atm, $(H\text{-}LDH/CTS)_{10}$ film showed a wondrous decrease in OTR with a value under the detection limit of commercial instruments (<0.005 cm^3/m^2 day atm).

9.4.4 Drug delivery

Selecting a nontoxic and effective drug delivery system with factors such as inert, biocompatible, mechanically durable, convenient for the patient, susceptible of attaining a high drug loading for the required blood levels, safe to accidental release, simple to apply, and easy to fabricate is enormously critical in the field of medicine to transfer and release the drug in a controlled fashion at the targeted site [81–83]. In research in the last decade, different strategies have been inspected for the delivery of nanomedicine by

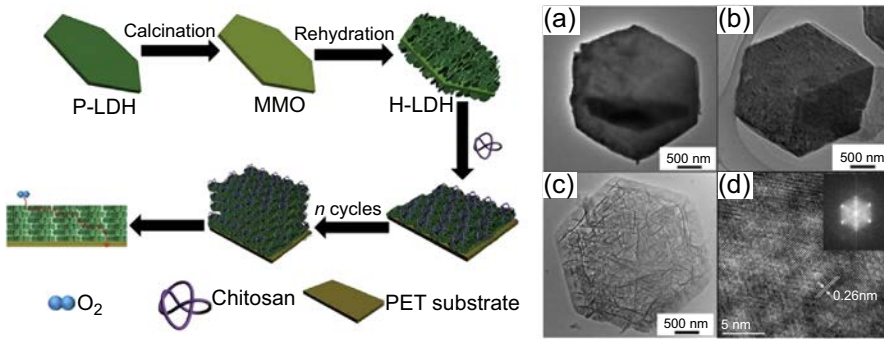

Figure 9.11 Schematic representation for the fabrication of (H-LDH/CTS)*n* films with excellent oxygen barrier properties. TEM images of the (a) P-LDH, (b) MMO, and (c) H-LDH. (d) The lattice fringe of H-LDH (inset: the fast Fourier transform pattern). Adapted from T. Pan, S. Xu, Y. Dou, X. Liu, Z. Li, J. Han, H. Yan, M. Wei, Remarkable oxygen barrier films based on a layered double hydroxide/chitosan hierarchical structure, Journal of Materials Chemistry A 3 (2015) 12350–12356. With kind permission of Royal Society of Chemistry.

using polymers, hydrogels, liposomes, and micelles. Although, drug carriers have many potential advantages as delivery systems, the premature drug release from these carriers usually induces to the challenge and revolution in these systems. LDHs as 2D materials and their NCs have remarkable characteristics that empower them for utilization as inorganic nanomedicines, as implied by published works [84]. A great deal of report has also proved that LDH nanomaterials can efficiently eliminate the limitations such as low solubility and low drug bioavailability of the free molecules in drug development from traditional formulations [81,85,86]. The LDHs are cheap and eco-compatible and have a high surface area, particle swelling property, memory effect, high anion exchange capacity, and stable physicochemical, which made them a very attractive group of lamellar solid compounds [82,87,88]. The release rate is mainly affected by the specific nature of the intercalated anion and the rate of the deintercalation process, depending on the electronic and steric structure of the guest molecule, drug–polymer interactions, fiber crystallinity, and hydrophilicity of drugs, whereas the easiness of its diffusion within the polymer matrix, depending on the dispersion of the inorganic lamellae [87,89,90]. In the past few years, many reports for release of drug from LDHs have been published. Bugatti et al. [87] prepared PCL nanohybrids based on ZnAl-LDH intercalated with benzoate derivatives as 2,4-dichlorobenzoate (BzDC) and p-hydroxybenzoate (*p*-BzOH), having antimicrobial properties. The release behavior of BzDC and *p*-BzOH from the exfoliated and microbiodegradable polymer composites showed a first stage, rapid as a "burst," corresponding to the release from the surface and followed by a much slower second stage, spreading for many months, up to an equilibrium value. These values are 100% and 50% for the BzDC and p-BzOH molecules, respectively. Miao et al. [89] fabricated biopolymer composite fibers based on a combination of ibuprofen-intercalated LDH (LDH-IBU) with two kinds of biodegradable polymers, PCL and PLA, via electrospinning for efficient drug loading and release. The uniform dispersion of LDH-IBU throughout biopolymer composites was demonstrated by TEM observations (Fig. 9.12).

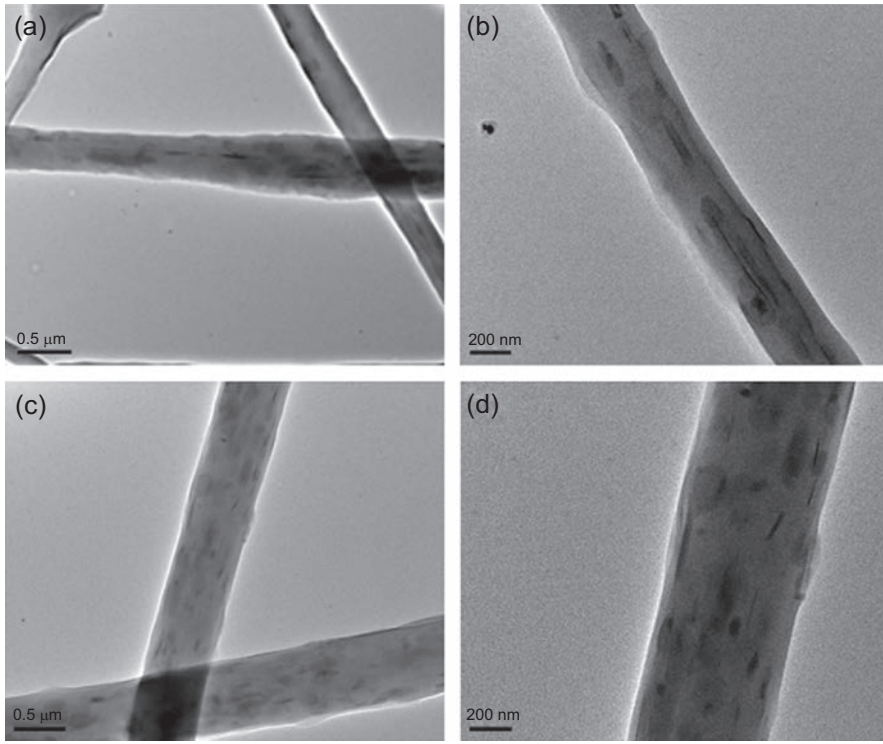

Figure 9.12 Low- and high-magnification TEM images of (a and b) 5 wt% LDH-IBU/PCL composite fibers and (c and d) 5 wt% LDH-IBU/PLA composite fibers.
Adapted from Y-E. Miao, H. Zhu, D. Chen, R. Wang, W.W. Tjiu, T. Liu, Electrospun fibers of layered double hydroxide/biopolymer nanocomposites as effective drug delivery systems, Materials Chemistry and Physics 134 (2012) 623–630. With kind permission of Elsevier.

They observed that the initial release rate of IBU from LDH-IBU/PCL composite fibers (40% release) is much slower than that from IBU/PCL fibers (70% release) within the first 2 h, while an opposite phenomenon is perceived in both IBU/PLA and LDH-IBU/PLA systems and almost 10% of the total quantity of drug was discharged from both IBU/PLA and LDH-IBU/PLA fibers within the same time period. The extremely slow drug release from PLA-based fibers than that from PCL-based fibers can be attributed to poor chain flexibility of PLA, leading to high T_g (about 60C) as well as restricting the chain mobility and the diffusion of the water uptake. To modulate the release rate of IBU from PLA-based fibers, they replaced 25% of PLA with poly(oxyethylene-b-oxypropylene-b-oxyethylene) (Pluronic) and observed the release more than 80% of IBU. It is related to the hydrophilicity of Pluronic and a plasticization effect, which synergistically accelerates IBU release rate [91]. Intercalation of the diclofenac, chloramphenicol, and ketoprofen in the interlayer space of the ZnAl hydrotalcite was done and then supported and dispersed in semicrystalline PLA to compare the drug release from the layered host and from the polymer-supported host. Drug release from all three drug-intercalated hydrotalcites along 24 h is about 100% of the initial amount in the case of ketoprofen, but only 80% and 60%

for chloramphenicol succinate and diclofenac, respectively. In all cases, a fast initial release is observed due to organic anions that weakly deposited on the external surface of LDH (almost 1 h for diclofenac, 2 h for chloramphenicol, or 5.5 h for ketoprofen). Afterward the release is slower that it relates to the anion exchange with anions in the solution and progresses through diffusion inside the interlayer space. In other method, different concentration of LDHs intercalated with Amoxicillin (AMOX) was encapsulated into PCL by the electrospinning technique [90]. The comparison of the fraction of AMOX released displayed that the release rate of AMOX protected into the LDH is slower than the drug alone and that the release time of PCL-LDH/AMOX was extended up to months for the most concentrated sample (Fig. 9.13).

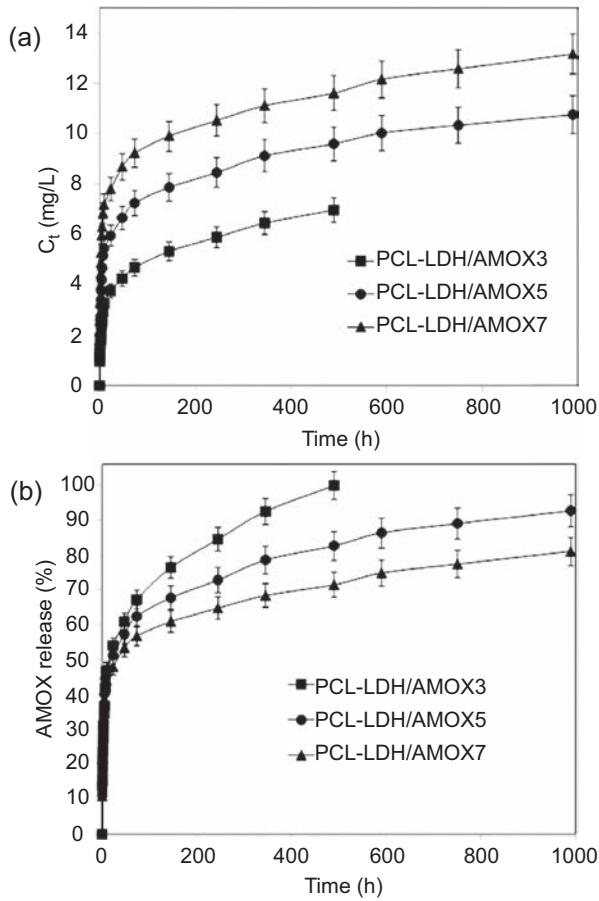

Figure 9.13 Amount of AMOX released, as absolute concentration (Ct, mg/L) (a) and as % of the maximum achievable concentration (b).
Adapted from E. Valarezo, L. Tammaro, S. González, O. Malagón, V. Vittoria, Fabrication and sustained release properties of poly (ε-caprolactone) electrospun fibers loaded with layered double hydroxide nanoparticles intercalated with amoxicillin, Applied Clay Science 72 (2013) 104–109. With kind permission of Elsevier.

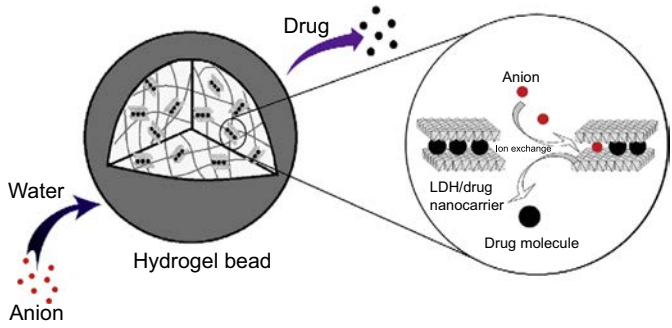

Figure 9.14 Schematic illustration showing the cephalexin release from CMC/LDH-CPX NC bead.
Adapted from S. Barkhordari, M. Yadollahi, Carboxymethyl cellulose capsulated layered double hydroxides/drug nanohybrids for Cephalexin oral delivery, Applied Clay Science 121 (2016) 77–85. With kind permission of Elsevier.

Barkhordari and Yadollahi [81] also applied physically cross-linked carboxymethyl cellulose (CMC) to encapsulate LDH–cephalexin (CPX) nanohybrids and prepared pH-sensitive NC in gastrointestinal tract conditions. They showed that the CMC/LDH-CPX NC bead system is a very promising drug carrier when compared with the LDH-CPX. The drug release decreases and CMC/LDH-CPX NC shrinks at acidic pH; as a result, the drug is protected against digestion within the stomach, while the release increased with the increase of the pH and the total release reached to 92% in 8 h at pH 7.4. The release mechanism of NC beads is indicated in Fig. 9.14.

In another similar interpretations led by Barkhordari et al. [92], ibuprofen-intercalated LDH systems were encapsulated into CMC and a same drug release pattern was observed in the alkali and acidic conditions.

LDH–drug hybrids are usually coated by polymers due to their sensitivity to acid, rapidly released in the stomach media, and low toxicity. For example, amount of 34.2% of 5-fluorouracil (5-FU) as electronegative model drug was loaded in LDH and PEGylated hyaluronic acid (HA-PEG) coated via electrostatic adsorption on the LDHs by hydrothermal method [93]. They demonstrated that the modification of HA-PEG on the LDH surface developed the biocompatibility and endocytosis ability of the drug delivery system. As shown in Fig. 9.15, LDH/HA-PEG had stronger fluorescence intensity and showed higher cellular uptake and target delivery abilities than the unmodified LDH.

In a similar work, drugs such as tetracycline (TET), doxorubicin (DOX), 5-fluorouracil (5FU), vancomycin (VAN), sodium fusidate (SF), and antisense oligonucleotides (ASO) were complexed to the LDH clay and dispersed in poly(D,L lactic acid-co-glycolic acid) (PLGA) (85/15) films [94]. In contrast with LDH–drug with a large burst phase of release, the drug–LDH–PLGA was led to a reduced burst phase of release with a slow continuous release after many weeks. Singh et al. [95] have prepared a new protein delivery system by loading human growth hormone (hGH) intercalated with an LDH nanoplate complex (LDH-hGH) within a cationic pH- and temperature-sensitive injectable PAEU hydrogel to obtain a controlled, sustained

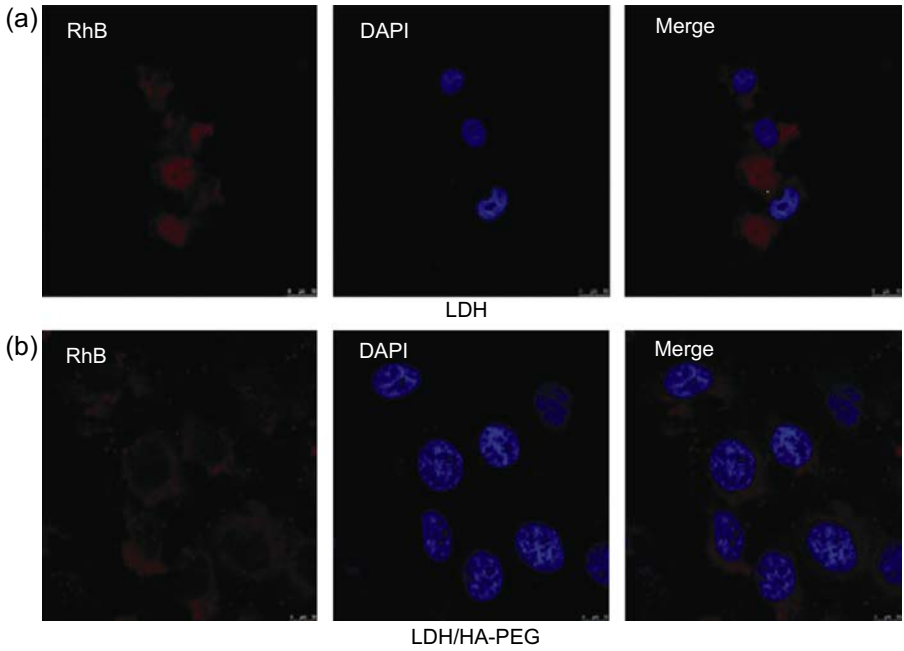

Figure 9.15 In vitro cell endocytosis of (a) LDH-RB and (b) LDHRB/HA-PEG evaluated by fluorescent inverted microscopy.
Adapted from A. Dong, X. Li, W. Wang, S. Han, J. Liu, J. Liu, J. Zhao, S. Xu, L. Deng, Layered doublehydroxide modified by PEGylated hyaluronic acid as a hybrid nanocarrier for targeteddrug delivery, Transactions of Tianjin University 22 (2016) 237–246. With kind permission of Springer.

release and enhanced bioavailability of hGH. In TEM image, large particle size of LDH-hGH (95–100 nm) than the LDH (50–80 nm) showed that hGH is coated onto the LDH surface (Fig. 9.16). They showed that the pure PAEU and a PAEU/LDH nanohybrid have been gradually destroyed after hydrogel production, and also in vivo weight loss was estimated 20 and 35 wt%, respectively, for 35 days (Fig. 9.17(a)). In optical micrograph it can be observed that the form of both hydrogels kept on steady for more than 4 weeks and the size slowly reduced due to copolymer degradation (Fig. 9.17(b)). The SEM images of pure PAEU and PAEU/LDH nanohybrid hydrogels indicated that before degradation, pure PAEU hydrogel had separate and big pores, compared to nanohybrid hydrogels. Also, after degradation, the pore bulk of pristine PAEU was more strictly affected than that of PAEU/LDH (Fig. 9.17(c)) [95].

In an interesting work, Wei et al. [86] intercalated indocyanine green (ICG) into amine-modified LDH interlayers and the coated chitosan on the external surfaces of LDHs–ICG through the cross-linking of LDHs–NH_2–ICG and chitosan by using glutaraldehyde (GA) as a cross-linked agent. The combination of chitosan and LDHs–NH_2–ICG not only produced an efficient NIR optical contrast agent to inhibit ICG molecules from leaching and/or metabolizing in physiological conditions but also developed organ-specific drug delivery systems that transmit therapeutic drugs to desired target organs by controlling the coating amounts of chitosan.

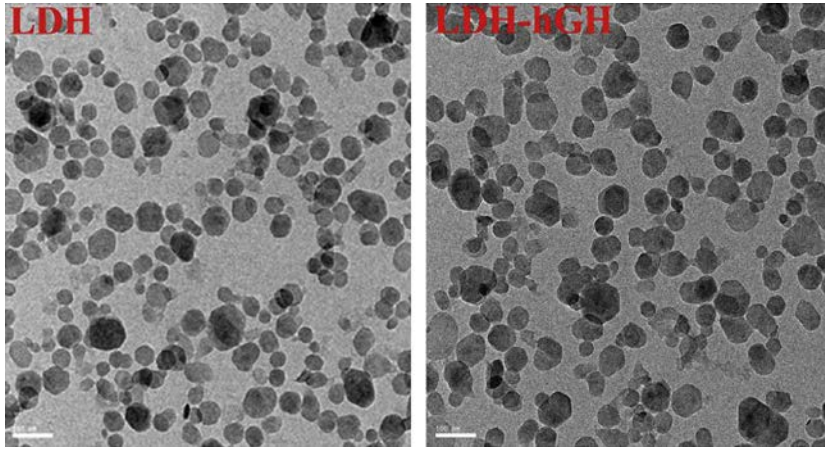

Figure 9.16 TEM images of pristine LDH and LDH-hGH nanoparticles.
Adapted from N.K. Singh, Q.V. Nguyen, B.S. Kim, D.S. Lee, Nanostructure controlled sustained deliveryof human growth hormone using injectable, biodegradable, pH/temperature responsivenanobiohybrid hydrogel, Nanoscale 7 (7) (2015) 3043–3054. With kind permission of Royal Society of Chemistry.

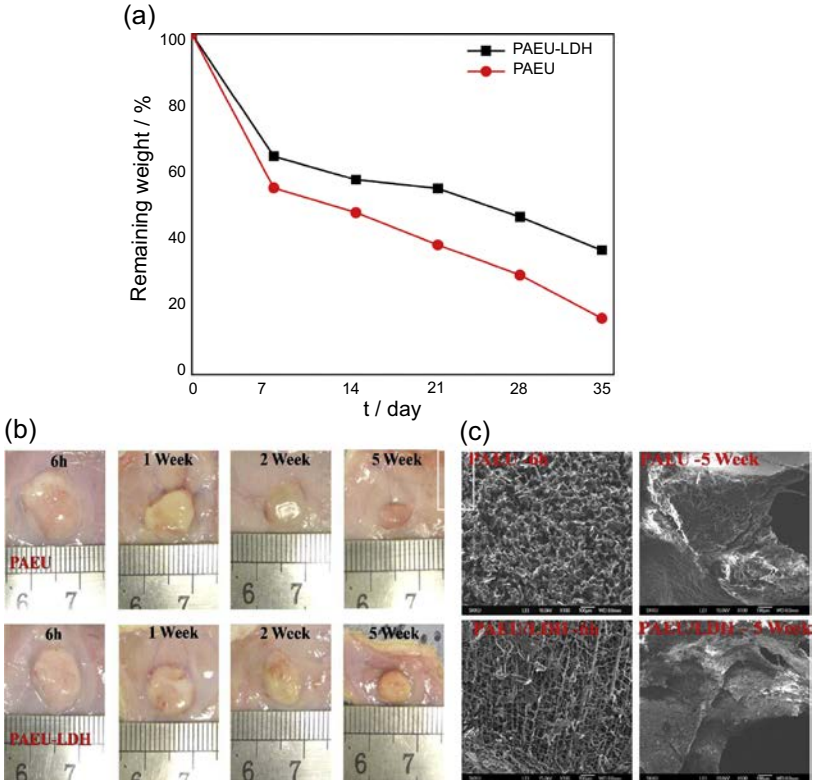

Figure 9.17 (a) In vivo degradation of PAEU and PAEU/LDH hydrogel (15 wt%, pH 6.3) determined by the mass loss method, (b) optical micrograph, and (c) SEM morphology of PAEU and PAEU/LDH hydrogels before and after degradation.
Adapted from N.K. Singh, Q.V. Nguyen, B.S. Kim, D.S. Lee, Nanostructure controlled sustained deliveryof human growth hormone using injectable, biodegradable, pH/temperature responsivenanobiohybrid hydrogel, Nanoscale 7 (7) (2015) 3043–3054. With kind permission of Royal Society of Chemistry.

Various research studies show that electrospun nanofibers due to significant features such as high porosity, high specific surface area, good structure controllability, and space grid structure are suitable for drug delivery, cell proliferation, and tissue repair. In view of that, Yang et al. [96] used a hybrid electrospinning to fabricate of flurbiprofen axetil-MgAl-LDHs/poly(lactic-co-glycolic acid) (FA-LDH/PLGA) composite nanofibers, which could significantly reduce the burst release phenomenon at the initial phase of drug release and appreciably extend the release time of the drug.

9.4.5 Adsorption

Properties such as the large surface area, high anion exchange capacity of LDHs, and flexible interlayer region are fundamentally important features to use LDHs for the removal of contaminants. Several mechanisms have been proposed to control the removal of contaminants from water and industrial wastewater: surface adsorption, interlayer anion exchange, chemical precipitation, conventional coagulation, reverse osmosis, electrodialysis, electrolysis, and reconstruction of calcined LDH precursors by the memory effect [40,97]. Factors such as PH, temperature, dosage of adsorbent, competitive anions, nature of precursor metals and crystallinity of LDHs, calcination and memory effect, layer charge and interlayer anion charge, and particle size can influence contaminant adsorption by LDH NC, which obviously reported in many literature works [40]. Arguably the most intensely studied application of biopolymer/LDH NCs is the removal of inorganic pollutants from aqueous solutions. Free-radical copolymerization of N-isopropylacrylamide (NIPAm) and the silylanized Mg/Al layered double hydroxides (SiLDHs) was performed by Hen et al. [98] for removing of Orange-II, As(III), and As(V) from water. The specific surface areas of PNIPAm and PNIPAm-co-SiLDH (with mass ratios 3:1) are determined to be 68 and 86 m^2/g, respectively. They found that the sorption capacity of PNIPAm-co-SiLDH (13.5 mg/g) to uptake Orange-II was seven times higher than that of PNIPAm (2.0 mg/g), and composites containing LDH/NO_3^- due to the larger exposed external surface showed the stronger sorption capacity for Orange-II than that of CO_3^{2-}. However, the sorption capacities of arsenate onto PNIPAm-co-SiLDH (0.14 and 0.45) are also greater than that onto PNIPAm (0.06 and 0.010), for both As(III) and As(V), respectively. In comparison to NO^{3-}-Mg/Al LDH, $SiLDH_N$ has a smoother surface, and PNIPAm-co-SiLDH exhibits the porous structure with a mean diameter around 8 μm. The EDS data proved that the surface-silanized LDHs as multifunctional cross-link agents have been dispersed in the PNIPAm (Fig. 9.18).

Chen and An [99] prepared a Mg–$FeCO_3$ LDHs-loaded cellulose fiber as a novel green adsorbent with relative standard deviation (RSD) of 3.3% (0.5 μg/L, $n=11$) for the adsorption of inorganic selenium species via coprecipitation with the Mg–$FeCO_3$ LDH layer. The adsorption of metal species is highly pH dependent, and the quantitative adsorption of selenite and selenate was accomplished at pH 3.8–8.0 and pH 5.8–7.0, respectively. This fact is probably related to the distribution of the chemical forms of different species of selenium and the surface charge of the sorbent. In other work, Mandal and Mayadevi [100] investigated the fluoride adsorption properties of three samples of raw cellulose, unsupported LDH, and cellulose-supported LDHs (CSLDH). They reported that defluoridation capacity of the CSLDHs was two to four times higher than

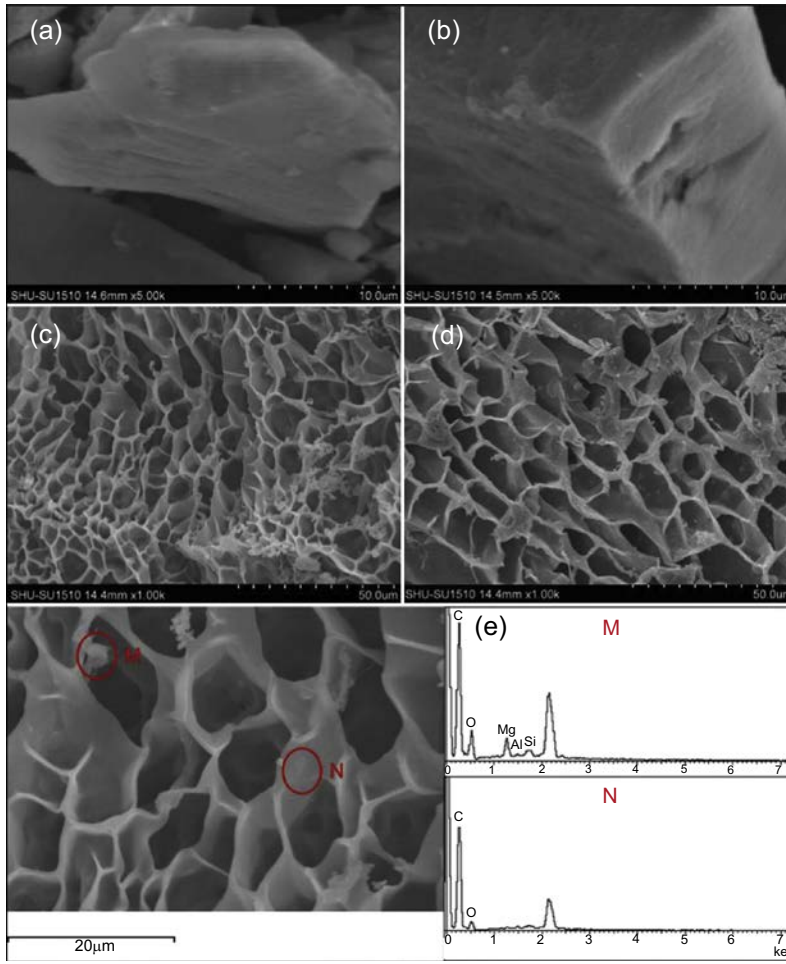

Figure 9.18 SEM images of prepared samples (a) NO_3–Mg/Al LDH, (b) $SiLDH_N$, (c) P/SN-2, (d) P/SC-2, and (e) EDS of P/SN-2.
Adapted from H. Chen, G. Qian, X. Ruan, R.L. Frost, Abatement of aqueous anionic contaminants by thermo-responsive nanocomposites: (poly (N-isopropylacrylamide))-*co*-silylanized magnesium/aluminun layered double hydroxides, Journal of Colloid and Interface Science 448 (2015) 65–72. With kind permission of Elsevier.

that of unsupported LDH, so that CSLDH with 27% loading of LDH showed maximum fluoride uptake capacity (5.29 mg/g) in fixed-bed column study. Hibino [101] investigated adsorption ability of SO_4^{2-}, I^-, and HPO_4^{2-} by using agarose–LDH hydrogels as anion adsorbent and compared with that of powdered LDH restacked. The results indicated that adsorption ability of hydrogels in low amounts of LDH is lower than that of the restacked LDH. When the ratio of LDH to agarose approached 1:1 by weight, this value was evaluated about the same as or slightly greater than that of the restacked LDH. This result can be related to accessibility of anion to the LDH nanoplates.

9.4.6 Other applications

As pointed out above, LDHs due to their properties such as the layered structure, large surface area, and ion exchange ability are of potential interest for amperometric or potentiometric sensors. Ai et al. [102] explored a composite systems based on the electrode coated with the Ni/Al-LDH nanoflakes and chitosan for preparing a cheap and simple amperometric glucose biosensor. The biosensor revealed a good linear range of 0.01–10 mM and appropriate operational stability with RSD <7.5% for the analysis of glucose in human blood serum. The result has a good accordance with that from the spectrophotometric method. Anion exchange membrane direct ethanol fuel cells (AEM DEFCs) that prepared using an alkaline anion exchange membranes, due to eco-friendly, extensive available, and high energy density have attracted more tendency than other alcohol fuels. Zeng et al. [103] synthesized composite membranes based on alkaline PVA/LDH composites via solution casting method, which exhibited high ionic conductivity of 26.6 mS/cm and lower ethanol permeability with 20 wt% LDH at 30°C, while the power density was 61.31 and 81.92 mW/cm^2 at 60 and 80°C, respectively. In Fig. 9.19, the presence of two strong peaks (003) and (006) signified interlayer spaces of 0.776 nm. Also, TEM image exhibited that Mg–Al LDHs have relatively uniform structure with thin hexagonal platelets of 100 nm size.

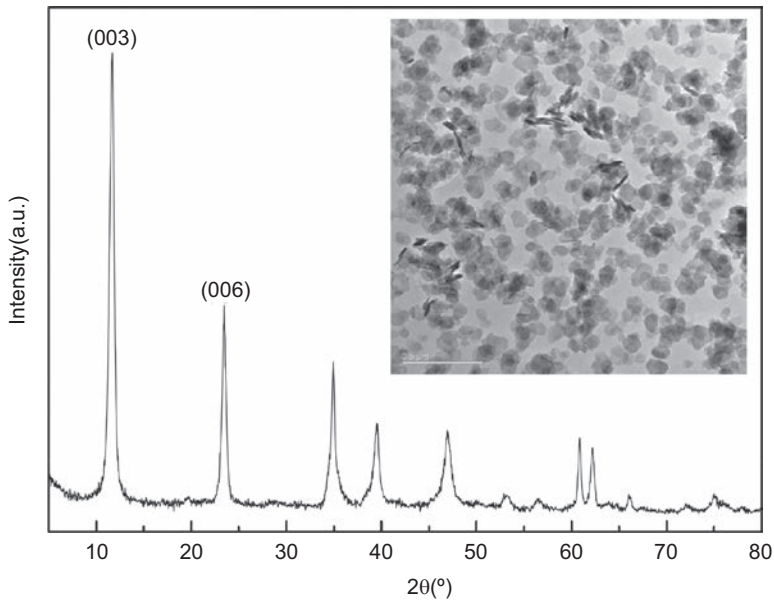

Figure 9.19 e XRD patterns of the MgeAl layered double hydroxides (LDHs). The inset shows the TEM image of MgeAl LDHs.
Adapted from L. Zeng, T. Zhao, Y. Li, Synthesis and characterization of crosslinked poly (vinyl alcohol)/layered double hydroxide composite polymer membranes for alkaline direct ethanol fuel cells, International Journal of Hydrogen Energy 37 (2012) 18425–18432. With kind permission of Elsevier.

9.5 Conclusions

By rapid growth and development of the society, specifically since the last decade of 20th century, the use of synthetic polymers such as plastic and rubber has been challenging an evident threat relevant to the soil, water, air, and overall to the whole environment due to their nonbiodegradability and toxicity. Usage of the biodegradable and natural polymers was proposed as an acceptable method. Based on the searches reported by various group of researchers in this chapter, it can be found that biopolymer/LDH NCs are an ecological alternative and possess a favorable potential to use a wide range of industrials. These NCs, due to their excellent properties rising from the nanoreinforcement of LDH, stimulated scientific and industrial attention. In this contribution, we intended to cover the current state of the art in the degradation characteristics and applications of polymer/LDH NC in various fields such as flame retardant, drug delivery, adsorption, and catalyst. The following pointed out main points of this chapter:

- Polymer/LDH NCs show the promoting flame-retardant property due to different functions such as heat absorption (endotherm), gaseous dilution, char formation, and dispersion.
- Properties such as presence of M(II) and M(III) (and MIV) cations, unlimited combination of MII and MIII with two or more types, kind of selected anions, and nearly uniform dispersion of cations in the brucitelike layers and anions in the interlayer spacing lead to catalyst application of LDHs in biopolymers.
- LDHs, due to their flexibility of chemical composition, pH-responsive solubility, and highly tunable structures, have a key role in analytical adsorption of polymer NCs.

Acknowledgments

The authors acknowledge the Research Affairs Division of Isfahan University of Technology (IUT), Isfahan, Iran. We also appreciate the National Elite Foundation (NEF), Tehran, Iran, the Iran Nanotechnology Initiative Council (INIC), Tehran, Iran, and Center of Excellence in Sensors and Green Chemistry Research (IUT), Isfahan, Iran, for financial support.

References

[1] Y.-L. Chung, H.-M. Lai, Preparation and properties of biodegradable starch-layered double hydroxide nanocomposites, Carbohydrate Polymers 80 (2010) 525–532.
[2] S. Chanprateep, Current trends in biodegradable polyhydroxyalkanoates, Journal of Bioscience and Bioengineering 110 (2010) 621–632.
[3] M. Hennous, Z. Derriche, E. Privas, P. Navard, V. Verney, F. Leroux, Lignosulfonate interleaved layered double hydroxide: a novel green organoclay for bio-related polymer, Applied Clay Science 71 (2013) 42–48.
[4] S.S. Ray, M. Bousmina, Biodegradable polymers and their layered silicate nanocomposites: in greening the 21st century materials world, Progress in Materials Science 50 (2005) 962–1079.

[5] D. Lennerová, F. Kovanda, J. Brožek, Preparation of Mg–Al layered double hydroxide/polyamide 6 nanocomposites using Mg–Al–taurate LDH as nanofiller, Applied Clay Science 114 (2015) 265–272.
[6] S. Mallakpour, M. Dinari, Manufacture and characterization of biodegradable nanocomposites based on nanoscale MgAl-layered double hydroxide modified with N, N′-(pyromellitoyl)-bis-L-isoleucine diacid and poly (vinyl alcohol), Polymer-Plastics Technology and Engineering 53 (2014) 880–889.
[7] S. Mallakpour, M. Dinari, Bionanocomposite materials from layered double hydroxide/N-trimellitylimido-L-isoleucine hybrid and poly (vinyl alcohol) structural and morphological study, Journal of Thermoplastic Composite Materials 29 (2016) 623–637.
[8] S. Omwoma, W. Chen, R. Tsunashima, Y.-F. Song, Recent advances on polyoxometalates intercalated layered double hydroxides: from synthetic approaches to functional material applications, Coordination Chemistry Reviews 258 (2014) 58–71.
[9] Q. Wang, D. O'Hare, Recent advances in the synthesis and application of layered double hydroxide (LDH) nanosheets, Chemical Reviews 112 (2012) 4124–4155.
[10] P.H.C. Camargo, K.G. Satyanarayana, F. Wypych, Nanocomposites: synthesis, structure, properties and new application opportunities, Materials Research 12 (2009) 1–39.
[11] A.M. Youssef, Polymer nanocomposites as a new trend for packaging applications, Polymer-Plastics Technology and Engineering 52 (2013) 635–660.
[12] Y. Wang, D. Zhang, Bioinspired assembly of layered double hydroxide/carboxymethyl chitosan bionanocomposite hydrogel films, Journal of Materials Chemistry B 2 (2014) 1024–1030.
[13] V. Katiyar, N. Gerds, C.B. Koch, J. Risbo, H.C.B. Hansen, D. Plackett, Poly L-lactide-layered double hydroxide nanocomposites via in situ polymerization of L-lactide, Polymer Degradation and Stability 95 (2010) 2563–2573.
[14] G. Totaro, L. Sisti, A. Celli, H. Askanian, V. Verney, F. Leroux, Poly (butylene succinate) bionanocomposites: a novel bio-organo-modified layered double hydroxide for superior mechanical properties, RSC Advances 6 (2016) 4780–4791.
[15] J. Leng, P.J. Purohit, N. Kang, D.-Y. Wang, J. Falkenhagen, F. Emmerling, A.F. Thünemann, A. Schönhals, Structure–property relationships of nanocomposites based on polylactide and MgAl layered double hydroxides, European Polymer Journal 68 (2015) 338–354.
[16] Z. Wei, G. Chen, Y. Shi, P. Song, M. Zhan, W. Zhang, Isothermal crystallization and mechanical properties of poly (butylene succinate)/layered double hydroxide nanocomposites, Journal of Polymer Research 19 (2012b) 1–10.
[17] R. Zhang, H. Huang, W. Yang, X. Xiao, Y. Hu, Preparation and characterization of bio-nanocomposites based on poly (3-hydroxybutyrate-*co*-4-hydroxybutyrate) and CoAl layered double hydroxide using melt intercalation, Composites Part A: Applied Science and Manufacturing 43 (2012) 547–552.
[18] A. Causa, G. Filippone, C. Domingo, A. Salerno, Study of the morphology and texture of poly (ε-caprolactone)/polyethylene oxide blend films as a function of composition and the addition of nanofillers with different functionalities, RSC Advances 5 (2015) 59354–59363.
[19] M.-F. Chiang, T.-M. Wu, Synthesis and characterization of biodegradable poly (L-lactide)/layered double hydroxide nanocomposites, Composites Science and Technology 70 (2010) 110–115.
[20] S. Mallakpour, M. Dinari, Novel bionanocomposites of poly (vinyl alcohol) and modified chiral layered double hydroxides: synthesis, properties and a morphological study, Progress in Organic Coatings 77 (2014) 583–589.

[21] M. Ardanuy, J. Velasco, Mg–Al Layered double hydroxide nanoparticles: evaluation of the thermal stability in polypropylene matrix, Applied Clay Science 51 (2011) 341–347.
[22] N. Raman, S. Sudharsan, K. Pothiraj, Synthesis and structural reactivity of inorganic–organic hybrid nanocomposites–a review, Journal of Saudi Chemical Society 16 (2012) 339–352.
[23] Y. Shu, P. Yin, B. Liang, H. Wang, L. Guo, Bioinspired design and assembly of layered double hydroxide/poly (vinyl alcohol) film with high mechanical performance, ACS Applied Materials & Interfaces 6 (2014) 15154–15161.
[24] Y. Cao, G. Li, X. Li, Graphene/layered double hydroxide nanocomposite: properties, synthesis, and applications, Chemical Engineering Journal 292 (2016) 207–223.
[25] N.A. Gonçalves, T.R.N. Caio, S.B. de Moraes, L.M.F. Lona, Synthesis and characterization of biodegradable poly (L-lactide)/layered double hydroxide nanocomposites, Polymer Bulletin 71 (2014) 2235–2245.
[26] S. Huang, X. Cen, H. Zhu, Z. Yang, Y. Yang, W.W. Tjiu, T. Liu, Facile preparation of poly (vinyl alcohol) nanocomposites with pristine layered double hydroxides, Materials Chemistry and Physics 130 (2011) 890–896.
[27] M.-F. Chiang, E.-C. Chen, T.-M. Wu, Preparation, mechanical properties and thermal stability of poly (L-lactide)/γ-polyglutamate-modified layered double hydroxide nanocomposites, Polymer Degradation and Stability 97 (2012) 995–1001.
[28] F.L. Theiss, G.A. Ayoko, R.L. Frost, Synthesis of layered double hydroxides containing Mg^{2+}, Zn^{2+}, Ca^{2+} and Al^{3+} layer cations by co-precipitation methods—a review, Applied Surface Science 383 (2016) 200–213.
[29] S. Mallakpour, M. Dinari, Intercalation of amino acid containing chiral dicarboxylic acid between Mg–Al layered double hydroxide, Journal of Thermal Analysis and Calorimetry 119 (2015) 1123–1130.
[30] S. Mallakpour, M. Dinari, V. Behranvand, Design of one-pot green protocol for the synthesis of novel modified LDHs with diacids based on amino acids: morphology and thermal examinations, Journal of the Iranian Chemical Society 13 (2016) 1635–1642.
[31] M.-F. Chiang, M.-Z. Chu, T.-M. Wu, Effect of layered double hydroxides on the thermal degradation behavior of biodegradable poly (L-lactide) nanocomposites, Polymer Degradation and Stability 96 (2011) 60–66.
[32] J. Qu, Q. Zhang, X. Li, X. He, S. Song, Mechanochemical approaches to synthesize layered double hydroxides: a review, Applied Clay Science 119 (2016) 185–192.
[33] Q. Zhou, V. Verney, S. Commereuc, I.-J. Chin, F. Leroux, Strong interfacial attrition developed by oleate/layered double hydroxide nanoplatelets dispersed into poly (butylene succinate), Journal of Colloid and Interface Science 349 (2010) 127–133.
[34] M. Zubitur, M. Gomez, M. Cortazar, Structural characterization and thermal decomposition of layered double hydroxide/poly (p-dioxanone) nanocomposites, Polymer Degradation and Stability 94 (2009) 804–809.
[35] M. Sajid, C. Basheer, Layered double hydroxides: emerging sorbent materials for analytical extractions, TrAC Trends in Analytical Chemistry 75 (2016) 174–182.
[36] F.L. Theiss, G.A. Ayoko, R.L. Frost, Removal of boron species by layered double hydroxides: a review, Journal of Colloid and Interface Science 402 (2013) 114–121.
[37] Y. Gao, J. Wu, Q. Wang, C.A. Wilkie, D. O'Hare, Flame retardant polymer/layered double hydroxide nanocomposites, Journal of Materials Chemistry A 2 (2014) 10996–11016.
[38] S. Li, B. Bhushan, Lubrication performance and mechanisms of Mg/Al-, Zn/Al-, and Zn/Mg/Al-layered double hydroxide nanoparticles as lubricant additives, Applied Surface Science 378 (2016) 308–319.

[39] D. Basu, A. Das, K.W. Stöckelhuber, U. Wagenknecht, G. Heinrich, Advances in layered double hydroxide (LDH)-based elastomer composites, Progress in Polymer Science 39 (2014) 594–626.
[40] K.-H. Goh, T.-T. Lim, Z. Dong, Application of layered double hydroxides for removal of oxyanions: a review, Water Research 42 (2008) 1343–1368.
[41] Z. Gu, J.J. Atherton, Z.P. Xu, Hierarchical layered double hydroxide nanocomposites: structure, synthesis and applications, Chemical Communications 51 (2015) 3024–3036.
[42] M.-F. Chiang, T.-M. Wu, Intercalation of γ-PGA in Mg/Al layered double hydroxides: an in situ WAXD and FTIR investigation, Applied Clay Science 51 (2011) 330–334.
[43] S. Mallakpour, M. Dinari, V. Behranvand, Ultrasonic-assisted synthesis and characterization of layered double hydroxides intercalated with bioactive N, N′-(pyromellitoyl)-bis-L-α-amino acids, RSC Advances 3 (2013) 23303–23308.
[44] S. Elbasuney, Surface engineering of layered double hydroxide (LDH) nanoparticles for polymer flame retardancy, Powder Technology 277 (2015) 63–73.
[45] S. Mallakpour, M. Dinari, M. Hatami, Modification of Mg/Al-layered double hydroxide with L-aspartic acid containing dicarboxylic acid and its application in the enhancement of the thermal stability of chiral poly (amide-imide), RSC Advances 4 (2014) 42114–42121.
[46] S. Mallakpour, M. Dinari, Facile synthesis of nanocomposite materials by intercalating an optically active poly (amide-imide) enclosing (L)-isoleucine moieties and azobenzene side groups into a chiral layered double hydroxide, Polymer 54 (2013) 2907–2916.
[46a] X. Zhang, et al., Biodegradable medical polymers: fundamental sciences, in: X. Zhang (Ed.), Science and Principles of Biodegradable and Bioresorbable Medical Polymers: Materials and Properties, Woodhead Publishing Series in Biomaterials: Number 117, 2017, pp. 1–33.
[47] L. Averous, E. Pollet, Biodegradable polymers, in: Environmental Silicate Nano-Biocomposites, Springer, 2012, pp. 13–39.
[48] E. Chiellini, R. Solaro, Biodegradable Polymers and Plastics, Springer Science & Business Media, 2012.
[48a] P. Dobrzynski, et al., Synthetic biodegradable medical polyesters: poly (trimethylene carbonate), in: X. Zhang (Ed.), Science and Principles of Biodegradable and Bioresorbable Medical Polymers: Materials and Properties, Woodhead Publishing Series in Biomaterials: Number 117, 2017, pp. 107–152.
[48b] S.M.A.S. Keshk, M. Gouda, Natural biodegradable medical polymers: cellulose, in: X. Zhang (Ed.), Science and Principles of Biodegradable and Bioresorbable Medical Polymers: Materials and Properties, Woodhead Publishing Series in Biomaterials: Number 117, 2017, pp. 279–294.
[49] I. Armentano, M. Dottori, E. Fortunati, S. Mattioli, J. Kenny, Biodegradable polymer matrix nanocomposites for tissue engineering: a review, Polymer Degradation and Stability 95 (2010) 2126–2146.
[50] M. Dziadek, E. Stodolak-Zych, K. Cholewa-Kowalska, Biodegradable ceramic-polymer composites for biomedical applications: a review, Materials Science and Engineering: C 95 (2016) 1175–1191.
[50a] S. Li, Synthetic biodegradable medical polyesters, in: X. Zhang (Ed.), Science and Principles of Biodegradable and Bioresorbable Medical Polymers: Materials and Properties, Woodhead Publishing Series in Biomaterials: Number 117, 2017, pp. 37–78.
[51] P. Visakh, Polyhydroxyalkanoates (PHAs), their blends, composites and nanocomposites: state of the art, new challenges and opportunities, in: R. Ipsita, P.M. Visakh (Eds.), Polyhydroxyalkanoate (PHA) based Blends, Composites and Nanocomposites, RSC Green Chemistry, 2014, pp. 1–17.

[52] V. Ojijo, S.S. Ray, Processing strategies in bionanocomposites, Progress in Polymer Science 38 (2013) 1543–1589.
[53] C.-Y. Ciou, S.-Y. Li, T.-M. Wu, Morphology and degradation behavior of poly (3-hydroxybutyrate-*co*-3-hydroxyvalerate)/layered double hydroxides composites, European Polymer Journal 59 (2014) 136–143.
[54] N. Gerds, V. Katiyar, C.B. Koch, H.C.B. Hansen, D. Plackett, E.H. Larsen, J. Risbo, Degradation of L-polylactide during melt processing with layered double hydroxides, Polymer Degradation and Stability 97 (2012) 2002–2009.
[55] S.S. Shafiei, M. Shavandi, G. Ahangari, F. Shokrolahi, Electrospun layered double hydroxide/poly (ε-caprolactone) nanocomposite scaffolds for adipogenic differentiation of adipose-derived mesenchymal stem cells, Applied Clay Science 127 (2016) 52–63.
[56] Y. Kuang, L. Zhao, S. Zhang, F. Zhang, M. Dong, S. Xu, Morphologies, preparations and applications of layered double hydroxide micro-/nanostructures, Materials 3 (2010) 5220–5235.
[57] H.-M. Zhang, P. Stewart, C.-H. Zhu, W.-J. Liu, A. Hexemer, E. Schaible, Thermal stability and thermal aging of poly (vinyl chloride)/MgAl layered double hydroxides composites, Chinese Journal of Polymer Science 34 (2016) 542–551.
[58] C.D. Papaspyrides, P. Kiliaris, Polymer Green Flame Retardants, Newnes, 2014.
[59] S. Mallakpour, M. Dinari, A. Nabiyan, A facile and simple synthetic strategy for the preparation of modified NiAl-layered double hydroxide as nanofiller for L-phenylalanine containing poly (amide-imide) s based nanocomposites, Designed Monomers and Polymers 18 (2015) 550–556.
[60] D.-Y. Wang, Novel Fire Retardant Polymers and Composite Materials, Woodhead Publishing, 2016.
[61] D.-Y. Wang, A. Leuteritz, Y.-Z. Wang, U. Wagenknecht, G. Heinrich, Preparation and burning behaviors of flame retarding biodegradable poly (lactic acid) nanocomposite based on zinc aluminum layered double hydroxide, Polymer Degradation and Stability 95 (2010) 2474–2480.
[62] Y.-C. Li, Y.-H. Yang, J.R. Shields, R.D. Davis, Layered double hydroxide-based fire resistant coatings for flexible polyurethane foam, Polymer 56 (2015) 284–292.
[63] J. Cai, H.-M. Heng, X.-P. Hu, Q.-K. Xu, F. Miao, A facile method for the preparation of novel fire-retardant layered double hydroxide and its application as nanofiller in UP, Polymer Degradation and Stability 126 (2016) 47–57.
[64] M. Zubitur, A. Mugica, J. Areizaga, M. Cortázar, Morphology and thermal properties relationship in poly (p-dioxanone)/layered double hydroxides nanocomposites, Colloid and Polymer Science 288 (2010) 809–818.
[65] K. Zhou, Y. Hu, J. Liu, Z. Gui, S. Jiang, G. Tang, Facile preparation of layered double hydroxide/MoS_2/poly (vinyl alcohol) composites, Materials Chemistry and Physics 178 (2016) 1–5.
[66] C.-X. Zhao, Y. Liu, D.-Y. Wang, D.-L. Wang, Y.-Z. Wang, Synergistic effect of ammonium polyphosphate and layered double hydroxide on flame retardant properties of poly (vinyl alcohol), Polymer Degradation and Stability 93 (2008) 1323–1331.
[67] G. Fan, F. Li, D.G. Evans, X. Duan, Catalytic applications of layered double hydroxides: recent advances and perspectives, Chemical Society Reviews 43 (2014) 7040–7066.
[68] Z.P. Xu, J. Zhang, M.O. Adebajo, H. Zhang, C. Zhou, Catalytic applications of layered double hydroxides and derivatives, Applied Clay Science 53 (2011) 139–150.
[69] R. Mahdi, C. Guérard-Hélaine, C. Laroche, P. Michaud, V. Prévot, C. Forano, M. Lemaire, Polysaccharide-layered double hydroxide–aldolase biohybrid beads for biocatalysed CC bond formation, Journal of Molecular Catalysis B: Enzymatic 122 (2015) 204–211.

[70] X. Kong, X. Rao, J. Han, M. Wei, X. Duan, Layer-by-layer assembly of bi-protein/layered double hydroxide ultrathin film and its electrocatalytic behavior for catechol, Biosensors & Bioelectronics 26 (2) (2010) 549–554.
[71] T. Zhan, Q. Yang, Y. Zhang, X. Wang, J. Xu, W. Hou, Structural characterization and electrocatalytic application of hemoglobin immobilized in layered double hydroxides modified with hydroxyl functionalized ionic liquid, Journal of Colloid and Interface Science 433 (2014) 49–57.
[72] M.V. Reddy, N.T.K. Lien, G.C.S. Reddy, K.T. Lim, Y.T. Jeong, Polymer grafted layered double hydroxides (LDHs-g-POEGMA): a highly efficient reusable solid catalyst for the synthesis of chromene incorporated dihydroquinoline derivatives under solvent-free conditions, Green Chemistry 18 (2016) 4228–4239.
[73] G.C. Pradhan, S. Dash, S.K. Swain, Barrier properties of nano silicon carbide designed chitosan nanocomposites, Carbohydrate Polymers 134 (2015) 60–65.
[74] M. Du, W. Ye, W. Lv, H. Fu, Q. Zheng, Fabrication of high-performance poly (vinyl alcohol)/MgAl-layered double hydroxide nanocomposites, European Polymer Journal 61 (2014) 300–308.
[75] M.-F. Chiang, T.-M. Wu, Preparation and characterization of melt processed poly (L-lactide)/layered double hydroxide nonocomposites, Composites Part B: Engineering 43 (2012) 2789–2794.
[76] M. Yadollahi, H. Namazi, S. Barkhordari, Preparation and properties of carboxymethyl cellulose/layered double hydroxide bionanocomposite films, Carbohydrate Polymers 108 (2014) 83–90.
[77] J. Xie, K. Zhang, J. Wu, G. Ren, H. Chen, J. Xu, Bio-nanocomposite films reinforced with organo-modified layered double hydroxides: preparation, morphology and properties, Applied Clay Science 126 (2016) 72–80.
[78] D. Wu, P.R. Chang, X. Ma, Preparation and properties of layered double hydroxide–carboxymethylcellulose sodium/glycerol plasticized starch nanocomposites, Carbohydrate Polymers 86 (2011) 877–882.
[79] Y. Dou, A. Zhou, T. Pan, J. Han, M. Wei, D.G. Evans, X. Duan, Humidity-triggered self-healing films with excellent oxygen barrier performance, Chemical Communications 50 (2014) 7136–7138.
[80] T. Pan, S. Xu, Y. Dou, X. Liu, Z. Li, J. Han, H. Yan, M. Wei, Remarkable oxygen barrier films based on a layered double hydroxide/chitosan hierarchical structure, Journal of Materials Chemistry A 3 (2015) 12350–12356.
[81] S. Barkhordari, M. Yadollahi, Carboxymethyl cellulose capsulated layered double hydroxides/drug nanohybrids for Cephalexin oral delivery, Applied Clay Science 121 (2016) 77–85.
[82] Y. Kuthati, R.K. Kankala, C.-H. Lee, Layered double hydroxide nanoparticles for biomedical applications: current status and recent prospects, Applied Clay Science 112 (2015) 100–116.
[83] S. Saha, S. Ray, R. Acharya, T.K. Chatterjee, J. Chakraborty, Magnesium, zinc and calcium aluminium layered double hydroxide-drug nanohybrids: a comprehensive study, Applied Clay Science 135 (2016) 493–509.
[84] M.A. Rocha, P.A. Petersen, E. Teixeira-Neto, H.M. Petrilli, F. Leroux, C. Taviot-Gueho, V.R. Constantino, Layered double hydroxide and sulindac coiled and scrolled nanoassemblies for storage and drug release, RSC Advances 6 (2016) 16419–16436.
[85] P. Sahoo, H. Panda, D. Bahadur, Studies on the stability and kinetics of drug release of dexamethasone phosphate intercalated layered double hydroxides nanohybrids, Materials Chemistry and Physics 142 (2013) 106–112.

[86] P.-R. Wei, S.-H. Cheng, W.-N. Liao, K.-C. Kao, C.-F. Weng, C.-H. Lee, Synthesis of chitosan-coated near-infrared layered double hydroxide nanoparticles for in vivo optical imaging, Journal of Materials Chemistry 22 (2012a) 5503–5513.
[87] V. Bugatti, G. Gorrasi, F. Montanari, M. Nocchetti, L. Tammaro, V. Vittoria, Modified layered double hydroxides in polycaprolactone as a tunable delivery system: in vitro release of antimicrobial benzoate derivatives, Applied Clay Science 52 (2011) 34–40.
[88] V. Rives, M. del Arco, C. Martín, Layered double hydroxides as drug carriers and for controlled release of non-steroidal antiinflammatory drugs (NSAIDs): a review, Journal of Controlled Release 169 (2013) 28–39.
[89] Y.-E. Miao, H. Zhu, D. Chen, R. Wang, W.W. Tjiu, T. Liu, Electrospun fibers of layered double hydroxide/biopolymer nanocomposites as effective drug delivery systems, Materials Chemistry and Physics 134 (2012) 623–630.
[90] E. Valarezo, L. Tammaro, S. González, O. Malagón, V. Vittoria, Fabrication and sustained release properties of poly (ε-caprolactone) electrospun fibers loaded with layered double hydroxide nanoparticles intercalated with amoxicillin, Applied Clay Science 72 (2013) 104–109.
[91] M.S. San Román, M.J. Holgado, B. Salinas, V. Rives, Drug release from layered double hydroxides and from their polylactic acid (PLA) nanocomposites, Applied Clay Science 71 (2013) 1–7.
[92] S. Barkhordari, M. Yadollahi, H. Namazi, pH sensitive nanocomposite hydrogel beads based on carboxymethyl cellulose/layered double hydroxide as drug delivery systems, Journal of Polymer Research 21 (2014) 1–9.
[93] A. Dong, X. Li, W. Wang, S. Han, J. Liu, J. Liu, J. Zhao, S. Xu, L. Deng, Layered double hydroxide modified by PEGylated hyaluronic acid as a hybrid nanocarrier for targeted drug delivery, Transactions of Tianjin University 22 (2016) 237–246.
[94] M. Chakraborti, J.K. Jackson, D. Plackett, S.E. Gilchrist, H.M. Burt, The application of layered double hydroxide clay (LDH)-poly (lactide-co-glycolic acid)(PLGA) film composites for the controlled release of antibiotics, Journal of Materials Science: Materials in Medicine 23 (2012) 1705–1713.
[95] N.K. Singh, Q.V. Nguyen, B.S. Kim, D.S. Lee, Nanostructure controlled sustained delivery of human growth hormone using injectable, biodegradable, pH/temperature responsive nanobiohybrid hydrogel, Nanoscale 7 (7) (2015) 3043–3054.
[96] C. Yang, T. Zhu, J. Wang, S. Chen, W. Li, Synthesis and characterization of flurbiprofen axetil-loaded electrospun MgAl-LDHs/poly (lactic-co-glycolic acid) composite nanofibers, RSC Advances 5 (2015) 69423–69429.
[97] E.I. Unuabonah, A. Taubert, Clay–polymer nanocomposites (CPNs): adsorbents of the future for water treatment, Applied Clay Science 99 (2014) 83–92.
[98] H. Chen, G. Qian, X. Ruan, R.L. Frost, Abatement of aqueous anionic contaminants by thermo-responsive nanocomposites: (poly (N-isopropylacrylamide))-*co*-silylanized magnesium/aluminun layered double hydroxides, Journal of Colloid and Interface Science 448 (2015) 65–72.
[99] M.-L. Chen, M.-I. An, Selenium adsorption and speciation with Mg–$FeCO_3$ layered double hydroxides loaded cellulose fibre, Talanta 95 (2012) 31–35.
[100] S. Mandal, S. Mayadevi, Cellulose supported layered double hydroxides for the adsorption of fluoride from aqueous solution, Chemosphere 72 (2008) 995–998.
[101] T. Hibino, Evaluation of anion adsorption properties of nanocomposite polymer hydrogels containing layered double hydroxides, Applied Clay Science 87 (2014) 150–156.

[102] H. Ai, X. Huang, Z. Zhu, J. Liu, Q. Chi, Y. Li, Z. Li, X. Ji, A novel glucose sensor based on monodispersed Ni/Al layered double hydroxide and chitosan, Biosensors & Bioelectronics 24 (2008) 1048–1052.
[103] L. Zeng, T. Zhao, Y. Li, Synthesis and characterization of crosslinked poly (vinyl alcohol)/layered double hydroxide composite polymer membranes for alkaline direct ethanol fuel cells, International Journal of Hydrogen Energy 37 (2012) 18425–18432.

Poly(vinyl alcohol)/carbon nanotube nanocomposites: challenges and opportunities

10

Shadpour Mallakpour, Shima Rashidimoghadam
Isfahan University of Technology, Isfahan, Islamic Republic of Iran

10.1 Introduction

10.1.1 Poly(vinyl alcohol)

Poly(vinyl alcohol) (PVA) is an odorless and tasteless, translucent, white or cream-colored granular powder, which is discovered by Herrman and Haehnel in 1928 [1]. PVA is a water-soluble, nontoxic, semicrystalline, biocompatible, and biodegradable polymer. It is widely utilized for various applications such as textile sizing, paper coating, flexible water-soluble packaging films, controlled drug delivery systems, dialysis membrane, wound dressing, and artificial skin. This broad range of applications is due to its outstanding properties such as high oxygen and aroma barrier properties, high tensile strength and flexibility, excellent film forming, emulsifying, and adhesive properties [2,3]. The melting point of PVA is 230°C and 180–190°C for the fully hydrolyzed and partially hydrolyzed grades, respectively. Its decomposition temperature is above 200°C and it can undergo pyrolysis at high temperatures. The vinyl alcohol tautomerizes to acetaldehyde, which is more stable than vinyl alcohol at room temperature. Thus, PVA is not built up in polymerization reactions from vinyl alcohol monomer. The basic monomer for PVA is vinyl acetate (VA). This polymer is prepared by the polymerization of VA to poly(vinyl acetate) (PVAc), followed by hydrolysis of PVAc to PVA with the use of either acid or base as a catalyst [4,5]. The sequence of reactions is shown in Fig. 10.1.

10.1.2 Carbon nanotubes

The discovery of the carbon nanotubes (CNTs) was credited to Iijima in 1991 [6]. Because of their exceptional properties such as tubelike morphology with large surface areas and aspect ratios, high electrical conductivity, excellent thermal conductivity, and high mechanical strength along their axes, CNTs are very valuable materials in most fields of materials science and technology [7–9]. They are novel allotropes of carbon with a seamless hollow cylindrical nanostructure, which are composed of carbon atoms linked in hexagonal shapes, with each carbon atom covalently bonded to three other carbon atoms. There are many various types of CNTs, but they are usually

Biodegradable and Biocompatible Polymer Composites. http://dx.doi.org/10.1016/B978-0-08-100970-3.00010-9

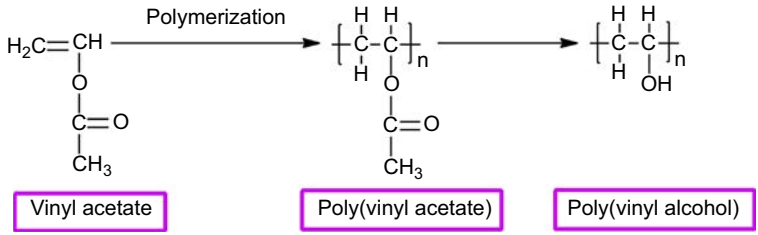

Figure 10.1 Synthesis of poly(vinyl alcohol).

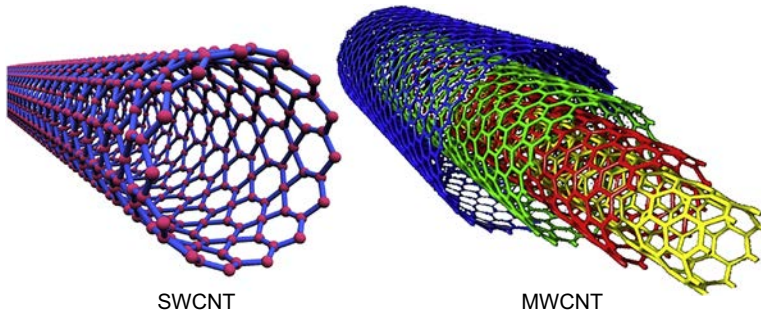

Figure 10.2 Types of carbon nanotubes. *MWCNT*, multiwalled carbon nanotube; *SWCNT*, single-walled carbon nanotube.

classified as either single-walled carbon nanotubes (SWCNTs) and multiwalled carbon nanotubes (MWCNTs) (Fig. 10.2).

SWCNTs comprise one atomic sheet of hexagonal carbon atom, which wrapped up to form a tube. The diameter of this tube typically ranges from 0.4 to over 3 nm, whereas MWCNTs have several concentric cylinders with diameter from 1.4 to over 100 nm [10].

10.1.2.1 Functionalization of carbon nanotube

Unfortunately, the uniform distribution and alignment of the CNTs in the polymer matrix is very difficult to attain because of the strong intertube van der Waals forces that attract the nanotubes together, resulting in the tubes to cluster [11]. It is essential to overcome this limitation because the homogeneity and stability of CNTs dispersion in a polymer matrix play a critical role in achieving high performance of the CNT–polymer composites [12]. The functionalization of CNTs has been suggested as an effective way to prevent the CNT aggregation, which leads to good dispersion of CNTs within a polymer matrix. Generally, there are two approaches for functionalization of CNTs, which involved covalent functionalization and noncovalent functionalization [13]. The covalent functionalization is performed by formation of covalent attachments between various functional groups and the π-conjugated skeleton of nanotubes. This functionalization occurs at the sidewall site (sidewall functionalization) of nanotubes or at the defect sites (defect functionalization) of

CNT. The disadvantage of this method is the destruction of the translational symmetry of CNTs by changing the hybridization of carbon atoms from sp^2 to sp^3, resulting in considerable changes in their physical properties such as electronic and transport. The covalent functionalization of CNTs with polymers (polymer grafting) is emerging as a very promising method for fabrication of CNT–polymer NCs. Covalent grafting of polymers to CNTs is carried out by two methods: "grafting to" and "grafting from." In the "grafting to" method, the polymer molecules with functional end/side groups (e.g., —OH, —NH_2, —COOH, and —COCl), are connected to surface of pure, oxidized, or prefunctionalized CNTs, via chemical reactions. In this method, the attached polymer content is limited. In "grafting from" technique, the polymer is attached to the CNT walls through in situ polymerization of monomers in presence of reactive CNTs or CNT-supported initiators. This approach promises high graft densities rather than in the case of the "grafting to" method. Noncovalent functionalization is mostly based on adsorption or wrapping of different organic moieties by hydrogen bonds, van der Waals force, π-stacking interactions, and electrostatic forces onto the skeleton of the CNTs. This kind of functionalization does not demolish the electronic network of the tubes, and consequently it does not influence the final structural properties of the CNTs but improves solubility and processability [14–16].

10.1.3 Carbon nanotube–polymer nanocomposites

Polymer NCs are organic/inorganic materials, in which low quantities of inorganic component in the nanoscale (typically less than 100 nm) is dispersed in a polymer. These materials have been extensively investigated due to their extraordinary combinations of properties of each of the components or giving novel and unique properties that are difficult to achieve from the individual components. As mentioned above, polymer NCs are filled with nanometer scale fillers, thus the filler–polymer interactions are enhanced in comparison with conventional composites. This leads to the high-performance composite materials, which are suitable for various applications [17–19]. There are three common techniques utilized to dispersion of nanofillers in polymer matrix to produce NCs: melt blending, in situ polymerization, and the solvent method. The melt blending method involves heating a polymer and the filler mixture under shear, usually in an extruder, above the melting point or above the glass transition temperature (T_g) of polymers. The drawback of this technique is that the uniform distribution of filler is difficult to achieve, especially in nonpolar polymers. In situ polymerization approach starts by preparing a monomer solution or liquid monomer containing the fillers followed by polymerization of obtained mixture by standard polymerization methods. In this method, covalent bonds are formed between the polymer and the filler surfaces. Solution blending is done by mixing filler and polymer in a solvent. After removal of the solvent, the composites are obtained. This method brings about a good molecular level of mixing and can overcome the limitations of melt mixing [20–23]. Different types of fillers, such as CNTs [24,25], carbon black [26,27], clay [28–30], metal oxides [31–34], layered double hydroxide (LDH) [35–37], and graphene [38] were used for the synthesis of polymer NCs. Among these

filler materials, CNTs have been receiving significant attention recently owing to their unique properties such as extraordinarily high aspect ratios, high electrical and thermal conductivity, chemical stability, unique atomic structures, and very high tensile strength, making them ideal reinforcing materials in NCs [39–41]. Since the fabrication of CNTs/polymer NCs in 1994 for the first time [42], they hold particular attention because the combination of polymers and CNTs allows one to prepare the NCs with enhanced properties promising to be utilized for various applications [43]. In this chapter, we described the incorporation of CNTs into PVA matrix to yield PVA/CNT NCs. We will not effort to report in detail all of the fabricated CNT–reinforced PVA composites but will present an updated overview on the different synthetic methods, characterization, and applications of various PVA/CNT NCs published in the years of 2014–2017. These NCs possess advantages of PVA such as high biodegradability and good mechanical properties.

10.2 Synthesis of poly(vinyl alcohol)/carbon nanotube nanocoposites

Compared to other NCs, PVA/CNT NCs have received a great deal of attention in recent years because their unique properties produce many potentially commercial applications. Due to strong interaction between PVA and SWCNTs as well as MWCNTs, PVA/CNT NCs show unique properties, which are not found in other polymer/CNT NCs. Therefore, numerous experimental investigations have been reported for fabrication of PVA/CNT NCs. This chapter is an overview of the recent advances in preparation, characterization, and properties of PVA/CNT (SWCNT and MWCNT) NCs.

Capacitive deionization (CDI) is a technology to deionize water by applying an electrical potential difference over two porous carbon electrodes [44]. Hou et al. fabricated a composite electrode by introduction of MWCNTs as filler into PVA matrix to attain high ion removal capacity and effective surface area for CDI. The results showed that the obtained NCs electrode demonstrated a high hydrophilicity, very good capacitive performance, and excellent electrochemical stability. The SEM and TEM micrographs of the MWCNTs, macroscopic view of the NCs, and optical micrographs of the water contact angle on the electrode surface are shown in Fig. 10.3. The contact angle formed by water drop on the NCs surface is 60.3 degrees, showing high hydrophilic properties (Fig. 10.3(d)). The NCs electrode can enhance inner surface sites to be penetrated by ions because of wetted surface area. Therefore, electrosorption of ions was enhanced by enhancing the hydrophilicity of the NCs electrode [45].

Mallakpour et al. reported the synthesis of PVA/amino acid–functionalized MWCNT NCs using the solution casting method. They functionalized the surface of MWCNTs by L-phenylalanine, and various amounts of L-phenylalanine-functionalized MWCNTs (1, 3, and 5 wt%) were incorporated in PVA matrix. TEM images (Fig. 10.4) showed uniform distribution of functionalized MWCNT in PVA matrix due to strong H-bonding between OH, NH, and carbonyl groups on the MWCNT surface and the hydroxyl groups of PVA (Fig. 10.5). The obtained NCs are expected to have potential application in new types of coatings and adhesives [46].

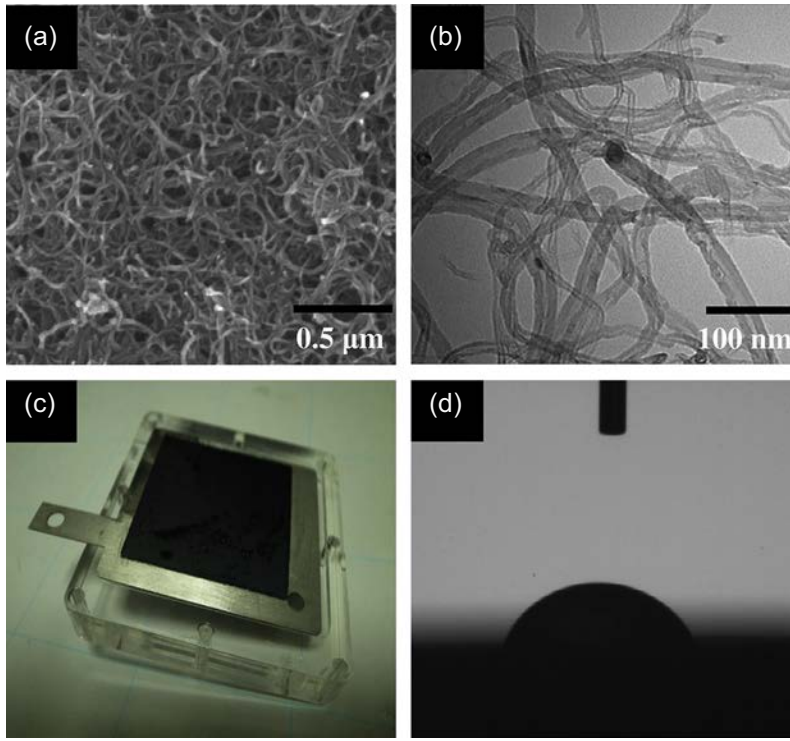

Figure 10.3 (a) SEM image and (b) TEM micrograph for the multiwalled carbon nanotubes (MWCNTs) used in the experiments, (c) macroscopic view of the MWCNT/poly(vinyl alcohol) composite electrode, and (d) optical micrographs of the water contact angle on the electrode surface.
Adapted from C.-H. Hou, N.-L. Liu, H.-L. Hsu, W. Den, Development of multi-walled carbon nanotube/poly(vinyl alcohol) composite as electrode for capacitive deionization, Separation and Purification Technology 130 (2014) 7–14. With kind permission of Elsevier.

Ding et al. prepared the MWCNTs-COOH/PVA composites via new, simple, less time-consuming, and environmentally friendly two-step method: electrospinning and swelling in water. Different concentrations of MWCNTs-COOH (5, 10, 20, 30, 40 mg/mL) were embedded in PVA. The results showed that the conductivity of NCs significantly improved by increasing the MWCNTs-COOH loading in the composites. Conductivity can be determined by the intertube contact area. When the concentration of MWCNTs-COOH increased, the intertube contact area was increased, resulting in higher electrical conductivity. The optimum MWCNTs-COOH concentration for the generation of high tensile strength was found to be 30 mg/mL [47].

Malikov et al. synthesized MWCNTs by chemical vapor deposition (CVD) over Fe–Co/alumina as catalyst. Afterward, they oxidized the fabricated MWCNTs by $KMnO_4$ solution to form carboxyl groups on wall defects and end caps. After incorporation of the oxidized MWCNTs in PVA matrix, they were connected to polymer via Fischer esterification reaction. The presence of defects on the MWCNT walls

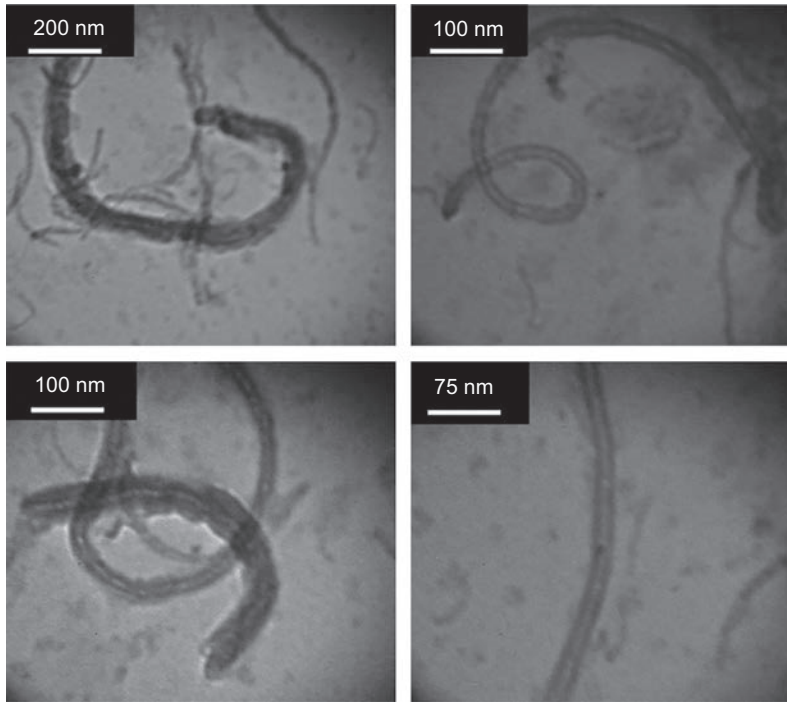

Figure 10.4 TEM photographs of poly(vinyl alcohol)/amino acid–functionalized multiwalled carbon nanotubes composite (5 wt%).
Adapted from S. Mallakpour, A. Abdolmaleki, S. Borandeh, L-Phenylalanine amino acid functionalized multi walled carbon nanotube (MWCNT) as a reinforced filler for improving mechanical and morphological properties of poly(vinyl alcohol)/MWCNT composite, Progress in Organic Coatings 77 (2014) 1966–1971. With kind permission of Elsevier.

is evident from TEM and SEM images and these micrographs revealed that PVA is attached primarily to these defects [48].

Amirilargani et al. incorporated MWCNTs into PVA matrix to fabricate PVA NC membranes with treatment of MWCNTs by poly(sodium 4-styrenesulfonate) (PSS), a noncovalent functionalization agent. HRTEM micrographs demonstrated that PSS completely covers the outer surface of the MWCNTs, and field emission SEM images confirmed that the uniform dispersion of PSS-wrapped MWCNTs in the PVA matrix was achieved (Fig. 10.6). The pervaporation performances of NC membranes with different contents of MWCNTs-PSS for the dehydration of isopropanol (IPA) were evaluated under different operating conditions. The results showed that membrane performance was improved by introduction of MWCNTs-PSS to the PVA matrix [49].

Rahy et al. dispersed CNTs in PVA matrix using simple and green method to obtain a composite with high mechanical properties. In this process, composite fibers were prepared using a PVA layer precoated on a polyethylene terephthalate (PET) film (Fig. 10.7).

The fibers were thermally annealed at the range of 130–180°C for 30 min under tension by taping both ends of each fiber to find an optimum annealing temperature.

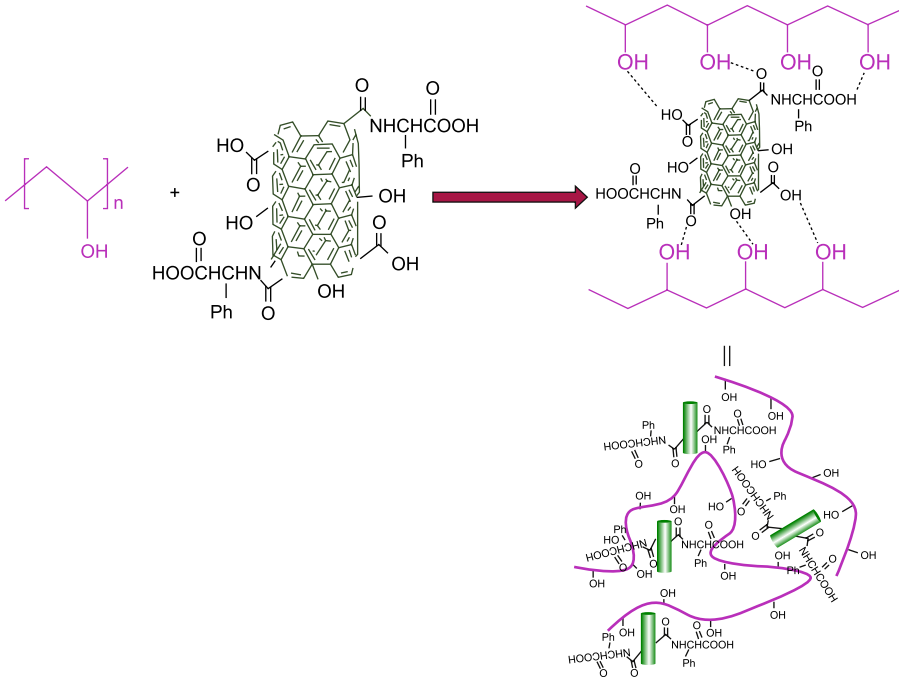

Figure 10.5 Interaction between poly(vinyl alcohol) and amino acid–functionalized multi-walled carbon nanotubes.
Adapted from S. Mallakpour, A. Abdolmaleki, S. Borandeh, L-Phenylalanine amino acid functionalized multi walled carbon nanotube (MWCNT) as a reinforced filler for improving mechanical and morphological properties of poly(vinyl alcohol)/MWCNT composite, Progress in Organic Coatings 77 (2014) 1966–1971. With kind permission of Elsevier.

The effect of thermal annealing on the mechanical properties of PVA/CNT composite fibers was investigated. The results showed the best results were achieved at 160°C: 1.9 GPa tensile strength and 117 GPa Young's modulus (Fig. 10.8). At the annealing temperature of 160°C, cross-linking of —OH groups of PVA was occurred, which increased mechanical strength of the composite fibers [50].

Kishore et al. showed that PVA-CNT composite can act as an organic insulator to manufacture Si/PVA/CNT/PVA/Al metal–insulator–semiconductor-type memory devices. They synthesized the CNT by CVD method using nickel-coated stainless steel (Ni/SS) prepared by electrophoretic deposition. CNT was dispersed into PVA without any difficult functionalization reaction and acted as an excellent charge storage node for the memory device [51]. Jose et al. investigated the effect of acid-functionalized MWCNT on the dielectric and conductivity properties of the PVA NC membranes. The pristine MWCNT was treated with 2:3 ratio H_2SO_4 and HNO_3 mixture. PVA/MWCNT NCs were fabricated by incorporation of various amounts of acid-functionalized MWCNT (0.5, 1, 1.5, and 2 wt%) into PVA matrix via solution casting technique. The possible interaction between polymer and filler is shown in Fig. 10.9.

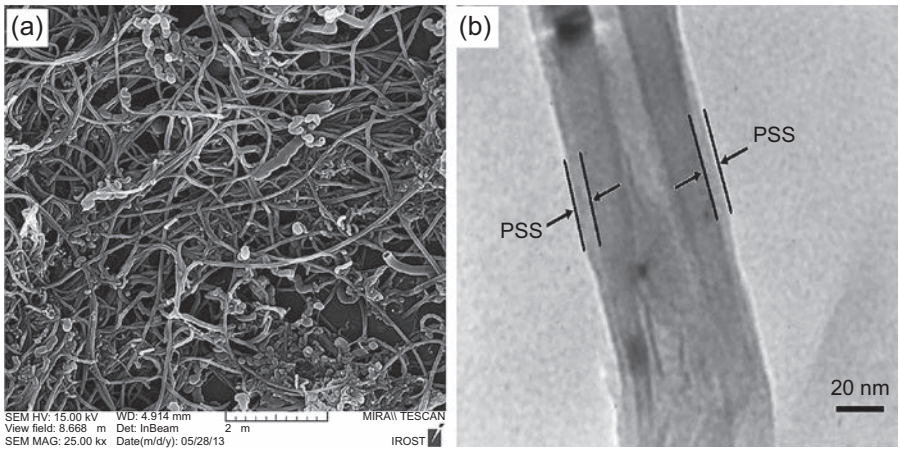

Figure 10.6 (a) Field emission SEM and (b) high-resolution TEM images of MWCNTs-poly(sodium 4-styrenesulfonate).
Adapted from M. Amirilargani, M.A. Tofighy, T. Mohammadi, B. Sadatnia, Novel poly(vinyl alcohol)/multiwalled carbon nanotube nanocomposite membranes for pervaporation dehydration of isopropanol: poly(sodium 4-styrenesulfonate) as a functionalization agent, Industrial & Engineering Chemistry Research 53 (2014) 12819–12829. With kind permission of American Chemical Society.

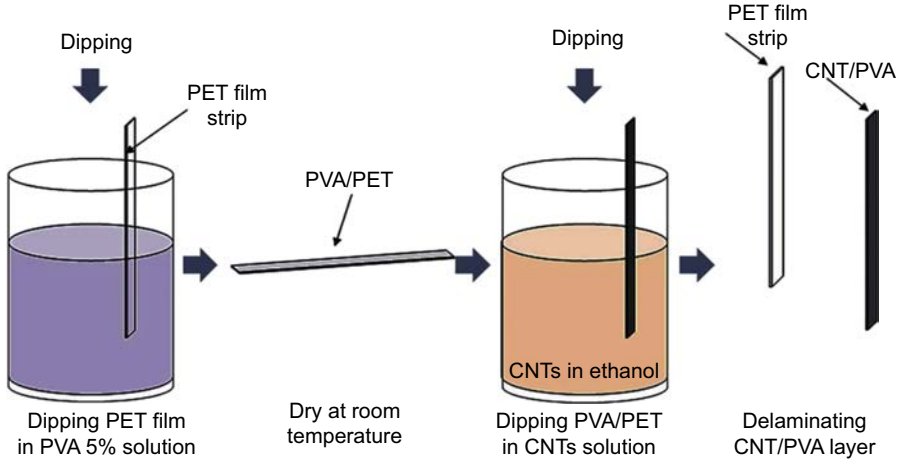

Figure 10.7 Schematic diagram of composite carbon nanotube (CNT) fabrication process. *PET*, polyethylene terephthalate; *PVA*, poly(vinyl alcohol).
Adapted from A. Rahy, A. Choudhury, C. Kim, S. Ryu, J. Hwang, S.H. Hong, D.J. Yang, A simple/green process for the preparation of composite carbon nanotube fibers/yarns, RSC Advances 4 (2014) 43235–43240. With kind permission of Royal Society of Chemistry.

They demonstrated that PVA/MWCNT NCs with 1.5 wt% loading of CNTs demonstrated better dielectric properties. The pervaporation performance of the prepared NC membranes was also studied. The NC membranes were utilized for the separation of azeotropic composition of water–ethanol mixture. The variation of flux and separation

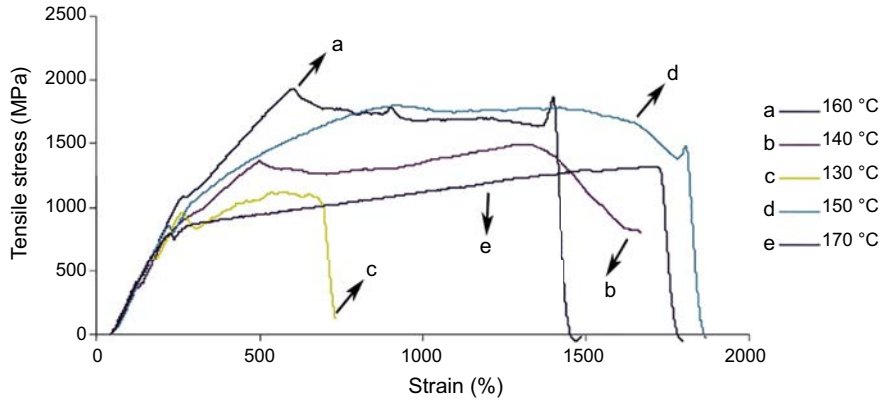

Figure 10.8 The effects of thermal annealing on the stress–strain behavior of the poly(vinyl alcohol)/multiwalled carbon nanotube composite fibers.
Adapted from A. Rahy, A. Choudhury, C. Kim, S. Ryu, J. Hwang, S.H. Hong, D.J. Yang, A simple/green process for the preparation of composite carbon nanotube fibers/yarns, RSC Advances 4 (2014) 43235–43240. With kind permission of Royal Society of Chemistry.

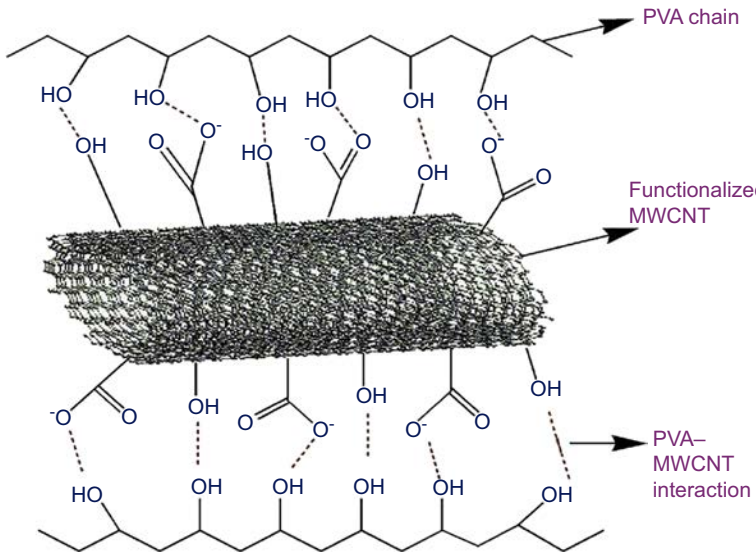

Figure 10.9 Schematic representation for the interaction and dispersion of acid-functionalized multiwalled carbon nanotube (MWCNT) and poly(vinyl alcohol) (PVA) in the polymeric matrix.
Adapted from J. Thomasukutty, C.G. Soney, M. Maya, T. Sabu, Functionalized MWCNT and PVA nanocomposite membranes for dielectric and pervaporation applications, Chemical Engineering & Process Technology 6 (2015) 233–241. Open access journal.

factor is shown in Fig. 10.10. As can be seen, NCs with 0.5 wt% loading of CNT show optimum PV performance [52].

Escobar et al. explored the mechanical properties of PVA reinforced with various amounts of mechanically oriented CNTs (0.25, 0.5, and 1 wt%). The results

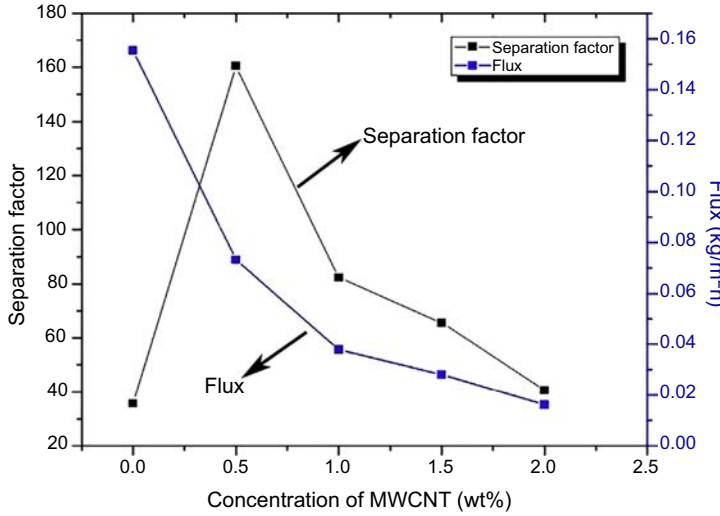

Figure 10.10 Variation of flux and separation factor of the poly(vinyl alcohol) nanocomposites with filler loading. *MWCNT*, multiwalled carbon nanotube.
Adapted from J. Thomasukutty, C.G. Soney, M. Maya, T. Sabu, Functionalized MWCNT and PVA nanocomposite membranes for dielectric and pervaporation applications, Chemical Engineering & Process Technology 6 (2015) 233–241. Open access journal.

demonstrated that the strength, stiffness, and hardness properties of the PVA enhanced the addition of CNTs below 0.5 wt%. Thus these materials can be used in structural applications. The thermal degradation temperature of the composite in about 100°C was enhanced by soaking the NC in ethanol, suggesting that, in particular for structural applications, is recommended a stabilization to enhance the resistance to degradation by humidity and temperature [53].

Lai et al. reported the preparation of environmentally friendly PVA/MWCNT composite fibers having a large amount of MWCNTs (>27.6 wt%) using wet-spinning process. The MWCNTs were functionalized by noncovalent and covalent functionalization method. Covalent functionalization was done to create several oxygen-containing groups on the sidewall of MWCNTs. Noncovalent functionalization was carried out by using PVA as the dispersant and matrix. The strong H-bond was formed between MWCNTs and PVA; thus uniform dispersion of MWCNTs in PVA matrix was obtained. They showed that as the content of MWCNTs increased, the mechanical properties of the PVA composite fibers enhanced significantly due to a uniform distribution of MWCNTs throughout PVA matrix and efficient stress transfer between MWCNTs and PVA matrix [54]. Preparation of cross-linked PVA NC membranes via introduction of various amounts of treated MWCNTs (TCN) into polymer matrix and using citric acid as the cross-linking agent was reported by Shameli et al. The NCs fabricated by solution casting and solvent evaporation method and employed as a separation element in a membrane reactor to improve the esterification of acetic acid with methanol using 15 wt% of Amberlyst 15 as the

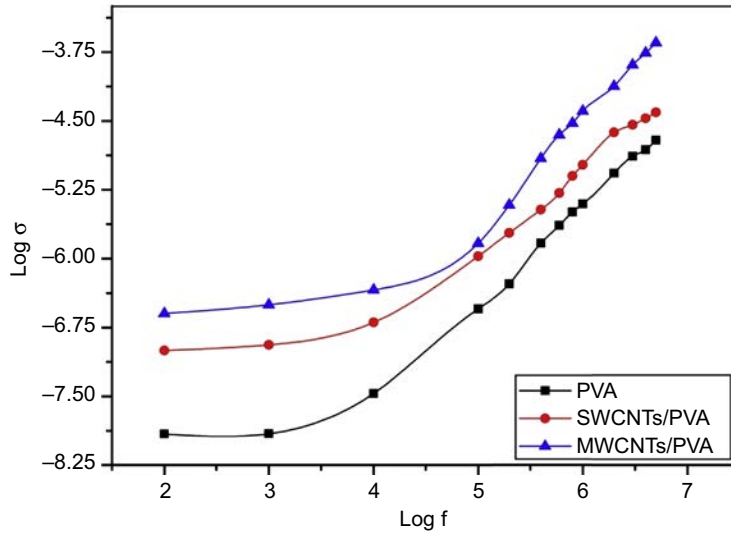

Figure 10.11 The AC conductivity of poly(vinyl alcohol) (PVA) with single-walled carbon nanotubes (SWCNTs) and multiwalled carbon nanotubes (MWCNTs).
Adapted from N.S. Alghunaim, Optimization and spectroscopic studies on carbon nanotubes/PVA nanocomposites. Results in Physics 6 (2016) 456–460. With kind permission of Elsevier.

heterogeneous catalyst. The results demonstrated that by increasing the amount of TCN, the acid conversion rate enhances. It was also indicated that the hybrid membranes had good separating properties for removing water from the reaction mixture. The final conversion of acid was increased from 52.30% to 99.25% using the membrane with 2 wt% TCN instead of the pure membrane at optimized condition and 4 h of operation [55]. Alghunaim utilized constant ratio of SWCNTs-COOH and MWCNTs-COOH for preparation of PVA-based NCs by dispersion methods with the aim of attaining the remarkable improvement in spectroscopic properties and AC conductivity at room temperature. Fig. 10.11 shows the AC conductivity of PVA, SWCNTs/PVA, and MWCNTs/PVA in frequencies ranging from 100 Hz to 5 MHz at room temperature.

The highest value of AC conductivity was recorded at 5 MHz, and AC conductivity of MWCNTs/PVA was higher than that of SWCNTs/PVA. This phenomenon can be explained by the fact that when CNTs are incorporated into polymer, effective conductive network is formed and CNTs begin to bridge gap separated between localized states and potential barrier, thus facilitating charge carrier transfer. As a result, it is concluded that the obtained NCs can be considered as semiconducting organic materials [56].

Composite nanofibers from PVA and different percentage of MWCNT (2–10 wt%.) were fabricated using electrospinning method by Wongon et al. They added sodium dodecylbenzenesulfonate (NaDDBS) surfactant into the MWCNTs solution system via ultrasonic technique for homogeneous distribution of MWCNTs in PVA/MWCNT

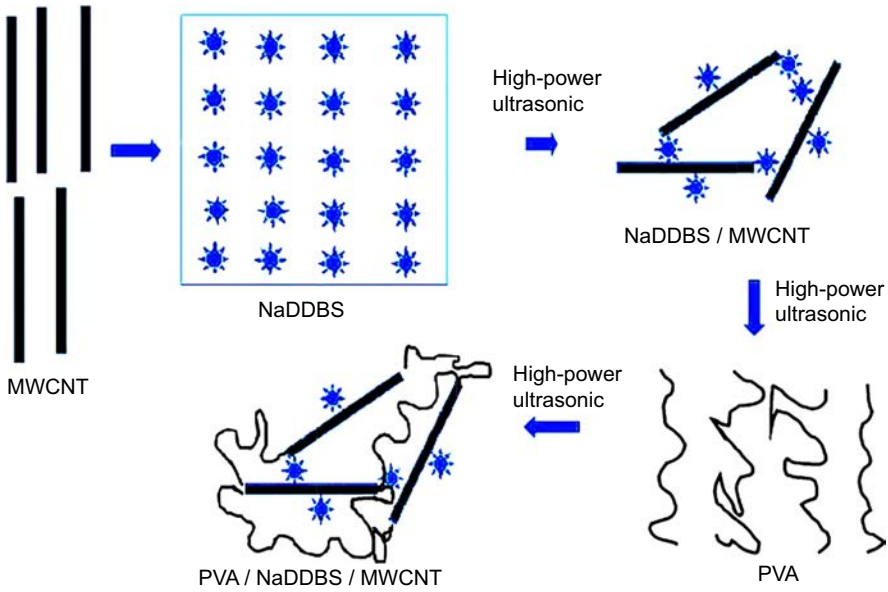

Figure 10.12 Schematic diagram of sodium dodecylbenzenesulfonate (NaDDBS) in poly(vinyl alcohol) (PVA)/multiwalled carbon nanotube (MWCNT)/NaDDBS/water system. Adapted from J. Wongon, S. Thumsorn, N. Srisawat, Poly(vinyl alcohol)/multiwalled carbon nanotubes composite nanofiber, Energy Procedia 89 (2016) 313–317. Open access journal.

composite nanofibers. The surfactant decreased the surface tension of CNTs and then decreased the CNTs aggregation (Fig. 10.12). SEM images showed that the MWCNT was uniformly dispersed in polymer matrix and the surface of PVA/MWCNT composite nanofibers was smooth [57]. Chen et al. utilized a novel method for fabrication of CNT/PVA NCs. In this method a hollow cylindrical CNT was synthesized and employed for fabrication of NCs by its in situ deposition under the spray of a PVA solution. They demonstrated that the properties of the obtained NCs are affected by the change in the amount of CNTs. The optimum CNT content for the generation of high electrical conductivity (1322 S/cm) and tensile strength (3.16 GPa) was found to be 56.8 wt%. These exceptional properties are superior to any other CNT/polymer NCs [58]. The adsorption behavior of heavy metal ions (Pb^{2+} and Cu^{2+}) from aqueous solutions was investigated onto the PVA/CNT NCs by Jing et al. The NCs were prepared by incorporation of CNTs into PVA–boric acid cross-linking via a facile technique. The results of adsorption experiments indicated that the NCs were good adsorbents for removing Pb^{2+} and Cu^{2+} ions and Freundlich adsorption isotherm fitted the experimental results [59].

Zhang et al. prepared the microcombed PVA/CNT NC films with excellent electrical and mechanical properties using simple, reliable, and reproducible method. The microcombed CNT/PVA composite films exhibited the electrical conductivity

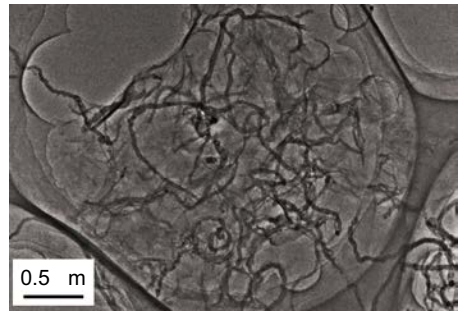

Figure 10.13 High-resolution TEM images of graphene/carbon nanotubes.
Adapted from H.-L. Ma, L. Zhang, Y. Zhang, S. Wang, C. Sun, H. Yu, X. Zeng, M. Zhai, Radiation preparation of graphene/carbon nanotubes hybrid fillers for mechanical reinforcement of poly(vinyl alcohol) films, Radiation Physics and Chemistry 118 (2016) 21–26. With kind permission of Elsevier.

of 1.84×10^5 S/m, Young's modulus of 119 GPa, tensile strength of 2.9 GPa, and toughness of 52.4 J/cm^3, which are much higher than reported values for uncombed samples. The enhancement in electrical conductivity could be attributed to the increased nanotube alignment, straightness, and packing by microcombing, which resulted in increased intertube contact area for more efficient electron transfer. Microcombing straightened the wavy CNTs and packed them denser and more uniformly, which improved their mechanical properties [60]. Ma et al. fabricated the graphene/CNT (G/CNTs) hybrid fillers by γ-ray radiation reduction of graphene oxide (GO) in presence of CNTs. The NC films were synthesized by incorporation of different amounts of G/CNTs (0.5, 0.75, and 1.0 wt%) hybrid fillers into the PVA matrix. High-resolution TEM analysis showed that the homogeneous dispersion of CNTs between the layers of graphene nanosheets was achieved due to the formation of interconnected 3D network structure (Fig. 10.13). This structure prevented the aggregation of nanotubes during the PVA NCs formation; thus the NCs with good mechanical properties were obtained [61].

Amrin et al. studied the dielectric relaxation and AC conductivity behavior of MWCNT-COOH/PVA NC films. The measurement temperature was varied in the range from 303 to 423K, and the frequency range was varied from 0.1 Hz to 1 MHz. The results showed that the dielectric constant increased with the incorporation of MWCNT-COOH in the PVA matrix. Also, with an increase in temperature and also with an increase in MWCNT-COOH amount, an increase in the dielectric constant was observed because of interfacial polarization [62].

Abdolmaleki et al. utilized microwave radiation for surface modification of MWCNTs-COOH using vitamin B_2 as a biological and safe molecule. The attachment of vitamin B_2 on the surface of MWCNTs was achieved via esterification reaction between —OH of vitamin B_2 and COOH groups of MWCNTs and also via formation of the π–π interactions between isoalloxazine ring of vitamin B_2 and the nanotube sidewall (Fig. 10.14). The different

amounts of MWCNTs-vitamin B_2 (3, 5, and 7 wt%) were incorporated into PVA matrix via solution casting method for preparation of PVA/MWCNTs-vitamin B_2 NC films.

The TEM analysis showed that the surface modification of MWCNTs was successfully carried out, and MWCNTs-vitamin B_2 is uniformly distributed in the PVA matrix with sizes around 20–60 nm (Figs. 10.15 and 10.16) [63].

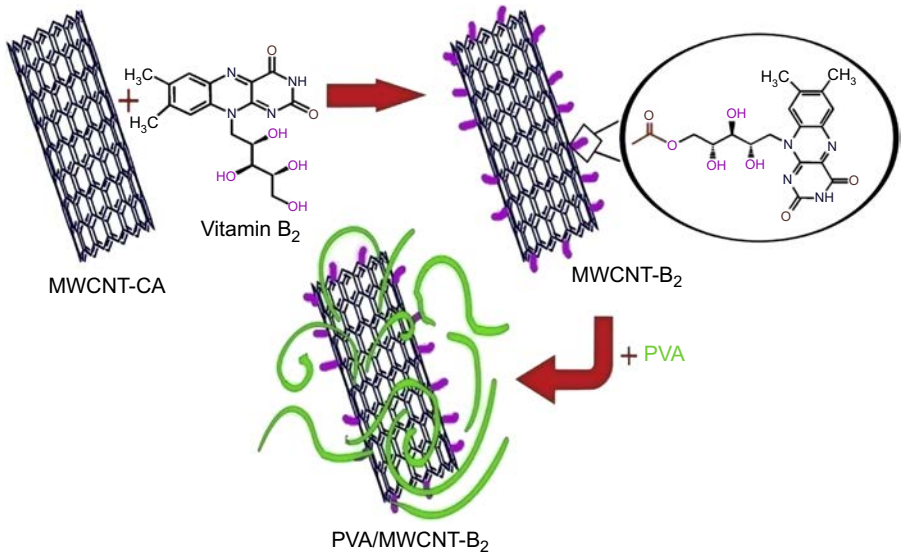

Figure 10.14 Surface modification of the multiwalled carbon nanotubes (MWCNTs) and schematic exhibition for preparation of poly(vinyl alcohol) (PVA)/MWCNTs-vitamin B_2 nanocomposite.
Adapted from A. Abdolmaleki, S. Mallakpour, F. Azimi, Microwave-assisted treatment of MWCNTs with vitamin B2: study on morphology, tensile and thermal behaviors of poly(vinyl alcohol) based nanocomposites, European Polymer Journal 87 (2017) 277–285. With kind permission of Elsevier.

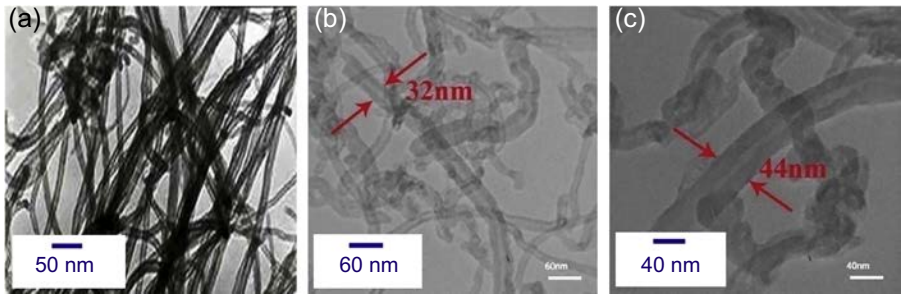

Figure 10.15 TEM images of multiwalled carbon nanotubes-COOH (a) and multiwalled carbon nanotubes-vitamin B_2 (b, c) with different magnifications.
Adapted from A. Abdolmaleki, S. Mallakpour, F. Azimi, Microwave-assisted treatment of MWCNTs with vitamin B2: study on morphology, tensile and thermal behaviors of poly(vinyl alcohol) based nanocomposites, European Polymer Journal 87 (2017) 277–285. With kind permission of Elsevier.

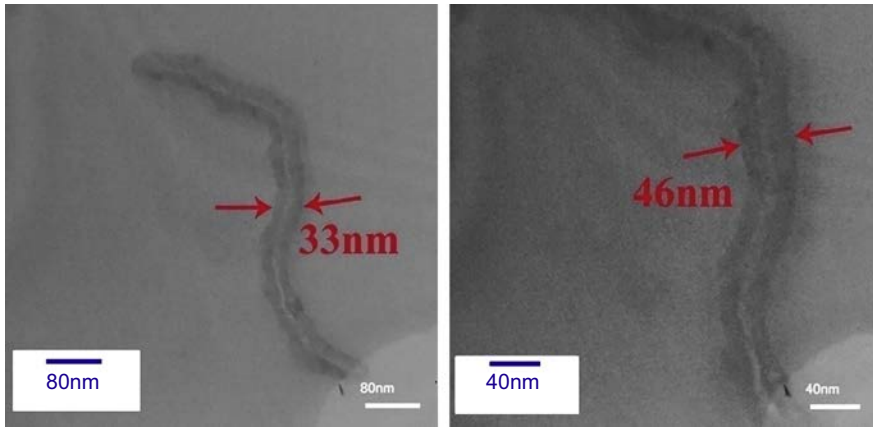

Figure 10.16 TEM images of poly(vinyl alcohol)/multiwalled carbon nanotubes-vitamin B_2 nanocomposites (7 wt%) with different magnifications.
Adapted from A. Abdolmaleki, S. Mallakpour, F. Azimi, Microwave-assisted treatment of MWCNTs with vitamin B2: study on morphology, tensile and thermal behaviors of poly(vinyl alcohol) based nanocomposites, European Polymer Journal 87 (2017) 277–285. With kind permission of Elsevier.

10.3 Conclusions

In recent years, polymer NCs have attracted considerable attention owing to their importance both in industry and in academia, as a result of their excellent properties and multifunctionality that are well usable in a variety of applications. With the purpose of fabrication of polymer NCs, several nanosized filler materials were incorporated into polymers. Owing to their superior properties such as high mechanical strength, large surface areas, and aspect ratios as well as their excellent thermal and electrical conductivities, CNTs can be employed as ideal fillers for preparation of high-performance polymer NCs. The polymer NCs that consist of PVA and CNTs are found to have unique characteristics and improved properties. This chapter presents the recent advances in synthesis and characterization, application, and resulting properties of PVA/CNT NCs. Because of strong interaction between surface of functionalized CNTs and functional groups of PVA, uniform dispersion of CNTs in PVA matrix is occurred and the obtained NCs show unique properties such as high ion removal capacity and effective surface area for CDI, higher electrical conductivity, high mechanical properties, and good adsorption capacity for removing Pb^{2+} and Cu^{2+} ions.

Acknowledgments

The authors wish to acknowledge financial support for this research from Research Affairs Division, Isfahan University of Technology (IUT), Isfahan, Iran. They also thank the Iran Nanotechnology Initiative Council (INIC), Tehran, Iran, National Elite Foundation (NEF), Tehran, Iran, and Center of Excellence in Sensors and Green Chemistry (IUT), Isfahan, Iran for their support.

References

[1] W.O. Herrmann, H. Wolfram, Process for the Preparation of Polymerized Vinyl Alcohol and Its Derivatives, 1928, US1672156, Munich, Germany.
[2] S. Rashidi, A. Ataie, Structural and magnetic characteristics of PVA/$CoFe_2O_4$ nanocomposites prepared via mechanical alloying method, Materials Research Bulletin 80 (2016) 321–328.
[3] C.C. Thong, D.C.L. Teo, C.K. Ng, Application of polyvinyl alcohol (PVA) in cement-based composite materials: a review of its engineering properties and microstructure behavior, Construction and Building Materials 107 (2016) 172–180.
[4] J.K. Fink, Poly(vinyl alcohol), in: Handbook of Engineering and Specialty Thermoplastics, John Wiley & Sons, Inc, 2011, pp. 39–68.
[5] C.M. Hassan, N.A. Peppas, Structure and applications of poly(vinyl alcohol) hydrogels produced by conventional crosslinking or by freezing/thawing methods, in: Biopolymers PVA Hydrogels, Anionic Polymerisation Nanocomposites, Springer Berlin Heidelberg, Berlin, Heidelberg, Germany, 2000, pp. 37–65.
[6] S. Iijima, Helical microtubules of graphitic carbon, Nature 354 (1991) 56–58.
[7] S. Dadras, M.V. Farahani, The effects of carbon nano tubes on electric and dielectric properties of CNTs doped KBr (CNTs/KBr) compound, Physica B: Condensed Matter 477 (2015) 94–99.
[8] M.A. Deyab, Effect of carbon nano-tubes on the corrosion resistance of alkyd coating immersed in sodium chloride solution, Progress in Organic Coatings 85 (2015) 146–150.
[9] B. Hao, P.C. Ma, Chapter 3-carbon nanotubes for defect monitoring in fiber-reinforced polymer composites A2-Peng, Huisheng, in: Q. Li, T. Chen (Eds.), Industrial Applications of Carbon Nanotubes, Elsevier, Boston, USA, 2017, pp. 71–99.
[10] M. Naebe, T. Lin, X. Wang, Carbon Nanotube Reinforced Electrospun Polymer Nanofibers, INTECH, Croatia, 2010.
[11] C. Mangeon, S. Mahouche-Chergui, D.L. Versace, M. Guerrouache, B. Carbonnier, V. Langlois, E. Renard, Poly(3-hydroxyalkanoate)-grafted carbon nanotube nanofillers as reinforcing agent for PHAs-based electrospun mats, Reactive and Functional Polymers 89 (2015) 18–23.
[12] M. Hasanzadeh, V. Mottaghitalab, R. Ansari, B. Hadavi Moghadam, A.K. Haghi, Issues in production of carbon nanotubes and related nanocomposites: a comprehensive review, Cellulose Chemistry and Technology 49 (2015) 237–257.
[13] V.D. Punetha, S. Rana, H.J. Yoo, A. Chaurasia, J.T. McLeskey Jr., M.S. Ramasamy, N.G. Sahoo, J.W. Cho, Functionalization of carbon nanomaterials for advanced polymer nanocomposites: a comparison study between CNT and graphene, Progress in Polymer Science (2016)http://dx.doi.org/10.1016/j.progpolymsci.2016.12.010.
[14] A. Pantano, Carbon Nanotube Based Composites: Processing, Properties, Modelling and Application, Smithers Rapra Technology, Shropshire, United Kingdom, 2012.
[15] A. Tiwari, S.K. Shukla, Advanced Carbon Materials and Technology, Wiley, NJ, USA, 2014.
[16] F.V. Ferreira, L. Cividanes, F. Sales Brito, B. Rossi Canuto de Menezes, W. Franceschi, E. Alves Nunes Simonetti, G. Patrocínio Thim, Functionalizing Graphene and Carbon Nanotubes, Springer International Publishing, NY, USA, 2016.
[17] K.Y. Castrejón-Parga, H. Camacho-Montes, C.A. Rodríguez-González, C. Velasco-Santos, A.L. Martínez-Hernández, D. Bueno-Jaquez, J.L. Rivera-Armenta, C.R. Ambrosio, C.C. Conzalez, M.E. Mendoza-Duarte, P.E. García-Casillas, Chitosan–starch film reinforced with magnetite-decorated carbon nanotubes, Journal of Alloys and Compounds 615 (Suppl. 1) (2014) S505–S510.

[18] N.N.K. Getangama, Dielectric Spectroscopy of Polyvinyl Alcohol Hydrogels and Nanocomposites, The University of Western Ontario, Canada, 2015.
[19] Z. Liu, L. Zhao, M. Chen, J. Yu, Effect of carboxylate multi-walled carbon nanotubes on the performance of thermoplastic starch nanocomposites, Carbohydrate Polymers 83 (2011) 447–451.
[20] A. Downing-Perrault, Polymer Nanocomposites Are the Future, University of Wisconsin-Stout, USA, 2005.
[21] A. Dufresne, S. Thomas, L.A. Pothen, Biopolymer Nanocomposites: Processing, Properties, and Applications, John Wiley & Sons, USA, 2013.
[22] J. Fawaz, V. Mittal, Synthesis of polymer nanocomposites: review of various techniques, in: Synthesis Techniques for Polymer Nanocomposites, Wiley-VCH Verlag GmbH & Co. KGaA, 2014, pp. 1–30.
[23] L. Nicolais, G. Carotenuto, In Situ Synthesis of Polymer-Embedded Nanostructures, John Wiley & Sons, USA, 2013.
[24] S. Mallakpour, S. Soltanian, Vitamin C functionalized multi-walled carbon nanotubes and its reinforcement on poly(ester-imide) nanocomposites containing L-isoleucine amino acid moiety, Composite Interfaces 23 (2016) 209–221.
[25] S. Mallakpour, A. Zadehnazari, Synthesis, morphology investigation and thermal mechanical properties of dopamine-functionalized multi-walled carbon nanotube/poly(amide-imide) composites, Reactive and Functional Polymers 106 (2016) 112–119.
[26] K. Jiang, T. Fei, F. Jiang, G. Wang, T. Zhang, A dew sensor based on modified carbon black and polyvinyl alcohol composites, Sensors and Actuators B: Chemical 192 (2014) 658–663.
[27] X. Xu, H. He, Y. Zhang, D. Zhang, Z. Yang, Influence of position on the microstructure of carbon black/polyvinyl alcohol composite obtained by the directional freeze-drying process, Journal of Macromolecular Science, B 53 (2014) 568–574.
[28] S. Mallakpour, H. Ayatollahi, Development of novel chiral poly(amide–imide)/bionanocomposites containing N,N′-(pyromellitoyl)-bis-phenylalanine units reinforced by organoclay and modified TiO_2, Journal of Thermoplastic Composite Materials 28 (2015) 3–18.
[29] S. Mallakpour, M. Khani, Characterization of nanocomposite laminates fabricated from aqueous dispersion of polyvinylpyrrolidone and l-leucine amino acid modified-montmorillonite, Polymer Bulletin 73 (2016) 2677–2688.
[30] S. Mallakpour, V. Shahangi, Bio-modification of cloisite Na^+ with chiral l-leucine and preparation of new poly(vinyl alcohol)/organo-nanoclay bionanocomposite films, Synthesis and Reactivity in Inorganic, Metal-Organic, and Nano-Metal Chemistry 43 (2013) 966–971.
[31] S. Mallakpour, A. Abdolmaleki, H. Tabebordbar, Production of PVC/α-MnO_2-KH550 nanocomposite films: morphology, thermal, mechanical and Pb (II) adsorption properties, European Polymer Journal 78 (2016) 141–152.
[32] S. Mallakpour, E. Khadem, Novel poly(N-vinyl-2-pyrrolidone) nanocomposites containing poly(amide–imide)/aluminum oxide nanostructure hybrid as a filler, High Performance Polymers 28 (2016) 55–63.
[33] S. Mallakpour, M. Madani, Functionalized-MnO_2/chitosan nanocomposites: a promising adsorbent for the removal of lead ions, Carbohydrate Polymers 147 (2016) 53–59.
[34] S. Mallakpour, M. Naghdi, Application of SiO_2 nanoparticles with double layer coverage consist of citric acid and l(+)-ascorbic acid for the production of poly(vinyl chloride)/SiO_2 nanocomposite films with enhanced optical and thermal properties, Polymer Bulletin 73 (2016) 1701–1717.
[35] S. Mallakpour, M. Dinari, Bionanocomposite materials from layered double hydroxide/Ntrimellitylimido-L-isoleucine hybrid and poly(vinyl alcohol): structural and morphological study, Journal of Thermoplastic Composite Materials 29 (2016) 623–637.

[36] S. Mallakpour, M. Dinari, M. Hatami, Modification of Mg/Al-layered double hydroxide with l-aspartic acid containing dicarboxylic acid and its application in the enhancement of the thermal stability of chiral poly(amide-imide), RSC Advances 4 (2014) 42114–42121.
[37] S. Mallakpour, M. Dinari, M. Talebi, Novel nanocomposites obtained by dispersion of LDH modified with N-tetrabromophthaloyl-glutamic in poly(amide-imide) having N-trimellitylimido-l-leucine and 4,4′-diaminodiphenylether units, Polymer Composites 37 (2016) 1323–1329.
[38] S. Mallakpour, A. Abdolmaleki, Z. Khalesi, S. Borandeh, Surface functionalization of GO, preparation and characterization of PVA/TRIS-GO nanocomposites, Polymer 81 (2015) 140–150.
[39] C.-X. Feng, J. Duan, J.-H. Yang, T. Huang, N. Zhang, Y. Wang, X.-T. Zheng, Z.-W. Zhou, Carbon nanotubes accelerated poly(vinylidene fluoride) crystallization from miscible poly(vinylidene fluoride)/poly(methyl methacrylate) blend and the resultant crystalline morphologies, European Polymer Journal 68 (2015) 175–189.
[40] K. Huang, S. Pisharath, S.-C. Ng, Preparation of polyurethane–carbon nanotube composites using 'click' chemistry, Tetrahedron Letters 56 (2015) 577–580.
[41] O. Osazuwa, M. Kontopoulou, P. Xiang, Z. Ye, A. Docoslis, Polymer composites containing non-covalently functionalized carbon nanotubes: a study of their dispersion characteristics and response to ac electric fields, Procedia Engineering 42 (2012) 1414–1424.
[42] P.M. Ajayan, O. Stephan, C. Colliex, D. Trauth, Aligned carbon nanotube arrays formed by cutting a polymer resin–nanotube composite, Science 265 (1994) 1212–1214.
[43] E. Zakharchenko, O. Mokhodoeva, D. Malikov, N. Molochnikova, Y. Kulyako, G. Myasoedova, Novel sorption materials for radionuclide recovery from nitric acid solutions: solid-phase extractants and polymer composites based on carbon nanotubes, Procedia Chemistry 7 (2012) 268–274.
[44] M.E. Suss, S. Porada, X. Sun, P.M. Biesheuvel, J. Yoon, V. Presser, Water desalination via capacitive deionization: what is it and what can we expect from it? Energy & Environmental Science 8 (2015) 2296–2319.
[45] C.-H. Hou, N.-L. Liu, H.-L. Hsu, W. Den, Development of multi-walled carbon nanotube/poly(vinyl alcohol) composite as electrode for capacitive deionization, Separation and Purification Technology 130 (2014) 7–14.
[46] S. Mallakpour, A. Abdolmaleki, S. Borandeh, l-Phenylalanine amino acid functionalized multi walled carbon nanotube (MWCNT) as a reinforced filler for improving mechanical and morphological properties of poly(vinyl alcohol)/MWCNT composite, Progress in Organic Coatings 77 (2014) 1966–1971.
[47] Z. Ding, Y. Zhu, C. Branford-White, K. Sun, S. Um-i-Zahra, J. Quan, H. Nie, L. Zhu, Self-assembled transparent conductive composite films of carboxylated multi-walled carbon nanotubes/poly(vinyl alcohol) electrospun nanofiber mats, Materials Letters 128 (2014) 310–313.
[48] E.Y. Malikov, M.B. Muradov, O.H. Akperov, G.M. Eyvazova, R. Puskás, D. Madarász, L. Nagy, Á. Kukovecz, Z. Kónya, Synthesis and characterization of polyvinyl alcohol based multiwalled carbon nanotube nanocomposites, Physica E: Low-dimensional Systems and Nanostructures 61 (2014) 129–134.
[49] M. Amirilargani, M.A. Tofighy, T. Mohammadi, B. Sadatnia, Novel poly(vinyl alcohol)/multiwalled carbon nanotube nanocomposite membranes for pervaporation dehydration of isopropanol: poly(sodium 4-styrenesulfonate) as a functionalization agent, Industrial & Engineering Chemistry Research 53 (2014) 12819–12829.

[50] A. Rahy, A. Choudhury, C. Kim, S. Ryu, J. Hwang, S.H. Hong, D.J. Yang, A simple/green process for the preparation of composite carbon nanotube fibers/yarns, RSC Advances 4 (2014) 43235–43240.
[51] S.C. Kishore, A. Pandurangan, Fabrication of solution processed carbon nanotube embedded polyvinyl alcohol composite film for non-volatile memory device, Journal of Nanoscience and Nanotechnology 14 (2014) 2381–2387.
[52] J. Thomasukutty, C.G. Soney, M. Maya, T. Sabu, Functionalized MWCNT and PVA nanocomposite membranes for dielectric and pervaporation applications, Chemical Engineering & Process Technology 6 (2015) 233–241.
[53] S.A. Medina Escobar, C.A. Isaza Merino, J.M. Meza Meza, Mechanical and thermal behavior of polyvinyl alcohol reinforced with aligned carbon nanotubes, Matéria (Rio de Janeiro) 20 (2015) 794–802.
[54] D. Lai, Y. Wei, L. Zou, Y. Xu, H. Lu, Wet spinning of PVA composite fibers with a large fraction of multi-walled carbon nanotubes, Progress in Natural Science: Materials International 25 (2015) 445–452.
[55] A. Shameli, E. Ameri, Synthesis of cross-linked PVA membranes embedded with multi-wall carbon nanotubes and their application to esterification of acetic acid with methanol, Chemical Engineering Journal 309 (2017) 381–396.
[56] N.S. Alghunaim, Optimization and spectroscopic studies on carbon nanotubes/PVA nanocomposites, Results in Physics 6 (2016) 456–460.
[57] J. Wongon, S. Thumsorn, N. Srisawat, Poly(vinyl alcohol)/multiwalled carbon nanotubes composite nanofiber, Energy Procedia 89 (2016) 313–317.
[58] Y. Chen, L. Zhang, H. Zhan, J.N. Wang, New processing method to fabricate high-performance carbon-nanotube/polyvinyl alcohol composite films, Carbon 110 (2016) 490–496.
[59] L. Jing, X. Li, Facile synthesis of PVA/CNTs for enhanced adsorption of Pb^{2+} and Cu^{2+} in single and binary system, Desalination and Water Treatment 57 (2016) 21391–21404.
[60] L. Zhang, X. Wang, R. Li, Q. Li, P.D. Bradford, Y. Zhu, Microcombing enables high-performance carbon nanotube composites, Composites Science and Technology 123 (2016) 92–98.
[61] H.-L. Ma, L. Zhang, Y. Zhang, S. Wang, C. Sun, H. Yu, X. Zeng, M. Zhai, Radiation preparation of graphene/carbon nanotubes hybrid fillers for mechanical reinforcement of poly(vinyl alcohol) films, Radiation Physics and Chemistry 118 (2016) 21–26.
[62] S. Amrin, V.D. Deshpande, Dielectric relaxation and ac conductivity behavior of carboxyl functionalized multiwalled carbon nanotubes/poly (vinyl alcohol) composites, Physica E: Low-Dimensional Systems and Nanostructures 87 (2017) 317–326.
[63] A. Abdolmaleki, S. Mallakpour, F. Azimi, Microwave-assisted treatment of MWCNTs with vitamin B2: study on morphology, tensile and thermal behaviors of poly(vinyl alcohol) based nanocomposites, European Polymer Journal 87 (2017) 277–285.

This page intentionally left blank

Bio-based aliphatic polyesters from dicarboxylic acids and related sugar and amino acid derivatives

11

Jordi Puiggalí[1], Angélica Díaz[1], Ramaz Katsarava[2]
[1]Escola d'Enginyeria de Barcelona Est-EEBE, Barcelona, Spain; [2]Agricultural University of Georgia, Tbilisi, Georgia

11.1 Introduction

Poly(alkylene dicarboxylate)s are playing an increasing role in the development of biodegradable materials for biomedical applications. Some recent examples can be mentioned: (1) Development of antimicrobial packaging films for hospital environments (e.g., functionalization of poly(butylene adipate) with quaternary phosphonium groups [1]); (2) tissue engineering applications (e.g., use of micropatterned (poly (butylene succinate) (PBS)) surfaces to favor alignment of stem cells [2], scaffolds with elastomeric properties that mimic the extracellular matrix [3]); (3) development of hydrogels from multifunctional alcohols and carboxylic acids (e.g., poly(glycerol sebacate) [4,5] and poly(octanediol citrate) [6]); and (4) development of drug delivery systems (e.g., polymers derived from sebacic acid due to their good solubility characteristics [7]). Furthermore, materials are highly interesting because most of monomers can be obtained from renewable resources as will be explained in more detail in the next section.

Nevertheless, it should also be taken into account the use of PBS and related copolymers in the fields of textiles and plastics because their easy and excellent processability together with their good thermal and mechanical properties make them a very interesting alternative to polyolefins. PBS is a highly crystalline material with a moderate molecular weight that may limit properties. Therefore, it has been modified with chain extenders and the incorporation of branched monomers to give a suitable commercial product (Bionolle) [8,9].

Furthermore, poly(alkylene dicarboxylate)s are highly interesting materials because they can be produced from monomers coming from renewable resources as will be explained in more detail in the next section.

Thermal and mechanical properties of poly(alkylene dicarboxylate)s can be easily improved by incorporation of rigid units in the main chain. In this way, different biodegradable aliphatic–aromatic copolyesters (e.g., poly(butylene succinate-*co*-terephthalate) (PBST), poly(ethylene succinate-*co*-terephthalate), and poly(butylene adipate-*co*-terephthalate) (PBAT)) have been produced in an industrial scale

Biodegradable and Biocompatible Polymer Composites. http://dx.doi.org/10.1016/B978-0-08-100970-3.00011-0

by different companies (e.g., PBAT by BASF (Ecoflex) and PBST by Tejin (Green Ecopet)) [10]. Green synthesis of terephthalic acid can be performed at a laboratory scale from isobutene or limonene, methyl coumalate, methyl pyruvate, furfural, *p*-cymene [11–16], and even in a commercial scale from isobutene [17].

Efforts have also been focused on the incorporation of cycloaliphatic rings (e.g., cyclohexanedicarboxylic acid and 1,4-cyclohexanedicarboxylate), which have the advantage that can be prepared from natural products such as terpenes but unfortunately at still too high costs [18]. Special interest merits the preparation of poly(alkylene dicarboxylate)s from carbohydrates derived from natural polysaccharides such as cellulose, starch, and mannans [19], being performed a consistent and extensive research as will be detailed in Section 11.3.

Properties of polyesters can also be improved by the incorporation of amide groups due to the capability of the derived polymers (i.e., poly(ester amide)s (PEAs)) to establish strong intermolecular hydrogen bonding interactions. These polymers may keep biodegradable characteristics due to the presence of ester groups. PEAs can be prepared from a wide variety of monomers and synthetic methodologies giving rise to polymers with random, blocky, and ordered microstructures and linear, branched, and hyperbranched architectures. Therefore, PEAs constitute a promising family of polymers to cover a wide spectrum of applications. PEAs derived by the incorporation of natural α-amino acids in the main chains play nowadays a fundamental role for biomedical applications considering in addition that functional groups can be easily introduced. Therefore, synthesis of these specific derivatives will be considered in Section 11.4.

Incorporation of nanoparticles could have a great influence on mechanical, thermal stability, crystallization behavior, barrier properties, and biodegradability of polymers. For example, an enhanced degradation is expected when silicate layers are incorporated in a biodegradable polyester matrix due to the presence of hydroxyl groups [20,21]. Furthermore, the incorporated nanoparticles may have a hydrophilic surface that could increase the susceptibility of the derived nanocomposite to microbial attack and also the swelling degree of the original hydrophobic matrix [22,23]. Sections 11.5 and 11.6 are focused on the recent research performed on nanocomposites based on poly(alkylene dicarboxylate) and PEA matrices.

11.2 Poly(alkylene dicarboxylate)s from renewable resources

Poly(alkylene dicarboxylate)s are a specific family of biodegradable polyesters that can be obtained from bio-based diols and dicarboxylic acids. These polymers can be employed as both commodity and specialty applications (e.g., hydrogels, scaffolds for tissue engineering or drug delivery systems) and have properties that can vary from those characteristics of elastomeric and rigid materials [24].

Poly(alkylene dicarboxylate)s are usually prepared by a thermal polycondensation process from diols and dicarboxylic acids (or alternatively their diesters or

dichlorides). Usually, polycondensation is performed in two steps (nitrogen atmosphere and high vacuum) and at high temperature to favor the removal of condensation by-products. In general, molecular weights are limited (e.g., M_n is usually lower than 30,000 g/mol) [25–27], being consequently proposed the use of catalysts such as titanium-based compounds [28–30], lipases [31–33], triflates [34–36], and organometal or metal oxide compounds [37].

Different poly(alkylene dicarboxylate)s can be prepared from fully bio-based monomers, being probably the more studied ones those derived from diols, such as 1,3-propanediol (PDO), 1,4-butanediol (BDO), 1,6-hexanediol (HDO), and 1,10-decanediol, and dicarboxylic acids such as succinic acid (SA), adipic acid, azelaic acid, sebacic acid, and other fatty diacids.

It is well established that bio-PDO can be obtained from fermentation of corn sugar by using a genetically modified strain of *Escherichia coli* [38]. PDO has gained great interest as a raw material due to its odd number of methylene units. BDO can be synthesized by reduction of SA [39,40], which can be obtained by fermentation of glycerol, glucose, and corn sugar [41]. HDO can be derived from 5-hydromethyl furfural (5-HMF), which has been considered as a relevant building block produced by depolymerization and fermentation of biopolymers [42]. In fact, 5-HMF can led to promising chemical intermediates and specifically to HDO by a simple direct hydrogenation, a process that can also be considered as an alternative reaction pathway [43]. 1,10-Decanediol can be produced by hydrogenation of sebacic acid [44], which can be prepared by alkali fusion at high temperatures and alkali concentrations of ricinoleic acid that naturally occurs in mature castor plant [45]. Adipic acid can be produced by chemocatalytic conversion of *cis*-muconic acid and D-glucaric acid [46], which are bio-based precursors produced by fermentation [47,48]. Other proposed pathways for adipic acid production are based on the oxidation of alcohols or fatty acid substrates using engineered yeast [49] and also a *Candida tropicalis* strain [50]. Other well-known examples of bio-based monomers correspond to pimelic acid, obtained by oxidation of ricinoleic acid from castor oil, azelaic acid prepared by ozonolysis cleavage of the alkene double bond of oleic acid and subsequent oxidation, and 1,9-nonanediol prepared by reduction of azelaic acid [51].

Fatty acids coming from plant oils (e.g., methyl oleate and ethyl erucate) have extensively been considered, and specifically the production of C_{19} and C_{23} α,ω-dicarboxylic acid esters have received great attention [52,53]. It has also been reported that genetically optimized yeast strains can be employed for the production of saturated aliphatic dicarboxylic acids with chain lengths varying from C11 to C18 from fermentation of vegetable oils [54]. Pyrolysis of fatty acids can also give rise to $CH_2{=}CH(CH_2)_nCOOR$ fragments that can be coupled to render long-chain α,ω-dicarboxylic acid esters after hydrogenation. In this way, 1,20-eicosanedioic acid was obtained from metathesis of undecenoic acid and employed to get new biodegradable polyesters [55,56].

Logically tunable properties can be attained by copolymerization using different diol or dicarboxylic units. The incorporation of comonomers has a great influence on both thermal and mechanical properties, crystallinity, and biodegradability. In general, the most studied systems are constituted by even units, being representative

the systems based on succinate/adipate [57,58], adipate/suberate [59], adipate/sebacate [60] dicarboxylate units. Nevertheless, copolyesters including odd units as those derived from BDO and azelate units have also extensively studied due to their peculiar crystallization behavior [61–63].

11.3 Poly(alkylene dicarboxylate)s and poly(ester amide)s from sugar-based monomers

Galbis et al. have recently written an excellent and complete review on sugar-based monomers derived from natural resources [64]. Therefore, most of the information concerning derived polymers can be found there, but nevertheless there are some points that merit to be remembered:

1. Abundant examples are mentioned about synthesis of different poly(alkylene dicarboxylate) s from monosaccharides such as alditols constituted by four (i.e., threitols such as erithritol), five (i.e., pentitols such as xilitol or arabinitol), and six carbon atoms (i.e., hexitols such as mannitol, glucitol, sorbitol, galactitol, or iditol); dianhydroalditols, and aldaric acids (e.g., tartaric, xylaric or arabinaric, and glucaric or galactaric acids for four, five, and six carbon atom–membered compounds, respectively). Most dianhydroalditol derivatives are based on dianhydrohexitols (e.g., isosorbide, isomannide, and isoidide). Fig. 11.1 shows the chemical formulae of the indicated sugar monomers.
2. The presence of functional hydroxyl side groups allows further chemical reactions to attach drugs and active compounds to the polymer chain. In addition, monomers can be submitted to cyclization reactions as it is the case of bicyclic mannitol, bicyclic glucitol, bicyclic galactaric acid, and bicyclic glucaric acid (Fig. 11.2).
3. Incorporation of polymethylene sequences without functionalized or cyclic side groups can be done by copolymerization with aliphatic diols, dicarboxylic acids, or both simultaneously. Copolymerization was fundamental to get polymers with tailored properties according to final composition.

Incorporation of bifunctional, sugar-based monomers with a bicyclic structure is of great interest, due to their ability to add stiffness to a polymer backbone. High-molecular-weight polycondensates containing high-molecular-weight polyesters have been prepared from sugar-based monomers with a bicyclic structure by solid-state modification (SSM) of semicrystalline polyesters. Basically, transesterification

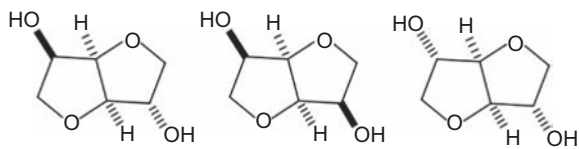

Figure 11.1 Chemical structure of representative dianhydrohexitols.

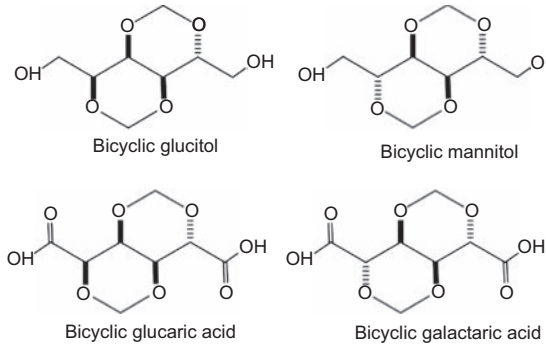

Figure 11.2 Chemical structure of representative bicyclic monosaccharide monomers.

reactions involved the mobile amorphous fraction [65]. Diols derived from isosorbide [66], 2,3:4,5-di-*O*-methylene-galactitol [67], 2,4:3,5-di-*O*-methylene-D-mannitol [68], and the bicyclic diol 2,4:3,5-di-*O*-methylene-D-glucitol [70] have been incorporated into polyesters by SSM. Fully bio-based polyesters have also been prepared using ethylene glycol, BDO or 1,10-decanediol, and the rigid isoidide dicarboxylic acid under rather mild conditions [69].

The homopolymer derived from 2,4:3,5-di-*O*-methylene-D-mannitol and dimethyl succinate showed an interesting combination of biodegradability and molecular stiffness, being also possible to tune the final characteristics by copolymerization with BDO [70]. Interestingly the enzymatic degradation rate of these copolymers was always greater than that determined for the parent PBS homopolymer.

PBS has also been modified by insertion of monocyclic acetals (e.g., 2,3-di-*O*-methylene-L-threitol and 2,3-di-*O*-methylene-L-tartaric acid), and an increase in both hydrolytic and enzymatic degradability together with an increase in the elongation at break was observed [71].

Bulk or solution polycondensation reactions have also been successfully performed with pentitols (e.g., 2,3,4-tri-*O*-methyl-L-arabinitol and 2,3,4-tri-*O*-methyl-xylitol), pentaric acids (e.g., 2,3,4-tri-*O*-methyl-L-arabinaric acid and 2,3,4-tri-*O*-methyl-xylaric acid), and using BDO and adipic acid as comonomers to tune final properties [72].

Cross-linked polyesters based on isosorbide, itaconic acid, and SA showed shape memory effects on heating above a glass transition temperature that was close to 75°C [73]. Furthermore, polymers based on isosorbide were interesting as bioelastomers with photoinduced antibacterial activity [74,75].

Polymers derived from isosorbide or isomannide and incorporating natural α-amino acids are probably the most studied PEAs based on sugar monomers and related to poly(alkylene dicarboxylate)s. These PEAs (Fig. 11.3) can be obtained by an esterification of the indicated monomers with α-amino acids (e.g., L-phenylalanine, L-leucine, L-isoleucine, and L-methionine) in the presence of *p*-toluenesulfonic acid and subsequent reaction with *p*-nitrophenyl esters of aliphatic dicarboxylic acids [76,77]. The formed O,O′-bis-α-aminoacyl derivatives had highly reactive amino groups that make feasible to attain rather high molecular weights in contrast with the problems

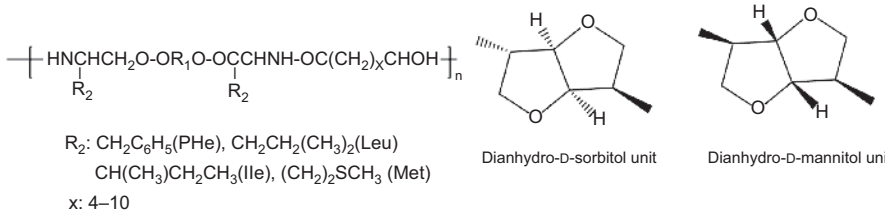

Figure 11.3 Chemical formula of poly(ester amide)s constituted by dianhydrohexitols, α-amino acids, and dicarboxylic acids.

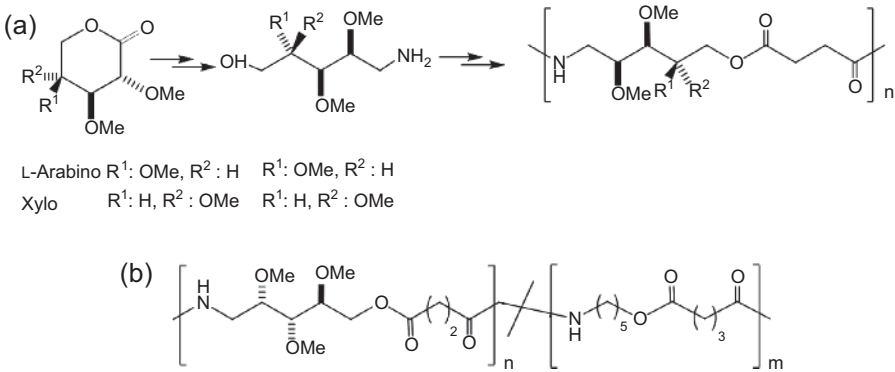

Figure 11.4 (a) Chemical formula of stereoregular poly(ester amide)s derived from 1-amino-1-deoxy-2,3,4-tri-*O*-methyl-L-arabinitol and 2,3,4-tri-*O*-methyl-D-xylitol. (b) Chemical structure of copoly(ester amide)s containing L-arabinose, 5-aminopentanol, succinyl, and glutaryl units.

observed in the synthesis of polyesters that were derived from the low reactivity of the sterically hindered secondary hydroxyl groups.

The obtained PEAs[1] were hydrolytically and enzymatically degradable, being degradation rates similar to those determined for related polymers derived from α,ω-alkylenediols. Therefore hydrolysis was not hindered by the presence of the rigid bicyclic units. Enzymatic degradation with lipases and α-chymotrypsin was effective and sensitive to the selected amino acid (i.e., the higher degradation rate was observed when the highly hydrophobic L-phenylalanine residue was employed) as well as on the length of the dicarboxylic acid (i.e., the rate increased as the number of methylene units did). PEAs derived from D-glucitol, D-mannitol, or L-iditol have been patented as intraocular delivery systems [78].

PEAs constituted by carbohydrate units (L-arabinose and D-xylose) showed a high susceptibility to hydrolytic degradation when compared with related compounds that incorporated different ratios of linear amino alcohols (e.g., 5-aminopentanol) (Fig. 11.4) [79,80]. Note that these PEAs were derived from dicarboxylic acids but

[1] For this kind of the PEAs see also Section 11.4.

the chemical structure was not in full agreement with poly(alkylene dicarboxylate)s because amino alcohols were used instead of diols and amino acids.

11.4 Biodegradable polymers composed of naturally occurring α-amino acids

Amino acid–based biodegradable (AABB) polymers represent a relatively new but a huge family of biodegradable biomaterials, which have been extensively developed since the early 1990s [24,81,82]. These polymers are composed of physiological and nontoxic building blocks such as naturally occurring α-amino acids, fatty diols, dicarboxylic acids, and carbonic acids that provide a high biocompatibility of the AABB polymers. Many of the said building blocks are obtained from renewable natural resources.

Three main classes of AABB polymers were designed on the basis of the said building blocks [24,81,82]: (1) PEAs composed of *three variable* building blocks such as α-amino acid, fatty diol, and dicarboxylic acid, (2) poly(ester urethane)s (PEURs) composed of *three variable* building blocks such as α-amino acid and two diols (one comes from bis-nucleophilic monomer, another one from bis-electrophilic monomer), and (3) poly(ester urea)s (PEUs) composed of *two variable* building blocks—α-amino acid and diol (in case of PEURs and PEUs, an additional (*nonvariable*) building block is carbonic acid). The basic starting compounds, common for all three classes of the AABB polymers, are bis-nucleophilic monomers—diamine–diesters (DADEs), which are cheap and vastly available compounds composed of 2 mol of α-amino acids and 1 mol of fatty diols. These monomers contain two hydrolyzable ester bonds per molecule, which being incorporated into the polymeric backbones provide biodegradability of the resulting polymers.

The most rational way for the synthesis of the DADE monomers is a direct condensation of α-amino acids with diols in the presence of *p*-toluenesulfonic acid, which serves as both the condensation reaction catalyst and α-amino groups protector (prevents the latter from undesirable interaction), as it is depicted in Fig. 11.5 for hydrophobic α-amino acids such as alanine, valine, leucine, isoleucine, phenylalanine, and methionine, containing only two functional groups such as α-amino and α-carboxylic groups [83]. In this case, 2 mol of *p*-toluenesulfonic acid is used in the condensation reaction, which is attached to α-amino groups of the amino acid (compound **I**).

In case of polyfunctional α-amino acids such as arginine (R), which contains the lateral guanidine group, the synthesis of the DADE monomers via direct condensation with a diol is still a suitable method because the guanidine group is inactive and does not enter into undesirable side reactions during either the synthesis of the DADE monomers via direct condensation reaction (Fig. 11.6) or the synthesis of polymers on the basis of these monomers [84,85]. In this case, 4 mol of *p*-toluenesulfonic acid should be used in the condensation reaction because 2 mol is attached

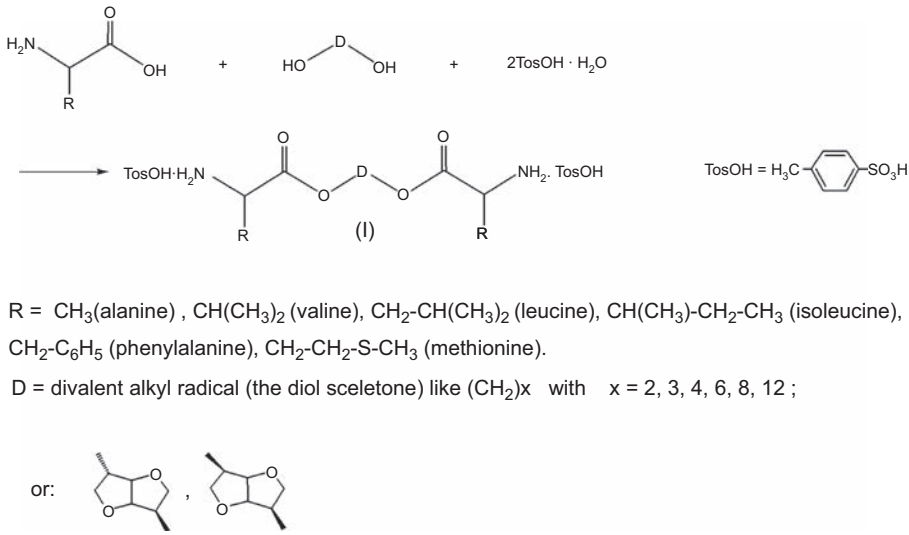

Figure 11.5 Synthesis of diamine–diester monomers on the basis of hydrophobic α-amino acids.

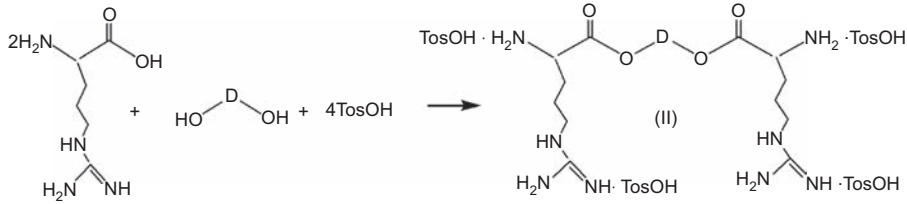

Figure 11.6 Synthesis of diamine–diester monomers on the basis of L-arginine.

to the lateral guanidine groups, and another 2 mol to α-amino groups of the amino acid (compound **II**).

The DADE monomers on the basis of hydrophobic α-amino acids are obtained as di-*p*-toluenesulfonic acid salts **I** and as tetra-*p*-toluenesulfonic acid salts **II** on the basis of arginine.

It has to be noted here that the most of the DADE monomers described in literature are synthesized on the basis of primary diols such as polymethylene-1,n-diols, although the DADE monomers were successfully synthesized, as indicated in the previous section, on the basis of secondary diols (1,4:3,6-diahydohexitols, DAHs) (Fig. 11.1), which are available in industrial quantities and are derived entirely from renewable resources (e.g., starch). The DAHs are synthesized by double dehydration of hexitols such as sorbitol (aka glucitol) and mannitol—1,4:3,6-dianhydro-D-sorbitol (aka 1,4:3,6-dianhydro-D-glucitol) (DAS) [76,77], and 1,4:3,6-dianhydromannitol (DAM) [77], accordingly.

The DADEs on the basis of bicyclic DAH and various hydrophobic α-amino acids were synthesized in good yields (70–95%) [77]. The DAH-based monomers are purified from organic solvents, which is a limitation since their cost is increased compared

to the DADE on the basis of polymethylene-1,n-diols, which are recrystallized from water. However, the use of DAH-based DADE as comonomers is reasonable in certain specific cases for modifying properties of the AABB polymers (to be discussed below).

The DADE salt monomers **I** are used for synthesizing various AABB polymers having the neutral structure of the macromolecular chains [24,81–83], whereas the DADE salt monomers **II** are used for synthesizing cationic AABB polymers, containing positively charged lateral guanidine groups along the macromolecular chains [84,85]. As to biocompatibility of diols used for synthesizing the DADE monomers, polymethylene-1,n-diols are known as nontoxic and easily metabolizable compounds and are widely used for constructing numerous biodegradable ester polymers such as aforementioned poly(alkylene carboxylate)s and poly(ortho-ester)s [86]. In the light of the said issue, it has to be noted that DAHs are widely used in pharmacy and, consequently, are nontoxic and represent suitable building blocks for constructing/modifying various polymers including biodegradable biomaterials [19,76,77] (see also below). DAHs are also highly interesting diol components for the synthesis of heterochain polymers such as polyesters [87–92], poly(ester-anhydride)s [93], polyethers [90], polyurethanes [89,94], polycarbonates [89], and related polymers.

Among three classes of the AABB polymers mentioned above, the PEAs and PEUs are the most promising biodegradable biomaterials because these polymers reveal a wide range of mechanical properties from elastic materials with elongation at break 800%–1000% [82] to high-strength materials with Young's modulus up to 6 GPa [82,95] being promising for numerous biomedical applications. The third class of AABB polymers, the PEURs, are mostly amorphous and pliable materials less appropriate for a wide range of biomedical applications. Along with the favorable mechanical properties, the AABB PEAs and PEUs are much more available because bis-electrophilic monomers used for their synthesis, diacid chlorides [82] and triphosgene [82,95], accordingly, are inexpensive and purchasable products. The PEURs are synthesized using bis-chloroformates of diols [96], which are less available and should be specially synthesized from diols by their interaction with phosgene [97].

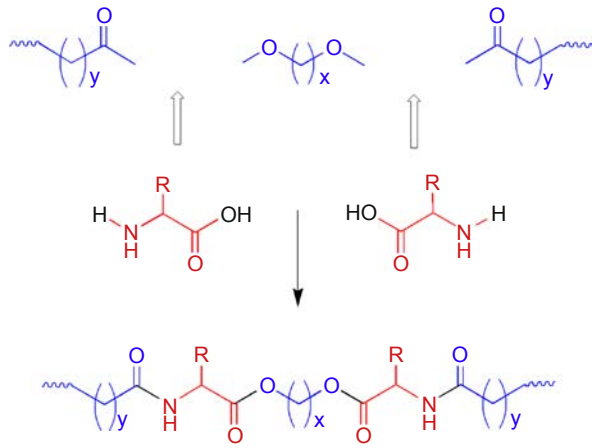

Figure 11.7 Schematic representation of the amino acid–based biodegradable poly(ester amide)s as products of the insertion of α-amino acids between ester bonds.

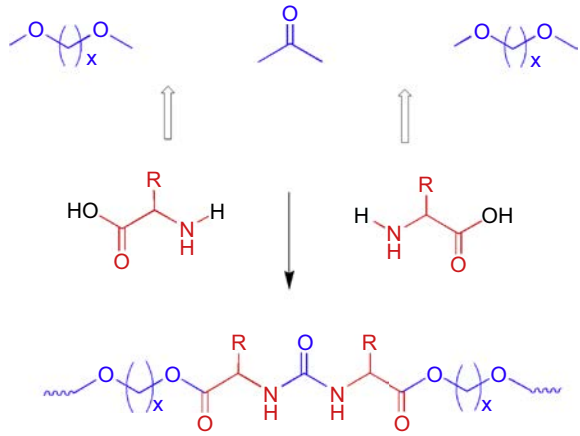

Figure 11.8 Schematic representation of the amino acid–based biodegradable poly(ester urea)s as products of the insertion of α-amino acids between carbonate bonds.

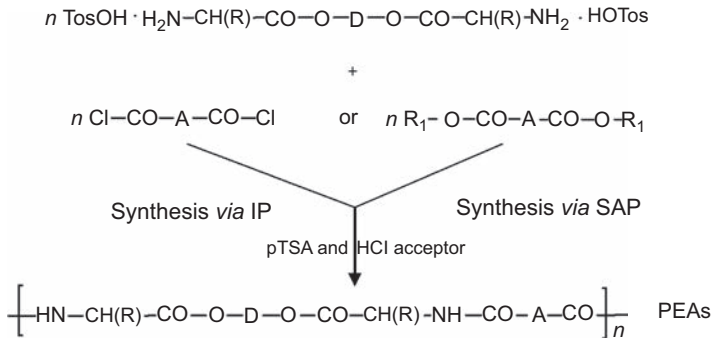

Figure 11.9 Synthesis of the amino acid–based biodegradable poly(ester amide)s (PEAs) via Interfacial Polycondensation (IP) and Solution Active Polycondensation (SAP).

The AABB PEAs relate to the family of poly(alkylene dicarboxylate)s—polyesters made of alkylenediols HO-$(CH_2)_x$-OH and dicarboxylic acids HOOC-$(CH_2)_y$-COOH. Schematically the AABB PEAs can be represented as products of the insertion of α-amino acids residues among carbonyl groups and ether oxygen atoms in poly(alkylene dicarboxylate)s (Fig. 11.7).

Analogously, the AABB PEUs relate to the family of poly(alkylene carbonate)s—polyesters made of alkylenediols HO-$(CH_2)_x$-OH and carbonic acid HO—CO—OH. Schematically the PEUs can be represented as products of the insertion of α-amino acid residues among carbonyl groups and ether oxygen atoms in poly(alkylene carbonate)s (Fig. 11.8).

The transition from poly(alkylene dicarboxylate)s and poly(alkylene carbonate)s to the AABB PEAs and PEUs by the "insertion" of amino acid residues in the main chains allows the establishment of strong intermolecular hydrogen bonding interactions that

could modify both physical–chemical and biological properties of the polymers (to increase hydrophilicity, to improve tissue compatibility, etc.).

11.4.1 Amino acid–based biodegradable poly(ester amide)s

The AABB PEAs are synthesized using either Interfacial Polycondensation (IP) or Solution Active Polycondensation (SAP), according to Fig. 11.9.

The IP, based on the use of diacid chlorides (purchasable products) and normally being carried out in two phase system—water/hydrophobic organic solvent, is a fast, simple, and cost-effective method. However, this method results in the high-molecular-weight PEAs only when using dichlorides of hydrophobic diacids, such as aromatic terephthaloyl chloride, or dichloride of long-chain diacids such as sebacic acid with A = $(CH_2)_8$, or higher dicarboxylic acids in Fig. 11.9 [98–103], and is less successful in case of easily hydrolyzable short-chain diacid chlorides. It has to be noted here that diacid chlorides are less suitable monomers in the traditional Solution Polycondensation (SP) [104] with aliphatic diamines such as the DADE because these electrophiles enter in numerous undesirable side reactions with tertiary amines and other acceptors of the liberated hydrogen chloride [104]; acid acceptors are used also for removing TosOH from amino groups of the DADE. These side reactions cause the disbalance of the equimolar ratio of electrophilic/nucleophilic functional groups, which, in turn, causes the termination of the chain growth process resulting in the formation of low-molecular-weight polymers with poor material properties. Therefore, in the case of short-chain diacids, preference should be given to SAP, which is based on the application of activated diesters, R_1–O–CO–A–CO–O–R_1 (where R_1–O is a leaving group, e.g., *p*-nitrophenoxy, *N*-oxysuccinimide [82,105,106]), which are more soft bis-electrophiles compared to bis-chlorides and less tend to undesirable chain termination side reactions.

The AABB PEAs, along with the widely tunable mechanical properties pointed out above, showed excellent biocompatibility [82] and are of interest for various biomedical applications in surgical devices and drug delivery systems. For example, the PEA [107] and their blends were used for constructing various medical biocomposites. One of them, registered as "PhagoBioDerm" in Republic of Georgia and produced as elastic films, represents novel wound-dressing device (artificial skin). Product consists of lytic bacteriophages, antibiotics, pain killers, and proteolytic enzymes. PhagoBioDerm showed an excellent therapeutic effect in the management of infected wounds and ulcers (of both trophic and diabetic origin) [108] and in the complex treatment of infected local radiation injuries caused by the exposure to ^{90}Sr [109]. The AABB PEAs are also promising for preparing electrospun fibrous mats loaded with various bactericides including bacteriophages [110–112].

Elastomeric functional AABB co-PEA on the basis of three monomers: (1) sebacic acid (1.00 equivalent), (2) the DADE monomer composed of L-leucine and HDO (0.75 equivalent), and (3) L-lysine benzyl ester (0.25 equivalent)—(co-PEA **8(L6)$_{0.75}$K(Bn)$_{0.25}$**) [113,114] showed excellent blood and tissue compatibility in both in vitro [115] and in vivo (pigs) [116] tests. The same co-PEA selectively supported the in vitro growth of epithelial cells [116]. The in vivo biocompatibility was tested in

porcine coronary arteries, comparing the polymer-coated stents with bare metal stents in 10 pigs [116]. All animals survived till were sacrificed 28 days later. Prior to sacrifice, angiography revealed identical diameter stenosis in both groups. Histology confirmed similar injury scores, inflammatory reaction, and area stenosis. These results support the notion that polymer has a high potential for cardiovascular applications.

The AABB PEAs on the basis of the DADE made of polymethylene 1,*n*-diols showed rather low glass transition temperature (T_g)—maximum up to 59°C [83]. The PEAs having higher T_g (up to 102°C) were prepared by using the DADE monomer composed of DAH [77], i.e., by synthesizing the PEAs containing bulky and rigid DAH fragments in the polymeric backbones (Fig. 11.3). This phenomenon was used for increasing the T_g of the leucine-based PEAs and co-PEA **8(L6)$_{0.75}$K(Bn)$_{0.25}$** [117]. The incorporation of bulky fragments of isosorbide (DAS) increased also Young's modulus of the polymers. At the same time the bulky fragments did not influence drastically the biodegradation of the PEAs both in vitro [76,77] and in composted soil and in an activated sludge [76].

The DSM team [118,119] has synthesized a version of the co-PEA **8(L6)$_{0.75}$K(Bn)$_{0.25}$** by SAP of four monomers—(1) di-*p*-toluenesulfonic acid salts of bis-(L-leucine)-

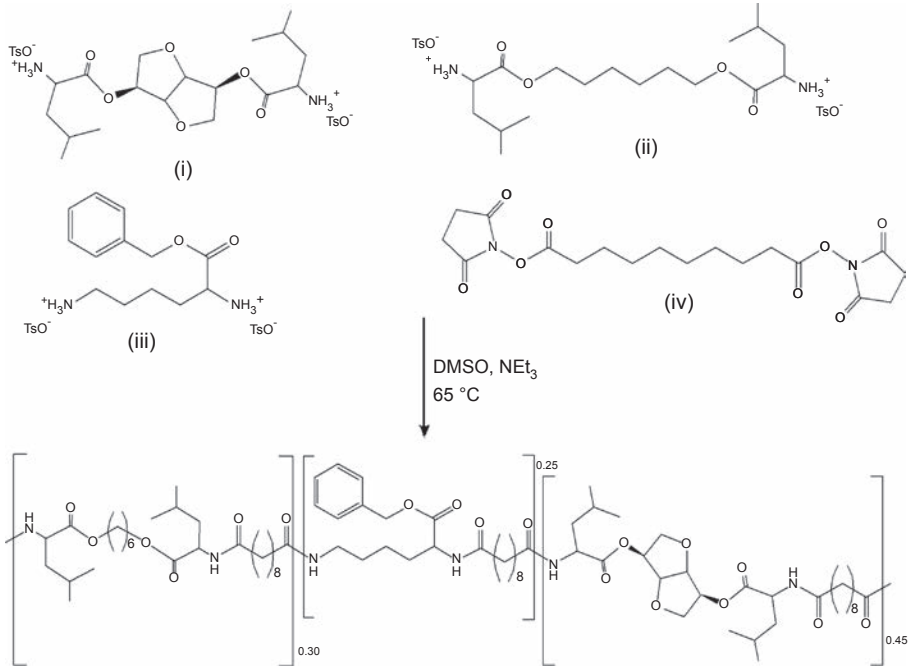

Figure 11.10 The synthesis of 1,4:3,6-dianhydro-D-sorbitol-containing amino acid–based biodegradable poly(ester amide) from the four monomers: (**i**) bis-(L-leucine)-1,4-dianhydro sorbitol diester, (**ii**) bis-(L-leucine)-1,6-hexane diol-diester, (**iii**) lysine benzyl-ester, and (**iv**) di-*N*-hydroxysuccinimide ester of sebacic acid.

1,4-dianhydro sorbitol diester (0.45 equivalent), (2) bis-(L-leucine)-1,6-hexane diol-diester (0.30 equivalent), (3) lysine benzyl-ester (0.25 equivalent), and (4) di-*N*-hydroxysuccinimide ester of sebacic acid (1.00 equivalent), as it is depicted in Fig. 11.10. This modified AABB PEA was successfully used for fabricating micronized particles—microfibrils [118] and microspheres [119] for intraocular delivery of a lipophilic drug, dexamethasone. The PEA showed excellent biocompatibility and provided sustained drug delivery.

11.4.2 Amino acid–based biodegradable poly(ester urea)s

The AABB PEUs are also synthesized using either IP or SAP, according to Fig. 11.11. The IP synthesis of the AABB PEUs, based on the use of purchasable triphosgene (which is more safe and convenient compared to gaseous phosgene Cl–CO–Cl) and being carried out in two phase system—water/hydrophobic organic solvent [95], is very fast, simple, and cost-effective. This synthesis results in the PEUs with higher molecular weights and better material properties as compared with AABB PEUs obtained via SAP, which is based on the use of activated carbonates R_1-CO-R_1 (where R_1-O is a leaving group, mostly *p*-nitrophenoxy [96] to be specially synthesized). The PEUs are relatively new and less studied AABB polymers. However, like the AABB PEAs they also revealed a high biocompatibility and an enzyme-catalyzed biodegradability [120–124]. For example, the PEU composed of L-leucine and HDO degraded in the presence of lipases and proteases [120]. An enzyme (α-chymotrypsin), being impregnated into the electruspun nanofibers, retained activity and catalyzed the degradation process. The **PEUs** composed of L-leucine or L-phenylalanine and various alkylenediols were also studied for in vitro biodegradation [120–124]. It was shown that the degradation rate of PEUs can be tuned by changing the diol chain length. PEUs degrade more quickly as compared with poly(L-lactic acid) (PLLA) and polycaprolactone (PCL).

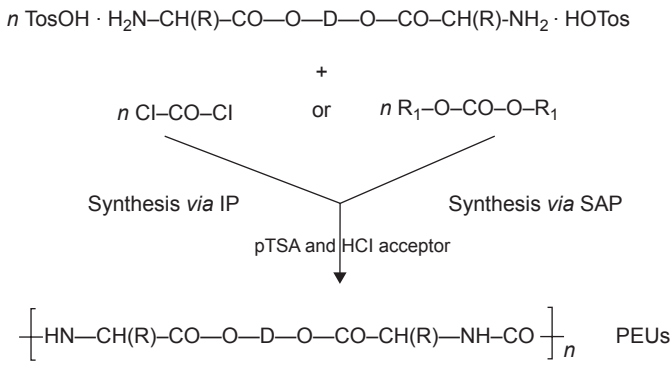

Figure 11.11 Synthesis of the poly(ester urea)s (PEUs) via Interfacial Polycondensation (IP) and Solution Active Polycondensation (SAP).

This class of AABB polymers is especially attractive as biodegradable biomaterials for the applications with tissues highly sensitive to acidic media because after ultimate biodegradation the PEUs release neutral products such as α-amino acid, fatty diol, and CO_2. Besides, the PEUs revealed self-buffering property [122–124]. Hence, after the biodegradation of the PEUs, no local acidic environment causing inflammation is built up.

The PEUs also revealed material properties suitable for their application in biomedicine. It was shown very recently that the PEU derived from L-leucine and HDO could be successfully electrospun to form microfiber scaffolds [120]. The high solubility of the PEU allowed the use of appropriate solvents to load different antibacterial drugs and even enzymes without being denatured. New scaffolds were biocompatible, as demonstrated by adhesion and proliferation of epithelial (Vero) and fibroblast (Cos-7) cells.

The PEUs cross-linked with terminally functionalized osteogenic growth peptide [122–124] revealed outstanding mechanical characteristics. The material obtained on the basis of the PEU composed of L-phenylalanine and HDO showed Young's modulus up to 6.1 ± 1.1 GPa.[2] These are the first degradable polymeric constructs with moduli in the range of 6.0 GPa, which is substantially higher than the moduli of other, commercially available, and widely used polyesters including tyrosine-derived polycarbonates (≈1–2 GPa), PLLA (≈3–3.5 GPa), and poly(propylene fumarate) (2.2 GPa) used in numerous regenerative medicine and orthopedic applications. Another significant limitation of the semicrystalline polyesters, such as PLLA and PCL, is very slow degradation of devices made of them. It can take years for these materials to degrade and resorb fully, and the associated acidification that results often leads to inflammation. When the semicrystalline PEUs were melt processed, the T_g remained the same but no melting peak was observed, indicating that no crystallinity was present.

This provides relatively quick and complete biodegradation of the AABB PEUs in contrast to, e.g., PLLA in which the high initial crystallinity forms large amounts of tiny and rough highly resistant particles after the amorphous phase was degraded. Such particles are now known as very inflammatory and thus well explain the late dramatic inflammatory response [125]. The obtained mechanical and biochemical data show that the new PEU materials may be apt to provide structural support and facilitate new tissue regeneration strategies in load bearing applications [122–124].

No AABB PEAs were synthesized on the basis of the DADE made of DAH so far. Because the incorporation of bulky fragments of DAH increased Young's modulus of the AABB PEAs, it is expected that the PEUs constituted of the DAH-based DADE will have higher mechanical characteristics compared to the polymethylene 1,n-diol-based PEUs above. One can assume that the incorporation of DAH fragments in the polymeric backbones can improve properties of the pliable AABB PEURs as well. A huge potential for modifying properties of the AABB polymers lies also in the application of bicyclic diols and diacids depicted in Fig. 11.2.

[2] For comparison, the elastic modulus of cortical bone within the mid-diaphysis of a long bone, along the axis of the bone, is approximately 18 GPa.

11.5 Nanocomposites from poly(alkylene dicarboxylate)s

Properties of polymers can be easily modified by the incorporation of nanoparticles (e.g., clay silicates, carbon nanotubes (CNTs), or SiO_2 particles), being probably their effect on biodegradation the most unpredictable due to contradictory influences. In the same way, the effect on thermal stability and crystallization behavior is also dependent on the type of nanoparticle and even on the final structure of the nanocomposite (e.g., in the case of silicate nanoclays, the organomodifier compound and the attainment of exfoliated or intercalated nanostructures). An extensive work has been performed with polyesters in general and different poly(alkylene dicarboxylate)s in particular. Therefore, only some recent and representative examples are discussed.

Commercial applications of PBS justify that it is probably the poly(alkylene dicarboxylate) most widely studied as a nanocomposite matrix. Ray et al. [126] have summarized the preparation methods and the control on microstructure of layered silicate nanocomposites. In general, the achievement of a fine dispersion of the nanofiller in the PBS matrix was difficult, being subsequently proposed different treatments to improve physical interactions between clay and PBS. Thus, urethane covalent bonds between surface silanol groups of silica layers and even between the organomodifier compound and silanol groups have been established using a diisocyanate coupling agent (Fig. 11.12) to increase the basal spacing and favor the polymer penetration into silicate layers [127].

Properties of PBS/clay nanocomposites have also recently been reviewed [128,129], being suggested melt intercalation as the best method to produce this kind of composites because it avoids the use of organic chemicals, is compatible with current industrial processes (e.g., extrusion and injection molding), and renders nanocomposites with good properties. Different examples can also be mentioned concerning the use of carbon nanofibers [130], CNTs [131,132], graphene [133], and silica nanoparticles [134] to prepare PBS nanocomposites.

PBS/SiO_2 nanocomposites prepared by the in situ polymerization showed that interactions between the hydroxyl end groups of PBS and the surface silanol groups of SiO_2 took place. In this way, particles acted as chain extenders at low concentration and gave rise to branching and cross-linking reactions at high concentrations [135].

PBS/microfibrillated cellulose (MFC) nanocomposites were obtained by melt stretching processing after treatment of MFC with acetyl chloride to improve interfacial compatibility [136]. Interestingly, the formation of a shish kebab superstructure consisting of aligned (MFC) and PBS lamellae was postulated through SEM and SAXS observations.

PBSA is a biodegradable random copolyester derived from BDO and succinic and adipic acids, which has also a wide applied interest. Properties (e.g., modulus, tensile strength, biodegradability, thermal) can be improved by the addition of nanoclays [128,137–139].

The effect of two different types of organomodified montmorillonites (OMMTs) (i.e., C30B and C20A) on the nonisothermal crystallization of poly(butylene succinate-*co*-adipate) (PBSA) was reported, being found a peculiar influence of silicate

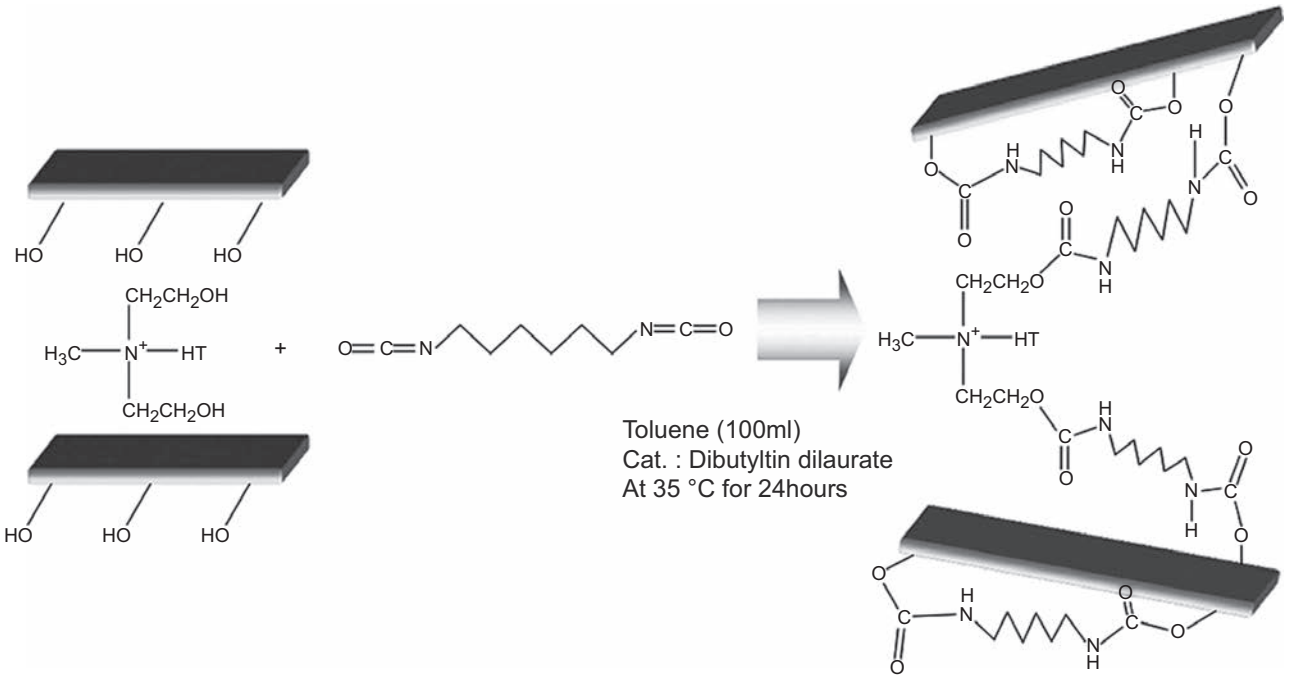

Figure 11.12 Increase of the silicate basal spacing of clay particles by surface urethane modification. Reproduced with permission from V. Ojijo, S.S. Ray, Progress in Materials Science 62 (2014) 1–57.

layers when an exfoliated structure was attained (i.e., with the incorporation of C30B). The behavior was explained as a consequence of the decrease of both spherulitic nucleation and crystal growth [140,141]. It was postulated that finely dispersed layers acted as obstacles for secondary nucleation. Cold crystallization was also influenced by the incorporation of exfoliated layers, and specifically a clear increase on the cold crystallization temperature was observed. In contrast, C20A was less compatible with the polymer matrix than C30B and an intercalated morphology was derived. In this case, a typical behavior characterized by a nucleating effect of nanoparticles and an increased crystallization rate was determined. In summary, crystal growth kinetics was delayed in delaminated nanocomposites, an opposed behavior to the increased rate usually detected for stacked/intercalated nanocomposites.

Nanocomposites from PBSA and synthetic fluorine mica were prepared by melt blending, being obtained exfoliated and intercalated silicate layers homogeneously dispersed in the polymer matrix. Nonisothermal crystallization studies demonstrated a negative effect of nanoparticles in the crystallization process due to increased activation energy, and therefore slower crystallization kinetics was derived [142].

The mechanical properties of PBSA were enhanced by the incorporation of 3 wt% of CNT-coated silk fibers coated with CNTs into PBSA while potential biodegradability was retained. Interactions between PBSA and CNT-coated silk fibers played a significant role, being the average interfacial shear strength of the nanocomposites close to 1.7 MPa, a value that was clearly higher than determined for similar composites lacking CNTs (i.e., 1.1 MPa) [143].

Nanocomposites of PBSA incorporating commercial halloysite nanotubes (HNTs) have also been prepared and characterized [144]. Scarce influence on the nucleation of PBSA and therefore a slight change in the isothermal crystallization kinetics was determined. Nevertheless, the presence of HNTs influenced on the melting behavior of PBSA because the typical melting–recrystallization process of less stable crystals during heating was hampered by the presence of HNTs. These nanoparticles caused also a decrease in thermal stability, an effect that contrasted with the observed one for clay containing nanocomposites. Addition of HNTs increased the flexural modulus up to 94% for a 20 wt% load, but the effect was lower than obtained after incorporation of the C15A OMMT. The rheological property measurements confirmed the achievement of a pseudonetwork structure at 5 wt% C15A loading, whereas the HNT-included system did not develop a network structure.

Water-assisted extrusion process has been revealed highly effective to attain a better dispersion and exfoliation levels of both native and organomodified montmorillonites in a PBSA matrix. The resulting films exhibited better barrier properties than typically extruded films, increasing this effect with the nanofiller content. Better properties were also determined for OMMT samples with respect to native montmorillonite (MMT) when samples with an equivalent load were compared [145].

The addition of clay nanoparticles into poly(ethylene succinate) (PES) has been studied. Results indicate an increase of the degree of crystallinity and consequently an improvement of its thermal and mechanical properties. Specifically, C30B clay particles (i.e., modified with methyl tallow bis(2-hydroxylethyl) quaternary

ammonium salt) were found to act as strong nucleating agent for PES crystallization [146]. Nanocomposites containing 5 wt% of the organomodified clay were prepared using solution-intercalation-film-casting technique and found a disordered intercalated structure from SAXS data and TEM micrographs. Favorable interactions between the polymer matrix and the clay organomodifier were postulated, being specifically detected a significant effect on the degree of crystallinity due to the nucleation role of the delaminated silicate layers. Nanocomposites showed also a highly significant improvement in thermal stability (i.e., the temperature at which 5% degradation occurs increased by approximately 40°C) as a consequence of the homogeneous dispersion of the silicate layers in the polymer matrix.

The in situ melt polycondensation method was applied to prepare biodegradable PES/graphene [147]. In this case, nanocomposites were obtained by polycondensation of SA with ethylene glycol containing a fine dispersion of exfoliated graphene oxide (GO) sheets through ultrasonic treatment. PES chains were effectively grafted onto these sheets, which were subsequently thermally reduced during reaction to graphene. The final nanocomposites showed a clear improvement of both thermal stability and mechanical properties even at low graphene loadings (i.e., the addition of 0.5 wt% of graphene increased the onset decomposition temperature by 12°C, and an improvement of 45% and 60% in tensile strength and in elongation at break was achieved).

The biodegradable copolyester poly(ethylene succinate-*co*-decamethylene succinate) (PEDS) is characterized by a relatively slow crystallization rate. To solve this problem, carboxyl-functionalized multiwalled carbon nanotubes (*f*-MWCNTs) were added, being also detected an improvement of mechanical properties [148]. A good dispersion of *f*-MWCNTs was observed at low load but aggregation began to develop at contents higher than 0.5 wt%.

Nanocomposites from cellulose nanocrystals (CNCs) and a PBS/PEG blend were also prepared by twin screw extrusion [149]. The use of a PEG/CNC masterbatch facilitated the dispersion of hydrophilic CNC nanoparticles in the hydrophobic PBS, being not detected an agglomeration of particles. A fractionated crystallization phenomenon of PEG was observed during cooling from the melt but no nucleating effect of CNC. The incorporation of a 4 wt% of CNC gave the best mechanical performance when modulus and elongation at break were considered.

Enzymatic hydrolysis of three nanocomposites prepared by in situ polymerization, based on a poly(propylene sebacate) matrix and having 2 wt% content of three types of nanoparticles (SiO_2, MWCNTs, and MMT) has recently been studied [150]. A similar degradation mechanism was found, but in all cases nanoparticles hampered the action of the enzymes. It was postulated that particles decreased the available matrix surface and also that significant interactions between nanoparticles and the polymer matrix were established. Results in any case illustrate the difficulty to predict the effect of fillers in the degradability. Thermal stability was enhanced by the incorporation of MWCNTs and MMT but was not influenced by the presence of SiO_2 [151].

11.6 Nanocomposites from poly(ester amide)s

Despite PEAs have a great interest as biocompatible and biodegradable materials for biomedical uses, their application as commodity materials is more restricted due to their high cost relative to conventional thermoplastics. Probably, one of the most economical PEAs is derived from BDO, adipic acid, and caprolactam (or alternatively 6-aminohexanoic acid). In this case, the use of biodegradable fillers such as starch [152–154] and reinforcing agents such as agrofibers with high tensile modulus (e.g., jute) was studied [155]. Furthermore, a good level of compatibility was found between plasticized wheat starch, and this aliphatic PEA and even coextruded films having PEA as hydrophobic outer layers have been proposed [156]. The use of corn starch as a filler gave rise to an increase in yield stress, a feature that is in contrast to the decrease typically observed in other starch-filled polymers [154].

This PEA was also melt-mixed with octadecyl-treated montmorillonites to get nanocomposites with improved mechanical and barrier properties [157,158]. Nanocomposites showed an intercalated structure on extrusion that became progressively delaminated as the shear rate increased, especially when the filler content was high. TEM morphological observations indicated that clay layers tended to be oriented parallel to the plane of the melt processed sheets, being possible to attain an 80% reduction of oxygen permeability with respect to the pure polymer.

The influence of nanoparticles (i.e., nano-$CaCO_3$ and nano-SiO_2) on the biodegradability of PEAs has also been evaluated being found that hydrolysis rate could be increased around the critical concentration where a percolation transition appeared (i.e., 5 wt% and 8 wt% for nano-SiO_2 and nano-$CaCO_3$-filled nanocomposites, respectively) [159].

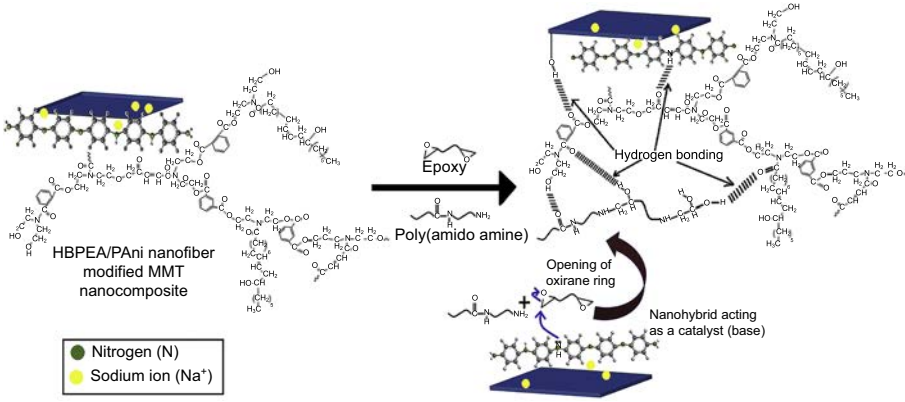

Figure 11.13 Interactions and curing reaction of hyperbranched poly(ester amide) (HBPEA) and nanohybrid using an epoxy-poly(amido amine) hardener system. *MMT*, montmorillonite; *PAni*, polyaniline.
Reproduced with permission from S. Pramanik, P. Bharali, B.K. Konwarh, N. Karak, Materials Science and Engineering: C 35 (2014) 61–69.

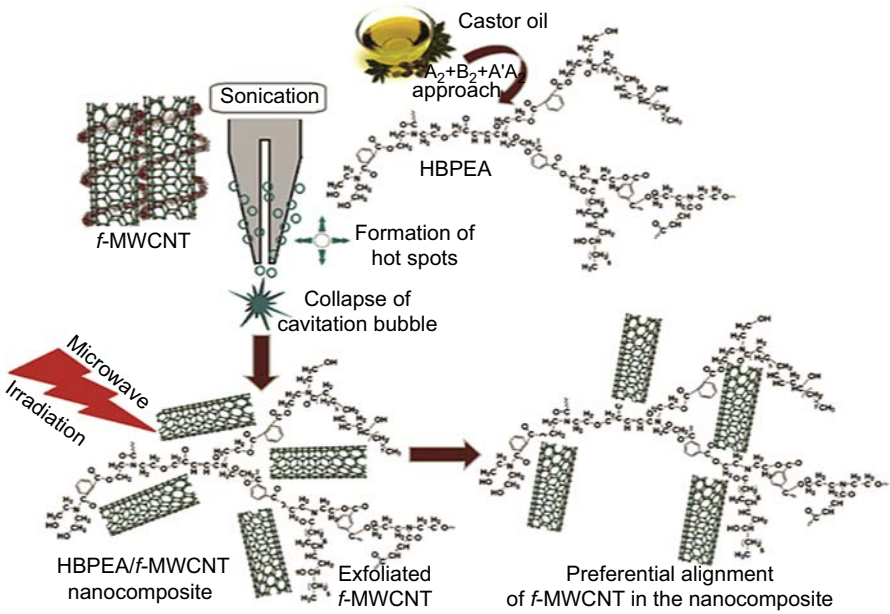

Figure 11.14 Preparation of the bio-based hyperbranched poly(ester amide) (HBPEA)–functionalized multiwalled carbon nanotube (*f*-MWCNT) nanocomposites by the synergism of ultrasonication and microwave irradiation.
Reproduced with permission from S. Pramanik, B.K. Konwarh, N. Barua, A.K. Buragohain, N. Karak, Biomaterials Science 2 (2014) 192–202.

An extensive work has also been carried out with PEAs having hyperbranched architectures due to their potential use as compatibilizers and the capability to provide a large number of functional groups.

Nanocomposites containing modified MMT (1, 2.5, and 5 wt%) were prepared from bio-based hyperbranched PEAs (HBPEAs) and polyaniline nanofibers. The prepared nanocomposites take advantage of the high antimicrobial activity of π-conjugated polymers such as polyaniline (PAni) [160], which is clearly enhanced when chains become organized in the nanoscale regime [161]. To this end, PAni chains were sandwiched between silicate layers giving rise to a nanohybrid that was then incorporated into an HBPEA matrix to get a long-term efficacy.

The hyperbranched polymer allowed getting a good interaction with the nanohybrid due to the presence of a large number of functional groups that provided high reactivity and compatibilizing ability. Furthermore, nanocomposites could be subsequently cured using a bisphenol-A-based epoxy resin and a poly(amido amine) hardener (Fig. 11.13) to render new thermosetting nanocomposites. These exhibited thermostability, good mechanical properties, and a remarkable activity against a wide spectrum of both bacterial (e.g., positive bacteria such as *Bacillus subtilis* and *Staphylococcus aureus*) and fungal (e.g., *Aspergillus niger*, *Fusarium oxysporum*, and *Coleotricum capcii*) strains and algal consortium (e.g., those comprising *Chlorella*, *Hormidium*, and *Cladophorella* species) [162].

Multifunctional bio-based nanocomposites were also obtained by incorporation of MWCNTs (1, 2.5, and 5 wt%) into the above-employed bio-based HBPEA. Nanotubes were functionalized in a single pot by covalent and noncovalent attachment of poly(glycidyl methacrylate) (PGMA) and PAni, respectively. Typical challenges of graphitic networks as chemical inertness, poor dispersion, and interfacial bonding were avoided, whereas high antibacterial efficacy was attained due to the synergism of MWCNTs and PAni nanofibers (Fig. 11.4) [163]. Pulsed ultrasounds were applied in the process because they were effective in the exfoliation and dispersion of MWCNT agglomerates in the HBPEA matrix [164,165]. Basically, ultrasounds led to the formation of high temperature and pressure domains as a consequence of cavitation, which favored exfoliation of noncovalently wrapped PAni nanofibers and increased the interaction with the HBPEA matrix.

An ultrasound-assisted noncovalent functionalization of MWCNTs with fatty amide of castor oil via CH-π interactions and their subsequent use as a reactive component in an in situ polymerization of HBPEA has also been reported [166]. Anchorage of ester-amide groups to the nanotubes was demonstrated as well as the intercalation and formation of dense polymer layers on the isotropically dispersed nanotubes. Nanocomposites showed a selective efficacy against the gram-positive bacteria (e.g., the death rate increased by 137.5% and by 107.6% for *Staphylococcus aureus* and *Bacillus subtilis*, respectively), maintained an acceptable mechanical performance, and had an enhanced thermal stability over pristine HBPEA [167].

PEAs incorporating α-amino acids appear as good candidates to be used as polymeric matrices because they are biocompatible and had good chemical stability and functionality together with other typical characteristics of PEAs such as high thermal stability, flexibility, high mechanical strength, good chemical resistance, and high biodegradability [167–169]. In addition, α-amino acids may lead to chiral properties and enhanced biodegradability [170–173].

HBPEAs based on various α-amino acids and having thioester moieties can easily be prepared through "click" chemistry [174]. The hyperbranched structure is attained by the dominant thiol-Michael addition of commercially available 1-thioglycerol to compounds derived from neutral α-amino acids. The resultant polymers can be used as a boxlike container to encapsulate metal ions taking also into account the strong affinity between sulfur atoms and Au [175]. The biocompatibility of selected HBPEA due to its biological origin makes it a good candidate for stabilizing gold nanoparticles. Specifically a water-soluble copolymer having a hydrophobic alanine-based HBPEA core containing thioether moieties, and numerous hydrophilic poly[2-(dimethylamino)ethyl methacrylate] (PDMAEMA) arms were found to render narrow-sized and ultrastable gold nanoparticles. These could act as not only a size-tunable nanoreactor due to their excellent catalytic activities under mild conditions but also a pH-sensitive matrix.

This copolymer showed also a reversible thermosensitive phase transitions caused by secondary aggregation of the large micelles driven by increasing hydrophobic interaction due to the dehydration of hydrophilic PDMAEMA arms on heating (Fig. 11.15).

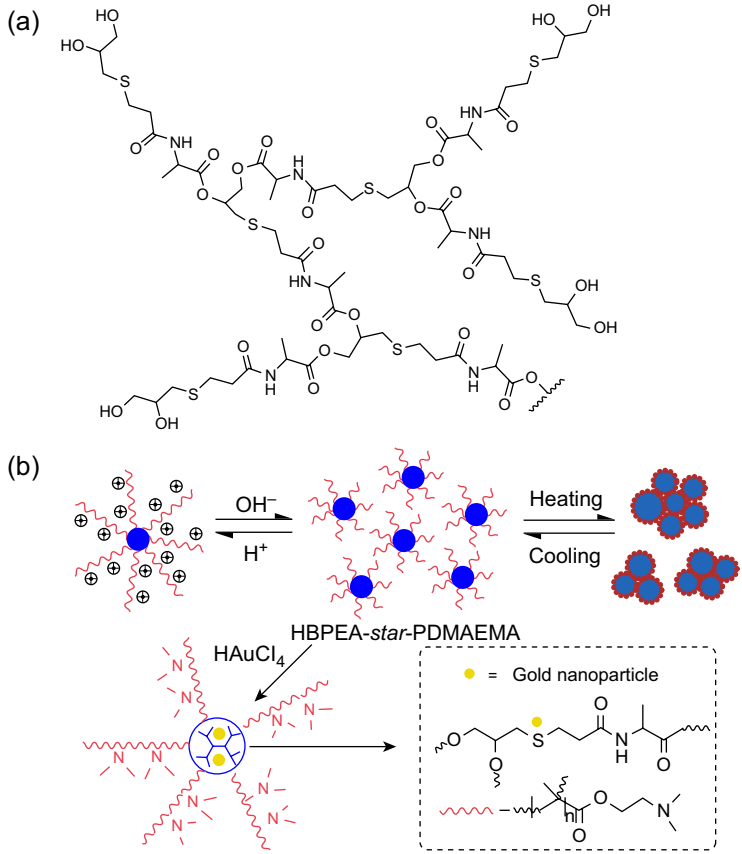

Figure 11.15 Chemical structure of hyperbranched poly(ester amide) (HBPEA) containing sulfur atoms able to interact with gold particles (a) and scheme showing the reversible thermosensitive transitions of copolymer having poly[2-(dimethylamino)ethyl methacrylate] (PDMAEMA) arms (b).
Reproduced with permission from Y. Bao, G. Shen, H. Liu, Y. Li, Polymer 54 (2013) 652–660.

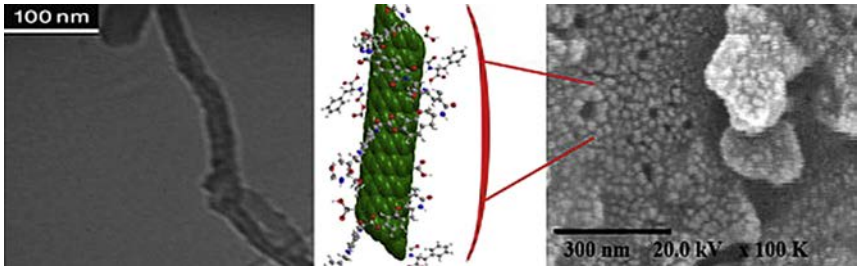

Figure 11.16 TEM (left) and field emission SEM (right) micrographs of the PAEI composite containing 15 wt% of multiwalled carbon nanotubes (MWCNTs). A scheme of the functionalized MWCNT is provided to illustrate its presence in the surface morphology micrograph.
Reproduced with permission from A. Abdolmaleki, S. Mallakpour, S. Borandeh, Applied Surface Science 287 (2013) 117–123.

Nanocomposites with well-dispersed MWCNTs were attained after their functionalization and the use of an L-phenylalanine containing poly(amide-ester-imide) [176] (PAEI) matrix (Fig. 11.16). The biodegradable PAEI was based on two different amino acids, which were synthesized via direct polycondensation of biodegradable *N*,*N*′-bis[2-(methyl-3-(4-hydroxyphenyl)propanoate)]isophthaldiamide and *N*,*N*′-(pyromellitoyl)-bis-L-phenylalanine diacid [177]. The functionalization process involved a typical chemical oxidation that allows creating carboxylic acid groups in the CNT surface followed by amidation with L-phenylalanine to increase molecular interactions and compatibility with the selected matrix. Furthermore, it was determined that thermal stability of new composites was significantly enhanced due to the good interfacial interactions between the amino acid–based PAEI and the amino acid–functionalized CNT.

Graphene nanoplatelets were also chemically functionalized with L-phenylalanine amino acid via direct Friedel–Crafts acylation in a polyphosphoric acid/phosphorus pentoxide medium [178]. This electrophilic substitution of C–H sites located on the graphite edges gave rise to a basal plane surface of graphite without any defects. The above-indicated chiral PAEI containing *S*-tyrosine and L-phenylalanine linkages was an interesting nanocomposite matrix because good interactions could be established. Specifically the influence of the different edge-selective functionalized graphite distributions on thermal and morphological features was evaluated. These nanocomposites were prepared by dispersion of functionalized nanoplatelets in 5, 10, and 15 wt% of PAEI solutions in DMAc via a vigorous stirring for 1 day, followed by ultrasonication for 1 h.

The in situ thermal polycondensation technique has been revealed effective to get nanocomposites from OMMTs and sodium chloroacetylaminohexanoate. The reaction led to new biodegradable PEAs based on an alternating disposition of glycolic acid and 6-aminohexanoic acid units, being the most dispersed structure obtained when the C25A organomodified clay was employed. Significant differences between the neat polymer and its nanocomposite with C25A were found from both isothermal and nonisothermal calorimetric analyses. Interestingly, the polymerization kinetics was highly influenced by the presence of the silicate particles because they reduced chain mobility and the Arrhenius preexponential factor [179].

In situ polymerization in the presence of C20A and C30B OMMTs rendered intercalated structures that contrast with the exfoliated structure found with the use of the C25A MMT [180]. Polymerization studies under nonisothermal and isothermal conditions indicated that C20A and C30B had a similar influence on the polymerization kinetics, and specifically a significant decrease on the activation energy and the Arrhenius preexponential factor with respect to the neat monomer was found. Nanoconfinement in the intercalated silicate galleries was postulated to favor the occurrence of polycondensation reactions that reduced the corresponding activation energy in comparison with the value determined for the exfoliated nanocomposite (i.e., that derived from C25A). This confinement led also to a decrease on the chain mobility, and consequently lower frequency factors than those calculated for the neat monomer were derived. Clear differences were also found with respect the polymerization carried out in the presence of the C25A clay because in this

case polymerization had similar activation energy to that determined for the neat monomer.

Melt mixing technique allowed also preparing intercalated nanocomposites from the organomodified C25A clay and the above-indicated biodegradable PEA [181]. The incorporation of nanoparticles had a clear influence on the crystallization rate because they increased the primary nucleation with respect to the neat polymer. The secondary nucleation constant also increased indicating a hampered crystal growth mechanism due to presence of clay particles. SAXS morphologic studies suggested that the lamellar insertion mechanism was favored for the nanocomposite during cold crystallization [181]. Similar results concerning crystallization kinetics were deduced for the intercalated nanocomposites prepared by in situ polymerization using the C20A and C30B clays [180]. Thermogravimetric studies showed also significant differences between the nanocomposite and the neat polymer because three and two decomposition steps were, respectively, detected [182]. The organomodifier compound decreased the onset mass loss temperature, whereas the silicate layers significantly decreased the degradation rate at the last stages of decomposition. Kinetic analyses demonstrated that the presence of the organomodified clay modified the mechanisms of degradation.

An exfoliated nanocomposite having the same components could alternatively be prepared by the film casting technique. In this case, both primary nucleation and crystal growth rate decreased significantly with the incorporation of nanoparticles. The degree of crystallinity and the size of crystalline domains decreased also significantly with the addition of the highly miscible organoclay [183].

An unsaturated poly(ester amide) derived from maleic and phthalic anhydrides, ethylene glycol, neopentylene glycol, and glycine was prepared by melt polycondensation [184]. Nanocomposites with hydroxyapatite (HAp) were successfully obtained by in situ polymerization, and flexural and degradable properties in function of the HAp content were evaluated. In fact, the incorporation of the bioceramic nanoparticles is usually performed to get prosthetic devices and implanted materials because HAp as a primary constituent of human hard tissues is biocompatible and nontoxic.

Novel nanocomposites based on poly(amide-ester-imide) (PAEI) containing L-leucine and nano-Mg-doped fluorapatite (Mod-MgFA) were prepared by means of ultrasonic irradiation [185]. Incorporation of F ions into HAp is interesting because it causes an increase in both thermal stability and crystallinity and a reduction in crystal strain [186]. Magnesium ions improved the adhesion strength between substrates and apatite coatings and are of interest for the development of artificial bones [187].

The surface of nanoparticles was modified with biodegradable optically active diacid *N*-trimellitylimido-L-leucine to increase their compatibility and dispersity into the polymer matrix. The derived nanocomposites having amide and imide linkages showed outstanding thermal properties while promising features were also expected from the incorporation of optically active units [188].

Polycondensation of vegetable seed oils (VSOs) derived from diol fatty amides and dicarboxylic acids/anhydrides rendered thermoset materials that could be used as protective coatings [189] with antimicrobial properties when manganese, cobalt, and copper ions were incorporated [190]. VSO-based waterborne PEA could, for example, be

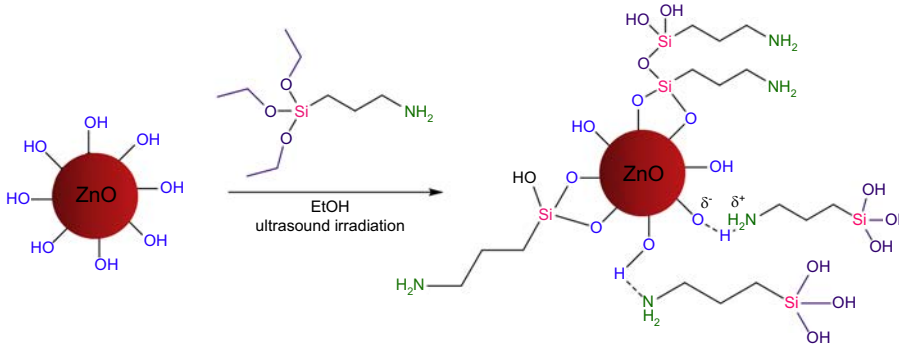

Figure 11.17 Surface modification of ZnO nanoparticles with γ-aminopropyltriethoxyl silane. Reproduced with permission from A. Abdolmaleki, S. Mallakpour, S. Borandeh, Polymer Bulletin 69 (2012) 15–28.

synthesized by a single pot reaction through microwave irradiation within 4–5 min by amidation and condensation of oil [191]. Nanocomposites of linseed oil–based PEAs with Cloisite 93A were obtained by a microwave-assisted mixing process. Irradiation played a crucial role on the final morphology because short exposure times led to intercalated structures, whereas longer times and lower Cloisite loads favored exfoliation [192,193].

PEA/ZnO bionanocomposites were obtained by incorporating ZnO nanoparticles treated with γ-aminopropyltriethoxyl silane as a coupling agent that facilitates the dispersion of particles into the polymer matrix under ultrasonic irradiation [194]. The aminosilane was selected due to its capability to interact with surface hydroxyl groups of ZnO through hydrogen bonding, ionic bonding, and covalent bonding (Fig. 11.17). Furthermore, good interactions with the polymer matrix could be established between NH_2 and the esteric or amidic C═O and N–H groups of PEA. ZnO was specifically selected because it is an environmentally friendly multifunctional semiconductor that has low toxicity and offers a wide range of potential applications (e.g., gas sensors, piezoelectric devices, electroacoustic transducers, UV light–emitting devices, or UV absorbers) [195–198].

11.7 Conclusions

Nowadays, great efforts are focused on the development of biodegradable polymers based on renewable resources. These materials can be employed as ecological products for commodity applications as well as specialties with applications in the biomedical field. Bioproduction of chemicals is a reality that allows getting monomers in a competitive production scale to traditional petrochemicals. Different aliphatic diols and dicarboxylic acids can be prepared from natural resources justifying the interest on biodegradable poly(alkylene dicarboxylate)s. Furthermore, incorporation of carbohydrates widens the range of possibilities and properties because it leads to polymers with an increased molecular stiffness. In addition, natural α-amino acids can

easily be incorporated to the above indicated polyesters (with or without sugar rings) giving rise to biodegradable PEAs. In this case, polymers display peculiar properties due to their capability to form strong intermolecular hydrogen bonds through their amide groups. Furthermore, the presence of α-amino acids guarantees the enzymatic biodegradability of these polymers and supports their high potential for applications in the biomedical sector as pointed out in this chapter.

Properties of aliphatic polyesters, PEAs, and related compounds can be easily improved by addition of nanoparticles. Results achieved in the recent reviewed publications have demonstrated that an immense potential has just been opened considering the different additives (e.g., clays, CNTs, graphene, "kind viruses" such as bacteriophages), the inherent properties of the polymer matrices, and the increasing scientific knowledge about nanocomposites.

References

[1] T. Anthierens, L. Billiet, F. Devlieghere, F. du Prez, Innovative Food Science & Emerging Technologies 15 (2012) 81–85.
[2] D.F. Coutinho, M.E. Gomes, N.M. Neves, R.L. Reis, Acta Biomaterialia 8 (2012) 1490–1497.
[3] J.P. Bruggeman, B.-J. de Bruin, C.J. Bettinger, R. Langer, Biomaterials 29 (2008) 4726–4735.
[4] Y. Wang, Y.M. Kim, R. Langer, Journal of Biomedical Materials Research Part A 66 (2003) 192–197.
[5] C.J. Bettinger, E.J. Weinberg, K.M. Kulig, J.P. Vacanti, Y. Wang, J.T. Borenstein, R. Langer, Advanced Materials 18 (2006) 165–169.
[6] A.R. Webb, V.A. Kumar, G.A. Ameer, Journal of Materials Chemistry 17 (2007) 900–906.
[7] J. Simitzis, S. Soulis, D. Triantou, L. Zoumpoulakis, P. Zotali, Journal of Materials Science: Materials in Medicine 22 (2011) 2673–2684.
[8] T. Fujimaki, Polymer Degradation and Stability 59 (1998) 209–214.
[9] Y. Ichikawa, T. Mizukoshi, Advances in Polymer Science 245 (2012) 285–314.
[10] M. Niaounakis (Ed.), Biopolymers Reuse, Recycling, and Disposal, Chap. 1: Introduction to Biopolymers, William Andrew Publishing, Elsevier, 2013, pp. 1–75.
[11] M.W. Peters, J.D. Taylor, M. Jenni, L.E. Manzer, D.E. Henton, Integrated Process to Selectively Convert Renewable Isobutanol to p-xylene, 2011, US Patent 20,110,087,000.
[12] C. Berti, E. Binassi, M. Colonna, M. Fiorini, G. Kannan, S. Karanam, M. Mazzacurati, I. Odeh, Bio-based Terephthalate Polyesters, 2010, US Patent 20,100,168,461.
[13] N. Jacquel, R. Saint-Loup, J.-P. Pascault, A. Rousseau, F. Fenouillot, Polymer 59 (2015) 234–242.
[14] J.J. Lee, G.A. Kraus, Green Chemistry 16 (2014) 2111–2116.
[15] Y. Tachinaba, S. Kimura, K.-I. Kasuya, Scientific Reports 5 (2015) 8249–8253.
[16] M. Colonna, C. Berti, M. Fiorini, E. Binassi, M. Mazzacurati, M. Vannini, S. Karanam, Green Chemistry 13 (2011) 2543–2549.
[17] Toray Industries, Inc., Toray and Gevo Sign Bio-paraxylene Offtake Agreement for the World's 1st Pilot-scale Fully Renewable, Bio-based Polyethylene Terephthalate (PET) Production, 2012, Available from: http://www.toray.com/news/rd/nr120627.html.
[18] A. Celli, P. Marchese, L. Sisti, D. Dumand, S. Sullalti, G. Totaro, Polymer International 62 (2013) 1210–1217.

[19] F. Fenouillot, A. Rousseau, G. Colomines, R. Saint-Loup, J.P. Pascault, Progress in Polymer Science 35 (2010) 578–622.
[20] S.S. Ray, K. Yamada, M. Okamoto, K. Ueda, Macromolecular Materials and Engineering 288 (2003) 203–208.
[21] N. Heidarzadeh, M. Rafizadeh, F.A. Taromi, L.J. Valle, L. Franco, J. Puiggalí, Polymers 8 (2016) 253.
[22] S.I. Han, J.S. Lim, D.K. Kim, M.N. Kim, S.S. Im, Polymer Degradation and Stability 93 (2008) 889–895.
[23] G. Chouzouri, M. Xanthos, Acta Biomaterialia 3 (2007) 745–756.
[24] A. Díaz, R. Katsarava, J. Puiggalí, International Journal of Molecular Sciences 15 (2014) 7064–7123.
[25] Y.K. Han, J.W. Um, S.S. Im, B.C. Kim, Journal of Polymer Science, Part A: Polymer Chemistry 39 (2001) 2143–2150.
[26] C.Y. Zhu, Z.Q. Zhang, Q.P. Liu, Z.P. Wang, J. Jin, Journal of Applied Polymer Science 90 (2003) 982–990.
[27] B. Saulnier, J. Coudane, H. Garreau, M. Vert, Polymer 47 (2006) 1921–1929.
[28] J. Yang, S. Zhang, X. Liu, A. Cao, Polymer Degradation and Stability 81 (2003) 1–7.
[29] J.S. Lim, S.M. Hong, D.K. Kim, S.S. Im, Journal of Applied Polymer Science 107 (2008) 3598–3608.
[30] D.N. Bikiaris, D.S. Achilias, Polymer 47 (2006) 4851–4860.
[31] Y.Y. Linko, Z.L. Wang, J. Seppala, Journal of Biotechnology 40 (1995) 133–138.
[32] H. Uyama, K. Inada, S. Kobayashi, Polymer Journal 35 (2000) 440–443.
[33] S. Kobayashi, H. Uyama, S. Namekawa, Polymer Degradation and Stability 59 (1998) 195–201.
[34] A. Takasu, Y. Iio, Y. Oishi, Y. Narukawa, T. Hirabayashi, Macromolecules 38 (2005) 1048–1050.
[35] A. Takasu, Y. Oishi, Y. Iio, Y. Inai, T. Hirabayashi, Macromolecules 36 (2003) 1772–1774.
[36] M. Garaleh, M. Lahcini, H.R. Kricheldorf, S.M. Weidner, Journal of Polymer Science, Part A: Polymer Chemistry 47 (2009) 170–177.
[37] N. Jacquel, F. Freyermouth, F. Fenouillot, A.P. Rousseau, J. Pascault, P. Fuertes, R. Saint-Loup, Journal of Polymer Science, Part A: Polymer Chemistry 49 (2011) 5301–5312.
[38] P. Werle, M. Morawietz, S. Lundmark, K. Sörensen, E. Karvinen, J. Lehtonen, in: Ullmann's Encyclopedia of Industrial Chemistry, Wiley-VCH Verlag GmbH & Co. KGaA, 2008.
[39] D.P. Minh, M. Besson, C. Pinel, P. Fuertes, C. Petitjea, Topics in Catalysis 53 (2010) 1270–1273.
[40] R. Luque, J.H. Clark, K. Yoshida, P.L. Gai, Chemical Communications 21 (2009) 5305–5307.
[41] C. Wang, A. Thygesen, Y. Liu, Q. Li, M. Yang, D. Dang, Z. Wang, Y. Wan, W. Lin, J. Xing, Biotechnology for Biofuels 6 (2013) 74–84.
[42] P. Gallezot, Chemical Society Reviews 41 (2012) 1538–1558.
[43] T. Buntara, S. Noel, P.H. Phua, I. Melian-Cabrera, J.G. de Vries, H.J. Heeres, Angewandte Chemie International Edition 50 (2011) 7083–7087.
[44] K.M. Zia, A. Noreen, M. Zuber, S. Tabasum, M. Mujahid, International Journal of Biological Macromolecules 82 (2016) 128–1040.
[45] H. Mutlu, M.A.R. Meier, European Journal of Lipid Science and Technology 112 (2010) 10–30.
[46] S.K. Bhatia, R.K. Bhatia, Y.-H. Yang, Reviews in Environmental Science and Biotechnology 15 (2016) 639–663.

[47] H.M. Jung, M.Y. Jung, M.K. Oh, Applied Microbiology and Biotechnology 99 (2015) 5217–5225.
[48] T.S. Moon, S.-H. Yoon, A.M. Lanza, J.D. Roy-Mayhew, K.L.J. Prather, Applied and Environmental Microbiology 75 (2009) 589–595.
[49] M.S. Smit, M.M. Mokgoro, E. Setati, J.M. Nicaud, Biotechnology Letters 27 (2005) 859–864.
[50] Y. Yang, W. Lu, X. Zhang, W. Xie, M. Cai, R.A. Gross, Biomacromolecules 11 (2010) 259–268.
[51] L. Hojabri, X. Kong, S.S. Narine, Biomacromolecules 11 (2010) 911–918.
[52] D. Quinzler, S. Mecking, Angewandte Chemie International Edition 49 (2010) 4306–4308.
[53] F. Stempfle, D. Quinzler, I. Heckler, S. Mecking, Macromolecules 44 (2011) 4159–4166.
[54] S. Huf, S. Krügener, T. Hirth, S. Rupp, S. Zibek, European Journal of Lipid Science and Technology 113 (2011) 548–561.
[55] M. Genas, Angewandte Chemie International Edition 74 (1962) 535–540.
[56] J. Trzaskowski, D. Quinzler, C. Bahrle, S. Mecking, Macromolecular Rapid Communications 32 (2011) 1352–1356.
[57] X. Li, Z. Hong, J. Sun, Y. Geng, Y. Huang, H. An, The Journal of Physical Chemistry B 113 (2009) 2695–2704.
[58] V. Tserki, P. Matzinos, E. Pavlidou, D. Vachliotis, C. Panayiotou, Polymer Degradation and Stability 91 (2006) 367–376.
[59] Z. Liang, P. Pan, B. Zhu, T. Dong, L. Hua, Y. Inoue, Macromolecules 43 (2010) 2925–2932.
[60] Z. Liang, P. Pan, B. Zhu, Y. Inoue, Polymer 52 (2011) 2667–2676.
[61] A. Díaz, L. Franco, J. Puiggalí, Thermochimica Acta 575 (2014) 45–54.
[62] A. Díaz, L. Franco, F. Estrany, L.J. del Valle, J. Puiggalí, Polymer Degradation and Stability 99 (2014) 80–91.
[63] I. Arandia, A. Mugica, M. Zubitur, A. Arbe, G. Liu, G. Wang, R. Mincheva, P. Dubois, A.J. Müller, Macromolecules 48 (2015) 43–57.
[64] J.A. Galbis, M.G. García-Martín, M.V. de Paz, E. Galbis, Chemical Reviews 116 (2016) 1600–1636.
[65] M.A.G. Jansen, L.H. Wu, J.G.P. Goossens, G. de Wit, C. Bailly, C.E. Koning, G. Portale, Journal of Polymer Science, Part A: Polymer Chemistry 46 (2008) 1203–1217.
[66] R. Sablong, R. Duchateau, C.E. Koning, G. de Wit, D. van Es, R. Koelewijn, J. van Haveren, Biomacromolecules 9 (2008) 3090–3097.
[67] C. Lavilla, E. Gubbels, A. Martínez de Ilarduya, B.A.J. Noordover, C.E. Koning, S. Muñoz-Guerra, Macromolecules 46 (2013) 4335–4345.
[68] E. Gubbels, C. Lavilla, A. Martínez de Ilarduya, B.A.J. Noordover, C.E. Koning, S. Muñoz-Guerra, Journal of Polymer Science, Part A: Polymer Chemistry 52 (2014) 164–177.
[69] J. Wu, P. Eduard, S. Thiyagarajan, J. van Haveren, D.S. van Es, C.E. Koning, M. Lutz, C. Fonseca Guerra, ChemSusChem 4 (2011) 599–603.
[70] C. Lavilla, A. Alla, A. Martínez de Ilarduya, S. Muñoz-Guerra, Biomacromolecules 14 (2013) 781–793.
[71] E. Zakharova, C. Lavilla, A. Alla, A. Martínez de Ilarduya, S. Munñoz-Guerra, European Polymer Journal 61 (2014) 263–273.
[72] M.G. García-Martín, R. Ruiz Pérez, E. Benito Hernández, J.A. Galbis, Macromolecules 39 (2006) 7941–7949.
[73] O. Goerz, H. Ritter, Polymer International 62 (2013) 709–712.

[74] H. Kang, X. Li, J. Xue, L. Zhang, L. Liu, R. Xu, B. Guo, RSC Advances 4 (2014) 19462–19471.
[75] C. Lorenzini, A. Haider, I.-K. Kang, M. Sangermano, S. Abbad-Andalloussi, P.-E. Mazeran, J. Lalevee, E. Renard, V. Langlois, D.-L. Versace, Biomacromolecules 16 (2015) 683–694.
[76] M. Okada, M. Yamada, M. Yokoe, K. Aoi, Journal of Applied Polymer Science 81 (2001) 2721–2734.
[77] Z. Gomurashvili, H.R. Kricheldorf, R. Katsarava, Journal of Macromolecular Science, Part A: Pure and Applied Chemistry 37 (2000) 215–227.
[78] G.C. Landis, W.G. Turnell, Y. Yumin, Delivery of Ophthalmologic Agents to the Exterior or Interior of the Eye, 2007, WO 2007/130477A2.
[79] I. Molina, M. Bueno, J.A. Galbis, Macromolecules 28 (2005) 3766–3770.
[80] I. Molina, M. Bueno, F. Zamora, J.A. Galbis, Journal of Polymer Science, Part A: Polymer Chemistry 36 (1998) 67–77.
[81] R. Katsarava, N. Kulikova, J. Puiggalí, Jacobs Journal of Regenerative Medicine 1 (3) (2016) 1–14 012.
[82] R. Katsarava, Z. Gomurashvili, Biodegradable polymers composed of naturally occurring α-amino acids, in: A. Lendlein, A. Sisson (Eds.), Handbook of Biodegradable Polymers - Isolation, Synthesis, Characterization and Applications, Wiley-VCH, Verlag GmbH & Co. KGaA, 2011, pp. 107–131. Ch. 5.
[83] R. Katsarava, V. Beridze, N. Arabuli, D. Kharadze, C.C. Chu, C.Y. Won, Journal of Polymer Science, Part A: Polymer Chemistry 37 (1999) 391–407.
[84] T. Memanishvili, N. Zavradashvili, N. Kupatadze, D. Tugushi, M. Gverdtsiteli, V.P. Torchilin, C. Wandrey, L. Baldi, S.S. Manoli, R. Katsarava, Biomacromolecules 15 (2014) 2839–2848.
[85] D. Yamanouchi, J. Wu, A.N. Lazar, K.C. Kent, C.C. Chu, B. Liu, Biomaterials 29 (22) (2008) 3269–3277.
[86] J. Heller, Biomaterials 11 (1990) 659–665.
[87] R. Storbeck, M. Rehahn, M. Ballauff, Makromolekulare Chemie 194 (1993) 53–64.
[88] R. Storbeck, M. BaUauff, Polymer 34 (1993) 5003–5006.
[89] D. Braun, M. Bergmann, Journal fuer Praktische Chemie 334 (1992) 298–310.
[90] M. Majdoub, A. Loypy, G. Heche, European Polymer Journal 30 (1994) 1431–1437.
[91] G. Schwarz, H.R. Kricheldorf, Journal of Polymer Science Part A: Polymer Chemistry 34 (1996) 603–611.
[92] H.R. Kricheldorf, Journal of Macromolecular Science-Reviews in Macromolecular Chemistry and Physics C37 (1997) 599–631.
[93] H.R. Kricheldorf, Z. Gomourachvili, Macromolecular Chemistry and Physics 198 (1997) 3149–3160.
[94] E. Cognet-Georjon, F. Mechin, J.P. Pascault, Macromolecular Chemistry and Physics 196 (1995) 3733–3751.
[95] R. Katsarava, D. Tugushi, Z.D. Gomurashvili, Poly(ester Urea) Polymers and Methods of Use, 2014, US Patent No. 8765164.
[96] T. Kartvelishvili, G. Tsitlanadze, L. Edilashvili, N. Japaridze, R. Katsarava, Macromolecular Chemistry and Physics 198 (1997) 1921–1932.
[97] U. Short, Glycols and bischloroformates, in: J.K. Stille, T.W. Campbell (Eds.), Condensation Monomers, John Wiley-Interscience, New York, 1972.
[98] N. Paredes, A. Rodriguez-Galan, J. Puiggalí, Journal of Polymer Science, Part A: Polymer Chemistry 36 (1998) 1271–1282.

[99] N. Parades, M.T. Casas, J. Puiggalí, B. Lotz, Journal of Polymer Science, Part A: Polymer Chemistry 37 (1999) 2521–2533.
[100] N. Paredes, A. Rodrıguez-Galan, J. Puiggalı, J. Peraire, Journal of Applied Polymer Science 69 (1998) 1537–1549.
[101] A. Rodrıguez-Galan, M. Pelfort, J.E. Aceituno, J. Puiggalı, Journal of Applied Polymer Science 74 (1999) 2312–2320.
[102] A. Rodrıguez-Galan, L. Fuentes, J. Puiggalı, Polymer 41 (2000) 5967–5970.
[103] M. Nagata, Macromolecular Chemistry and Physics 200 (1999) 2059–2064.
[104] P.W. Morgan, Condensation Polymers: By Interfacial and Solution Methods, Interscience, New York (, 1965.
[105] R.D. Katsarava, Russian Chemical Reviews 60 (1991) 722–737.
[106] R. Katsarava, Active Polycondensation - from peptide chemistry to amino acid based biodegradable polymers, in: H.R. Kricheldorf (Ed.), Polycondensation 2002", Macromolecular Symposia, 199, Wiley-VCH, 2003, pp. 419–429.
[107] R. Katsarava, Z. Alavidze, Polymer Blends as Biodegradable Matrices for Preparing Biocomposites, 2004, U.S. Patent 6703040.
[108] K. Markosishvili, G. Tsitlanadze, R. Katsarava, J.G. Morris, A. Sulakvelidze, International Journal of Dermatology 41 (2002) 453–458.
[109] D. Jikia, N. Chkhaidze, E. Imedashvili, I. Mgaloblishvili, G. Tsitlanadze, R. Katsarava, J.G. Morris Jr., A. Sulakvelidze, Clinical and Experimental Dermatology 30 (2005) 23–26.
[110] S.K. Murase, L.-P. Lv, A. Kaltbeitzel, K. Landfester, L.J. del Valle, R. Katsarava, J. Puiggali, D. Crespy, RSC Advances 5 (2015) 55006–55014.
[111] S.K. Murase, L.J. del Valle, S. Kobauri, R. Katsarava, J. Puiggalí, Polymer Degradation and Stability 119 (2015) 275–287.
[112] L.J. del Valle, L. Franco, R. Katsarava, J. Puiggalí, AIMS Molecular Science 3 (1) (2016) 52–87.
[113] G. Jokhadze, M. Machaidze, H. Panosyan, C.C. Chu, R. Katsarava, Journal of Biomaterials Science Polymer Edition 18 (2007) 411–438.
[114] C.C. Chu, R. Katsarava, Elastomeric Functional Biodegradable Copolyester Amides and Copolyester Urethanes, U.S. Patents: 6503538, 2003, p. 7304122 (2007; 7408018(2008)).
[115] K.M. DeFife, K. Grako, G. Cruz-Aranda, S. Price, R. Chantung, K. Macpherson, R. Khoshabeh, S. Gopalan, W.G. Turnell, Journal of Biomaterials Science 20 (2009) 1495–1511.
[116] S.H. Lee, I. Szinai, K. Carpenter, R. Katsarava, G. Jokhadze, C.C. Chu, Y. Huang, E. Verbeken, O. Bramwell, I. De Scheerder, M.K. Hong, Coronary Artery Disease 13 (2002) 237–241.
[117] Z. Gomurashvili, H. Zhang, J. Da, T.D. Jenkins, J. Hughes, M. Wu, L. Lambert, K.A. Grako, K.M. DeFife, K. Macpherson, V. Vassilev, R. Katsarava, W.G. Turnell, From drug-eluting stents to biopharmaceuticals: poly(ester amide) a versatile new bioabsorbable biopolymer, in: A. Mahapatro, A.S. Kulshrestha (Eds.), ACS Symposium Series 977: Polymers for Biomedical Applications, ACS Symposium Series 977: Polymers for Biomedical Applications, vol. 10–26 , Oxford University Press, 2008.
[118] M. Kropp, K.-M. Morawa, G. Mihov, A.K. Salz, N. Harmening, A. Franken, A. Kemp, A.A. Dias, J. Thies, S. Johnen, G. Thumann, Polymers 6 (2014) 243–260.
[119] V. Andrés-Guerrero, M. Zongc, E. Ramsay, B. Rojas, S. Sarkhel, B. Gallego, R. de Hoz, A.I. Ramírez, J.J. Salazar, A. Triviño, J.M. Ramírez, E.M. del Amo, N. Camerong, B. de-las-Heras, A. Urtti, G. Mihov, A. Dias, R. Herrero-Vanrell, Journal of Controlled Release 211 (2015) 105–117.

[120] A. Díaz, L.J. del Valle, D. Tugushi, R. Katsarava, J. Puiggalí, Materials Science and Engineering: C 46 (2015) 450–462.
[121] M. Planellas, M.M. Pérez-Madrigal, L.J. del Valle, S. Kobauri, R. Katsarava, C. Alemán, J. Puiggalí, Polymer Chemistry 6 (2015) 925–937.
[122] K.S. Stakleff, F. Lin, L.A. Smith Callahan, M.B. Wade, A. Esterle, J. Miller, M.L. Becker, Acta Biomaterialia 9 (2013) 5132–5142.
[123] G. Policastro, F. Lin, A. Esterle, F. Harris, M. Graham, R. Katsarava, K.S. Stakleff, M.L. Becker, OGP functionalized phenylalanine-based poly(ester urea) for enhancing osteoinductive potential of human mesenchymal stem cells, in: 249th ACS National Meeting & Exposition, March 22-26, Denver, CO, USA, 2015.
[124] J. Yu, F. Lin, P. Lin, Y. Gao, M.L Becker, Macromolecules 47 (2014) 121–129.
[125] M. Vert, Biomacromolecules 6 (2005) 538–546.
[126] S.S. Ray, K. Okamoto, M. Okamoto, Macromolecules 36 (2003) 2355–2367.
[127] S.Y. Hwang, E.S. Yoo, S.S. Im, Polymer Journal 44 (2012) 1179–1190.
[128] V. Ojijo, S.S. Ray, Processing strategies in bionanocomposites, Progress in Materials Science 38 (2013) 1543–1589.
[129] V. Ojijo, S.S. Ray, Progress in Materials Science 62 (2014) 1–57.
[130] S.K. Lim, S.I. Lee, S.G. Jang, K.H. Lee, H.J. Choi, I.J. Chin, Journal of Macromolecular Science, Part B: Polymer Physics 50 (2011) 100–110.
[131] L. Tan, Y. Chen, W. Zhou, S. Ye, J. Wei, Polymer 52 (2011) 3587–3596.
[132] L. Song, Z. Qiu, Polymers for Advanced Technologies 22 (2011) 1642–1649.
[133] X. Wang, H. Yang, L. Song, Y. Hu, W. Xing, H. Lu, Composites Science and Technology 72 (2011) 1–6.
[134] S.I. Han, J.S. Lim, D.K. Kim, M.N. Kim, S.S. Im, Polymer Degradation and Stability 93 (2008) 889–895.
[135] A.A. Vassiliou, D. Bikiaris, K. El Mabrouk, M. Kontopoulou, Journal of Appled Polymer Science 119 (2011) 2010–2024.
[136] M. Zhou, M. Fan, Y. Zhao, et al., Carbohydrate Polymers 140 (2016) 383–392.
[137] S. Sinha Ray, J. Bandyopadhyay, M. Bousmina, Polymer Degradation and Stability 92 (2007) 802–812.
[138] K.M. Dean, S.J. Pas, L. Yu, A. Ammala, A.J. Hill, D.Y. Wu, Journal of Applied Polymer Science 113 (2009) 3716–3724.
[139] G. Chen, J.S. Yoon, Polymer International 54 (2005) 939–945.
[140] S. Sinha Ray, M. Bousmina, Polymer 46 (2005) 12430–12439.
[141] S.S. Ray, J. Bandyopadhyay, M. Bousmin, European Polymer Journal 44 (2008) 3133–3145.
[142] S. Sinha Ray, M. Bousmina, Macromolecular Chemistry and Physics 207 (2006) 1207–1209.
[143] H.S. Kim, B.H. Park, J.S. Yoon, H.J. Jin, Polymer International 56 (2007) 1035.
[144] F.-G. Chiu, Polymer Test 54 (2016) 1–11.
[145] S. Charlon, N. Follain, E. Dargent, J. Soulestin, M. Sclavons, S. Marais, The Journal of Physical Chemistry C 120 (2016) 13234–13248.
[146] S.R. Suprakas, E.M. Mamookho, Polymer 50 (2009) 4635–4643.
[147] J. Zhao, X. Wang, W. Zhou, E. Zhi, W. Zhang, J. Ji, Journal of Applied Polymer Science 130 (2013) 3212–3220.
[148] X. Li, Z. Qin, Industrial & Engineering Chemistry Research 55 (2016) 3797–3803.
[149] L.N. Luduena, E. Fortunati, J.I. Moran, et al., Journal of Applied Polymer Science 133 (2016) 43302–43311.

[150] D.N. Bikiaris, N.P. Nianias, E.G. Karagiannidou, A. Docoslis, Polymer Degradation and Stability 97 (2012) 2077–2089.
[151] K. Chrissafis, E. Roumeli, K.M. Paraskevopoulos, N. Nianias, D.N. Bikiaris, Journal of Analytical and Applied Pyrolysis 96 (2012) 92–99.
[152] T. Ferre, L. Franco, A. Rodriguez-Galan, J. Puiggali, Polymer 44 (2003) 6139–6152.
[153] L. Avérous, N. Fauconnier, L. Moro, C. Fringant, Journal of Applied Polymer Science 76 (2000) 1117–1128.
[154] L. Willett, F.C. Felker, Polymer 46 (2005) 3035–3042.
[155] A.K. Mohanty, M.A. Khan, G. Hinrichsen, Influence of chemical surface modification on the properties of biodegradable jute Fabrics-polyester amide composites, Composites Part, A: Applied Science and Manufacturing 31 (2000) 143–150.
[156] O. Martin, L. Averous, Journal of Applied Polymer Science 86 (2002) 2586–2600.
[157] M. Krook, A.C. Albertsson, U.W. Gedde, M.S. Hedenqvist, Polymer Engineering & Science 42 (2002) 1238–1246.
[158] M. Krook, G. Morgan, M.S. Hedenqvist, Polymer Engineering & Science 45 (2005) 135–141.
[159] X. Liu, Y. Zou, G. Cao, D. Luo, Materials Letters 61 (2007) 4216–4221.
[160] Q. Jia, S. Shan, L. Jiang, Y. Wang, D. Li, Journal of Applied Polymer Science 125 (2012) 3560–3566.
[161] Z. Du, C. Li, L. Li, M. Zhang, S. Xu, T. Wang, Materials Science and Engineering: C 29 (2009) 1794–1797.
[162] S. Pramanik, P. Bharali, B.K. Konwarh, N. Karak, Materials Science and Engineering: C 35 (2014) 61–69.
[163] S. Pramanik, B.K. Konwarh, N. Barua, A.K. Buragohain, N. Karak, Biomaterials Science 2 (2014) 192–202.
[164] F.H. Gojny, M.H.G. Wichmann, U. Kopke, B. Fiedler, K. Schulte, Composites Science and Technology 64 (2004) 2363–2371.
[165] R. Konwarh, S. Pramanik, D. Kalita, C.L. Mahanta, N. Karak, Ultrasonics Sonochemistry 19 (2012) 292–299.
[166] S. Pramanik, N. Barua, A.K. Buragohain, J. Hazarika, A. Kumar, N. Karak, The Journal of Physical Chemistry C 117 (2013) 25097–25107.
[167] M. Okada, Progress in Polymer Science 27 (1) (2002) 87–133.
[168] L.S. Nair, C.T. Laurencin, Progress in Polymer Science 32 (2007) 762–798.
[169] A. Rodríguez-Galán, L. Franco, J. Puiggalí, Polymers 3 (2011) 65–99.
[170] S. Mallakpour, P. Asadi, M.R. Sabzalian, Amino Acids 41 (2011) 1215–1222.
[171] S. Mallakpour, F. Tirgir, M.R. Sabzalian, Journal of Polymer Research 18 (2011) 373–384.
[172] P. Karimi, A.S. Rizkalla, K. Mequanint, Nature Materials 3 (2010) 2346–2368.
[173] G. Tsitlanadze, T. Kviria, R. Katsarava, C.C. Chu, Journal of Materials Science 15 (2004) 185–190.
[174] Y.M. Bao, X.H. Liu, X.L. Tang, Y.S. Li, Journal of Polymer Science, Part A: Polymer Chemistry 48 (23) (2010) 5364–5374.
[175] Y. Bao, G. Shen, H. Liu, Y. Li, Polymer 54 (2013) 652–660.
[176] A. Abdolmaleki, S. Mallakpour, S. Borandeh, Applied Surface Science 287 (2013) 117–123.
[177] A. Abdolmaleki, S. Mallakpour, S. Borandeh, Materials Research Bulletin 47 (2012) 1123–1129.
[178] S. Mallakpour, A. Abdolmaleki, S. Borandeh, Chemical Society 12 (2015) 2065–2073.
[179] L.T. Morales, L. Franco, M.T. Casas, J. Puiggalí, Journal of Polymer Science, Part A: Polymer Chemistry 47 (2009) 3616–3629.

[180] L.T. Morales-Gámez, I. Jones, L. Franco, J. Puiggalí, Express Polymer Letters 5 (2011) 717–731.
[181] L. Morales-Gámez, L. Franco, M.T. Casas, J. Puiggalí, Polymer Engineering & Science 51 (2011) 1650–1661.
[182] L.T. Morales-Gámez, L. Franco, J. Puiggalí, Thermochimica Acta 512 (2011) 142–149.
[183] L.T. Morales, L. Franco, M.T. Casas, J. Puiggalí, Journal of Polymer Science Part, B: Polymer Physics 48 (2010) 33–46.
[184] M. Ganjaee Sari, B. Ramezanzadeh, M. Shahbazi, A.S. Pakdel, Journal of Applied Polymer Science 121 (2011) 2591–2596.
[185] S. Mallakpour, M. Khani, F. Mallakpour, M. Fathi, Journal of Polymer Research 23 (2016) 198–211.
[186] M.H. Fathi, E. Mohammadi Zahrani, Journal of Crystal Growth 311 (2009) 1392–1403.
[187] G. Qi, S. Zhang, K.A. Khor, W. Weng, X. Zeng, C. Liu, Thin Solid Films 516 (2008) 5172–5175.
[188] S. Mallakpour, A. Zadeh Nazari, Advances in Polymer Technology 32 (2013) 21333–21344.
[189] M. Alam, D. Akram, E. Sharmin, F. Zafar, S. Ahmad, Arabian Journal of Chemistry 7 (2014) 469–479.
[190] F. Zafar, H. Zafar, E. Sharmin, S.M. Ashraf, S. Ahmad, Journal of Inorganic and Organometallic Polymers and Materials 21 (2011) 646–654.
[191] F. Zafar, H. Zafar, M. Yaseen Shah, E. Sharmin, S. Ahmad, Vegetable seed oil based waterborne polyesteramide: a green material, in: L.D. Khemani, M.M. Srivastava, S. Srivastava (Eds.), Chemistry of Phytopotentials: Health, Energy and Environmental Perspectives, Springer, Berlin Heidelberg, 2012, pp. 127–130.
[192] U. Riaz, S. Ahmad, Journal of Applied Polymer Science 121 (2011) 2317–2323.
[193] F. Zafar, E. Sharmin, H. Zafar, M. Yaseen Shah, N. Nishat, S. Ahmad, Industrial Crops and Products 67 (2015) 484–491.
[194] A. Abdolmaleki, S. Mallakpour, S. Borandeh, Polymer Bulletin 69 (2012) 15–28.
[195] B. Shouli, L. Xin, L. Dianqing, C. Song, L. Ruixian, C. Aifan, Sensors and Actuators B: Chemical 153 (2011) 110–116.
[196] Z. Wang, Chinese Science Bulletin 54 (2009) 4021–4034.
[197] N. Saito, H. Haneda, T. Sekiguchi, N. Ohashi, I. Sakaguchi, K. Koumoto, Advanced Materials 14 (2002) 418–421.
[198] Y. Tu, L. Zhou, Y.Z. Jin, C. Gao, Z.Z. Ye, Y.F. Yang, Q.L. Wang, Journal of Materials Chemistry 20 (2010) 1594–1599.

This page intentionally left blank

Fundamentals of bionanocomposites

12

Rajesh K. Saini[1], *Anil K. Bajpai*[1], *Era Jain*[2]
[1]Government Model Science College, Jabalpur, India; [2]Saint Louis University, Saint Louis, MO, United States

12.1 Introduction

Composites materials are materials, with characteristics different from those of individual component materials, composed of two or more constituent materials with significantly different physical and chemical properties. They show unique and special properties of individual components. They are basically composed of two major constituents, i.e., matrix (a continuous phase, which is a polymer, metal, or ceramic, and plays a role to maintain the fibers in the proper direction and arrangement in space and protect them from abrasion and the environment) and reinforcement (particle-reinforced, short fiber–reinforced, and continuous fiber–reinforced elements that increase the physical and mechanical properties of the matrix) [1,2]. Usually the systems incorporated are in the form of particles, whiskers, fibers, lamellae, or a mesh. Most of the resulting materials show improved mechanical properties and a well-known example is inorganic filler-reinforced polymers.

The term bionanocomposites (occasionally called biocomposites, nanocomposites, nanobiocomposites, green composites, biohybrids, or bio-based plastics (bioplastics)) was introduced several years ago (first time by Theng in 1970) to define an emerging class of biohybrid materials that show dimensions in the nanometer range (1–100 nm), resulting from the combination of biopolymers such as polysaccharides, proteins, and nucleic acids with inorganic solids at the nanometric scale. They can be widely used in a variety of areas owing to multidimensional properties such as biocompatibility, antimicrobial activity, and biodegradability and show good properties (mechanical, optical, barrier, etc.) as compared to micro- or macrocomposites [3,4], in which at least one of the phases exhibits dimensions in the nanometer rang. Such inorganic fraction consists of finely divided solids, spanning from clays to phosphates or carbonates, whose origin can be either natural or synthetic. As in any multiphase material, the most significant challenge in bionanocomposites is to attain materials with superior performance, by the subtle management of the individual properties of its components. Notably, the biocompatible and biodegradable characteristics of biopolymers, alongside with the mechanical and thermal properties of the inorganic counterpart, bridge the gap between functional and structural materials [5–7]. In the last decade, preparation of nanocomposites based on biorenewable polymers has been intensively studied. Most of the studies on bionanocomposites are related to polylactic acid (PLA), polycaprolactone (PCL), proteins and polysaccharides, incorporating layered silicates of the smectite group, widely used

Biodegradable and Biocompatible Polymer Composites. http://dx.doi.org/10.1016/B978-0-08-100970-3.00012-2

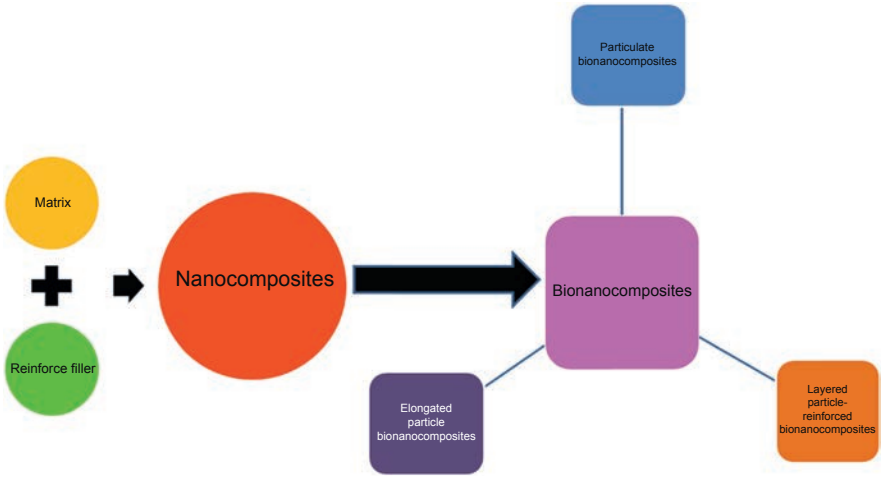

Figure 12.1 Types of bionanocomposites.

in regenerative medicine, drug delivery, tissue engineering, electronics, and food packaging. However, recent studies show that the use of microfibrous clay minerals such as sepiolite and palygorskite results in an interesting reinforcement of polymer as well as biopolymer matrices in the development of clay–polymer nanocomposites [8].

On the basis of types of matrix used, origin, shape, and the size of reinforcements, bionanocomposites can be categorized into three different classes: particulate (isodimensional particles are used as reinforcements), elongated particle (carbon nanotubes (CNTs) and cellulose nanofibrils as reinforcement), and layered structure (flocculated/phase-separated nanocomposites, intercalated nanocomposites, exfoliated nanocomposites) biocomposites (Fig. 12.1).

Organic and inorganic materials are usually quite different from each other in their properties. Inorganic materials such as glass and ceramics are hard but not impact resistant, that is, they are brittle, whereas organic polymers/oligomers are resilient. However, organic polymers generally suffer from some of the inherent drawbacks such as instability to heat and tendency of natural degradation on aging. In general, inorganic species usually have good mechanical and thermal stability as well as optical properties. Organic moiety would provide flexibility, toughness, hydrophobicity, and new electronic or optical properties. Organic–inorganic hybrid materials could then have desired combinations of the features of both organic and inorganic components. Common composite materials are light and have superior mechanical properties. Fiber-reinforced plastics and particulate-filled composites are two common examples of mechanical composites. There are two components in such composites: polymer-based matrix and reinforcing fillers (fibers or particles) [9,10]. The fibers provide strength and stiffness to the composite, whereas the polymer matrix acts as lightweight binder and distributes external load to the fibers [11]. In addition to increasing the rigidity of the polymer matrix, the particles are added to modify rheology to aid in processing [12,13]. Because of the new and different properties of these nanocomposite materials that the traditional macroscale composites do not have, the preparation, characterization, and applications of organic/inorganic hybrid materials have become a fast expanding area of research in materials science.

12.2 Classification of composites

12.2.1 Classification based on source

Depending on the sources from which composites are obtained, they can be classified into natural composites and synthetic composites.

12.2.1.1 Natural composites

Most of the biological materials are the combination of organic and ceramic phases. The matrices used by nature in biocomposites include cellulose, chitin, collagen, and proteoglycans and reinforced usually with $CaCO_3$, hydroxyapatite, and silica. Among many others, wood and bone are well-known examples of natural composites. Wood is a composite of strong cellulose fiber with cementing material known as lignin. Bone is an organic–inorganic composite of strong but soft fibrils of collagen (a protein) and hard but brittle thin plates of hydroxyapatite (a mineral) containing several configurations with varying architectures.

12.2.1.2 Synthetic composites

Attempts have been made during the last three decades for rapid increase in the production of synthetic composites, in particular those incorporating fine fibers in various plastics. Predictions suggest that the demand for composites will continue to increase steadily with metal- and ceramic-based composites making a more significant contribution. Several attempts have also been made to develop processing methods in synthetic ceramics and composites to produce microstructure similar to those of biomaterials. Natural biomineralization process is, however, difficult to be copied completely in the artificial systems.

12.2.1.3 Classification based on dimensions of the filler particles

Three types of nanocomposites can be distinguished, depending on how many dimensions of the dispersed particles are in the nanometer range [14,15]:

- When three dimensions are in the order of nanometers, they are called isodimensional nanoparticles, such as spherical silica nanoparticles obtained by in situ sol–gel methods or by polymerization promoted directly from their surface, but also can include semiconductor nanoclusters and others.
- When two dimensions are in the nanometer scale and the third is larger, they form elongated structures such as nanotubes or whiskers as, for example, CNTs or cellulose whiskers, which are extensively studied as reinforcing nanofillers yielding materials with exceptional properties.
- When only one dimension is in the nanometer range, the filler is in the form of sheets of one to a few nanometers thick and to hundreds to thousands nanometer long. This family of composites can be gathered under the name of polymer-layered crystal nanocomposites. These materials are almost exclusively obtained by the intercalation of the polymer (or a monomer subsequently polymerized) inside the galleries of layered host crystals

12.2.1.4 Classification based on matrix used

Depending on the nature of matrix (continuous phase), composite materials can be classified into three groups.

12.2.1.4.1 Ceramic–matrix nanocomposites

Ceramic–matrix nanocomposites (CMCs) include a great variety of materials in which a matrix (polycrystalline ceramic, glass, or their mixture) is reinforced by the addition of particles, flacks, fibers, or even voids. The designs of these multicomponent systems enhance the ability to obtain high strength and toughness at elevated temperatures. In most cases, CMCs encompass a metal as the second component. Ideally both components, the metallic one and the ceramic one, are finely dispersed in each other to elicit the particular nanoscopic properties. Nanocomposites from these combinations were demonstrated in improving their optical, electrical, and magnetic properties as well as tribological, corrosion-resistant, and other protective properties. The fabrication routes for ceramic matrix composites are varied and include mixing of the reinforcement with the powdered matrix and pressing, techniques involving slurries, and vapor deposition methods, e.g., (lithium aluminosilicate) LAS–glass–ceramic and LAS-50% SiC composites. CMCs can be used in medical devices, implants, load bearing structural parts, wear or friction surfaces, automotive, aerospace, and power generation applications (engines, turbines, etc.) [16].

12.2.1.4.2 Polymeric matrix composites

The most commonly used matrices for composites are polymeric in nature, and polymeric composite material represents about 90% of all composites. These materials are made up of either particles or fiber reinforcement. In the simplest case, appropriately adding nanoparticulates to a polymer matrix can enhance its performance, often in very dramatic degree, by simply capitalizing on the nature and properties of the nanoscale filler. This strategy is particularly effective in yielding high-performance composites, when good dispersion of the filler is achieved and the properties of the nanoscale filler are substantially different or better than those of the matrix, for example, reinforcing a polymer matrix by much stiffer nanoparticles of ceramics, clays, or CNTs. Applications of polymeric matrix composites in various fields include aerospace, boats, domestic, leisure, electronic, and medical industries [17].

12.2.1.4.3 Metal–matrix nanocomposites

In these composites, metals or metallic alloys are used as continuous matrices and the reinforcement or discontinuous phase is generally ceramics. The reinforcement is in the form of particulates, whiskers, or fibers, e.g., TiC, SiC, or alumina particles are used in Al metal–matrix nanocomposites (MMCs) and carbon fiber is used in Mg MMCs. They have many advantages over monolithic metals including a high specific modulus, higher specific strength, better thermal properties, lower coefficients of thermal expansion, and high wear resistance. Some of MMCs for aerospace applications are Cu-based matrices, which have been reinforced by carbon fibers or SiC fibers [18].

12.2.1.5 Types of polymer–clay composites

From structural point of view, polymer–clay composites can be generally classified into three types [19] of composites as shown in Fig. 12.2.

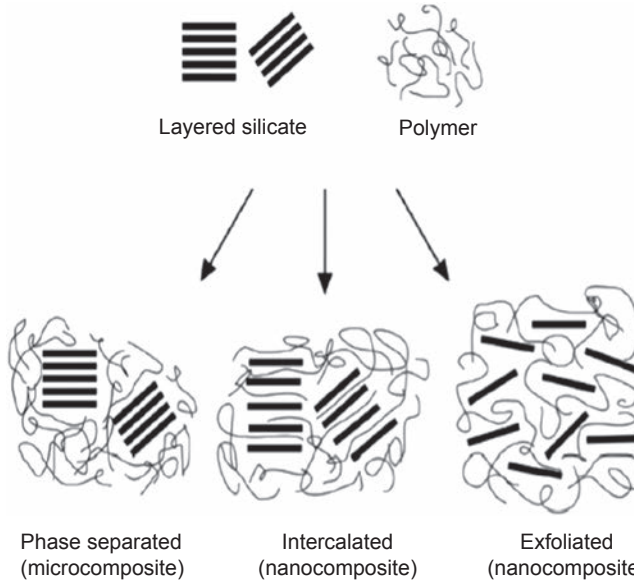

Figure 12.2 Types of layered particle-reinforced bionanocomposites.

1. Conventional composites
The organization of the clay nanolayers in conventional composites (phase separated) is retained when mixed with the polymer, but there is no intercalation of the polymer into the clay structure. Consequently, the clay fraction in these composites plays little or no functional role and act mainly as filler for economic considerations.
2. Intercalated nanocomposites
A single (or sometimes more than one) extended polymer chain is intercalated between the silicate layers resulting in a well-ordered multilayer morphology built up with alternating polymeric and inorganic layers.
3. Exfoliated nanocomposites
When the silicate layers are completely and uniformly dispersed in a continuous polymer matrix, an exfoliated or delaminated structure is obtained. Extensive polymer penetration, resulting in disorder and eventual delamination of the silicate layer, produces exfoliated structures consisting of individual 1-nm-thick silicate layers suspended in the polymer matrix.

12.3 Types of biopolymers used in bionanocomposites

Biopolymers are those polymers that occur in nature and have exhibited potential application in many fields such as agriculture [20,21], hygienic products [22,23], wastewater treatment [24,25], and drug delivery [26]. Thus so far, many kinds of materials have been used for preparing superabsorbents, among them the naturally available resources such as polysaccharides and inorganic clay minerals have shown particular advantages and drawn considerable attention [27]. The utilization of low cost, annually renewable, and biodegradable polysaccharides for deriving superabsorbents has offered commercial

and environmental superiorities [28–30]. Presently, the natural polysaccharides including starch [31,32], cellulose [33], chitosan [34], alginate [35], and gelatin [36] have been used for deriving superabsorbents, and the resultant materials have also shown potentials as substitutes for existing petroleum-based superabsorbent materials.

Polysaccharides, stereoregular polymers of monosaccharides (sugars), are unique raw materials in that they are very abundant natural polymers (they are referred to as biopolymers); inexpensive (low-cost polymers); widely available in many countries; renewable resources; stable and hydrophilic biopolymers; and modifiable polymers. They also have biological and chemical properties such as nontoxicity, biocompatibility, biodegradability, polyfunctionality, high chemical reactivity, chirality, chelation, and adsorption capacities. The excellent adsorption behavior of polysaccharides is mainly attributed to the following:

- high hydrophilicity of the polymer due to hydroxyl groups of glucose;
- presence of a large number of functional groups (acetamido, primary amino, and/or hydroxyl groups);
- high chemical reactivity of these groups;
- flexible structure of the polymer chain.

Table 12.1 offers representative functional groups and classes of organic compounds in biomass. The symbol R is shorthand for residue, and its placement in a formula indicates that what is attached at that site varies from one compound to another, according to Teli and Waghmare [37].

12.3.1 Carboxymethyl cellulose

Among numerous polysaccharides [35,38,39], cellulose is the most abundant natural polymer with excellent biodegradability and biocompatibility. However, the poor solubility of cellulose in water and most organic solvents and the poor reactivity make it difficult to be directly modified to fabricate other useful materials. However, the derivative modification of cellulose can overcome these drawbacks. Carboxymethyl cellulose is a representative cellulose derivative with carboxymethyl groups (–CH_2–COONa) bonded to some of the hydroxyl groups on cellulose backbone. It can be easily synthesized by the alkali-catalyzed reaction of cellulose with chloroacetic acid and has been widely used as a thickening agent and stabilizing agent. The polar carboxyl groups render the cellulose soluble, chemically reactive and strongly hydrophilic, and so the application of carboxymethyl cellulose in superabsorbent fields becomes attractive and promising [34]. It is a nontoxic high-viscosity product, which is used in food science as a viscosity modifier or thickener and to stabilize emulsions in various products including ice cream. It is also a constituent of many nonfood products, such as toothpaste, water-based paints, detergents, textile sizing, and various paper products.

12.3.2 Chitosan

Chitosan is a cationic polysaccharide obtained by deacetylating chitin, which is the major constituent of the exoskeleton of crustaceous water animals. Chitin accounts for

Table 12.1 The representative functional groups and classes of organic compounds in biomass

Formula of functional group	Name	Class of compounds
	Hydroxyl	Alcohols, carbohydrates
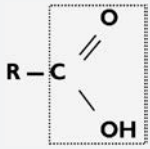	Carboxyl	Fatty acid, proteins, organic acids
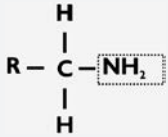	Amino	Proteins, nucleic acids
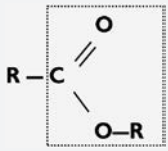	Ester	Lipids
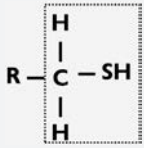	Sulfydryl	Cysteine (amino acid) proteins
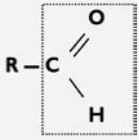	Carbonyl, terminal end	Aldehydes, polysaccharides
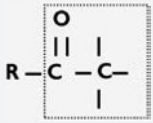	Carbonyl, internal	Ketones, polysaccharides
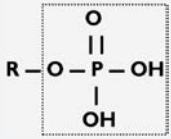	Phosphate	DNA, RNA, ATP

approximately 70% of the organic components in such shells. Chitosan was reportedly first discovered by Rouget in 1859, when he boiled chitin in concentrated potassium hydroxide solution. This resulted in the deacetylation of chitin. In 1934, two patents, one for producing chitosan from chitin and other for making films and fibers from chitosan, were obtained by Rigby. Unlike oil and coal, chitosan is a naturally regenerating

resource (e.g., crab and shrimp shells) that can be further enhanced by artificial culturing. Chitosan can selectively bind desirable materials such as cholesterol, fats, metal ions, proteins, and tumor cells. Chitosan has also shown affinity for proteins, such as wheat germ agglutinin and trypsin. Other properties that make chitosan very useful include inhibition of tumor cells, antifungal effects, acceleration of wound healing, stimulation of immune system, and acceleration of plant germination [39]. Due to chitosan's many attractive properties such as reactivity, biodegradability, natural origin, and abundance, it has many areas of application including waste and water treatment, medical areas, biotechnological areas, and fabrications [40].

12.3.3 Alginate

Alginate, first described by Stanford in 1881 [41], is an anionic polysaccharide mainly occurring as a structural component in marine brown algae (Phaeophyta) [42]. In brown algae, alginate is the most abundant polysaccharide comprising up to 40% of the dry matter [43], mainly occurring in the cell walls and intercellular spaces where it consists of an insoluble mixture of calcium, magnesium, sodium, and potassium salts [44].

Alginate is a family of linear binary copolymers of (1→4) glycosidically linked α-L-guluronic acid (G) and its C-5 epimere, the α-D-mannuronic acid (M) residue [45]. Its main function is to contribute to the strength and flexibility of the seaweed plant, and the composition of the alginate varies both within different species of algae and within different parts of the plant [46]. Industrially, alginate has for many decades been used for its gelling, viscosifying, and stabilizing properties and for its ability to retain water [47]. Alginates also have recognized potential in the removal of toxic heavy metals from industrial waste by biosorption [48].

12.3.4 Gelatin

Gelatin is a protein derived from collagen and commonly used plasma expander [49]. Being a protein, gelatin is composed of a unique sequence of amino acids. Characteristic features of gelatin are the high content of the amino acids such as glycine, proline, and hydroxyproline. Gelatin is a multifunctional ingredient, which gives texture and stability to the finished product due to one or more of the following properties: gel formation, thickening, foaming/whipping, film forming, binding, elasticity, water binding, emulsifying solubility, biodegradability, biocompatibility, and pH-induced surface charge [49]. This multifunctionality has led to the use of gelatin as a highly valued ingredient in many products. The presence of multifunctional groups, such as $–NH_2$ and –COOH, in the gelatin chain makes it a suitable candidate to bind with drugs such as doxorubicin forming drug–polymer conjugate [50] or poly(ethylene glycol) to form reticuloendothelial system evading conjugate [51]. Furthermore, cell surface and extracellular matrix contain fibronectin, which contain specific sites for binding to cells and a range of macromolecules including collagen and gelatin [51]. Moreover, gelatin can be fabricated as microspheres and nanospheres depending on the technique used for the fabrication and found to enhance tumoral cell phagocytosis [52]. Another important property of protein

molecules is interaction with metal ions, because nitrogen atoms of the imidazole group of the histidine residue and the sulfhydryl group of the fine cysteine residue are potential adsorbents for metal ions [53].

12.3.5 Guar gum

Guar gum (GG) is derived from the seeds of the guar plant *Cyanaposis tetragonolobus* (Leguminosae); it is a branched polymer with β-D-mannopyranosyl units linked (1–4) with single-membered a-D-galactopyranosyl units occurring as side branches [54]. GG and its derivatives have been used in various areas (e.g., in the preparation of thicker, ion exchange resins, suspending agents [55]). However, little information regarding the introduction of GG into superabsorbents has been reported [56].

12.3.6 Pectin

Pectin is a kind of plant-derived polysaccharide enriched with galacturonic acid and galacturonic acid methyl ester units as a component of extracellular matrix. It has high biological compatibility [57] and contains carboxyl groups as the functional groups with apatite forming ability in body environment. Pectin forms skeletal tissues of plants by combining with proteins and other polysaccharides, which are chemically stable and physically strong. Pectin can take various forms ranging from fluid sol to dense gels with high-molecular-weight and polyanionic character depending on the degree of the chemical reaction. These properties enable pectin polymers to carry signal molecules and support various biologically active substances [58]. The structure of pectin is primarily composed of repeating units of galacturonic acid joined by 1→4 glycosidic linkages, which create a linear polymer [59]. The linear structure is cleaved by the presence of neutral sugar side chains such as rhamnose. Furthermore, the carboxyl groups of galacturonic acid may either remain as free acids, which are able to be esterified with methanol or neutralized with cations. In detail, pectin is primarily a polymer of D-galacturonic acid (homopolymer of [1→4]α-D-galactopyranosyluronic acid units with varying degrees of carboxyl groups methylesterified) and rhamnogalacturonan (heteropolymer of repeating [1→2]α-L-rhamnosyl-[1→L]α-D-galactopyranosyluronic acid disaccharide units), making it an α-D-galacturonan [60]. According to Thibault, this rhamnogalacturonan main chain is combined with galactose, arabinose, mannose, and glucose as side chain [61].

12.3.7 Aliphatic polyester–based nanocomposites

The main sources of aliphatic biodegradable polyesters are renewable sources or petroleum. The polyesters such as polylactides (PLAs) and polyhydroxyalkanoates (PHAs) are derived from renewable resources, whereas PCL, polyesteramide (PEA), and polybutylene succinate (PBS); copolyesters such as poly[(butylene succinate)-co-adipate] (PBSA); and aromatic polyesters such as polybutylene adipate terephthalate (PBAT) are from petroleum [62]. PLA is a biopolymer that has high strength, thermal plasticity, biodegradability, and biocompatibility but its brittleness, slow crystallization

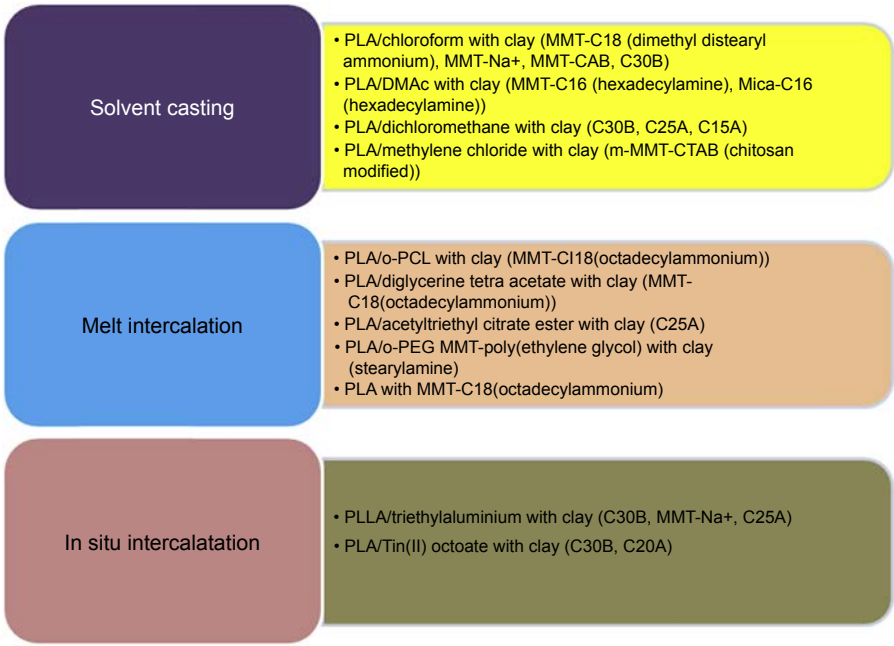

Figure 12.3 Polylactic acid–based clay bionanocomposites and their method of preparation.

rate, and gas permeability limit its uses. Therefore, different reinforce fillers such as clays, CNTs, silica, graphene, polyhedral oligomeric silsesquioxanes (POSSs), and hydroapatite are incorporated in PLA via solution casting method to improve its properties (Fig. 12.3). Wu and Wu [63] prepared PLA and montmorillonite (MMT) bionanocomposites by treating the MMT with n-hexadecyl trimethylammonium bromide (CTAB) cations and then modifying it with chitosan to enhance the miscibility with PLA during the solvent casting process and obtain exfoliated structures [64,65]. Recently, cocamidopropyl betaine (CAB) pH-dependent (negative charge at higher pH values and a positive charge in acidic conditions) surfactant belongs to the betaine group, which contains both quaternary ammonium and carboxyl moieties, derived from coconut oil, and is used to modify the MMT surface to ensure proper dispersion in the PLA matrix. Many authors used melt intercalation methods to prepare clay/PLA bionanocomposites and investigated the effects of the aspect ratio of the silicates, the organic modifier, and the silicate loading, on the formed structure whether intercalated, intercalated–flocculated, and nearly exfoliated, and coexistence of intercalated and exfoliated states. Researchers used oligo-PCL (o-PCL), polyethylene glycol (PEG) [66], oligo-PEG [67], PCL [68], in small amounts as compatibilizers and plasticizers to enhance the dispersibility and melt processibility of PLA. The type of clay and how it influences dispersion during the melt intercalation process has been elucidated in many studies. In situ polymerization method is an appropriate method to produce nanocomposites with a good dispersion of clay but not widely applied to prepare PLA/clay nanocomposites because of its limitations such as the need for organometallic

catalysts, degradation-sensitive monomer, and in some cases the need for solvent(s), which make it unsuitable for industrial applications. Furthermore, melt intercalation is an environmentally benign process, which is preferred in the industrial processing of polymers. However, producing exfoliated structures through melt intercalation is not always easy. Therefore, alternative routes, such as preparing master batches through in situ polymerization before melt blending in a polymer, have been explored. The primary advantage of this particular technique is the possibility of obtaining nanocomposites with a high degree of exfoliation, which may not be achieved when using the direct melt intercalation process [69].

Recently, PLA–CNTs–based bionanocomposites were synthesized by solvent casting and melt mixing due to suitable distribution and dispersion of the filler inside the polymer matrix to ensure low percolation thresholds combined with high mechanical performance and high shear and a prolonged mixing time should help to well disperse the CNTs in the PLA matrix [70–72]. However, functionalization of the surface of the CNTs is an important step to enhance its dispersability within the PLA matrix. This step is primarily performed through acid oxidation to introduce –OH and –COOH functional groups. These functional groups could then serve as route for further functionalization into the desired surface functional groups. Use of carboxyl multiwalled carbon nanotubes (MWCNTs) in the preparation of PLA/CNTs than unmodified and hydroxyl-modified MWCNTs showed better dispersion in the PLA matrix due to affinity between the carboxylic group and the PLA.

PHAs (poly(3-hydroxybutyrate) (PHB), the copolymer, poly(3-hydroxybutyrate-co-3-hydroxyvalerate) (PHB/HV), and the elastomeric poly(3-hydroxyoctanoate) (PHO)) are biodegradable, biocompatible, and able to be produced by bacterial fermentation from renewable resources because they found as discrete cytoplasmic inclusions in bacterial cells, synthesized by a variety of bacterial species under nutrient-limiting conditions with excess carbon, and belong to polyhydroxyesters of 3-, 4-, 5-, and 6-hydroxyalkanoic acids (HAs) [73]. However, they are not good as conventional thermoplastics due to their high crystallinity, brittleness, and poor thermal stability at temperatures near their melting point. Therefore, CNTs, HAs, layered double hydroxides (LDHs), and silver have been used to enhance properties of PHB matrix. They are mostly prepared by melt intercalation (care has to be taken to avoid thermal- and thermomechanical degradation during processing, that occur rapidly near the melting point, which is primarily based on a random chain scission due to the macromolecular chain cleavage) and solution casting methods [74,75]. PHA/clay nanocomposites have also been prepared using the solution casting technique, in which chloroform is primarily the solvent of choice but is not environmentally friendly due to the use of copious amounts of hazardous solvents [76–78]. Due to hydrophobic, organic modification of the clay surface, it enhances its dispersion in the PHB matrix and determines the type of structure that results when clays are incorporated into PHA matrices [75,79].

Poly(butylene succinate) (PBS) is an aliphatic thermoplastic polyester synthesized by the condensation polymerization of glycol, 1,4-butanediol, and an aliphatic dicarboxylic acid, succinic acid [80]. It is a biodegradable polyester, and various nanoparticles such as CNTs, graphene, nanosilica, clay, and carbon nanofibers (CNFs) have

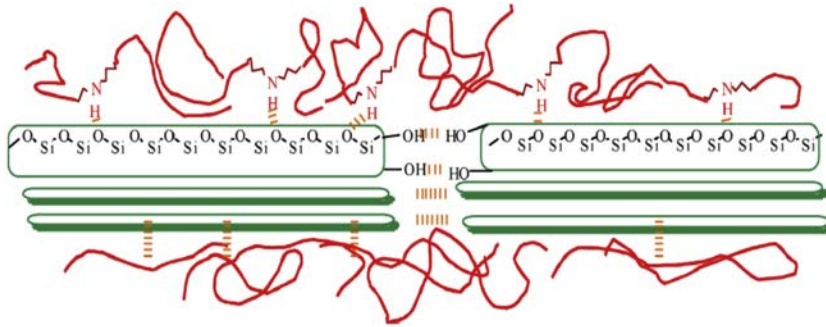

Figure 12.4 Formation of possible hydrogen bonds between PBS and clay surface, which leads to the flocculation of the dispersed silicate layers, and hence, high aspect ratio of dispersed clay particles.

been incorporated in it to improve properties such as its softness, gas barrier, and thermal stability. The bionanocomposites of PBS/clay are synthesized by melt compounding technique. Some researchers studied the structure and mechanical properties of PBS/clay nanocomposites prepared by melt intercalation method and showed that properties depend on the clay type, clay content, and organic modification [81]. The strong flocculation of the dispersed intercalated silicate layers was due to the edge–edge interactions of the clay (Fig. 12.4).

Solution casting method was used to synthesize PBS/clay bionanocomposites by MMT modified by cetyl pyridinium chloride (CPC) and cetyl trimethylammonium bromide (CTAB) salts, and PBS/CPC showed intercalated structure, whereas PBS/CTAB showed a mixture of both intercalated and partially exfoliated structures [82,83]. The in situ polymerization technique has not been the preferred route for the preparation of PBS/clay nanocomposites.

PBSA is a biodegradable random copolymer thermoplastic polyester synthesized by polycondensation of 1,4-butanediol with succinic and adipic acids [80,84]. Various reinforce fillers are used as nanoreinforcement materials to improve its modulus, strength, barrier properties, biodegradability, and thermal stability of PBSA matrix. Clays are by far the most commonly used nanoparticles, although PBSA nanocomposites based on CNTs [85] have been reported by researchers.

Poly(ε-caprolactone) (PCL) (first biopolymer nanocomposite) is obtained from polymerization of crude oil, a fully biodegradable hydrophobic, semicrystalline polymer, aliphatic polyester polymer, and can be prepared by either ring-opening polymerization of ε-caprolactone using a variety of anionic, cationic, and coordination catalysts or free radical ring-opening polymerization of 2-methylene-1,3-dioxepane [86]. The thermal, mechanical, and barrier properties with good biodegradability of PCL matrix can be improved by incorporation of clays, CNTs, graphene, and silica. PCL-based nanocomposites were prepared using the in situ polymerization technique [87,88]. The nature of bionanocomposites of PCL/clay depends not only on the type of clay modification but also on the processing route and parameters used, as the type and

localization of the functional group on the modifying agent have a tremendous effect on the ability to yield nanocomposites.

Despite solvent casting, in situ polymerization, and melt blending, some researchers used two-step processes, such as the use of master batches for synthesizing PCL/clay bionanocomposites.

PCL/CNT nanocomposites with imparting good electromagnetic interference shielding properties were also synthesized and studied by researchers by melt blending (prepared through melt mixing in tetrahydrofuran (THF) and subsequent recovery of the CNTs) and coprecipitation (involved the dispersion of CNTs in a PCL/THF solution, ultrasonication, and finally precipitation in heptane), respectively [89]. During the melt mixing process, thicker MWCNTs were more broken than the thinner ones, due to higher percolation concentration for the thicker MWCNTs but thinner CNTs would be better able to resist changes in their length during such mixing processes. However, the uniform dispersion of CNTs in the PCL matrix can be achieved by introducing carboxylic and hydroxylic groups by functionalization of the surface of the CNT as well as by ionic modification and covalently grafting compounds onto the CNTs.

12.3.8 Polysaccharides-based nanocomposites

Polysaccharides such as starch, cellulose, and chitin/chitosan are major part of biosphere, used to prepare bionanocomposites through solvent intercalation or melt processing and not through in situ polymerization. Mostly clays, CNTs, graphene, LDHs, POSSs, and silica are used as nanofillers to improve the properties of matrix. At present, most research has been focused on clays such as MMT due to their low cost, availability, versatility, and friendliness to the environment. Starch is an inexpensive biopolymer that consists of a linear α-D-glucan amylose and a highly branched amylopectin, used as a packaging material [90]. At room temperature, starch is largely insoluble in water and retains its granular structure. However, its poor mechanical properties and a high water affinity limit its uses. Hence, nanoparticles have been used to improve some of these properties. The melting point of native starch is very high due to the many intermolecular hydrogen bonds that exist between the chains. Processing of starch/clay nanocomposites is dependent on the properties of the starch. The disruption of the starch crystalline structure is achieved through either a solvent process or a thermomechanical process. During preparation of starch-based nanocomposites, it is necessary to reduce glass transition and the melting temperature of the starch by use of water and/or plasticizers that are not volatile, such as glycerol and sorbitol, or nitrogen-based plasticizers [91]. The plasticized starch is usually known as “thermoplastic starch (TPS)” and can be processed via melt compounding with a nanofiller alone or as a polymer blend system, e.g., TPS/polyvinyl alcohol (PVA)–clay, TPS/PLA–clay, and TPS/PCL–clay. However, on heating, starch is converted into largely amorphous viscous paste after the destruction of most of the intermolecular hydrogen links and plasticizers are mixed mechanically at certain temperature regimes. However, TPS alone cannot always meet all of the requirements of a packaging material, so clay such as naturally abundant, environmentally friendly acceptable filler is incorporated

Figure 12.5 Common methods for synthesizing starch blends–based bionanocomposites

to improve the properties by using solution casting [90–93] and melt mixing [90,91] techniques. The type of plasticizer and its concentration in the matrix has been shown to influence clay dispersion in the TPS/clay nanocomposites [94,95].

Due to drawbacks of starch such as high viscosity, poor melt properties, and brittle nature of products, blending method can be used to prepare desire products of starch with other biodegradable polymers such as PVA, PCL, natural rubber, PLA, PVA, and PBSA [96–99] (Fig. 12.5). More hydrophilic polymers influence the resultant nanocomposites structures. Therefore in case of major starch matrix, better dispersion should be realized with hydrophilic (MMT-Na^+) clays (due to the polar–polar interaction between the clay surface and the starch) than with hydrophobic (organoclays) clays, and inverse process is used when starch is the minor matrix and a more hydrophobic biopolymer is the major matrix [97].

Researchers prepared nanocomposites based on MMT-Na^+, PBSA, and PVA/starch by various methods with improved properties, and a better dispersion of clay was expected. The incorporation of nano-silicon dioxide (nano-SiO_2) into the polymer blend matrix using the solution casting technique enhances the dispersion of nanofillers as intermolecular hydrogen bond was formed between nano-SiO_2 and starch/PVA and that the strong chemical bond C—O—Si was also formed in the nano-SiO_2/starch/PVA hybrid materials [100]. Presently, CNTs are used as nanoreinforcement fillers for starch-based bionanocomposites due to their extraordinary mechanical and electrical properties and incorporated by the solution casting technique, rather than melt extrusion [101–103]. The better uniform dispersion of nanofiller in polymeric matrices strongly depends on the ability to disperse the CNTs homogeneously throughout the matrix without destroying their integrity. However, their nonreactive surfaces and

strong aggregative properties make it difficult to disperse CNTs in polymer matrices and, hence, limit their application as reinforcement nanofillers. Functionalization of CNTs can be used as suitable method for dispersion of CNTs in starch matrix [101]. It is expected that such successes in the dispersion of CNTs in solution should help in the preparation of various polymer/CNT composites using the solution casting method.

Some workers prepared nanocomposites based on LDH (LDH crystallites in starch (or acid-modified starch) dispersions under hydrothermal treatment conditions) and silica using the solvent casting technique as well as by reactive extrusion techniques [104,105]. The process resulted in well-dispersed starch–LDH nanocomposites. When Zn–Al LDH fillers is used for fabrication of TPS matrix with carboxymethyl cellulose as the stabilizer in an aqueous solution, uniformly dispersed bionanocomposites are obtained because the introduction of carboxymethyl cellulose improved the stability in water due to its hydrophobicity.

Cellulose is the most abundant biopolymer composed of linear polymer consisting of a β (1→4) linked D-glucose synthesized by plants and bacteria, which decomposes at temperatures below its melting point due to presence of numerous hydroxyl functional groups that result in strong hydrogen bonds. The glucose monomer units in cellulose form inter- and intramolecular hydrogen bonds, leading to the formation of cellulose microfibrils. Presently, various nanofillers such as clay, CNTs, graphene, LDH, and silica are used for preparing cellulose-based bionanocomposites. However, the hydroxyl groups must be replaced with other functional groups such as acetate or methyl functional groups to improve the properties of cellulose-based plastic.

Cellulose/clay nanocomposites can be prepared from solution casting techniques; because of the high crystallinity of cellulose derived from cotton and its high molecular weight, it does not melt before the onset of the decomposition temperature. Apart from the solvent type, clay surface modification directly affects the level of dispersion achieved in the cellulose acetate/clay nanocomposites [106]. It is possible to obtain CA/clay nanocomposites with good clay dispersion by modification of the clay surface, optimization of the process parameters, and the precise choice of solvent.

Chitin is the most abundant biopolymer composed of an acetylated polysaccharide composed of N-acetyl-D-glucosamine groups linked by a β(1→4) linkage as ordered crystalline microfibrils in the structural components of crustacean and insect exoskeletons and in the cell walls of fungi and microorganisms. Chitosan, poly-β(1,4)-2-amino-2-deoxy-D-glucose, is obtained from chitin by deacetylation; has active amine groups and hydroxyl groups; and shows polycationic nature in acidic medium. Researchers are synthesizing chitosan nanocomposites with clay [107–109] and graphene [110] by using the solution casting having intercalated and exfoliated structures. Wang et al. [109] used solution casting method for preparing a new quaternized carboxymethyl chitosan/rectorite nanocomposite without destroying the structure of the rectorite layer and high intercalation. CNT-based nanocomposites are less studied as the interaction between chitosan and CNTs depends on pH of the chitosan solution, poor dispersibility CNT in a polymeric media. However, it can be increased by increasing number of functional groups on CNTs that form hydrogen bonds with the chitosan chains to improve the interfacial compatibility [111].

12.3.9 Polypeptide–polymer nanocomposites

Proteins are highly multifunctional complex amphoteric polymers composed of different amino acids bonded together by amide bonds. They have better gas barrier properties but lower water vapor permeability. Presently, milk protein–based, soybean protein–based, gelatin-based, corn zein–based, and wheat gluten–based nanocomposites were studied due to their multifunctionality, and localized charges allow nanofillers to disperse and produce well-dispersed nanocomposites [90]. Melt extrusion, solvent casting, and a sequential combination of the two techniques can be adopted for synthesizing protein-based bionanocomposites. Surface modification of nanofillers is a better method.

12.4 Preparation of nanocomposites

Bionanocomposites are usually prepared using three main techniques: (1) in situ polymerization, (2) solution casting, and (3) melt processing. Recently, other preparation techniques, such as electrospinning and processing under supercritical conditions (e.g., supercritical carbon dioxide is promising to be a particularly approach because this solvent is greener than other organic solvents), have gained interest. Typically, three approaches have been adopted to synthesize polymer nanocomposites: solution blending, melt blending, and in situ polymerization. For all the three techniques, proper dispersion of the nanoparticles is always a goal during processing. For instance, in the case of clays, exfoliation of the stacked silicate platelets into individual platelets dispersed homogeneously in the polymer matrix is always the ultimate aim.

1. **In situ polymerization method:** In this method the nanoparticles are premixed with the liquid monomer or monomer solution. Then polymerization is initiated by heat, radiation, or suitable initiators. Unlike melt intercalation, a layered silicate is mixed with monomer before polymerization takes place in situ. Because of the low monomer viscosity (comparing to melt viscosity), it is much easier to achieve uniform mixing of particles in the monomer using a high shear mixer. In addition, the low viscosity and high diffusivity result in a higher rate of monomer diffusion into the interlayer region. It is also possible to control nanocomposite morphology through the combination of reaction conditions and clay surface modification. For most thermoset polymers, in situ polymerization is the only viable method to prepare nanocomposites.
2. **Solution blending method:** In solution blending (i.e., based on a solvent system in which the polymer or prepolymer is soluble), a solvent or solvent mixture is used to disperse the nanoparticles and dissolve the polymer matrix. Depending on the interactions of the solvent and nanoparticles, the nanoparticle aggregates can be disintegrated in a good solvent due to the weak van der Waals forces that stack the layers together. Solution intercalation is based on a solvent system in which the polymer is soluble and the phyllosilicate is swellable and dispersible. For preparing nanocomposites based on other polymers, the polymer and the phyllosilicate are normally dissolved/swollen separately in solvent and then the two solutions are mixed allowing the intercalation to occur by the polymer chains replacing the solvent molecules within the interlayer spaces of the phyllosilicate. Polymer chains can then be adsorbed onto the nanoparticles. However,

on solvent removal, the nanoparticles tend to reagglomerate. Few exfoliated nanocomposites were prepared via this method. Another disadvantage of this method is the large amount of solvent needed, resulting in a high product cost. The types of polymers that can be used to synthesize nanocomposites ultimately depend on the selection of proper solvent, limiting the applicability of this method. Nevertheless, this is an attractive route to prepare nanocomposites based on water-soluble polymer and layered silicate nanocomposites because most water-soluble polymers are polar and hydrophilic enough to interact with the silicate surface without the need of cation exchange modification on the silicate surface. It is well known that inorganic layered silicates are able to exfoliate in water and form colloidal particles. Several polymer nanocomposites, including polyethylene oxide (PEO), PVA, and polyacrylic acid (PAA), were prepared via this method. Some polymer/CNF nanocomposites are also synthesized by this method [112,113].

3. **Melt processing:** Instead of using solvent as the medium, nanoparticles can be directly mixed with a molten polymer. This process eliminates the use of solvent and is compatible with industrial polymer extrusion and blending processes. It offers an economically attractive route in fabricating polymer nanocomposites. A wide variety of polymer/clay nanocomposites have been prepared via this route, i.e., nylon 6, polystyrene (PS), and polypropylene (PP). Melt intercalation offers a "simple" way of preparing nanocomposites. However, care has to be taken to "fine-tune" the layered silicates surface chemistry to increase the silicate compatibility with the polymer matrix. Many studies have shown that the polar interactions of polymer and clay surface play a critical role in achieving particle delamination/dispersion. For nonpolar polymers, e.g., PP, a polar compatibilizer such as maleic anhydride–modified PP (PP-MA) is commonly added to improve the compatibility of PP and clay and thus the clay nanoparticle dispersion. Polymer/CNF nanocomposites have also been synthesized via this method. Shear stress is extremely important to disintegrate and disperse nanoparticles; therefore it needs to be controlled at an appropriate level. Too strong shear force tends to break single fibers into many shorter pieces reducing the reinforcement efficiency and deteriorating properties in which high aspect ratio of the nanoparticle is essential [15]. It is a better process for preparing clay-containing bionanocomposites (depends on the transport/diffusion of polymer chains from the bulk melt into the silicate interlayers), over either the in situ intercalative polymerization or polymer solution intercalation techniques as well as it is an environmentally friendly method because no organic solvents are used and biopolymers that were not suitable for in situ polymerization are used. The characteristic properties of bionanocomposites formed by this process depend up the thermodynamic interaction between the polymer and the nanoparticle [114,115]. Two primary factors, i.e., processing conditions and enthalpic interaction between the polymer and the nanoparticle, play an important role to determine the level of dispersion of the nanoparticles within the polymer matrix during melt processing: In the absence of such favorable interactions, the dispersion of the nanoparticles within the polymer matrix becomes difficult, and indeed, only microcomposites result. Therefore, careful optimization of the processing parameters is required for the majority of thermally sensitive biopolymers. The optimization of the processing temperature and pressure is also important to avoid the degradation of biopolymer matrices. The only drawback of this process is that certain biopolymers are degraded by either the mechanical shearing force or the temperature applied during processing, which leads to the degradation due to cleavage of polymer chains and consequently to a decrease in molecular weight. During the melt processing of nanocomposites based on clays, for instance, high shear sustained over long periods is required for the "peeling" off of the platelets. However, such high shear and prolonged stay within the melt processing machine, whether an extruder or internal mixer, would result in the degradation of certain polymers.

4. **Other methods:** By tailoring the interactions between the monomer, the surfactant, and the clay surface, exfoliated nanocomposites (e.g., nylon-6, PCL, epoxy, and polycarbonate) have been successfully synthesized via the ring-opening polymerization. The functional group in the organic cation can catalyze the intralayer polymerization and facilitate layer separation. Free radical polymerization has also been employed to synthesize many thermoplastic nanocomposites. Efforts have been made to anchor initiators in the interlayer region to improve the intralayer polymerization rate for exfoliated nanocomposites. Reactive groups containing carbon–carbon double bonds were introduced to the clay surface via several approaches. Clay exfoliation/delamination has been dramatically enhanced by this way [114]. In addition, the restacking process is a newly imposed approach in which nanocomposites are obtained via a transformation of the host material into a colloidal system and precipitation in the presence of the polymer. This method differs from other methods because a previously formed host layered crystal is not used. These nanocomposites show interesting microstructural phase changes as well as enhanced thermal stability relative to both parent phases [116]. A variety of synthetic techniques have been developed to provide cleanly dispersed nanoparticles within polymer matrices. In "grafting-to" methods, functional polymers are connected to nanoparticle surfaces through the polymer chain end, or through multidentate pendent functionality, whereas the "grafting-from" methodology starts from nanoparticles decorated with small molecule ligands from which the polymerization chemistry can be initiated (Fig. 12.6). Both approaches can be utilized effectively in the preparation of cleanly dispersed nanocomposites. In addition, nanoparticles can be synthesized directly in functional polymer materials, in which the polymer either replaces or is used in conjunction with conventional, small molecules surfactant (ligands) typically used in the nanoparticle synthesis, whereas this approach often gives lower-quality nanoparticles samples (in terms of crystallinity and/or size distribution) relative to those produced using small surfactant molecules [115]. The selection of any of the techniques depends on the type of biopolymer involved and, to a large extent, the nanoparticle in question.

Electrospinning of biodegradable polymer solutions is a popular method to produce nanofiber scaffolds for tissue engineering applications. Poly(L-lactic acid)/exfoliated MMT clay/salt solutions were electrospun followed by salt leaching/gas foaming. The resultant scaffold structure contained both nano- and microsized pores offering a combination of cell growth and blood vessel invasion microdimensions along with nanodimensions for nutrient and metabolic waste transport.

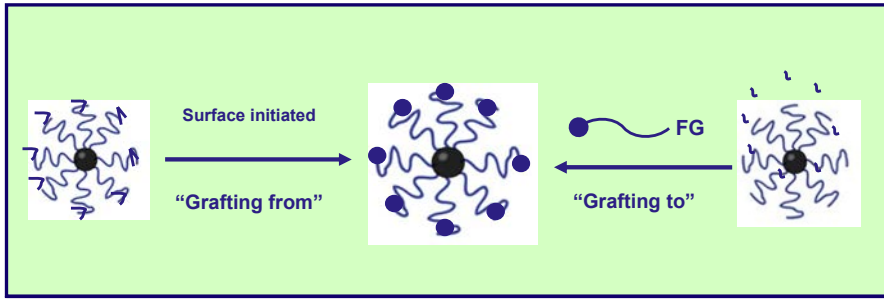

Figure 12.6 Schematic depiction of two practiced methods for surface functionalization of nanoparticles with polymers.

12.5 Properties of bionanocomposites

In the past 50 years, the field of biomedical research has advanced and researchers are attempting to replace body tissues with natural or synthetic biomaterials with novel properties that make them especially suitable to have an intimate contact with living tissue and are produced through processes that often employ or mimic biological phenomena. Presently many bionanocomposites materials are used as biomaterials in biomedical fields. Therefore, these materials must possess the following properties to qualify as biomaterials.

12.5.1 Biocompatibility

Biomaterials (polymers, metals, ceramics, and composites) are generally used to recognize a nondrug substance, either natural or synthetic material for biomedical applications, save lives, relieve suffering, and improve the quality of life for a large number of patients every year because they are suitable for inclusion in systems that interact with human tissue and body fluids and that augment or replace the function of badly damaged tissue or organs in a reliable, safe, and physiologically acceptable manner without causing adverse effects on blood or other tissues [117–119]. They must show nontoxicity, immunogenicity, functionality, sterilizability, and *biocompatibility.* Biocompatibility refers to the ability of a material to perform with an appropriate host response in a specific situation and is used for a specific application without having toxic or injurious effects on biological function [120,121].

In this context, such materials should be easy to manipulate, radiopaque, dimensionally stable, nonabsorbable, and nontoxic [122]. The determination of the biocompatibility of materials and implanted devices involves detailed characterization of the material (e.g., bulk and surface chemical composition; density; porosity; and mechanical, electrical, and degradation properties) and extensive testing, first at the protein/cell/tissue or in vitro level and then in vivo animal models and ultimately in human clinical trials [123]. Fig. 12.7 shows implanted biomaterial reaction in higher organism.

Biomaterials used in blood-contacting applications are exposed to a challenging biological environment. The main parameter of blood compatibility, which is commonly investigated, is platelet response to the foreign material. Platelets may adhere to a foreign surface, following which they may or may not activate: Conversely, they may activate although they do not adhere to a surface; if they do adhere to a surface, they may spread, covering the surface with a "passivating" layer. The platelet, or direct thrombogenic response, in the short term, may be the most significant element of the biocompatibility of a material. However, for longer-duration implanted devices, the effects on other components of the host response to foreign objects may also have a significant effect on the biocompatibility of the implant [124,125].

Cell culture assays are used to assess the biocompatibility of a material or extract through the use of isolated cells in vitro. These techniques are useful in evaluating the toxicity or irritancy potential of materials and chemicals. They provide an excellent way to screen materials prior to in vivo test [126].

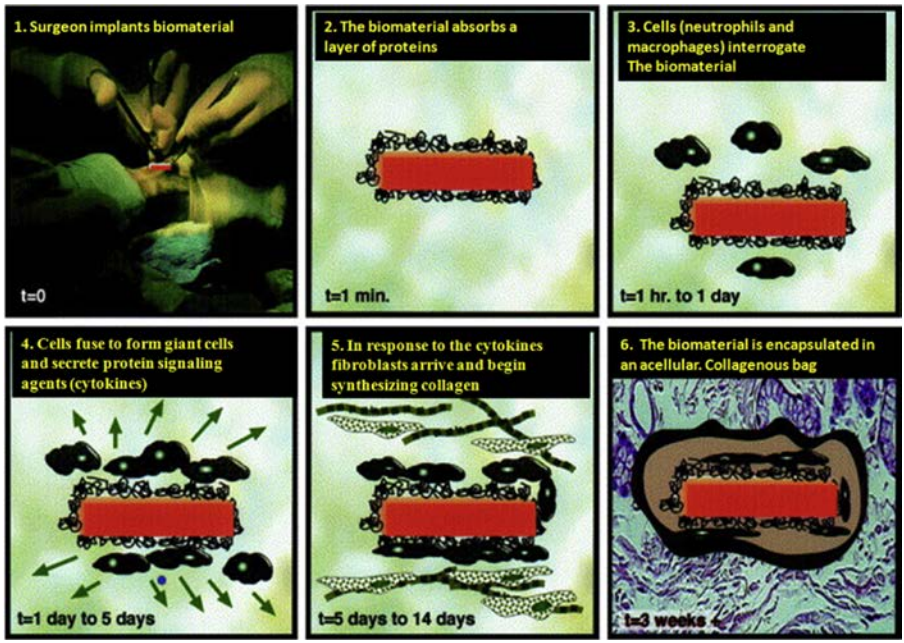

Figure 12.7 The foreign body reaction is the normal reaction of a higher organism to an implanted synthetic material and is schematically illustrated here. (1) A surgeon implants a biomaterial in a surgical site (an injury). (2) Quickly, the implant adsorbs a layer of proteins, the normal process for a solid surface in biological fluids. (3) Cells (neutrophils and then macrophages) interrogate and attack the "invader," i.e., the biomaterial. (4) When the macrophages find they cannot digest the implant, they fuse into giant cells to engulf the object. However, it is too large to completely ingest. The giant cells send out chemical messengers (cytokines) to call in other cells. (5) Fibroblast cells arrive and begin synthesizing collagen. (6) The end stage of the reaction has the implant completely encased in an acellular, avascular collagen bag. There are macrophages between the collagen sac and the implant.

There are three cytotoxicity tests commonly used for medical devices:

1. The direct contact procedure is recommended for low-density materials, such as contact lens polymers.
2. The agar diffusion assay is appropriate for high-density materials, such as elastomeric closures.
3. The MEM elution assay uses different extracting media and extraction conditions to test devices.

The effects of the chemical structure and the surface properties of polymer biomaterials that influence their biocompatibility include (1) the interfacial free energy, (2) balance between the hydrophilicity and the hydrophobicity on the surface, (3) the chemical structure and functional groups, (4) the type and the density of surface charges, (5) the molecular weight of the polymer, (6) conformational flexibility of the polymer, and (7) surface topography and roughness.

12.5.2 Biodegradability

Polymer, whether human-made or natural, degrades during use, with progressive loss of properties such as appearance, mechanical strength, and overall integrity. Recently, biodegradable polymeric materials have gained much attention by researchers because these materials degrade within the body as a result of natural biological processes, eliminating the need to remove a drug delivery system after release of the active agent has been accomplished. With regard to biodegradable polymers, it is essential to recognize that degradation is a chemical process (brought about by factors such as light, heat, water, ultrasound) that may take place through bulk hydrolysis, and polymer erosion takes place in uniform manner that depends on dissolution and diffusion processes. For some degradable polymers, most notably the polyanhydrides and polyorthoesters, the degradation occurs only at the surface of the polymer, resulting in a release rate that is proportional to the surface area of the drug delivery system [127]. The origin of all degradation processes is the initial bond–breaking reactions, i.e., scission of bonds. Input of many forms of energy can cause the scission. The primary bond scission reactions may end the extent of deterioration but may also give rise to secondary chemical reactions, leading to more bond scission and recombination reactions. Polymer degradation can be classified into photo, thermal, mechanical, hydrolytic, oxidative, biodegradation, radiation, and chemical degradation [128]. For degradable polymers, two different erosion mechanisms have been proposed: (1) surface or heterogeneous erosion and (2) bulk or homogeneous erosion (Fig. 12.8). In the case of surface eroding polymer matrices, polymer degradation is much faster than water intrusion into the polymer bulk. Degradation occurs, therefore, mainly in the outermost polymer layers. Consequently, erosion affects only the surface and not the inner parts of a matrix (heterogeneous process). Bulk eroding polymers in contrast degrade slowly, and water uptake by the system is much faster than polymer degradation. Thus, the entire system is rapidly hydrated, and polymer chains are cleaved throughout the device. Consequently, erosion is not restricted to the polymer surface (homogeneous process) [129].

12.5.3 Mechanical property

Mechanical properties of biomaterials are very important for pharmaceutical applications. For example, the integrity of the drug delivery device during the lifetime of the application is very important to obtain. FDA approval is not given unless the device is designed to protect a sensitive therapeutic agent, such as protein must maintain its integrity to be able to protect the protein until it is released out of the system. Changing the degree of cross-linking has been utilized to achieve the desired mechanical properties of the hydrogel. Increasing the degree of cross-linking of the system will result in a stronger gel. However, a higher degree of cross-linking creates a more brittle structure. Hence, there is an optimum degree of cross-linking to achieve a relatively strong and yet elastic hydrogel. Copolymerization has also been utilized to achieve the desired mechanical properties of hydrogel. Incorporating a comonomer that will contribute to H-bonding can increase the strength of hydrogel [130].

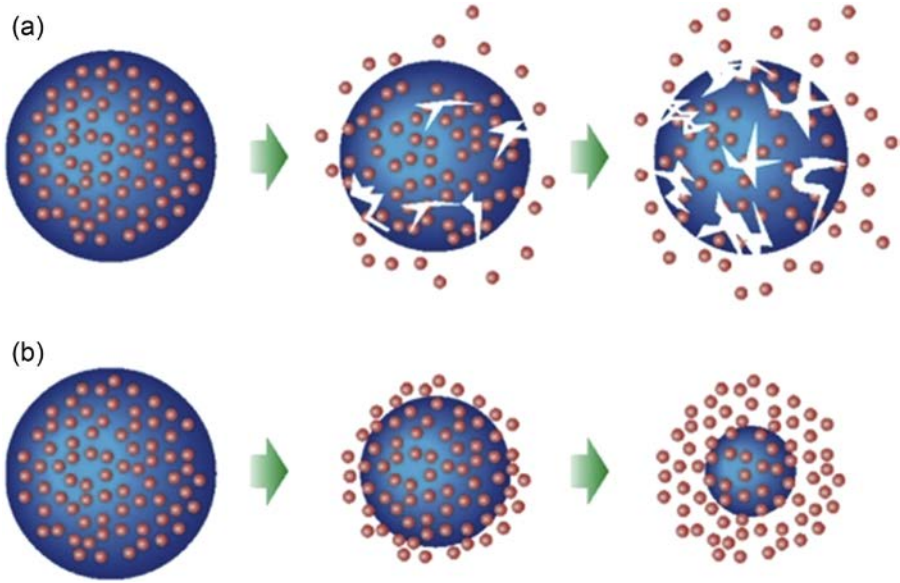

Figure 12.8 Drug delivery from (a) bulk eroding, and (b) surface eroding biodegradable systems.

12.5.4 Swelling property

The swelling kinetics of hydrogels can be classified as diffusion-controlled (Fickian) and relaxation-controlled (non-Fickian) swelling. When water diffuses into the hydrogel much faster than the relaxation of the polymer chains, the swelling kinetics is relaxation controlled. A nice mathematical analysis of the dynamics of swelling has been presented by Peppas and Colombo [131]. Besides the nature the cross-linking ratio is one of the most important factors that affects the swelling of blends. It is defined as the ratio of moles of cross-linking agents to the moles of polymer repeating units. The higher the cross-linking ratio, the more the cross-linking agent incorporated in the hydrogel structure. Highly cross-linked blends have a tighter structure and will swell less compared to the same blends with lower cross-linking ratio. Cross-linking hinders the mobility of the constituent polymer chains, thus lowering the swelling ratio.

The chemical structure of the polymer may also affect the swelling ratio of the blend hydrogels. Hydrogels containing hydrophilic groups swell to a higher degree compared to those containing hydrophobic groups. Hydrophobic groups collapse in the presence of water, thus minimizing their exposure to the water molecule. As a result, the hydrogels will swell much less compared to hydrogels containing hydrophilic groups 20. Superabsorbent polymers, which may be termed as materials capable of absorbing and holding large amount of water, have gained considerable attention and may be very useful in the biomedical fields. These materials have extensive commercial applications such as “infant diapers,” “feminine hygiene products,” and “incontinency products.” These materials can be fruitfully prepared by radiation grafting technique [132].

References

[1] C. Defonseka, Introduction to Polymeric Composites with Rice Hulls, Smithers Rapra, Shropshire, England, 2014, pp. 1–2.
[2] E. Bayraktar, Materials Science and Materials Engineering (2016). http://dx.doi.org/10.1016/B978-0-12-803581-8.04108-4.
[3] E. Ruiz-Hitzky, P. Aranda, M. Darder, Bionanocomposites, in: Kirk–othmer Encyclopedia of Chemical Technology, October 17 , 2008. Published Online http://dx.doi.org/10.1002/0471238961.bionruiz.a01.
[4] M. Darder, P. Aranda, E. Ruiz-Hitzky, Advanced Materials 19 (2007) 1309–1319.
[5] Y.A. Arfat, S. Benjakul, T. Prodpran, K. Osako, Food Hydrocolloids 39 (2014) 58–67.
[6] H.J. Park, M.S. Chinnan, Jornal of Food Engineering 25 (1995) 497–507.
[7] T. Prodpran, S. Benjakul, A. Artharn, International Journal of Biological Macromolecules 41 (2007) 605–614.
[8] A.C.S. Alcântara, M. Darder, P. Aranda, Applied Clay Science 96 (2014) 2–8.
[9] A. Kelly (Ed.), A Concise Encyclopedia of Composite Materials, Elsevier, Oxford, 1994, pp. xvii–xxix.
[10] R.N. Rothon, M. Hancock, General principles guiding selection and use of particulate materials, in: R.N. Rothon (Ed.), Particulate-filled Polymer Composites, 1995, pp. 1–45.
[11] F.P. Gerstle Jr., Composites, in: in: J.I. Kroschwitz, H.F. Mark, N.M. Bikales, C.G. Overberger, G. Menges (Eds.), Encyclopedia of Polymer Science and Technology, vol. 3, John Wiley and Sons, New York, 1985.
[12] G.V. Jackson, M.L. Orton, Filled thermosets, in: R.N. Rothon (Ed.), Particulate-filled Polymer Composites, 1995, pp. 317–370.
[13] H.S. Katz, Particulate fillers, in: S.T. Peters (Ed.), Handbook of Composites, second ed., Chapman Hall, London, 1998, pp. 242–253.
[14] R. Pyrz, B. Bochenek, Bulletin of the Polish Academy of Sciences Technical Sciences 55 (2) (2007) 251–260.
[15] M. Alexandre, P. Dubois, Materials Science and Engineering 28 (2000) 1–63.
[16] S. Zhang, D. Sun, Y. Fu, H. Du, Surface and Coatings Technology 167 (2003) 113–119.
[17] E. Manias, Nature Materials 6 (1) (2007) 9–11.
[18] F. He, Q. Han, M.J. Jackson, International Journal of Nanoparticles 1 (4) (2008) 301–309.
[19] R.E. Gorga, M. Okamoto, F. Hussain, M.J. Hojjati, Composite Materials 40 (17) (2006) 1511–1575.
[20] M. Chu, S.Q. Zhu, H.M. Li, Z.B. Huang, S.Q. Li, Journal of Applied Polymer Science 102 (2006) 5137–5143.
[21] F. Puoci, F. Iemma, U.G. Spizzirri, G. Cirillo, M. Curcio, N. Picci, North American Journal of Agricultural and Biological Sciences 3 (2008) 299–314.
[22] M. Kamat, R. Malkani, Indian Journal of Pediatrics 70 (2003) 879–881.
[23] K. Kosemund, H. Schlatter, J.L. Ochsenhirt, E.L. Krause, D.S. Marsman, G.N. Erasala, Regulatory Toxicology and Pharmacology 53 (2009) 81–89.
[24] H. Kasgoz, A.Z. Durmus, A. Kasgoz, Polymers for Advanced Technologies 19 (2008) 213–220.
[25] Y.Q. Wang, H.F. Zhang, Y.P. Wu, J. Yang, L.Q. Zhang, European Polymer Journal 41 (2005) 2776–2783.
[26] M. Sadeghi, H.J. Hosseinzadeh, Journal of Bioactive and Compatible Polymers 23 (2008) 381–404.
[27] S.S. Ray, M. Bousmina, Progress in Materials Science 50 (2005) 962–1079.

[28] A. Pourjavadi, H. Hosseinzadeh, M. Sadeghi, M.J. Compos, Materials 41 (2007) 2057–2069.
[29] T. Yoshimura, I. Uchikoshi, Y. Yoshiura, R. Fujioka, Carbohydrate Polymers 61 (2005) 322–326.
[30] J.P. Zhang, Q. Wang, A.Q. Wang, Carbohydrate Polymers 68 (2007) 367–374.
[31] P. Lanthong, R. Nuisin, S. Kiatkamjornwong, Carbohydrate Polymers 66 (2006) 229–245.
[32] A. Li, J.P. Zhang, A.Q. Wang, Bioresource Technology 98 (2007) 327–332.
[33] A.L. Suo, J.M. Qian, Y. Yao, W.G. Zhang, Applied Polymer Science 103 (2007) 1382–1388.
[34] Y. Chen, Y.F. Liu, H.M. Tan, J.X. Jiang, Carbohydrate Polymers 75 (2009) 287–292.
[35] S.B. Hua, A.Q. Wang, Carbohydrate Polymers 75 (2009) 79–84.
[36] K.P. Talaro, A. Talaro, Foundations in Microbiology, fourth ed., McGraw-Hill College, Blacklick, Ohio, USA, 2002.
[37] M.D. Teli, N.G. Waghmare, Carbohydrate Polymer 78 (2009) 492–496.
[38] L. Wu, M.Z. Liu, Carbohydrate Polymer 72 (2008) 240–247.
[39] Q. Li, E.T. Dunn, E.W. Grandmaison, M.F.A. Goosen, Journal of Bioactive and Compatible Polymers 7 (1992) 370–397.
[40] D.W. Lee, H. Lim, H.N. Chong, W.S. Shim, The Open Biomaterials Journal 1 (2009) 10–20.
[41] K.I. Draget, O. Smidsrod, G. Skjak-Braek, Alginates from algae, in: Biopolymers, A. Wiley-VCH Verlag GmbH, 2002, pp. 215–244.
[42] T.J. Painter, Algal polysaccharides, in: The Polysaccharides, Academic Press, London, 1983, pp. 196–286.
[43] K.I. Draget, O. Smidsrod, G. Skjak-Braek, Alginates from algae, in: A. Steinbuchel, S.K. Rhee (Eds.), Polysaccharides and Polyamides in the Food Industry, Wiley-VCH Verlag GmbH & Co, Weinheim, 2005, pp. 1–30.
[44] A. Haug, O. Smidsrod, Nature 215 (1967) 757.
[45] O. Smidsrod, Journal of the Chemical Society, Faraday Transactions, 57 (1974) 263–274.
[46] I. Andresen, O. Skipnes, O. Smidsrod, K. Ostgaard, P.C. Hemmer, ACS Symposium Series 48 (1977) 361–381.
[47] E. Onsoyen, *Carbohydrates in Europe* 14 (1996) 26–31.
[48] T.A. Davis, B. Volesky, A. Mucci, Water Research 37 (2003) 4311–4330.
[49] S. Young, M. Wong, Y. Tabata, A.G. Mikos, Journal of Controlled Release 109 (2005) 256–274.
[50] E. Leo, M.A. Vandelli, R. Cameroni, F. Forni, International Journal of Pharmaceutics 155 (1997) 75–82.
[51] E. Engvall, E. Ruoslahti, International Journal of Cancer 20 (1977) 1–5.
[52] C. Coester, P. Nayyar, J. Samuel, European Journal of Pharmaceutics and Biopharmaceutics: Official Journal of Arbeitsgemeinschaft Fã¼r Pharmazeutische Verfahrenstechnik e.V 62 (2006) 306–314.
[53] J. Bajpai, R. Shrivastava, A.K. Bajpai, Journal of Applied Polymer Science 103 (2007) 2581–2590.
[54] A.M. Goldstein, E.N. Alter, J.K. Seaman, in: R.L. Whistler (Ed.), Guargum. Industrial Gums, second ed., Academic Press, New York, 1973, pp. 303–321.
[55] H.L. Greenwald, L.K.S. Luskin, in: R.L. Davidson (Ed.), Handbook of Water Soluble Gums and Resins, McGraw Hill, New York, 1980, p. 19.
[56] H.T. Lokhande, P.V. Varadara, Bioresource Technology 42 (1992) 119–122.
[57] H.E. Kokkonen, J.M. Ilvesaro, M. Morra, H.A. Schols, J. Tuukkanen, Biomacromolecules 8 (2007) 509–515.

[58] T. Manabe, Pectinsitunokagaku, in: Pectin, Saiwai-Shobou Co., Ltd., Japan, 2001, p. p.1.
[59] C.H. Chen, M.T. Sheu, T.F. Chen, Y.C. Wang, W.C. Hou, D.Z. Liu, Biochemical Pharmacology 72 (2006) 1001.
[60] L.W. Doner, ACS Symposium Series 310 (1986) 13.
[61] J.F. Thibault, Phytochemistry 22 (1983) 1567–1571.
[62] Y. Doi, K. Fukuda (Eds.), Biodegradable Plastics and Polymers, Studies in Polymer Science, vol. 12, Elsevier Science, Amsterdam, 1994, p. 627.
[63] T.M. Wu, C.Y. Wu, Polymer Degradation and StabilityPolymer Degradation and Stability 91 (2006) 2198–2204.
[64] A.R. McLauchlin, N.L. Thomas, Polymer Degradation and StabilityPolymer Degradation and Stability 94 (2009) 868–872.
[65] E. Jaffar Al-Mulla, Fibers and Polymers 12 (2011) 444–450.
[66] S. Gumus, G. Ozkoc, A. Aytac, Journal of Applied Polymer Science 123 (2012) 2837–2848.
[67] M. Shibata, Y. Someya, M. Orihara, M. Miyoshi, Journal of Applied Polymer Science 99 (2006) 2594–2602.
[68] A. Hasook, S. Tanoue, Y. Iemoto, T. Unryu, Polymer Engineering and Science 46 (2006) 1001–1007.
[69] M.A. Paul, C. Delcourt, M. Alexandre, P. Degée, F. Monteverde, A. Rulmont, Chemical Physics 206 (2005) 484–498.
[70] T. Villmow, P. Pötschke, S. Pegel, L. Häussler, B. Kretzschmar, Polymer 49 (2008) 3500–3509.
[71] J.T. Yoon, S.C. Lee, Y.G. Jeong, Composites Science and Technology 70 (2010) 776–782.
[72] S. Barrau, C. Vanmansart, M. Moreau, A. Addad, G. Stoclet, J.M. Lefebvre, Macromolecules 44 (2011) 6496–6502.
[73] S. Philip, T. Keshavarz, I. Roy, Journal of Chemical Technology and Biotechnology 82 (2007) 233–247.
[74] E. Hablot, P. Bordes, E. Pollet, L. Avérous, Polymer Degradation and Stability 93 (2008) 413–421.
[75] P. Bordes, E. Pollet, S. Bourbigot, L. Avérous, Macromolecular Chemistry and Physics 209 (2008) 1473–1484.
[76] S. Wang, C. Song, G. Chen, T. Guo, J. Liu, B. Zhang, Polymer Degradation and Stability 87 (2005) 69–76.
[77] G.X. Chen, G.J. Hao, T.Y. Guo, M.D. Song, B.H. Zhang, Journal of Applied Polymer Science 93 (2004) 655–661.
[78] M.D. Sanchez-Garcia, J.M. Lagaron, Journal of Applied Polymer Science 118 (2010) 188–199.
[79] A. Botana, M. Mollo, P. Eisenberg, R.M. Torres Sanchez, Applied Clay Science 47 (2010) 263–270.
[80] T. Fujimaki, Polymer Degradation and Stability 59 (1998) 209–214.
[81] S. Sinha Ray, K. Okamoto, P. Maiti, M. Okamoto, Journal of Nanoscience and Nanotechnology 2 (2002) 171–176.
[82] Y.F. Shih, T.Y. Wang, R.J. Jeng, J.Y. Wu, C. Teng, Journal of Polymers and the Environment 15 (2007) 151–158.
[83] Y.F. Shih, T.Y. Wang, R.J. Jeng, J.Y. Wu, D.S. Wuu, Journal of Applied Polymer Science 110 (2008) 1068–1079.
[84] M.S. Nikolic, J. Djonlagic, Polymer Degradation and Stability 74 (2001) 263–270.
[85] P.B. Messersmith, E.P. Giannelis, Journal of Polymer Science Part A: Polymer Chemistry 33 (1995) 1047–1057.
[86] M.A. Woodruff, D.W. Hutmacher, Progress in Polymer Science 35 (2010) 1217–1256.

[87] P.B. Messersmith, E.P. Giannelis, Chemistry of Materials 5 (1993) 1064–1066.
[88] N. Pantoustier, B. Lepoittevin, M. Alexandre, P. Dubois, D. Kubies, C. Calberg, Polymer Engineering & Science 42 (2002) 1928–1937.
[89] J.M. Thomassin, X. Lou, C. Pagnoulle, A. Saib, L. Bednarz, I. Huynen, The Journal of Physical Chemistry C 111 (2007) 11186–11192.
[90] F. Chivrac, E. Pollet, L. Avérous, Materials Science & Engineering 67 (2009) 1–17.
[91] P. Ren, T. Shen, F. Wang, X. Wang, Z. Zhang, Journal of Polymers and the Environment 17 (2009) 203–207.
[92] C. Zeppa, F. Gouanvé, E. Espuche, Journal of Applied Polymer Science 112 (2009) 2044–2056.
[93] V.P. Cyras, L.B. Manfredi, M.T. Ton-That, A. Vázquez, Carbohydrate Polymers 73 (2008) 55–63.
[94] X. Tang, S. Alavi, T.J. Herald, Carbohydrate Polymers 74 (2008) 552–558.
[95] B.S. Chiou, D. Wood, E. Yee, S.H. Imam, G.M. Glenn, W.J. Orts, Polymer Engineering & Science 47 (2007) 1898–1904.
[96] C.J. Pérez, V.A. Alvarez, I. Mondragón, A. Vázquez, Polymer International 56 (2007) 686–693.
[97] S.Y. Lee, M.A. Hanna, Polymer Composites 30 (2009) 665–672.
[98] K.M. Dean, M.D. Do, E. Petinakis, L. Yu, Composites Science and Technology 68 (2008) 1453–1462.
[99] S. Bocchini, D. Battegazzore, A. Frache, Carbohydrate Polymers 82 (2010) 802–808.
[100] S. Tang, P. Zou, H. Xiong, H. Tang, Carbohydrate Polymers 72 (2008) 521–526.
[101] A. Star, D.W. Steuerman, J.R. Heath, J.F. Stoddart, International Edition 41 (2002) 2508–2512.
[102] L.M. Famá, V. Pettarin, S.N. Goyanes, C.R. Bernal, Carbohydrate Polymers 83 (2011) 1226–1231.
[103] Z. Liu, L. Zhao, M. Chen, J. Yu, Carbohydrate Polymers 83 (2011) 447–451.
[104] L. Yan, P.R. Chang, P. Zheng, Carbohydrate Polymers 84 (2011) 1378–1383.
[105] Y.L. Chung, H.M. Lai, Carbohydrate Polymers 80 (2010) 525–532.
[106] F.J. Rodríguez, M.J. Galotto, A. Guarda, J.E. Bruna, Journal of Food Engineering 110 (2012) 262–268.
[107] M. Darder, M. Colilla, E. Ruiz-Hitzky, Applied Clay Science 28 (2005) 199–208.
[108] H. Oguzlu, F. Tihminlioglu, Macromolecular Symposia 298 (2010) 91–98.
[109] X. Wang, B. Liu, J. Ren, C. Liu, X. Wang, J. Wu, Composites Science and Technology 70 (2010) 1161–1167.
[110] Y. Pan, T. Wu, H. Bao, L. Li, Carbohydrate Polymers 83 (2011) 1908–1915.
[111] Y.T. Shieh, H.M. Wu, Y.K. Twu, Y.C. Chung, Colloid and Polymer Science 288 (2010) 377–385.
[112] L.J. Lee, C. Zeng, X. Cao, X. Han, J. Shen, G. Xu, Composites Science and Technology 65 (2005) 2344–2363.
[113] R.A. Vaia, E.P. Giannelis, Macromolecules 30 (1997) 7990–7999.
[114] T. Kuila, S. Bhadra, D. Yao, N.H. Kim, S. Bose, J.H. Lee, Recent advances in graphene based polymer composites, Progress in Polymer Science 35 (11) (2010) 1350–1375.
[115] P.K. Sudeep, T. Emrick, Polymer Reviews 47 (2007) 155–163.
[116] S.S. Ray, M. Okamoto, Progress in Polymer Science 28 (2003) 1539–1641.
[117] M.F. Maitz, I. Tsyganov, M.T. Pham, E. Wieser, Annual Report, 2002, IIM, FZR-362.
[118] B.D. Ratner, D. Hoffman, F.J. Schoen, J.E. Lemons, An introduction to materials in medicine, in: Biomaterial Science, Academic press, San Diego, 2004.

[119] B. Menaa, F. Menaa, C. Aiolfi-Guimaraes, O. Sharts, International Journal of Nanotechnology 7 (1) (2010) 1.
[120] D.F. Williams, Biomaterials 29 (20) (2008) 2941–2953.
[121] J.M. Anderson, Annual Review of Materials Research 31 (81) (2001) 1–401.
[122] A.H. Gartner, S.O. Dom, Advances in endodontic therapy, Dental Clinics of North America 36 (2) (1992) 357–378.
[123] S. Paulo, Brazilian Oral Research 19 (3) (2005) 1806–8314.
[124] B. Montdargent, F. Maillet, M.P. Carreno, M. Jozefowicz, M. Kazatchkine, D. Labarre, Biomaterials 14 (1993) 203–208.
[125] G.M. Bernacca, M.J. Gulbransen, R. Wilkinson, D.J. Wheatley, Biomaterials 19 (1998) 1151–1165.
[126] ISO 10993, Biological Evaluation of Medical Device, Part 5, Test for in Vitro Cytotoxicity, 1999.
[127] F. Alexis, Polymer International 54 (2005) 36–46.
[128] N. Grassie, Polymer Degradation and Steblization, Cambridge University Press, 1985. 1445.
[129] V.V. Ranade, M.A. Hollinger (Eds.), Drug Delivery Systems, second ed., 2003, pp. 1–69.
[130] N.A. Peppas, P. Bures, W. Leobomdung, H. Ichikawa, European Journal of Pharmaceutics and Biopharmaceutics 50 (2000) 27–46.
[131] N.A. Peppas, P. Colombo, Journal of Controlled Release 45 (1997) 35–40.
[132] S. Kiatkamjorwong, N. Meechi, Radiation Physics and Chemistry 49 (6) (1997) 689–696.

Further reading

[1] T. Kushibiki, H. Matsuoka, Y. Tabata, Biomacromolecules 5 (2004) 202–208.

This page intentionally left blank

Advances in bionanocomposites for biomedical applications

13

Rajesh K. Saini[1], *Anil K. Bajpai*[1], *Era Jain*[2]
[1]Government Model Science College, Jabalpur, India; [2]Saint Louis University, Saint Louis, MO, United States

13.1 Introduction

Mechanical composite materials continue to be an integral part of our daily lives. Composites have a wide range of applications (Fig. 13.1), from sports equipment to transportation vehicles. Composites make it possible for tennis rackets, kayaks, boats, and many other recreational sports equipment to be both lightweight and strong. They are found in aircraft components, ranging from the seat frames to sections of the wings [1,2]. The rotor blades of helicopters are made of composite because they have much greater tolerance for fatigue than metals. Automobile tires are made of rubber reinforced with steel thread to extend life and to increase performance at high speeds. Historic and more contemporary examples of composite materials appear to favor mechanical properties for applications. However, with the application of electrical, thermal, magnetic, and optical properties in our everyday lives, nonmechanical composites have also become important [3]. These materials are not as apparent to the everyday user because they may be encased in protective packaging, but they provide essential functions in many systems, such as personal computers.

The dimensional scale for electronic devices has now entered the nanorange. The electrical conductivity of carbon nanotubes (CNTs) in insulating polymers has also been a topic of considerable interest. The utility of polymer-based nanocomposites in these areas is quite diverse involving many potential applications including photovoltaic cells and photodiodes, supercapacitors, sensors, printable conductors, light-emitting diodes, field effect transistors electromagnetic interference shielding, transparent conductive coatings, electrostatic dissipation, electromechanical actuators, and various electrode applications [4–6].

13.2 Dental applications

National Institutes of Health published the report on the denture materials that states that there are more than 100 million people missing teeth and that the need for implant dentistry is very high. In the last 50 years, researchers focused on the synthesis of biomaterials (materials intended to interface with biological systems to evaluate, treat, augment, or replace any tissue, organ, or function of the body)-based medical dental

Biodegradable and Biocompatible Polymer Composites. http://dx.doi.org/10.1016/B978-0-08-100970-3.00013-4

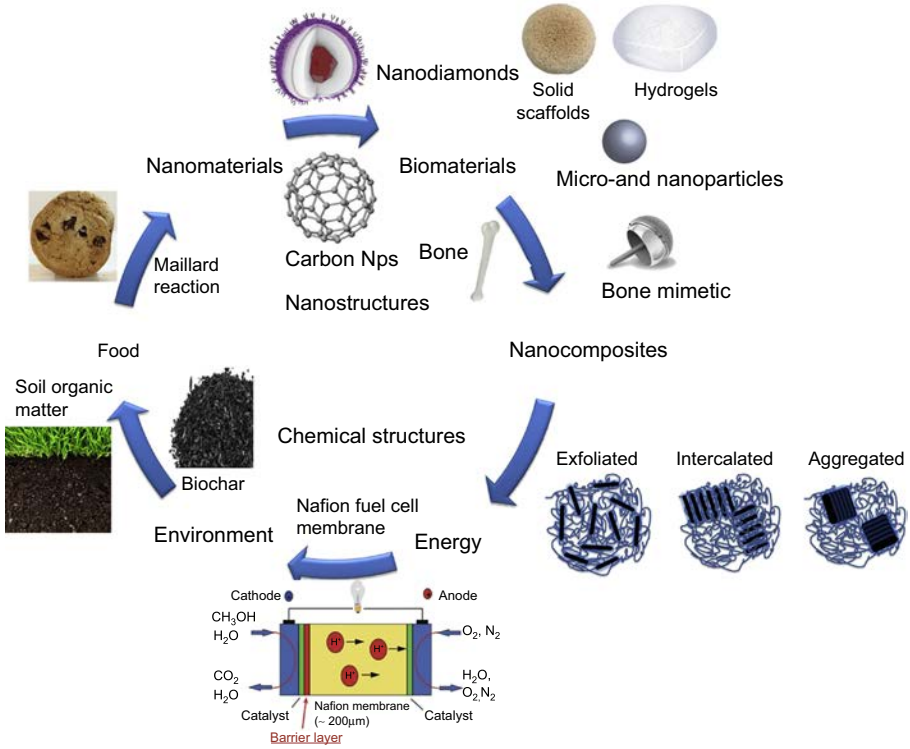

Figure 13.1 Applications of nanocomposites.

implants for treatment of millions of patients every year. Teeth are hardest materials in our body mainly consists of hydroxyapatite ($Ca_5(PO_4)_3(OH)$). National Bureau of Standard of the US government has set specification standards for selection and grading of dental amalgam implants. Out of various materials, polymer-based materials have gained much attention due to their greatest versatility in properties and processing, on the basis of the conditions found in the body, taking into consideration that the circumstances under which polymers are most susceptible, including those of elevated temperature, electromagnetic radiation, and atmospheric oxygen, and also used extensively in dentistry as composite (resin–ceramic) restorative materials, implants, dental cements, and denture bases and teeth [7,8]. Composite resin had average particle sizes that far exceeded 1 μm and microfillers and used for adhesive dental restoration as the realization of minimum cavity preparation and superior esthetics, restorative materials, cavity liners, pit and fissure sealants, cores and buildups, inlays, onlays, crowns, provisional restorations, cements for single or multiple tooth prostheses and orthodontic devices, endodontic sealers, and root canal posts [9], because of ease of their formulation tailored to their particular requirements as restoratives, sealants, cements, provisional materials, etc. The predominant base monomer used in commercial dental composites has been bis-GMA, which due to its high viscosity is mixed with other dimethacrylates, such as triethylene glycol dimethacrylate (TEGDMA), diurethane dimethacrylate (UDMA), or other monomers [10]. However, "macrofill" materials

are difficult to polish, and lack of surface smoothness makes its applications limited. For long-term esthetics, "nanofills" are used because they are generally weak due to their relatively low filler content, and a compromise was needed to produce adequate strength by increasing the filler level by incorporating highly filled, prepolymerized resin fillers within the matrix to which additional "microfill" particles were added [11]. Nowadays, organically modified ceramics; flowable composites containing adhesive monomers, such as Vertise Flow (Kerr) and Fusio Liquid Dentin (Pentron Clinical); and epoxy-based silicone system have been developed by researchers for better dental implant materials [12]. These materials possess good mechanical properties and provide verified lower shrinkage than typical dimethacrylate-based resins, likely due to the epoxide curing reaction that involves the opening of an oxiranering and currently recommended for liners and small restorations, and are serving as the entry point for universal self-adhesive composites [13,14].

13.3 Orthopedic applications

Bone is a natural extracellular matrix (ECM) living tissue composed of organic–inorganic complex (60% mineral (nanohydroxyapatite (nHA, $Ca_{10}(PO_4)_6(OH_2)$)), 30% matrix (collagen, major structural protein of connective tissue), and 10% water by weight), and its high strength with special elastic properties makes it suitable for structural framework, protective shield for internal organs and marrow, mechanical strength, blood pH regulation and maintenance of the calcium and phosphate level for metabolic processes, and it provides stores of ions necessary for normal bodily function and forms the part of endoskeleton of vertebrates [15–18]. Bone-related injuries causing hospitalization due to fractures and grafting procedures have become a global phenomenon. To address the need for intervention in these causes, many materials are currently in use to repair or replace bone and must exhibit adequate mechanical properties coupled with controlled degradation rates and appropriate biological behavior in terms of interaction with living tissues [19]. Polymer nanocomposites based on hydroxyapatite ($Ca_{10}(PO4)_6(OH)_2$) have been investigated for bone repair and implantation. Hydroxyapatite, a major constituent of hard tissue, exhibits undesirable mechanical properties if directly employed, and therefore, polymer-based matrix composites are desired. Biodegradation of the matrix is also desired to allow infiltration of new bone growth at the repair site. Natural polymers (polysaccharides, polypeptides, collagen, chitosan) or synthetic biodegradable polymers are often employed as the matrix in these studies. Collagen-derived gelatin and poly-2-hydroxyethylmethacrylate/poly (3-caprolactone) nanocomposites based on hydroxyapatite are examples of bone repair systems.

Various types of synthetic substitutes such as metals, ceramics, polymers, and composites have been developed to comply with biofunctionality and biocompatibility as per the requirements and the type of function that needs replacement. Mostly hydroxyapatite-based bioabsorbable nonallogenic bone substitutes (ceramics) are commercially available for clinical use because they are biocompatible and their strength can be improved by using natural and synthetic polymers by coprecipitation method [20–23]. Polymer composites of plaster of Paris (PP) (calcium sulfate hemihydrate)

have a porous structure, which is suitable for osteoblast proliferation, and have been clinically used as bone substitute materials. When gypsum ($CaSO_4 \cdot 2H_2O$) is heated to 150°C, it will lose three-fourths of its water to form calcium sulfhate hemihydrate ($CaSO_4 \cdot ½H_2O$) as shown in the following equation, and when it is grinded into powder form, it is referred as PP [24].

$$CaSO_4 \cdot 2H_2O \rightarrow CaSO_4 \cdot ½H_2O + 1½H_2O$$

Through many experimental studies, researchers showed the potential of the biomaterial formed by combining an appropriate ratio of particulate dentin, which is mainly composed of hydroxyapatite and PP, which increases the stability of graft material and promotes bone healing, to be used in soft tissue restoration and for membrane function [25].

Although the nanoscale modeling of synthetically manufactured hybrids and composites is still in infancy, mimicking natural microstructures while using synthetic molecules may lead to new generation materials whose toughness characteristics will be comparable with the materials available in the nature. A formidable challenge remains on the optimizations of their morphology and bioactivity in these novel hybrid composites [26]. Existing orthopedic implants typically consist of single bioinert materials such as metals, ceramics, or polymers and offer relatively cores, combination of two or three components [27]. The development of bonelike composites with improved mechanical properties and enhanced biocompatibility calls for a biomimetic approach using natural bone as guide [28].

13.4 Tissue engineering

The unique combination of hard and soft components in an engineered bionanocomposite closely resembles the amalgamation in natural ECM or tissues [29–33]. Resulting materials possess extraordinary properties and exceptional mechanical strength making bionanocomposites of special significance in tissue regeneration [34–36]. The developments of bionanocomposites provide new avenues for fulfilling certain needs of the emerging technologies in matrix formation, tissue regeneration, and drug delivery and will be instrumental in accelerating evolution of new therapeutics [30]. The greatest challenge in designing of bionanocomposites for tissue regeneration is to have high mechanical strength coupled with high biocompatibility and bioactivity [31,37,38].

For tissue engineering applications, several biopolymers have been combined with nanofillers in different categories such as silicate-based materials such as clays and silica nanoparticles, ceramics such as nanohydroxyapatite (nHA) [31], inorganic nanoparticles of calcium triphosphate [31], synthetic layered double hydroxides (LDHs) [38], carbon-based nanomaterials, such as graphene and CNT [39], and metal/metal oxides (gold, silver, iron oxide) [38,40]. In addition to reinforcing the mechanical strength of the biopolymers, each of these nanofillers also impart additional functionality to the composite. For example, CNTs impart electrical conductivity, while inorganic filler or silicate-based fillers consist of minerals, which are essential for maintenance of several body functions [41]. For instance, calcium is vital for bone development, silicon as

present in ceramics is important for skeletal formation. Silicon causes human stem cells to differentiate into osteogenic lineage and promotes collagen type I synthesis [42]. Thus, incorporating such functional nanoparticles within biopolymers endows them bioactive characteristics useful for tissue regeneration and maintenance [31].

Due to their extraordinary mechanical properties of bionanocomposites, much interest lies in mimicking the bone structure as they allow for multilevel integration of material, structural, and biological properties constituted by the polymer and nanofiller combination [31,40]. Intuitively, many of the bionanocomposites try to achieve bone-like structure by combining the natural bone mineral/ceramic that is nanohydroxyapatite (nHA) and collagen [31]. Some other natural biopolymers, which have been combined with HAs, are silk fibroin, bovine serum albumin, alginate, and chitosan. The synthetic polymers include both degradable and nondegradable polymers such as polylactic glycolic acid (PLGA), polylactic acid (PLA), poly-L-lactic acid (PLLA), polycaprolactone (PCL), polyurethane, ultrahigh-molecular-weight polyethylene, poly(etherketone), and polyvinyl alcohol (PVA) [31]. Inclusion of nanofillers such as HAs increases surface roughness and changes porosity, which is closer to natural bone and facilitates osteoblast spreading and bone regrowth. Other inorganic ceramic nanofillers structurally similar to components of native bone are tricalcium phosphate, bioactive glass, glass ceramic (apatite–wollastonite) have also shown formation of potential high mechanical strength and mineralization inducing scaffold for bone tissue engineering [31,34,37,42]. Furthermore, by a triple combination of natural and synthetic polymers with nHA, mechanical properties and hierarchical structure closely mimicking natural bone might be obtainable (Fig. 13.2). For instance, mechanical

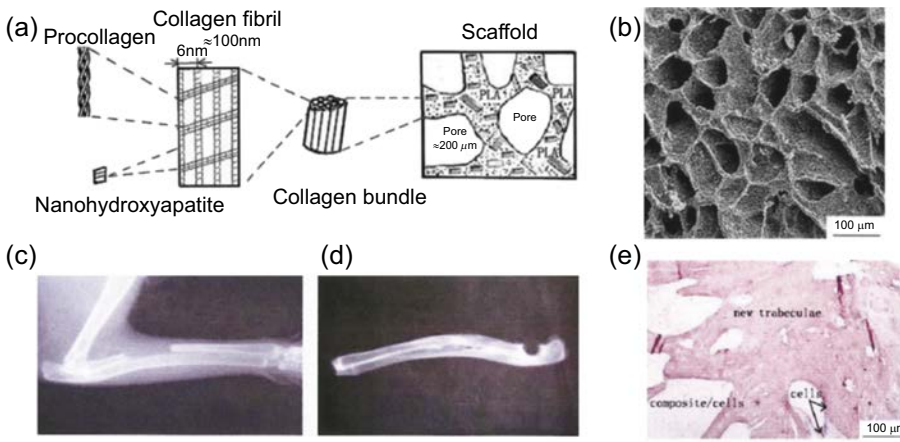

Figure 13.2 A bone scaffold composite of nano-HA/collagen/PLA. (a) Schematic of hierarchical structure of the nano-HA/collagen/PLA composite. (b) Scanning electron microscopy morphology of nano-HA/collagen/PLA composite. (c and d) Implantation of the nano-HA/collagen/PLA composite in a large cortical bone defect results in a completely connected bone after 12 weeks. (e) Decalcified histology HE staining of implant at 12 weeks (compare to 8 weeks) shows more new trabeculae replace the composite. *HA*, hydroxyapatite; *PLA*, polylactic acid.
Reproduced from S.S. Liao, F.Z. Cui, W. Zhang, Q.L. Feng, Journal of Biomedical Materials Research – Part B 69b (2004) 158–165.

strength of a composite of n-HA/collagen/PLA had compressive modulus of 1 MPa and an elastic modulus of 47.3 MPa by changing the PLA ratio in the composite, which was comparable to lower compression range of natural cancellous bone and elastic range of trabecular bone, respectively. On implantation in a rabbit segmental defect, it integrated well with defect and partially substituted with new bone after 12 weeks (Fig. 13.2) [43,44].

Future improvements within this research line could be aimed toward the replacement of HA in biopolymer-based implants by alternative inorganic, or even organic–inorganic, substrates. Besides nHA or nHA-like ceramic nanofillers, SiO_2-based silicon ceramics [37,45], $Mg_2\ SiO_4$ (forsterite) are also actively pursued for bionanocomposites for bone tissue engineering. The silanolan groups found in silicon ceramics interact with calcium and phosphate ions depositing an amorphous calcium phosphate similar to the natural bone [38]. The bionanocomposites of silica (or bioglass)–polymers show variegated bioactivity, and how do these compare to nHA containing bionanocomposites is still to be established [37,45]. The bionanocomposites of forsterite–polymer show superior mechanical properties to nHA–polymer or bioglass–polymer composites [46].

Layered or fibrous clay-based silicate particles combined with either natural or synthetic polymers are used for developing bionanocomposites for tissue engineering. Intercalation of clays with natural polymers, such as proteins such as gelatin, collagen, or zein (storage corn protein) and polysaccharides such as chitosan, cellulose, starch, or alginate, not only increases the mechanical strength but also reduces the degradation rate. Specifically, bionanocomposites of chitosan–clays have been made in different forms to enhance their properties for use in tissue engineering. The clay component in the composites for vast number of studies has been montmorillonite (MMT). The interest in these natural polymers is due to the obvious fact that these either constitute the natural ECM components such as collagen or are structurally similar to natural ECM components such as gelatin, which is a denatured collagen, or chitosan, which resembles the proteoglycans especially for bone and tissue matrix. However, a matrix derived from just the natural polymers is usually weak inclusion of a nanofiller that boosts their mechanical stability. Moreover, these biopolymers have abundant charged and functional group, which can bond via hydrogen bond or van der Waals interaction to silanol groups found in clay or similar nanofillers forming a strong matrix [47,48].

Similarly, addition of small amounts of surface-modified clay nanoparticles (natural MMT = layered silicate) to brittle polymers such as PLGA can improve its toughness and elongation during tensile tests from 7% for the neat polymer to 210% for the polymer nanocomposite (Fig. 13.3(a) and (b)) [49]. This reinforcement and toughness has been attributed to the physical cross-linking between polymer chains and MMT silicate nanoparticles by multiple crazing and shear yielding (Fig. 13.3(c)). Similarly, increase in polymer is seen on MMT combination with PLLA [50,51] and PLA [52]. However, in some cases it has been reported that addition of clay reduces crystallinity of these polymers and accelerates degradation in process. No reports of bionanocomposite formation on effect of clay degradation characteristics have been reported so far. Lastly, combination of fibrous clays such as sepiolite, a magnesium silicate, with biopolymers such as collagen gives rise to hybrid materials with a high degree of

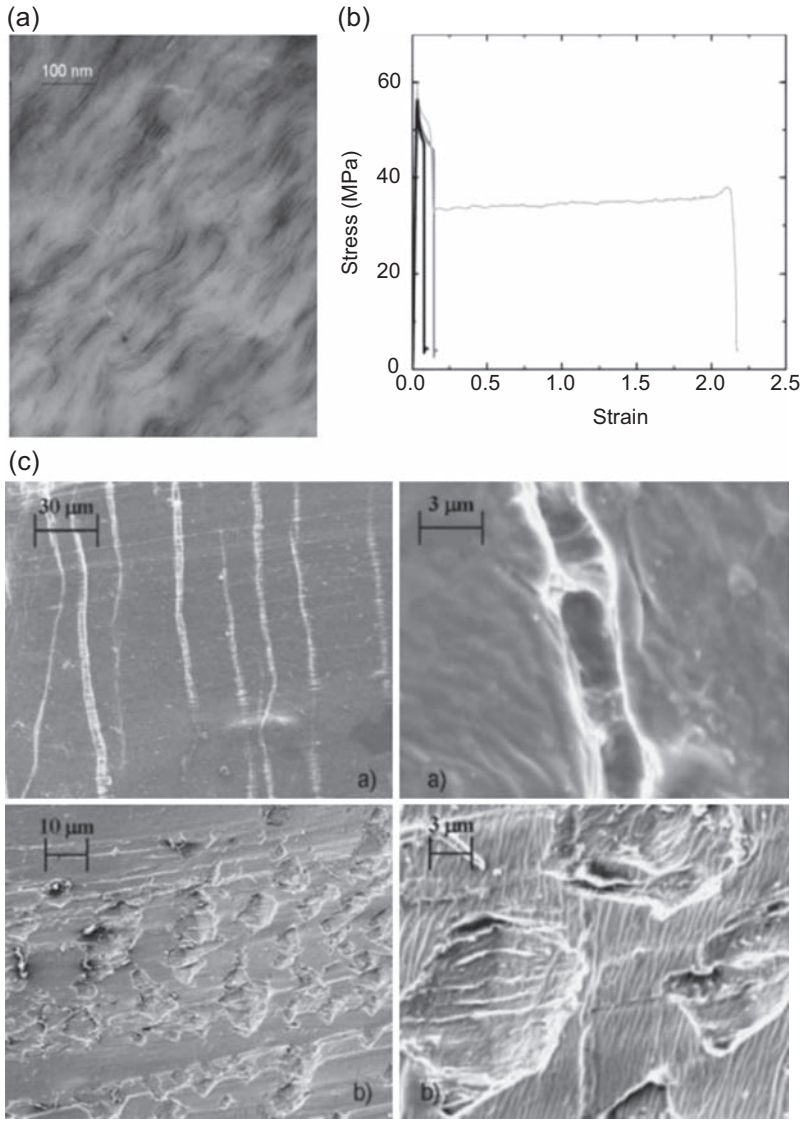

Figure 13.3 A bionanocomposite of poly(D,L-lactide-co-glycolide) (PLG) and montmorillonite (MMT) (30B: Cloisite 30B). MMT was modified with methyl, tallow, bis-2-hydroxyethyl, quaternary ammonium chloride. (a) Transmission electron microscopy (TEM) images of poly(D,L-lactide-co-glycolide) (PLG)/30B bionanocomposites showing a mixed intercalated and dispersed clay particles within PLG. The clay particles display a curved morphology rather than a rigid particle–like shape. (b) Uniaxial tensile test measured at a crosshead speed of 5 mm/min shows a 210% elongation (2.1 strain) of PLG/30B (—) bionanocomposite compared to neat PLG (—) and PLG/silica (—). (c) Scanning electron microscopy images of PLG/30B bionanocomposite: (A) right after yielding shows multiple crazes perpendicular to stretching direction, and (B) after break the polymer fibrils in crazes arrange parallel to stretching direction; the tensile direction is horizontal to the images.
Reproduced from W. Xu, S. Raychowdhury, D.D. Jiang, H. Retsos, E.P. Giannelis, Small 4 (2008) 662–669.

organization [53,54]. The high affinity between collagen and sepiolite fibers leads to their alignment with the collagen chains. Further cross-linking of the polymer reduces degradation and enhances mechanical properties leading to a longer persistence on implantation in body.

Besides reinforcing bulk material properties, hydrogel properties can be also augmented by the use of the nanofillers. By the addition of optimal nanofillers to hydrogels, their inherent low mechanical strength expands their range of biomedical applications [40]. These bionanocomposites can be obtained by physical mixing of the hydrogel precursor components and the preformed nanoparticles and then inducing gelation. In other cases, nanoparticles may itself act as cross-linkers and thus on mixing with the hydrogel precursor can cause it gelation. Either way the nanoparticles are then entrapped inside the hydrogel. Most of the nanofillers in this category require modification of their surface by attachment of the polymeric chains to increase interaction between the hydrophilic network and nanoparticle. The hydrogel bionanocomposites offer a unique tailor ability of the hydrogel properties by means of the nanoparticle used in the composite. For example, colloidal metal particles of gold, silver, or platinum particles can be used to change optical properties of hydrogels. While introduction, iron oxide particles impart magnetic properties and CNTs impart conductive properties. These specific properties lend them useful for applications such as biosensing, nerve tissue conduits, and stimuli sensitive system. In one particular example, CNTs were coated with methacrylated gelatin (GelMA) and embedded in a porous network of GelMA. Addition of just 0.5% CNT to the GelMA increased the tensile modulus and induced threefold increase in spontaneous beating frequency of the seeded cardiomyocytes. Additionally, the cells were highly aligned and could be excited using a much lower electrical voltage, which was attributed to presence of conductive CNTs. Engineered cardiac tissue when released from the substrate displayed cyclical contraction in fluid environment (Fig. 13.4) [42]. CNTs' surface has also been modified with amyloid fibers to increase dispersion and interaction with fibrous hydrogels. Such approaches can be helpful to design hydrogels for various biomedical applications. However, further investigation in their cytocompatibility is still required. Other carbon-based nanofillers such as graphene have also been used in context of tissue engineering. Graphene sheets conjugated to hydrogel networks of elastin such as polypeptide or other synthetic hydrogels have been used to form stimuli responsive and high resilient nanocomposites. Such composites with high tensile strength can be useful for development of elastomeric scaffolds for tissue under constant mechanical stress and electrical stimulation such as heart.

Silicate-based nanoclays have been commonly used to create bionanocomposite hydrogels of mechanical strength elasticity. Nanoclays impart ultraelongation and superstiffness to the hydrogels due to high interaction with biopolymer attributed to their anisotropic plate–like morphology and high aspect ratio [42,47,48]. Both natural (MMT and halloysite) or synthetic polymers such as laponite are used often. Advantages of using synthetic laponite over natural MMT clay include single layer dispersions of nanoparticles, high purity, gelation properties [42,47,48]. MMT presents a plate-like layered structure, whereas halloysite is a hollow nanotube that can be used for controlled drug delivery. Synthetic silicate nanoparticles or nanoplatelets

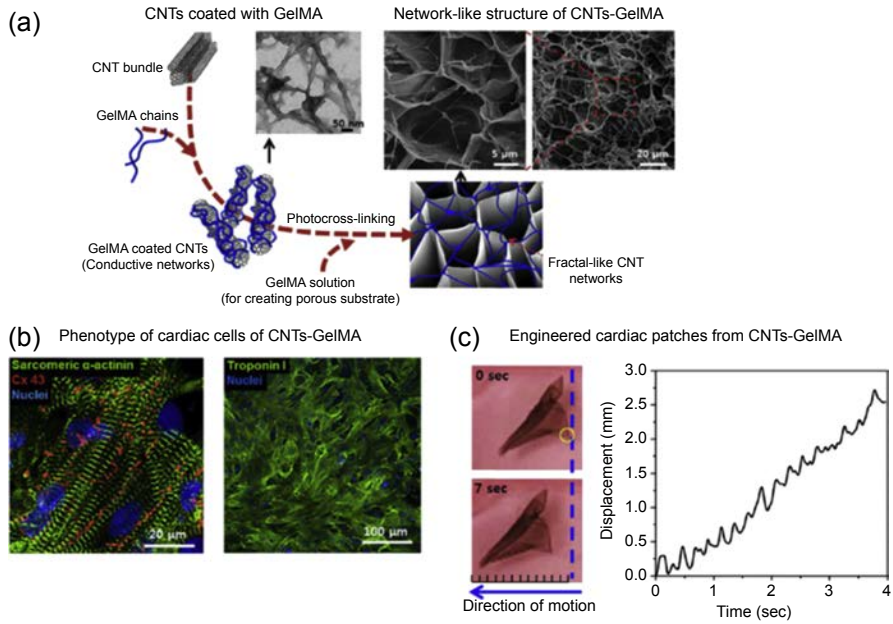

Figure 13.4 Nanocomposite hydrogels from carbon nanotubes (CNTs) and methacrylated gelatin (GelMA). (a) Schematic of GelMa-CNTs nanocomposite fabrication and microstructure network. (b) Cardiac cells seeded on CNTs-GelMA nanocomposites retained their phenotype as determined by the expression of sarcomeric α-actinin and troponin I. (c) The engineered cardiac patch obtained by seeding cardiac cells on CNTs-GelMA surface showed macroscopic mechanical displacement due to continuous contraction and relaxation of the patch.
Reproduced from A.K. Gaharwar, N.A. Peppas, A. Khademhosseini, Biotechnology and Bioengineering 111 (2014) 441–453.

form highly robust and tissue adhesive when mixed with hydrogels [55–57]. Such systems also are shear thinning and may be used for minimally invasive therapies.

Magnetic scaffolds may have some interest in tissue engineering. Recently, hydrogel–gold–iron oxide scaffolds were shown to be a system with high biocompatibility and useful setup to study influence of magnetic field on cells. Additionally, cultured cells on the collagen-iron oxide scaffold internalized iron oxide and became magnetized lending them susceptible to magnetic cell levitation and study of cells in more natural 3D environments [58].

An important factor besides the composition of the bionanocomposite is the architecture of the whole composite itself. One of the main requirements for making a tissue engineering scaffold is to generate a porous bed with interconnected pores. Thus, methods used to make conventional tissue engineering scaffolds have also been used for generating bionanocomposites as well. These include fiber bonding, phase separation, solvent casting (SC), particle leaching (PL), gas or CO_2 foaming (GF), and emulsification/freeze-drying, which have been employed to generate foamlike bionanocomposites with a suitable porosity and interconnected pores. One of the aims of generating foamlike

bionanocomposites is to control the pore size and direction. Pores sizes ranging from nanomicron scale are desirable for various transport processes and cell attachment. On the other hand, unidirectional pores give, a layered/hierarchical structure similar to natural bionanocomposites such as nacre. One way to obtain unidirectional pores is by freezing the composite-forming mixture in a single direction, thus inducing aligned pores.

The choice of method to design the framework of the bionanocomposite not only influences pore structure and porosity but also influences the bioactivity of the composite on whole. For example, bionanocomposites prepared by combination of SC/PL always invariably have the risk of having residual organic solvent, which might affect cell activity. In a study comparing bionanocomposites, properties formed by either SC/PL and GF/PL showed scaffold made with GF/PL to be mechanically and biologically superior. The compression and tensile moduli of the GF/PL scaffolds increased by 99% and 1331%, respectively, compared with the SC/PL scaffolds [59]. In other works, these have also been formed as fibers by fiber-spinning to form bionanocomposites. Fiber bionanocomposites were reported to have high structural stability and potential to form bone and cartilage tissue ligaments. This is due to the porous nature of fiber scaffolds promoting cellular infiltration, along with strong mechanical properties of fibers. Some other design factors that influence performance of bionanocomposite as scaffolding material or tissue regeneration capabilities are (1) ratio of the nanocomposites to polymer, (2) nanofiller aspect ratio, and (3) structure and organization of the inorganic nanofiller itself [39,47,48]. For example, both size and shape of the nHA have significant influence on mechanical strength and cell response especially osteoblast. It has been shown that nanocomposite coating of nHA and PCL over basic calcium phosphate scaffold was most effective in integrating and increasing mechanical strength and osteoblast differentiation when nanosized needle-shaped HA particles were used compared to micron-sized rod or spherical particles [60].

Lastly, multifunctional high performance tissue regenerating bionanocomposites can be made by simultaneous addition and release of drugs, growth factors, and cytokines. This is a very helpful strategy where the same material provides both the support matrix and cues for differentiation and proliferation. Such strategies have been adopted in nHA–polymer composites for bone tissue regeneration where bone morphogenic protein was immobilized in nHA to regulate osteogenic process [61,62]. In other example, adsorption of iron on the clay was used to make a magnetic bionanocomposite, which was used to enhance osteoblast proliferation and align them on the electrospun fibers [63]. Other examples of such novel applications include inclusion of a morphogenetic protein to promote tissue regeneration in an HA–alginate–collagen system and the addition of a vitamin in a Ca-deficient HA–chitosan nanocomposite. Such customizable composites with multifunctional abilities highlight important tools for development of systems for tendon or bone repair or tissue engineering in general.

13.5 Drug delivery

Drug delivery technology represents one of the broader areas of science, which involves multidisciplinary scientific approach, contributing to human health care. The treatment of acute diseases or chronic illnesses has been achieved by delivery of drugs

to the patients for many years. The traditional methods and routes of drug administration result in a rate of drug uptake that is controlled by the drug properties (solubility, charge, molecular size, etc.) and the characteristics of the site of administration (pH, surface area, presence of enzymes, active transport mechanisms, etc.). The applicability of polymer nanotechnology and nanocomposites to emerging biomedical/biotechnological applications is a rapidly emerging area.

Biocompatibility and nanosized dimensions are very beneficial characteristics for use of some bionanocomposites for drug delivery. An advantage of using the polymer bionanocomposites for drug delivery is that nanocomposites usually present torturous diffusion path for encapsulated small molecule/drug forming effective barrier and sustained delivery with minimal to no burst release [64]. Polymer matrix nanocomposites have been proposed for drug delivery/release applications. The addition of nanoparticles can provide an impediment to drug release allowing slower and more controlled release, and reduced swelling and improved mechanical integrity of hydrogel-based nanocomposites. Several examples of drug delivery using bionanocomposites exist. Like other applications, organic/inorganic nanofillers such as clays and ceramic-based nanofillers can be used. Additionally, silicate nanoparticles [65] and carbon-based nanofillers such as graphene and CNTs [39] have also been considered for controlled drug delivery. CNTs are of particular interest due to their high barrier crossing abilities especially blood–brain barrier; relatively large surface area and hollow core and ability to be functionalized and entrap multifunctional particles inside make them versatile and potential tool for drug delivery [39]. Usually the nanofiller component acts as a drug carrier. The drug loading and release from bionanocomposite has been found to be dependent on the nanofiller chemistry (ionic interactions, intercalation, or hydrogen bonding), amount of nanofiller in the composite, degree of dispersion, and aspect ratio of the particles [66].

Traditionally, clays have long history of use as drug excipients, which help in either formation of stable suspension, emulsion, or drug adsorption and maintenance of stability. Depending on the type of clay/nanofiller and drug type, the drug may adsorb onto the surface of the clay either by ion-exchange or intercalation in the lamellar spaces. The drug loading onto clays can be enhanced and controlled by surface modification of the clays itself using different biopolymers. Biopolymer nanoclay composites offer several advantages such as film forming ability, bioadhesion, and cell uptake [48]. Fibrous (sepiolite, palygorskite) and more popularly layered clays (MMT and laponite) have been used as fillers, which restrict water access (thus controlling drug release) into biopolymers or drug carriers in bionanocomposites. Clay bionanocomposites with chitosan, alginate, and carboxymethyl cellulose (CMC) formed as microspheres via different routes have been used for controlled delivery of beta blockers and different nonsteroidal antiinflammatory drugs [66]. For example, chitosan–palygorskite [48], or alginate–chitosan–clay [67], microspheres were used for controlled delivery of diclofenac. The particles avoided degradation in gastric fluid while slowly degrading and controlling release of diclofenac in the intestinal region [48,67].

Silica-based bionanocomposites made by spray drying as nanospheres have also been used as a drug delivery system. The silica–alginate hybrid nanoparticles were biocompatible and endocytosed by the fibroblast where they were degraded, as potential carriers for targeted drug delivery [65] (Fig. 13.5). In the same context,

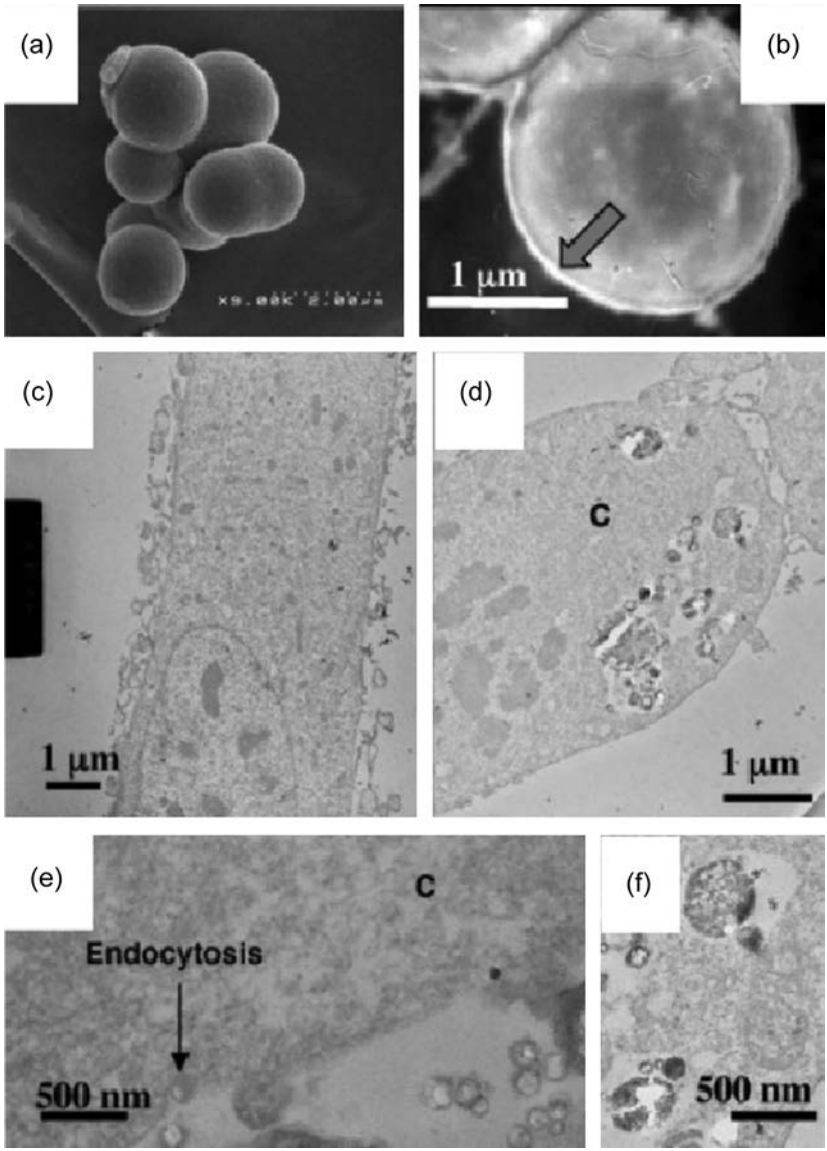

Figure 13.5 Silica–alginate hydrogel bionanocomposite. (a) Scanning electron microscopy and (b) transmission electron microscopy (TEM) images of spray-dried silica–alginate nanocomposites. (c) TEM images of fibroblast cells. (d–f) TEM images of fibroblast cultured in with silica–alginate hydrogel showing endocytosis of nanocomposites by fibroblast cells. Reproduced from I.I. Slowing, B.G. Trewyn, S. Giri, V.S.Y. Lin, Advanced Functional Materials 17 (2007) 1225–1236.

carrageenan–silica aerogels were synthesized by CO_2 supercritical drying method [38,65]. Notably, targeted drug delivery can also be achieved by simultaneous inclusion of the magnetic nanoparticles in the multifunctional and biodegradable bionanocomposites. The drug can then be accumulated and be delivered at the precise target by making use of their superparamagnetic properties and ability to release the transported drug [68].

Injectable drug delivery can also be envisaged for stimuli-responsive polymers and nanoparticle composites. For example, Pluronic, a temperature-sensitive polymer, usually cannot be used for long-term delivery of drugs due to its faster dissolution rate. However, combination of Pluronic with laponite nanoparticles (synthetic layered clay) caused a shift in the Pluronic phase transition temperature made the hydrogel more resistant to dissolution, which considerably extended release of loaded drug [69].

Furthermore, the bionanocomposites have also been used for gene delivery and vaccine delivery [48]. Pioneering work by Choy and colleagues has shown DNA-loaded LDH as efficient nonviral vector for gene therapy. They further confirmed intercalation of DNA in the interlayer space of a magnesium–aluminum LDH by an ion-exchange mechanism, whereby DNA double-helix chains are oriented parallel to the basal plane of the LDH. The bionanocomposites facilitate transport into the cells by shielding the negative charge of DNA, whereby the slightly acidic pH of lysozyme dissolved the LDH and transfer DNA to cell nucleus [70,71]. In other type of hybrid bionanocomposite, DNA biding to nanofillers can be achieved by hydrogen bonding, for example, in clays [48].

For vaccine delivery, the use of inorganic–organic bionanocomposite is very recent and the field is yet to see major developments. Some of the nanofillers, which might be helpful, are iron oxide, calcium phosphate, and LDH [72]. In one example, sepiolite clay surface was modified with xanthan to deliver influenza vaccine. The idea was inspired by the fact that adsorption of influenza on a surface similar to nasal mucosa, natural location of influenza can stabilize it [73]. The formation of stable suspension of this bionanocomposite offers possibility for nasal delivery of vaccine [74] (Fig. 13.6). The bionanocomposite offered high-level seroprotection and increased efficacy of the vaccine attributed to increased irritation of nasal mucous by microfibrous structure of the clay itself [74]. Further developments have shown that bionanocomposite-based vaccine delivery system can also offer thermal stability of vaccines, which is an important consideration for stocking of prepandemic vaccines [75].

13.6 Wound dressings

Bionanocomposite with drug release properties holds great potential as for wound-dressing applications, as they usually have high water uptake and noncytotoxicity together and high mucoadhesivity. Moreover, a wound-dressing material should be robust, highly flexible and elastic, and tear resistance (self-healing) to bear the forces exerted by different body shapes. Many of these requirements are fulfilled by several bionanocomposite discussed above making them ideal biomaterial for wound dressing.

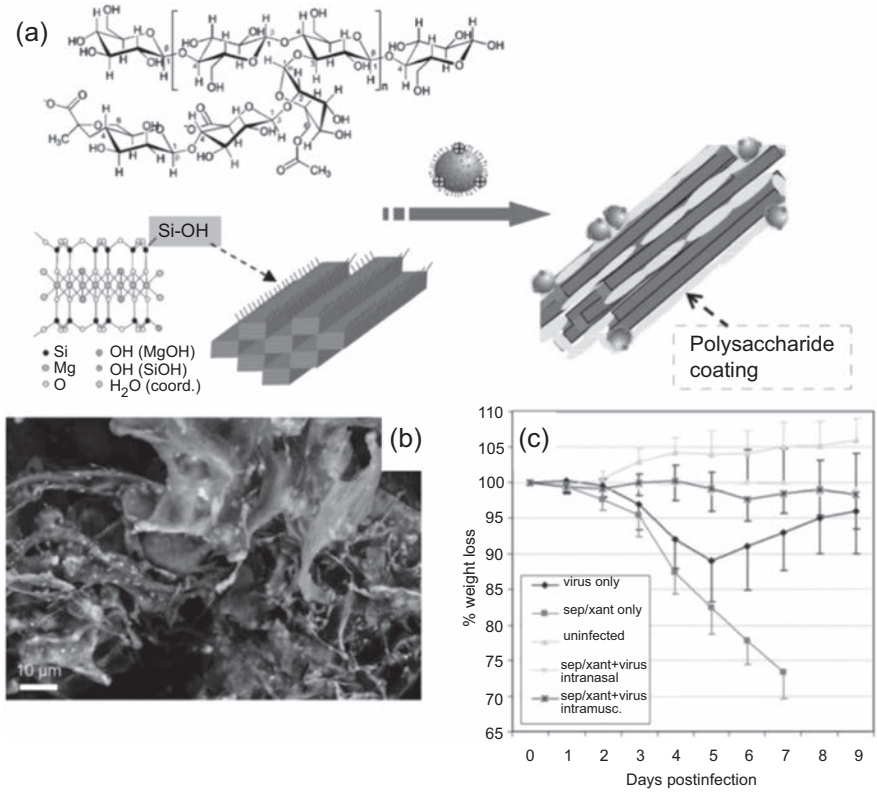

Figure 13.6 (a) Schematic of assembly of virus/bionanocomposite materials: The virus-loaded bionanocomposites are prepared by assembling a negatively charged polysaccharide, such as xanthan, with sepiolite fibers, giving virus/bionanocomposites by anchorage of influenza virus particles. (b) Field emission scanning electron microscopy images at low pressure (c.40 Pa) showing the tissuelike aspect of the biohybrid xanthan–sepiolite material. (c) Changes in body weight after challenge of mice with the influenza virus. Daily monitoring of body weights showed that control mice (both saline and viral particle alone) lost substantial amounts of weight, whereas the virus/bionanocomposite-vaccinated animals maintained their initial weight after the challenge.
Reproduced from E. Ruiz-Hitzky, M. Darder, P. Aranda, M.A.M. del Burgo, G. del Real, Advanced Materials 21 (2009) 4167–4171.

Plethora of metallic, ceramic, and polymeric nanoparticles are being investigated for development wound dressing for accelerated and aesthetic wound healing [76–78]. Much of the interest in development of bionanocomposites for healing and wound-dressing applications stems from the specific properties of nanofillers themselves. Recent developments in effective antimicrobial wound dressing incorporating silver nanoparticles have instigated a deeper quest for development of such composites for enhanced wound healing [79–82].

Similarly, ZnO nanoparticles and chitosan are known for their antimicrobial properties; silicate clays such as MMT have hemostatic properties. Combination of the healing qualities of these nanoparticles with flexible elastic polymer networks constitutes an ideal material for wound dressing [83–85].

Additionally, due to these multifunctional properties, these bionanocomposites are also useful as tissue adhesives, hemostats, and antimicrobial agents.

Silver nanoparticles (AgNPs) deposited by self-assembly on surface of bacterial cellulose were effective as antimicrobial wound-dressing material [86]. In another example, AgNPs were deposited on mussel-inspired poly(dopamine methacrylamide-co-methyl methacrylate, MADO) nanofibers by a one-step electrospinning process [87]. The method allowed uniform deposition of the AgNPs on the polymer surface, while catechol redox chemistry protected AgNPs from oxidation. This endowed the wound dressing with them with long-term antimicrobial activity and sustained release. The ECM-like matrix of the wound dressing combined with antimicrobial properties was effective in healing partial thickness wound much faster in presence of the composite (Fig. 13.7). Similar studies have been reported in combination with other polymers such as PVA, chitosan [88], and electrospun CMC fibers. Although wound dressing with AgNPs is used clinically and no toxic effects have been reported, reducing the required amount of AgNPs and increasing efficacy by means of such bionanocomposites is of therapeutic benefit [89].

Ceramic nanoparticles because of semicrystalline nature and release of ionic products on dissolution have shown enhanced wound healing and angiogenesis. Some ceramic nanomaterials of interest as wound-dressing materials include silica, silicate clays, bioglass, and zinc oxide nanoparticles.

Amine-functionalized silica nanoparticles carrying N-diazeniumdiolate groups were used for nitric oxide (NO) release to facilitate wound healing [90]. Incorporation of the functionalized particles in a PEG and chitosan matrix offered further control NO release. Wounds treated with the NO-releasing composite showed complete wound closure in 12 days, whereas the untreated wounds had delayed wound healing [91]. Moreover, silica nanoparticles can be entrapped in collagen wound dressing to overcome the burst release of drugs from the collagen-only dressings. Additionally, silica nanoparticles increased durability of collagen dressing by decreasing rate of enzymatic degradation of collagen by metalloprotease [92].

Considering the blood clotting ability of aluminosilicate clay, such as MMT, MMT and laponite nanoparticle biopolymer composites have been widely explored for their hemostatic activity. Moreover, being charged particles with both negative and positive charge, these interact strongly with growth factors such as vascular endothelial growth factor (VEGF) delivery, which have been used for enhancing angiogenesis and promoting wound healing [47,93]. Addition of the VEGF-functionalized clay nanoparticles to collagen stabilizes the hydrogel network due to strong physical interactions. Incorporation of VEGF within laponite–collagen gel enhances angiogenesis in vivo and may be useful in promoting wound healing [93]. Moreover, nanosilicate-based hydrogels can also be used as injectable system for accelerated hemostasis by as much as 77% in traumatic injury, which can be due to nanosilicates attracting

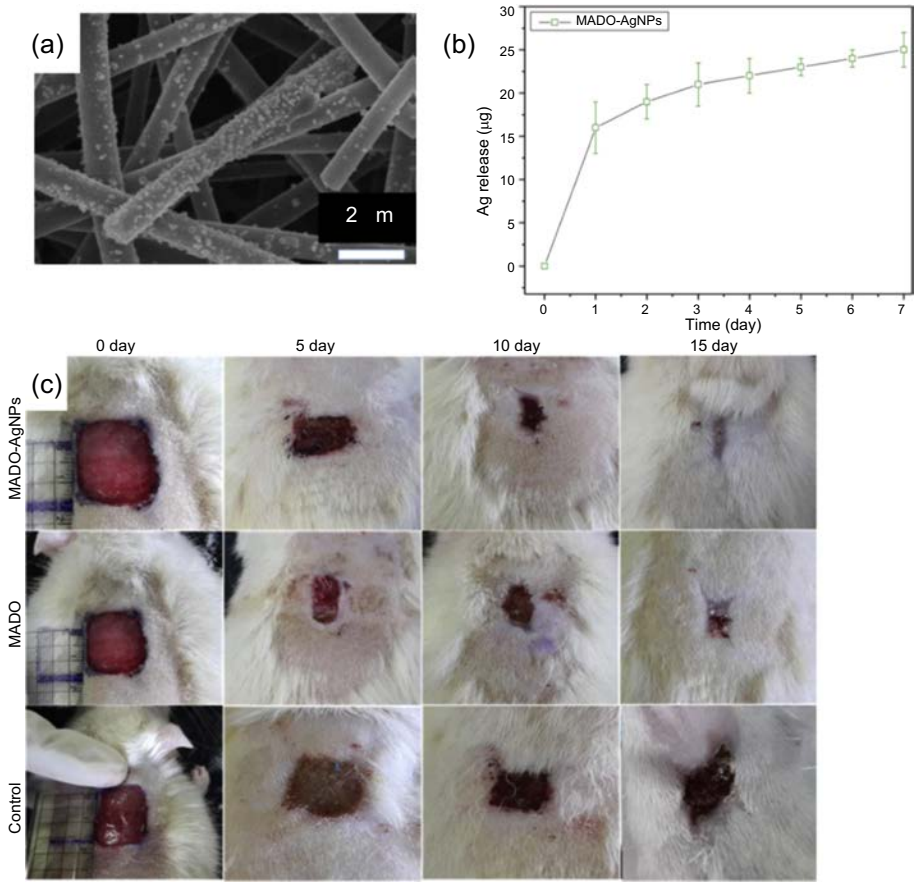

Figure 13.7 (a) Field emission scanning electron microscopy images of electrospun MADO-AgNPs nanofibers. (b) In vitro release profile of Ag from MADO-AgNPs scaffold as a function of time. (c) Wound appearance at 0, 5, 10, and 15 days after grafting with MADO-AgNPs, MADO nanofiber, and bare.
Reproduced from A. GhayamiNejad, A.R. Unnithan, A. Ramachandra, K. Sasikala, M. Samarikhalaj, R.G. Thomas, Y.Y. Jeong, S. Nasseri, P. Murugesan, D.M. Wu, C.H. Park, C.S. Kim, ACS Applied Materials & Interfaces 7 (2015) 12176–12183.

plasma components, to wound site. Similarly, controlled release antimicrobial wound dressing of gelatin–MMT was made by intercalation of ciprofloxacin by electrostatic attraction in layered silicate MMT nanoparticles [94]. Like collagen–clay composites, gelatin degradation rate was also retarded by presence of MMT.

Lastly, combination of bacterial cellulose and MMT resulted in robust and highly swellable bionanocomposites wound-dressing materials. Moreover, sodium, calcium, and copper ions could be loaded by the ion-exchange property of the MMT. Bionanocomposite loaded with Cu-MMT had highest antimicrobial activity against gram-negative *Escherichia coli* and gram-positive *Staphylococcus aureus* [95].

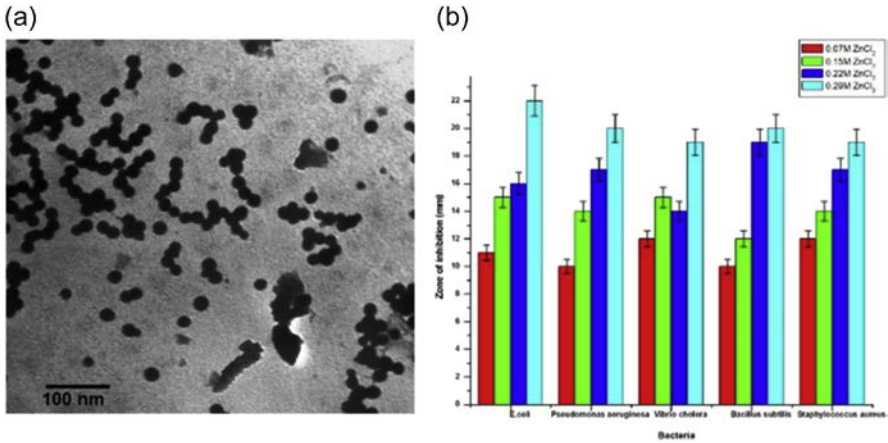

Figure 13.8 Composite of polyvinyl alcohol cryogel with zinc oxide. (a) Transmission electron microscopy images of polyvinyl alcohol (PVA) cryogel–ZnO nanocomposite (PVA = 2 g, $ZnCl_2$ = 0.07 M, freeze–thaw cycle = 5). (b) Bar diagram showing the antibacterial effect of different concentration of zinc chloride on various bacteria (PVA = 2 g, freeze–thaw cycle = 5). Reproduced from A. Chaturvedi, A.K. Bajpai, J. Bajpai, S.K. Singh, Materials Science and Engineering C: Materials for Biological Applications 65 (2016) 408–418.

Similar to AgNPs, zinc oxide nanoparticles (ZnO NPs) possess antimicrobial activities, which are strongly correlated to the size and ability of nanoparticles to release free Zn^{2+} ions from ZnO colloidal solution [96].

ZnO NPs incorporated in chitosan/chitin wound-dressing bandages demonstrated blood clotting ability and antibacterial characteristics [97,98]. Other studies showed that PVA macroporous cryogel prepared by repeated freeze–thaw incorporating of ZnO NPs in cryogel networks showed effective antimicrobial activity against gram-positive and gram-negative bacteria [99] (Fig. 13.8). Although ZnO is FDA approved, research on the safety profile of ZnO needs further investigations when used as nanoparticles [100].

13.7 Biosensors applications

Conjugated polymers with various nanoscale filler inclusions have been investigated for sensor applications including gas sensors, biosensors, and chemical sensors. The nanofillers employed include metal oxide nanowires, CNTs, nanoscale gold, silver, nickel, copper, platinum, and palladium particles [101]. With CNTs, the electrical resistance was found to be significantly changed by exposure to specific gases such as NO_2 and NH_3 [102]. A nanocomposite of single- carbon nanotube (SWCNT)/polypyrrole yielded a gas sensor with sensitivity similar to SWCNT alone [103]. The sensing capability of these nanocomposites can be based on conductivity changes due to gas or chemical interactions with either the nanofiller or the conjugated polymer, pH changes, electrochromic or electrooptical property changes, catalytic

activity, chemiluminescent property, or biological recognition. Examples of sensors for dopamine detection include a poly(anilineboronic acid)/CNT composite [104] and a polyaniline/gold composite hollow sphere system [105].

References

[1] D.H.A. Bowen, in: A. Kelly (Ed.), Concise Encyclopedia of Composite Materials, Elsevier, Oxford, 1994, pp. 7–15.
[2] R.F.A. Haresceugh, in: A. Kelly (Ed.), Concise Encyclopedia of Composite Materials, Elsevier, Oxford, 1994, pp. 1–7.
[3] R.E. Newnham, J.R. Giniewicz, Comprehensive Composite Materials 1 (2000) 431–463.
[4] M. Baibarac, P.J. Gomez-Romero, Nanoscience and Nanotechnology 6 (2006) 1–14.
[5] R.H. Baughman, A.A. Zakhidov, W.A. De Heer, Science 297 (2002) 787–792.
[6] M. Moniruzzaman, K.I. Winey, Macromolecules 39 (2006) 5194–5205.
[7] D.F. Williams, Biodegradation of Medical Polymers, in: D.F. Williams (Ed.), Concise Encyclopedia of Medical and Dental Materials, Pergamon Press and The MIT Press, 1990, pp. 69–74.
[8] M. Donachie, in: J.R. Davis (Ed.), Biomaterials, Metals Handbook Desk Edition, second ed., ASM International, 1998, pp. 702–709.
[9] M. Sun-Hong, J.L. Ferracane, L. In-Bog, Dental Materials 26 (2010) 1024–1033.
[10] A. Peutzfeldt, European Journal of Oral Sciences 105 (1997) 97–116.
[11] S.C. Bayne, H.O. Heymann, E.J. Swift Jr., Journal of the American Dental Association 125 (1994) 687–701.
[12] H. Wolter, W. Glaubitt, K. Rose, Materials Research Society Symposia Proceedings 271 (1992) 719–724.
[13] W. Weinmann, C. Thalacker, R. Guggenberger, Dental Materials: Official Publication of the Academy of Dental Materials 21 (2005) 68–74.
[14] N. Ilie, R. Hickel, Dental Materials Journal 25 (2006) 445–454.
[15] H. Bundela, A.K. Bajpai, Express Polymer Letters 2 (3) (2008) 201–213.
[16] J. Vuong, C. Hellmich, Journal of Theoretical Biology 287 (2011) 115–130.
[17] A. Fritsch, C. Hellmich, L. Dormieux, Journal of Theoretical Biology 260 (2009) 230–252.
[18] J.A. Sowjanya, J. Singh, T. Mohita, S. Sarvanan, A. Moorthi, N. Srinivasan, N. Selvamurugan, Colloids and Surfaces B: Biointerfaces 109 (2013) 294–300.
[19] J. Song, V. Malathong, R. Carolyn, J. Bertozzi, Journal of the American Chemical Society 127 (2005) 3366–3372.
[20] T.W. Bauer, R.C. Geesink, R. Zimmerman, J.T. McMahon, Journal of Bone and Joint Surgery 73-A (1991) 1439–1452.
[21] R.W. Bucholz, Clinical Orthopaedics 395 (2002) 44–52.
[22] J.W. Frame, Journal of Dentistry 3 (1975) 177–187.
[23] K. Kanellakopolou, E.J. Giamarellos–Bour boulis, Drugs 59 (2000) 1223–1232.
[24] M.A.W. Merkx, J.C. Maltha, Oral and Maxillofacial Surgery 32 (2006) 1–6.
[25] C. Chandara, K.A.M. Azizli, Z.A. Ahmad, E. Sakai, Waste Management 29 (2009) 1675–1679.
[26] S.C. Mendes, R.L. Reis, Y.P. Bovell, A.M. Chunna, C.A. Blitterswijk, J.D. Bruijn, Biomaterials 22 (2001) 2057–2064.
[27] X.D. Ma, X.F. Qiam, J. Yin, Z.K. Zhu, Journal of Materials Chemistry 12 (2002) 663–666.

[28] A.K. Bajpai, J. Bajpai, S. Shukla, Reactive and Functional Polymers 50 (2001) 9–21.
[29] H.J. Gao, B.H. Ji, I.L. Jager, E. Arzt, P. Fratzl, Proceedings of the National Academy of Sciences of the United States of America 100 (2003) 5597–5600.
[30] C.J. Wu, A.K. Gaharwar, P.J. Schexnailder, G. Schmidt, Materials 3 (2010) 2986–3005.
[31] N.G. Sahoo, Y.Z. Pan, L. Li, C.B. He, Nanomedicine-UK 8 (2013) 639–653.
[32] P. Fratzl, R. Weinkamer, Progress in Materials Science 52 (2007) 1263–1334.
[33] Z.Y. Tang, N.A. Kotov, S. Magonov, B. Ozturk, Nature Materials 2 (2003) 413–U418.
[34] B.W. Sheldon, W.A. Curtin, Nature Materials 3 (2004) 505–506.
[35] R. Vaia, J. Baur, Science 319 (2008) 420–421.
[36] R.A. Vaia, H.D. Wagner, Materials Today 7 (2004) 32–37.
[37] E. Stodolak-Zych, A. Fraczek-Szczypta, A. Wiechec, M. Blazewicz, Acta Physica Polonica 121 (2012) 518–521.
[38] M. Darder, P. Aranda, E. Ruiz-Hitzky, Advanced Materials 19 (2007) 1309–1319.
[39] R.G. Mendes, A. Bachmatiuk, B. Buchner, G. Cuniberti, M.H. Rummeli, Journal of Materials Chemistry B 1 (2013) 401–428.
[40] C. Aime, T. Coradin, Journal of Polymer Science Part B: Polymer Physics 50 (2012) 669–680.
[41] A. Hoppe, N.S. Guldal, A.R. Boccaccini, Biomaterials 32 (2011) 2757–2774.
[42] A.K. Gaharwar, N.A. Peppas, A. Khademhosseini, Biotechnology and Bioengineering 111 (2014) 441–453.
[43] S.S. Liao, F.Z. Cui, Tissue Engineering 10 (2004) 73–80.
[44] S.S. Liao, F.Z. Cui, W. Zhang, Q.L. Feng, Journal of Biomedical Materials Research – Part B 69b (2004) 158–165.
[45] L. Calandrelli, M. Annunziata, F. Della Ragione, P. Laurienzo, M. Malinconico, A. Oliva, Journal of Materials Science: Materials in Medicine 21 (2010) 2923–2936.
[46] M. Diba, M. Kharaziha, M.H. Fathi, M. Gholipourmalekabadi, A. Samadikuchaksaraei, Composites Science and Technology 72 (2012) 716–723.
[47] J.I. Dawson, R.O.C. Oreffo, Advanced Materials 25 (2013) 4069–4086.
[48] E. Ruiz-Hitzky, M. Darder, F.M. Fernandes, B. Wicklein, A.C.S. Alcantara, P. Aranda, Progress in Polymer Science 38 (2013) 1392–1414.
[49] W. Xu, S. Raychowdhury, D.D. Jiang, H. Retsos, E.P. Giannelis, Small 4 (2008) 662–669.
[50] J.H. Lee, T.G. Park, H.S. Park, D.S. Lee, Y.K. Lee, S.C. Yoon, J.D. Nam, Biomaterials 24 (2003) 2773–2778.
[51] S.S. Ray, K. Yamada, M. Okamoto, K. Ueda, Nano Letters 2 (2002) 1093–1096.
[52] G. Ozkoc, S. Kemaloglu, M. Quaedflieg, Polymer Composites 31 (2010) 674–683.
[53] N. Olmo, M.A. Lizarbe, J.G. Gavilanes, Biomaterials 8 (1987) 67–69.
[54] N. Olmo, A.M. del Pozo, M.A. Lizarbe, J.G. Gavilanes, Collagen and Related Research 5 (1985) 9–16.
[55] A.K. Gaharwar, P. Schexnailder, V. Kaul, O. Akkus, D. Zakharov, S. Seifert, G. Schmidt, Advanced Functional Materials 20 (2010) 429–436.
[56] A.K. Gaharwar, V. Kishore, C. Rivera, W. Bullock, C.J. Wu, O. Akkus, G. Schmidt, Macromolecular Bioscience 12 (2012) 779–793.
[57] P.J. Schexnailder, A.K. Gaharwar, R.L. Bartlett, B.L. Seal, G. Schmidt, Macromolecular Bioscience 10 (2010) 1416–1423.
[58] G.R. Souza, J.R. Molina, R.M. Raphael, M.G. Ozawa, D.J. Stark, C.S. Levin, L.F. Bronk, J.S. Ananta, J. Mandelin, M.M. Georgescu, J.A. Bankson, J.G. Gelovani, T.C. Killian, W. Arap, R. Pasqualini, Nature Nanotechnology 5 (2010) 291–296.
[59] S.S. Kim, M.S. Park, O. Jeon, C.Y. Choi, B.S. Kim, Biomaterials 27 (2006) 1399–1409.
[60] S.I. Roohani-Esfahani, S. Nouri-Khorasani, Z.F. Lu, R. Appleyard, H. Zreiqat, Biomaterials 31 (2010) 5498–5509.

[61] B.J. Jeon, S.Y. Jeong, A.N. Koo, B.C. Kim, Y.S. Hwang, S.C. Lee, Macromolecular Research 20 (2012) 715–724.
[62] Y. Liu, Y. Lu, X.Z. Tian, G. Cui, Y.M. Zhao, Q. Yang, S.L. Yu, G.S. Xing, B.X. Zhang, Biomaterials 30 (2009) 6276–6285.
[63] H.M. Lewkowitz-Shpuntoff, M.C. Wen, A. Singh, N. Brenner, R. Gambino, N. Pernodet, R. Isseroff, M. Rafailovich, J. Sokolov, Biomaterials 30 (2009) 8–18.
[64] S.H. Cypes, W.M. Saltzman, E.P. Giannelis, Journal of Controlled Release 90 (2003) 163–169.
[65] I.I. Slowing, B.G. Trewyn, S. Giri, V.S.Y. Lin, Advanced Functional Materials 17 (2007) 1225–1236.
[66] C. Aguzzi, P. Cerezo, C. Viseras, C. Caramella, Applied Clay Science 36 (2007) 22–36.
[67] Q. Wang, J.P. Zhang, A.Q. Wang, Carbohydrate Polymers 78 (2009) 731–737.
[68] S.T. Tan, J.H. Wendorff, C. Pietzonka, Z.H. Jia, G.Q. Wang, ChemPhysChem 6 (2005) 1461–1465.
[69] C.J. Wu, G. Schmidt, Macromolecular Rapid Communications 30 (2009) 1492–1497.
[70] J.H. Choy, S.Y. Kwak, J.S. Park, Y.J. Jeong, J. Portier, Journal of the American Chemical Society 121 (1999) 1399–1400.
[71] J.H. Choy, S.Y. Kwak, Y.J. Jeong, J.S. Park, Angewandte Chemie International Edition 39 (2000) 4042–4045.
[72] Z.P. Xu, Q.H. Zeng, G.Q. Lu, A.B. Yu, Chemical Engineering Science 61 (2006) 1027–1040.
[73] E. Ruiz-Hitzky, M. Darder, P. Aranda, M.A.M. del Burgo, G. del Real, Advanced Materials 21 (2009) 4167–4171.
[74] J.P. Amorij, W.L.J. Hinrichs, H.W. Frijlink, J.C. Wilschut, A. Huckriede, The Lancet Infectious Diseases 10 (2010) 699–711.
[75] D.T. Brandau, L.S. Jones, C.M. Wiethoff, J. Rexroad, C.R. Middaugh, Journal of Pharmaceutical Sciences 92 (2003) 218–231.
[76] K.A. Rieger, N.P. Birch, J.D. Schiffman, Journal of Materials Chemistry B 1 (2013) 4531–4541.
[77] R.S. Balkawade, D.K. Mills, The FASEB Journal (2012) 26.
[78] I. Kalashnikova, S. Das, S. Seal, Nanomedicine-UK 10 (2015) 2593–2612.
[79] J. Jain, S. Arora, J.M. Rajwade, P. Omray, S. Khandelwal, K.M. Paknikar, Molecular Pharmaceutics 6 (2009) 1388–1401.
[80] T. Maneerung, S. Tokura, R. Rujiravanit, Carbohydrate Polymers 72 (2008) 43–51.
[81] K. Chaloupka, Y. Malam, A.M. Seifalian, Trends in Biotechnology 28 (2010) 580–588.
[82] J.L. Song, N.L. Birbach, J.P. Hinestroza, Cellulose 19 (2012) 411–424.
[83] C.A. Vaiana, M.K. Leonard, L.F. Drummy, K.M. Singh, A. Bubulya, R.A. Vaia, R.R. Naik, M.P. Kadakia, Biomacromolecules 12 (2011) 3139–3146.
[84] X.Q. Li, H.F. Wang, H.L. Rong, W.H. Li, Y. Luo, K. Tian, D.Q. Quan, Y.G. Wang, L. Jiang, Journal of Colloid and Interface Science 445 (2015) 312–319.
[85] C.Y. Chu, F.C. Peng, Y.F. Chiu, H.C. Lee, C.W. Chen, J.C. Wei, J.J. Lin, PLoS One (2012) 7.
[86] J. Wu, Y.D. Zheng, W.H. Song, J.B. Luan, X.X. Wen, Z.G. Wu, X.H. Chen, Q. Wang, S.L. Guo, Carbohydrate Polymers 102 (2014) 762–771.
[87] A. GhayamiNejad, A.R. Unnithan, A. Ramachandra, K. Sasikala, M. Samarikhalaj, R.G. Thomas, Y.Y. Jeong, S. Nasseri, P. Murugesan, D.M. Wu, C.H. Park, C.S. Kim, ACS Applied Materials & Interfaces 7 (2015) 12176–12183.
[88] C.W. Li, R.Q. Fu, C.P. Yu, Z.H. Li, H.Y. Guan, D.Q. Hu, D.H. Zhao, L.C. Lu, International Journal of Nanomedicine 8 (2013) 4131–4145.

[89] M. Walker, D. Parsons, International Wound Journal 11 (2014) 496–504.
[90] J.H. Shin, S.K. Metzger, M.H. Schoenfisch, Journal of the American Chemical Society 129 (2007) 4612–4619.
[91] A.J. Friedman, G. Han, M.S. Navati, M. Chacko, L. Gunther, A. Alfieri, J.M. Friedman, Nitric Oxide-Biology and Chemistry 19 (2008) 12–20.
[92] G.S. Alvarez, C. Helary, A.M. Mebert, X.L. Wang, T. Coradin, M.F. Desimone, Journal of Materials Chemistry B 2 (2014) 4660–4670.
[93] J.I. Dawson, J.M. Kanczler, X.B.B. Yang, G.S. Attard, R.O.C. Oreffo, Advanced Materials 23 (2011) 3304.
[94] B.D. Kevadiya, S. Rajkumar, H.C. Bajaj, S.S. Chettiar, K. Gosai, H. Brahmbhatt, A.S. Bhatt, Y.K. Barvaliya, G.S. Dave, R.K. Kothari, Colloids and Surfaces B: Biointerfaces 122 (2014) 175–183.
[95] M. Ul-Islam, T. Khan, W.A. Khattak, J.K. Park, Cellulose 20 (2013) 589–596.
[96] K.R. Raghupathi, R.T. Koodali, A.C. Manna, Langmuir 27 (2011) 4020–4028.
[97] P.T.S. Kumar, V.K. Lakshmanan, T.V. Anilkumar, C. Ramya, P. Reshmi, A.G. Unnikrishnan, S.V. Nair, R. Jayakumar, ACS Applied Materials & Interfaces 4 (2012) 2618–2629.
[98] P.T.S. Kumar, V.K. Lakshmanan, M. Raj, R. Biswas, T. Hiroshi, S.V. Nair, R. Jayakumar, Pharmaceutical Research-Disorder 30 (2013) 523–537.
[99] A. Chaturvedi, A.K. Bajpai, J. Bajpai, S.K. Singh, Materials Science and Engineering C: Materials for Biological Applications 65 (2016) 408–418.
[100] S.J. Soenen, W.J. Parak, J. Rejman, B. Manshian, Chemical Reviews 115 (2015) 2109–2135.
[101] D.W. Hatchett, M. Josowicz, Chemical Reviews (2008) On web 01/03/2008.
[102] J. Kong, N.R. Franklin, C. Zhou, M.G. Chapline, S. Peng, K. Cho, H. Dai, et al., Science 287 (2000) 622–625.
[103] K.H. An, S.Y. Jeong, H.R. Hwang, Y.H. Lee, Advanced Materials 16 (2004) 1005–1009.
[104] S.R. Ali, Y. Ma, R.R. Parajuli, Y. Balogun, W.Y.C. Lai, H. He, Analytical Chemistry 79 (2007) 2583–2587.
[105] X. Feng, C. Mao, G. Yang, W. Hou, J.J. Zhu, Langmuir 22 (2006) 4384–4389.

This page intentionally left blank

14 Quality- and sustainability-related issues associated with biopolymers for food packaging applications: a comprehensive review

Carlo Ingrao, Valentina Siracusa
University of Catania, Catania, Italy

14.1 Introduction

Packaging has been defined as a socioscientific discipline that operates in society to ensure the delivery of goods to the related ultimate consumers in the best condition intended for their usage [1]. It is also defined as a coordinated system of preparing goods for transport, distribution, storage, retailing, and end use. It can be considered as a means of ensuring safe delivery in sound condition at optimum cost, and a techno-commercial function aimed at optimizing the delivery costs, while maximizing sales and, hence, profits [1].

The packaging sector represents almost 2% of the gross national product in developed countries and, in particular, food packaging is approximately 50% by weight of total packaging sales [1,2]. This is why this chapter was focused just on the use of packages for food applications investigating briefly but exhaustively the related technology, quality, and sustainability issues.

Food packaging lies at the very heart of the modern food industry and can be considered as being characterized by a multidisciplinary nature. In the process of package design and manufacture, technologists are required to bring to their professional duties a wide-ranging background drawn from a multitude of disciplines (i.e., chemistry, physics, food technology, environmental and industrial engineering, economy, and so on) [1]. However, planning a food package is a serious and complicated procedure, because different requirements, sometimes contradictory to each other, should be taken into account [3]. As a matter of fact, food packages play multiple key roles, not just because they contain, protect, and preserve foods in all phases of their distribution chains but also because they report on essential information for their better handling by consumers. In line with the definitions provided at the beginning of this section, packages are designed mainly to maintain the benefits of food processing after the process is complete, thus enabling foods to travel safely for long distances from the production to the marketing sites, and still be wholesome at the consumption time [2]. This well shows why supply chains of unpacked foods would be impossible to

Biodegradable and Biocompatible Polymer Composites. http://dx.doi.org/10.1016/B978-0-08-100970-3.00014-6

be developed because, as stated by Robertson [1], they would be a messy, inefficient, and costly exercise and, additionally, modern consumer marketing would be virtually impossible.

Despite the important functions that a package is required to have, it is generally considered by consumers to be somewhat superfluous and, at worst, a serious waste of resources and an environmental menace. Such should be attributed to those functions being either unknown or not considered in full, so much so that it often happens that, by the time most consumers come into contact with a package, its job is almost over [1]. This emphasizes well on the need to discuss what both the packaging materials and functions are, so that consumers could best understand how to handle not only the food contained but also the package itself, especially at its end of life when the food has been consumed.

14.2 Roles of food packaging

Packaging performs a series of disparate tasks: it protects foods from outside influence and damage; contains them making it possible to easily transport and store them; and communicates with consumers during its service life [1,2,4].

Any package must contain the product to function successfully; otherwise product loss and pollution would be widespread. So it is clear that the containment function of a package makes a huge contribution to protect the environment from the myriad of products that are moved from one place to another on numerous occasions each day in any modern society [1]. In this context, it should be observed that the right planning and manufacturing of a package can generate energy and raw material saving along with less environmental impacts [3]. A positive contribution in this regard is made when packages are designed to reduce food waste (from packing to distribution and sale of foods), thus becoming an important tool to decrease the overall environmental impact associated with a food supply chain [5]. In this regard, Zhang et al. [6] applied Life Cycle Assessment (LCA) to investigate the effects of active packaging systems on the minimization of food losses. They found a breakeven point across diverse impact categories between conventional and active packaging solutions, thus highlighting the need for guidelines for active packaging development striving for a positive eco-profile of the food and packaging system [6].

In contrast, when inadequate conditions and systems of preservation, protection, storage, and transportation of foods occur, major pollution of the environment is caused subsequently, also as a result of the increased amount of food waste [1,2].

A food package is conceived to retard product deterioration; retain the beneficial effects of processing; increase or, at least, maintain the quality and safety of the food contained; and reduce the risk of generating waste by extending the shelf life of foods. When a food is packed, it becomes protected from outside external influences of chemical (i.e., water, water vapor, gases, and odors), biological (i.e., microorganisms and dust), and physical (i.e., shocks, vibrations, and compressive forces) nature [1,2]. Therefore, a food package, especially when it comes to a packaging film, should be designed and manufactured to be lightweight, flexible, and transparent, thus properly

acting as a barrier material against gases and water vapor. A good balance between material, temperature, and thickness should also be created to avoid mass transfer from and to the external environment and, as a result, guarantee a satisfying internal system for food containment, protection, and conservation [7]. Moreover, a food package provides consumers with indications mainly regarding ingredients, nutritional properties, expiry date, brand, and price, as well as with recommendations for food cooking and package disposal. Thus, it is understandable that distinctive or innovative packages may enhance the product image and/or differentiate the food products in the market, thus boosting sales in increasingly competitive societies [2].

Additionally, a food package has other functions that can be considered as "secondary" but, however, are increasingly gaining importance, such traceability and convenience.

According to Marsh and Bugusu [2], traceability has the objective of improving supply management; facilitating trace-back for food safety and quality purposes; and differentiating and marketing foods with subtle or undetectable quality attributes. Thus, food manufacturing companies have realized that packaging can serve, also, as a tool to allow and favor traceability of foods all over their distribution chains and, for this purpose, they have been incorporating unique codes onto the package labels of their food products.

Furthermore, packaging plays a vital role in meeting the increasing demands of consumers for convenience, as modern industrialized societies have brought about tremendous changes in lifestyles and in the ways of handling, preparing, and consuming foods [1]. As a consequence, the packaging industry is called to follow those changes by producing packages that satisfy convenience features such as ease of access, handling, and disposal; product visibility; resealability; and the ability of being heated within microwaves, which is often named as "microwavability." These are the so-called "convenient" packages that promote innovation and sales but, at the same time, may also influence the amount and type of packaging waste requiring disposal, with potentially greater environmental impacts.

14.3 Biodegradable polymers utilized in food packaging: a brief overview

As already mentioned, packaging of foods serves to maintain their quality, freshness, and safety during distribution and storage until consumption, and for this purpose, package design and construction, as well as the selection of packaging materials and technologies, play essential roles. In this regard, it should be noticed that today's food packages often combine several materials to best exploit their main features and functions toward foods. Materials that have traditionally been used in food packaging include glass, metals, paper and paperboards, and plastics [2]. The latter can be considered as one of the most used materials for packaging purposes. Indeed, in 2015, its consumption represented almost 40% of the total European plastic demand, which was equal to 49 Mtons [8]. Plastics are made by polycondensation or polyaddition of monomer: there are two major categories of plastics, namely, thermosets and thermoplastics. The former are polymers that solidify or set irreversibly when heated and

cannot be remolded. They are strong and durable, and for this reason, they are used primarily in automobiles and construction applications. In contrast, thermoplastics are polymers that soften on exposure to heat and return to their original condition at room temperature. These plastics can easily be shaped and molded into various forms and products, thus they are ideal for food packaging purposes [2]. In particular, a wider variety of polymeric resins can be considered for their manufacturing: polyethylene terephthalate (PET), polyvinylchloride (PVC), polyethylene (PE), polypropylene (PP), polystyrene (PS), and polyamide (PA). Indeed, these resins have been increasingly utilized as packaging materials mainly in the light of their good mechanical performances such as tensile and tear strength, good barrier to oxygen, carbon dioxide, anhydride and aroma compounds, and heat sealability [9]. Additionally, they are largely available at relatively low costs and present several desired features such as softness, lightness, and transparency [9], which facilitate and favor their usage and handling. However, these polymers are produced from crude oil and other fossil fuels, such as natural gas and coal, because of their chemistry lending itself to the readily accessible constituents of those fuels. In this regard, it should be highlighted that, in agreement with Colwill et al. [10] and Ingrao et al. [11], resource depletion is not the only one problem to be faced when dealing with synthetic plastic production, as the emission of carbon dioxide (CO_2) from fossil fuel combustion should be considered too. As a matter of fact, CO_2 is a major contributor to global warming (GW) and could have potentially devastating social, economic, and environmental consequences in the future, if not duly addressed [10]. In addition, the massive consumption of polymeric materials is accompanied by a consistent generation of wastes that cause several environmental pollution problems. According to Eurostat [12], 15.24 Mtons of plastic packaging waste was generated in 2014. Plastics are mainly produced for durable scopes and, therefore, can persist undegraded for decades in the environment where they are disposed of. With regard to this point, Blanco et al. [13,14] documented that their end life prediction and, hence, their persistence in the environment go well beyond the predictable one. In particular, the marine litter issue is increasingly raising great environmental concern because it is harmful to ocean ecosystems, wildlife, and humans. Besides cigarette residues, food wrappers and containers, plastic bags, beverage plastic bottles, and plastic cutlery are the most important sources of debris [8]. In this regard, a recent study from Jambeck et al. [15] indicated that, only in 2010, 4.8–12.7 Mtons of plastics ended up in the oceans. In addition, as discussed in Siracusa et al. [9], during their service, life packaging materials are often so contaminated by foodstuff and biological substances that recycling is impracticable or, most of the times, economically nonconvenient. Consequently, several tons of plastic-based materials and goods are incinerated or land filled, increasing every year the problem of municipal waste disposal. In this regard, Michaud et al. [16] investigated the plastic waste management sector and considered a group of selected environmental impact indicators. They concluded that, where feasible, mechanical recycling is the most environmentally sustainable option as it performs best in almost all of those indicators. For contrast, incineration (with energy recovery) can be considered as the intermediary option, and landfill is confirmed as having the worst environmental performance.

Such concerns emphasize on the need for alternatives to fossil fuel–based products and processes: as a matter of fact, the continuous search for more environmentally sustainable solutions has been receiving the attention of a broad research community at the global level [11,17]. In this context, the concept of eco-friendly materials has been accepted by several countries worldwide, and indeed, new advanced materials are under constant development and improvement [11]. For instance, biopolymers with their biodegradability, eco-friendly manufacturing processes, and vast range of types and applications can be considered as quite valid to replace the traditional, synthetic polymers on an equal function and quality basis [11,18]. For this reason, the development of biopolymers has occurred largely in response to the growing concerns regarding the sustainability of conventional polymers and the environmental pollution caused by plastic packaging waste treatment. In this regard, this chapter was designed to discuss, briefly but exhaustively, about the quality- and sustainability-related issues of biopolymers, thereby exploring their feasibility of usage for food packaging purposes. Biopolymers can be considered to be mainly a solution to waste disposal problems associated with synthetic plastics and represent a loosely defined family of polymers that are designed to degrade through a series of actions performed by living organisms. Additionally, they offer a possible alternative to traditional nonbiodegradable polymers where, mainly due to food contamination, recycling can neither be pursued nor is economically convenient [8,11,19]. This is the instance case of trays made out of expanded PS and generally used for packaging of fresh foods such as meat. According to Ingrao et al. [20], such trays act as a sponge because, for marketing and aesthetic reasons, they are conceived also to absorb the blood released by the fresh meat contained. As a consequence, they get contaminated with a variety of microorganisms that make them suitable not for being recycled but disposed off in sanitary landfills, as municipal solid wastes (MSWs). If those trays were constituted by expanded poly(lactic acid) (PLA), or other suitable biopolymers, they could be composted along with the MSW organic fraction and other biomasses. In this way, the contamination due to the prolonged contact with the fresh meat content would no longer be a problem [11]. Biodegradability is, in fact, one of the main reasons for the interest in bio-based polymers: it is a functional requirement and, at the same time, answers to the need and urgency of environmental sound disposal scenarios [9,11]. In addition, the compostability attribute is important and required for biopolymer-based packaging products, so that they can be disposed of in compost plants and processed into compost matrixes to be utilized, in turn, as fertilizers or soil conditioners [9], with several environmental benefits that would occur subsequently. Moreover, in the course of the years it has been documented that production of biopolymers, especially of second generation, is less energy demanding and greenhouse gas (GHG) emitting than that of synthetic polymers [11].

All that stated, biopolymers could be considered valid alternative materials to those produced from fossil resources and it is quite so in nearly every function, from packaging and single use to durable products. As a matter of fact, they are gaining increasingly larger shares of the global market, thus replacing synthetic polymers in a wide range of applications, from packaging to medical, automotive, and many more [21].

14.3.1 Polylactic acid: one of the most widespread biopolymers for packaging applications

Biodegradable polymers can be derived from natural resources, such as PLA, or partially made from renewable and synthesized resources, as it happens for bio-based PET [22]. There exist three main categories of biodegradable polymers that were clearly highlighted in Siracusa et al. [9]:

1. *Natural biodegradable polymers*: These are derived from natural raw materials and renewable resources, such as polysaccharides (from starch and cellulose, lignin), proteins (gelatin, casein, wool, silk), and lipids (fats and oil), and can be either naturally or synthetically produced.
2. *Polymers of PHA's family*: These are obtained from microbiologically produced materials or genetically modified bacteria such as poly(hydroxybutyrate), poly(hydroxyvalerate), polyhydroxyhexanoate, and poly(hydroxyalkanoates) (PHAs).
3. *Synthetic biodegradable polymers*: These are obtained by chemical polymerization of biomonomers such as PLA, polycaprolactone, polybutylene succinate, polybutylene succinate adipate, aliphatic–aromatic copolyesters, polybutylene adipate/terephthalate, and polymethylene adipate/terephthalate.

One of the most promising biopolymers is PLA, which belongs to the first category of biopolymers and, as is known, is a linear, aliphatic polyester that is synthesized from hydroxycarboxylic acid, as the starting lactic acid (LA) monomer [1,11]. The latter is of great interest due to its versatility of applications in the food, pharmaceutical, textile, leather, and chemical industries [11]. PLA can exist in three stereochemical forms that are poly(L-lactide) (PLLA), poly(D-lactide) (PDLA), and poly(DL-lactide) (meso-lactide) [4,11].

To date, there exist two methods for LA production at the industrial level, namely, chemical synthesis and microbial fermentation [23]. The former is principally based on the hydrolysis of lactonitrile by strong acids, thus giving rise to the racemic mixture of D- and L-LA [11], which, however, does not guarantee the best crystalline melting point for PLA production [23]. For this reason, PLA processability can be improved based on melting point depression by randomly incorporating small amounts of lactide enantiomers of opposite configuration into the polymer [23].

There exist other synthesis technologies and strategies such as the catalyzed degradation of sugars; the oxidation of propylene glycol; the reaction of acetaldehyde, carbon monoxide, and water at high temperature and pressure conditions; the hydrolysis of chloropropionic acid; and the nitric acid oxidation of propylene [11]. The majority of them use by-products from other industries, which, overall, contributes to making the chemical process both economically and environmentally expensive, especially where petroleum-based raw materials are the major contributors.

Therefore, to use renewable resources instead of the chemical ones and obtain economic and environmental sound monomers, the microbial fermentative production of LA is increasingly gaining interest and attention. The carbon sources utilizable for this purpose should be cheap and characterized by rapid production rate; high yield; little or no by-product formation; little or no pretreatment required for their fermentation; and year-round availability [23]. They could be sugar in pure form (i.e., glucose,

sucrose, and lactose) or sugar-containing crops such as whey, maize, sugarcane and cassava bagasse, potato, wheat, tapioca, and so on [11].

LA fermentation offers advantages in terms of the usage of renewable carbohydrate biomasses, low production temperature, low energy consumption, and the production of optically high pure LA by selecting an appropriate strain of microorganisms. The conditions for LA production through microbial fermentation depend on several factors such as suitable production strains; carbon source; cell recycling and immobilization; pH; and avoided contaminations [23].

In their study, Juodeikiene et al. [23] documented about the sustainability metrics that are needed to be accounted for identification and development of a cost-effective and sustainable viable processes for LA production, namely, material efficiency; total energy efficiency; economic added value; and land use. They compared the microbial approach to the chemical one, and documented that biotechnological process for wheat biomass conversion into LA gives higher energy efficiency by 47% than that of the chemical route, and lower costs for production by almost 17%. Moreover, the mass efficiency of the fermentation process resulted as 36% lower than the chemical one and lower amount of waste is produced in the case of bio-based rather than chemical LA. This is one of the main reasons why the majority of the big LA production industries have switched to a fermentation-based technology [23], and the biotechnological process is increasingly stimulating research, development, and innovation at the global level. To further restrain the input material production burdens of both economic and environmental nature, by-products and residues from agriculture and the food industry could be used as valid alternatives to dedicated starchy biomass in LA fermentation [11]. This could be the case of using wastes and/or wastewaters outlet from the starchy food industries, as highlighted by Ingrao et al. [8] in the conclusions and future perspectives of their paper.

LA is highly demanded for industrial application due to the growth that PLA bioplastics market is increasingly recording [23]. Such should be attributed, in turn, to PLA being a versatile polymer, recyclable and compostable, with high transparency, high molecular weight, good processability, and resistance to water solubility [9]. For these reasons, it has shown the highest commercial potential and is now produced on a comparatively large scale for lots of applications [1]. Along with commercialization, a large number of papers dealing with PLA have been published in the scientific literature over the years, including a number of reviews, such as Auras et al. [24], Avérous [25], and Jamshidian et al. [26], and a book entirely devoted to PLA [27]. The reader is referred to all of them for further details on this polymer.

PLA achieved its first commercial success in medical applications such as resorbable sutures, orthopedic implants, and controlled drug release [23,24]. Thereafter, it has been widely studied for usage in medical applications because of its bioresorbability and biocompatible properties in the human body. Because PLA manufacturing processes have been lowering its production costs, PLA has been finding use in different applications: for instance, low polymerization degree PLA was used in large-scale agricultural systems to help in controlled-release or degradable mulch films [23]. In addition, as a consequence of the production cost reduction, in the last 10–15 years, PLA has been increasingly implied as a packaging material all across

Europe, Japan, and the United States, mainly in the area of fresh food products such as meats and cured meats, cheese, fruits, and vegetable [24,27]. PLA production has grown annually and currently it is estimated that worldwide production will reach at least 800 ktons by 2020 with Japan and the United States, the two major producers [28]. Medical studies have indeed documented that the level of LA migrating to food from packages is much lower than the amount of LA in common food ingredients, thus concluding about the applicability of LA-derived polymers as packaging materials [24]. The most used forms of PLA-based packaging systems that are currently available on the market are foil bags, wraps, bags and trays, drinking and salad cups, as well as beverage bottles [11]. Nevertheless, when PLA is intended to be used in 100% replacement of petroleum-based thermoplastics, some problems could occur. For instance, for food packaging applications where high gas and barrier protection properties are required, replacement of PLA is not practicable, as its brittleness could be an obstacle. In this and other cases where PLA cannot be used in alternative to synthetic conventional polymers, PLA modification and blending with other polymers, also using nanocomposite-based coatings for improved barrier effect, could be considered, thus obtaining high-performance biodegradable polymers [4]. In a previous study, El-Hadi [29] showed that improvements can be made to make PLLA suitable for packaging purpose, by developing polymeric blends based on PLLA and poly((R)-3-hydroxybutyrate) (PHB), together with tributyl citrate (TBC) as a plasticizer. In contrast, Claro et al. [30] developed flexible PLA/acetate and PLA/chitosan films with improved thermal and mechanical properties without the addition of a plasticizer and additive to yield extruder compositions with melt temperatures above those of acetate and chitosan. Based on the findings of the study, PLA/acetate films showed an increase of 30°C in initial degradation temperature and an increase of 3.9% in elongation at break, whereas PLA/chitosan films showed improvements in mechanical properties as an increase of 4.7% in elongation at break, thus presenting the greatest increase in elongation at break and proving itself to be the best candidate for food packaging applications.

In addition, to optimize PLA properties, organomodified montmorilonites have been extensively used to obtain nanocomposites. Although the subject literature is full of studies dealing with PLA nanocomposites, there is still few information about the influence of organoclays on the biodegradation process, which is relevant to know, because one of the main purposes related to the final disposal of biopolymers as PLA is composting [31]. In this context, in their review paper, Souza et al. [31] documented that food quality and safety, as well as the effect to human health and the environment, are relevant issues to be considered in the field of PLA nanocomposites being made from organoclays.

All that stated, it can be concluded that research is more and more required to enhance the quality and performance of this material, thereby optimizing and favoring its usage in the food packaging sector and thus expanding the application range. Effort is still required to be directed toward PLA development to make it an acceptable and effective option to the more traditional petroleum-based polymers [32]. Thus far, numerous studies have been focused on further understanding and improving the physical, chemical, and mechanical properties of PLA and derived polymers. Others

have been developed to investigate and improve the compatibility of such materials for food packaging applications not only in human health and safety terms, as done in several medical studies, but also in terms of food losses. This latter aspect has repercussions in the environmental sphere as those losses need to be managed and treated with several environmental impacts and economic costs, even of high magnitude. Therefore, economic and environmental studies are, overall, desirable for identification and communication of more sustainable ways of package production, use, and disposal.

14.4 Packaging, sustainability, and the use of life cycle assessment

During the last decades, sustainable development has been one of the most popular and universal concerns; in another hand, the issue that future generations will be able to experience the same standards of living and opportunities for growth has been attracting much attention [20,33]. The industry is increasingly realizing that the environmental impacts that their products have on the environment do not start and end with the manufacture of a product, as they start with the design and end at the ultimate disposal of the product after its service life [3]. In this context, the environmental impacts caused by the packaging industry have been raising serious concerns [34] as well as the attention from the scientific community at the international level. In particular, to perform the functions that have been discussed thus far in this chapter, a package causes several environmental impacts in almost all phases of its life cycles, mainly due to the exploitation of natural and primary energy resources as well as the emissions of gases impacting on climate change, human health, and ecosystem quality [20,35]. Thus, to obtain packages with environmentally sustainable properties, application of Life Cycle Thinking (LCT) to their design is essential. As a consequence, the design of a product should be performed to evaluate and mitigate the technological, environmental, and economic repercussions that the manufacturing of a product has on the next phases of utilization and end of life. In this context, LCA is acknowledged worldwide to be a valid tool for this purpose: it substantiates the LCT approach by a clear and structured methodology, which is ruled by the International Standards 14040 and 14044 [36,37]. It is a systematic tool that enables identification and quantification of the environmental impacts associated with a product in its life cycle [20], considering several indicators such as GW, nonrenewable energy, respiratory inorganic matter, acidification, and eutrophication. Preparation of both raw and auxiliary materials from resource extraction, transportation, product manufacture, end use, and ultimate disposal is generally accounted in LCAs [38].

LCA is carried out through the following four phases according to the aforementioned standards: Goal and Scope Definition; Life Cycle Inventory (LCI); Life Cycle Impact Assessment (LCIA); and Life Cycle Interpretation.

The first phase describes the purpose and background of the study and reports on information about the reasons the study has been conducted based on the

background itself. In this LCA elaboration phase, the Functional Unit (FU) and the system boundaries are defined. The FU is a key element and represents the unit of product that is going to be studied and compared, and provides a reference to which the inputs and outputs can be related [1]. The system boundaries include all the resources, materials, energies, and processes and stages through which the system is developed and modeled. It can also be asserted that the system boundaries include all the unit operations which the system is generally broken down to facilitate its modeling and the development of the next phases of LCI and LCIA. Both the FU and the system boundaries should be defined to be consistent with the aim and scope of the LCA, which is intended to be developed, and best represent the system under investigation.

After this phase is concluded, the LCI is carried out. It involves the compilation and quantification of both inputs and outputs and comprises data collection and calculation, which is acknowledged worldwide to be the most consuming part in LCA. The inputs are represented by the resources, materials, and energies implied by the system investigated, whereas the outputs are the material emissions in air, water and soil, as well as the exploitation of natural and primary energy resources. The quality aspect of the data is crucial, and in an ideal world, all the data required would be obtained from the correct sources. In practice, this is seldom possible and, therefore, generic data have to be used, at least for part of the LCI [1]. Specific data that are collected on site (primary data) are, indeed, combined with background data that are extrapolated from databases of acknowledged scientific value and relevance and, if needed, properly adjusted. Among those databases, Ecoinvent accommodates most of the background materials and processes often required in LCA case studies [39]. Anyway, difficulties are sometimes experienced in obtaining quality data for each individual unit operation [1], especially when several manufacturing companies (also from different countries) are involved.

The LCI results are then used for development of the LCIA phase. The latter is indeed carried out aggregating in a limited set of Impact Categories (ICs) all the output flows quantified in the LCI phase [40]. This is done based on the midpoint approach using predetermined classification and characterization schemes and factors. Then, the ICs can be grouped into Damage Categories (DCs), namely, environmental compartments suffering the damage caused by the product in its life cycle, thus extending the assessment to the endpoint approach. In particular, the latter provides that the phases of "normalization" and "weighing" are included in the assessment coming after the midpoint phases, namely, the "classification" and "characterization."

In particular, the midpoint approach is generally used to quantify the LCIA results in the form of specific characterization values represented by equivalent indicators such as $kgCO_{2eq}$ for "Global Warming," $kgPM_{2.5\cdot eq}$ for "Respiratory Inorganics," and $kgC_2H_3Cl_{eq}$ for "Carcinogens."

As regards the endpoint approach, the "weighing" results are estimated by means of equivalent numerical parameters expressed as "weighing points" or "damage points" or "eco-points" or, more simply, "points." This makes it possible to represent quantitatively the environmental impacts associated not only with the system investigated but also with all the included materials and processes, so as to highlight the most

impacting ones [8]. In particular, the weighing points can be obtained multiplying the dimensionless results from the "normalization" phase by a given weighing factor.

For greater understanding, it should be observed that both LCI and LCIA are generally carried out using specific software and calculation tools where inventory databases and the various steps and factors for the environmental impact assessment are implemented and available.

Results from the LCI and LCIA are combined together and reported to give a complete and unbiased account of the study. This is done in the last LCA elaboration phase, namely, the Interpretation, to support reaching conclusions and recommendations in accordance with the defined goal and scope of the study. As clearly stated by Robertson [1], the Life Cycle Interpretation comprises three main elements:

- identification of the significant issues based on the results of the LCI and LCIA phases;
- evaluation of results, which considers completeness, sensitivity, and consistency checks; and
- conclusions and recommendations for reducing material use and environmental burdens.

According to Jeswani et al. [41], LCA has evolved significantly over the past decades, thanks to the valuable work carried out by several research groups worldwide.

As stated by Robertson [1], it has emerged as a valuable decision support tool for both policy makers and company owners in assessing the cradle-to-grave impacts of a product or process, as a consequence of the following:

- *government regulations*, which are moving in the direction of life cycle accountability and the concept that a manufacturer is responsible not only for direct production impacts but also for impacts associated with product inputs, use, transport, and disposal;
- *business*, which is participating in voluntary initiatives that contain LCA and product stewardship components; and
- *environmental preferability*, which has emerged as a criterion in both consumer markets and government procurement guidelines. Together these developments have placed LCA in a central role as a tool for identifying cradle-to-grave impacts both of products and the materials from which they are made.

Over the years, LCA has been applied to investigate a huge number of sectors such as automotive, buildings and construction, energy, electronics, agriculture, food production and packaging, and so many others [20,42]. In the packaging sector, LCA can be applied to determine the environmental impacts that a package generates on- and off-site, namely, those associated not only with the manufacturing process but also with the phases of transport, use, and disposal [3]. In this regard, it can be used to identify package production solutions that minimize those impacts, thus contributing to production of more eco-friendly packaging products [20]. If one considers that in Europe-27 almost 82 Mtons of packaging waste were generated in 2014, as the most up-to-date data based on Eurostat [12], it is clear that waste prevention and management solutions and strategies are urgent to be implemented. In this regard, LCA can help to highlight that a reduction of the amount of raw material utilized for production of a package (without compromising its functions) allows for reduced impacts not only in the package preparation phase but also in the phases of package handling and transport, and disposal. This emphasizes well on the economic and environmentally unsustainability of overdesigned and oversized

packages. In particular, if the material utilized in addition to the specific standards does not enhance the functions and performances of a package toward the food content, it becomes useless and can be avoided, thus avoiding the environmental impacts associated with its whole life cycle. Such was documented by Siracusa et al. [43] in their paper regarding application of LCA to bilayer film bags for vacuum food packaging applications.

Additionally, LCA can be used to compare packaging waste treatment scenarios to find the most environmentally sustainable option. With regard to this point, Cosate de Andrade et al. [44] investigated three different treatment scenarios for PLA disposal and, in particular, focused on mechanical recycling, chemical recycling, and composting. In their study, the authors documented that mechanical recycling presented the lowest environmental impact, followed by chemical recycling and composting. In a previous study, Rossi et al. [45] compared the life cycle GHG and environmental impacts of six end-of-life options of two biodegradable materials, PLA and thermoplastic starch (TPS), used for dry packaging. Yano et al. [46] compared different waste treatment scenarios for household plastic containers and quantified the GHG emissions reduction achievable by replacement of fossil-derived materials with bio-based materials. These were made of 100% PLA, and PLA combined with polybutylene succinate adipate, alternatively. In agreement with Cosate de Andrade et al. [44], Rossi et al. [45] and Yano et al. [46] showed that separate waste collection and mechanical recycling are the most favorable options and thus should be promoted. In particular, Yano et al. [46] highlighted that replacement of fossil-derived materials with biomass-based materials could reduce life cycle GHG emissions by 14%–20%. Not to mention that if the separate collection ratio ideally reached 100%, replacement with biomass-based materials could potentially reduce GHG emissions by almost 32%. Additionally, as is known, industrial composting generates environmental gains for the use of the compost matrixes as fertilizers or soil conditioners. However, as documented by Rossi et al. [45], industrial composting causes high environmental impacts that make it the worst disposal scenario for a biopolymer-based package. This should be attributed not only to the consumption of operational energies and fuels associated with the compost plant management, but also to the emission of biogenic methane that comes from the organic matter decomposition and significantly impacts on the "climate change" DC [8,11].

Toniolo et al. [47] investigated the environmental effects of different disposal scenarios on the environmental impacts of packaging systems produced from recycling postconsumer bottles made of PET. The study allowed the authors to document and stress on the importance of using, where possible, recycled materials for reduced environmental impacts in the life cycles of packages. For what concerns to this issue, in their LCA, Siracusa et al. [43] showed that using 25% PA granule is a great opportunity for environmental improvement in the production of the aforementioned multilayer polymer bags.

Finally, LCA can be used as a tool for comparative assessments of various alternative packaging materials, to identify those with the lowest environmental impact. See, just by way of example, the work done by Ingrao et al. [8,11] that performed both Carbon Footprint and LCA to compare the use of expanded PS and PLA for

production of fresh-food packaging trays. Along time, several other papers have been conducted in the field and have greatly enriched the subject literature and knowledge. For consistency with the aim and scope of this chapter, those regarding investigation of PLA-based package supply chains were discussed in the review section below.

14.5 Applications of life cycle assessment and related tools in the supply chains of packages made out of polylactic acid: a comprehensive review

This section was dedicated to overview research papers regarding assessment of the environmental impacts associated with food packages, with particular regard to those made out of PLA. The literature review was performed focusing just on peer-reviewed papers from international journals of acknowledged scientific relevance, in which they were considered by the authors as recipient of the majority of the studies conducted in the field. Several studies were detected not only for comparison between natural and synthetic materials but also for investigating improvements and innovations in the usage of biodegradable polymers. For instance, Bohlmann [48] performed LCI and GW assessment with cradle-to-grave approach to compare PLA to PP in food packaging applications. Vidal et al. [49] assessed the environmental impacts of new biodegradable multilayer films made out of modified starch and PLA and those of conventional multilayer film based on PP and PA6. In another study, Hermann et al. [50] compared bio-based materials (paper, PLA, bio-based polyethylene, and a bio-based polyester) as well as conventional ones (polypropylene, polyethylene) usable for manufacturing of moisture-sensitive food packages. In addition, Dobon et al. [51,52] performed socioeconomic and environmental evaluations of a flexible best-before-date communicative device on a packaging consumer unit consisting of a nanoclay-based PLA tray filled with pork chops. Later, Gironi and Piemonte [53] and Papong et al. [54] investigated the field of drinking-water bottles exploring through application of LCA the use of PLA rather than PS in the production phase. In the field of trays and similar packages, Madival et al. [42] performed LCA to investigate the supply chain of thermoformed clamshells for packing of fresh strawberries comparing PLA to PET and PS. In addition, Roes and Patel [55] compared a sugarcane bagasse food tray to food trays made out of PET, PLA, and molded pulp, alternatively. Likewise, Suwanmanee et al. [56] perform LCA to highlight environmental impacts of single use boxes for food packaging comparing petroleum-based (PS) to biodegradable polymers (PLA and PLA/starch). Furthermore, Fernández et al. [57] presented a multicriteria optimization methodology for injection molding food package considering both synthetic and biodegradable polymers. The authors concluded that PLA would be the preferred option on an environmental criteria basis and, in contrast, PET is more economically competitive. Therefore, in agreement with the authors, it is clear that the final choice on which polymer to consider for usage is strictly dependent on which decisive factor is preferred and chosen.

Finally, as part of a research aimed at investigating the usage of biopolymers for food packaging applications, Ingrao et al. [8,11] documented that, in production terms, PLA is slightly less environmentally impacting than PS. However, its supply chain still represents a problem in that the cultivation of the starchy crops generally used for its production are often performed in countries (i.e., the Americas) being far away from the majority of the processing plants. As a result, the PLA granule delivery phase involves long distances and different transport means and subsequently causes significant impacts in terms of nonrenewable energy resource exploitation and GHG emission. This emphasizes on the importance of the transport and logistics system to be considered and, at the same time, on the need to search for alternative ways of PLA granule production that avoid involving those large pieces of land for cultivation.

14.6 Conclusions

The increasing consideration of natural resources and energy conservation has recently renewed the interest on bio-based materials and, in particular, on new ecologically friendly materials based on renewable natural resources. In this regard, biopolymers with their biodegradability, eco-friendly manufacturing processes could be considered as quite valid to replace the traditional, synthetic polymers in several applications including food packaging. Among them, PLA is a highly versatile polymer that is suitable for food packaging applications, especially where the package, mainly due to the prolonged contact with the food contained, cannot be recycled at the end of its service life. It is produced from LA through fermentation of the biomass and biomass residual streams outlet from agriculture and food industry, thereby making PLA-based products 100% recyclable and compostable after their disposal. The physical and mechanical properties of PLA can be manipulated through the polymer architecture. In this regard, it has been documented and highlighted in the subject literature that PLA can be blended with other polymers to improve its functions and performances toward the food content, thus enlarging its range of applications.

Production of PLA is characterized by CO_2 sequestration and energy savings, which makes it be acknowledged worldwide as an environmentally sustainable material. However, its supply chain still represents a problem as the cultivation of the starchy crops generally used for its production is often performed in countries (i.e., the Americas) being far away from the majority of the processing plants. Therefore, the PLA granule delivery phase is one of the most environmentally impacting in its whole life cycle as it involves long distances to be traveled and different types of means to be used. Additionally, this aspect contributes to making PLA and, more generally, biopolymers still more expensive compared to the fossil fuel-based ones. For this reasons, the authors of this chapter believe that the feasibility of using first-generation biopolymers should be reconsidered, and more globally sustainable options of materials and technologies should be developed. In this regard, innovation is important to be made for enhanced environmental sustainability and economic convenience of biopolymers, thus making it more competitive in the global market.

References

[1] G.L. Robertson, in: Food Packaging – Principles and Practice, third ed., Taylor & Francis Group LLC, Boca Raton, 2013 (Chapters 1, 2 and 23).

[2] K. Marsh, B. Bugusu, Food packaging – roles, materials and environmental issues, Journal of Food Science 72 (3) (2007) 39–55.

[3] A. Zabaniotou, E. Kassidi, Life cycle assessment applied to egg packaging made from polystyrene and recycled paper, Journal of Cleaner Production 11 (2003) 549–559.

[4] V. Siracusa, C. Ingrao, The use of polylactic acid in food packaging, in: Reference Module in Food Science, Elsevier, Amsterdam, 2016, pp. 1–5.

[5] H. Williams, F. Wikström, Environmental impact of packaging and food losses in a life-cycle perspective: a comparative analysis of five food items, Journal of Cleaner Production 19 (2011) 43–48.

[6] H. Zhang, M. Hortal, A. Dobon, J.M. Bermundez, M. Lara-Lledo, The effect of active packaging on minimizing food losses: life cycle assessment (LCA) of essential oil component-enabled packaging for fresh Beef, Packaging Technology and Science 28 (9) (2015) 761–774.

[7] V. Siracusa, C. Ingrao, Correlation amongst gas barrier behaviour, temperature and thickness in BOPP films for food packaging usage: a lab-scale testing experience, Polymer Testing 59 (2017) 277–289.

[8] C. Ingrao, M. Gigli, V. Siracusa, An attributional life cycle assessment application experience to highlight environmental hotspots in the production of foamy polylactic acid trays for fresh-food packaging usage, Journal of Cleaner Production 150 (2017) 93–103.

[9] V. Siracusa, P. Rocculi, S. Romani, M. Dalla Rosa, Biodegradable polymers for food packaging: a review, Trends in Food Science & Technology 19 (2008) 634–643.

[10] J.A. Colwill, E.I. Wright, S. Rahimifard, A holistic approach to design support for bio-polymer based packaging, Journal of Polymers and the Environment 20 (4) (2012) 1112–1123.

[11] C. Ingrao, C. Tricase, A. Cholewa-Wójcik, A. Kawecka, R. Rana, V. Siracusa, Polylactic acid trays for fresh-food packaging: a carbon footprint assessment, Science of the Total Environment 537 (2015) 385–398.

[12] Eurostat, Packaging Waste by Waste Operations and Waste Flow, 2017, Available at http://ec.europa.eu/eurostat/web/waste/key-waste-streams/packaging.

[13] I. Blanco, L. Abate, M.L. Antonelli, The regression of isothermal thermogravimetric data to evaluate degradation E_a values of polymers: a comparison with literature methods and an evaluation of lifetime prediction reliability, Polymer Degradation and Stability 96 (2011) 1947–1954.

[14] I. Blanco, L. Abate, M.L. Antonelli, F. Bottino, The regression of isothermal thermogravimetric data to evaluate degradation E_a values of polymers: a comparison with literature methods and an evaluation of lifetime prediction reliability. Part II, Polymer Degradation and Stability 98 (2013) 2291–2296.

[15] J.R. Jambeck, R. Geyer, C. Wilcox, T.R. Siegler, M. Perryman, A. Andrady, R. Narayan, K. Lavender Law, Plastic waste inputs from land into the ocean, Science 347 (2015) 768–771.

[16] J-C. Michaud, L. Farrant, O. Jan, Environmental Benefits of Recycling – 2010 Update. Available at: http://www.wrap.org.uk/sites/files/wrap/Environmental_benefits_of_recycling_2010_update.3b174d59.8816.pdf.

[17] A. Paiva, S. Pereira, A. Sá, D. Cruz, H. Varum, J. Pinto, A contribution to the thermal insulation performance characterization of corn cob particleboards, Energy and Buildings 45 (2012) 274–279.

[18] A. Sukan, I. Roy, T. Keshavarz, Dual production of biopolymers from bacteria, Carbohydrate Polymers 126 (2015) 47–51.
[19] A.K. Mohanty, M. Misra, G. Hinrichsen, Biofibres, biodegradable polymers and biocomposites: an overview, Macromolecular Materials and Engineering 276–277 (1) (2000) 1–24.
[20] C. Ingrao, A. Lo Giudice, J. Bacenetti, A. Mousavi Khaneghah, A. de Souza Sant'Ana, R. Rana, V. Siracusa, Foamy polystyrene trays for fresh-meat packaging: a life-cycle inventory data collection and environmental impact assessment, Food Research International 76 (2015) 418–426.
[21] M. Niaounakis, in: Biopolymers: Processing and Products, first ed., Elsevier, Amsterdam, 2015.
[22] T.A. Hottle, M.M. Bilec, A.E. Landis, Sustainability assessments of bio-based polymers, Polymer Degradation and Stability 98 (9) (2013) 1898–1907.
[23] G. Juodeikiene, D. Vidmantiene, L. Basinskiene, D. Cernauskas, E. Bartkiene, D. Cizeikiene, Green metrics for sustainability of biobased lactic acid from starchy biomass vs chemical synthesis, Catalysis Today 239 (2015) 11–16.
[24] R. Auras, B. Harte, S. Selke, An overview of polylactides as packaging materials, Macromolecular Bioscience 4 (2004) 835–864.
[25] L. Avérous, Polylactic acid: synthesis, properties and applications, in: N. Belgacem, A. Gandini (Eds.), Monomers, Polymers and Composites from Renewable Resources, Elsevier Limited Publication, New York, 2008, pp. 433–450.
[26] M. Jamshidian, E.A. Tehrany, M. Imran, M. Jacquot, S. Desobry, Poly-lactic acid: production, applications, nanocomposites, and release studies, Comprehensive Reviews in Food Science and Food Safety 9 (2010) 552–571.
[27] R. Auras, L.-T. Lim, S.E.M. Selke, H. Tsuji (Eds.), Poly(lactic acid): Synthesis, Structures, Properties, Processing, and Application, John Wiley & Sons, Inc., New York, 2010.
[28] M. Karamanlioglu, R. Preziosi, G.D. Robson, Abiotic and biotic environmental degradation of the bioplastic polymer poly(lactic acid): a review, Polymer Degradation and Stability 137 (2017) 122–130.
[29] A.M. El-Hadi, Development of novel biopolymer blends based on poly(L-lactic acid), poly((R)-3-hydroxybutyrate), and plasticizer, Polymer Engineering and Science 54 (6) (2014) 1394–1402.
[30] P.I.C. Claro, A.R.S. Neto, A.C.C. Bibbo, L.H.C. Mattoso, M.S.R. Bastos, J.M. Marconcini, Biodegradable blends with potential use in packaging: a comparison of PLA/chitosan and PLA/cellulose acetate films, Journal of Polymers and the Environment 24 (4) (2016) 363–371.
[31] P.M.S. Souza, A.R. Morales, M.A. Marin-Morales, L.H. Innocentini Mei, PLA and montmorilonite nanocomposites: properties, biodegradation and potential toxicity, Journal of Polymers and the Environment 21 (3) (2013) 738–759.
[32] I.S.M.A. Tawakkal, M.J. Cran, J. Miltz, S.W. Bigger, A review of poly(lactic acid)-based materials for antimicrobial packaging, Journal of Food Science 79 (8) (2014) 1477–1490.
[33] R. Accorsi, R. Manzini, E. Ferrari, A comparison of shipping containers from technical, economic and environmental perspectives, Transportation Research Part D: Transport and Environment 26 (2014) 52–59.
[34] I. Leceta, P. Guerrero, S. Cabezudo, K. de la Caba, Environmental assessment of chitosan-based films, Journal of Cleaner Production 41 (2013) 312–318.
[35] M. Bertolini, E. Bottani, G. Vignali, A. Volpi, Comparative life cycle assessment of packaging systems for extended shelf life milk, Packaging Technology and Science 29 (2016) 525–546.

[36] ISO (International Organization for Standardization), 14040-Environmental Management – Life Cycle Assessment – Principles and Framework, 2006.
[37] ISO (International Organization for Standardization), 14044-Environmental Management – Life Cycle Assessment – Requirements and Guidelines, 2006.
[38] D. Henton, P. Gruber, J. Lunt, J. Randall, Polylactic acid technology, in: A.K. Mohanty, M. Misra, L.T. Drzal (Eds.), Natural Fibers, Biopolymers, and Biocomposites, CRC Press, Boca Raton, FL, USA, 2005, pp. 527–577.
[39] R. Frischknecht, G. Rebitzer, The ecoinvent database system: a comprehensive web-based LCA database, Journal of Cleaner Production 13 (2005) 1337–1343.
[40] L. De Benedetto, J.J. Klemes, The environmental performance strategy map: an integrated LCA approach to support the strategic decision-making process, Journal of Cleaner Production 17 (2009) 900–906.
[41] H.K. Jeswani, A. Azapagic, P. Schepelmann, M. Ritthoff, Options for broadening and deepening the LCA approaches, Journal of Cleaner Production 18 (2010) 120–127.
[42] S. Madival, R. Auras, S.P. Singh, R. Narayan, Assessment of the environmental profile of PLA, PET and PS clamshell containers using LCA methodology, Journal of Cleaner Production 17 (2009) 1183–1194.
[43] V. Siracusa, C. Ingrao, A. Lo Giudice, C. Mbohwa, M. Dalla Rosa, Environmental assessment of a multilayer polymer bag for food packaging and preservation: an LCA approach, Food Research International 62 (2014) 151–161.
[44] M.F. Cosate de Andrade, P.M.S. Souza, O. Cavalett, A.R. Morales, Life cycle assessment of poly(lactic acid) (PLA): comparison between chemical recycling, mechanical recycling and composting, Journal of Polymers and the Environment 24 (4) (2016) 372–384.
[45] V. Rossi, N. Cleeve-Edwards, L. Lundquist, U. Schenker, C. Dubois, S. Humbert, O. Jolliet, Life cycle assessment of end-of-life options for two biodegradable packaging materials: sound application of the European waste hierarchy, Journal of Cleaner Production 86 (2015) 132–145.
[46] J. Yano, Y. Hirai, S.-I. Sakai, J. Tsubota, Greenhouse gas emissions from the treatment of household plastic containers and packaging: replacement with biomass-based materials, Waste Management Research 32 (4) (2014) 304–316.
[47] S. Toniolo, A. Mazzi, M. Niero, F. Zuliani, A. Scipioni, Comparative LCA to evaluate how much recycling is environmentally favourable for food packaging, Resources Conservation and Recycling 77 (2013) 61–68.
[48] G.M. Bohlmann, Biodegradable packaging life-cycle assessment, Environmental Progress & Sustainable Energy 23 (4) (2004) 342–346.
[49] R. Vidal, P. Martinez, E. Mulet, R. Gonzalez, B. Lopez-Mesa, P. Fowler, J.M. Fang, Environmental assessment of biodegradable multilayer film derived from carbohydrate polymers, Journal of Polymers and the Environment 15 (3) (2007) 159–168.
[50] B.G. Hermann, K. Blok, M.K. Patel, Twisting biomaterials around your little finger: environmental impacts of bio-based wrappings, International Journal of Life Cycle Assessment 15 (4) (2010) 346–358.
[51] A. Dobon, P. Cordero, F. Kreft, S.R. Østergaard, M. Robertsson, M. Smolander, M. Hortal, The sustainability of communicative packaging concepts in the food supply chain. A case study: Part 1. Life cycle assessment, International Journal of Life Cycle Assessment 16 (2) (2011) 168–177.
[52] A. Dobon, P. Cordero, F. Kreft, S.R. Østergaard, M. Robertsson, M. Smolander, M. Hortal, The sustainability of communicative packaging concepts in the food supply chain. A case study: Part 2. Life cycle costing and sustainability assessment, International Journal of Life Cycle Assessment 16 (6) (2011) 537–547.

[53] F. Gironi, V. Piemonte, Life cycle assessment of polylactic acid and polyethylene terephthalate bottles for drinking water, Environmental Progress & Sustainable Energy 30 (3) (2010) 459–468.
[54] S. Papong, P. Malakul, R. Trungkavashirakun, P. Wenunun, T. Chom-in, M. Nithitanakul, E. Sarobol, Comparative assessment of the environmental profile of PLA and PET drinking water bottles from a life cycle perspective, Journal of Cleaner Production 65 (2014) 539–550.
[55] A.L. Roes, M.K. Patel, Environmental assessment of a sugar cane bagasse food tray produced by roots biopack — results of a shortcut-life cycle assessment, Journal of Biobased Materials and Bioenergy 5 (1) (2011) 140–152.
[56] U. Suwanmanee, V. Varabuntoonvit, P. Chaiwutthinan, M. Tajan, T. Mungcharoen, T. Leejarkpai, Life cycle assessment of single use thermoform boxes made from polystyrene (PS), polylactic acid, (PLA), and PLA/starch: cradle to consumer gate, International Journal of Life Cycle Assessment 18 (2) (2013) 401–417.
[57] A. Fernández, C. Javierre, J. González, D. Elduque, Development of thermoplastic material food packaging considering technical, economic and environmental criteria, Journal of Biobased materials and Bioenergy 7 (2) (2013) 176–183.

Index

'*Note*: Page numbers followed by "f" indicate figures and "t" indicate tables.'

A

AABB. *See* Amino acid-based biodegradable (AABB) polymers
AABB PEAs. *See* Amino acid-based biodegradable poly(ester amide)s (AABB PEAs)
AABB PEUs. *See* Amino acid-based biodegradable poly(ester urea)s (AABB PEUs)
Acetylation, 15, 68
Active blood vessel system, 244–247
ADP glucose, 14
Adsorption, 41, 286–287, 287f
Alginate, 358
Aliphatic polyester-based nanocomposites
  copolyesters, 359–361
  montmorillonite (MMT), 359–361
  multiwalled carbon nanotubes (MWCNTs), 361
  PLA-CNTs-based bionanocomposites, 361
  poly(butylene succinate) (PBS), 361–362, 362f
  poly(ε-caprolactone) (PCL), 362–363
  poly[(butylene succinate)-*co*-adi-pate] (PBSA), 362
  polylactic acid-based clay bionanocomposites, 359–361, 360f
  reinforce fillers, 359–361
  solution casting method, 362
  tetrahydrofuran (THF), 363
Aliphatic polyesters, 33
Alkaline phosphatase (ALP), 241
Alkalization, 171
Amino acid-based biodegradable (AABB) polymers, 325f–326f
  classes, 323
  1,4:3,6-diahydohexitols (DAHs), 325
  diamine-diesters (DADEs) synthesis, 323, 324f
  polymethylene-1,n-diols, 325
  poly(ester amide)s, 327–329
  poly(ester urea)s, 329–330
Amino acid-based biodegradable poly(ester amide)s (AABB PEAs), 328f
  diamine-diesters (DADEs), 327
  PhagoBioDerm, 327
  synthesis of, 326f, 327
Amino acid-based biodegradable poly(ester urea)s (AABB PEUs), 329–330, 329f
γ-Aminopropyltriethoxysilane (APS), 45
Amoxicillin (AMOX), 281–282, 282f
Amylopectin, 14, 363–364
Amylose, 14
Angiogenesis, 244–247
Animal fibers, 55–56
Antheraea pernyi, 138
Antibacterial effect, 93
Aromatic polyanhydrides, 19
Arsenic, 252–253
Asbestos fiber, 115
Automobile tires, 379

B

Bagasse, 65
Bamboo fibers, 65–66, 66f
  functionalization, reinforced polymer composites, 170–172, 171f
  surface modification, 130–131
Banana plants *(Musa sapientum)*, 60, 60f
Benzenediazonium-functionalized abaca fibers, 175
1,2,4,5-Benzenetetracarboxylic dianhydride, 176–177
Benzoylation, 68
Benzylation, 70
Betel nut fibers, 62, 63f
BGs. *See* Bioactive glasses (BGs)
Bioactive ceramics, 95–96

Bioactive fillers, 85
Bioactive glasses (BGs), 240–241
Biocompatibility, 34, 369–370, 370f
  tests, 100
Biocompatible material, 187
Biocomposites, 57, 116
Biodegradability, 115–116, 269, 371, 372f
Biodegradable composite biomaterials
  clinical considerations, 95
  composite ceramics and bioglass fillers, 97f
    bone tissue, 95–96
    salt leaching method, 97
    scaffold, 96–97
  composite nanoparticle fillers, 98–100, 99f
  composite scaffolds
    mass loss/degradation percentage, 86–87
    in vitro degradation experiment, 87–88, 87f
  material interface, biological systems
    cell-material interface, 88
    in vitro assessment, biomaterials, 88–90, 89f
    in vivo response, biomaterials, 90–92, 91f
  polymeric biomaterials/postsurgery implications, biodegradation, 94–95, 94f
  surgical implants, 86
  tissue engineering, 86
    bioactivity, of fillers, 93
    scaffolds, 92, 93f
Biodegradation, 3, 330, 381
  polymeric biomaterials and postsurgery implications, 94–95
  tissue exposure to filler, 84
Biofilm life cycle, 102, 103f
Bioglass fillers, 95–97
Biomass, 55, 268, 356
Biomaterial
  defined, 83
  medical devices, factors, 83–84
  in vitro assessment, 88–90
  in vivo response, 90–92, 91f
Biomolecules, 49, 189–190
Bionanocomposites, 223
  biomedical applications, 380f
    biosensors applications, 395–396
    dental applications, 379–381
    drug delivery, 388–391
    orthopedic applications, 381–382
    tissue engineering, 382–388
    wound dressings, 391–395
  biopolymers used, 355–356
    alginate, 358
    aliphatic polyester-based nanocomposites, 359–363
    carboxymethyl cellulose (CMC), 356
    chitosan, 356–358
    gelatin, 358–359
    guar gum (GG), 359
    organic compounds in biomass, 356, 357t
    pectin, 359
    polypeptide-polymer nanocomposites, 366
    polysaccharides-based nanocomposites, 363–365
  classification
    filler particles, 353
    matrix used, 353–354
    natural composites, 353
    polymer-clay composites, 354–355, 355f
    synthetic composites, 353
  fiber-reinforced plastics, 352
  inorganic materials, 352
  organic-inorganic hybrid materials, 352
  organic moiety, 352
  preparation of, 366, 368f
    clay exfoliation/delamination, 368
    electrospinning, 368
    free radical polymerization, 368
    melt processing, 367
    in situ polymerization method, 366
    solution blending method, 366–367
  properties
    biocompatibility, 369–370, 370f
    biodegradability, 371, 372f
    mechanical property, 371
    swelling property, 372
  types of, 352, 352f
  uses of, 351–352
Bionanocomposites (bio-NCs), 187
Bionolle, 317

Biopolymer/layered double hydroxide nanocomposites (LDH NCs), 288, 288f
adsorption, 286–287, 287f
catalyst and electrocatalyst, 276f
biprotein/LDH ultrathin film, 276–277
Brønsted-type base sites, 275–276
chromene-incorporated dihydroquinoline derivatives, 277, 277f
hydroxyl-functionalized ionic liquid (HFIL), 276–277
LDH-Hbcop and HFIL-LDH-Hbcop, 276–277, 277f
drug delivery, 285f
advantages, 279–280
Amoxicillin (AMOX), 281–282
cephalexin release, CMC/LDH-CPX NC bead, 283, 283f
2,4-dichlorobenzoate (BzDC), 279–280
factors, 279–280
ketoprofen, 281–282
LDH-drug hybrids, 283
LDH-IBU/PCL composite fibers, 279–280, 281f
LDH-IBU/PLA composite fibers, 279–280, 281f
p-hydroxybenzoate (*p*-BzOH), 279–280
pristine LDH and LDH-hGH nanoparticles, 283–284, 285f
in vitro cell endocytosis, 283, 284f
flame retardant
char residue, cone calorimetry testing, 274–275, 274f
cone calorimetry test, 271–272, 273f
montmorillonite clay (MMT), 272–273
PPDO/LDH-DDS, 275, 275f
standards and indices, 271–272
thermogravimetric analysis, 271–272
X-ray diffraction (XRD), 272–273
packaging, 278–279, 279f
Biopolymers, 187, 355–366
defined, 3
natural biopolymers, 4–15. *See also* Natural biopolymers
synthetic biopolymers, 15–28. *See also* Synthetic biopolymers
uses of, 3
Bioresorbability, 239–240
Biosensors, 195–196, 254, 288
applications, 395–396
Bisphenol A (BPA), 252
Bleaching, 70–71
Bombyx mori, 138
Bone tissue, 95–96
Bovine serum albumin (BSA), 121–122
Bragg's law, 75–76
Brown coir, 64
Brown jute *(Corchorus olitorius)*, 58
1,4-Butanediol (BDO), 319

C

Calcium phosphate, 84–85
Caldimonas manganoxidans, 269
Candida albicans, 253–254
Candida antarctica (lipase B), 18
Candida tropicalis, 319
Capacitive deionization (CDI), 300
ε-Caprolactone, 225
Carbon nanostructures, 98
Carbon nanotubes (CNTs), 379. *See also* Chit/carbon nanotube nanocomposites (CNT NCs)
composition, 297–298
functionalization of, 298–299
polymer nanocomposites, 299–300
types of, 297–298, 298f
Carboxymethyl cellulose (CMC), 356
Cash crops, 55
CDI. *See* Capacitive deionization (CDI)
Cell adhesion, 34, 34f
Cell-material interface, 88
Cell-polymer interaction, 34
Cell spreading, 34
Cellulose, 11–13, 13f, 71–73, 356, 365
Cellulose acetate, 13
Cellulose-supported LDHs (CSLDH), 286–287
Ceramic-matrix nanocomposites, 354
Cetyl pyridinium chloride (CPC), 362
Cetyl trimethylammonium bromide (CTAB), 362
Chemical conjugation
γ-aminopropyltriethoxysilane (APS), 45
hydrolysis, 45, 46f
silane coupling agent, 44, 45f
self-condensation, 45, 46f
Chemical retting, 57

Chemical vapor deposition (CVD), 37f
  initiation, 38
  propagation, 38
  termination, 38
Chemotherapeutic ion, 100
China grass, 66
Chit/carbon nanotube nanocomposite fiber
  adsorption process, 197–198
  Chit-based MWNT/PU composite fiber, 195–196, 196f
  depolymerization process, 197–198
  electrical conductivity, 195–196
  fracture mechanism, 196–197, 197f
  liquid densification and polymer infiltration, 196–197
  postspin twisting procedure, 195–196
Chit/carbon nanotube nanocomposite films, 194f
  biomolecules, 189–190
  carbohydrates, 192–193
  Chit/MWCNT-Gl NC, 192–193, 192f
  gamma irradiation, 193–194
  magnesium oxide (MgO), 194, 195f
  MWCNT-COOH, 189–190, 193
  MWCNT-Val, 189–190, 190f
  MWCNT-VC, 191f
    effect of, 191
    morphological properties, 191
  N,N'-carbonyldiimidazole (CDI), 192–193
  tensile strength and Young's modulus, 193
Chit/carbon nanotube nanocomposite foam, 201f
  digital photographs, 198, 199f–200f
  ice-templating procedure, 198
  sublimation-helped compression procedure, 198
Chit/carbon nanotube nanocomposites (CNT NCs)
  application of, 188
    adsorption and membrane, 201–209
    drug delivery, 210–211
    electroanalytical sensors, 212–215
    tissue engineering, 209–210
  charge density, 187
  chemical structure, 187, 188f
  nanofillers, 188
  preparation, 188
  synthesis and characterization
    fibers, 195–198
    films, 189–194
    foam, 198–200
    polar groups, 189
    surface modification, 189
  uses of, 188
Chitin, 9–11, 356–358, 365. *See also* Polysaccharides
Chit matrix, 188
Chitosan, 9–11, 356–358. *See also* Polysaccharides
Chit/silica-coated CNTs (Chit/SCNTs) membranes, 207
Citric acid (CA), 92
CMC. *See* Carboxymethyl cellulose (CMC)
Coconut/coir fibers, 64–65, 65f
  functionalization, reinforced polymer composites, 172–174, 173f
  surface modification
    ethylene dimethylacrylate (EMA), 133
    properties, 131
    water absorption behavior, 132, 132f
Collagen
  biosynthesis, 4
  biosynthetic pathway, 5–6, 5f
  disulfide bondings, 4
  hydrolysis, 5
  protease enzymes, 5–6
  triple helix structure, 4
Composites, 57
  delivery mediators
    bone morphogenic protein (BMP), 107
    HANPs, protein encapsulation/release, 107–108, 108f
    hydrogels, 107
    stoichiometric proportion, 109
Composite ceramics, 95–97
Composite fillers, 83, 84f
Composite materials, 83, 84t
Composite nanoparticle fillers, 98–100, 99f
Convenient packages, 403
Conventional composites, 355
"Coordination-insertion" mechanism, 225–226
Copolymerization, 320
Corn starch, 15

Cotton fibers, 365
surface modification
contact angles, untreated and modified cotton fibers, 118–119, 120f
divinylbenzene (DVB), 121
Escherichia coli, 120
2-hydroxy-4-acryloyloxybenzophenone (HAB), 121
multiwall carbon nanotubes (MWCNTs), 121
ozone gas treatment, 118–119
photoluminescence behavior, 120
Pseudomonas aeruginosa, 120
scanning electron microscopical (SEM) images, 118–119, 119f
sodium chlorite/potassium permanganate redox bleaching system, 122
3-(4′-vinylbenzyl)-5,5-dimethylhydantoin (VBDMH), 121
water contact angle (WCA), 121
Covalent functionalization, 298–299
Covalent grafting, 298–299
Crosslinking points, 83, 84f
CVD. *See* Chemical vapor deposition (CVD)
Cyanaposis tetragonolobus (Leguminosae), 359
Cycloaliphatic rings, 318

D

Damage Categories (DCs), 410
Decolorizing agents, 9
Decortication, 57
Defect functionalization, 298–299
Degradation, 269
kinetics, 85
Degree of polymerization (DP), 71–73
Dehydrochlorination, 20
Demineralization, 11
Dental applications, 379–381
Desorption, 41
electrostatic interaction, 42–43, 43f
hydrophobic interaction, 42–43, 43f
sodium dodecyl sulfate (SDS), 43, 43f
vs. polymer matrix (polylactic acid (PLA)), 43, 44f
surfactants, 42
1,4:3,6-Diahydohexitols (DAHs), 325
Diamine-diesters (DADEs), 323, 324f
Dianhydrohexitols, 320, 320f
2,4-Dichlorobenzoate (BzDC), 279–280
Differential scanning calorimetry (DSC), 76
Differential thermal analysis (DTA), 76
Diisocyanate, 25
Dilute acids, 5
Dimethacrylates, 379–381
Dimethylformamide (DMF), 41
Divinylbenzene (DVB), 121
DL-dithiothreitol (DTT), 248
Dodecyltrimethylammonium bromide (DTAB), 125–126
Double networks (DN), 85
Doxorubicin (DOX), 211
Drug carriers, 247–248
Drug delivery, 388–389
biocompatibility and nanosized dimensions, 389
biopolymer/layered double hydroxide nanocomposites (LDH NCs), 285f
advantages, 279–280
Amoxicillin (AMOX), 281–282
cephalexin release, CMC/LDH-CPX NC bead, 283, 283f
2,4-dichlorobenzoate (BzDC), 279–280
factors, 279–280
ketoprofen, 281–282
LDH-drug hybrids, 283
LDH-IBU/PCL composite fibers, 279–280, 281f
LDH-IBU/PLA composite fibers, 279–280, 281f
p-hydroxybenzoate (*p*-BzOH), 279–280
pristine LDH and LDH-hGH nanoparticles, 283–284, 285f
in vitro cell endocytosis, 283, 284f
Chit/carbon nanotube nanocomposite
bovine serum albumin (BSA), 210–211
doxorubicin (DOX), 211
O-CNTs-LChit-DOX, 211, 212f
polysaccharides, 210–211
drug excipients, 389
Pluronic, 391
polycaprolactone/metal oxide nanocomposites, 251f
biodegradable macromolecules, 248
DL-dithiothreitol (DTT), 248

Drug delivery *(Continued)*
doxorubicin (DOX) carrier, 248, 249f
drug carriers, 247–248
ketoconazole (KCZ), 250
modified Fe_3O_4 NPs, 248–250, 249f
nonmagnetic micelles, 248–250, 249f
PCL/Si-Dox film, 250–251, 252f
PCL-SS-PDMAEMA copolymer, 248, 249f
surface drug delivery system, 250
silica-alginate hydrogel bionanocomposite, 389–391, 390f
vaccine delivery, 391
virus/bionanocomposite materials, 391, 392f
Dry etching, 39–40

E

Electroanalytical sensors, 215
Chit/carbon nanotube nanocomposite, 212
blood coagulation and anticoagulation, 214–215
CNT-Chit in channel 1, 214–215, 215f
Cu-Chit/MWCNT/GC electrode, 213, 213f
fiber optic probe, 214–215, 215f
MWCNT/GCE and Cu-Chit/MWCNT/GCE, 213, 213f
rutin, 213–214, 214f
Electron beam radiations, 40
Electrospinning process, 234–235
Elongation at break, 77
Empty fruit bunches, 62–63
Endocrine disrupting chemicals (EDCs), 252
Entangled fibers, 57
Epoxy-based silicone system, 379–381
Escherichia coli, 120, 319
Ethylene dimethylacrylate (EMA), 133
Exfoliated nanocomposites, 355
Extracellular matrix (ECM), 86

F

Fatty acids, 319
Fibers. *See also* Fiber yielding plants/trees
classification, 55–56, 56f
types, 55
Fiber cleaning, 57
Fiber extraction, 57
Fiber modification
acetylation, 68
benzoylation, 68
benzylation, 70
bleaching, 70–71
chemical treatment, 67
compounds containing methylol groups, 71
coupling agent, 67
malenization, 68–69
mercerization (alkali treatment), 67–68
physical treatment, 67
scouring, 70
silane treatment, 69–70
toluene diisocyante treatment, 71
Fiber-reinforced plastics, 352
Fiber yielding plants/trees
bamboo, 65–66, 66f
banana plants *(Musa sapientum)*, 60, 60f
betel nut fibers, 62, 63f
coconut/coir fiber, 64–65, 65f
flax, 61–62, 61f
hemp (*Cannabis sativa* L.), 61, 61f
jute, 58, 58f
kenaf *(Hibiscus cannabinus)*, 58, 59f
oil palm (*Elaeis guineensis* Jacq.), 62–63, 63f
okra bamia (lady's finger) plant, 62, 62f
ramie *(Boehmeria nivea)*, 66–67, 67f
roselle *(Hibiscus sabdariffa)*, 59, 60f
sisal fibers *(Agave sisalana)*, 58, 59f
sugarcane (*Saccharum officinarum* L.), 65, 66f
wild almond *(Sterculia foetida)* tree, 63–64, 64f
Field emission scanning electron microscopy (FESEM), 269
Filaments, 57
Filler components
antibacterial agents and biofilm, 102–105, 103f–104f
clinical considerations, 105–107
composite biomechanical properties, degradation, 105, 106f
ion release kinetics, POC-BG composite scaffolds, 100–102, 101f

Fillers
bioactivity, 93
bioglass fillers, 95–97
components, 100–107
composite nanoparticle fillers, 98–100, 99f
tissue exposure, 84
types, 83
Flax fibers *(Linum usitatissimum)*, 61–62, 61f
functionalization, reinforced polymer composites, 165–166
surface modification
chemical modifications, 123
glycidyl methacrylate (GMA), 122
octadecylphosphonic acid (ODPA), 122
tensile strength modification, 122–123, 123f
Food packaging, 401–402
Damage Categories (DCs), 410
eco-friendly materials, 405
Functional Unit (FU), 409–410
Impact Categories (ICs), 410
Life Cycle Assessment (LCA) applications, 413–414
Life Cycle Inventory (LCI), 410
Life Cycle Thinking (LCT), 409
municipal solid wastes (MSWs), 405
plastics, 403–404
polylactic acid (PLA)
applications, 407–408
biodegradable polymers, 406
lactic acid (LA), 407
polymeric resins, 403–404
roles of, 402–403
thermoplastics, 403–404
Fourier transform infrared spectroscopy, 74–75
Fusio Liquid Dentin (Pentron Clinical), 379–381

G

Gallium, 100
Gelatin, 358–359
amino acid compositions, 7–9, 8t
collagens, 7–9
extraction, natural resources, 9, 10f
industrial extraction, 9, 10f
manufacturing process, 9
structure, 7–9, 7f
GG. *See* Guar gum (GG)
Gliadins, 6–7
Global warming, 265–266
Glucose-6-P, 14
Glutaraldehyde (GA), 284
Gluten
biosynthesis, 6–7, 6f
molecular weight, 6–7
uses of, 7
Glycidyl methacrylate (GMA), 122
Grafting, 47, 48f
Guar gum (GG), 359
Gypsum, 381–382

H

Halloysite nanotubes (HNTs), 333
Hemicellulose, 73
Hemp fibers (*Cannabis sativa* L.), 61, 61f, 123
functionalization, reinforced polymer composites, 162t
chemical treatments, 161
γ-methacryloxypropyltrimethoxysilane (MPS), 162
potassium permanganate (KP), 162
Young's modulus, 161
surface modification
bag retting and white rot fungal treatments, 125
chemical treatments, 124
dodecyltrimethylammonium bromide (DTAB), 125–126
flame retardancy, 125
MPS functionalization, 124
silane treatment, 124
X-ray diffractogram, unmodified and modified hemp fibers, 125–126, 126f
Young's modulus, 124
Hexadecanol, 129
1,6-Hexanediol (HDO), 319
Human bone marrow mesenchymal stem cells (h-BMSCs), 241
Hydrogels, 386
Hydrogen peroxide, 244–247
Hydrothermal synthesis, 227

2-Hydroxy-4-acryloyloxybenzophenone (HAB), 121
Hydroxyapatite (HAp), 340
Hydroxyl-functionalized ionic liquid (HFIL), 276–277

I

Immobilization methods, 49, 50f
Impact Categories (ICs), 410
Induced osteogenic effect, 93
Initiation, 38
In situ polymerization, 299–300
  ε-caprolactone, 233
  dichloroethane and N,N-dimethylformamide, 235–237
  electrospinning apparatus, 234–235, 236f
  electrospinning process, 234–235
  electrospun nanofibers, 235–237
  grafted TiO_2 NPs (g-TiO_2), 234, 235f
  method, 366
  PCL/Fe_3O_4@GO NC, 233–234, 234f
  PCL/Fe_3O_4 NCs, 233, 233f
  PCL nanofibrous scaffolds, 235–237, 237f
Intercalated nanocomposites, 355
Interfacial Polycondensation (IP), 327
Interpenetrated networks, 85, 109–111, 110f
Ion-doped polymer, 102–103
Ion-imprinted polymers (IIPs), 205–206
Ionizing radiations, 40
Isocyanate group back titration (IBT) method, 129

J

Jute fibers, 58, 58f
  functionalization, reinforced polymer composites
    chemical treatments, 160
    maleic anhydride-grafted PP, 158–159
    multiwalled carbon nanotubes (MWCNTs), 161
    poly(lactic acid) (PLA), 160
    SEM images, 159–160, 160f
    silane-treated jute fibers, 158–159, 159f
    Young's modulus, 158
  surface modification
    chemical treatments, 127
    MWCNTs-modified jute fibers, 127
    oleoyl chloride, 126–127
    pyromellitic dianhydride (PMDA), 127

K

Kenaf fibers *(Hibiscus cannabinus)*, 58, 59f
  functionalization, reinforced polymer composites, 166t
    KP-modified kenaf fibers, 163
    nano-magnesium carbonate, 164
    polypropylene (PP) composites, 164, 164f–165f
    polyurethane (PU), water uptake behavior, 163, 163f
  surface modification, 129–130
Ketoconazole (KCZ), 250
Ketoprofen, 281–282

L

Lactic acid, 22
Layered double hydroxide (LDH), 265–266. *See also* Polymer/layered double hydroxide nanocomposites (LDH NCs)
LDH-drug hybrids, 283
Life Cycle Assessment (LCA), 402
Life Cycle Inventory (LCI), 410
Life Cycle Thinking (LCT), 409
Lignin, 13, 73
Lignocellulosic fibers, 55–56, 115, 136–138, 157
Linum usitatissimum, 122
Lipase, 24
Living polymerization, 225–226

M

Macrofill materials, 379–381
Magnetically/multifunctional Chit/carbon nanotube nanocomposites
  hydrophilic shell, 208
  imprinting method, 205–206
  ion-imprinted polymers (IIPs), 205–206
  magnetically retrievable IIP-Chit/CNT, 205–206, 206f
  mChit/CNT formation, 204–205, 205f
  multifunctional composite, 207, 207f
  proton exchange membrane, 207
  pseudo-second-order kinetics, 205
  saturation adsorption capacity, 206
  thermodynamic constants, 205
  water contact angles, 208, 208f
Magnetic separation, 204–205

Maleated polyethylene (MPE), 130
Maleated polypropylene (MPP), 130
Malenization, 68–69
Marine brown algae (Phaeophyta), 358
Material interface, biological systems
  cell-material interface, 88
  in vitro assessment, biomaterials, 88–90, 89f
  in vivo response, biomaterials, 90–92, 91f
Mattress fibers, 64–65
Mechanical property, 371
Melt blending method, 299–300
Melt extrusion
  advantage, 230–231
  chloroform, 231–233
  PLA/PCL/TiO_2 NCs, 231, 231f
  ring-opening polymerization, 231–233, 232f
  room-temperature notched surfaces, 231–233, 232f
  twin-screw microcompounder, 231–233
Melt processing, 367
Melt transesterification, 27
Mercerization (alkali treatment), 67–68
Metal ions, 100
Metal-matrix nanocomposites (MMCs), 354
Metal oxides (MOs)
  hydroxylation, 226
  quantum confinement, 226
  synthesis methods, 227–228
Methacrylated gelatin (GelMA), 386
Methyl methacrylate (MMA), 168
Microemulsion, 227
Microfibrillated cellulose (MFC), 331
Microfill, 379–381
Microlithography, 47–48, 48f
Micromanipulation, 49
MMCs. *See* Metal-matrix nanocomposites (MMCs)
Modulus of elasticity, 77
Molecular level scale BG-PCL (MBG-PCL), 242–243
Monocytes, 90
Montmorillonite clay (MMT), 272–273
MOs. *See* Metal oxides (MOs)
Multiwalled carbon nanotubes (MWCNTs), 121, 161, 298
Municipal solid wastes (MSWs), 405

N

Nanocomposites (NCs)
  CNT NCs. *See* Chit/carbon nanotube nanocomposites (CNT NCs)
  layered double hydroxide (LDH). *See* Polymer/layered double hydroxide nanocomposites (LDH NCs)
  poly(alkylene dicarboxylate)s, 331–334
  polycaprolactone/metal oxide. *See* Polycaprolactone/metal oxide nanocomposites
  poly(ester amide)s, 335–341
Nanodiamond (ND) material, 98
Nanofillers, 98, 265–266, 299–300
Nanohydroxyapatite (nHAP), 383–384
Nanomaterials, 83
Natural biopolymers
  defined, 4
  microorganisms, 4
  polysaccharides, 9–15
  proteins, 4–9
Natural composites, 353
Natural fiber-reinforced polymer composites, 157–186
Natural fibers, 55
  characterization
    Fourier transform infrared spectroscopy, 74–75
    mechanical properties, 77
    scanning electron microscopy (SEM), 75
    thermal analysis, 76–77
    water absorption, 77–78
    X-ray diffraction, 75–76
  chemical composition, 72t
    cellulose, 71–73
    extractive and ash, 74
    hemicellulose, 73
    lignin, 73
    pectin, 73
    wax, 74
  features of, 157
  origins of, 55–56, 56f
  physical properties, 74, 74t
  properties/advantages over conventional fibers, 56–57
  surface modification. *See also* Surface modification
    bamboo fiber, 130–131
    biodegradability, 115–116

Natural fibers *(Continued)*
chemical techniques, 116–118
coir fibers, 131–133
cotton fibers, 118–122
flax fibers, 122–123
hemp fibers, 123–126
jute fibers, 126–127
kenaf fibers, 129–130
mechanical properties, 115–116, 117t
oil palm fibers, 133–134
physical techniques, 116–118
ramie fibers, 128–129
sisal fiber, 134–136
Natural polymers, 33
ND surface (ND-ODA), 98
N,N'-carbonyldiimidazole (CDI), 192–193
Noncovalent functionalization, 298–299
Nonionizing radiations, 40
Nucleation, 227–228

O

Octadecylphosphonic acid (ODPA), 122
Octanediol (OD), 92
Oil palm fibers (*Elaeis guineensis* Jacq.), 62–63, 63f
functionalization, reinforced polymer composites, 174–175
surface modification, 133–134, 134f
Okra bamia (lady's finger) plant, 62, 62f
Oleoyl chloride, 126–127
Organically modified ceramics, 379–381
Organic moiety, 352
Organomodified montmorillonites (OMMTs), 331–333
Orthopedic applications, 381–382
Osseous tissue, 239–240
Osteoconductivity, 239–240
Osteogenecity, 239–240
Osteoinductivity, 239–240
Ozone gas treatment, 118–119

P

Packaging, 278–279, 279f. *See also* Food packaging
defined, 401
material, 363–364
Patterns, 47–48, 48f
PBS. *See* Poly (butylene succinate) (PBS)
PCL. *See* Polycaprolactone (PCL)
PDO. *See* Poly(p-dioxanone) (PDO)
PEAs. *See* Polyester amides (PEAs)
Pectin, 73, 359
Petroleum-based polymers, 187
PGAs. *See* Polyglycolides (PGAs)
PhagoBioDerm, 327
Phagocytosis, 90
Phenylboronic acid (PBA), 248–250
Phosphoglucomutase, 14
p-Hydroxybenzoate (*p*-BzOH), 279–280
PLA. *See* Polylactic acid (PLA)
Plant fibers, 55–56, 115, 157
Plasma polymerization/deposition, 40
Plasma treatment, 39–40, 39f
Plaster of Paris (PP), 381–382
Plastics, 403–404
Pluronic, 391
Poly(3-hydroxybutyrate) (PHB), 269
Poly(alkyl cyanoacrylates), 20–21, 21f
Poly(amide-ester-imide) (PAEI), 338f, 339
Poly (butylene succinate) (PBS), 17–18, 18f, 317, 321, 361–362
applications, 331
properties, 331
Poly(butylene succinate-*co*-adipate) (PBSA)
mechanical properties, 333
nanocomposites, 333
Poly(ε-caprolactone) (PCL), 362–363
Poly(ethylene succinate) (PES), 333–334
Poly(ethyleneimine) (PEI), 121–122
Poly(lactic acid) (PLA), 160, 169, 176
Poly(methyl methacrylate) (PMMA), 135–136
Poly(p-dioxanone) (PDO), 18
Poly(sodium 4-styrenesulfonate) (PSS), 302
Poly(vinyl alcohol) (PVA)
applications, 297
melting point, 297
synthesis, 297, 298f
Polyanhydrides, 19–20, 20f
Polyaniline (PAni), 336
Poly[(butylene succinate)-*co*-adi-pate] (PBSA), 362
Polycaprolactone (PCL), 22–24, 24f, 25t, 223
characteristics, 224
properties, 224, 224t
rigid nanofillers, 225
synthesis, 225–226, 226f

Polycaprolactone/metal oxide nanocomposites
degradation, 238–239
melt extrusion, 230–233
potential application, 254
drug delivery, 247–251
tissue engineering, 239–247
water treatment, 252–254
in situ polymerization
ε-caprolactone, 233
dichloroethane and N,N-dimethylformamide, 235–237
electrospinning apparatus, 234–235, 236f
electrospinning process, 234–235
electrospun nanofibers, 235–237
grafted TiO_2 NPs (g-TiO_2), 234, 235f
PCL/Fe_3O_4@GO NC, 233–234, 234f
PCL/Fe_3O_4 NCs, 233, 233f
PCL nanofibrous scaffolds, 235–237, 237f
solution casting method
dichloromethane (DCM), 228–229
FE-SEM images, 228–229, 229f
polymer matrix, 228
SEM micrographs, 230, 230f
TGA thermograms, 228–229, 229f
strong interfacial bonding, 228
Polycarbonates, 26–27, 27f
Poly(vinyl alcohol)/carbon nanotube nanocoposites (PVA/CNT NCs), 304f, 310f–311f
AC conductivity, 306–307, 307f
acid-functionalized multiwalled carbon nanotube (MWCNT), 303, 305f
capacitive deionization (CDI), 300
chemical vapor deposition (CVD), 301–302
electrospinning method, 307–308
flux and separation factor, 304–305, 306f
graphene/carbon nanotubes, 308–309, 309f
isopropanol (IPA), 302
multiwalled carbon nanotubes (MWCNTs), 300, 301f
MWCNTs-COOH, 301
MWCNTs-poly(sodium 4-styrenesulfonate), 302, 304f
nickel-coated stainless steel (Ni/SS), 303
poly(sodium 4-styrenesulfonate) (PSS), 302
poly(vinyl alcohol)/amino acid-functionalized MWCNT, 300, 302f–303f
sodium dodecylbenzenesulfonate (NaDDBS), 307–308, 308f
solution casting method, 300
thermal annealing, stress-strain behavior, 302–303, 305f
vitamin B_2, 309–310, 310f
wet-spinning process, 306–307
Polyester amides (PEAs), 19
Polyesters, 33
properties, 318
Polyfunctional α-amino acids, 323–324
Polyglycolides (PGAs), 15–17, 16f, 17t
Polylactic acid (PLA), 21–22, 22t, 23f
Polylactic glycolic acid, 27–28, 28f
Polymer-clay composites, 354–355, 355f
Polymer degradation, 238–239
Polymeric matrix composites, 354
Polymerization, 47, 48f
Polymer/layered double hydroxide nanocomposites (LDH NCs)
analytical methods, 266
biodegradable polymers, 268f
biocompatibility, 267–268
blending and copolymerization, 269
natural polymers, 268
synthetic polymers, 268
delamination, 266
investigation biodegradability, 269–270, 270f–271f
layer thickness and lateral dimensions, 267
overview, 265–266
properties, 267
synthesis, 266
Polymer matrix, 83, 84f, 85
Polymer wettability, 33–34
Polypeptide-polymer nanocomposites, 366
Polyplastics, 265–266
Polypropylene (PP), 158–159, 164, 164f–165f
benzenediazonium-functionalized abaca fibers, 175
SEM images, 159–160, 160f
silane-treated jute fibers, 158–159, 159f

Polypropylene (PP) *(Continued)*
untreated and alkalized kenaf fibers, 164–165, 165f
Poly(alkylene dicarboxylate)s
biomedical applications, 317
nanocomposites, 331
enzymatic hydrolysis, 334
halloysite nanotubes (HNTs), 333
microfibrillated cellulose (MFC), 331
organomodified montmorillonites (OMMTs), 331–333
PBS/SiO_2 nanocomposites, 331
poly (butylene succinate) (PBS), 331
poly(butylene succinate-*co*-adipate) (PBSA), 333
poly(ethylene succinate) (PES), 333–334
silicate basal spacing, clay particles, 332f
in situ melt polycondensation method, 334
and poly(ester amide)s, sugar-based monomers, 322f
bicyclic monosaccharide monomers, 320, 321f
cross-linked polyesters, 321
dianhydrohexitols, 320, 320f
enzymatic degradation, 322
poly (butylene succinate) (PBS), 321
solid-state modification (SSM), 320–321
stereoregular poly(ester amide)s, 322–323, 322f
renewable resources
1,4-butanediol (BDO), 319
1,6-hexanediol (HDO), 319
1,3-propanediol (PDO), 319
thermal polycondensation process, 318–319
thermal and mechanical properties, 317–318
Poly(ester amide)s (PEAs), 318, 320–323
amino acid-based biodegradable poly(ester amide)s, 327–329
nanocomposites, 341f
corn starch, 335
graphene nanoplatelets, 339
hydroxyapatite (HAp), 340
hyperbranched PEAs (HBPEAs), 335f–336f, 336
melt mixing technique, 340
multiwalled carbon nanotube (MWCNT), 337
PEA/ZnO bionanocomposites, 341
poly(amide-ester-imide) (PAEI), 338f, 339
polyaniline (PAni), 336
poly[2-(dimethylamino)ethyl methacrylate] (PDMAEMA), 337, 338f
vegetable seed oils (VSOs), 340–341
Polysaccharides, 356
cellulose, 11–13, 13f
chitin and chitosan, 10f
extraction procedures, 11, 12f
general structure, 9, 11f
natural synthesis pathway, 11, 12f
properties, 9–10
uses of, 10–11
starch
applications, 14
extraction methods, 15, 15t
synthesis, plant cells, 14, 14f
Polysaccharides-based nanocomposites
cellulose, 365
chitin, 365
starch, 363–364, 364f
Polyurethane (PU)
condensation and addition reactions, 25
physical and chemical properties, 24–25
synthetic pathways, 25, 25t, 26f
uses of, 24–25
water uptake behavior, 163, 163f
Porous beads, Chit/carbon nanotube nanocomposites
Chit beads surface, 201–203, 202f
Chit-controlling kind, 204
Chit-SWNT beads preparation, 203, 203f
elastic property, 201–203
methyl orange (MO) and Au NPs, 201–204
Precipitation, 227–228
Primary radical recombination, 38
Primary radical termination, 38
Propagation, 38
1,3-Propanediol (PDO), 319
Protease enzymes, 5–6
Proteins, 366

collagen
biosynthesis, 4
biosynthetic pathway, 5–6, 5f
disulfide bondings, 4
hydrolysis, 5
protease enzymes, 5–6
triple helix structure, 4
gelatin, 7–9, 7f, 8t, 10f
gluten, 6–7, 6f
Proton exchange membrane, 207
Pseudomonas aeruginosa, 120
Pseudo-second-order kinetics, 205
Pseudostem, 60
PVA. *See* Poly(vinyl alcohol) (PVA)
Pyromellitic dianhydride (PMDA), 127

Q

Quantum confinement, 226

R

Radiation, 40
Ramie fibers *(Boehmeria nivea)*, 66–67, 67f
functionalization, reinforced polymer composites, 167–168, 167f
surface modification, 128–129, 129f
Reactive oxygen species (ROS), 244–247
Redox initiator system, 140
Retting process, 61
Reverse micelle, 227
Reversible addition-fragmentation chain transfer (RAFT), 128, 277
Ring-opening polymerization (ROP), 16–17, 16f
advantages, 225
ε-caprolactone, 225
melt extrusion, 231–233, 232f
Roselle *(Hibiscus sabdariffa)*, 59, 60f
Roughening, 48–49

S

Scaffolds, 86, 92
Scanning electron microscopy (SEM), 75, 189
Schotten–Baumann condensation, 20
Scouring, 70
Sidewall functionalization, 298–299
Silane coupling agent, 44, 45f
Silane treatment, 69–70
Silanization, 171
Silica-alginate hydrogel bionanocomposite, 389–391, 390f
Silica-kaolinite-modified cotton fibers, 118–119
Silicon, 382–383
Silk fibers, 55–56
surface modification, 138–139
Silver nanoparticles (AgNPs), 393
Single-walled carbon nanotubes (SWCNTs), 298
Sisal fibers *(Agave sisalana)*, 58, 59f
functionalization, reinforced polymer composites
epoxy matrix, 169
methyl methacrylate (MMA), 168, 169f
NaOH and clay treatments, 169–170, 170f
NaOH-treated sisal fibers, 168
poly(lactic acid) (PLA), 169
treatments, 168
surface modification, 134–136, 136f
Sliver, 57
Sodium dodecyl sulfate (SDS), 43, 43f
Sodium hydroxide, 5
Sol-gel route, 227
Solution Active Polycondensation (SAP), 329
Solution adsorption, 41
Solution blending, 299–300, 366–367
Solution casting method, 300, 362
dichloromethane (DCM), 228–229
FE-SEM images, 228–229, 229f
polymer matrix, 228
SEM micrographs, 230, 230f
TGA thermograms, 228–229, 229f
Solvent evaporation technique, 228
Solvothermal method, 227
Spinning, 57
Stannous octoate, 24
Starch
applications, 14
drawbacks, 364
extraction methods, 15, 15t
melting point, 363–364
synthesis, plant cells, 14, 14f
thermoplastic starch (TPS), 363–364
Stripping, 70
Sugar-based monomers, 320–323

Sugarcane (*Saccharum officinarum* L.), 65, 66f
Superabsorbents, 355–356
Surface hydrophilicity/hydrophobicity, 33
Surface/interfacial reactions, 39
Surface modification
  bamboo fiber, 130–131
  biological method
    cell seeding and growth, 50, 52f
    chemical conjugation, 50, 51f
    immobilization methods, 49, 50f
    physical adsorption, 49
    self-cross-linking, 49
  carbon nanotubes (CNTs), 189
  categories of, 115, 116f
  coir fibers, 131–133
  cotton fibers, 118–122
  flax fibers, 122–123
  hemp fibers, 123–126
  jute fibers, 126–127
  kenaf fibers, 129–130
  lignocellulosic plant fibers, 136–138
  mechanical method
    micromanipulation, 49
    roughening, 48–49
  oil palm fibers, 133–134
  overview, 33–37, 36f
  physicochemical method
    combination, 47–48
    gas phase/radiation, 37–40
    liquid and bulk phases, 41–46
  ramie fibers, 128–129
  sisal fiber, 134–136
Surface wettability, 34
Surfactants, 42
Swelling property, 372
Synthetic biopolymers
  poly(alkyl cyanoacrylates), 20–21
  poly(butylene succinates) (PBSs), 17–18
  polyanhydrides, 19–20
  polycaprolactone (PCL), 22–24
  polycarbonate, 26–27
  polyester amides (PEAs), 19
  polyglycolides (PGAs), 15–17
  polylactic acid (PLA), 21–22
  polylactic glycolic acid, 27–28
  polymerization techniques, 15, 16f
  polyurethanes, 24–26
Synthetic composites, 353
Synthetic polymers, 33

T

Tensile strength, 77
Terephthalic acid, 317–318
Termination, 38
Terpenes, 318
Tetrahydrofuran (THF), 363
Thermal analysis, 76–77
Thermal polycondensation process, 318–319
Thermogravimetric analysis (TGA), 76
Thermoplastics, 403–404
Thermoplastic starch (TPS), 363–364
Tissue engineering, 86, 387f
  bioactivity, of fillers, 93
  Chit/carbon nanotube nanocomposite, 209–210, 210f
  chitosan-clays, 384
  hydrogel, 386
  magnetic scaffolds, 387
  methacrylated gelatin (GelMA), 386
  nano-HA/collagen/PLA, 383–384, 383f
  nanohydroxyapatite (nHAP), 383–384
  PLG and montmorillonite (MMT), 384–386, 385f
  polycaprolactone/metal oxide nanocomposites, 240f, 244f
    active blood vessel system, 244–247
    alkaline phosphatase (ALP), 241
    angiogenesis, 244–247
    BG-ceramic (BGC), 242
    bioactive glasses (BGs), 240–241
    bioresorbability, 239–240
    chicken chorioallantoic membrane (CAM) assay, 244–247, 245f
    fabrication process, composite scaffolds, 243, 243f
    human bone marrow mesenchymal stem cells (h-BMSCs), 241
    mechanical features, tissues, 239–240
    molecular level scale BG-PCL (MBG-PCL), 242–243
    osseous tissue, 239–240
    osteoconductivity, 239–240
    osteogenecity, 239–240
    osteoinductivity, 239–240
    reactive oxygen species (ROS), 244–247
    wound healing activity, 244–247, 246f
    ZnO-containing films, 240
  scaffolds, 92, 93f

silicate-based materials, 382–383
silicon, 382–383
Tissue integration, 34, 34f
Toluene-2,4-diisocyanate (TDI), 129
Toluene diisocyante treatment, 71
Transmission electron microscopy (TEM), 189
2,2,2-Trifluoroethyl methacrylate (TFEMA), 128
Twin-screw microcompounder, 231–233
Type A gelatin, 9
Type B gelatin, 9

U

Ultrasonication, 13

V

van der Waal forces, 49, 298–299
Vascular endothelial growth factor (VEGF) delivery, 393–394
Vegetable seed oils (VSOs), 340–341
Vertise Flow (Kerr), 379–381
Vinyl acetate (VA), 297
3-(4′-Vinylbenzyl)-5,5-dimethylhydantoin (VBDMH), 121
Vinyltrimethoxysilane, 137
Vitamin B_2, 309–310, 310f
Vitamin C (VC), 191, 191f
Vulcanized rubber, 83

W

Water absorption, 77–78
Water contact angle (WCA), 33–34, 34f, 121, 208, 208f
Water retting, 57
Water treatment, polycaprolactone/metal oxide nanocomposites, 252–254, 253f
Wax, 74
Wettability, 33
White coir, 64
White jute *(Corchorus capsularis)*, 58
White ramie, 66
Wild almond *(Sterculia foetida)* tree, 63–64, 64f
Wool fibers, 139–141, 141f, 142t
Wound dressings, 391
aluminosilicate clay, 393–394
ceramic nanoparticles, 393
silver nanoparticles (AgNPs), 393, 394f
vascular endothelial growth factor (VEGF) delivery, 393–394
ZnO nanoparticles and chitosan, 393, 395
Wound healing activity, 244–247, 246f

X

Xanthoceras sorbifolia, 137
X-ray diffraction (XRD), 75–76, 189

Y

Young's modulus, 84, 124

Z

Zinc oxide (ZnO), 100

This page intentionally left blank

Biodegradable and Biocompatible Polymer Composites: Processing, Properties and Applications provides a comprehensive review on the processing, properties, environmental impact, and applications of biodegradable and biocompatible polymer composites.

This book begins by discussing the current state of the art, new challenges, and opportunities for various biodegradable and biocompatible polymer composite systems. Interfacial characterization of composites and the structure–property relationships in various composite systems are explained in detail via the theoretical model. Processing techniques for various macro and nanocomposite systems and the influence of processing parameters on properties of the composite are also reviewed in detail. The characterization of microstructure, elastic, viscoelastic, static and dynamic mechanical, thermal, rheological, optical, and electrical properties are highlighted, as well as a broad range of applications.

This provides a useful reference resource for both researchers and engineers working in composite materials science, biotechnology, and nanotechnology, as well as students attending chemistry, physics, materials science, and engineering courses.

About the Editor

Dr. Navinchandra Gopal Shimpi is presently wokring as Associate Professor in Deparment of Chemistry, University of Mumbai,Mumbai since April 2014. Previously he was associated with University Institute of Chemical Technoloyg, Jalgaon. Dr. Navinchandra has completed Ph. D from North Maharashra University, Jalgaon in 2006. He is recipent of Young Scientist Award from Asian Polymer Association in 2014 and Dnyanjoti Puraskar in 2008 from Shirsathe Foundation, Jalgaon. So far Dr. Navinchandra Shimpi has published more than 65 papers in International Journals of good impact factor and delivered more than 40 lectures as an invited speaker. He has generated Rs 1.2 cr for outstanding research from various funding agencies. He is at present having one research project from UGC, New Delhi and one consultancy project from Indofil Chemicals Ltd, Thane. So far seven students have completed their Ph.D, two have submitted their thesis and eight are doing their Ph. D under his guidance. Dr. Navinchandra Shimpi is having two granted patent and four are under examination. Moreover, Dr. Shimpi has guided 15 students for their M.Tech disseratiation. Besides this Dr. Shimpi have organized Five national and international confences with Five Staff Development programs and four professional certficates courses. Dr. Navinchandra G.Shimpi is Associate Editor of International Journal of Chemical Studies and worked as Lead Guest Editor for Advancement in Polymeric Nanomaterials and Nanocomposites a special issue of International Journal of Polymer Science

Related titles

Caroline Baillie and Randika Jayasinghe, *Green Composites*, 2nd Edition, Woodhead Publishing, 9780081007839

Mizi Fan and Feng Fu, *Advanced High Strength Natural Fibre Composites in Construction*, Woodhead Publishing, 9780081004111

Alan Lau and Ada Pui Yan Hung, *Natural Fibre-Reinforced Biodegradable and Bioresorbable Polymer Composites*, Woodhead Publishing, 9780081006566

ISBN 978-0-08-100970-3

9 780081 009703

ELSEVIER

WP WOODHEAD PUBLISHING

An imprint of Elsevier

elsevier.com/books-and-journals